

AD-A239 844



AGARD-CP-480

(1)

AGARD-CP-480

AGARD

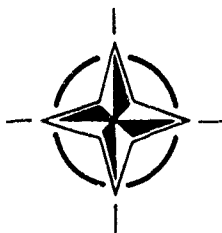
ADVISORY GROUP FOR AEROSPACE RESEARCH & DEVELOPMENT

7 RUE ANCELLE 92200 NEUILLY SUR SEINE FRANCE

AGARD CONFERENCE PROCEEDINGS 480

Low Temperature Environment Operations of Turboengines (Design and User's Problems)

Fonctionnement des Turboréacteurs en
Environnement Basse Température
(Problèmes Posés aux Concepteurs
et aux Utilisateurs)



NORTH ATLANTIC TREATY ORGANIZATION

For public release;
Distribution Unlimited

Distribution and Availability on Rack Cover

AGARD

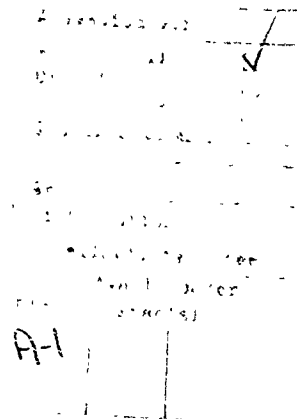
ADVISORY GROUP FOR AEROSPACE RESEARCH & DEVELOPMENT

7 RUE ANCELLE 92200 NEUILLY SUR SEINE FRANCE

AGARD CONFERENCE PROCEEDINGS 480

Low Temperature Environment Operations of Turboengines (Design and User's Problems)

Fonctionnement des Turboréacteurs en
Environnement Basse Température
(Problèmes Posés aux Concepteurs
et aux Utilisateurs)



Papers presented at the Propulsion and Energetics Panel 76th Symposium
held in Brussels, Belgium, 8th--12th October 1990.



North Atlantic Treaty Organization
Organisation du Traité de l'Atlantique Nord

91 8 26 094

91-08951



**Best
Available
Copy**

The Mission of AGARD

According to its Charter, the mission of AGARD is to bring together the leading personalities of the NATO nations in the fields of science and technology relating to aerospace for the following purposes:

- Recommending effective ways for the member nations to use their research and development capabilities for the common benefit of the NATO community;
- Providing scientific and technical advice and assistance to the Military Committee in the field of aerospace research and development (with particular regard to its military application);
- Continuously stimulating advances in the aerospace sciences relevant to strengthening the common defence posture;
- Improving the co-operation among member nations in aerospace research and development;
- Exchange of scientific and technical information;
- Providing assistance to member nations for the purpose of increasing their scientific and technical potential;
- Rendering scientific and technical assistance, as requested, to other NATO bodies and to member nations in connection with research and development problems in the aerospace field.

The highest authority within AGARD is the National Delegates Board consisting of officially appointed senior representatives from each member nation. The mission of AGARD is carried out through the Panels which are composed of experts appointed by the National Delegates, the Consultant and Exchange Programme and the Aerospace Applications Studies Programme. The results of AGARD work are reported to the member nations and the NATO Authorities through the AGARD series of publications of which this is one.

Participation in AGARD activities is by invitation only and is normally limited to citizens of the NATO nations.

The content of this publication has been reproduced
directly from material supplied by AGARD or the authors.

Published May 1991

Copyright © AGARD 1991
All Rights Reserved

ISBN 92-835-0618-9



*Printed by Specialised Printing Services Limited
40 Chigwell Lane, Loughton, Essex IG10 3TZ*

Recent Publications of the Propulsion and Energetics Panel

CONFERENCE PROCEEDINGS (CP)

Viscous Effects in Turbomachines
AGARD CP 351, September 1983

Auxiliary Power Systems
AGARD CP 352, September 1983

Combustion Problems in Turbine Engines
AGARD CP 353, January 1984

Hazard Studies for Solid Propellant Rocket Motors
AGARD CP 367, September 1984

Engine Cyclic Durability by Analysis and Testing
AGARD CP 368, September 1984

Gears and Power Transmission Systems for Helicopters and Turboprops
AGARD CP 369, January 1985

Heat Transfer and Cooling in Gas Turbines
AGARD CP 390, September 1985

Smokeless Propellants
AGARD CP 391, January 1986

Interior Ballistics of Guns
AGARD CP 392, January 1986

Advanced Instrumentation for Aero Engine Components
AGARD CP 399, November 1986

Engine Response to Distorted Inflow Conditions
AGARD CP 400, March 1987

Transonic and Supersonic Phenomena in Turbomachines
AGARD CP 401, March 1987

Advanced Technology for Aero Engine Components
AGARD CP 421, September 1987

Combustion and Fuels in Gas Turbine Engines
AGARD CP 422, June 1988

Engine Condition Monitoring — Technology and Experience
AGARD CP 448, October 1988

Application of Advanced Material for Turbomachinery and Rocket Propulsion
AGARD CP 449, March 1989

Combustion Instabilities in Liquid-Fuelled Propulsion Systems
AGARD CP 450, April 1989

Aircraft Fire Safety
AGARD CP 467, October 1989

Unsteady Aerodynamic Phenomena in Turbomachines
AGARD CP 468, February 1990

Secondary Flows in Turbomachines
AGARD CP 469, February 1990

Hypersonic Combined Cycle Propulsion
AGARD CP 479, December 1990

Low Temperature Environment Operations of Turboengines (Design and User's Problems)
AGARD CP 480, May 1991

ADVISORY REPORTS (AR)

Through Flow Calculations in Axial Turbomachines (*Results of Working Group 12*)
AGARD AR 175, October 1981

Alternative Jet Engine Fuels (*Results of Working Group 13*)
AGARD AR 181, Vol.1 and Vol.2, July 1982

Suitable Averaging Techniques in Non-Uniform Internal Flows (*Results of Working Group 14*)
AGARD AR 182 (in English and French), June/August 1983

Producibility and Cost Studies of Aviation Kerosines (*Results of Working Group 16*)
AGARD AR 227, June 1985

Performance of Rocket Motors with Metallized Propellants (*Results of Working Group 17*)
AGARD AR 230, September 1986

Recommended Practices for Measurement of Gas Path Pressures and Temperatures for Performance Assessment of Aircraft Turbine Engines and Components (*Results of Working Group 19*)
AGARD AR 245, June 1990

The Uniform Engine Test Programme (*Results of Working Group 15*)
AGARD AR 248, February 1990

Test Cases for Computation of Internal Flows in Aero Engine Components (*Results of Working Group 18*)
AGARD AR 275, July 1990

LECTURE SERIES (LS)

Operation and Performance Measurement of Engines in Sea Level Test Facilities
AGARD LS 132, April 1984

Ramjet and Ramrocket Propulsion Systems for Missiles
AGARD LS 136, September 1984

3-D Computation Techniques Applied to Internal Flows in Propulsion Systems
AGARD LS 140, June 1985

Engine Airframe Integration for Rotorcraft
AGARD LS 148, June 1986

Design Methods Used in Solid Rocket Motors
AGARD LS 150, April 1987
AGARD LS 150 (Revised), April 1988

Blading Design for Axial Turbomachines
AGARD LS 167, June 1989

Comparative Engine Performance Measurements
AGARD LS 169, May 1990

AGARDOGRAPHS (AG)

Manual for Aeroelasticity in Turbomachines
AGARD AG 298/1, March 1987
AGARD AG 298/2, June 1988

Measurement Uncertainty within the Uniform Engine Test Programme
AGARD AG 307, May 1989

Hazard Studies for Solid Propellant Rocket Motors
AGARD AG 316, September 1990

REPORTS (R)

Application of Modified Loss and Deviation Correlations to Transonic Axial Compressors
AGARD R 745, November 1987

Rotorcraft Drivetrain Life Safety and Reliability
AGARD R 775, June 1990

Theme

The low temperature environment and its impact on aircraft propulsion reliability continues to be of major concern to military and commercial aviation. The Propulsion and Energetics Panel and Flight Mechanics Panel have sponsored Specialists' Meetings and Symposia in the past directed at problems and challenges concerning cold weather operation. This Symposium on Low Temperature Environment Operations of Turbo-Engines is particularly relevant now because in recent years engine and component design technology advancement permits better accommodation of cold weather variables in engine development and anti-icing design considerations.

This Symposium will address engine design and user's problems as well as new testing technologies. The Symposium encompasses four sessions:

- Session I deals with user's requirements and operational experience.
- Session II addresses engine starting conditions, improvements in engine performance and reliability due to electronic engine control, life cycle management, and specific examples of anti-icing design methods and results.
- Session III addresses fuels and lubricants and their performance at low temperature.

Icing conditions, analytical prediction models, testing technology, and recent test results are included in Session IV

In summary, this Symposium ties together the requirements and operational community and the engine design and testing community while presenting a balanced analytical and empirical view of the state-of-the-art.

Thème

L'environnement basse température et son impact sur la fiabilité des systèmes de propulsion des aéronefs reste l'une des préoccupations majeures de la communauté de l'aviation civile et militaire.

Dans le passé, les Panels AGARD de propulsion et d'Energétique et de la Mécanique du Vol ont organisé des réunions de spécialistes et des symposia sur les problèmes posés et les défis soulevés par le fonctionnement des moteurs d'avion par temps froid.

Ce symposium sur le fonctionnement des turboréacteurs en environnement basse température est particulièrement pertinente aujourd'hui puisque les progrès réalisés récemment dans les technologies de conception des moteurs et des composants ont permis une meilleure prise en compte des variables liées au temps froid dans le développement des réacteurs et la conception des systèmes d'antigivrage.

Le symposium examinera les problèmes rencontrés par les concepteurs et les utilisateurs des turboréacteurs, ainsi que les nouvelles technologies d'essai. Il est organisé en quatre sessions:

- La Session I porte sur les besoins des utilisateurs et l'expérience opérationnelle.
- La Session II concerne les conditions de mise en route des réacteurs, les améliorations apportées aux performances et à la fiabilité des moteurs grâce à la régulation électronique réacteur et à la gestion de la durée d'utilisation, et propose quelques exemples spécifiques de méthodes et de résultats dans le domaine de la conception des systèmes d'antigivrage.
- La Session III examine les carburants et les lubrifiants et leurs performances à basse température.
- La Session IV traite des conditions de givrage, les modèles prédictifs analytiques, les technologies d'essai et présente des résultats d'essais récents.

En résumé, ce symposium a pour objet de réunir la communauté des exigences opérationnelles et celle de l'étude et des essais des réacteurs, en présentant une synthèse équilibrée, à la fois analytique et empirique, de l'état de l'art dans ce domaine.

Propulsion and Energetics Panel

Chairman: M. l'Ing Princ. de l'Armement Ph. Ramette
Société Européenne de Propulsion
24, rue Salomon de Rothschild
bP 303 — 92156 Suresnes Cedex
France

Deputy Chairman: Prof. Dr A. Uçer
Middle East Technical University
ODTU
Makina Muh. Bölümü
Ankara, Turkey

PROGRAMME COMMITTEE

Mr William W. Wagner (Chairman)
Technical Director (Code TD)
Naval Air Propulsion Center
(Code PE 3), P.O. Box 7176
Trenton, New Jersey 08628-0176
United States

Dr Robert C. Bill
Chief, Engine & Transmission Div
US Army Propulsion Directorate
(AVSCOM) Mail Stop 77-12
21000 Brookpark Road
Cleveland, Ohio 44135
United States

Major Ibrahim Corbacioglu
1 NCI hava İkmal Ve Bakım
Merkezi K lığı
Eskischir
Turkey

Professor Dr Dietmar K Hennecke
Fachgebiet Flugantriebe
Technische Hochschule Darmstadt
Petersenstrasse 30
6100 Darmstadt
Germany

Professor Rene Jacques
Ecole Royale Militaire
30, avenue de la Renaissance
1040 Bruxelles
Belgium

Ing. de l'Armement Christophe Meyer
Service Technique des Programmes
Aéronautiques
4, avenue de la Porte d'Issy
00460 Armées
France

Mr Manuel Mulero Valenzuela
Departamento de Motopropulsion y
Energia, (INTA)
Crta. Torrejon a Ajalvir, Km. 4
28850 Torrejon de Ardoz, Madrid
Spain

Mr Don M. Rudnitski
Head, Engine Laboratory
Division of Mechanical Engineering
National Research Council of Canada
Ottawa, Ontario K1A 0R6
Canada

Mr David J Way
PN2 Division
Propulsion Department
Royal Aerospace Establishment (Pyestock)
Farnborough
Hants GU14 0LS
United Kingdom

HOST NATION COORDINATOR

Major L. Gabriel

PANEL EXECUTIVE

Mr Gerhard Gruber

Mail from Europe:
AGARD—OTAN
Attn: PEP
7 rue Ancelle
92200 Neuilly sur Seine
France

Mail from US and Canada:
AGARD—NATO
Attn: PEP
APO New York 09777

Telephone: 33 (1) 4738-5785 Telex: 610176 (France) Telefax: 33 (1) 4738-5799

ACKNOWLEDGEMENT

The Propulsion and Energetics Panel wishes to express its thanks to the National Authorities from Belgium for the invitation to hold this meeting in Brussels, and for the facilities and personnel which make the meeting possible.

Contents

	Page
Recent Publications of PEP	iii
Theme/Thème	v
Propulsion and Energetics Panel	vi

Reference

SESSION I — COLD WEATHER OPERATIONAL EXPERIENCE AND REQUIREMENTS

Low Temperature Environment Operation of Turbo Engines — A Military Operator's Experience and Requirements by M. Summerton	1
Canadian Forces Cold Weather Experience in the Maintenance and Operation of Fighter Engines by C. Ouellette	2
Analyse des Problèmes de Demarrage par Temps Froid avec les Turbomoteurs d'Hélicoptère de Type ASTAZOU par W. Pieters	3
Avions d'Affaires Mystere-FALCON — Expérience Opérationnelle par Temps Froid par C. Domenc	4
Vulnerability of a Small Powerplant to Wet Snow Conditions by R. Meijn	5
Ice Tolerant Engine Inlet Screens for CH113/113A Search and Rescue Helicopters by R. Jones and W.A. Lucier	6

SESSION II — SYSTEM DESIGN CONSIDERATIONS

Cold Starting Small Gas Turbines — An Overview by C. Rodgers	7
Cold Start Optimization on a Military Jet Engine by H. Gruber	8
Cold Weather Ignition Characteristics of Advanced Small Gas Turbine Combustion Systems by S. Sampath and I. Critchley	9
Cold Weather Jet Engine Starting Strategies Made Possible by Engine Digital Control Systems by R.C. Wibbelsman	10
Cold Start Investigation of an APU with Annular Combustor and Fuel Vaporizers by K.H. Collin	11

	Reference
Control System Design Considerations for Starting Turbo-Engines during Cold Weather Operation by R.Pollak	12
Cold Start Development of Modern Small Gas Turbine Engines at PWC by D.Breitman and F.Yeung	13
Design Considerations based upon Low Temperature Starting Tests on Military Aircraft Turbo-Engines by H.-F.Feig	14
Climatic Considerations in the Life Cycle Management of the CF-18 Engine by R.W.Cue and D.E.Muir	15
Application of a Water Droplet Trajectory Prediction Code to the Design of Inlet Particle Separator Anti-Icing Systems by D.L.Mann and S.C.Tan	16
Captation de Glace sur une Aube de Prerotation d'Entrée d'Air par R.Henry et D.Guffond	17
Development of an Anti-Icing System for the T800-LHT-800 Turboshaft Engine by G.V.Bianchini	18
Engine Icing Criticality Assessment by E.Brook	19
Ice Ingestion Experience on a Small Turboprop Engine by L.W.Blair, R.L.Miller and D.J.Tapparo	20

SESSION III – FUEL EFFECTS AND LUBRICANTS BEHAVIOUR

Fuels and Oils as Factors in the Operation of Aero Gas Turbine Engines at Low Temperatures by G.L.Batchelor	21
The Effect of Fuel Properties and Atomization on Low Temperature Ignition in Gas Turbine Combustors by D.W.Naegeli, L.G.Dodge and C.A.Moses	22
Givrage des Circuits de Carburant des Turboréacteurs par F.Garnier	23
The Influence of Fuel Characteristics on Heterogeneous Flame Propagation by M.F.Bardon, J.E.D.Gauthier and V.K.Rao	24
The Development of a Computational Model to Predict Low Temperature Fuel Flow Phenomena by R.A.Kamin, C.J.Nowack and B.A.Olmstead	25
Paper 26 withdrawn	

SESSION IV – ICING CONDITIONS AND TESTING

Paper 27 withdrawn	
Environmental Icing Testing at the Naval Air Propulsion Center by W.H.Reardon and V.J.Truglio	28

	Reference
Icing Research Related to Engine Icing Characteristics by S.J.Riley	29
Modelisation Numérique de l'Evolution d'un Nuage de Gouttelettes d'Eau en Surfusion dans un Caisson Givrant par P.Creismeas et J.Courquet	30
Icing Test Capabilities for Aircraft Propulsion Systems at the Arnold Engineering Development Center by C.S.Bartlett, J.R.Moore, N.S.Weinberg and T.D.Garretson	31
Icing Test Programmes and Techniques by E.Carr and D.Woodhouse	32
A Documentation of Vertical and Horizontal Aircraft Soundings of Icing Relevant Cloudphysical Parameters by H.-E.Hoffmann	33
Developments in Icing Test Techniques for Aerospace Applications in the RAE Pyestock Altitude Test Facility by M.Holmes, V.E.W.Garratt and R.G.T.Drage	34
Entrée d'Air d'Hélicoptères: Protection pour le Vol en Conditions Neigeuses ou Givrantes par X.de la Servette et P.Cabrit	35

LOW TEMPERATURE ENVIRONMENT OPERATION OF TURBO ENGINES - A MILITARY OPERATOR'S EXPERIENCE AND REQUIREMENTS

by
Lieutenant Colonel M Summerton CEng MRAeS REME
School of Aeronautical Engineering
Army Air Corps Centre
Middle Wallop
Stockbridge
Hampshire SO20 8DY

SUMMARY

The United Kingdom's commitment to NATO includes the regular use of Royal Marine and Army helicopters in low temperature conditions. This paper specifically addresses the operation of the Westland LYNX helicopter with its Rolls Royce GEM engines during winter deployments in Norway where the near-arctic conditions present certain operating and working difficulties.

This paper considers these difficulties both generally, from a human and physical point of view, and then more specifically with regard to the engines themselves. Finally, it concludes with a few areas for improvement, with the emphasis on reliability, ease of maintenance, and effective development and testing before entry into service.

INTRODUCTION

The aim of this paper is to help set the scene, as a prelude to more detailed and esoteric discussion of low temperature engine problems. The paper has been kept deliberately short and essentially practical, and does not seek to investigate and solve the relatively few problems that the British Army experiences.

The paper deals exclusively with helicopter operations, conducted from field locations without the benefit of hangarage.

BACKGROUND

The British Army has some 360 aircraft, the majority of which are LYNX and GAZELLE helicopters based in the United Kingdom and West Germany. This fleet includes a squadron of aircraft which are operated by the Royal Marines who are a part of the Royal Navy.

This Royal Marine squadron, together with an Army flight of six GAZELLES, deploys from January to March each year to Norway where they participate in NATO exercises.

These deployments constitute the majority of our cold weather experience but we also get a certain amount from our aircraft based in West Germany, though the conditions there rarely approach the severity of Norway. Neither of these areas compare with places like Canada and the arctic regions, however, but with winter temperatures ranging from +5 to -30°C, with freezing rain, snow and ice, the climatic conditions are considered more than representative of the problems.

THE NATURE OF WINTER OPERATIONS

When considering low temperature operations, it is important for those associated with the specification and design of aircraft, to understand the essential practical nature of such operations. It is important because winter conditions present problems which are unique and which tend to aggravate any fundamental weaknesses of design and

manufacture. Above all, aircraft should be as reliable and maintenance-free as possible, but where maintenance is unavoidable, it should be capable of being completed in the shortest possible time, with the minimum quantities of tools and equipment. To understand why, consider how our Royal Marine squadron operates in Norway.

Operating Conditions. Initially, the Marines operate from ships, flying off pitching decks regularly doused with cold sea-spray. Having landed all of their vehicles, equipment and supplies, the road parties deploy inland to several different field locations, sometimes in wooded areas, and sometimes in and around villages or towns. Once in position they are joined by their aircraft, which tend to end up in deep, fresh snow, unlike the vehicles which are normally sited on, or close to, cleared tracks and roads.

Once inland, away from the moderating influence of the relatively warm sea, and perhaps well above sea level, they experience a variety of weather conditions including:

- a. Day-time temperatures in the region -10 to -15°C.
- b. Cold soak night-time temperatures down to -30°C.
- c. Driving snow which drifts and builds up on flat surfaces.
- d. Cloud, mist and rain.
- e. Freezing fog and freezing rain.
- f. Wind.

The Practical Difficulties. Operating in the above conditions, there are many practical difficulties. Keeping warm becomes a major preoccupation, especially if there is any wind, where only a moderate breeze can reduce a temperature of -7°C down to -24°C. At such temperatures, there is a progressively worsening risk of frostbite, which at the lower end can result in flesh freezing within a minute. Such a threat requires engineers to work in pairs on a buddy-buddy system, to monitor each other for any signs of frostbite or cold exposure. Low temperatures can also cause instant adhesion of bare skin to very cold surfaces, and cold burns. At temperatures as 'mild' as -10°C, bare metal contact is quite painful.

In such conditions, effective protective clothing is absolutely essential, but unfortunately, a glove that is warm is guaranteed to be totally unsuitable for detailed technical work such as adjusting engine controls and wire-locking components.

The obvious answer to the problem is to move the aircraft under cover whenever you need to carry out significant work, but this can only be done if there are suitable large buildings close to the landing site, and where the route to the buildings is sufficiently flat, and clear of snow and ice. In practice, the work involved in getting an aircraft under cover, is not normally

justifiable, but it can be done if the need is great enough.

The alternative is to leave the aircraft where it is and rig a shelter over the area being worked on, and apply local heat. This still requires considerable effort, however, and it creates a huge thermal signature which could badly compromise a unit's location.

Besides personal protection, there is also a need to protect the aircraft, with covers. However, the act of fitting the covers can represent quite a difficult task in itself, especially if they happen to be covered in snow and ice from previous use. The problem is compounded by the need to apply camouflage netting and by deep snow, where the aircraft will settle on its skis at one height, but all ground activity is conducted 30 to 40 cms lower.

Other practical problems also present themselves:

- a. It is difficult getting tools and equipment out to the aircraft, especially in a full tactical setting where they will be widely dispersed around a location.
- b. If tools and equipment are dropped in the snow they can be very difficult to find.
- c. Before working on the aircraft you have to remove portions of the camouflage and protective covers.
- d. When you climb onto an aircraft you must be careful to remove all snow and ice from your boots, otherwise you can slip very easily.
- e. Protective hoods tend to restrict peripheral vision and hearing, making you more prone to dropping tools and banging your head on aircraft structure. Likewise, the wearing of NBC equipment is especially limiting.
- f. When carrying out technical work you have to leave your gloves off most of the time and you therefore need frequent warming-up. Job times are often doubled or trebled.

ENGINE PROBLEMS

With the exception of the points which are considered below, the operation of our GEM engines in cold weather present relatively few problems. From the flying point-of-view, once the engines are started and are stabilised at correct temperatures and pressures, then the only subsequent concern is for the adherence to snow and ice limitations.

From the engineering point-of-view, the picture is equally good: if you compare defect rates, spares usage, and data from engine health monitoring systems, then there is no detectable difference between cold and temperate engine operation.

Of far greater concern is fundamental engine reliability and maintainability, because, as illustrated above, any technical work that has to be carried out on an aircraft, in cold conditions, is extremely difficult.

Having put the subject in its correct context, let us now consider the problems that we do have.

Cold Soak. When an aircraft has been cold-soaked below -26°C , we have to heat the engines and gearbox to bring the main rotor gearbox sump temperature back to -26°C before we can attempt a start.

The act of having to rig up the heat source and the time it takes, however, is unacceptable.

Cold soak can also lead to the freezing and stiffness of engine controls, especially teleflex controls which may have got moisture inside them.

Starting. Successful starting is almost exclusively a function of adequate levels of electrical power. If we have well-charged aircraft batteries or we use an external DC supply, then we find the GEM engine relatively easy to start. If, however, electrical power is low then we experience:

- a. Stagnation/failure to start.
- b. Excessive light-up times, (30-50 secs rather than 22 secs).
- c. Wet starts and excessive turbine temperatures.

Operating from woods, in deep snow, and probably scattered over a wide area, arranging external power from either a vehicle or a ground rig can at best be unacceptably slow and inconvenient, and at worst, impossible. Our aircraft may also be operating totally remote from such support. We therefore prefer to use internal battery power as the norm. However, after overnight exposure to temperatures of -10°C and below, or a 24 hour soak at even milder temperatures, we find that many of our batteries have only marginal power for successful starting. The only solution in this case is to anticipate conditions and remove the battery to a warm area, but this in turn can impose a technical burden that is even worse than the lack of external power.

The problem of low battery power is almost certainly aggravated by increased engine turning resistance. We always check our engines for free rotation in case of any technical failure, or in case of any water having run-back into the engine and freezing in contact with rotating assemblies. In spite of the use of lower viscosity oil, however, it is noticeable that engine resistance is greater in comparison with temperate operation.

In our experience the only other factor that affects engine starting, is fuel volatility. Given the choice we would use F40 AVTAG which has a flash point of only -40°C , but we are normally supplied with F34 AVTUR which has a much higher flash point of $+38^{\circ}\text{C}$. At the other end of the scale we would prefer not to use the navy's F44 AVCAT which has an even higher flash point, for shipborne safety. Subjectively, we would say that there is a 5°C difference in the ambient temperature at which AVTUR will successfully start an engine, compared with AVCAT, (ie. a particular marginal engine and battery combination might manage an AVCAT start at -5°C , whereas AVTUR could manage it at -10°C).

In all cases of difficult starting, slight advancement of the engine speed select lever beyond the 'Ground Idle' gate normally helps, but T6 limits need careful monitoring.

Snow and Ice The most significant limitation on the use of helicopters in cold weather is the hazard caused by snow and ice. In our Ministry of Defence, the various climatic conditions in which our aircraft may be required to operate, are defined in DEFENCE STANDARD 00-970. These standards mandatorily require operation in

temperatures down to -26°C and no damage from cold soak down to -40°C . On the icing side, the standard defines nine different conditions that an aircraft may be required to operate in. These conditions can be summarised as:

- a. Clear air ice.
- b. Mixed snow and ice.
- c. Falling snow.
- d. Re-circulating snow (caused by hovering in ground effect).
- e. Freezing fog.
- f. Freezing rain/drizzle.

In practice, we find that unless the weather is almost clear blue skies, then we are greatly limited in when we can fly. These limitations are due to:

- a. A general lack of visibility.
- b. Ice accretion on rotors which destroys lift and causes severe vibration.
- c. General ice accretion on the airframe which, for example, might break off and damage a tail rotor, or enter an engine as a foreign object.
- d. Ice accretion on or around engine intakes, restricting air flow, or threatening ingestion.
- e. Snow and slush deposits which threaten ingestion.

We are advised that an ordinary-sized snowball is capable of flaming-out a GEM engine, and that a 15cc lump of ice can cause serious damage to the engine's axial flow, LP compressor.

The impression that we have gained, as operators, erroneously or not, is that we specify mandatory temperature requirements, but we do not appear to specify and achieve particular snow and ice requirements. As a consequence, when we conduct our cold weather testing, to establish in-service operating limits, we end up having to restrict the aircraft's operation to what we find, rather than just confirming what the designer has achieved in satisfaction of a contract specification.

In the case of the LYNX, this has resulted in us having spent many years trying to develop a satisfactory snow and ice guard, capable of extending the aircraft's snow and ice clearances to reasonably acceptable operational limits. This has now been achieved. From this experience we would note the extent to which the engine designer is very much dependant on the aircraft designer, to achieve a satisfactory intake design, and further, we would observe that an aircraft's snow and ice clearance is only as good as its worst feature. We hope that both our ministry and industry have learnt the appropriate lessons.

CONCLUSIONS

In conclusion, based on our experience of the LYNX/GEM combination, we would like to see the following general improvements:

- a. Even more reliable and maintainable

engines, to minimise the amount of work that has to be carried out in low temperature conditions.

- b. Lower cold-start limits to avoid any necessity for having to pre-heat engines and gearboxes.
- c. Better batteries that are less prone to losing their charge, or an alternative design of autonomous starting system which is less dependent on battery condition.
- d. In conjunction with the above, even more dependable starting.
- e. Fully integrated airframe and engine intake design to provide full airframe, transmission and engine protection from snow, slush and ice.
- f. More thorough specification, development and cold weather testing before delivery to service.

The state-of-the-art on helicopters may still not allow us to achieve, sufficiently economically, the level of snow and ice performance to which we would ideally aspire, but what is quite clear to us, is that between our ministry and industry, we must specify and actually achieve, realistic requirements that sensibly reflect the operational need. In the meantime, in the context of both temperate and cold weather operations, we must continue to strive to make our aircraft and engines as reliable and maintainable as possible.

Discussion

1. W. Wagner, US Navy

Please address starting limitations concerning lubricants or viscosity problems at low temperature.

Which problems effect engines or power drive system components?

Author.

We have no lubricant problem with the GEM engine in cold weather. Oil temperatures and pressures have to be monitored during start-up, and they take longer to stabilize, but this does not cause any problems.

We do not change engine oil when operating at low temperatures but we do change transmission oil to a lower viscosity type.

A check of serviceability statistics reveals no detectable difference between temperate and cold weather operations.

2. W. Wagner, US Navy

Please identify the engine design problems which this assemblage of design and manufacturing community could address

Author.

Fundamental reliability is the most important requirement both in temperate and in cold weather conditions.

A properly integrated airframe and engine inlet design is of equal importance, but whether you start with the assumptions of an ice-tolerant engine or not is a question of philosophy. If you have a robust, ice tolerant engine, then the integration of the engine into the airframe is not as critical, and the protection afforded to the engine can be reduced. Neither of our two main helicopters have fundamental engine design problems viz-a-viz cold weather operation.

LOW TEMPERATURE ENVIRONMENT OPERATIONS OF TURBO ENGINES

by

Lt Christian Ouellette
Mechanical and Propulsion Engineering Officer
Base Aircraft Maintenance Engineering Organization
Canadian Forces Base Cold Lake
Medley, Alberta
Canada

INTRODUCTION

Good morning Ladies and Gentlemen, Bonjour Madames et Messieurs, my name is Lt Christian Ouellette and I am here representing the Operational and Maintenance community of the Canadian Armed Forces, and more specifically the branch of Air Command. I am the Mechanical and Propulsion Engineering Officer at Canadian Forces Base Cold Lake, situated in the Central Eastern portion of the province of Alberta.

It is my distinct pleasure to share with you some of our experiences in the maintenance and operation of Turbo Engines under cold weather conditions.

Canada is a vast country, bordered by two oceans and the arctic circle. Our Armed Forces, with its varied commitments of Peacekeeping, the North Atlantic Treaty Organization (NATO) and the North American Air Defence (NORAD) plan, have the unenviable task of patrolling and protecting the vast reaches of the North American Northern Region.

Never a dull moment it seems. From the time we first turn over an aircraft at dawn, our missions vary from hunting down the odd arctic Bear-H, to escorting MIG-29s who have a tendency to wander and lose their way.

This morning's presentation will cover the following areas:

- (a) The climate conditions which we are faced with in Canada;
- (b) a summary of our operational role and commitments;
- (c) a brief look at some maintenance problems and practices associated with the cold weather environment;
- (d) the "Hung Start" problem associated with CF-18, GE-F404 engine; and
- (e) a quick review on the status of the infamous J-85-CAN-15 compressor stall problem.

CLIMATIC CONDITIONS

Canadian Forces Base Cold Lake, appropriately named, is located along the 54th parallel. The following is a graph depicting the temperature norms of the area over a 12 month period. Although our MEAN temperature low is only about -18 deg C, we face ARCTIC type conditions for over 35% of the November to February time frame. Wind chill factors reach in excess of 1625 Watts per square meter, a point at which exposed flesh freezes.

Inuvik, situated above the 68th parallel, is one of our four main Forward Operating Locations (FOLs). Weather conditions during the winter months are generally bitter, compounded further by constant prevailing winds from the East, driving temperatures down into extreme lows. The outside temperature (excluding the wind chill factor) is below -20 deg C for over 150 days per year.

OPERATIONAL ROLE

Our Air Force utilizes the CF-5 Freedom Fighter as our "Basic Fighter Pilot Trainer". We operate about 40 CF-5 aircraft out of 419 Sqn at CFB Cold Lake. The nucleus of our air defence posture is our front line Fighter and Interceptor, the CF-18 Hornet. A total of 125 CF-18s are spread amongst 8 squadrons, located in Baden-Soellingen—Germany, Bagotville—Quebec and Cold Lake—Alberta.

Our operational commitments are as follows:

- (a) Basic Fighter Pilot Training at 419 Sqn on the CF-5, and at 410 Sqn on the CF-18;
- (b) NORAD peacetime alert role and wartime deployment capability;
- (c) Air to Air Intercept;
- (d) Air Superiority and NATO training; and
- (e) Air to Air/Air to Ground peacetime training.

At CFB Cold Lake, our 3 CF-18 Squadrons combined, over the winter months of November to February, fly an average of 860 sorties per month. 419 Sqn alone, with the CF-5, averages 490 sorties per month during the cold weather season.

MAINTENANCE PROBLEMS AND PRACTICES

Severe weather conditions pose a series of the challenging problems to the maintenance community. The types of obstacles encountered are as follows:

- (a) **Personnel Protection Against Cold**
When servicing/starting aircraft in extreme conditions, safety of personnel is first and foremost. Crew members must protect themselves from the bitter temperatures by adding layer upon layer of clothing, making it difficult at times to perform routine servicing tasks;
- (b) **Power Take-Off Shaft Shearing**
Special precautions must be observed on engines which drive exterior gearboxes (such as the accessory drive system on the CF-5). In extreme cold weather the oil in the gearbox gels and the drive shaft will shear on engine start. Usual precautions as follows:
 - (i) motor the engine prior to starting;
 - (ii) apply heat (portable heater) to the gearbox;
 - (iii) run engine for minimum time before applying loads on generators, pumps
- (c) **Hydraulic Seal Leaks**
Hydraulic system "O" rings on cold soaked equipment will tend to leak. The normal cure is to let the system warm up at idle, eliminating the leaks once the system warms up.

(d) Fire Extinguishers

When the temperature drops to -40 deg C and below, fire extinguishers may not work as advertised (particularly CO_2 extinguishers) for they do not generate enough pressure to adequately push out the extinguishant. At Cold Lake we have special extinguishers which we have identified by a broad blue band on the case

(e) Fluid Servicing Carts

Servicing carts containing fluids may cause contamination problems. Carts are generally stored in the hangar at a temperature of 70 deg F. While hangar doors are often opened several times per day, the temperature quickly drops to that of the outdoors. During cold weather, the temperature of the cart shell (always metal) can be subject to temperature fluctuations of up to 100 deg F. This causes condensation within the cart and contaminates both the cart and the system replenished by that cart. In the CF-5 world we get frequent complaints from SPAR, one of our 3rd line maintenance contractors, about water contamination in the CF-5 Accessory Drive System. The only solution to this problem is to check the carts daily for water contamination, and drain water when found

(f) Starting Problems

In general the gas turbine engine starts easier under cold weather conditions, however some problems do occur. Failures to start can usually be attributed to either improper ignitor plug depth, burned out plugs or wetting of the plug (caused by introducing fuel into the engine before firing the plug).

(g) Overpower/Stalls

All gas turbine engines develop greater power in cold temperatures, thereby becoming more prone to stall. While stall prevention measures will vary according to the equipment, general rules such as "No Erratic Operation or Sudden Power Changes" will generally apply.

!!! HUNG START PROBLEM/F404-GE-400 ENGINE

The CF-18, F404 Engine is experiencing periodic Hung Start and Roll Back problems during cold weather operations. As recently as last spring, while on deployment to Inuvik, up to 6 hung starts per day were experienced, in an average temperature environment of -42 deg C. Present operating instructions call for motoring of the engine for 2 minutes prior to start. If a hung start is experienced, there are a series of checks to be carried out, verifying integrity to electrical connections, density settings etc. If no fault found, motor engine for an additional 2 minutes and repeat procedure until start occurs. If after repeated tries, the hung start persists, remove and replace Main Fuel Control. The situation in Inuvik often requires in excess of 15 minutes of engine cranking and throttle movement to achieve engine start.

Given the critical nature of operations at Forward Operating Locations, delayed aircraft starts are totally unacceptable. Further investigation into the Main Fuel Control start schedule is required and has been recommended.

CF-5/J-85-CAN-15 COMPRESSOR STALL HISTORY

Since the introduction into service of the CF-5 in the 1960s, the problem of sudden compressor stalling has plagued the fleet. This phenomenon was first identified during cold weather evaluations of the aircraft in the late 1960s, and continues to be a problem to this day.

The following traces back the history of the stall problem, outlining lessons learned, along with our present status:

- Feb 75 Investigation by NRC showed that engine anti-ice increased the stall margin.
- Nov 76 The interrelationships between RPM and EGT cutback, and T2 sensor outputs were discussed. The potential problem that incorrect T2 sensing could adversely affect stall characteristics was identified.
- Mar 78 Flight tests concluded and recommended a modification to activate anti-ice concurrent with the Afterburner.
- Jan 79 A temperature soaking procedure to prevent compressor stalls at very cold temperatures, mainly during ground runs, was recommended and implemented at 419 Squadron, until the Gas-Filled T2 sensor mod was installed.
- May 82 Underwent flight testing of a modified T2 sensing system, with a recommendation for relocation of the Resistance Temperature Detector (RTD) and adjustment of the MFCU to start RPM cutback at -15 deg C.
- Nov 82 Testing of the automatic engine anti-ice engagement system, whereby anti-ice is selected for 10 seconds following A/B initiation. Aircraft were modified and a reduction in stall numbers was recorded.
- Oct 84 MFCUs were biased by $+30$ deg F to compensate for inaccurate T2 sensing. Technique was somewhat effective in reducing stalls.
- Oct 87 Modification CF-055, Gas Filled T2 sensor was implemented.

PRESENT STATUS

- Installed:
 - auto engine anti-ice engagement system
 - GFT2 sensor/modified T5 amplifier
 - various AOI and unit flying order changes
- Modifications underway
 - automatic takeoff doors: automatically open for flight below $M = 0.45$
 - P3 lag tube: damps out rapid fluctuations of the P3 tap, which is an input to the MFCU
- Projected
 - the definition of the true icing limits for the aircraft, and the correct RPM cutback schedule
 - considering a new replacement T5 amplifier

PRESENT STALL RATE SITUATION

The following is a graph depicting the J-85 Stall rate, per 1000 hrs, over a 3 year average. The total number of stalls per year have gone from:

- 1987 — 76
- 1988 — 53
- 1989 — 36
- 1990 — even less

Discussion

J. R. E. Smith, Sverdrup

What were the fixes applied to make the fire extinguisher units effective at low temperatures?

Author:

The fire extinguishers acquired for cold weather conditions are still CO₂ types, but with a greater built-in discharge pressure. How this is accomplished, I am not certain. However, we have identified these extinguishers with a wide blue band to ensure we do not use them in temperature conditions above -26 C ambient.

2. W. Alwang, Pratt and Whitney

What was the nature of the T2 sensing problem and how was it corrected?

Author:

The T2 sensor was formally located near the under surface of the aircraft where air is collected by two scoops, one for each engine, and is ducted to the MFCVs. The problem was that the total temperature of the sample air picked up by the scoops was not representative for CIT, hence EGT and engine cutback were noch occurring on schedule, increasing the stall margin.

The RTD sensor was relocated to an area in the engine bay where a representative value of CIT could be obtained. Further sensing errors continued, so MFCV was biased to correct, and some improvement was seen.

Eventually the introduction of a gas-filled sensor eliminated the sensing error and was successful in reducing the stall rate.

3. R. Toogood, Pratt and Whitney Canada

You have spoken at some length on the CFT stall problem. Have you experienced any significant cold weather problems as yet with the CF 18 aircraft?

Author:

Our experience with the CF18 in cold weather is that the aircraft performs better. Our only complaint is with the scheduling of the MFCV during cold weather start-up. Our hung-start problem is critical during certain operations, and is considered totally unacceptable. This issue is apparently being addressed during paper 10.

4. P. Sabla, GEAC

What is the normal start-up procedure that permits plug wetting?

Author:

Our present start-up procedure for the CF-5 is as follows

- motor engines to 14.5%
- engage ignition
- advanced power lever, introduce fuel.

Our wet start problem is not caused by an erroneous start procedure, but rather by pilot error in selecting power lever too early. PILOT error will continue to be a problem, therefore perhaps the issue of a safeguard against accidental wetting can be addressed.

How is failure to spark detected?

Author:

We rely on the inability of the engine to fire-up as an indicator.

5. C. Rodgers, Sundstrand Power Systems

Do all CAF aircraft fly from prepared bases?

Do you provide portable heating for aircraft flying from unprepared forward bases?

Author:

Our fleet of CF-18 is based at prepared main operating bases (FOLs) where we make use of facilities on site, which in the most cases are inadequate. In other words, storage facilities for both aircraft and equipment are in short supply. Although portable heat is available at FOLs, i.e. Herman Nelson's, conditions generally render them little or no use. Heating is generally used for personal rather than A/C. We prefer to conduct starting operations with cold soaked A/C, avoiding the problems of expansion and contraction associated with introducing heat in severe conditions.

6. W. Wagner, US Navy

You referred to hung starts at extreme low temperatures with CF 18 aircraft. Would today's full authority digital electronic controls eliminate this problem?

Comment by R. Wibbelsman, GE:

The floor indicated it would correct the situation, and the problem will be addressed in detail in paper 10 tomorrow.

ANALYSE DES PROBLEMES DE DEMARRAGE PAR TEMPS FROID AVEC LES TURBOMOTEURS D' HELICOPTERE DE TYPE ASTAZOU.

par
Lieutenant Ir. W. PIETERS
Offr Maint
255 Cie Maint d' Aviation Légère
Flugplatz Butzweilerhof
Butzweilerstrasse
5000 KOLN 30
RFA

RESUME

Pendant les périodes d' hiver assez sévères au début des années 80, l' armée belge a connu de considérables problèmes de démarrage sur ses hélicoptères de type ALOUETTE équipés de turbomoteurs ASTAZOU.

Le rapport reprend les méthodes de détection des phénomènes employées par les utilisateurs, les actions immédiates prises au sein de l' armée et les solutions élaborées en collaboration avec les constructeurs ainsi que leurs conséquences budgétaires.

SUMMARY

During the heavy winter periods in the beginning of the 80th, the Belgian army had considerable starting problems on his helicopters ALOUETTE equipped with ASTAZOU turbo engines.

The papers discuss the different detection methods of the phenomena employed by the users, the immediate actions undertaken by the army and the solutions worked out in collaboration with the constructors as well as their budgetary consequences.

NOMENCLATURE

- 255: Abréviation utilisé dans le texte, indiquant la 255 Compagnie Maintenance et Dépôt d' Aviation Légère, faisant l' entretien des hélicoptères de la Force Terrestre de l' armée belge.
T4: Température à la sortie de la turbine.
P2: Pression à la sortie du compresseur.
RG: Révision générale, allouant un nouveau potentiel au turbomoteur.
VNIP: Visite Non Interruptive de Potentiel, le potentiel du moteur reste le même après son passage en usine.
FB: Francs Belges.
IT: Instruction Technique.
FF: Francs Français (avec 1 FF=6,5 FB).

1. INTRODUCTION.

a. Situation de l' armée belge.

L' armée belge, stationnée partiellement en Allemagne de l' Ouest et en Belgique, utilise des hélicoptères pour répondre à ses fonctions lui imposées dans le cadre des conventions de l' OTAN. Ainsi elle dispose actuellement de (Situation clôturée le 01 jan 90):

- FORCE TERRESTRE: 56 hélicoptères ALOUETTE II, dont 16 avec moteur ARTOUSTE et 40 avec moteur ASTAZOU. En utilisation depuis 1958, ils ont des missions d' observation et de liaison. Notons que l' armée a conclu récemment un contrat pour l' achat de 46 hélicoptères AGUSTA 109 dont 28 recevront une mission antichar et 18 auront une mission d' observation et de liaison. Leur livraison est prévue dès le mois de juin 1991. Une trentaine (32) d' ALOUETTES II resteront quand-même en service comme hélicoptère de liaison, mais uniquement en version ASTAZOU.
- FORCE AERIEENNE: 5 hélicoptères SEAKING prévus spécialement pour des opérations de sauvetage en mer.
- FORCE NAVALE: 3 hélicoptères de type ALOUETTE III, avec des missions de sauvetage en mer.
- GENDARMERIE: 3 hélicoptères de type PUMA.

Les hélicoptères de la Force Terrestre feront l' objet de cet exposé. Ils sont utilisés dans des conditions climatiques très variées, allant d' un climat maritime modéré en Belgique à un climat continental plus vers l' Est. En principe les conditions climatiques sont assez favorables point de vue température, avec une humidité

relativement élevée. Normalement, on ne connaît guère de problèmes dus à des températures extrêmement basses. Cependant, les années 80 ont été marquées par une succession de quelques périodes d'hiver très sévères ainsi que quelques périodes nettement plus modérées. Pendant ces périodes d'hiver sévères, des problèmes se sont manifestés.

b. Position du problème.

Pendant les périodes d'hiver au cours des années 80, l'armée belge a connu de considérables problèmes de démarrage sur ses hélicoptères de type ALOUETTE II pourvu de turbomoteurs de type ASTAZOU II A2.

L'exposé reprendra toutes les phases du problème, de sa détection jusqu'aux solutions élaborées ainsi que ses conséquences budgétaires.

2. THEORIE ELEMENTAIRE DE LA PHASE DE DEMARRAGE DES MOTEURS ASTAZOU.

Le circuit de démarrage se compose de 4 parties (annexe A)

- la micropompe (1)
- le robinet 4 voies (2)
- la prise d'air du carter turbine (3)
- les allumeurs-torches (4)

Le fonctionnement est le suivant. Dès la mise en marche, la micropompe aspire le carburant et en première phase purge son circuit. Quand la pression s'élève, le carburant est refoulé vers le robinet 4 voies qui contient une bille. La pression du carburant repousse la bille sur son siège et ouvre ainsi la voie vers les allumeurs-torches en bouchant la sortie du kérosène vers la prise d'air P2 qui est une prise d'air totale à la sortie du compresseur centrifuge. Le kérosène est injecté dans la chambre de combustion et enflammé par les allumeurs-torches.

Une fois que l'allumage est réalisé, la micropompe est coupée automatiquement; la pression carburant retombe à zéro et la bille du robinet 4 voies est soulevée de son siège car d'un côté elle est soumise à la pression totale P2 et de l'autre côté elle reçoit la pression statique régnant au niveau des allumeurs-torches laquelle est plus basse. Ce courant d'air sèche les tuyauteries et évite l'encrassement des allumeurs-torches par carbonisation du kérosène.

3. LA SURCHAUFFE AU DEMARRAGE.

a. Température idéale de démarrage.

Le constructeur a défini dans son manuel de vol une température idéale de démarrage T4 de 450 °C pour moteur froid et de 550 °C pour moteur chaud; on considère qu'un moteur est chaud quand la T4 résiduelle est de plus de 100 °C et de moins de 150 °C. En respectant ces plages de température lors du démarrage, le bon fonctionnement du turbomoteur ne devrait pas être problématique.

b. Surchauffe au démarrage.

Dans son manuel d'entretien édition Déc 1987, le constructeur a, d'une manière empirique, donné des températures de surchauffe au démarrage. Ce sont des températures à ne pas dépasser lors du démarrage sous peine d'endommagement de la turbine. Voici les contrôles qu'il a prévus:

SI T4 > 750 °C pendant t > 5 sec: Le moteur doit retourner en usine pour révision.

SI T4 > 750 °C pendant t < 5 sec: Le moteur peut être maintenu en service après
OU T4 > 700 °C mais < 750 °C certains contrôles spécifiques à la 255.

La température de surchauffe dépend principalement de la matière de construction des aubes des disques de turbine.

c. Les causes de surchauffe au démarrage.

Pour nos hélicoptères, quelques causes "classiques" de surchauffe au démarrage sont connues.

- (1). Une tension de batterie trop faible provoque une tension primaire et secondaire d'allumage trop basse. L'allumage est retardé tandis qu'un excès de carburant s'accumule dans le carter turbine. Ce surplus de carburant s'enflamme d'une manière brutale lors de l'allumage, il en résulte une température de démarrage excessive.
- (2). Un fonctionnement déficient du robinet 4 voies. La bille se trouvant dans le corps du robinet peut se bloquer et perdre son étanchéité par le givre ou par l'encrassement. Ainsi, du carburant envoyé par la micropompe peut entrer dans la chambre de combustion aussi bien par la prise d'air P2 que par les allumeurs-torches. Il en résulte un apport excessif de carburant par la prise de pression qui aboutit à une surchauffe au démarrage lors de sa mise à feu.
- (3). En dehors de ces causes primaires, il existe quelques causes secondaires de surchauffe au démarrage, notamment:

- La présence d'eau dans le carburant. L'Administration Fédérale de l'Aviation indique qu'une concentration de 30 ppm peut être dangereuse car elle peut provoquer le blocage du robinet 4 voies lors du refroidissement du carburant.
- Le bypass de la pompe de carburant mal réglé pourrait provoquer une pression de carburant trop élevée.
- Un mauvais fonctionnement du régulateur barostatique qui permet la régulation du débit carburant en fonction de l'altitude.
- Une pression micropompe trop élevée.
- Une entrée d'air obstruée, même partiellement.

4. LES SURCHAUFFES AU DEMARRAGE DANS LES ESCADRILLES. ANALYSE DES INCIDENTS ET ACCIDENTS.

a. Les périodes d'hiver 1982/83 jusqu'à 1984/85.

L'annexe B représente un état récapitulatif des incidents et accidents pour lesquels un avis technique a été établi par la 255 pendant la période 1982-1984. Sur un total de 70 hélicoptères, on compte 23 accidents/incidents dont 5 dus aux surchauffes au démarrage. Deux de ces incidents étaient causés par un erreur de pilotage; les trois autres avaient une cause purement technique: le gel du robinet 4 voies par temps froid. Le coût d'une révision générale s'élève à environ un million de FB (prix 85 non actualisé) sans compter l'immobilisation de l'hélicoptère, les frais de dépannage éventuels, le main d'oeuvre... Il va de soi que des incidents successifs, comme ils se sont produits au début 1985, sont très lourds à supporter. Non seulement, ils consomment entre 15 et 20 % du budget prévu pour l'année, mais ils ont également une influence directe sur la disponibilité des machines et sur le planning des heures de vol.

b. Analyse des problèmes.

Les problèmes de surchauffe au démarrage étaient relativement bien connus. De temps en temps, des surchauffes se produisaient suite à une mauvaise manipulation du pilote ou à un défaut technique. Les deux cas mentionnés en 1982 en sont la preuve. La 255 avait d'ailleurs déjà édité depuis le mois de juin 1978 une instruction technique pour attirer l'attention du pilote sur ce phénomène. Ces instructions techniques émises par la 255, qui, en matière de sécurité de vol, priment sur tout autre document (sans être en contradiction avec celui-ci naturellement), traitent des problèmes spécifiques rencontrés sur nos hélicoptères.

L'IT II B4 n° 3 en question parlait de la température idéale de démarrage, comme défini ci-dessus et indiquait les causes possibles de son dépassement. En ce qui concerne les températures maximales autorisées au démarrage, elle référait simplement au manuel de vol. Cette IT devait être portée à la connaissance des pilotes régulièrement et pour marquer son importance, des briefings spéciaux étaient donnés systématiquement.

Les trois incidents de début 1985 étaient considérés comme une suite plus ou moins aléatoire dont la cause présumée était le givrage de l'eau de condensation dans le robinet 4 voies. C'est pourquoi que le commandement se limitait à envoyer quelques notes de rappel de l'IT traitant du vol en atmosphère neigeuse et givrante. On imposait également la mise en place des housses de protection dès l'arrêt de la machine. Les mesures prises paraissaient adéquates car au cours de l'année, il ne se produisait plus de surchauffe.

c. La période d'hiver 1985-1986.

Pendant la période d'hiver 1985-1986 quatre surchauffes au démarrage se produisaient dans un délai de trois semaines (annexe C). C'était un désastre, deux moteurs devaient subir une RG, les deux autres devaient subir une VNIP. Les frais de réparation s'élevaient à environ 7,5 millions de FB. Les causes des incidents étaient à chaque fois soit un robinet 4 voies gelé, soit une batterie trop faible, soit une combinaison des deux facteurs. Le résultat était catastrophique car il ne restait plus aucun moteur de réserve pour le dépannage des machines immobilisées.

d. Analyse des problèmes.

Au début de l'hiver des briefings spéciaux avaient encore été donnés sur le problème de surchauffe au démarrage; la réaction des autorités ne se faisait pas attendre. Des sanctions pécuniaires pour le responsable de l'incident furent proposées et la 255 fut incitée à sortir des nouvelles IT; mais le premier pas envers la solution du problème était la mise sur pied d'une commission d'enquête pour traiter le problème dans sa globalité. Début mai 1986, la commission d'enquête sortait ses résultats.

Comme première cause principale des problèmes, la commission indiquait la faible charge de la batterie, elle proposait alors de faire particulièrement attention au voltage et aux tests de batterie pendant les périodes d'hiver. Elle proposait également de faire remplacer la génératrice DYNASTAR par une génératrice à courant de chargement supérieur et de faire construire, en collaboration avec le constructeur, un circuit de protection pour couper automatiquement la séquence de démarrage si la tension batterie descendait en dessous du seuil dangereux de 14 Volt.

Comme deuxième cause principale, le bon fonctionnement du robinet 4 voies était mis en question. La commission proposait de chercher une solution en collaboration avec le constructeur ou bien en déplaçant le robinet 4 voies ou bien en plaçant un système de préchauffage du robinet 4 voies. Elle proposait également de faire la mesure du degré hygrométrique du carburant en début d'hiver.

En ce qui concerne le problème de la batterie, il avait déjà été remarqué au début 1985, suite à une consommation anormale d'éléments de batterie que celles-ci étaient souvent insuffisamment chargées et que la méthode de charge et de décharge par impulsions pouvait être améliorée. Ce problème s'aggravait en hiver car la batterie perdait de sa capacité. Sur base de ces arguments, la décision était prise de former les responsables de la charge des batteries directement en usine chez la firme VARTA et d'être beaucoup plus sévère lors du contrôle des éléments. Les frais de remplacement des éléments batterie pour la période 1985/87 s'élevaient à 5,5 millions de FB. En outre, de nouveaux chargeurs de batterie étaient acquis pour une valeur totale de 600.000 FB. La proposition de placer un circuit de coupure du démarrage couplé à la tension batterie n'était pas étudié.

Les déficiences constatées au niveau du robinet 4 voies étaient doubles. Le mauvais fonctionnement provenait d'un encrassement de la bille suite aux différents démarrages, provoquant une augmentation évolutive des T4. Le deuxième phénomène se faisait sentir en hiver, par temps froid et degré hygrométrique élevé, par le blocage du robinet suite au gel des vapeurs de condensation.

Pour remédier à ces problèmes, une nouvelle version d'une IT II B1 n° 5A sortait au mois de novembre 1985, après contact téléphonique avec la firme TURBOMECA. L'IT rendait obligatoire la mise en place des coiffes de protection sur un sol couvert de neige et lors d'une température de moins de 5 °C. Elle imposait également au pilote de refaire une mise en marche du moteur après son arrêt jusqu'à une légère augmentation de T4, car cette opération permettait de remplir le robinet 4 voies de kérosène et d'éviter le gel de celui-ci. Elle prévoyait également le nettoyage et le séchage du filtre et du tuyau P2 ainsi que la bille et son siège du robinet 4 voies à chaque visite multiple de 25 heures.

Les trois incidents du début de 1986 prouvaient que les actions entreprises ne suffisaient pas encore, c'est pourquoi en mars et en novembre 1986 paraissaient des nouvelles versions des IT II B4 n° 3 contenant des prescriptions plus claires et simplifiées quant aux températures de décisions ainsi que les actions à prendre par le pilote et les mécaniciens en cas de température ou tension anormales.

La modification du robinet 4 voies était de la compétence de la firme TURBOMECA. Les propositions de la 255 étaient un réchauffement du robinet 4 voies par voie électrique, une solution toute simple et efficace, et éventuellement une modification du système lui-même. La modification enfin proposée par la firme était le déplacement du robinet 4 voies (plus près du moteur, donc avec moins de risques de gel) et une protection calorifique des tuyauteries du robinet 4 voies. La modification coûtait environ 7000 FF par turbine avec un délai de livraison de 8 mois. Quelques moteurs ont subi cette modification.

e. La période d'hiver 1986-1987.

Suite à l'étude faite en 1985 et 1986, on pouvait espérer une nette amélioration des problèmes pour l'hiver suivant. En effet, deux surchauffes au démarrage étaient remarquées mais les dégâts causés à la turbine étaient négligeables grâce à de bonnes réactions des pilotes. Le fait que le problème était bien connu et que des mesures suffisantes étaient prises, avait porté ses fruits.

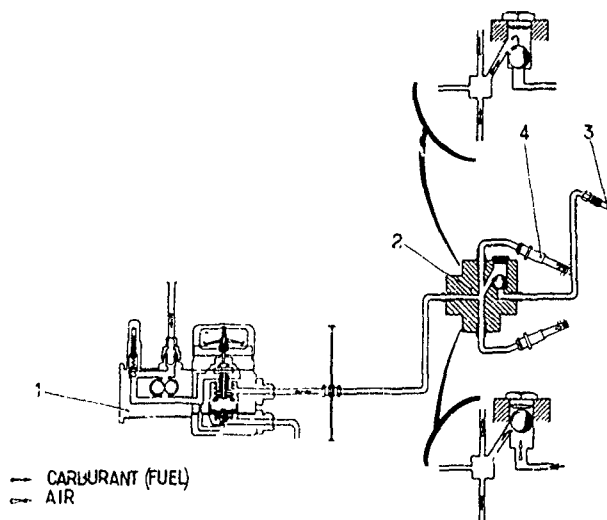
5. CONCLUSIONS GENERALES.

Le problème de surchauffe au démarrage était dû à deux phénomènes tout à fait indépendants. D'abord il y avait des causes purement techniques comme la défaillance de la batterie et du robinet 4 voies, qui ont été résolues d'une manière satisfaisante mais pas tout à fait complète. En effet, les solutions définitives, à savoir un circuit électrique de coupure du démarrage en fonction de la tension batterie ainsi qu'un système de préchauffage du robinet 4 voies n'ont pas été retenues. En outre, le risque d'erreur de manipulation (facteur humain) a été réduit à un minimum par une sensibilisation et une instruction adéquate.

Enfin il ne faut pas non plus exagérer le phénomène car depuis 1987 il n'y a plus jamais eu de problèmes de surchauffe au démarrage dus au temps froid, d'un côté parce que des conditions extrêmes de température sont devenues assez rares dans nos régions, peut-être, comme prétendent les "verts" à cause d'un réchauffement de la terre par effet de serre mais surtout parce que les pilotes sont bien conscients du phénomène et en cas de situation anormale, ils ont à leur disposition des instructions simples et claires.

REFERENCES

1. Manuel d'Entretien et Manuel de Vol S.A. 3180 ALOUETTE ASTAZOU, SUD AVIATION, Société Nationale de Constructions Aéronautiques, PARIS, FRANCE.
2. Documents classifiés de la 255 Compagnie Maintenance et Dépôt d'Aviation Légère.



Annexe A: CIRCUIT DE CARBURANT DE DEMARRAGE

Nombre d' hélicoptères: 70
 Nombre total d' incidents: 23
 Nombre total de surchauffes: 5

Date	Cause présumée	Prix Réparation (FB)
15 Fev 82	Non application des procédures	827.600 (RG)
17 Nov 82	Non application des procédures	1.254.800 (RG)
14 Jan 85	Bille robinet 4 voies gelée	691.637
04 Jan 85	Bille robinet 4 voies gelée	1.015.500 (VNIP)
14 Jan 85	Bille robinet 4 voies gelée	1.019.250

Annexe B: ACCIDENTS/INCIDENTS DE LA PERIODE 1982-1985

Surchauffe n° 1

Date: 05 Fev 86
 Appareil: A 81
 GTM n° 500 à 1322:30 hr
 Cellule: 3539:20 hr
 Incident: 1 surchauffe de 750 °C d' environ 2 sec
 Données supplémentaires:

Lieu: Vogelsang

L' hélicoptère était stationné sans ses housses de protection sur un emplacement enneigé. Lors du passage d' une autre machine, cette neige a pu s' élever du sol, entrer le moteur et s' accumuler dans le circuit d' alimentation jusqu' au robinet 4 voies. En plus, la procédure de remise en marche après arrêt n' a pas été exécutée.

Prix de réparation: 219.784 FF.

Surchauffe n° 2

Date: 11 Fev 86
 Appareil: A 42
 GTM n° 678 à 813:40 hr
 Cellule: 4612:35 hr
 Incident: 1 surchauffe de 700 °C, après coupure démarrage à 590 °C
 Données supplémentaires:

Lieu: Merzbruck (AIX)

Démarrage après une ventilation trop longue d' environ 15 sec, ce qui est nocif pour le démarreur, le relais démarreur et la batterie.

Cause présumée: Gel du robinet 4 voies bien que la machine ne stationna que 5 minutes dans une température légèrement négative.

Prix de réparation: 150.656 FF, soit le prix de l' expertise car la turbine n' a pas été endommagée.

Surchauffe n° 3

Date: 25 Feb 86

Appareil: A 78

GTM n° 551 à 1361:55 hr

Cellule: 3570:40 hr

Incident: Deux démarrages successifs anormaux de 630 °C, suivi d' une surchauffe de 750 °C pendant 1 sec. Le 19 Fév 86 une première surchauffe de 730 °C pendant 1 sec avait déjà eu lieu.

Données supplémentaires:

La température extérieure était de -5 °C. Un contrôle le lendemain indiquait que le robinet 4 voies était bloqué par le gel.

Cause présumée: Gel du robinet 4 voies et suite aux tentatives successives de démarrage, un affaiblissement de la batterie.

Prix de réparation: 171.549 FF plus remplacement de la DYNASTAR et le relais démarreur suite au refroidissement insuffisant entre les démarrages.

Surchauffe n° 4

Date: 25 Feb 86

Appareil: A 93

GTM n° 376 à 1573:35 hr

Cellule: 4505:40 hr

Incident: 1 surchauffe de 800 °C pendant 1 sec.

Cause présumée: Réaction retardive de la part du pilote pour arrêter la phase de démarrage, la batterie ne possédant pas le voltage minimum nécessaire pour effectuer un démarrage correct.

Lieu: Ecole d' Aviation Légère à BRASSCHAAT.

Prix de réparation: 229.178 FF

Annexe C: ACCIDENTS/INCIDENTS DE LA PERIODE D' HIVER 1985-1986

Surchauffe n° 1

Date: 13 Jan 87

Appareil: A 95

GTM n° 718

Incident: Lors d' une première mise en route, la température de 700 °C a été atteinte, lors du deuxième démarrage, elle était de 600 °C. Le robinet 4 voies a été préchauffé par un "crimp gaine heater" emprunté aux paracommandos. Après cette opération, un démarrage normal était possible.

Données supplémentaires:

Lieu: Schaffen

Température extérieure: -17 °C

Grâce à une intervention correcte du pilote, la turbine n' a subi aucun dégât.

Surchauffe n° 2

Date: 15 Jan 87

Appareil: A 79

Incident: A Cologne, un démarrage au moyen d' un groupe a été réalisé après préchauffage du robinet 4 voies à l' air chaud. Après un vol d' environ 3 heures, la turbine a été coupée et remise en route immédiate, jusqu' à une augmentation de T4 de 300 °C. Les housses de protection ont été mises en place aussitôt. Après 25 minutes, un nouveau démarrage a été tenté selon la procédure normale durant lequel une montée anormale de T4 jusqu' 600 °C a été remarquée. Après préchauffage du robinet 4 voies, un démarrage normal a pu avoir lieu.

Données supplémentaires:

Lieu: Soest

Température: -12 °C et vent d' Est assez fort et froid.

Annexe D: ACCIDENTS/INCIDENTS DE LA PERIODE D' HIVER 1986-1987

AVIONS D'AFFAIRES MYSTERE-FALCON
EXPERIENCE OPERATIONNELLE PAR TEMPS FROID

C. DOMENC
Responsable Propulsion
DASSAULT- AVIATION
Boîte Postale n° 24
33701 MERIGNAC CEDEX - FRANCE

- FAMILLE DES AVIONS MYSTERE-FALCON

Brève présentation des différents modèles, de leur domaine de vol, des caractéristiques de leurs moteurs, des systèmes de démarrage.

- EXPERIENCE DU DEMARRAGE PAR TEMPS FROID

Campagne d'essais jusqu'à - 40°C dans le cadre de la certification, comportement des systèmes de démarrage électrique à basse température, procédures opérationnelles correspondantes.
Domaine de démarrage en vol.

- EXPERIENCE EN CONDITIONS GIVRANTES

Brève description des systèmes de protection contre le givre, prélèvements d'air moteur, méthode de certification, expérience en service.

1. - INTRODUCTION

Depuis la certification en 1965 du MYSTERE-FALCON 20, la Société DASSAULT a produit plus de 1000 avions d'affaires à réaction qui ont accumulé 5 millions d'heures de vol en service.

Cette famille d'avions comprend les bi-réacteurs de type FALCON 20 et FALCON 10, ainsi que les tri-réacteurs de type FALCON 50 et FALCON 900.

Actuellement seuls les tri-réacteurs sont en production, mais un nouveau bi-réacteur, le FALCON 2000, est en cours de développement pour compléter la gamme.

2. - FAMILLES DES AVIONS MYSTERE-FALCON

A. - Caractéristiques principales.

Type	Nbre de passagers	Moteur	Rayon d'action (avec réserves NBAA-IFR)	Mach Maximum	Altitude Maximum
FALCON 20	8/10	2 GENERAL ELECTRIC CF 700	1400 Nm	0 85/0 88	42000 ft
DERIVES DU FALCON 20 : F20G/F200 F20-5*	8/10	2 GARRETT ATF3	2200 Nm	0 865	42000 ft
	8/10	2 GARRETT TFE 731-5AR	2200 Nm	0 85/0 88	42000 ft
FALCON 10	4/7	2 GARRETT TFE 731-2	1600 Nm	0 87	45200 ft
FALCON 50	8/14	3 GARRETT TFE 731-3	3200 Nm	0 86	49000 ft
FALCON 900	8/19	3 GARRETT TFE 731-5AR	3900 Nm	0 87	51000 ft

* Re-motorisation des F20 en Service.

Tous ces avions étaient de technologie très moderne au moment de leur certification tant en ce qui concerne les systèmes, dont les moteurs, que l'aérodynamique et la structure.

En raison de leurs performances ils sont tous entièrement équipés de commandes de vol servo-commandées. C'était une première pour un avion civil lors de la certification du FALCON 20, et cela a contribué à l'agrément particulier de pilotage de ces avions unanimement apprécié.

L'optimisation des voilures par le calcul a commencé avec le FALCON 10 et a été complètement réalisée pour le FALCON 50 et le FALCON 900 dont la voilure est optimisée en régime supercritique. Tous ces avions ont des dispositifs hypersustentateurs de bord d'attaque et de bord de fuite des voilures pour permettre l'emploi de pistes courtes utilisées par l'aviation d'affaires.

Les formes arrières de fuselage ont été particulièrement étudiées sur les tri-réacteurs FALCON 50 et 900 pour réduire la traînée en croisière.

Les voilures sont à structure intégrale sur tous les modèles. Un FALCON 10 est en service depuis quelques années avec une voilure à caisson en composite carbone. Les matériaux composites sont utilisés sur le FALCON 50 et surtout sur le FALCON 900.

B. - Domaine de vol typique

A titre d'exemple on trouvera ci-après le domaine d'emploi du FALCON 900 en température/altitude, avec la zone de décollage effectivement démontrée jusqu'à 14000 ft (LA PAZ) et le domaine de rallumage en vol garanti jusqu'à 30 000 ft

C. - Moteurs

Avion	Moteur	Décollage			Croisière 40000 ft M = 0.8 Cs (lb/lb/hr) (non installée)	Observations
		Poussée lb	Taux de compression	Taux de dilution		
F20	CF 700	4300/4500	6.5	2	0.967	Fan arrière
F200	ATF3	5200	21	2.9	0.80	Triple corps
F10	TFE 731-2	3230	13	2.7	0.81	Fan avant avec réducteur
F50	TFE 731-3	3700	14.7	2.8	0.814	Fan avant avec réducteur
F900	TFE 731-SAR	4500	14.7	3.6	0.759	Fan avant avec réducteur et tuyère à mélangeur

- Remarques générales sur ces moteurs :

■ le CF700 était le premier petit réacteur à double flux. Une roue turbine/fan était rajoutée derrière un générateur type CJ610. Préfiguration des UDF actuels de GENERAL ELECTRIC.

■ l'ATF3 est le seul petit réacteur double flux, triple corps, avec le corps haute pression juxtaposé à l'arrière d'un double corps fan/basse pression.

■ les TFE 731 ont été les premiers réacteurs utilisant une régulation électronique.

■ les taux de dilution modérés permettent de limiter le diamètre du moteur à des valeurs compatibles avec un montage sur le fuselage arrière.

- Caractéristiques de ces moteurs liées au démarrage, en particulier à basse température :

■ Pointe du couple résistant, à - 40°F (- 40°C).

	CF 700	ATF3	731-5AR
Vitesse prise démarreur (tours/minutes)	850	1200	1350
Couple résistant (Lb.Ft)	65	40	35
Puissance mécanique correspondante (Watts)	7800	6777	6710

Ces puissances sont compatibles avec un système de démarrage électrique. Le CF700, malgré son faible taux de compression, est plus exigeant car le compresseur dans son entier est entraîné par le démarreur, alors que seul le compresseur HP (centrifuge) de faible inertie et de taux de compression modéré (2 à 2.5) est entraîné sur l'ATF3 (N3) et sur le 731 (N2).

On peut noter que sur le TFE 731 le fan est couplé au compresseur BP par un réducteur qui nécessite une quantité d'huile augmentée, d'où un impact sur le couple résistant, mais moins fort que si le démarreur devait entraîner l'ensemble.

■ Les dispositifs de géométrie variable d'entrée d'air (CF 700, ATF3) et les vannes de décharge aident à diminuer le couple résistant au démarrage.

■ La régulation électronique des ATF3 et TFE 731 dose le débit carburant au démarrage en fonction de la température ambiante. Un enrichissement automatique est prévu au-dessous d'une température interturbine de 400°F. Une commande manuelle permettant de maintenir l'enrichissement au-delà de 400°F pour les démarrages à basse température est montée sur les FALCON 10 et 50.

■ La charge des accessoires avion est faible. Il n'a pas été nécessaire d'utiliser un by-pass des pompes hydrauliques. La génératrice électrique sert de démarreur et ne retrouve sa fonction génération qu'après la fin du démarrage. Selon les cas, il peut être nécessaire de temporiser la mise en ligne de la génératrice pour laisser le moteur accélérer entre la fin de la séquence de démarrage et le ralenti.

D. - Système de démarrage

- Sur ces avions de bilan électrique modéré, l'analyse a montré que le meilleur compromis en poids et en prix était d'utiliser une génération électrique en courant continu 28 volts, la génératrice servant aussi de démarreur. Pour permettre le démarrage autonome des moteurs, deux batteries (Nickel-Cadmium) sont nécessaires. Les génératrices (une par moteur) utilisées sur les FALCON ont une puissance de 9 Kw (sauf FALCON 200 : 10.5 Kw), les batteries sont de 36 Ah sur les FALCON 20 et 200, de 23 Ah sur les autres modèles.

- Le couplage des batteries en série ou en parallèle au cours du démarrage est choisi selon leur résistance interne de façon à maintenir une tension satisfaisante aux bornes du démarreur jusqu'à une température ambiante assez basse :

- . Série uniquement sur le FALCON 20 CF700.
- . Parallèle ou série (à basse température, sur sélection du pilote) sur les FALCON 10, 50 et 200.
- . Parallèle uniquement sur le FALCON 900.
- . Une assistance par la génératrice de l'APU, ou par celle d'un moteur déjà démarré est possible sur les FALCON.

- L'état de charge des batteries et leur température sont des paramètres essentiels du démarrage à basse température.

3. - EXPERIENCE DU DEMARRAGE PAR TEMPS FROID

3.1. - FALCON 20 - CF 700

- Une campagne a eu lieu en FINLANDE et NORVEGE en 1966 jusqu'à moins 28°C.
- Après exposition d'une nuit sans protection particulière, les démarrages se font correctement avec les batteries de 36 Ah en série.
- Le seul ennui rencontré est l'obturation d'une tuyauterie de régulation, modifiée ultérieurement par GENERAL ELECTRIC.

3.2. - FALCON 10 TFE 731-2

- Deux campagnes d'essais ont eu lieu la première en 1974 en ISLANDE et au CANADA (FROBISHER BAY) jusqu'à - 30°C, la deuxième en 1975 au CANADA (FROBISHER BAY et YELLOW KNIFE) jusqu'à - 45°C.

- La procédure de démarrage au-dessous de 5°C consiste à coupler les batteries en série pour démarrer le premier moteur et en parallèle pour démarrer le second

■ Démarrage sans protection particulière des batteries ou des moteurs après un séjour prolongé au froid.

.. Avec des batteries de 23 Ah le premier moteur démarre jusqu'à - 10°C/-15°C. Avec des batteries de 36 Ah cette limite passe à - 25°C/- 30°C : un démarrage marginal à -30°C a durée 65 secondes avec allumage au bout de 45 secondes et ITT maximum 820°C pour une limite de 860°C.

.. Le second moteur démarre dans tous les cas, après un séjour prolongé entre - 30°C et - 40°C.

.. Le premier moteur a pu être démarré, avec les batteries de 23 Ah, après un séjour de 4 heures à - 30°C, après deux tentatives infructueuses qui avaient réchauffé les batteries de - 10°C à 0°C et diminué la pointe initiale de courant de 1000 A/12.5V à 825A/11.5V.

■ Démarrage du premier moteur avec systèmes de réchauffage branchés sur des panneaux d'alimentation extérieure.

.. Réchauffage des batteries par couverture électrique chauffante CSA 120V/80W.

Après une nuit et une matinée passées à - 40°C/- 43°C, la température des batteries se maintient à - 5°C et le moteur démarre. La température de l'huile était de - 43°C.

Le démarrage est difficile le fan tourne lentement, on considère qu'au-delà de - 35°C il vaut mieux réchauffer le moteur.

.. Réchauffage des moteurs par ventilateur CTC 120V/850W.

L'installation de ce ventilateur dans l'entrée d'air avec les caches entrée d'air et tuyauterie normaux ou avec une couverture molletonnée à trois épaisseurs isolantes enveloppant toute la nacelle a permis de ramener la température d'huile respectivement de - 43°C à - 27°C et à - 18°C. La couverture permet de gagner 10 à 20°C sans vent, 20 à 30°C avec un vent de 10 Kts.

Le démarrage a été facile.

- Durant ces essais, des anomalies de fonctionnement des calculateurs électroniques du moteur lors de la chute de tension en début de démarrage ont amené le motoriste à modifier cette version initiale des calculateurs.

Avec des batteries de 23 Ah, la chute de tension initiale batteries en série, si les batteries ne sont pas réchauffées, peut amener une insuffisance momentanée de l'allumage et un passage en mode manuel du calculateur moteur. Tout rentre dans l'ordre quand le démarreur prend de la vitesse ce qui s'accompagne d'une augmentation de sa force contre-électromotrice, d'où une remontée de la tension et une baisse du courant débité par des batteries.

- La pression d'huile, moteur non réchauffé, peut atteindre 80 à 100 psi et demande 4 à 5 minutes avant de revenir dans la plage habituelle inférieure à 55 psi.

- un indicateur N2 qui se bloquait au froid a été modifié.

3.3. - FALCON 50 TFE 731-3

- Des essais ont eu lieu en FINLANDE, puis au CANADA (FROBISHER BAY - FORT CHURCHILL - CAMBRIDGE BAY) en 1980 jusqu'à - 39°C.

- Les moteurs et les batteries sont très proches de ceux du FALCON 10, la génératrice/démarreur est d'un modèle différent, l'APU qui n'existe pas sur FALCON 10 est optionnel sur FALCON 50.

- La première série d'essais en FINLANDE a montré la nécessité de réchauffer les batteries au-dessous de - 10°C/- 15°C ce qui est homogène au FALCON 10.

Les couvertures chauffantes de 80W du FALCON 10 se sont avérées insuffisantes, des couvertures mieux adaptées de 120W et 150W ont été essayées au CANADA. Les 150 W, trop puissantes, donnaient des élévations de température des batteries excessives (65 à 70°C). Les couvertures de 120W ont été retenues (échauffement de 55°C) avec, dans le kit grand froid issu des essais, une coupure de réchauffage à une température batterie de 25°C.

- L'APU et les moteurs doivent être réchauffés au-dessous de -35°C. Le fan ne peut être tourné à la main sans réchauffage à - 35°C.

L'APU est réchauffé par un ventilateur de 850 W placé dans l'entrée d'air, obturateurs d'entrée d'air et tuyère en place.

Les moteurs ont été réchauffés soit par deux ventilateurs (entrée d'air et tuyère) de 850W, soit par un prélèvement d'air branché sur l'avion qui suppose l'APU ou un moteur en fonctionnement. Le réchauffage du moteur permet la rotation du fan, mais l'huile contenue dans le relais d'accessoires reste à la température ambiante.

- Un démarrage après 3H30 à - 27°C sans aucun réchauffage a été essayé. Les batteries étaient à -15°C, l'huile moteur à - 17°C / - 23°C, le caisson APU à - 14°C.

Après un démarrage correct de l'APU sa génératrice est coupée pour simuler l'avion sans APU. Deux essais de démarrage d'un moteur batteries en série sont interrompus par le pilote à cause de la perte d'indication N2 (tension trop faible). La troisième tentative, batteries en parallèle est normale, les batteries étant maintenant à + 15°C.

- Avec les batteries réchauffées et une ambiance de - 31.5°C (température d'huile - 31°C) le démarrage est possible batteries en parallèle ou en série, mais dure 40 sec avec ITT = 660°C en parallèle, pour 26.5 sec et ITT = 475°C en série.

Si l'assistance d'une génératrice moteur ou APU est utilisée celle-ci fournit environ 30% du courant soit 460 Amp.

- Avec les batteries et les moteurs réchauffés (température inférieure à - 35°C) le premier moteur est démarré batteries en série, les autres batteries en parallèle avec assistance éventuelle des génératrices.

A - 39°C, batteries à + 28°C, huile à - 35°C (relais d'accessoires) le moteur démarre en 21 sec, ITT = 550°C.

- Des essais comparatifs d'huile MOBIL JET II et EXXON 2380 n'ont montré aucune différence perceptible des caractéristiques de démarrage malgré leurs viscosités différentes.

Un contacteur électrique du circuit de démarrage a dû être réchauffé.

3.4. - FALCON 900 - TFE 731-5AR

- Des essais ont eu lieu en 1986 et 1987 à FROBISHER BAY jusqu'à - 39°C.

- Cet avion est proche du FALCON 50, les moteurs ont un peu plus d'huile, l'APU étant de base sur cet avion le couplage des batteries est uniquement parallèle et l'assistance au démarrage par la génératrice de l'APU est systématique.

- Un essai a montré qu'il était possible de démarrer sans assistance et sans réchauffage après 12H passées entre -15°C et -19°C.

- Le réchauffage des batteries par les mêmes couvertures de 120W que sur le FALCON 50 à des températures inférieures à - 15°C a été utilisé (hors l'essai ci-dessus)

Le réchauffage des moteurs au-dessous de - 35°C, au lieu d'utiliser les ventilateurs de 850W a été fait à partir de groupes de piste permettant de souffler de l'air chaud sur les zones à réchauffer, en particulier sur les charnières des capots avant d'ouvrir ceux-ci pour réchauffer le réservoir d'huile et le relais d'accessoires ce qui n'était pas fait sur le FALCON 50. Un brassage du fan à la main d'une quinzaine de tours assure son déblocage.

- Le réchauffage de l'APU, quand il est lubrifié par de l'huile type I (ESSO 2381), n'est en principe pas nécessaire. Mais le temps de démarrage observé conduit à recommander le réchauffage à température inférieure à - 35°C.

- Pour couvrir le cas de panne de l'APU, un moteur a été démarré sans assistance à - 39°C, batteries à + 30°C, après un réchauffage de 15 minutes (T huile = 35°C). Le démarrage est long (1 minute 48 secondes) sans surchauffe (ITT = 548°C), c'est un cas marginal.
Avec assistance, le temps de démarrage est d'une trentaine de secondes.

3.5. - FALCON 200 - ATF3

- Une campagne d'essais a eu lieu en 1982 à YELLOW KNIFE jusqu'à - 48°C.

- Par rapport aux TFE 731 équipant les FALCON 10, 50 et 900, l'ATF3 n'a pas de réducteur de fan ce qui est un peu favorable.

L'avion est équipé de batteries de 36 Ah (37 Kg contre 25 Kg pour la batterie de 23 Ah). Leur résistance interne plus faible donne moins de chute de tension initiale que les batteries de 23 Ah.

- Sans protection particulière il a été possible de démarrer jusqu'à - 25°C.

- Avec réchauffage des batteries (température inférieure à - 30°C) par les couvertures de 120W, il a été possible de démarrer à des températures de l'ordre de - 45°C sans réchauffer le moteur, après avoir tourné le fan à la main. Quelques stagnations de régime entre la fin de démarrage et le ralenti, rattrapables en avançant la commande de gaz ont été observées et corrigées par le motoriste dans une version ultérieure du calculateur.

3.6. - RESUME DES PROCEDURES DE DEMARRAGE PAR TEMPS FROID

- Pour les FALCON équipés de moteurs GARRETT TFE 731 ou ATF3 il est recommandé de tourner le fan à la main avant un démarrage à température négative.

- Jusqu'à - 10°C/- 15°C (batteries de 23 Ah) ou - 25°C (batteries de 36 Ah) aucun réchauffage n'est nécessaire, le démarrage autonome est possible en sélectionnant le démarrage LOW TEMP, batteries en série, pour le premier moteur (sauf FALCON 900 ----> assistance APU).
Pour une exposition prolongée au-dessous de ces températures, il faudra prévoir un réchauffage des batteries.

- Au-dessous de - 35°C il faudra également réchauffer le réacteur (modèle TFE731) et l'APU de préférence avec un groupe de piste (air chaud).

- Le deuxième réacteur démarre toujours batteries en parallèle, le troisième également.

- Une pression d'huile forte peut être atteinte, en particulier s'il n'y a pas eu de réchauffage du relais d'accessoires.

- Les carburants utilisés au CANADA étaient du JET A1 ou du JET B.

- Le dispositif d'enrichissement manuel, peu utilisé sur les F10 et F50 n'a pas été reconduit sur le F900.

3.7. - DOMAINE DE DEMARRAGE EN VOL

- Le domaine d'altitude démontré sur les FALCON 20, 10, 50 et 900 est 0 - 30000 ft et 0-35000 ft sur le FALCON 200. En cas de panne du calculateur électronique l'altitude est limitée à 20 000 ft pour éviter les surchauffes (débit carburant plus fort).
- Le domaine vitesse/régime de démarrage en moulinet est ou non défini. C'est l'intérêt du démarrage électrique que d'être disponible à tout instant et pratiquement indépendamment des conditions d'altitude/vitesse, une consigne, du genre $N2 < 15\%$: utiliser le démarreur, peut suffire.

4. - EXPERIENCE EN CONDITIONS GIVRANTES

4.1. - DESCRIPTION SOMMAIRE DES SYSTEMES D'ANTIGIVRAGE

- Tous les FALCON sont équipés de circuits d'anti-givrage par air chaud prélevé sur les réacteurs. Ils protègent l'intégralité des bords d'attaque des voilures, ainsi que les entrées d'air des réacteurs.
 - La zone réchauffée de l'entrée d'air varie selon l'application :
 - . FALCON 20 CF 700. Entrée d'air à double conduit (un pour le compresseur et un pour le fan arrière). Réchauffage des lèvres entrée commune et entrée compresseur, de mâts structuraux du conduit de fan, du fond de ce conduit.
 - . FALCON 10, TFE 731. Réchauffage des lèvres et d'une portion aval du canal d'entrée d'air.
 - . FALCON 200 (ATF3), 50, 900, 20-5 (TFE 731). Réchauffage des lèvres uniquement.
 - . Moteur central FALCON 50 et 900 : en plus des lèvres, réchauffage des 180° supérieurs du conduit en S.
 - La technologie des échangeurs de chaleur est la suivante :
 - . Pour le bord d'attaque (becs mobiles) des voilures F20/F10/F50-900, l'air chaud distribué par un tube perforé circule dans des canaux usinés dans la paroi externe et refermés par une paroi interne.
 - . Pour les lèvres d'entrée d'air, il y a eu évolution : double peau (comme pour les voilures) sur la nacelle CF 700, simple caisson de bord d'attaque avec distribution d'air par tube "piccolo" sur les autres nacelles, évacuation par une double peau réchauffant un morceau du canal d'entrée d'air sur le FALCON 10, évacuation directe sur les autres avions.
 - . Pour les conduits en S des moteurs centraux F50 et F900, canaux en OMEGA rapportés.
 - Les prélèvements d'air (avec moteurs GARRETT) consistent en un mélange BP + HP pour les voilures et conduits en S, en HP pur pour les lèvres d'entrées d'air. Des vannes régulatrices de pression sont généralement utilisées pour moduler le débit prélevé en fonction du régime réacteur.
- Par exemple pour un FALCON 900, en montée, on prélève environ 1% de HP pour les lèvres d'entrées d'air et 7% de mélange HP + BP pour les voilures et le conduit en S.

- Les moteurs eux-mêmes ont, ou non, un système d'antigivrage. Le CF700 et les TFE731-2 et -3 initiaux (F20
- F10 - F50) étaient équipés d'une vanne de prélèvement et de réchauffage de l'entrée compresseur sur CF 700 (IGV) et du "spinner" elliptique d'origine sur le TFE.

Puis GARRETT a certifié des "spinners" coniques et supprimé tout réchauffage sur tous ses moteurs.

4.2. - METHODES DE CERTIFICATION

- Voilures : calcul des zones de captation, essai éventuel d'un panneau en soufflerie de givrage, mesure des températures de peau en vol et extrapolation aux limites, vol en givrage naturel. Détermination par calcul des régimes réacteur minimum nécessaires et vérification en vol.

- Nacelles : dossiers de calcul éventuels en conditions givrantes (GRUMMAN : TFE 731-2/F10 - ROHR : ATF3/F200), essais éventuels de l'installation motrice en soufflerie de givrage (CEPr SACLAY : nacelles CF700/F20, 731-2/F10, manche à air centrale 731-3/F50), mesure des températures de peau en air sec en vol, extrapolation aux limites du domaine, vol en conditions givrantes naturelles.

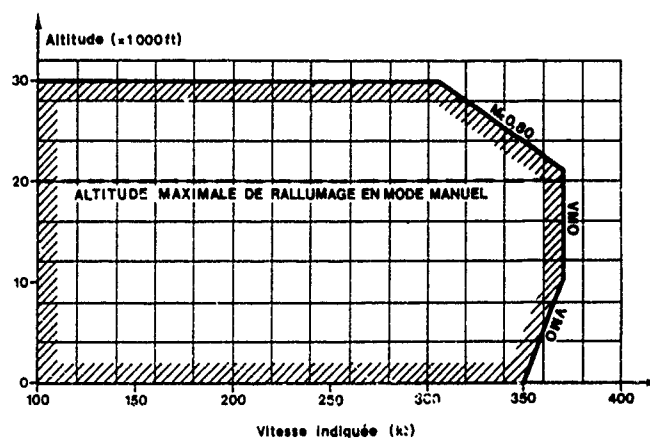
- Des essais de mise en service retardée de l'anti-givrage peuvent être faits à la demande des autorités de certification soit en soufflerie de givrage pour l'installation motrice, soit en vol pour la voilure

4.3. - EXPERIENCE EN SERVICE

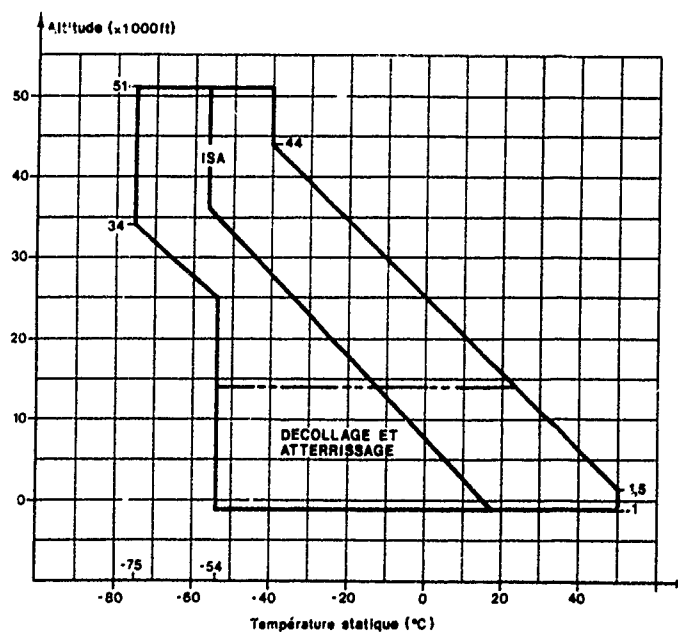
- Hors panne de vanne de prélèvement, aucun cas de protection insuffisante n'a été rapporté
- Des précautions d'emploi en jour chaud et en condition statique sont nécessaires, en particulier pour éviter la surchauffe des bords d'attaque de voilure.

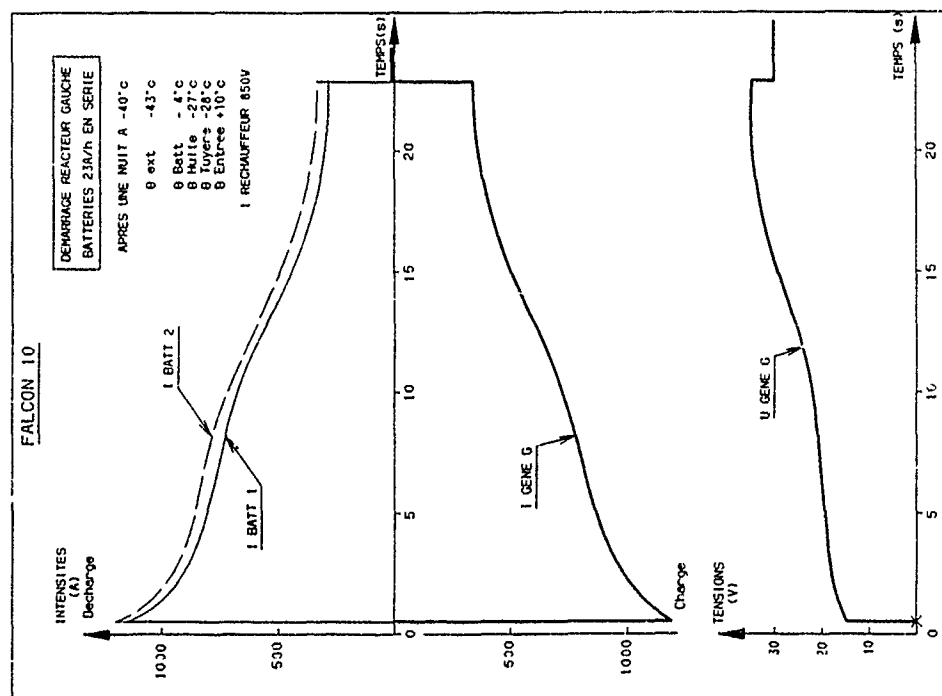
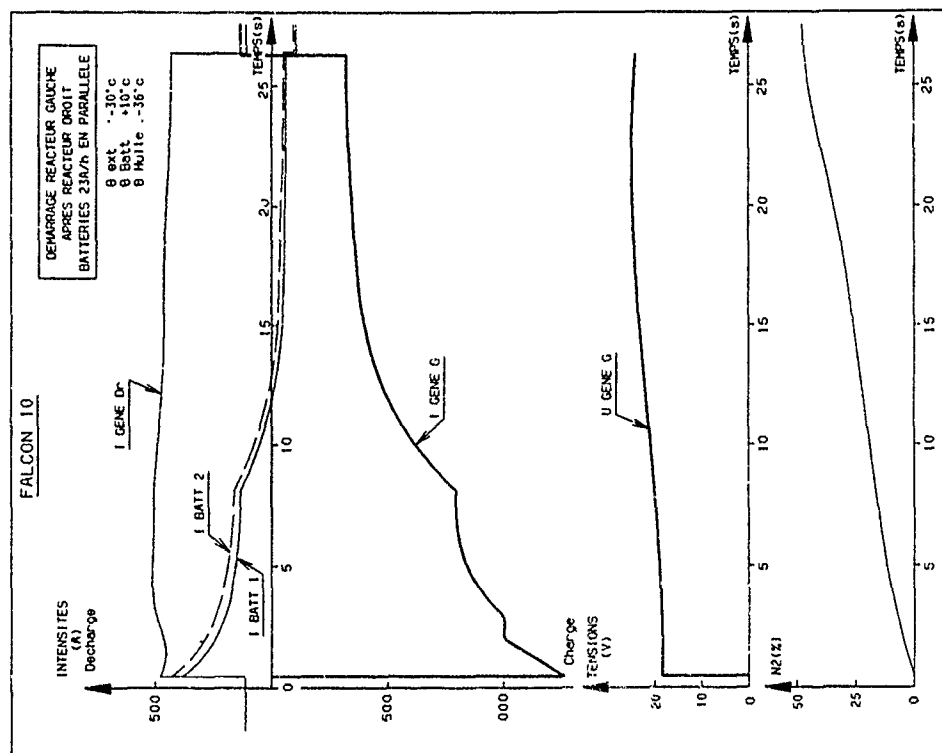
MYSTERE-FALCON 900

DOMAINE DE RALLUMAGE EN VOL



DOMAINE TEMPERATURE / ALTITUDE





VULNERABILITY OF A SMALL POWERPLANT TO WET SNOW CONDITIONS

by

R. Meijn
Manager Environmental Control and
Ice Protection Systems

FOKKER Aircraft B.V.
P.O. Box 7600
1117 ZJ Schiphol-Oost
The Netherlands

0. Abstract

Several temporary flame-out incidents were experienced in descent through light icing conditions and precipitation during regular scheduled flights. Previously, both engine and aircraft had been qualified against FAR 33/JAR E and FAR/JAR 25 including tunnel-testing and natural icing trials. Test-flights in natural icing conditions with video observation of the interior of the air intake revealed ice accretion at the interface between engine-casing and intake-duct in mixed conditions of cloud, snow, hail and rain while the aircraft exterior remained free of ice. Extensive ground testing of the engine indicated less tolerance to ice ingestion than had been demonstrated in engine certification tests. Powerplant ice protection was enhanced by additional anti-icing of the engine flexible seal by bleed air. This paper discusses factors influencing unexpected ice formation and associated uncertainties in the qualification process of a small turboprop powerplant.

1. Description of powerplant ice protection system

The aircraft is a twin-engine turboprop, designed for operation in icing conditions to FAR/JAR 25, Appendix C. The engine is a three-shaft turbo-prop in the 2000 horsepower-class with a maximum pressure-ratio of 15,2 (max cruise). The composite propeller is driven by the two-stage free turbine through a reduction gear-box.

The engine air intake is excentric and is provided with a by-pass channel for foreign object separation.

The engine has flexible mounting and consequently a flexible element is required between engine-casing and intake duct.

A 0,2 inch (5 mm) gap with recessed compression seal (silicone elastomer) is located between a light alloy adaptor flange on the engine and a flange on the composite duct.

Figure 1a gives a cross-section of the construction.

The abovementioned gap runs across areas of water or snow impingement.

The composite air intake is de-iced by an electro-thermal system, utilizing semi-conductor switching.

It consists of five sections which are cyclically heated: the propeller blades and spinner, the inner lip 1 and 2 surfaces, the duct floor and the duct side-walls.

The control of cyclically heated elements is dependent on outside air temperature.

The power-density for the cyclically heated parts is 12,5 W/in².

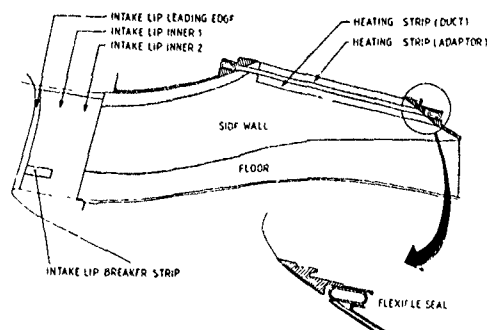


Figure 1a : Cross-sectional view of duct (split-up) and bifurcation (detail).

The leading edge is continuously heated and temperature controlled, originally between 40 °C and 50 °C.

The group of continuously heated elements also comprises strips at either side of the gap; a strip just below the cavity of the seal of the intake and a strip on the adaptor flange. Associated power-density is 12,5 W/in².

Figure 1b shows the heater sections for the original duty-cycle down to -7,5 °C.

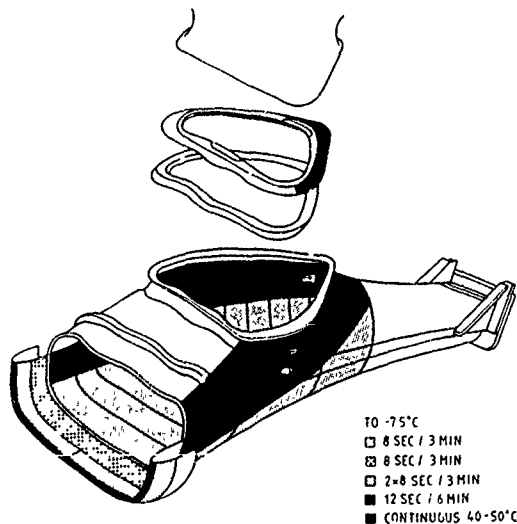


Figure 1b : Engine air intake de-icing configuration.

Powerplant de-icing is governed by two (LH/RH) De-icing Control Units, which monitor various input and output parameters and are capable of detecting partial system malfunction.

2. Qualification tests

The engine was qualified to FAR 33 and JAR E. FAR 33 addresses: water cloud icing conditions per Appendix C of FAR 25 and ice ingestion, in particular ice from the air intake, a 1 inch hailstone and water, 4% of the engine core massflow by weight.

Ice ingestion tests at sea-level with a typical air intake system yielded a maximum ice volume and shape that could be ingested without damage to the engine compressor; an associated limit for ice ingestion was declared in engine certification documents.

Since mechanical damage was considered the limiting factor, most tests had been conducted at relatively high engine speeds, i.e. high engine power-settings.

Operational limits for ice ingestion associated with flame-out were not defined, as by tradition flame-out was supposed to be covered by sea-level water ingestion tests.

The powerplant was certified to FAR 25 and JAR 25. FAR § 25.1093 specifies water cloud icing conditions per Appendix C and "snow, both falling and blowing"; however, temperature, density, water/ice ratio and crystal structure are undefined (ref.: AC 20-73 and FAA ADS-4).

In the absence of definition, test-facilities and test-traditions in Europe, the paragraph addressing snow has been deleted from JAR § 25.1093.

ACJ § 25.1093(b) recommends water cloud conditions at altitude for qualification of the powerplant.

For previous applications of the engine, the powerplant had been subjected to icing tests in a sea-level tunnel-facility.

Consequently, for subject derivative engine this tradition was followed with Liquid Water Content adjusted for the difference in airspeed.

The majority of the tests, including ice shedding after delayed activation of the de-icing system, were performed at high power-settings, representing prolonged conditions of ice encounters.

Note that ACJ § 25.1093(b), 2.4.3, 2.4.5 and 2.4.7 suggest ice shedding at high engine power.

At idle power-settings satisfactory ice protection capabilities were easily demonstrated since electrical de-icing is independent on engine-speed.

In addition to abovementioned ice-tunnel testing a fully-instrumented prototype-aircraft was subjected to dry air tests and natural icing trials.

Dry air tests comprised a wide range of testconditions, including (simulated) failure conditions.

Flight-tests in natural atmospheric icing conditions were executed to verify powerplant ice protection system effectiveness, especially in relation with system delayed activation, ice accumulation on unprotected areas and aircraft flight handling characteristics.

Continuous maximum icing conditions were found; subsequent encounters with de-activated ice protection system resulted in ice build-up that would have accumulated in intermittent maximum icing conditions.

During flight-tests no anomalies occurred; not even when the engine ingested about 0.5 inch (13 mm) of ice accumulated on the intake-lip.

It was concluded that the powerplant ice protection system performed satisfactorily.

3. Operational incidents

During the winter of 1988 with more than 30 aircraft in service and about 50.000 hours of flight accumulated, several occurrences were reported of a sudden temporary loss of torque. In general, the so-called flame-out incidents occurred under the following conditions:

- flight-phase: descent, power 10 to 35% torque
- IOAT -2 to +3 °C
- altitude 8.000 to 14.000 ft
- IAS 160 to 180 kts

Analyzing a total of 6 confirmed occurrences the following common factors were recognized:

- incidents occurred at relatively low power settings
- together with the altitude effect, this meant that engine massflow was low
- powerplant ice protection system had been activated prior to the incident, together with continuous ignition
- prior to each incident the aircraft had encountered light icing conditions, while in most cases rain was reported by the flight-crew and in some cases snow
- however, no or little ice was seen on the airframe
- in each case ambient temperatures were near freezing level

The abovementioned sudden losses of engine power were characterized by a drop in torque to zero percent, followed by a drop in gas temperature. Next, when gasgenerator speed had dropped to the level where relight is possible, power restored automatically.

The aircraft did not leave its intended flight-path and flight safety was not impaired.

Previously, there had been several exposures to severe water cloud icing conditions in which the powerplant ice protection system performed as designed and engine operation remained undisturbed.

In response to the first incidents operational restrictions were imposed, mainly addressing power as a means of increasing engine tolerance to ice ingestion.

However, the power needed to obtain the intended benefit was too high for regular operations, especially descent.

Evidently, an unknown phenomenon, not experienced during qualification testing, had to be identified before an effective solution could be defined.

4. Flight-tests: engine water injection

Following aforementioned incidents, investigations were initiated to retrieve the cause of the power-interruptions.

A first series of flight-tests was conducted to analyse the engine tolerance at altitude to sudden water ingestion.

Water was used, because it could easily be injected repeatedly into the engine compressor in well-defined quantities at known rates.

The aircraft installation consisted of a large hydraulic cylinder; total volume of water to be injected ranged up to 0.53 US gal (2 litres) maximum at a flow-rate of more than 0.53 US gal/s (maximum).

More than 150 water injections were performed in various configurations at altitudes between 5.000 and 18.000 feet altitude at different power-settings (torque); a total of 73 flame-outs were induced.

Boundaries for flame-out were established at several anti-surge bleed (Handling Bleed) massflows; it appeared that more bleed increased the engine's tolerance to water ingestion. However, from the test results it was concluded that flame-out behaviour was rather different from that reported in the incidents, which therefore remained unexplained.

Later, comparative water and ice ingestion tests were conducted on a sea-level testbed. Ice appeared to be much more critical regarding effect on engine behaviour, also on a basis of mass times enthalpy.

From the tests it was concluded that the flame-out incidents were unlikely to have been caused by ingestion of rain or water accumulated in the engine air intake. However, it was recognized that tolerance to water ingestion reduced considerably with increasing altitude independent of power-setting; restoration was achieved by alteration of anti-surge bleed valve control. The tolerance to water ingestion increased significantly with 8% Handling Bleed. Finally, it was concluded that engine behaviour with sudden water injection and increased anti-surge bleed had no relation to that with ice ingestion (at sea-level); consequently, further ice ingestion tests were required.

5. Flight-tests: video observation inside the air intake

As a result of the incidents, the engine air inlet de-icing system was re-evaluated to observe ice build-up and shedding characteristics inside the duct in natural icing conditions. Ice accretion was recorded using three miniature colour video cameras mounted at different positions in the air intake of a prototype aircraft.

The fields of view were chosen as follows:

1. rear of air intake duct including the bifurcation and the lower half of the engine inlet interface
2. floor of the intake duct
3. top (ceiling) of the intake duct and forward part of the engine inlet casing

Figure 5a shows the positions of the cameras in the intake duct.

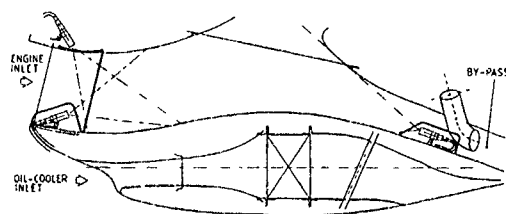


Figure 5a : Positions and fields of view of cameras mounted in the air intake duct.

Initially, exploratory flights were conducted in atmospheric conditions of opportunity, including: light cloud icing conditions, snow, hail and rain. As a result of these video-observations it emerged that significant ice accumulation developed at the rear of the intake duct at the bifurcation. Further flight-tests were performed with only one video camera mounted on the intake lip, viewing the rear of the intake duct.

With video observation in natural snow conditions significant ice accumulation was found in the area of the adaptor flange.

The unheated slot into which a considerable portion of ice keyed, formed a comfortable point of attachment for precipitation which otherwise would have been repelled from adjacent continuously heated strips.

Ice lodged in the cavity of the seal and bridged across the continuously heated strips to the cyclically heated side-wall. Complete shedding was inhibited by the ice being keyed; Figure 5b gives an impression of the way ice mushroomed in the seal gap.

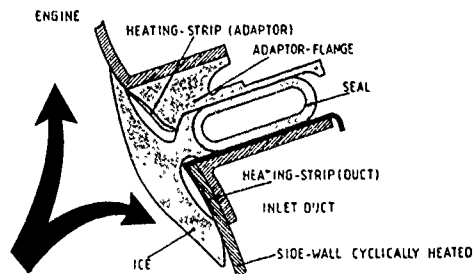


Figure 5b : Principle of ice accretion in the seal cavity.

Ice accreted until aerodynamic forces prevailed over the adhesive forces between ice and duct wall and the strength of the foundation provided by the unheated slot.

Periodic shedding was frequently observed; the central part disappeared in the by-pass duct, whilst the remainder was sometimes ingested by the engine.

This mechanism appeared to be dependent on the dimensions of the accumulated ice, whereas also power-setting appeared to influence patterns of ice shedding; Figure 5c shows the location of ice accumulation and the direction of shedding.

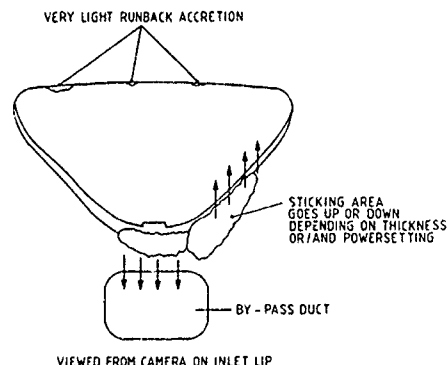


Figure 5c : Location of ice accumulation and shedding pattern.

Apart from the seal area, ice accumulated on the (lefthand) rear side-wall (influence of propeller-swirl) where it accreted between the heating-cycles to such an extent that it sometimes resisted complete shedding.

In general, the observed ice accumulation in the area where it could potentially enter the engine under critical conditions was estimated to have a volume of 5 to 6 in³ (82 to 98 cm³).

These figures are estimated by projecting the side-wall and seal surface as a triangle of 30 in² (196 cm²) with an average thickness of 0.16 to 0.20 inch (4 to 5 mm).

The largest volume of ice which was seen to be ingested by the engine was estimated to be 3 to 4 in³ (49 to 66 cm³); it did not produce a flame-out condition, nor was engine operation noticeably affected.

However, it is quite conceivable that double that volume would occasionally have entered the engine, which is indeed in the order of the volume that is presently estimated to cause a flame-out at altitude.

Note that ice accretion as described was formed in mainly wet snow conditions;

OAT -7 to -2 °C at an altitude of 8,000 to 14,000 feet, with an airspeed of 150 to 170 knots (IAS). At the same time no or little ice was collected on windshield wipers, wing leading edges and air intake lip.

These conditions match those associated with reported incidents quite well. Hence, it was concluded that the ultimate cause of the flame-out incidents had been traced.

Ice protection capabilities in cloud icing conditions were judged satisfactory and quite similar to those previously qualified in sea-level tests.

Protection against conditions of wet snow and mixed conditions was upgraded by modifying the air intake de-icing system as will be outlined in the next paragraph.

Effectiveness was demonstrated during natural icing trials with a prototype-aircraft with one powerplant de-icing system modified, the opposite system unaltered, both monitored by means of video observation.

Subsequently, the effectivity of the modifications was verified and confirmed during and in-service trial for about 210 days (1260 flight-hours; status April 1990, trial is continuing) also utilizing a small video camera on the air intake lip.

In general, video-recordings were of high quality taking into account the variation of natural (day-)light inside the air intake due to changing atmospheric conditions and changing aircraft heading and attitude; details of both intake duct and engine inlet could be clearly distinguished. The commercially available video system exhibited excellent serviceability (KIMO CCD Color Camera, Model EM 102; diameter 0.7 inch (17,5 mm), length 2.1 inch (53 mm)).

6. Improved ice protection of powerplant

Engine de-icing system performance was improved by raising the control temperature of the sensors embedded in the leading edge of the intake lip; these sensors also control the continuously heated strips at the edges of the gap at the engine interface. Control temperatures were raised to 50 °C falling, for activation of the heating-cycle and 70 °C rising, for de-activation.

Associated with this modification the cycle-interval of the side-walls was halved to once every three minutes.

Originally, this cycle was determined to minimize the chances of runback ice in the engine-casing, which posed a potential hazard of damage to the impeller upon ice ingestion.

However, this was based on ice-tunnel testing rather than in-service experience.

To completely eliminate ice accumulation in the vicinity of the seal gap, de-icing of the slot by means of engine compressor bleed air was introduced; Figure 6a shows the basic principle. An asymmetrical spray-pipe was inserted in the seal cavity, covering an area reaching forward of the by-pass duct range and extended at the lefthand-side to the forward radius of the engine aperture to account for any asymmetric ice accretion due to propeller-swirl.

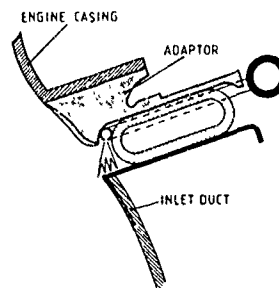


Figure 6a : Seal anti-icing by means of compressor bleed air impingement.

The spray-pipe has a 3/16 inch (4,8 mm) diameter, incorporating 88 holes of 0.04 inch (1 mm) at a pitch of 0.28 inch (7 mm). Total bleed air consumption under cruise conditions is about 2 lb/min (0,015 kg/s) at 150 °C (1.0 lb/min.ft; 0,025 kg/s.m).

The flexible seal was provided with slots to feed the spray-pipe by means of flat radial tubes from a common manifold.

Figure 6b shows a bottom-view photograph of the production spray-pipe.

The de-icing flow is controlled by a solenoid valve, while system operation is monitored by a pressure-switch.

A flow-limiter protects against excessive flow in the event of failure of the supply-pipe.

Figure 6c shows the system general arrangement.

7. Conclusions, lessons learned

The following comments are relevant to the design and qualification process of the de-icing system of a typical small powerplant:

- Detailed advisory material for qualification to airworthiness requirements and traditional testing may not address certain critical (natural) icing conditions. In the case of the subject powerplant, wet snow appeared to be critical.
- Small high pressure-ratio (turboprop) engines may be surprisingly sensitive to ice ingestion at altitude in terms of flame-out; traditional ice ingestion tests addressing mechanical damage do not reveal engine tolerance to flame-out.
- An engine air intake having an internal bifurcation (foreign object separation) or any other stagnation area, may be prone to ice accumulation in wet snow conditions: OAT -10 to 0 °C, TAT -5 to +5 °C. These conditions are generally not identified by the flight-crew in the absence of external ice accretion.

In addition, ice build-up in wet snow conditions appears to be different from that in cloud icing conditions, which are subject of traditional qualification tests.

- sudden water ingestion tests at altitude are unlikely to produce the effects of ice ingestion: these tests are no substitute

- finally, it is concluded that commercially available miniature video systems are quite suitable for observation of ice accretion inside an engine air intake during flight in natural icing conditions.

Performance in test-aircraft as well as in an operational trial was excellent.

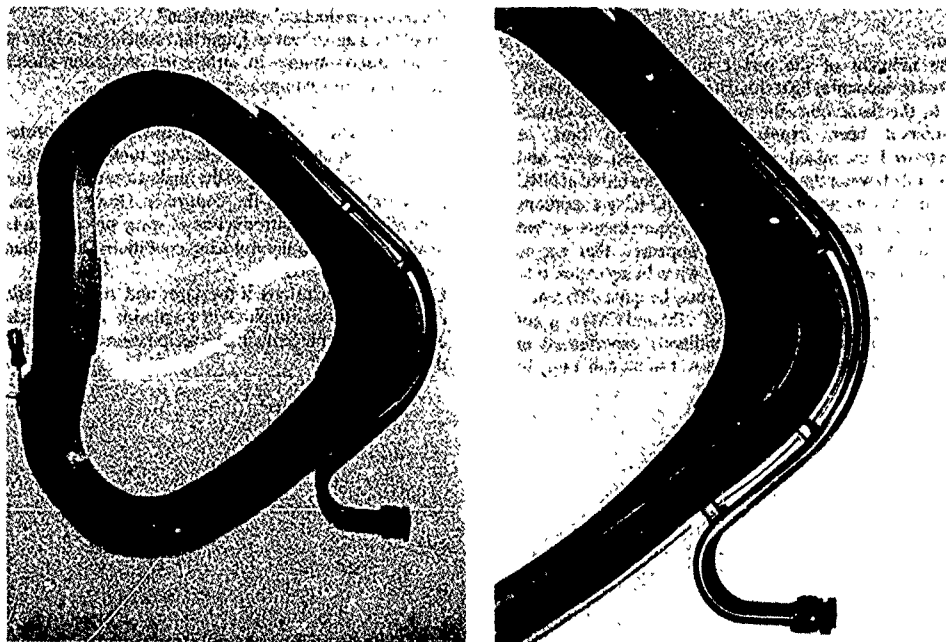


Figure 6b : Spray-pipe mounted on adapter-flange.

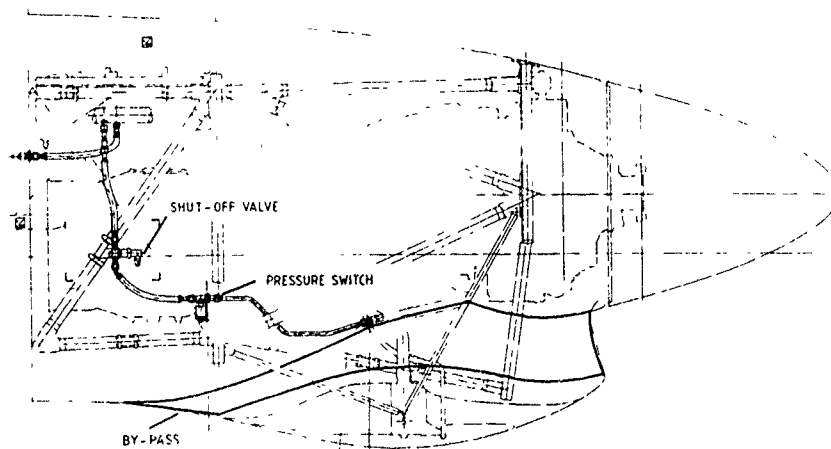


Figure 6c : General arrangement of bleed air supply to spray-pipe.

Discussion

1. W. Grabe, NRC Ottawa

Only light icing conditions were noted by pilots prior to flameouts, yet this problem was not encountered under heavy icing conditions at NRC. How come?

While problems were caused by wet snow, supercooled water icing at NRC should show the weak areas at the intake split. Why did it not do it?

Author:

At the moment of the power interruptions, the crew reported to encounter light cloud icing conditions. However, prior to the flame-outs, the aircraft had during a certain time-interval been exposed to what can best be characterized as mixed conditions of (wet) snow and (supercooled) water droplets. The conditions tested at NRC during qualification only addressed cloud icing conditions at sea-level in accordance with the requirements as laid down in IAR/FAR (ACI) 25. It appeared that engine tolerance to ice ingestion at altitude when being exposed to natural icing conditions (wet snow) may be quite different.

First of all, conditions tested at NRC (IM and CM) may not be that severe as the mixed conditions experienced in natural precipitation conditions (i.e. wet snow, hail, rain). In

addition, the engine tested at NRC was basically a gas generator and only airspeed was varied to account for different flight conditions. In-flight video observations of the flow pattern inside the air intake duct indicated that, for instance, propeller swirl significantly influences the location of stagnation areas.

2. R. Toogood, Pratt and Whitney Canada

Would you care to comment on the differences in inlet prototype configurations used in the ice tunnel and that of the initial production configuration?

Would you agree that an important conclusion of this study is that discontinuities in surface ice protection should be avoided at critical impingement locations?

Author: The differences between the prototype configuration last tested in the icing tunnel and the initial production configuration of the intake duct basically involve (software) changes to the controller. However, these are subordinate to the introduction of spray pipe, which is the result of testing in natural icing conditions rather than ice tunnel tests.

One of the conclusions of the paper and the presentation is indeed that discontinuities in stagnation areas which are exposed to impingement of precipitation involves a high design risk.

ICE TOLERANT ENGINE INLET SCREENS FOR CH113/113A SEARCH AND RESCUE HELICOPTERS

by

R.B. Jones
Senior Project Engineer
Boeing Canada Arnprior

W.A. Lucier
Manager Engineering
Boeing Canada Arnprior
Baskin Drive East
Arnprior, Ontario KFS 3M1
Canada

SUMMARY

The Canadian Forces CH113/113A Search and Rescue Helicopters occasionally encounter unavoidable icing conditions in their operating environment. The original engine inlet safeguards were not designed for, nor capable of sustained operations in icing environments, necessitating removal of the inlet screens in these conditions. This arrangement resulted in unacceptable risk of foreign object damage to the engine, and compromised operational safety.

Ice tolerant inlet screens have been developed as a remedy to this problem. The flat faced, inverted cone screens with a bypass opening accommodate progressive ice congestion during the various operational modes with minimal engine performance degradation. Comprehensive testing has confirmed the capability to operate in simulated severe icing conditions for a minimum of thirty minutes, meeting the objective "get out of trouble" capability. Operational experience and testing has substantiated improved tolerance to the full range of meteorological conditions for the fleet of CH113 Helicopters.

Activity is continuing to equip the remaining CH113A Helicopters with the ice tolerant engine inlet screens. Other international operators of the Boeing Helicopters Model 107 Type helicopters have expressed interest in the developments achieved, and independent evaluations are under way.

1.0 INTRODUCTION

Small gas turbine engines generally lack the tolerance to foreign object damage (FOD) and ice ingestion problems afforded to large turbofan powerplants in commercial jetliners. As such, inlet screens and particle separators are employed as protection to the vulnerable compressor blades in many helicopters and smaller fixed wing aircraft. The Canadian Forces CH113/113A Search and Rescue Helicopters, derivatives of the Boeing Helicopters 107 series tandem rotor helicopter, were originally equipped with conical wire mesh screens to minimize FOD problems for its two internally mounted engines. The CH113A helicopter also employed a particle separator. These systems proved to be effective at minimizing engine damage due to foreign debris under most operating

regimes. In icing conditions though, the CH113/113A screens had exhibited a tendency to become congested with ice, and consequently the screens have to be removed for winter operations. The unprotected engines are exposed to increased risk of FOD during operations in this period.

The CH113/113A Helicopters are rated at a maximum all up weight of 21,400 pounds, and are powered by twin General Electric T58-8F engines. The engine features a 10 stage axial in-line compressor, and variable inlet guide vanes to ensure efficient and stall free operation. The military power rating for each engine is 1350 shaft horsepower. At normal SAR operating weights and full fuel, the aircraft lacks single engine capability with the present power available. Canadian Forces experience has shown that the inlet guide vanes and first stage compressor blades of the T58 engine are particularly vulnerable to FOD in the absence of protective screens¹.

The inlet configuration for the CH113 helicopter consists of a straight cylindrical duct. This arrangement, with minimal obstruction, is known to offer virtually undistorted inlet flow and the recovery of a large percentage of the ram air effect, although offering little protection from sand and small particle debris. Electrical resistance heating and engine bleed air are employed to prevent ice build-up. The original particle separator system used with the CH113A variant provided improved resistance to debris damage, at the expense of a somewhat obstructed inlet. This latter arrangement also provided heating to breeze surfaces, although operational experience and testing has shown that ice could develop at the separator in some conditions².

Several factors have contributed to the need for improvements to the engine inlet protection systems for the CH113/113A. The very nature of search and rescue (SAR) operations, particularly in light of Canada's geography and environment, places a high demand on availability and reliability. SAR missions are most often conducted in coastal or mountainous regions and frequently in adverse weather conditions. Although the aircraft was not designed, nor authorized for flight into icing conditions, tolerance to unexpected, unavoidable icing conditions, or marginal conditions is highly desirable in the SAR role and particularly for a "get out of trouble" capability. The consequences of an aborted mission or a forced

landing could be serious due to both the role and environment served by the CH113/113A.

The limitations in single engine performance provides further impetus for enhanced protection against FOD and ice ingestion problems, underscoring the need for full time safeguards for the engine. The loss of a single engine is considered a critical emergency for the CH113/113A. The risk of dual engine failure can be significant in some circumstances of foreign debris ingestion, particularly during any in-flight ice shedding or severe inlet congestion due to ice or wet snow.

Although the possibility of developing a modified inlet duct system was initially considered, this option was dismissed in favour of an ice tolerant inlet screen due largely to the limitations inherent to the internal mounting of the engines. The problem addressed in the current work was therefore to develop a FOD ice screen to be installed externally in front of the straight duct. This approach was expected to yield a passive device to be employed in all seasons with minimal change to the existing engine inlet and duct configuration.

2.0 ICING CONDITIONS

The logical start to an analysis of the rate of ice accretion is the definition of the icing conditions, and herein lies an intensive challenge due to the variability of these conditions. While modelling the ice accretion rate for one particular set of parameters may be achievable, the certification requirement and the real world icing conditions are subject to a broad range of variation in the contributing factors, including: atmospheric parameters, surface properties, and engine operating condition and flight parameters.

Particularly difficult to define is the starting point, i.e. the icing cloud and the snow cloud. The Coalescence Theory model for precipitation gives a mechanism of rain drop growth in warm cloud, whereas the Wegener-Bergeron-Findeisen theory gives a cold cloud model in which supercooled water droplets and ice coexist, but coalescence takes place in such a cloud as well³. These two models are not mutually exclusive nor contradictory, therefore the liquid/solid water content is yet another variable. As well as this, the dependence of the type of icing cloud or snow conditions on the suspended atmospheric particles adds more to the complex picture. This is also influenced in ground effect hover with recirculating snow and ice laden air, resulting in a localized whiteout.

The problem of variability of atmospheric conditions for the Search and Rescue role for this helicopter in Canada is aggravated by seasonal and geographical realities. Canada has long coast lines on both the Atlantic and Pacific Oceans, and a vast interior speckled by an array of freshwater lakes that are among the world's largest and most numerous. This, combined with our ranges of terrain and latitude, contributes to a full spectrum of icing conditions that may be encountered. A rescue on the East coast far out into the shipping lanes can face weather changes in

a similar way to a mountain rescue involving altitude change on the West coast, and it is the variability of conditions: wet snow, dry snow, cold weather icing, warm weather icing and perhaps most worrisome, freezing rain that presents the real flight problem. Trying to predict the onset and effect of potential icing conditions can be humbling even when the consequences are less severe, such as when operating a personal automobile. It is not unusual to observe trees and fences glazed with freezing rain, and yet no accumulation will form on the windshield. Mysteriously, in what would seem to be comparable conditions to the casual observer, keeping even a heated windshield clear of ice build-up will be a virtually impossible task.

The rate of icing on the different surfaces is important for the type of screen considered and this introduces a further parameter i.e. the local air flow. A lesson learned at the start of testing invalidated an assumption that the blade downwash air travelled directly downwards in ground effect hover and ground run. It was found that the cross flow caused by the blade drag was very significant, especially for the ice accretion rate from the side of the engine inlet.

Earlier work with an ice detector installed on the helicopter did not yield successful results, leading to the removal of the detector. It was possible that it would mislead the air crew, especially as to the type of icing. The two basic types of ice formation experienced during tests were clear glaze ice and rime ice (milky white). The glaze ice varied from hard to soft, which introduced the danger of it breaking off, but the rime ice was always hard. This was of particular influence in the final detail design which had to be refined because of the type of build-up on different parts of the screen. The same also applied to the snow conditions: the wet snow often produced a soft glaze ice which could easily break off and enter the engine.

The certification requirements, as defined in Airworthiness Regulations FAR 25 (which is not strictly applicable for military helicopters), do not completely clarify the icing conditions and accretion rates to be considered for the design case⁴. The certification requirements also provide little guidance with respect to the failure criterion for different flight conditions. There are obviously two extreme cases: flame out due to air starvation and engine failure due to FOD resulting from an ingested ice piece. In either case for the CH113/113A, a single engine failure would result in degraded performance and a mission abort. In the case of a dual engine failure, an autorotation to the ground or sea surface would be necessary unless power can be recovered. The regime of flight and the local terrain or sea state would play an important role in the safe execution of the autorotative landing and survival. It would certainly be desirable to work towards some intermediate failure criterion, such as 70% screen blockage, versus the extremes raised with their inherent loss of affected engine power.

As a result of the difficulties in rigorously modelling the range in ice accretion rate, it was determined that testing and closely monitored prototype installations would most effectively cover this aspect of the development. Icing simulations were conducted at the National Research Council Canada (NRC) Ottawa test rig facilities. No testing was done with artificial snow as previous studies reported unreliable results, and it was felt that natural snow, whether wet or dry, would yield more credible testing⁵. Design features influenced by the icing conditions would call upon the test findings, as well as past experience in similar developments, such as that for the CH147 Chinook.

3.0 OPTIONS TO REMEDY THE ICING PROBLEM

Several candidate solutions to the CH113/113A engine inlet icing problems were considered. The number of potential remedies evaluated was reflective of the difficulty in fully defining the scope of the design parameters, as raised in the preceding discussion on icing conditions. The parameters considered in the evaluation of the candidates included:

- a) icing performance
- b) suitability for year round FOD protection,
- c) inlet flow distortion,
- d) aerodynamic drag penalty, and
- e) electrical power demand.

The solution commonly employed for inlet protection has generally been integrated into the duct, such as an S-duct, a vortex generator bank, or an axisymmetric duct with swirl vanes⁶. These and any similar solutions demanding extensive modification to the engine inlet duct configuration were immediately discounted due to physical space restrictions and program constraints. It should be noted that these criteria dismissed several possible solutions that could be of merit in other applications. Only solutions external to the inlet duct were considered further in the current investigation.

First among solutions considered were modifications to, or enhanced variants of, the original conical screen arrangement. This system had proven to be effective at preventing FOD ingestion in most environments, but operational experience and NRC ice test rig results confirmed its vulnerability to ice congestion. The test results suggested that in some conditions, sufficient ice build-up could occur within a few minutes to cause the engine to flame out. The aircraft operating instructions reflected this limitation by directing that the screens be removed in possible icing conditions. With these screens removed the engines were open to Ice/FOD ingestion, and engine damage occurred in this configuration.

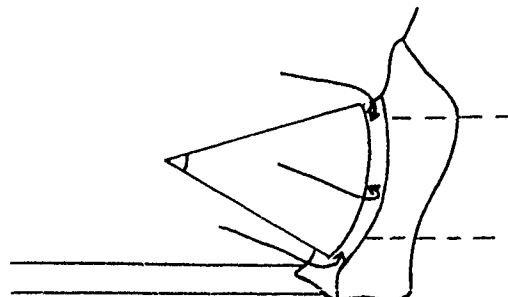
It was suspected that the original particle separator utilized on the CH113A was also responsible for a number engine failures caused by liberated ice developed at the separator. Testing in the NRC ice rig verified this possibility; the particle separator was

removed and replaced with a straight heated duct, comparable to the CH113 configuration. This new duct provided a improved heating capacity versus the prior arrangement, and commonality for any subsequent modifications evolving from the present investigation addressing the inlet screen icing problem.

A Boeing Helicopters proposal to the Swedish Armed Forces in 1974, and work done by Kawasaki Heavy Industries, describes a heated wire mesh screen similar in geometry to the original conical screen. This solution was burdened with prohibitively high manufacturing costs per screen on small production runs combined with excessive electrical power requirements: approximately 15 KW per screen to anti-ice 40 per cent of the screen surface under extreme icing conditions for short periods (up to 15 minutes), and 5 KW continuous under moderate icing conditions. These factors negated the feasibility of a heated variant of the conical screen.

A "dog house" type of protective inlet cover has been developed and used successfully by Columbia Helicopters. The simple arrangement is based on the concept of an enclosed space with a small entrance parallel to the incoming air stream. Dry air can be drawn in, leaving the moisture laden air and any suspended FOD particles to rush past. This concept was also studied by Kawasaki Heavy Industries from 1971 to 1981 for the 107 Type helicopter. The concept was dismissed because of potential for ice accretion and ingestion in severe icing conditions. The Columbia experience however, has proved more positive and the dog house configuration remains in service on their fleet of 107 Type helicopters.

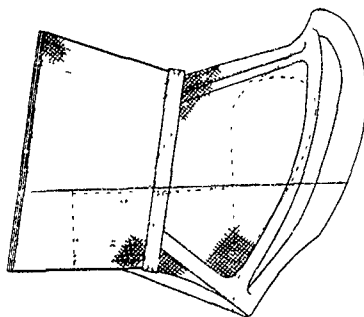
A variation of this concept is a panel or screen cone in front of the intake inlets pointing into the air stream so that the air has to go around the corner lip to enter the engine. This concept was not studied in detail due to its similarity to the original cone and because of the anticipated penalty in summer with the absence of FOD protection.



Kawasaki Heavy Industries developed an interesting double screen with bypass. It is not known whether the concept had been prototyped, or if the large frontal area would introduce excessive drag. One interesting aspect of Kawasaki's testing of this screen was the evaluation of Ice Repellant Coatings. Screens tested with and without the coating under simulated snow conditions unfortunately were almost simultaneously blocked by snow and ice. However, only a minimal shedding force was required on the Ice Repellant Coated screen to remove the accumulated snow.

In the 1950/1960's, Boeing Helicopters explored a design concept utilizing a flat face engine inlet screen. The approach, like the dog-house concept, exploited the expectation that an air stream would shed the majority of its entrained liquid water in flowing around a sharp obstruction. In this case, the ice congested flat face would force the axial flow of inlet air to accelerate radially inward around the face in order to enter the engine through the side of the screen. Any airborne water droplets, snow or ice would safely pass the engine inlet.

The results of the initial Boeing Helicopters investigation proved the viability of the flat face screen arrangement, and recommended that the original cylindrical sides to the screen be tapered toward the inlet, forming an inverted cone, to induce greater separation of any moisture content. The flat faced screen design, however, was never fully developed, nor tested for the Model 107 application. Further investigation into the performance of the flat faced screen with cylindrical sides was conducted at the Naval Air Propulsion Test Center, Trenton, New Jersey, in November, 1974. Their tests in up to 20 minutes in severe icing conditions resulted in a fully congested screen face, but little ice build-up on the side mesh. Based on these positive findings, and the applicability to the CH113/113A, this solution concept was resurrected in the current investigation.



The flat faced screen features accommodated a number of modes of operation. In fast forward cruise in icing conditions the front face ices over rapidly and the air has to turn sharply to enter the sides of the cone. The sides remain clear of deposit in forward flight, especially with the introduction of the cut back, and would thus provide the path for inlet air.

In ground effect hover or ground running, the inlet air flow is less unidirectional, and the screen surfaces would be expected to ice over more uniformly. Continued operation with such ice development would necessitate some form of open bypass to maintain a path to feed the engine air. The restricted and distorted air flow in this contingency mode of operation was expected to yield reduced but continued engine performance.

In both icing and non-icing conditions, the flat faced screen arrangement would provide full time protection against fod ingestion for particles larger than the wire mesh void size. Any bypass opening should also provide shielding against direct ingress.

The flat faced screen, including the suggested tapered sidewalls and a bypass feature, was selected over the alternate configurations to be the thrust of development. It has already been emphasized that this choice of final solution for this helicopter installation does not detract from the merits of other solutions for different configurations.

The following table summarizes the options considered, their merits and their drawbacks for the current application. Presented are the various screen arrangements discussed herein, as well as the plenum inlet arrangement, and the option of going to an externally mounted engine with an inlet screen configuration similar to that of the Chinook Helicopter.

TYPE OF ICE PROTECTION	MOST EFFECTIVE FOR WHICH CONDITIONS	PENALTIES	FEASIBILITY FOR CH113/113A
DOG HOUSE	ICE, SNOW, LARGE PARTICLES	RAM AIR LOSS ENG' POWER LOSS FOD, SIDE INGRESS	FEASIBLE
HEATED SCREEN	ICE, FOD, NOT WET SNOW	REQUIRES EXCESSIVE ELECTRICAL POWER AND PRONE TO FAILURE	NOT FEASIBLE
SOLID CONE WITH BYPASS	ICE, SNOW ONLY	LOSS OF ENGINE POWER SUMMER AND WINTER	FEASIBLE
DOUBLE SCREEN	ICE, FOD, DRY SNOW, UNKNOWN, WET SNOW	HIGH AERODYNAMIC DRAG	FEASIBLE
S DUCT SIDE ENTRANCE	ICE, FOD, DRY SNOW, SMALL PARTICLES	SPACE LOSS INLET DISTORTION	NOT FEASIBLE
AXISYMMETRIC WITH SWIRL VANES	SMALL PARTICLES, FOD	SPACE LOSS INCREASED INLET DRAG	NOT FEASIBLE
VORTEX SEPARATOR	SAND, SALT SPRAY	SPACE LOSS INCREASED DRAG, CAN BLOCK	NOT FEASIBLE
PLENUM	ICE, FOD, DRY SNOW	RAM LOSS SPACE LOSS	NOT FEASIBLE
EXTERNALLY MOUNTED ENGINES WITH CHINOOK SCREEN	ICE, FOD, WET SNOW, DRY SNOW	NOT SUITABLE FOR RETROFIT	NOT FEASIBLE
INVERTED CONE WITH BYPASS	PROVEN IN ICE, FOD, WET, DRY SNOW	NONE	FEASIBLE

4.0 DEVELOPMENT OF THE ICE TOLERANT INLET SCREEN

The process of designing and optimizing the ice tolerant inlet screens for the CH113/113A helicopter, based upon the flat faced inverted cone concept, was largely iterative. Although recognized as a protracted approach, these iterations were necessary due to the difficulty in anticipating the icing, screen and engine performance in the range of meteorological and operating conditions to be encountered.

The principle design features pursued in the development were:

- a) A flat front screen face perpendicular to the streamlines. During most (i.e. non-icing) conditions, engine intake air would be expected to enter the inlet via this front face.
- b) An inverted screen cone with sides parallel as possible to the stream lines of the air entering the engine. In the case of a congested front face, engine intake air would be expected to enter via the side panels.
- c) A shielded open bypass area in the screen to facilitate continued, although reduced, engine performance in the extreme case of a fully congested inlet screen (i.e. both face and sides).
- d) A solid fibreglass attachment collar to serve as a flush interface to the existing inlet fairing assembly.

The major design objectives were to:

- a) minimize the aircraft performance penalty of aerodynamic drag induced by the inlet screens,
- b) minimize the engine performance penalty resulting from intake air starvation or distortion,
- c) minimize the probability of any ice accretion within the screen that would introduce the risk of damaging ice ingestion, and
- d) provide full time protection against FOD.

4.1 Inlet Airflow Requirements

The project assumptions were that the existing air induction system with the original conical screens met all CH113/113A flight envelope requirements, and therefore, any new screen design, as a minimum, had to maintain the diameter and area of the engine inlet opening, and screen open mesh area. These assumptions precluded the need to calculate and

theoretically verify airflow characteristics through the air inlet to the engine, and allowed for testing to verify that the new design did not introduce any detrimental turbulence to the airflow.

The determination of screen geometry and the sizing of the various elements was the first task undertaken in the development of the new screens. The basic strategy utilized was to size the inverted cone sides to suit the geometry of the inlet duct while achieving a flow area not less than that provided by the screen being replaced (i.e. 418 sq. in.), even in the case of a fully congested front face. The diameter of the inverted cone rear ring was chosen so as to enclose the streamlines of the air entering the intake duct. The cone recess angle was chosen largely based upon physical constraints, although it compared favourably to that earlier proposed by Boeing Helicopters. The angle was deemed suitable in that it was adequate to induce water shedding but would not yield an excessively large screen face. The length of the truncated inverted cone was thus governed by the requirement for side flow area. By extension of the geometry of the inverted cone, the face diameter was established.

The bypass dimensions were chosen so that the minimum open area shown in the table was set equal to the normal open intake (i.e. 65 sq. in.).

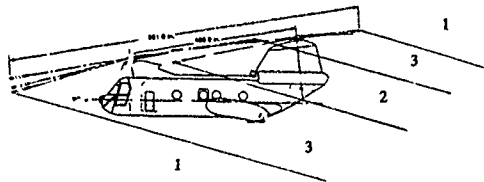
	AREA (SQ. IN.)	OPEN MESH (SQ. IN.)
ORIGINAL CONICAL	418	235
CH113: SIDEWALL	575	324
BYPASS	65	NA
CH113A: SIDEWALL	575	324
BYPASS	65	NA

The basic principle that air loses its liquid water content in bending sharply around the blocked flat face of the ice tolerant inlet screen suggests that the front face should be normal to the streamlines of the impinging local airflow. For a helicopter the direction of the streamlines varies with flight condition from hover to forward cruise. It was concluded that the ice tolerant inlet screen's front face should be oriented normally to the forward cruise airstream to maximize its performance in the "get out of trouble" case. The optimum angle of incidence of airflow to the engine inlet for forward cruise at 110 knots and blade downwash effects was derived as follows with vector addition of the primary airflow sources. This derivation excludes any influence of aircraft pitch, or airflow disturbances induced by aircraft aerodynamics or local inlet effects.

Forward Speed, $V = 110 \text{ knots} = 186 \text{ ft/sec. (corresponding to } V_{ne} \text{ at maximum gross weight)}$

Air Density, $\rho = 0.0023769 \text{ slugs/ft}^3$

The helicopter geometric data is shown below.



As seen there are three flow regions below the two sets of blades; the first is outside the radius of both blade sets, the second is in the region where the blade set overlap, and the third is the area under each of the blade sets where they do not overlap. The engine intake air can be drawn from either of the last two regions depending on the forward speed so both cases will be analyzed.

Case 1 INNER DISC TOTAL AREA

$$= \pi \left(\frac{50}{2} \right)^2 \times 2$$

$$= 3927 \text{ ft}^2$$

Case 2 OVERLAP DISC TOTAL AREA

$$= \pi \left(\frac{50}{2} \right)^2 \times 2 - 2 \left(\frac{50}{360} \pi \left(\frac{50}{2} \right)^2 - A_A \right)$$

$$\text{Where } A_A = \sin 20 \cos 20 \times 25^2$$

$$= 200 \text{ ft}^2$$

$$\therefore A = 3927 - 2 \times (273 - 200)$$

$$= 3781 \text{ ft}^2$$

From momentum theory for an ideal actuator disc

$$\text{Vertical Lift} = W = 2 A V_v^2. (\text{Ref. 8})$$

Where W = Weight of Helicopter (lb),

P = Air density (slug/ft³),

A = Rotor Area (ft²)

V_v = Vertical air speed ft/sec.

$$V_v = \sqrt{\frac{W}{2 \rho A}}$$

$$\text{Case 1 } V_v = \sqrt{\frac{19500}{2 \times 0.0023769 \times 3927}}$$

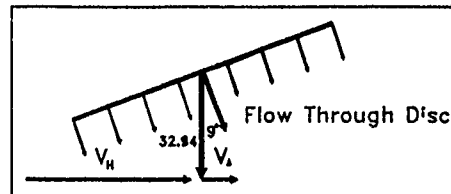
$$= 32.31 \frac{\text{ft}}{\text{sec}}$$

$$\text{Case 2 } V_v = \sqrt{\frac{19500}{2 \times 0.0023769 \times 3781}}$$

$$= 32.94 \frac{\text{ft}}{\text{sec}}$$

This vertical velocity is for an ideal actuator disc, however, for a tandem rotor helicopter the disc efficiency is between 85% and 95% depending on the speed range and for the worst condition can drop as low as 70% with ice on the blades.

Consider the flow just from the front rotor which has a horizontal component due to the tilt of the blade disc:



$$V_A = 32.9 \times \tan(9^\circ) = 5.21 \frac{\text{ft}}{\text{sec}}$$

$$V_H = V_A + V$$

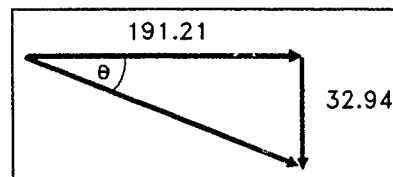
$$V = 110 \text{ k} = 186 \frac{\text{ft}}{\text{sec}}$$

$$V_H = 186 + 5.21 = 191.21 \frac{\text{ft}}{\text{sec}}$$

$V = 110 \text{ k} = 186 \text{ ft/sec}$ so the total horizontal velocity at engine inlet

$$= 186 + 5.21 = 191.21 \text{ ft/sec} = 191.21 \text{ ft/sec}$$

and the total vertical velocity at engine inlet = 32.94 ft/sec.



$$\therefore \tan \theta = \frac{32.94}{191.21}$$

$$\theta = 9.77^\circ$$

The angle of the flow to the ENGINE CENTRE LINE = 9.77 (For the case of ice build-up $V = 1.3 V_v$, the angle is 12.62°). (Ref. 9)

Therefore, the calculated optimum orientation of the screen faces would be tilted upward approximately 10 degrees from the horizontal, while slightly divergent from the plane of the aircraft centreline. It is interesting to note that the rear rotor set downwash is only effective in the inlet region if the angle is 23 degrees. From geometry, if the forward flight speed is greater than 45 knots, the engines inlet airflow is only influenced from the forward rotor.

The inverted front cone dimensions and the optimum angle corresponding to cruise conditions enabled the location of the left front cone to be centred just in front of the intake face. However, when integrating the front cone to the attachment collar, the desired angle of incidence could not be maintained for the right hand screen due to interference with the synchronizing shaft cover (tunnel) in front of the right hand intake. An inclination angle of 17 degrees was the minimum allowable for the given screen dimensions at the right hand side. This physical constraint superseded the optimum calculated orientation. This angle of incidence would be aligned to the expected inlet air flow at a forward cruise speed of 64 knots.

Tufting tests conducted by AETE during the certification phase of the final screen configuration substantiated the adequacy of the orientation for the screens.

The above geometric constraints were employed as design objectives in the manufacture of the first prototype screen, and in fact remained fixed throughout the development and final design. CAD facilities were employed and very effective at implementing these critical geometric parameters in preparing the engineering drawings for the designs completed.

4.2 Structural Considerations

The basic materials selected for the build of the prototype remained unchanged throughout the development. The screen mesh for the various inlet areas was type 304 stainless steel wire with 1/4 x 1/4 inch mesh. The underlying structure was manufactured of welded type 321 stainless tube, plate and sheet. The attachment collar was fabricated with a fibreglass - vinyl ester composite moulded to conform with the inlet fairing of the helicopter. The supporting structure and aft most edge of the screen mesh were embedded in the moulded collar during the manufacture. These materials enabled the designs to meet the various structural requirements including static strength, resistance to impact, and resistance to vibration induced fatigue.

This mention of structural requirements introduces a very interesting aspect of the design¹⁰. The impact load case for the front face of the screen, and consequently for the supporting structure right back to the support collar, was influenced by competing requirements. In order to reduce the impact load case, the structure needed to be flexible to absorb the energy of impact. However, the structure also had to be sufficiently strong to transmit the load developed without failure. The design of the structure with sufficient strength and flexibility to reduce the impact load resulted in a narrow window for structural design. The loading on the front face was derived by an iterative assumed load/deflection/resultant load calculation. This converged to the final impact load given by the rigid object strike to the front face.

Another interesting aspect in the design analysis was the determination of the structural contribution of the screen mesh, whose stress/strain relationship was found by test to be inherently non-linear.

4.3 Prototype Development

The earliest prototype developed was modular in concept. This design was applied to the CH113A, whose inlet configuration differed slightly from that of the CH113. Unlike subsequent models, the bypass feature was not integrated into the side of the screen. An optional bypass was achieved with interchangeable front faces - one flush face providing no bypass (i.e. suitable during non-icing seasons), and one face incorporating a forward bypass.

Testing plans for this first design were comprised of engine test cell work, intended to observe the flow distortions and engine performance at various stages of blockage, and icing tests. Due to program constraints, difficulties in emulating the aircraft inlet, and test facility problems; the findings of the engine tests with the first prototype were inconclusive.

The simulated icing test plan was comprised of 28 sorties for a total of 14.1 flying hours. The results of these icing trials suggested that the flush faced screen did not provide a sufficient time margin in icing to enable the pilot to recover safely before engine flame-out due to blockage. Ice build-up was also found to occur in the yet unchanged particle separator duct, which led to a engine FOD incident. This arising contributed to the decision to eliminate the particle separator for the CH113A helicopters.

This arrangement was abandoned in favour of an aft bypass system for subsequent designs.

The bypass location chosen in the next iteration was at the top aft area between the front cone rear small ring and the collar of the engine inlet screen. The bypass opening was covered by a piece of screen resulting in a shape like the open gill of a fish. This piece of screen, referred to as the "ear", was designed to provide shielding against direct ingress from the front while introducing minimal frontal aerodynamic drag. This configuration was subject to extensive ice rig and engine test cell qualifications, as detailed in Section 5.

4.4 Final Design Configuration

The final design configuration also utilized an aft bypass, but with the opening situated at the outboard side of the screen. The prototype of this configuration was subject to an extended flight test program, detailed below, before fitment to the CH113 fleet. Minor refinements were accomplished based upon the results of testing and operational experience with the prototype. This "fine tuning" of the screens was a critical phase in the development. Sites of localized

ice accretion were eliminated by contouring air flows, some elements were strengthened, a localized heating problem was remedied, and a removable bypass screen insert was developed to discourage bird nesting.

5.0 QUALIFICATION TESTING

The importance of the testing aspect of the development of the ice tolerant inlet screen has been stressed through out this paper. The team for the various qualification tests of the final configuration was comprised of representatives from the Canadian Forces National Defence Headquarters (NDHQ), the Aerospace Engineering Test Establishment (AETE), the National Research Council (NRC) and Boeing. The availability of the unique NRC ice test rig and the technical support of the ice rig staff was crucial to the development and certification. The use of the Standard Aero engine test cell and the support from Standard Aero made the engine testing possible.

5.1 Tufting Test

A tufting flight test was conducted by AETE in Ottawa to provide suitable airflow visualization throughout the CH113A operating speed range for confirmation of the optimum inlet screen angle. The test comprised two sorties for a total of 8.4 flying hours with a test helicopter and a photo chase aircraft. Six inch long tufts were affixed to the test aircraft's skin spaced every 4 inches for 7 ft along the top of the aircraft in front of both engine inlets and along the aft pylon within 3 feet of the engine inlets. In addition, a hoop positioned 32 inches in front of the engine inlets allowed the attachment of three 12-inch long tufts floating freely in the airstream for the purpose of indicating the direction of the airflow entering the engines.

The behaviour of the tufts was filmed from the photo chase helicopter. The film of these flights was difficult to analyze and showed rapid oscillation of the tufts, especially on the long tuft located to give the angle of airflow at the engine inlet. The estimated average air flow angles were observed to be approximately 10 degrees for the left hand screen, and 15 degrees for the right hand screen. These figures, although subject to wide scatter in the test results (i.e. +/- 8 degrees), substantiated the calculated screen orientations.

5.2 Engine Test Cell Qualifications

The ice tolerant inlet screens incorporating the aft top bypass feature were tested in December 1986 at the Standard Aero engine test cell with a production (T58-8F) engine. The main objective for testing the prototype screen and new fairing configuration in a test cell environment was to determine whether or not any detrimental effects on engine performance were

being imposed by the progressive increase in inlet area restriction on the prototype screen design. In addition, it was desired to determine whether use of the new inlet configuration would produce unacceptable inlet conditions which could affect the condition of the engine.

To fulfill the objective of the engine test cell trials, the following test points were defined as part of the final test plan:

- a) Perform two initial standard performance runs to establish base line data and verify repeatability of data;
- b) Create various air intake flow restrictions to simulate progressive screen blockage due to icing;
- c) Test with the fairing without particle separator and with the existing CH113A fairing for performance comparison;
- d) Conduct standard engine performance runs between main configuration change; to verify base line data repeatability;
- e) Perform a one hour endurance run with "optimum" air inlet blockage. The optimally blocked screen configuration involved 100% blockage of the top and front of the screen and 75% blockage of the bottom of the screen with the bypass area open. This configuration provided an element of swirl in the inlet flow conditions creating the worse inlet condition.
- f) Perform "slam" accelerations as well as "load chops" and "load bursts" with the screen totally blocked to demonstrate the engine's ability to neither stall nor surge with the screens completely iced.
- g) Monitor engine vibration levels throughout the test as an indication of inlet flow distortion caused by the various degrees of screen blockage.

In summary, the engine cell performance tests indicated a two percent (2%) power loss with front face completely blocked and 75% of sidewalls blocked. Thirty-seven percent (37%) power loss with both front face and sidewalls completely blocked - engine air entering solely through bypass opening. In the unlikely situation where such extreme inlet screen blockage might be experienced for both engines, there would be sufficient power remaining (i.e. 1700 HP) for cruise. During the tests the engine did not stall or surge during all "slam accelerations", "load chops", and "load bursts".

The results of this testing verified that the installed engine performance matched that of the original inlet configuration. The inlet distortion was monitored by recording the vibration of the first set of compressor blades using the zoom feature of a spectrum analyzer, and no adverse effects were noted in testing with the new induction system. The conclusions drawn at the end of this test phase were that the ice tolerant inlet screens and the new H46 inlet system performed satisfactorily. Even with all of the screen blocked and the bypass partially blocked, engine performance was acceptable. The design was subsequently approved for flight testing by Boeing and NDHQ technical authorities.

Finally, based on the analysis of the engine test cell trials, the proposed inlet screen design was approved, with respect to the propulsion system, for use during actual icing trials. It was recommended to proceed with flight trials.

5.3 Simulated Icing Trials

The Icing Spray Rig of the Low Temperature Laboratory of the Division of Mechanical Engineering, NRC, was employed for the simulation of icing environments. The rig, located in Ottawa, consists of an array of 161 steam atomizing water nozzles producing an icing cloud 16.4 feet deep and 75.5 feet wide. The array can be rotated about a single supporting mast 75.5 feet high to take advantage of wind direction. Liquid water content (LWC) can be varied over the range of 2.0×10^{-7} to 1.5×10^{-6} slugs per cubic foot (slug/ft³) and droplet sizes ranging from 1.2 to 2.4 thousandths of an inch depending on temperature and wind velocity. The second stage of testing in the NRC ice rig with the ice tolerant inlet screen and top aft bypass was the most crucial part of the test program. Basically, the performance objective was for 30 minutes of operation in severe icing conditions. The thrust of this testing was ice accretion, and no rigorous measure of any engine performance degradation was conducted at this test phase.

AETE was tasked to evaluate the ice tolerant inlet screen and develop the icing trial methodology. This methodology was based on knowledge from previous ice testing and a logical choice of cloud conditions. The FAR 25 stratiform cloud case was chosen rather than the cumuliform because this case is related to a larger horizontal extent (10.8 miles) of cloud giving more accretion time. Similarly the choice of droplet size of 1.2 thousandths of an inch, which was suggested by NRC personnel to represent a good average value for FAR testing, was considered prudent. These decisions enabled the test method to become simply a matter of controlling the accretion of ice as a function of the LWC and exposure time. The maximum LWC available from the rig, corresponding to the selected test parameters, was chosen. The available range of LWC was from 3.9×10^{-7} to 1.4×10^{-6} slug/ft³. With the helicopter on the ground the best icing cloud coverage was obtained at winds of approximately 10 miles per hour, with the spray

nozzles below the mid-mast position and the helicopter positioned approximately 100 feet away from and facing the array of spray nozzles. For in ground effect (IGE) hover the nozzle array was raised completely to the top of the mast, however, for the tandem rotor helicopter a wind velocity of at least 15.5 to 24.9 miles per hour was required to obtain a good cloud coverage.

The conclusion from this testing was that the prototype inlet screen allowed sufficient airflow for normal operation of the engines for up to 30 minutes at flight idle under severe simulated icing conditions. There was evidence of ice on the front of the struts which indicates that some of the air entering the front face exits through the bypass which is a very desirable feature, however, this was not confirmed. It was concluded that the bypass must be moved more to the side and that all struts in the bypass area must be relocated. It was recommended that further testing be conducted to investigate the capability of a modified CH113/113A helicopter to operate in all types of snow conditions and in visible moisture in the range of 32°F to 39°F.

The recommended modifications were embodied on the subsequent prototype, and the qualifications, with these revisions, resumed in genuine meteorological conditions versus the simulated environments.

5.4 Performance flight test.

Performance tests were conducted by AETE and 424 Squadron personnel March 1987. The tests were to determine and quantify any significant degradation in engine performance with the prototype bypass ice tolerant inlet screen and modified H-46E air induction system installed. The tests comprised seven sorties for a total of 2.2 hours of ground testing and 7.3 hours of flight testing.

In summary, the helicopter's performance with the protective inlet screens installed was acceptable.

5.5 Rain/Snow Flight Trials.

Results of the icing trials were sufficiently promising to warrant further investigation of the capabilities of the prototype screens¹¹. AETE was tasked to develop the test program and perform the flight testing. Tests were conducted to investigate different types of accretion on the test aircraft and on the prototype ice tolerant inlet screens in the following three meteorological conditions^{12 13}:

- a) cold rain in the range of 32°F to 39°F OAT;
- b) wet snow in the range of 26.6°F to 35.5°F OAT; and
- c. dry snow in the range of 15.8°F to 28.4°F.

Ground idle, (IGE) hover and low speed forward flight tests were conducted at CFB Gander in cold rain, wet snow, and dry snow conditions. Cold rain tests were conducted only at flight idle and no accretion of ice was observed. The worst cases in wet and dry snow were experienced during the 30 minute IGE hover flights. Unlike the original CH113/113A inlet screens, the prototype CH113/113A ice tolerant inlet screen, now equipped with the outboard rear bypass, was capable of operating during these trials in visible moisture below 39°F OAT.

The results of the flight tests with the side bypass were summarized as follows: Fleet fitment of the side bypass ice tolerant inlet screens was recommended with the following refinements incorporated in production versions:

- a) The fiberglass attachment collar was to be extended in the area beneath the left hand ice tolerant inlet screen assembly to cover the exposed heated surfaces of the engine air inlet fairing assembly in this area.
- b) All surfaces of the fiberglass attachment collar extending inside the ice tolerant inlet screen assembly were to be trimmed and all acute corners were to be smoothed out to reduce the collection of snow or ice.
- c) An additional 1 inch of the lower quadrant of the mesh screen was to be embedded in the fiberglass attachment collar to delay ice accretion inside the mesh screen.

These modifications to the screen assemblies further reduced or eliminated their susceptibility to the formation of ice inside the screen assembly. The two sets of CH113 prototype ice tolerant inlet screens were flown in normal operations for the duration of the icing season. The screen performance was acceptable. No engine performance degradation was reported. Therefore, the commitment was made to proceed with the CH113 fleet fitment of production inlet screens.

5.6 Qualification Summary

The following chart summarizes the ice tolerant inlet screen project with respect to the method used to achieve non-turbulent engine inlet airflow, minimum degradation in engine performance and minimum aerodynamic drag.

FEATURE	TESTING
Front Cone	Proved by extensive testing.
Bypass Area	Final design same area as screen tested in engine cell.
Frontal Drag & Engine Performance	Performance flight test.
Engine Inlet Distortion CH113A	Tested in engine cell. No anomalies reported during ground and flight testing.
Engine Inlet Distortion CH113	No anomalies reported during ground and flight testing.

Sufficient testing has been completed at the NRC ice rig, the engine test cell and during free flight in icing and snow conditions to establish both the airworthiness and effectivity of the ice/FOD deflector installation on the CH113/113A.

6.0 OPERATIONAL EXPERIENCE

The CH113 fleet of 6 aircraft has been flying with the ice tolerant inlet screens for over a year with no engine inlet icing or ice FOD related problems reported. It has been difficult to ascertain the extent of any ice development on the new screens in normal use. The engine inlets are not visible to aircrew in flight, and any accretion would be expected to melt during post landing operations and shutdown. The positive performance of the new ice tolerant inlet screens has contributed to improved pilot confidence in the aircraft capability, particularly in adverse weather conditions.

The first CH113A helicopter modified has also been flying for a year with the screens installed with no reported operational problems.

One set of screens has also been supplied to Kawasaki Heavy Industries for evaluation by the Japanese Self Defence Forces. To date, there has been no feedback regarding any operational performance results.

7.0 CONCLUSIONS

An ice tolerant engine inlet screen has been developed to provide protection against foreign object damage and resistance to inlet congestion. The design features a flat mesh face, an inverted conical side and a shielded bypass opening. The findings of a comprehensive test program proved that the screens would provide a minimum of thirty minutes of operation in severe icing conditions, and satisfactory performance in wet snow or dry snow.

These positive results have led to an improved tolerance to unexpected and unavoidable icing conditions for the engines of the CH113/113A Search and Rescue Helicopter fleet, and improved aircrew confidence in the aircraft's reliability in inclement weather.

During engine cell tests for the ice tolerant inlet screen, a unique method of monitoring any influence of detrimental inlet flow distortion was derived. This technique employed a spectrum analyzer to record the vibrational characteristics at the blade passing frequency for the compressor first stage. The result was a relatively simple and real-time verification of any undesirable compressor blade excitation when operating in the presence of the various inlet configurations.

8.0 ACKNOWLEDGEMENT

We would like to thank The National Research Council, Department of Mechanical Engineering for sponsorship in publishing this work. In addition, we acknowledge the support of the individuals and organizations contributing to the design and tests conducted, specifically the Canadian Forces Project Officers, the Aerospace Engineering Test Establishment, the staff of the National Research Council Ice Rig facility, and the staff of the Standard Aero Engine Test Cell.

9.0 REFERENCES

1. AETE PROJECT REPORT 85/52, "CH113/113A Helicopter Engine Inlet Ice FOD Screens", 17 NOV 1987.
2. AETE PROJECT REPORT 79/55, Leigh MK 12A Ice Detector Trials on CH113A Helicopter, Cold Lake, Alberta, 22 Dec 1980.
3. Vincent J. Shaefer, John A. Day. A Field Guide to the Atmosphere 1981.
4. FAR 25 Airworthiness Standards, Appendix C, 1974.
5. X. De la Servette and P. Cabrit. Helicopter Air Intake Protection Systems, AGARD Lecture Series 148 1986.
6. J. Ballard, Impact of IPS and IRS configurations on engine installation design, AGARD Lecture Series 148 1986.
7. CFTO C-12-113-000/MB-000 Aircraft Operating Instructions CH113/113A. 1987-08-31.
8. E.L. HOUGHTON AND A.G. BROCK, Aerodynamics for Engineering Students, 1960.
9. BOEING ARNPRIOR ENGINEERING REPORT DE-89-091 Rev. B, Aerodynamic Report 27 Jun 1990.
10. BOEING ARNPRIOR ENGINEERING REPORT DE-89-025, "STRESS REPORT", 27 FEB 1989.
11. AETE PROJECT REPORT 87/30, "CH113/113A ENGINE INLET ICE FOD SCREEN FOLLOW-ON TESTING", 9 AUG 1988.
12. AGARD-AR-223, Advisory Report, Rotorcraft Icing- Progress and Potential, Sept 1986.
13. FAA Advisory Circular No. 29-02 Change, Certification for Transport Category of Rotorcraft, May 1985.

Discussion

1. H. Saravanamuttoo, Carleton University

Was this system designed to allow flight in known icing conditions or to permit continued flight if unexpected icing was encountered?

Author:

The system was designed and tested to permit continued flight if icing is encountered in flight and no attempt was made to certify the helicopter for deliberate flight into icing. Essentially this is a get out of trouble capability. There may be a next stage in the project for continued icing certification together with the re-introduction of blade de-icing.

2. W. Grabe, NRC Ottawa

Anti-icing screens have been around for a long time, e.g. Sikorski gave a paper on it at a NAPTC conference some 20 years ago. What is different about this screen? How is its design special?

Author:

Yes, there are other good screens in service: the sister tandem rotor helicopter the Chinook has externally mounted engines and conical screens with a removable bypass screen which is effective in icing and is a good "fod" screen. The design in this paper is special only because of its geometrical shape which was developed to be ice-tolerant and the concept originated from studies 20 years ago. The side bypass and the cutback on the cone sides produce the unique multi-mode operation for cruise and hover.

COLD STARTING SMALL GAS TURBINES — AN OVERVIEW (Démarrage Temps Froid des Petites Turbines à Gaz)

by

C. Rodgers
Chief Concept Design
Sundstrand Power Systems
4400 Ruffin Road
San Diego, California 92123
United States

ABSTRACT

The requirements to operate aircraft gas turbines over a large range of environmental conditions prove particularly demanding to the systems designer, especially when rapid starting of a cold engine is stipulated at sub-zero ambient temperatures. As a consequence the occurrence of cold climatic extremes are discussed and a trend is observed toward designing aircraft for specific areas and deployment, rather than worldwide usage.

Cold engine cranking torque characteristics are basically controlled by the lubricant viscous drag in the mechanical drive train and accessories. To further complicate matters, this viscous drag is dependent upon the magnitude of the applied start torque. Either actual viscous drag test data or realistic methods of predicting engine cold cranking torque levels with high lubricant viscosity may be required before definitive starter specifications can be issued. Experience with start systems for small gas turbine Auxiliary Power Units (APU's) has shown that the total weight required for successful rapid starting at -54°F can approach the weight of the APU powerhead itself. As a consequence, most cold start requirements are relaxed to -40°C or higher.

Briefly addressed, but of critical importance, is the role of the combustion designer who provides a key input in designing and developing a combustor capable of rapid consistent light-off over a wide operating range at the earliest possible speed, thereby permitting the transition from negative (cranking) to positive engine assist during start.

Methods of reducing APU viscous drag and start energy requirements that deserve future study are the all electric gearbox-less APU, and the possibility of a self-start pulse combustor concept.

ABREGE

Les demandes d'utilisation des turbines d'avion dans une gamme étendue de conditions d'environnement s'avèrent de plus en plus exigeantes pour le concepteur des systèmes; ceci est spécialement le cas du démarrage rapide d'un moteur froid par températures très basses. La probabilité de rencontrer des conditions très froides doit être discutée, on observe une tendance à concevoir des avions pour des régions spécifiques et des conditions particulières, plutôt que pour une utilisation universelle.

Les couples caractéristiques d'entraînement d'un moteur froid dépendent essentiellement de la trainée visqueuse de l'huile dans les boîtes d'entraînement et les boîtes accessoires. La question se complique un peu du fait que la trainée visqueuse dépend de la grandeur du couple de démarrage appliqué. Avant d'écrire les spécifications définitives du démarreur, il faut soit des résultats d'essai mesurant la trainée visqueuse réelle, soit des méthodes réalistes de prévision des couples d'entraînement du moteur froid. L'expérience a montré que pour le démarrage de petits APV, la masse totale nécessaire pour réussir un démarrage à -54°C pouvait approcher la masse du générateur de puissance lui-même. En conséquence, la plupart des exigences de démarrage temps froid se limitent à des températures supérieures ou égales à -40°C .

Nous mentionnerons brièvement mais en soulignant son importance le rôle du concepteur du système de combustion; celui-ci apporte une contribution décisive en concevant et développant une chambre de combustion capable d'allumage rapides dans un domaine d'utilisation très étendu, à des vitesses de rotation les plus basses possible; ceci permet de passer rapidement d'un couple résistif à un couple moteur pendant le démarrage. Parmi celles qui méritent des études plus approfondies, les solutions permettant de réduire la trainée visqueuse d'un APU et les besoins en énergie électrique sont l'APU tout-électrique sans boîte d'entraînement et le concept possible d'une turbine à volume quasi-constant.

NOMENCLATURE

Area	Reference Area
AMAD	Aircraft Mounted Accessory Drive
ATS	Air Turbine Starter
ATSM	Air Turbine Starter Motor
APU	Auxiliary Power Unit
D	Diameter
ECS	Environmental Control System
EGT	Exhaust Gas Temperature
EPU	Emergency Power Unit
F	Axial Load
JFS	Jet Fuel Starter
JP	Jet Petroleum
HP	Horsepower
I_p	Polar Moment of Inertia
KPa	Kilo Pascal
M.E.	Main Engine
N	Rotational Speed
PASS	Pneumatic Air Start System
P	Pressure
Q	Oil Flow
SLS	Sea Level Standard
TIT	Turbine Inlet Temperature
T	Torque
VSCF	Variable Speed Constant Frequency
VLSI	Very Large Scale Integration
U	Tip Speed
V_{ref}	Combustor Reference Velocity
W	AIRFLOW
V_o	Isentropic Spouting Velocity
μ	Viscosity
ρ	Density

SUBSCRIPTS

b Burner

1.0 Introduction

Cold weather and cold environmental starting of aircraft main propulsion engines represents a significant design burden for self-sufficient fighter aircraft operation from unimproved forward bases. Although military and commercial aircraft typically operate from permanent bases with both personnel and equipment preheating capabilities, emergency in-flight power outage may require start up of the aircraft secondary power system after extensive soaking at -57°C conditions.

The many elements of the start system and the synergistic effect of cold weather are often difficult to accurately predict. A conservative cold start analysis may present an unpalatable system weight penalty. A more palatable analysis can mature to prove disastrous when into the final qualification stage. In retrospect, lessons learned would deem improved definition of the synergistic effects of fuel and lubricant viscosity effects, thermal soaking, and transient performance during preliminary design. It is the intent of this presentation to briefly expose most of the known pitfalls in cold weather starting, such that the designer is provoked and appreciative of the task involved.

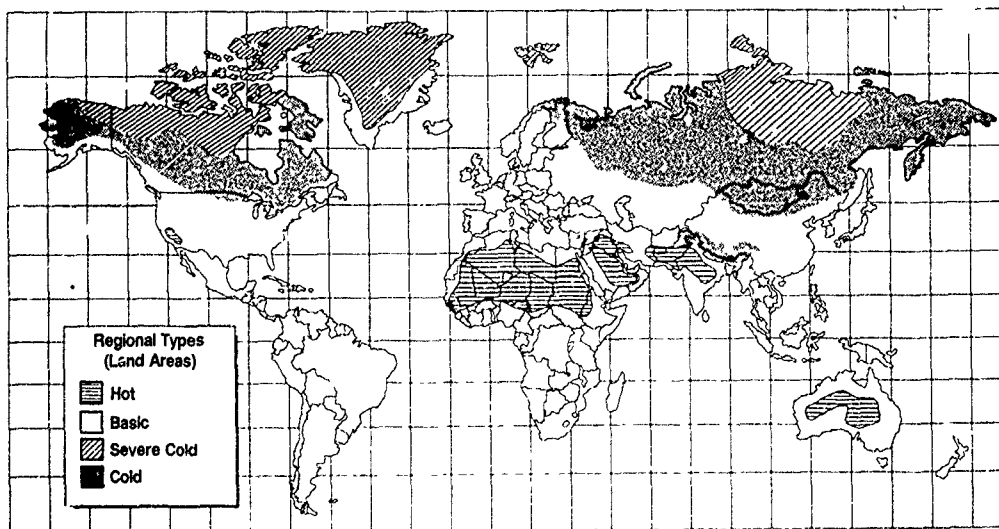
In preparation for addressing the cold weather problem, a review of climatic weather extremes and previous cold start technology is presented.

2.0 Cold Weather Extremes

The design of cold weather start systems for aircraft gas turbines is critically dependent upon the design specification, specifically, the low temperature extreme soak condition. Low temperature extremes for worldwide usage (excluding the air, land and ice shelf areas south of 60° degrees) are shown on Figure 1, and set forth in MIL-STD-210B and in the revised updated version MIL-STD-210C. Both standards do not give definite limits, but they offer design criteria and starting points for engineering analyses to determine design criteria.

The detailed requirement values used in MIL-STD-210B represent risk values. It would often be cost prohibitive and/or technologically impossible to design military equipment to operate anywhere in the world under the most extreme environmental stresses for all but a certain small percent of the time. The design criteria for operations in MIL-STD-210B are based where possible, on hourly data from the most extreme month and area in the world. From hourly data it is possible to determine the total number of hours a given value of a climatic element is equaled or surpassed. If a value of a climatic extreme occurs (or is surpassed) in about 7 hourly observations in the 7:4 hour observations of a 31-day month, then this value occurs roughly 1 percent of the time. The risk values pertaining to low temperature are as follows:

Low Temperature Risk Values					
Risk Value	1%	10%	12%	50%	?
Temperature ($^{\circ}\text{C}$)	-61	-54	-51	-46	-40



LPP00032-1

Figure 1. Climatic Extremes

The one percent extreme is used as the design criteria for all climatic elements except low temperature and rainfall rate. The 20 percent extreme is used for low temperature.

NATO has adopted a Standard Agreement which covers climatic environmental conditions affecting the design of material for use by NATO forces operating in a ground role. This document, STANAG No. 2831, is similar to MIL-STD-210C.

Five categories pertain to cold weather and are listed in the following table. Where a range of temperature is given, it reflects the high and low temperatures during a 24-hour period in which the severe temperature occurs. These values are for operational conditions corresponding to the values given in MIL-STD-210C which serve as starting points for engineering analyses.

The five locations of these climatic categories are:

- Mild Cold - Areas which experience mildly low temperatures such as the coastal areas of Western Europe under prevailing maritime influence, Southeast Australia and the Lowlands of New Zealand.
- Intermediate Cold - Areas which experience moderately low temperatures such as Central Europe including South Scandinavia, Japan and South Eastern Canada
- Cold - Colder areas which include Northern Norway, Prairie Provinces of Canada, Tibet and parts of Siberia but excludes those areas detailed in the two colder categories
- Severe Cold - The coldest areas of the North American Continent.
- Extreme Cold - The coldest areas of Greenland and Siberia

The values listed in STANAG 2831 represent the air temperature, which, on average, was attained or exceeded for all but approximately 1 percent of a month during the coldest month of the year.

A detailed evaluation of MIL-STD-210B, -210C and STANAG 2831, plus cold weather starting specification requirements for USAF aircraft was made in Reference 1.

The A-10, F-15 and F-16 aircraft are all qualified to -40°C. The minimum ground operation temperature specifications for the C-17 and the B-1B are -40°C and -34°C respectively. The

F-15 was most likely the first aircraft to be qualified at -40°C. Many of the justifications used to relax the cold temperature requirement for the F-15 pertain to most or all of the other aircraft as well.

The feasibility of starting an aircraft at -51°C was considered poor using the technology available and the expense required to obtain -51°C capability was considered unrealistic. Batteries were considered to be unacceptable for use below zero degrees. Hydraulic start systems were also limited in cold weather due to poor viscosity characteristics and while increased volume would provide the necessary energy, the weight penalty was unacceptable. Lack of full human functionality at -40°C and lower was used as justification, and the standard itself was often deemed to be unrealistic.

The results of the Reference 1 survey are summarized as follows:

1. MIL-STD-210B is an interpretable document which offers guidelines that allow significant deviance from the intended design criteria.
2. MIL-STD-210C will make no attempt at setting any design criteria
3. The U.S. Air Force sets cold weather requirements on a system-by-system basis.
4. Start systems appear to be a limiting factor with cost and space/weight penalties being main drivers. Start system technology has not kept pace with other areas.
5. The designing trend leans toward aircraft for use in specific areas rather than for use worldwide.

It was emphasized that MIL-STD-210 was an attempt to apply the lessons learned in World War II to future aircraft designs. Future systems must not be designed for the conditions they experience in peacetime, but for the conditions that they may encounter in the advent of war.

3.0 Review Of Previous Start Technology

Extensive design data and design techniques for aircraft gas turbine engine start systems have been published by the Society of Automotive Engineers (SAE) Starter Committee AE6, most notable of which are listed in References 2 through 8. The SAE Starter committee was first formed in 1962, and meets biannually to formulate standards for aircraft engine starting systems.

Cold Temperature Extremes for NATO Operational Conditions			
Category		Temperature	Lowest Recorded Temperature
Mild Cold	°C	-6 to -19	-24
Intermediate Cold	°C	-21 to -31	-42
Cold	°C	-37 to -46	-56
Severe Cold	°C	Constant -51	---
Extreme Cold	°C	Constant -57	-71

References 9 and 10, Starting Systems Technology, SAE special publications SP 598 1984, and SP 678 1986 provide latest design data for most aircraft start system components, including gas turbine auxiliary power units, emergency power units (EPUs), air turbine starters (ATS), and air turbine starter motors (ATSM), and hydraulic and electric starters.

The author and his affiliation (References 11 - 16) have devoted efforts toward the optimization of the start systems for both prime propulsion engines and small auxiliary power units. Previous start papers published by the author are found in References 11 - 16, and were motivated by a primary goal to improve start system reliability, particularly for self-sufficient jet fuel starters (JFS), which may provide the only means of aircraft dispatch.

4.0 Starting Methods

A frequently used method of starting aircraft prime propulsion gas turbine engines is by means of a small auxiliary power unit providing compressed (bleed) air to an accessory drive gearbox-mounted air turbine starter. This APU may be carried on-board or mounted externally on ground support equipment. The majority of these APU's deliver a bleed pressure ratio of approximately 4.0 at standard day conditions, as constrained by oil auto-ignition temperature limits no higher than 250°C for mostly commercial aircraft applications. The general effects of ambient temperature and altitude on small gas turbine performance at rated conditions are shown in Figure 2. The basic power lapse rate towards lower power on hot days is dictated by the decrease of cycle efficiency with turbine inlet temperature (T.I.T.) to ambient temperature ratio, air density with hot days decreasing output power, and cold days increasing output power. The temperature and altitude lapse rates shown are typical of single-shaft APU's with centrifugal compressors operating at rated TIT and constant rotational speed. Slightly different hot day power lapse rates may be exhibited with variable speed operation. Note that the power lapse rate change with ambient temperature may be approximated by

$$\frac{HP}{HP_{SLS}} \propto \left(\frac{T_{SLS}}{T} \right)^2$$

It is observed in Figure 2 that rated output power decreases about 30 percent from SL 15°C to SL 52°C conditions. Normally APU's are sized to meet full aircraft secondary power requirements at critical hot day conditions, and are therefore capable of delivering excess power at cooler ambient temperatures, as dependent upon load change with ambient temperature. Usually, 90 percent of APU operating time is spent at ambient temperatures below 35°C and therefore exposure to maximum TIT's may be limited.

Six common methods of starting aircraft prime propulsion gas turbine engines shown in Figure 3 are:

1. Mechanical Link - With small gas turbine jet starters of the two-shaft power turbine or single-shaft with torque converter configuration, (Figure 4)

2. Pneumatic Link - With small integral bleed or load compressor auxiliary power units (Figure 5), either mounted on-board, or from external ground carts.
3. Electrical - From aircraft batteries, on-board APU, or ground power supplies.
4. Hydraulic - From on-board APU or ground hydraulic cart.
5. Windmill - With possible assist from APU.
6. Cartridge - Solid propellant breech firing into the high temperature air turbine starter or direct rotor impingement

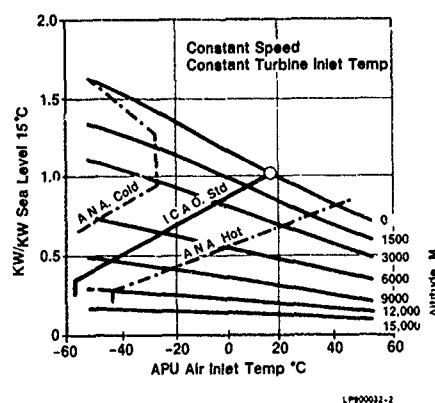


Figure 2. Typical Power Lapse Rate Single Shaft Radial Gas Turbine

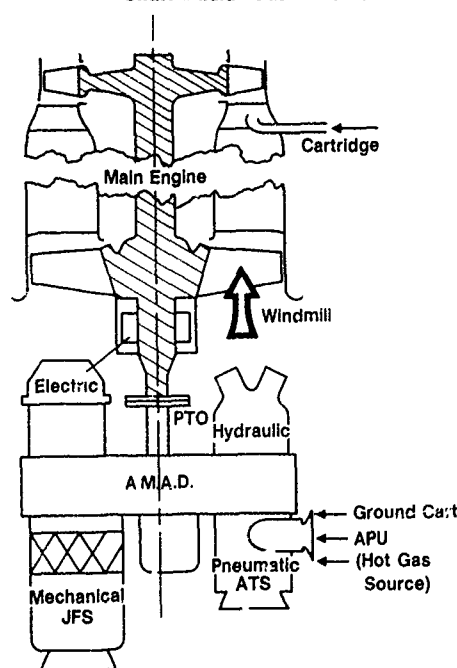
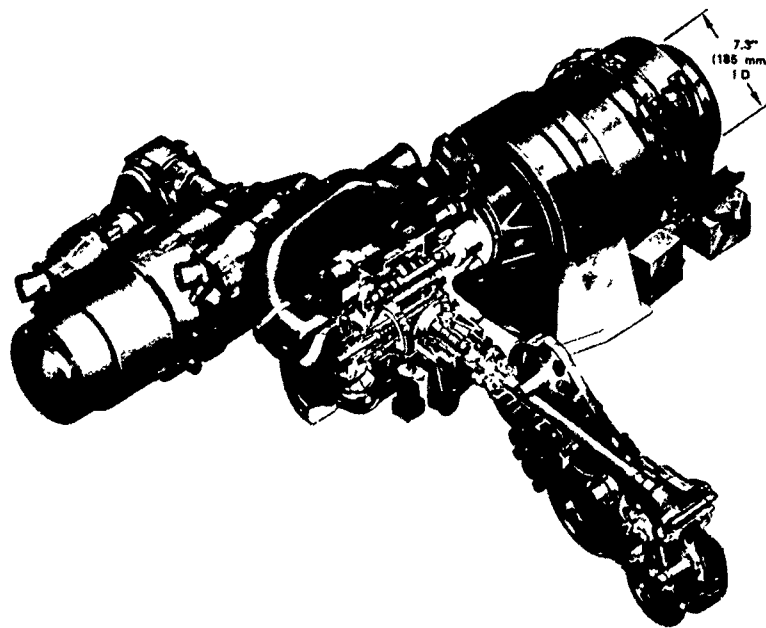
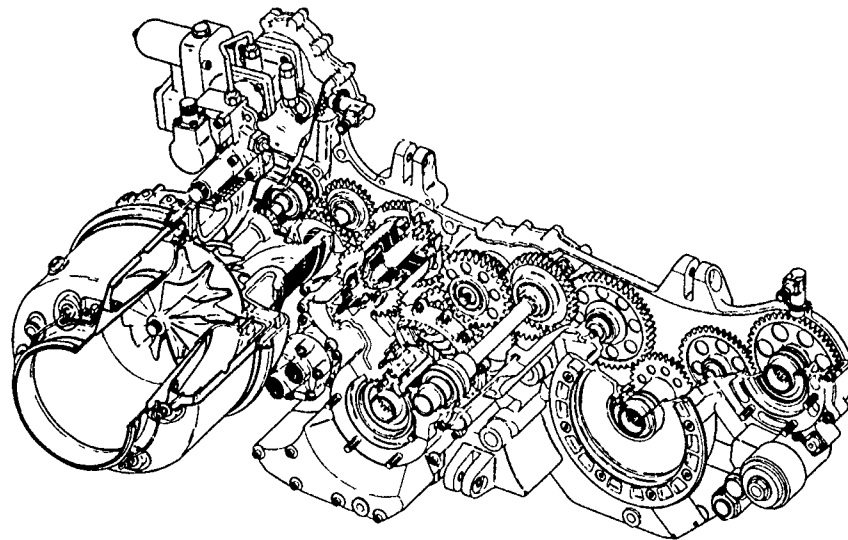
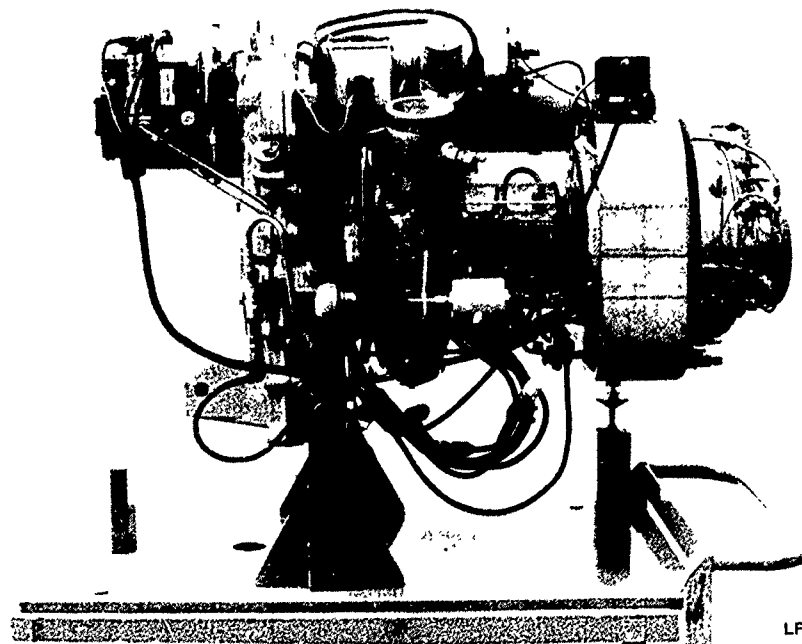
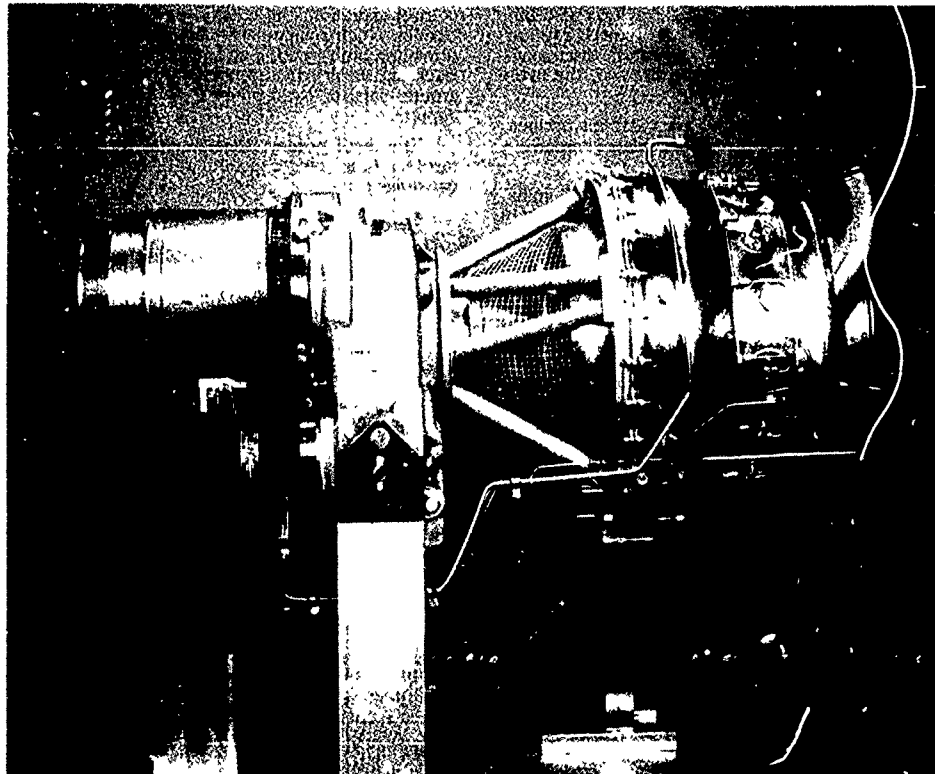


Figure 3. Engine Start Methods



LP900032-4

Figure 4. Jet Fuel Starters



LP900032-5

Figure 5. Pneumatic APUs

Since each of these start methods may also be applied in turn to start the on-board APU, caution is advised during start system integration discussions to clarify which starter is being addressed, the main engine, or the APU.

A summary of the various start systems options is listed in Table 1 and a more detailed comparison can be found in Reference 17.

Start system survey data for selected U.S. military aircraft and helicopter is shown in Table 2 which identifies the aircraft, main engine, on-board APU or JFS, and APU/JFS start mode. Examination of Table 2 data indicates the dominance of hydraulic start option. Since hydraulics are usually routed throughout the aircraft for flight

control actuation, the energy source is convenient, besides which accumulators can serve dual roles in providing both braking and back-up start assist. Back-up starting is also possible using a hydraulic ground cart, or hand pump for medium place helicopters.

The three primary start systems for small gas turbines (excluding expendable turbojets which use cartridges) are:

- Hydraulic
- Pneumatic
- Electric

Table 1. Summary Comparison of Secondary Power System Design Approaches		
SYSTEM TYPE AND USAGE	ADVANTAGES	DISADVANTAGES
Pneumatic Link. Large Commercial Aircraft EFA ATF B1 B2 •	<ul style="list-style-type: none"> • APU can be remotely located for flexibility in installation location and environment • Similar ECS airflow requirements • System is compatible for ground cart backup main engine starting 	<ul style="list-style-type: none"> • Low system efficiency, resulting in relatively large APU power rating required • Pressure ratio limited by bleed air temperature auto-ignition hazard
Mechanical Link. F-15 F-16	<ul style="list-style-type: none"> • High system efficiency results in relatively low APU power rating required • Power turbine or torque converter provides high stall torque 	<ul style="list-style-type: none"> • Requires close APU coupling to main engines • Significant penalty for backup main engine start capability • Mechanical coupling equipment and controls tends to be complex • Incompatible with ECS
Electric Link.	<ul style="list-style-type: none"> • APU can be remotely located for flexibility in installation location and environment • Offers increased system integration capability and simplification with all electric aircraft 	<ul style="list-style-type: none"> • Relatively high-power starter/generator technology not demonstrated • No backup main engine starting from standard ground carts • Incompatible with ECS
Hydraulic Link. Most Helicopters	<ul style="list-style-type: none"> • APU can be remotely located for flexibility in installation location and environment 	<ul style="list-style-type: none"> • Power transfer hydraulic system tends to be complex • Backup starting from ground carts is difficult since aircraft hydraulic system must be penetrated • Incompatible with ECS
Windmill	<ul style="list-style-type: none"> • Possible with clean inlet and exhaust installation 	<ul style="list-style-type: none"> • Limited operating envelope • Slow acceleration
Cartridge	<ul style="list-style-type: none"> • High power density 	<ul style="list-style-type: none"> • Poor start reliability under cold conditions • Excessive smoke logistics • Fail to fire breech danger

Table 2. Starting Data - U. S. Military Aircraft

AIRCRAFT	F-15	F-16	F-18	B-1	KC-135	C-141	Black Hawk	AH-64
Main Engine Model	F-100	F-100	GE404	F-100	CFM56	TF33	T700	T700
Ip lb.ft.sec ²	3.2	3.2	2.65	5.92	5.92	8.9	0.11	0.11
Core N krpm	13.5	13.5	14.5	14.5	14.5	9.0	43	43
IpN ² X10 ⁻⁶	583	583	557	1244	1244	720	203	203
APU								
			GTCP	GTCP		GTCP		GTCP
Model	JFS190	T62JFS	36-200	165-9	T40LC	85-106	T40	36-150
Ip lb ft sec ²	0054	.0032	0071	022	0045	.026	0031	.0068
N krpm	65	61.6	62	38.0	64.3	41	61.6	62
IpN ² X10 ⁻⁶	22.8	12.1	27.3	31.8	18.6	75.6	11.8	26.1
Approx Weight lb	100	84	160	230	190	320	96	100
APU START SYSTEM								
Type	Hydraulic	Hydraulic	Hydraulic	Hydraulic	Hydraulic	Hydraulic	Hydraulic	Hydraulic
Weight lb	75	47	51	110	63	119	56	46
Low Temp °C	-40°C	-40°C	-40°C	-29°C	-40°C	0	-40°C	-32°C
Starter Displacement in ³ /rev	0.3	0.42	0.37	0.60	0.65	0.37	0.68	0.365
Accumulator Volume in ³	2x2.5	2x200	290	1200	500	2x400	200	299
Approx System Weight lb	75	50	51	110	61	119	62	40

4.1 APU Hydraulic Start

Until recently, most quick start military gas turbine APU installations used hydraulic start systems, as opposed to electric systems. The reasons stemmed from compatibility with the aircraft hydraulic system, and cold weather starting. Electrical systems usually require battery electrolyte heating at temperatures below -28°C , but can be started at lower temperatures with battery shorting, if time is not critical. Hydraulic start systems are mainly in use for sub-Arctic environments, but nevertheless, are also prone to increasing fluid viscosity pressure drops effects, and thus reduced starter output torque. Hydraulic start system sizing for -54°C conditions, in particular, require large hydraulic accumulator volumes and therefore penalize aircraft gross take-off weight. As with batteries, APU preheating may be necessary.

The effect of soaked temperature conditions on the performance of a typical hydraulic starter using MIL-H-83232 fluid is shown in Figure 6. For temperatures less than -40°C the use of MIL-H-5606 fluid is recommended.

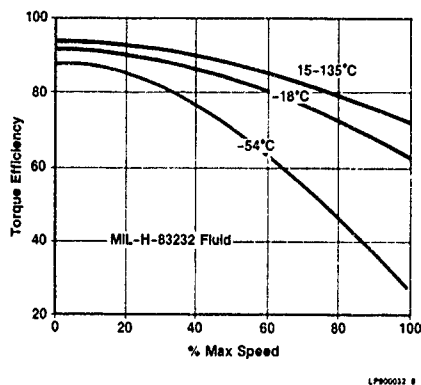


Figure 6. Typical Hydraulic Starter Performance

4.2 APU Pneumatic Start

High pressure pneumatic air start systems (PASS) (see Reference 17 and 18) are being proposed and used to circumvent the low temperature problems of the electric and hydraulic approaches. Stored air in high pressure bottles is expanded across an air motor attached to the APU gearbox or directly impinged on the turbine rotor. Current system pressure levels are 1,000 psig, with higher levels, 4,000 psig, being considered to reduce storage volume. Further air storage volume reduction is possible with development of small high pressure fuel rich air/JP combustors capable of heating the cold expanding air (sometimes at -73°C or lower) to 900°C . The cryogenic temperatures experienced with PASS components and prolonged high pressure recharge compressor times offer challenges to match the high start reliability standards of hydraulic starters.

4.3 APU Electric Start

Increased avionics, electrical systems, and power levels has created renewed interest in the full electrical aircraft. Advanced VSCF type generators, capable of operation as starters are being studied for both large prime propulsion and APU gas turbines. Switched reluctance starter-generators have also been identified as a potential future technology approach. These starter-generators generally operate at 150 percent of rated power during a start to meet the engine start torque requirements, and may also require a dual ratio gearbox. None of them have yet demonstrated satisfactory starts in an actual aircraft. Battery charge considerations under cold weather conditions as typified in Figure 7 is a fundamental constraint. Reference 19 describes a battery shorting technique used to make successful -54°C start with a small gas turbine. The engine ECU incorporated a "WINTER" mode which initiated a pre-program in the microprocessor to periodically connect and disconnect the battery from the starter windings in accordance with a programmed sequence of on/off cycles, causing the battery to be warmed internally from its own cell resistance

5.0 Engine Starting Characteristics

It is difficult to estimate with any reasonable accuracy the starting characteristics of small gas turbines because of the synergistic nature of the problem. Engine starting characteristics are influenced (among other intangibles) by:

- Temperature and altitude
- Initial engine design selection
- Engine performance
- Engine fuel control scheduling
- Mechanical features and associated viscous drag
- Acceleration rate
- Starter selection and torque characteristics

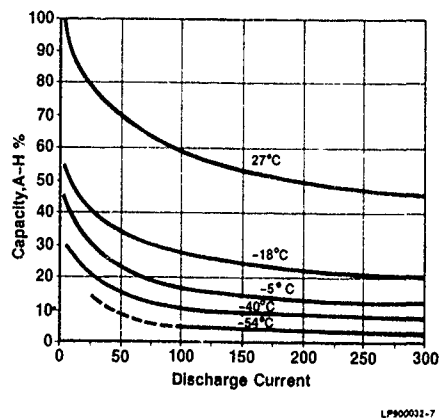
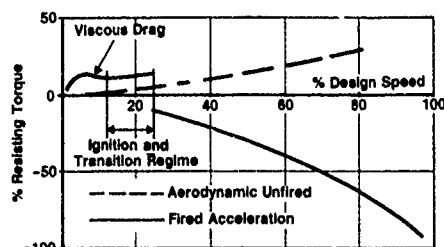


Figure 7. Typical Battery Characteristics

Due to the complex interrelation of these factors, engine starting characteristics are realistically only obtained by actual test under controlled conditions with a specific start system. Although extrapolation of these characteristics to other operating conditions and start systems without actual test is not recommended, it is often necessary.

The three major torques during engine acceleration shown in Figure 8 are:

- Unfired cranking torque
- Viscous torque
- Fired torque



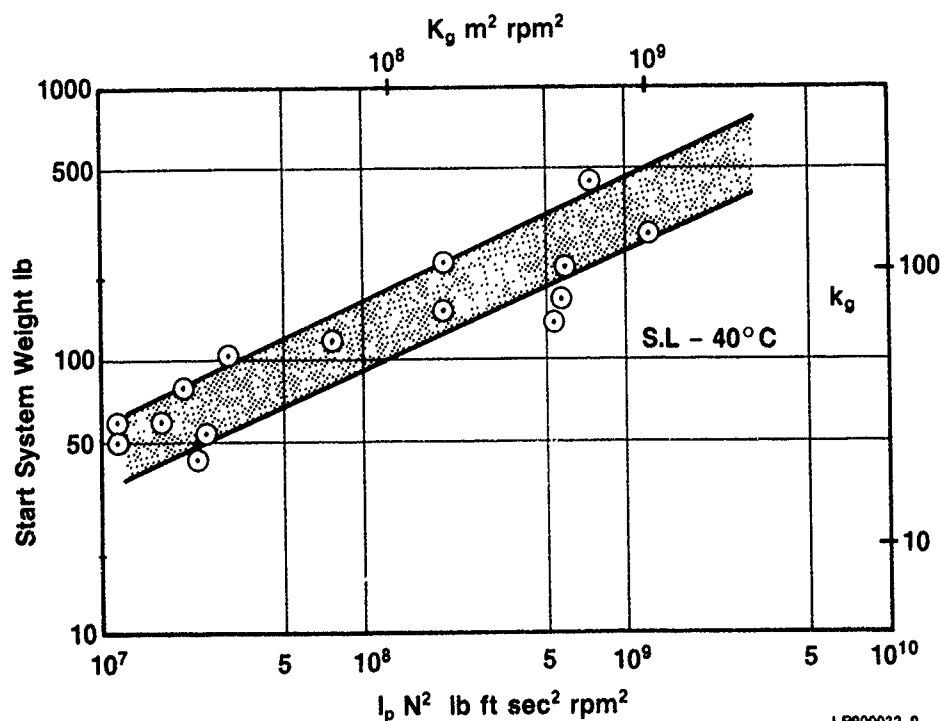
L-908622-8

Figure 8. Idealized Engine Torque Characteristics

During the initial start phase (below approximately 20 percent design speed), the aerodynamic and viscous drags at normal ambient temperatures may be relatively small in relation to the basic starter applied torque. In such cases, the starter applied torque is approximately equal to the basic flywheel acceleration torque as determined from the rotating assembly inertia and acceleration.

Under these conditions, examination of several small gas turbines with different start systems has shown that the starting difficulty (or amount of starting energy required) can be correlated with the product of the rotating assembly polar moment of inertia and the square of the rotational speed, $I_p N^2$.

Since the start system weight is a function of the stored starting energy, general trends have been established for start system weight as a function of $I_p N^2$ as shown in Figure 9. These trends are useful in early engine design to indicate the potential effect of compressor and turbine geometry and design speed upon start system weight for equal start times at normal ambient conditions. Both APU and main engine (core) $I_p N^2$, data are shown on Figure 9 for a wider correlation base of gas turbine engine types. The use of the core inertia and speed is a fundamental correlating parameter for turbofans, particularly with the trend to higher bypass ratios and three spool configurations.



LP800232 2

Figure 9. Start System Weight Correlation

A review of the hypothetical starting times for a typical main propulsion engine using a pneumatic link start system comprising a small APU, ducting, and air turbine starter was described in Reference 15, where relative sea level start times for the idealized case with only aerodynamic and no viscous drag effects considered showed.

Ambient °C	Relative Time %
15	100
34	130
-54	63

The longer main engine start time for the SL 130°F is typical of pneumatic link systems, and consequently often sized the APU. The computed reduced start time at -54°C is purely hypothetical and contrary to normal sub-zero trends, where viscous drag becomes dominant and causes relative start time to increase substantially above that of SL 15°C. These start times reflect the basic power lapse rate of the smaller gas turbine APU with output power increasing significantly at lower ambient temperatures. Both the main engine and APU, are, however, impacted adversely by cold weather drag effects.

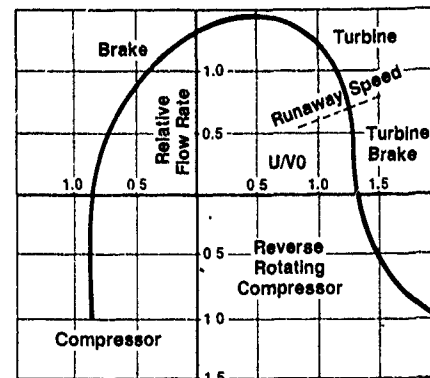
At -54°C ambient conditions, hydraulic start systems weight for small APUs may approach that of the APU power plant itself, forcing the APU designer to scrutinize all possible sources of reducing rotor inertias. Such scrutiny is common practice in turbocharger design, for example, where fast accelerations are required for response and smoke abatement. Rotor blade number and disk configurations are whittled to the minimum necessary for structural integrity at design or overspeed conditions. The APU engine turbine blade number tradeoff is extremely weight effective, and turbine efficiencies of up to three percentage points may be sacrificed for non-continuous duty operation.

5.1 Unfired Cranking

Engine performance behavior during the initial cranking phase, prior to light off, are often predicted using steady state compressor, combustor and turbine component characteristics, yet it is well known that the transient and steady-state component performances may be different. For example, the first start of a gas turbine normally requires a longer time than subsequent starts.

Difficulties encountered in computing low speed "unfired" cranking torque are:

- Accurate low speed characteristics definition of the compressor, combustor and turbine.
- Operation of the turbine near or beyond "runaway" conditions, as illustrated in Figure 10



LP00032-10

Figure 10. Four Quadrant Turbine Operations

Analysis of low speed unfired cranking torques for small gas turbine APUs indicates that the approximate magnitude of the net aerodynamic cranking torque conservatively relates to that of the torque required to drive the compressor (only). For fixed compressor geometry and zero bleed conditions this can be simply expressed as:

$$\text{Aerodynamic Cranking Torque} \approx \frac{\text{Compressor Design HP} \times 5250}{\text{Design Speed rpm}} \left(\frac{\% \text{ Design } N}{100} \right)^2$$

In effect, this presumes the turbine operates near runaway conditions producing no expansion torque and requiring minimal input.

Aerodynamic cranking torque, is best determined from actual torque measurements, but may be derived from APU speed deceleration traces after a cold unfired starter crank.

5.2 Viscous Drag

The mechanical features of the engine starter drive train and support bearings are possibly the most dominant single factor controlling cranking at sub-zero ambient temperatures. Inadequate clearances and dissimilar metal contraction rates have been known for example to cause interference binding preventing starting. High oil viscosity throughout the train and bearings increases drag torque by an order of magnitude. Parasitic losses in the oil and fuel pumps increase also with the change in viscosity.

At normal ambient temperatures, the mechanical losses in the drive train, bearings, and accessories are on the order of 1 to 4 percent of the design power rating dependent upon train reduction ratio, type, number of bearings, and accessories. Additional parasitic losses may stem from engine driven equipment such as cooling fans, generators and hydraulic pumps. Miniature gas turbines (less than 20 hp) tend to exhibit higher mechanical losses on the order of one-tenth of rated power, since it is not always cost effective to scale engine driven accessories, especially when ultra high rotational speeds are employed.

High speed rolling element bearing losses for small gas turbines can be estimated using the data of Reference 20 approximated to give:

$$\text{HP loss/bearing} = 0.20 (\mu Q)^{0.2}$$

$$\left(\frac{DN}{10^6} \right)^2 + .0002D \left(\frac{N}{10^6} \right)^{0.5} F$$

Where the bearing bore, diameter D is given in mm, and the viscosity μ is in centistokes. For light axial loads the power loss is dominated by viscous shearing, and with typical "DN" values of 2×10^6 , can be further approximated to yield:

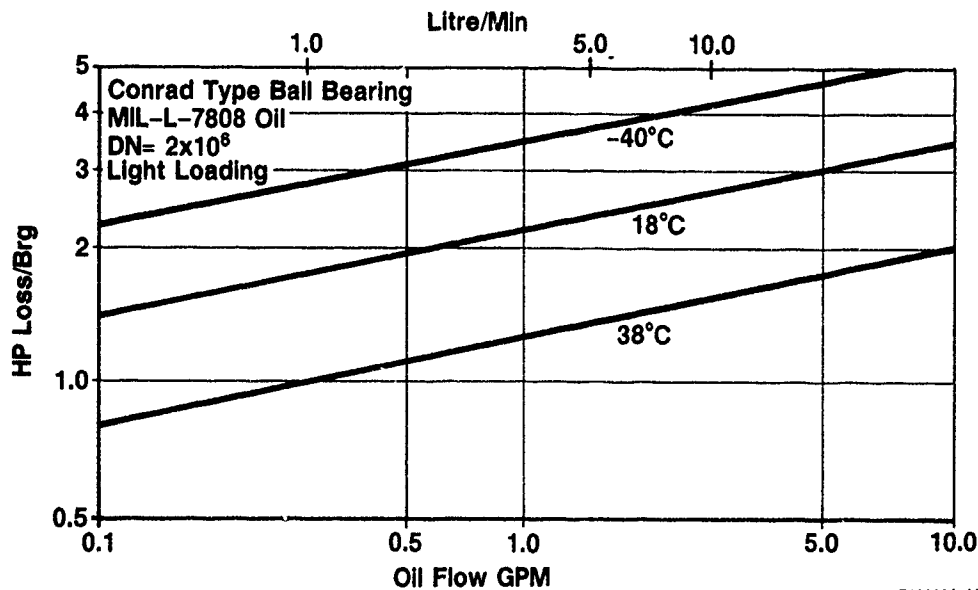
$$\text{HP loss/bearing} = 0.80 (\mu Q)^{0.2}$$

This relationship is shown plotted on Figure 11.

During preliminary engine design, a mechanical design configuration is selected after many design iterations to best compromise all the design criteria and constraints. The creative designer will generate an efficient design in which mechanical losses are minimized to avoid impacting such factors as cost, performance and oil cooler requirements. Although these mechanical losses at normal ambient temperatures and design speed may be small (2-5 percent) and seemingly negligible relative to the aerodynamic drag, oil viscous shearing at start initiation results in larger mechanical than aerodynamic drag.

The T-47 gas turbine APU (Figure 5) gearbox was subjected to extensive cold crank tests during initial development. The effect of oil sump temperature on its cranking torque at 15 percent speed is shown in Figure 12.

The cranking torque ratio shown is that composing mechanical drag from the starter drive train via the main reduction gear bearings, accessories, and aerodynamic drag. Total mechanical losses at design speed for this engine were approximately four percent of the total engine output. Light aircraft type oils, MIL-7808 and MIL-23699 were used but nevertheless cranking torque increased by a factor of 4.0 at -54°C with higher oil viscosity. Cranking tests results with the gearbox deprived are also included and indicate up to a 20 percent reduction drag.



LP900032-11

Figure 11. Bearing Losses

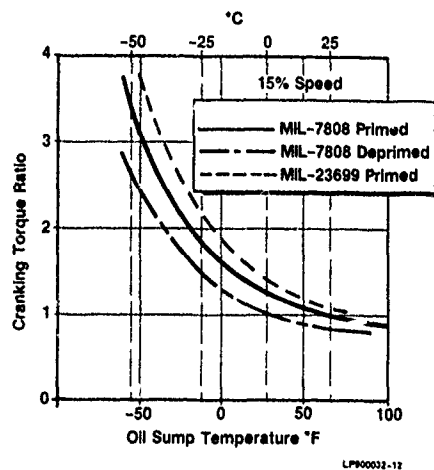


Figure 12. Effect of Oil Sump Temperature on Cranking Torque

Examination of the apparent oil viscosity variation (based on ambient temperature) and the increase in cranking torque indicated a relationship similar to that presented in Reference 21 based upon cold starting of diesel and automotive engines where:

$$\frac{\text{Cranking Torque}}{\text{Cranking Torque Reference}} \propto \left(\frac{\mu}{\mu_{\text{ref}}} \right)^n$$

The reference conditions define the cranking torque and apparent oil viscosity at design ambient. The exponent n varies from 0.2 to 0.3. This relationship may be applied to project mechanical drag at sub-zero ambient conditions providing:

- Mechanical drag at the reference condition is known to be reasonably accurate by estimation or direct measurements.
- Aerodynamic torque is assumed negligible in the range of 0 to 15 percent speed.

In the event that a reference torque condition is unavailable, the representative breakaway torques (torque at zero speed) in Figure 13 may be used in a first cut start analysis. Higher breakaway torques at -54°C have been experienced resulting in stored energy start system weights that can approach the dry APU powerhead weight itself. The same APUs when employed as a starter for larger prime propulsion gas turbines are burdened with the incompatibility of starter torque output dependent upon the square of air density (Figure 2), yet main engine cranking torque is basically dependent upon lubricant viscosity. Fortunately, a main engine restart at altitude occurs with the lubricant already preheated. Altitude and sub-zero starting conditions, however, will continue to require excessively heavy start systems until viscous shear losses can be reduced by either.

- Applications of external starting torque direct to the high speed shaft itself, with uncoupling of all but necessary viscous parasitic shear sources.
- Advancement in applied tribology to reduce viscous shear effects in gas turbine accessory and main shaft components.

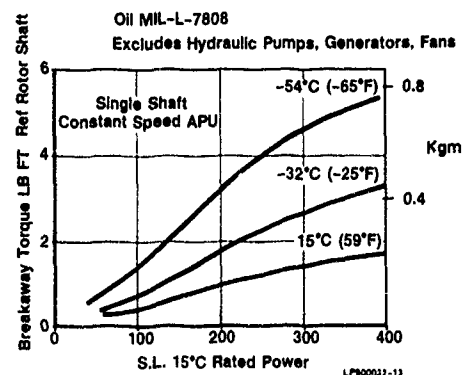


Figure 13. Typical APU Breakaway Torques

5.3 Fired Acceleration

The transition from unfired cranking torque resisting acceleration, to fired torque assisting acceleration, occurs upon ignition and combustor light off with fuel burn scheduled by the engine control unit (ECU). The synergistic starting effects culminate during this transition phase. With instantaneous thermal and fluid response this transition would hypothetically materialize by a vertical shift from unfired to fired torque levels at constant speed. In practice the transition takes a finite speed interval as dictated by the system response.

Thermal transient response effects become even more significant during fast accelerations. Substantial increases have been observed in transient fuel flow demands for small gas turbines at the author's affiliation, directly relating to heat losses to the "cold" castings and flame quenching effects on combustion efficiency. Heat exchanged gas turbine engines are notorious in this respect as the large mass of the heat exchanger acts as thermal reservoir absorbing heat during start and dissipating heat (with possible bearing soakback problems) on shutdown.

The phenomena of increased viscous drag with higher applied starter torque and faster accelerations is discussed in Reference 14. The effect is related to the increase in oil viscosity under high pressure shear rates.

Cold starting characteristics of a load compressor type APU are shown on Figure 14 at S.L. -40°C conditions, with 0.95 and 0.68 cu. in. hydraulic start motors. Acceleration fuel scheduling of the EGT topping type was the same for both. Increasing the start stall torque by approximately 50% (0.95 cu. in. motor) increases the initial engine resisting torque by a similar percentage. The increase of APU resisting torque with acceleration rate complicates start system optimization and starter selection and necessitates experimental determination of its magnitude. The EGT topping fuel schedule eventually produces the same APU assisting torque characteristics after acceleration past starter cut-out.

Small gas turbines are particularly sensitive to tip clearance effects since clearance gap to blade height ratios tend to be larger than those of larger gas turbines. In most instances, the minimum engine operating clearances are established by transient engine tests to determine limiting rub clearances gaps. Some tuning can be accomplished by matching thermal responses of the rotors and stationary shrouds and by appropriate material selection. Computation of engine transient performance using steady-state component performance characteristics does entail small errors due to the effect of transient clearance effects on both component efficiency and pressure flow characteristics.

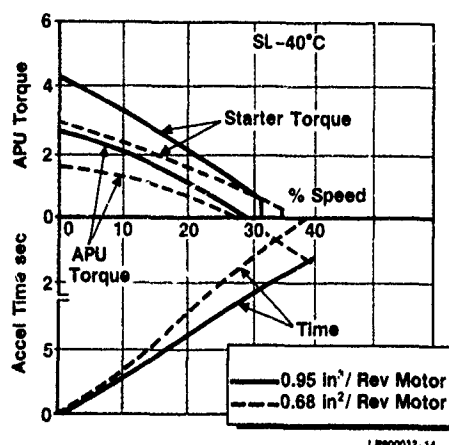


Figure 14. Effect of Higher Starter Torques

5.4 In-Flight APU Starting

In-flight starting of the APU after cold soak conditions is dependent upon:

- The inlet and exhaust duct pressure recovery or loss,
- Aircraft location of the inlet and exhaust,
- Gearbox breakaway torque after cold soak,
- Combustor characteristics under ram conditions.

The static pressure at the exhaust must never be greater than the static pressure at the inlet when a start is attempted since this can result in flame-back out of the APU inlet. Although high inlet ram recovery can increase APU power, it increases velocities through the combustor and may interfere with APU starts, which is discussed in the next section. Starting above the tropopause with low pressures and temperatures results in compressor operation at lower Reynolds numbers and higher relative Mach numbers which can reduce surge margin. Advanced ECU's are now capable of identifying surge and responding by re-metering the start fuel schedule to avoid surge confrontation.

6.0 Combustor Design Considerations

The previous effects are relatively small when compared with the transient behavior of the combustor. Transient combustor efficiencies as low as 20 percent have been experienced for small short reverse flow annular combustors on cold starts following ignition and light-off, as indicated on Figure 15.

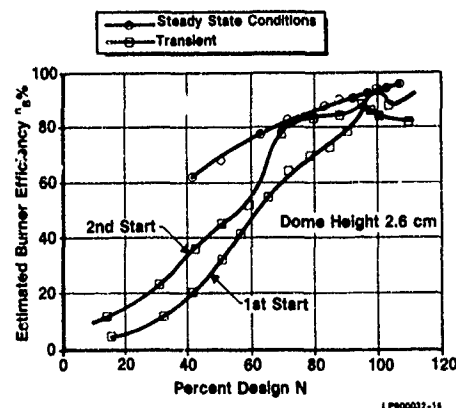


Figure 15. Transient Burner Efficiencies

Of primary importance to increasing engine acceleration assisting torque is early ignition and good fuel atomization, which affects the transition from engine resisting to positive acceleration torque characteristic. A major constraint for reliable early ignition under a wide range of operating conditions is in the design of the fuel injection (atomization) system.

All these transient effects can be simulated with sophisticated analytical models, but the acid test is start demonstration under exposed cold soak conditions.

The capability to fill the fuel manifold faster, combined with higher ignition spark rate, and improved start nozzle fuel atomization, is required to provide an earlier transition from unfired cranking to positive engine assist torque. Under Arctic conditions, high fuel viscosity and poor fuel atomization may cause a delayed light-off, which combined with higher viscous parasitic drag can result in an aborted or hung start.

Low combustor reference velocities and loadings are preferred for reliable ignition (especially at altitude), fuel air ratio stability limits, and low combustor pattern factors. Combustor reference velocity is defined as:

$$V_{ref} = W_b / (A_{ref} \cdot \rho)$$

where W_b = Combustor airflow
 A_{ref} = Combustor reference area
 ρ = Combustion gas density

The combustor reference area is typically calculated from the mean diameter and chamber dome height since most gas turbine combustors are of the reverse flow or axial through-flow types. Combustor maximum diameter becomes governed by the necessity to minimize frontal area compatible with that of the compressor and/or turbine. The only remaining "free" combustor sizing variables are usually dome height and length. Choice of length (volume) influences the combustor heat release rate and loading, which are additional important combustor design criteria.

$$\text{Combustor Loading} = W_b / \left[(P_b)^{1/8} \text{Vol} e^{T_b/540} \right]$$

Lower combustor reference velocities permit wider fuel/air ratio limits during start in the manner shown in Figure 16, and therefore tend to promote improved fuel atomization and blow out limits under high altitude operation.

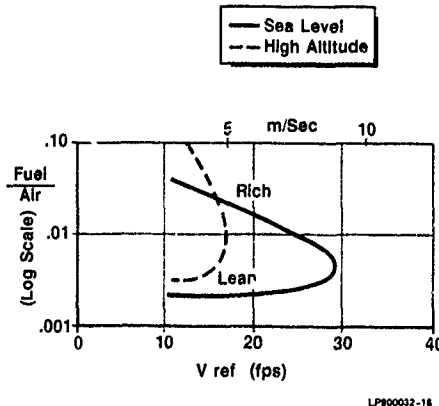


Figure 16. Typical Small Burner Ignition Limits

The typical effect of engine speed and flight Mach number on unfired combustor reference velocity is shown in Figure 17. Higher Mach numbers, or more specifically, engine inlet/exit pressure ratios, increase the reference velocities and eventually may cause blow-out upon ignition attempts.

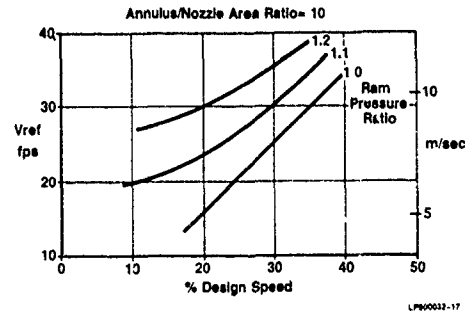


Figure 17. Typical Effect of Ram Pressure Ratio on V_{ref}

Note that under ram conditions, flow is being rammed through the engine at zero speed and may actually decrease slightly as the engine initially breaks away and picks up speed, as dependent upon the turbine flow characteristics at low pressure ratios and speeds.

Combustor reference velocities are determined also by the ratio of the combustor reference area to the turbine nozzle area. Thus, for a given combustor area, higher engine pressure ratios with corresponding smaller turbine nozzle areas provide lower combustor reference velocities.

As mentioned previously, good fuel atomization is critical for small gas turbines. In this respect Figure 18 shows the result of tests on a series of swirl pressure atomizers, of differing sizes appropriate to 200 hp APU, using two different fuels of 4 and 25 centistokes viscosity. Using 4 centistokes is appropriate to typical JP-4, at an ambient of -40°C . A viscosity of 25 centistokes is appropriate to a heavy diesel oil near its cloud point, and represents a worst case, appropriate, for example, to Air Force ground carts burning diesel fuels. The two curves define the fuel pressure required for adequate atomization and any chosen fuel flow, when using a 0.8 Joule ignition system. The scale effects of swirl pressure atomization is clearly shown by the impossibility of providing adequate fuel atomization for fueling rates of 5 and 1 kg/hr or less, for viscosities of 25 and 4 centistokes respectively as, at such fuel flows, the fuel pressure required is infinite. On the other hand, fuel flows much above 15 kg/hr show little effect of fuel viscosity, and fuel pressure required for adequate fuel atomization is modest at about 35 psi. Thus, a very significant difference in flame performance using swirl pressure atomizers, as between large and small gas turbines, exists. This focuses, in the small gas turbine, more strongly than in the large turbine, on those fuel properties affecting fuel atomization, with emphasis primarily on fuel viscosity and, to a smaller degree, on surface tension.

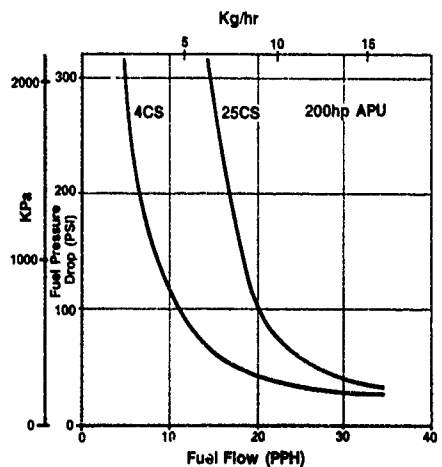


Figure 18. Minimum Fuel Pressure for Good Atomization

Fuel atomization effects are dominant on ignition as the fuel evaporation rate is inversely proportionate to the square of the fuel droplet size. Fuel volatility has a secondary important influence, but hydrogen content and end boiling point have, in comparison, little influence. This is well illustrated in the small Gemini APU (Figure 19) where unusually excellent ignition is obtained, with very viscous non-volatile diesel fuels, in the extreme conditions of Arctic operation, by use of extremely fine atomization from a novel rotating cup fuel injector.

In addition, fuel viscosity has a further important influence on ignition since the fuel spray angle is significantly reduced with viscous fuels. With this reduction, the fuel spray may not be in correct relationship to the ignitor spark and ignition will not occur. A separate start injector makes it easier to take account of this, so that in the worst case, most viscous fuels such as JP-5 having up to 16.5 centistokes viscosity at -40°C , and No. 2 diesel having up to 25 centistokes viscosity at -12°C , can be ignited.

7.0 Control System

Once combustion is accomplished, the magnitude of engine assisting torque is governed by:

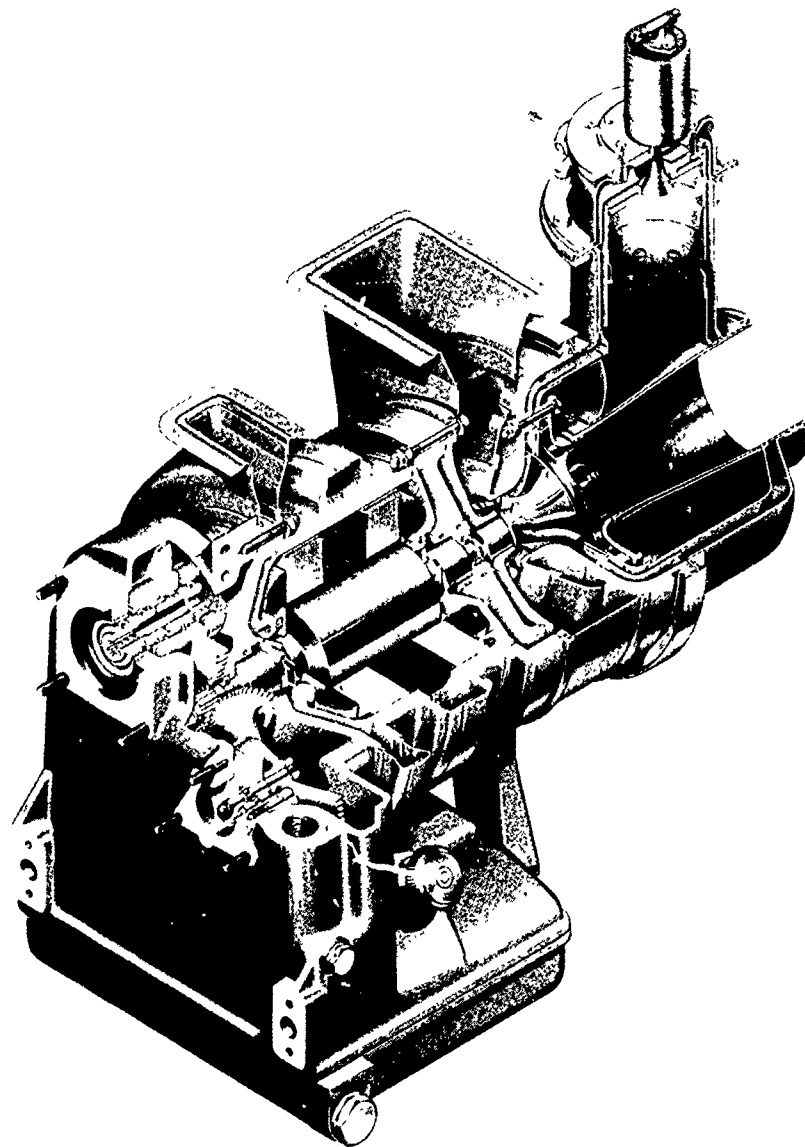
- Engine performance and temperature and temperature limitations.
- Compressor surge margin.
- Fuel control scheduling.
- Parasitic applied torques.
- Transient thermal mass affects.

Larger, higher pressure ratio gas turbines use complex controls systems to skirt the compressor surge line and accelerate within predefined mechanical operational limitations. Smaller, low-cost APUs have, until recently, used simplified "open loop" type acceleration control systems.

The advent of electronic controls for small gas turbines has permitted the utilization of closed loop acceleration, fuel control scheduling where fuel may be topped as a function of a single or multiple control variable.

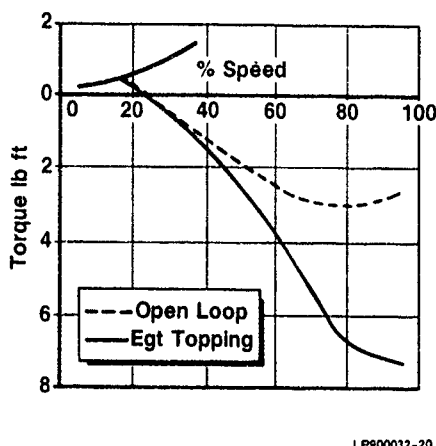
Most recent APUs provide higher starting torques by metering fuel close to the design transient T.I.T. limitations. Typically, two fast response thermocouples are positioned in the exhaust to measure exhaust gas temperature (EGT) which is a speed dependent indicator of T.I.T. Two EGT thermocouple outputs are normally averaged to provide the control input signal. However, if there is a disagreement of a predetermined differential between the two readings, the lower one is disregarded and the higher of the two is used for control. If, by certain predetermined criteria, neither probe is providing valid data, then a shutdown is initiated.

A comparison of APU starting torques with open loop and EGT topping control systems is shown on Figure 20. Torques at low-end speed remain essentially unchanged, being established by light-off speed and viscous effects. Above 32 percent speed, the EGT topping control exhibits higher torques than open loop control, until at 80 percent speed, accelerating torque is approximately doubled, providing faster start time.



LP900032-19

Figure 19. 10 Kw Turboalternator



LP900032-20

Figure 20. Effect of Closed Loop Control

8.0 Alternate Approaches

It has been shown that the critical phases in cold weather starting are fuel atomization and ignition, plus the transition from unfired to fired torques as dependent upon viscous drag and engine thermal response. Alternate starting methods currently under study and development to improve conditions are described as follows.

8.1 "All-Electric" APU

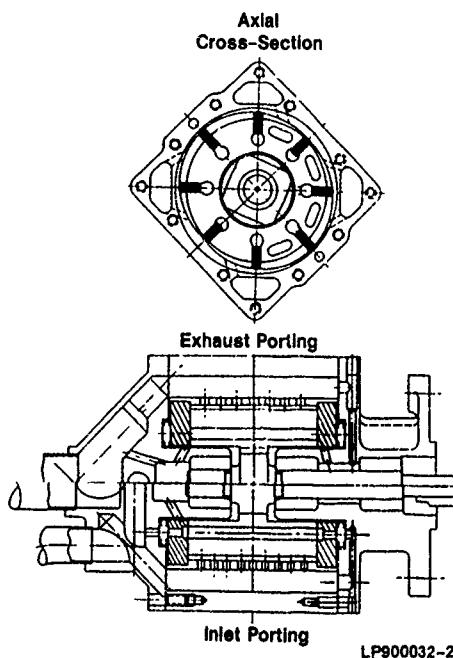
The development of a small "Gemini" Turboalternator APU is described in Reference 22 where the gas turbine directly drove a high speed solid Lundell alternator at 93,500 rpm. Several accessory drive systems were studied, but cost and reliability considerations finally constrained the configuration to that shown in Figure 15, with a conventional reduction gearbox arrangement and lower speed accessories.

The increasing demand for electrical secondary power and dramatic electronic power conditioning component technology advances are requiring a reappraisal of the Turboalternator concept, without a gearbox, where in the alternator could also be used as a starter. The accessory fuel pump, oil pump, etc., would be driven electrically from the conditioned alternator output. Viscous drag during cold starting could be significantly reduced in this arrangement. A disadvantage of this approach is that the alternator inertia may be similar in magnitude to the gas turbine rotating assembly thus prolonging the start time, and the requirement for battery preheating under Arctic conditions.

The replacement of metallic components in the small Gemini gas turbines by the ceramic components is described in Reference 16. The replacement permitted the demonstration of an extremely fast start of 2 1/2 seconds duration from zero to 100 percent rated speed.

8.2 Hot Gas Vane Motor

The inability of most current front-line military aircraft to provide self-sufficient starting at -34°C conditions has prompted the USAF to sponsor the development of a high torque, high power density "Hot Gas Vane Motor" program described in Reference 23. The concept is to provide the hot motor (Figure 21) as a F-16 aircraft retrofit Arctic start kit, for the existing hydraulic start motor (Figure 3). Demonstration starts have been completed using both hydrazine and air/JP gas generators, and development is continuing with a flight weight unit for eventual overall installation. Small high pressure air/JP gas generators as depicted in Figure 22 have found several recent applications in high energy start and emergency power system:



LP900032-21

Figure 21. Hot Gas Vane Motor

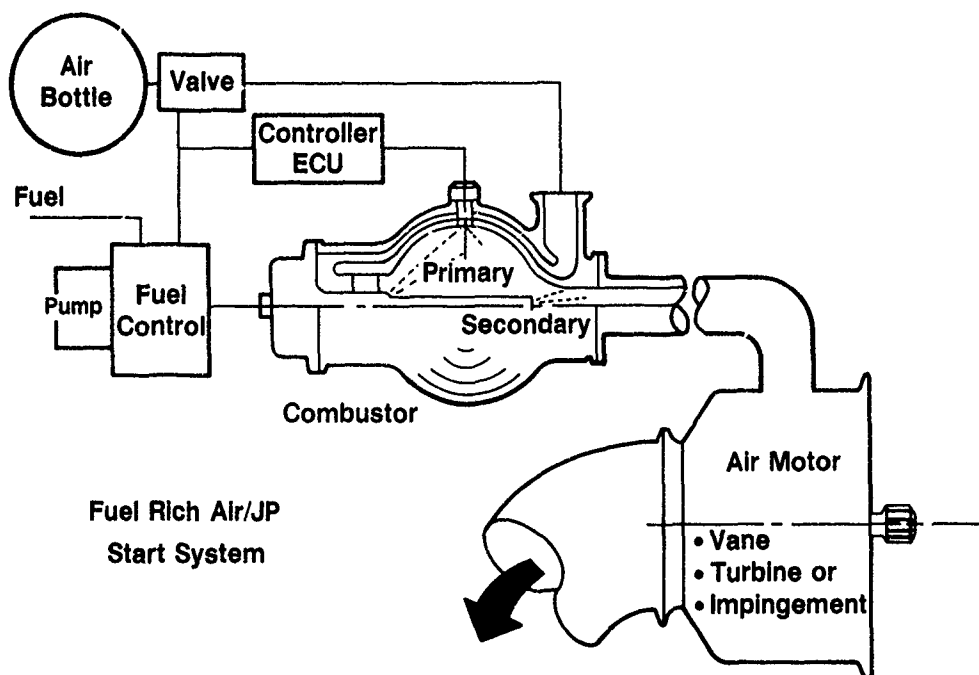
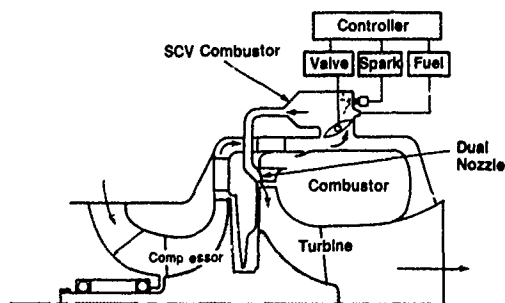


Figure 22. Fuel Rich Air/JP Start System

LP900032-22

8.3 Self-Start APU Concept

Blackburn Reference 24 fully describes a pulse combustor method and apparatus for starting a gas turbine engine, (Figure 23). The first process of the concept method is to inject fuel into the quiescent combustion chamber of an at-rest engine and ignite the mixture of fuel and ambient air. The resulting pressure rise of the combusted gas within the chamber volume expands through the turbine and imparts rotational energy to it.



L9000032-23

Figure 23. Self-Start APU Concept

The gas expansion does not reverse flow into the engine compressor because flapper valves between the compressor and the combustor act as a check valve. The absence of compressor through-flow as the combustion gases are expanding through the turbine minimizes the power required to drive the compressor. Hence, most of the turbine output torque is utilized to accelerate the inertia of the compressor-turbine rotor. Once expansion (i.e., blow-down) is completed, the flapper valves automatically open to allow the now-rotating compressor to scavenge and recharge the combustor volume with fresh air. Fuel is then injected again and ignited to commence another cycle of the "ratcheting" start process.

Attempts to develop constant volume type gas turbines have so far been unsuccessful essentially due to combustor valving inadequacies, heat losses, and non-optimum choice of combustor volume to turbine nozzle area ratio. Exploratory research in the combustor process has been initiated at the author's association with a goal of eventually developing a small self-start APU of the type shown in Figure 23 which potentially would not require a stored energy (battery or accumulator) start assist system.

8.4 High Altitude, High Speed Start

With the use of significantly high starter torque input it is possible to accelerate the engine to near full (100 percent) speed where the combustor inlet pressure and temperature are substantially higher than the ambient conditions, as dependent upon compressor design pressure ratio. Combustor loading is also reduced and fuel requirements increased making combustor and fuel spray conditions more ideal for light-off and operation.

Often specialized start injectors are a requirement for high altitude ignition, i.e., a means of fuel atomization specific to high altitude low speed ignition. By means of high speed ignition such complexity is eliminated. The difficulty with the high speed light-off concept is the high starter torque requirement, even though the unfired windage torque is reduced at altitude. Two potential methods of providing the required high starter torque are:

- Hydraulic starter motor with increased accumulator volume and capability to operate at up to 150 percent overspeed.
- Hot gas generator driving a vane starter motor or direct impingement on the rotating assembly (Figure 22).

Additionally, the use of variable compressor inlet guide vanes can help reduce high unfired windage torque.

In summary, a high altitude start method is feasible where the engine light-off is scheduled to take place at about 80-100 percent rated speed, rather than the conventional practice of about 5-40 percent speed.

9.0 Conclusions

Specific power levels of gas turbines continue to increase paced by continuing advancements in key technologies such as aerothermodynamics, computational fluid mechanics, and high temperature materials. Power sections consequently continue to diminish in size and increase in speed for a given power rating. Associated technology developments in engine driven mechanical equipment such as reduction gearboxes, generators and hydraulic pumps proceed at a more modest rate. This technological disparity precipitates disproportionate sizing of the engine powerhead and driven equipment, spawning increased viscous drag and potentially reduced cold start reliability.

Increased viscous effects are mitigated to some degree by advanced engine ECUs with inherent capability to tailor the starting sequence for all environments. The nemesis of the advanced ECU is fixed cost which can represent more than half the cost of an advanced small APU. Implementing VLSI technology will serve to deter disproportionate cost trends and should be pursued to realize cost effective advanced digitally controlled APUs.

High energy starters and sophisticated electronic controls may not have as much immediate payback as simply reducing the rotating assembly inertia. Advanced material development however, can be equally expensive and time consuming. Thus, all options should be examined in detail, including the all electric gearbox-less APU with switched reluctance high speed generator.

The requirements to operate aircraft gas turbines over a large range of environmental conditions prove particularly demanding to the designer, especially when rapid starting of a cold engine is stipulated at sub-zero ambient temperatures.

Cold engine cranking torque characteristics are basically controlled by the lubricant viscous drag in the mechanical drive train and accessories. To further complicate matters, this viscous drag is dependent upon the magnitude of the applied start torque. Either actual viscous drag test data or realistic methods of predicting engine cold cranking torque levels with high lubricant viscosity may be required before definitive starter specifications can be issued. Experience with start systems for small gas turbine APUs had shown that the total weight required for successful rapid starting at -54°C can approach the weight of the APU powerhead itself.

It is evident that starting torque characteristics of small gas turbines are a function of many interdependent criteria and thus, quite synergistic. Indeed, isolation of the individual cause and effect of many of the criteria involved may be intangible. Nevertheless, an effort has been made to describe these criteria and their apparent effects which may prove sufficiently intriguing to simulate renewed interest in the development of improved starting prediction procedures.

Hopefully, the considerations presented will be employed by the gas turbine mechanical or systems engineer to more realistically appraise the complex starting problem issue, and may serve to make him more cognizant of the effects of engine parasitic viscous drag sources on starting during the critical engine preliminary design phase. Briefly addressed, but of critical importance, is the role of the combustion designer who provides a key input in designing and developing a combustor capable of rapid consistent light-offs over a wide operating range at the earliest possible speed thereby permitting the transition from negative (cranking) to positive engine assist during start.

Methods of reducing APU viscous drag and start energy requirements that deserve future study are the all electric gearbox-less APU, and possibility of the self-start pulse combustor concept.

10.0 ACKNOWLEDGMENTS

The author would like to acknowledge the efforts of the following people in preparation and editing of the manuscript. Jack Shekelton, Mcchele Wilson, Patu McNally and Trudy Lentz, and to Sundstrand Power Systems for publication authority, and the combined efforts of the SAE Starting Committee in their continuing function to improve aircraft gas turbine starting technology.

REFERENCES

1. AIR 781A - Auxiliary Power Sources for Aerospace Applications.
2. AIR 781 - Guide for Determining Engine Starter Drive Torque Requirements
3. ARP 906A - Glossary, Aircraft Engine Starting and Auxiliary Power
4. AIR 944A - Pneumatic Ground Power Supplies for Starting Aircraft
5. ARP 949A - Turbine Engine Starting System Design Requirements
6. AIR 1174 REV A - Index of Starting System Specifications and Requirements
7. AIR 1467 REV A - Gas Energy Limited Starting Systems
8. MIL-STD-210B - Military Standard Climatic Extremes for Military Equipment
9. SAE SP-398 - "Starting Systems Technology." 1984.
10. SAE SP-678 - "Starting Systems Technology II." 1986.
11. Rodgers, C., "Starting Torque Characteristics of Small Gas Turbines and APUs," ASME 79-GT-95. 1979.
12. Rodgers, C., "Impingement Starting and Power Boosting of Small Gas Turbines." ASME 84-GT-188. 1984
13. Rodgers, C., "Secondary Power Unit Options for Advanced Fighter Aircraft." AIAA-85-1280. 1985
14. Rodgers, C., "Fast Start APU Technology" SAE 86-1712/SP-679. 1986.
15. Rodgers, C., "Pneumatic Link Secondary Power Systems for Military Aircraft" SAE 88-1499. 1988.
16. Rodgers, C., Bornemisza, T., "Fast Start Ceramic APU" SAE 89-2254. 1989.
17. Rhoden, J. A., "Modern Technology Secondary Power Systems for Next Generation Military Aircraft." SAE 84-1606. 1984.
18. Gazzera, R. W., "Advanced Pneumatic Start Systems for APUs." SAE 36-1713. 1986.
19. Drury, E.A., "Low Temperature Starting of the V1 Battle Tank." ASME 82-GT-190, 1982.
20. Trippett, R.J., "A High Speed Rolling Element Bearing Loss Investigation" Trans ASME Vol. 100 Jan. 1978.
21. Meyer, W.E., DeCarolis, J.J., Stanley, R.L., "Engine Cranking at Arctic Temperatures," Society of Automotive Engineers Transactions, Vol. 63, 1955, Pg. 515.
22. Rodgers, C., "Performance Development History - 10 KW Turboalternator", SAE 740849. 1974.
23. Dusenberry, G., Carlson, D., "Development of a Hot Gas Vane Motor for Aircraft Starting Systems." SAE 861714. 1986.
24. Blackburn, R., Moulten, J., "Semi Constant Volume Pulse Combustor for Gas Turbine Starting". AIAA 89-2449

Discussion

1. H. Saravanamuttoo, Carleton University

What difficulty do you have in obtaining realistic compressor data at very low speeds, say 30-40% of design? Compressor characteristics are very seldom available below 50%, a typical idle speed.

Author:

- Reference to Figures 2 and 12 show that viscous power losses increase more rapidly than thermo-dynamic power increase, with decreasing ambient temperatures.
- We test our compressors to as low as 20% speed. I am not knowledgeable of low speed efficiency levels of larger more sophisticated multiple-spool axial compressors.
- Removal of misfired cartridges is indeed a dangerous task.

2. P. Sabla, MGR CAD GEAC

Why in figure 9 does weight go up by the factor 5 (data points) for the same energy level. Is this driven by design requirements or by external requirements?

Author:

The weight factor (see Figure 9) is actually less than two, and results from the correlation of many different APU and main engine configurations produce a relatively wide correlation band.

3. R. Wibbelsman, GE

The moment of inertia depends very much on the design of the engine and is also a function of the mission of the aircraft. At high Mach engines the rotor is stronger and heavier and impacts on the torque.

COLD START OPTIMIZATION ON A MILITARY JET ENGINE

by
H. Gruber
Hans-Sachs-Str. 16b
8038 Gröbenzell
Germany

1. INTRODUCTION

Cold-start testing at temperatures of approximately minus 40°C (233 K) was performed on 2 RB 199 engines at a West German altitude test facility.

The engines were of the same build standard with exception of the seal configuration (labyrinth or brush), and running times.

One part of the test was performed with F34 fuel, the other with F40.

The

- facilities
- test methods
- and test results

will be presented in this report.

2. TEST FACILITIES

The general layout of the altitude test cell in which the test series were performed is shown in figure 1. The engine test set-up was largely identical to that of sea level test configurations.

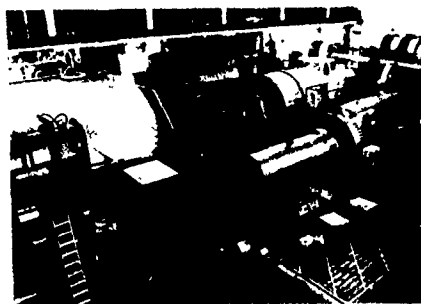


Figure 1: Altitude Test Facility

The induction air path through the test facility and test cell is described in figure 2.

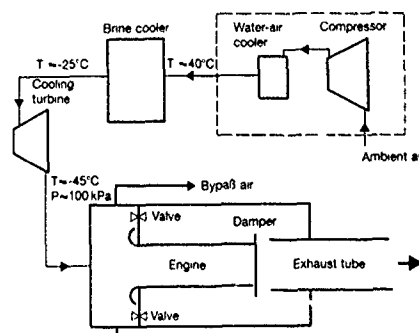


Figure 2: Cooling-Air Flow in Test Cell

After the air had passed through the compressor, the temperature was reduced to approximately 40°C by a water-air cooler. The cooling-air temperature was then reduced by another 65°C to minus 25°C by an additional downstream brine cooler before entering a cooling turbine, which then lowered the temperature to the level required for test-cell induction, in this case minus 40°C to minus 45°C.

The induction air temperature remained at this level from starting to idle speed. To maintain this, it was necessary to bypass a certain amount of air in relation to the specific engine operating conditions.

Up to idle speed, pressure in front of and behind the engine was approximately 100 kPa. A movable damper installed behind the engine prevented the rotation of the engine spools during the cooling phase. Additionally, the high-pressure spool was blocked by internal resistance from the Slave-Loading-System. The intermediate-pressure spool would not turn when both high and low-pressure spools were static.

An additional locking pin was installed radially to block the fan, thereby preventing the low-pressure spool from rotating when the damper was opened.

A steel pipe holding approximately 25 liters of fuel was installed in the test cell directly ahead of the fuel backing pump. This portion of fuel very quickly reached the required minus 40°C during the test cell cooling phase.

Figure 3 shows the temperature drop with respect to cooling time.

After approximately 4 hours, the engine as well as the fuel and oil had been completely cooled.

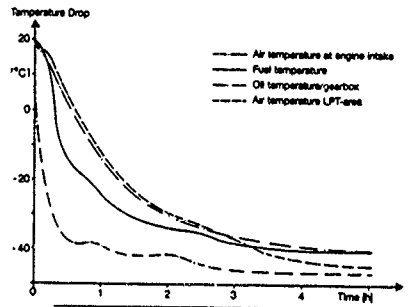


Figure 3: Temperature Drop During Cooling Phase

3. ENGINE STANDARD

The general layout of constructive features of the three-spool engine RB 199 is shown in figure 4.

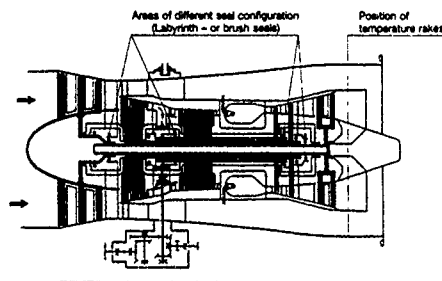


Figure 4: Cross-Section of Three-Spool Engine RB199

The assemblies incorporating labyrinth seals during the first test phase and brush seals during the second test phase are specially identified.

The exhaust gas temperature, which supplied important information for engine monitoring during the starting phase, was measured by rakes located behind the low-pressure turbine.

4. TEST METHODS

The cold-starting tests were to be performed in accordance with the standard starting procedure (at 15 °C) shown in figure 5.

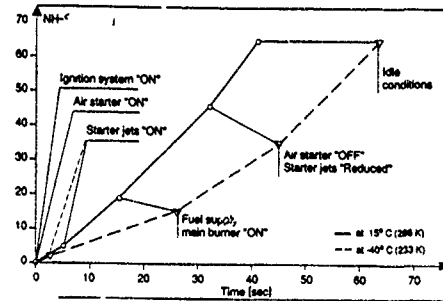


Figure 5: Starting Procedure

The damper (figure 2) was opened approximately 1 minute before starting; the fan-locking pin was removed as the starting sequence was initiated. After reaching idle speed, the engine was to be accelerated to maximum power.

During the starting phase, load (50 kW at the high-pressure spool) was applied to, and bleed-air (approximately 0.22 kg/s.c. from high-pressure compressor area) was taken from the engine.

The following main parameters were to be monitored:

- Time
- Temperatures and pressures in the test cell
- Engine speed
- Turbine-area temperatures

The testing comprised

- 11 starting attempts at minus 30°C using F34
- 5 starting attempts at minus 30°C using F40
- 12 starting attempts at minus 40°C using F34
- 16 starting attempts at minus 40°C using F40

All of these attempts were carried out with a high margin of success.

5. TEST RESULTS

5.1 Combustion chamber ignition characteristics

It was difficult to reliably evaluate the ignition characteristics of the combustion chamber during the individual starting phases with the instrumentation available. Combustion chamber ignition generally means a rapid increase ($\geq 50^\circ/\text{second}$) of the turbine outlet temperature. During testing, this rapid increase was not observed until the low-pressure spool began to rotate ($\geq 2\% \text{ NL}$).

This may have been caused by an improvement of the flow and combustion characteristics in the combustion (greater pressure drop) and turbine areas once the low-pressure spool began to rotate. Unusually high temperatures at the high-pressure compressor outlet indicate a blockage of airflow in the combustion chamber and turbine before the low-pressure spool has begun to rotate.

5.1.1 Influence of the igniter plug location

Figure 6 shows a simplified drawing of the combustion chamber head featuring the arrangement of the starter jets, igniter plugs and vaporizers.

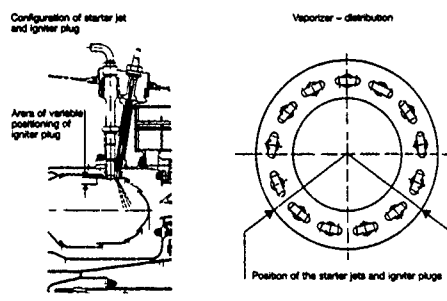


Figure 6:
Combustion Chamber Detail

The location of the igniter plug in relation to the combustion chamber head was varied from + 1.74 mm to - 1.34 mm

The plus-sign indicates:

- the igniter plug protrudes into the combustion chamber

The minus-sign indicates:

- the igniter plug is located "outside" the combustion chamber

The test evaluations did not reveal any tendencies regarding ignition characteristics even though other tests indicated that the location of the igniter plug did indeed influence ignition characteristics.

5.1.2 Influence of the starter jets

The influence of the starter jets is greatest during the first phase of starting, since their proper functioning is critical to the ignition of the main fuel

5.1.2.1 Starter jet flow numbers

Starter jets with flow numbers 0.3 and 0.6 ($FN = \sqrt{\dot{V}/\Delta p}$) were available for the test engine.

Starts were performed using both starter jet sizes and both F34 and F40 fuel. The starts using FN 0.6 were successful in every case, whereas only half the tests using the smaller jets offered the desired results.

The major advantages of the larger jets were, as expected, the increased rate of engine acceleration to the point of main fuel jet activation, improved heating-up of the combustion chamber and, consequently, improved combustion propagation of the main fuel.

In order to prevent excess fuel delivery and the corresponding danger of hotstarts, the flow number 0.45 was determined in an additional short test phase as being optimal for all further tests.

All starter jets were removed and cleaned after every third or fourth cold start. The flow values dropped by as much as 5% between starts. The spray angle remained practically unchanged.

According to general experience, combustion propagation should have been better with F40 than with F34. This, however, could not be confirmed by the test data. The differences between F34 and F40 were within test result scatter.

5.1.2.2. Starter jet configuration

At the beginning of testing it was observed that the starter jet fuel had ignited on only one side of the combustion chamber. Figure 7 shows the exhaust gas temperature profile obtained from rake measurements during starting phase 1. It is plain to see that the maximum value was measured at the right-hand starter jet. This was documented by a video-camera, as well. By the time the main fuel is ignited, approximately 23 seconds after the starter jets are activated, both starter jets are burning. It was assumed that the uneven ignition of the starting fuel during the initial starting phase was due to a difference in timing caused by the different lengths of fuel-feed tubes to the port and starboard starter jets. The equalization of the pipe lengths led to an increased average temperature level, which meant that an higher amount of energy was present within the combustion chamber and the turbine area.

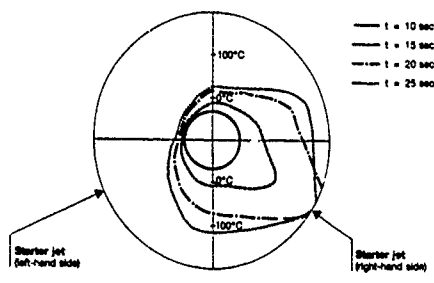


Figure 7:
Exhaust Gas Temperature Distribution During Cold-Starting

It is suspected that the starter jet feed lines contained residual fuel vapors, whose effect on fuel delivery increases with an increase in fuel line length. "Wet cranks", performed prior to the starting tests would surely have helped preclude any such difficulties.

The exhaust gas temperature, which is a primary factor in evaluating the effect of pipe-length equalization, subsequently showed a greater rate of increase during the starting tests that followed.

5.2 Starting procedure optimization

The starting procedures for cold-starting were substantially modified compared to the sequence at 15 °C (figure 5).

During starting at minus 30°C and minus 40°C, a sufficient high-pressure spool speed (19-23%) could not be reached with normal starter jet assistance alone. It would have been helpful to keep the starter jets activated for a longer period of time to augment the thermal energy available in the combustion chamber, thereby improving the conditions for the ignition of the main fuel. This, however, would have resulted in a very short overlap of starter engagement and main fuel jet activation. Experience shows that a long period of starter engagement with the combustion chamber "lit" or partially "lit" is required for successful cold-starting. This could be accomplished by varying the starter engagement time in relation to engine intake temperature, as is the case with other engines.

The following starting sequence was found to be optimal for the test engine:

starter jet open: after 2 to 5 seconds
main jets open : after 20 + 5 seconds

This required that the main fuel feed be activated at a certain point in time rather than at a specific engine speed. The point at which the main fuel jets were activated corresponds to 12 - 15% high-pressure spool speed at minus 30°C and minus 40°C. During ambient starts (engine-intake temperature = 15°C) 19 - 23% high-pressure spool speed was reached, compared to 25% during hotstarts (engine-intake temperature = 50°C).

5.3 Torque profile

Figure 8 shows the torque profiles for cold-starting of the test engines with different seal configurations.

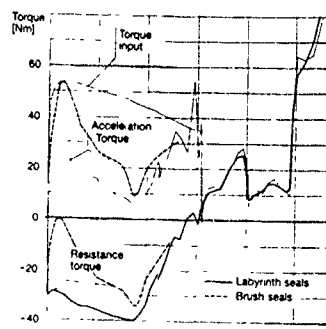


Figure 8:
Torque During Cold-Starting

It must be taken into consideration that the engine equipped with the brush seals had been operated for approximately 180 hours prior to cold-start testing and could therefore not be representative of a new brush-seal equipped engine.

The comparison between the different engine builds showed that:

- the differences in the resistance curves for both engines were small.
- the low-pressure spool breakaway of the brush seal engine was not affected by engine intake temperature between minus 30°C and minus 40°C. The low-pressure spool breakaway occurred at approximately 19% high-pressure spool speed, which is slightly higher than that of the engine equipped with labyrinth seals. It appears that the labyrinth configuration was indeed affected by engine-intake temperature.

It is assumed that the friction of the cold brush seals was lower than that of the cold labyrinth seals. This may be due to the relatively long running time of the brush seal engine and the fact that the brush seal pins did not come into contact with any rotating parts at these low temperatures.

6. CONCLUSIONS

These results are based on tests with two engines of different seal configuration and with different running times. They are certainly useful as a basis for general assertions concerning the behaviour of those engines; they do not, however, allow any final conclusions to be drawn. Further extensive testing would be necessary.

The following points of interest, relevant to the RB199 engine cold-starting were noted;

- The differences between the ignition propagation properties of fuels F34 and F40 were within the measurement scatter.
- The starting characteristics of the engines equipped with brush and labyrinth seals differed only slightly. The relatively long running time of the engine equipped with brush seals prior to testing must be taken into account.
- The configuration and size of the starter jets is of fundamental significance to the ignition propagation in the combustion chamber and, subsequently, to the success of the starting process.
- The optimization of the starting process entails changing from an engine-speed-determined main fuel supply activation point to a time-determined point.
- A further, marked improvement in starting characteristics may be achieved by generally changing to an intake temperature-related starter-engagement sequence, as is the case with a number of other engines.

Discussion

1. C. Moses, Southwest Research Institute

You stated that there was very little difference in the starting characteristics of the two fuels. Was this also true when you used the smaller fuel nozzles?

Author:

The situation was comparable with both flow nozzle sizes

2. P. Sabla, GEAE

Was the inlet air dry? How was the moisture removed?

Author:

The inlet air was not dried. We ran all the tests with unconditioned air, that means with normal ambient conditions.

3. D. Hennecke, Technische Hochschule Darmstadt

Do your test cell arrangement and your test procedure ensure that you have steady-state temperature conditions when you start the engine?

Author:

Figure 3 of my report shows the temperature drop with respect to cooling time. During this phase a low amount of wet air was passing through the engine although the damper was filled behind the engine. The spools did not rotate. The temperature level in and around the engine was controlled all the time by temperature probes. After approximately 4 hours, the engine as well as the fuel and oil had been cooled down to the required -40°C .

4. C. Rodgers, Sundstrand Power Systems

Was ignition of the starter jets programmed at 5% n?

Did a revision of the cold start fuel schedule require reprogramming of the ECU?

Author:

The ignition of the starter jets was initiated at 5% n by the engine driver.

The tests were not performed with a DECU, but the experience gained during the tests later on was introduced in fuel scheduling of another engine programme.

COLD WEATHER IGNITION CHARACTERISTICS OF ADVANCED SMALL GAS TURBINE COMBUSTION SYSTEMS

I. Critchley, P. Sampath, F. Shum
Pratt & Whitney Canada Inc., 6375 Dixie Rd.,
Mississauga, Ontario, Canada L5T 2E7

SUMMARY

Low temperature and high altitude starting requirements of present day small aero-gas turbine engines are discussed from the viewpoint of their influence on the design of the combustors and ignition systems. Use of electric starters, common in small engines, creates particular challenges to starting especially under cold soak sea level and altitude start up conditions.

The main factors in combustion system design affecting starting performance are discussed; including combustor sizing, fuel placement, fuel atomization, fuel scheduling and igniter selection. Experience of Pratt and Whitney Canada (P&WC) with small engines for different applications are also covered.

Low emission requirements may adversely affect starting performance, necessitating use of elaborate fuel/ignition systems, some recent developments are described.

Nomenclature

ΔP = Pressure drop
 SMD = Sauter Mean Diameter
 T_0 = Ambient temperature
 T_3 = Combustor air inlet temperature
 T_5 = High pressure turbine exit temperature
 T_{TL} = Time to light
 T_a = Air temperature
 T_f = Fuel temperature

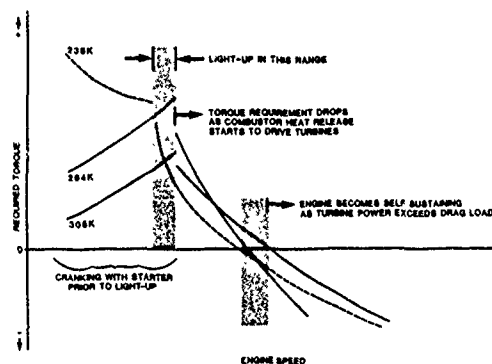
INTRODUCTION

The ability of an aircraft gas turbine to light-up and accelerate easily and reliably is of crucial importance both for ground and altitude starts. The achievement of this goal under adverse conditions of low soaking temperatures, or at low temperature and pressure during altitude operations, imposes severe constraints on the combustion system. Typical cold start requirements for small aircraft gas turbines would be for air temperatures down to 220K and with fuel viscosities up to 12 centistokes. Altitude relighting capability is needed typically up to 11,000 meters for main power plants and in excess of 12,500 meters for the new generation of Auxiliary Power Units (APU), which may be required to start and rapidly generate emergency power after cold soaking at high altitude.

Small aircraft gas turbines are typically equipped with electric starters, the starting torque being set to be greater than the maximum drag torque during cranking conditions. However all the major drag sources; compressor aerodynamic load, windage in compressor & turbine discs,

friction in bearings and gears, accessory loads and lubricant viscosity effects, tend to increase the initial drag at low temperature as seen in Figure 1. Lower battery voltages during cold soak/altitude operations and the higher drag therefore tend to reduce engine cranking speeds and air flows during start-up and hence reduce the combustor air pressure drop available for atomization and mixing within the combustor.

FIG 1- TYPICAL STARTING TORQUE REQUIREMENTS



Adding to these difficulties is the increased viscosity of the fuel at low temperatures which will result in a more coarsely atomised fuel spray and hence be more difficult to light. Low pressures and temperatures adversely affect both the initial ignition process and the subsequent flame propagation because of slow evaporation and reaction rates. Even after a stable flame has been established its efficiency and therefore the ability of the engine to accelerate are significantly lowered under extreme conditions of low temperature and pressure. Reduction of the combustion efficiency occurs at a time when increased engine drag necessitates more energy from the combustion system.

All these factors combine to increase the difficulty of starting under adverse conditions and can result in the inability to light, accelerate or lead to torching and consequently turbine damage which may not be immediately apparent. Other possibilities are hung starts or extremely long times to light and idle. Solutions to these problems impose restraints on the combustion system and increase the complexity of the fuel and ignition systems. This is particularly undesirable on small aero gas turbines where these systems can be a significant contribution to the total engine cost and weight.

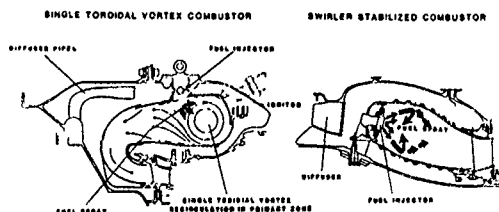
Advanced engines with their demand for lower specific fuel consumption and

specific weight operate at higher engine pressure ratios and turbine inlet temperatures. These requirements have driven combustor designs to be more compact for durability, to have lower combustor pressure drop for performance and to operate with leaner primary zones for smoke and emissions control. All these requirements have made the problem of designing for cold and high altitude starting more challenging than ever before.

DESIGN CONSIDERATIONS

The first requirement of the combustor is good ignition performance, necessitating a combustion system with adequate fuel atomization, optimum fuel placement and a reliable and effective ignition system. However, the combustor primary zone must be sized with sufficient volume for reasonable air loadings [1]. The combustor primary zone flow structure and fuel - air ratio must be set to achieve rapid ignition and subsequent flame stabilization and propagation around the combustor annulus. A recirculating primary zone flow is commonly used. The structure of the recirculating flow will vary with different designs and may be driven by swirling air through the fuel nozzles or, as is more common in small engines, a single toroidal vortex, Figure 2, driven by wall cooling flows around the front end of combustor. The fuel nozzles are positioned to spray the fuel into the combustor so as to maximize the residence time of the fuel in the primary zone. The nozzles may be mounted radially spraying upstream or axially through the dome of the combustor or tangentially as shown in Figure 3.

FIG 2. TYPICAL COMBUSTION SYSTEMS FOR GAS TURBINE ENGINES

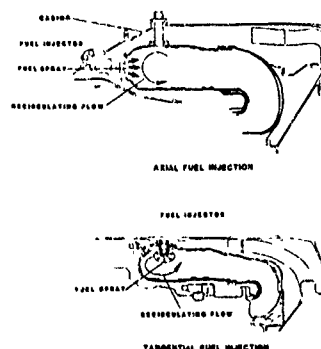


The igniters (usually 2 to provide redundancy) are positioned in a fuel rich region of the primary zone. However, care must be taken to prevent excessive fuel wetting which can lead to premature igniter failure or spark quenching.

Circumferential positioning of the igniters will depend on the degree and direction of any residual swirl from the diffuser air outlet which may be present in the primary zone and the trajectory of the fuel spray. In practice, igniter position and penetration are determined by development testing. Optimum penetration will be a compromise between improving ignition and excessive igniter tip temperatures as penetration increases.

The number of fuel injectors is generally selected as a compromise to satisfy both combustor performance requirements and cost and weight

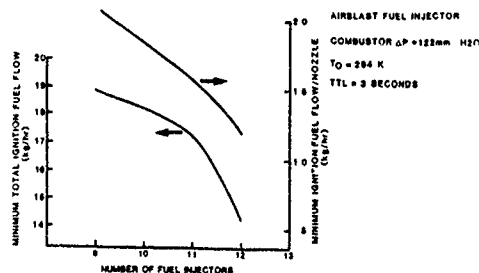
FIG 3: FUEL INJECTOR MOUNTING ARRANGEMENTS



considerations. The number selected will influence combustor exit temperature distribution as well as ignition and starting performance. Engine manufacturers generally use empirical correlations developed to suit their own combustion systems. Figure 4 shows the minimum ignition fuel flow for an airblast fuel injector system with different numbers of fuel injectors; the minimum ignition fuel flow required decreases with increasing number of fuel injectors.

Primary zone fuel air ratio control is an important aspect of combustor design affecting ignition, combustion efficiency and emissions performance. One of the means of reducing emissions is to design the primary zone to be fuel lean, however, a rich primary zone is usually required for good ignition and flame stability. Elimination of local fuel rich pockets in the primary zone will reduce smoke but may adversely impact ignition, Figure 5. In most cases detailed combustor hole pattern development and fuel spray optimization are necessary to meet both cold ignition and emissions requirements.

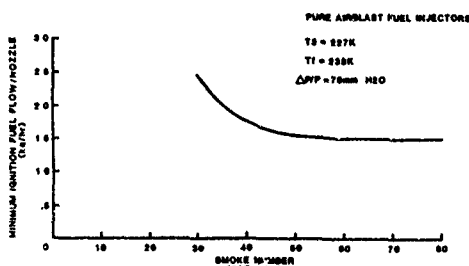
FIG 4. MINIMUM IGNITION FUEL FLOW FOR DIFFERENT NUMBER OF FUEL INJECTORS



FUEL DELIVERY SYSTEM

The fuel system design, including fuel injector, manifold and scheduling plays an important role in cold ignition performance. Good atomization is crucial for good ignition. Figure 6 shows a comparison of droplet size between pressure and airblast atomizers, showing the superior performance of airblast injectors except under starting conditions.

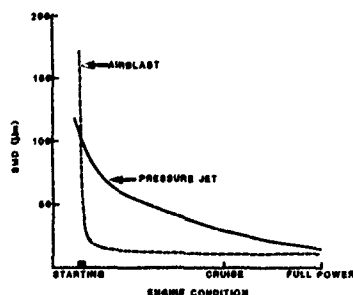
FIG 5: RELATIONSHIP BETWEEN MINIMUM IGNITION FUEL FLOW AND SMOKE EMISSIONS



Pressure Atomizers

Pressure atomizers have been used successfully for many years on gas turbine engines. However, on engines with a high turn-down ratio (ratio of maximum to minimum fuel flow), low fuel pressure and thus poor atomization will result at the starting conditions. This problem can be overcome to some extent by staging of the fuel whereby some fuel injectors near the igniters receive fuel at a higher pressure which will improve their ignition performance. Staging is achieved by use of a flow divider valve which may be single or multi-port providing several levels of staging to aid a gradual flame propagation.

FIG 6: COMPARISON OF SPRAY SAUTER MEAN DIAMETERS FOR PRESSURE JET AND PURE AIRBLAST ATOMIZERS



Staging of the fuel can result in torching or flame propagation difficulties. Correct proportioning of the fuel to the various stages is required to prevent long manifold fill-up times with consequent fuel dribbling and pooling which can lead to torching during starts. Recent PT6 engines use a 2 stage system with primary and secondary fuel injectors. Figure 7 shows how the peak transient combustor exit temperature can be reduced by optimizing the number of primary and secondary fuel injectors. An optimum fuel flow split between stages exists when the temperature peaks associated with the light up of each stage are equalized and neither predominates. In this case this was achieved with 10 primary injectors.

Engine hanging can also occur as a result of fuel staging where the engine

will light but fail to accelerate. In this case, the primary fuel injectors may have low combustion efficiency under adverse conditions. If the engine then fails to develop sufficient air pressure for the fuel control to schedule an increase in fuel flow, the secondary fuel injectors may not have sufficient fuel pressure for good atomization. This can be overcome by increasing the starting fuel flow; increasing starting fuel flow eliminates hanging and the engine always accelerates at temperatures above its lighting limit. However, this is not always a viable solution since over-fueling can lead to excessive exhaust temperatures during light-up. The hanging can also be eliminated by use of a single manifold (unstaged) system, Figure 9. However, such a system usually has a fairly high ambient temperature ignition limit, although this can be lowered by increasing the starting fuel flow.

FIG 7: VARIATION OF PEAK TEMPERATURE DURING STARTING WITH NUMBER OF PRIMARY FUEL INJECTORS

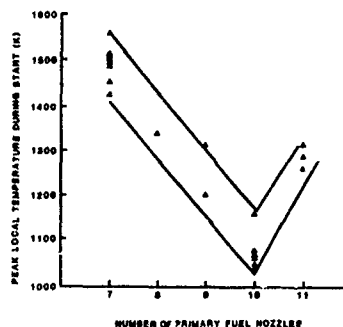
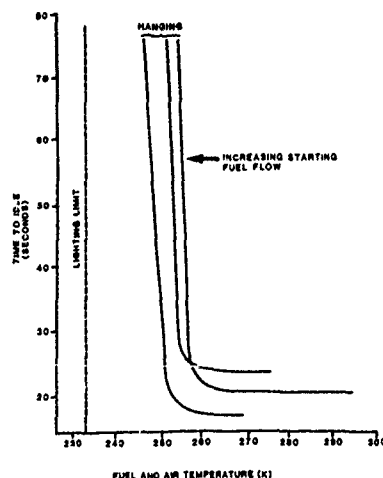
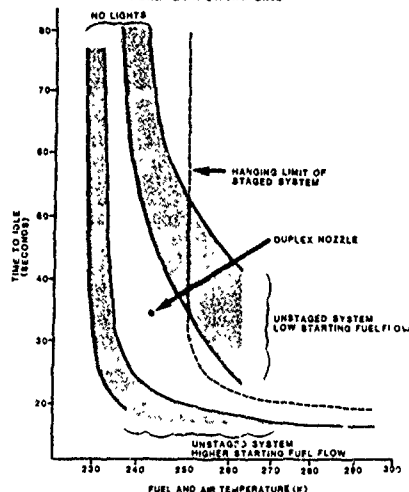


FIG 8: EFFECT OF STARTING FUEL FLOW ON HANGING



An alternate approach to improve starting performance and to eliminate hanging is use duplex fuel injectors. Figure 9; lighting should not be a problem although the limit was not established in this testing. However, the complexity of duplex injectors and the need to maintain adequate fuel passage sizes limits their use to low turndown ratio applications.

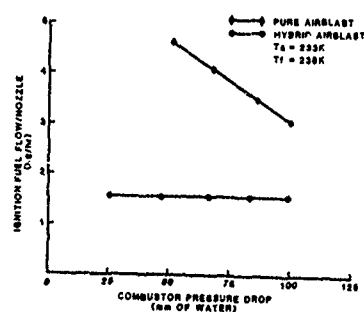
FIG 9: COMPARISON OF STAGED AND UNSTAGED FUEL "LOW ON HANGING"



Airblast Atomizers

Advanced gas turbine engines with their requirements for better spray quality and longer life generally use airblast fuel injectors. This type of injector is particularly suited to small engines since fuel passages can be larger than for pressure atomizers which are prone to blockage in small engines. As a result of the dependence on air pressure drop across the combustor for atomization, droplet sizes are usually coarse at starting conditions, particularly at low temperatures when the fuel is more viscous and cranking speeds are low. For small gas turbine engines, under extreme conditions, the combustor air pressure drop could be as low as 25 mm of water. Development of airblast fuel injectors for small engines has concentrated on improving atomization at these low pressure drops. Testing at

FIG 10: COMPARISON OF IGNITION PERFORMANCE BETWEEN HYBRID AND PURE AIRBLAST SYSTEMS

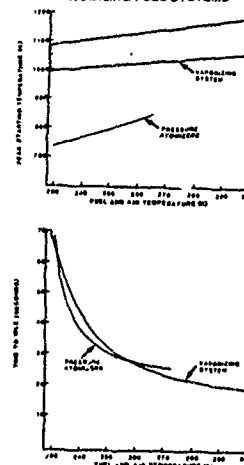


P&WC has successfully demonstrated ignition with airblast fuel injectors at combustor pressure drops down to 38 mm of water at fuel and air temperatures of 230K.

Piloted fuel systems are used to enhance starting and to alleviate torching from overfueling at low temperature and pressure conditions. Piloted systems usually employ a hybrid fuel nozzle or a torch igniter. A torch igniter consists of a combined igniter and pressure jet atomizer. Problems of coking and blockage can be minimized by mounting the atomizer in a relatively cool region or by purging. Application of torch igniters is most common on vaporizing fuel systems but has been used in some airblast applications.

Hybrid fuel injectors consist of a pressure atomizing primary and an airblast secondary nozzle. Fuel is introduced to the primary fuel circuit first for initial light-up and subsequent propagation to the remaining airblast fuel injectors. Figure 10 shows a comparison of minimum ignition fuel flow for a pure airblast and a hybrid airblast system at cold conditions. For the hybrid system, the minimum ignition fuel flow is independent of combustor pressure drop. With the pure airblast system, time-to-light is governed by the manifold fill-up time and the achievement of favourable conditions at the igniter. This can result in much slower ignition with possible pre-ignition fuel accumulation and torching at ignition. With the hybrid system, ignition can be achieved at extremely low combustor air pressure drops and with a much quicker time-to-light. Ignition is usually instantaneous and a controlled light-around without any torching is achieved.

FIG 11: STARTING CHARACTERISTICS OF A PT6 ENGINE WITH VAPORIZING AND PRESSURE ATOMIZING FUEL SYSTEMS



Vaporizers

Vaporizing fuel systems are widely used in small gas turbine engines; this type of system requires the use of an external flame source like a torch igniter for lighting. Once developed, lighting performance is governed by the torch igniter and is very similar to pressure atomizing systems as shown in Figure 11. However, problems may occur with flame

propagation around the combustor depending on vaporizer design and spacing. Slow flame propagation may cause unburned fuel to accumulate during start-up and can lead to high exhaust temperatures, Figure 11 and long starting times.

FUEL MANIFOLD AND CONTROLS

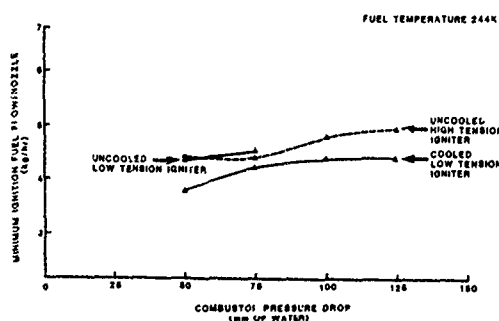
Fuel manifold design plays a role in the success of the starting system. A small diameter manifold can give excessive line pressure losses which can ultimately affect the combustor outlet temperature distribution. A large diameter manifold will require a long filling time leading to dribbling and torching. It is necessary to find a compromise between these two requirements. Spiking the initial fuel flow can reduce the manifold filling time and the torching tendency, a solution which has become more viable with the advent of electronic fuel controls. The accurate fuel scheduling off any required engine operating parameter provided by electronic controls is also of great benefit to starting performance since it is possible to operate with a small margin between sub-idle surge and the acceleration demand.

Air assist systems use high pressure air which can be introduced into the fuel manifold to aerate the fuel thereby assisting atomization during light-ups. This kind of system has been used for heavy fuels in industrial applications.

IGNITION SYSTEM

Most small gas turbine engines use ignition system energies in the range 1 to 4 joules. Both low tension (L.T.) semi-conductor (approx. 4kV) and high tension air gap (typically 24 kV) systems are employed. For a given output energy, both systems give similar ignition performance as shown in Figure 12. Air cooling to the igniter can also affect ignition performance. In this case, Figure 12, the provision of air cooling aided ignition which suggests that rich conditions prevailed near the igniters. Igniter cooling air is not always beneficial to starting and the effect depends on the environment adjacent to the igniter.

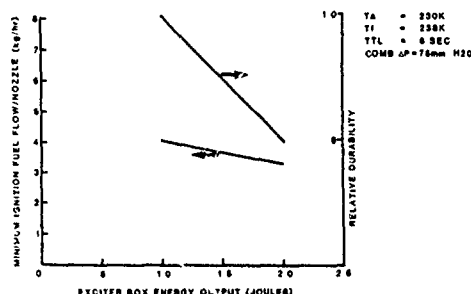
FIG 12: EFFECT OF IGNITER TYPES ON IGNITION



The most dominant effect on ignition performance is the energy supplied at the igniter tip, increasing energy level will improve ignition performance but will be

detrimental to igniter durability, Figure 13. The final choice will be the minimum energy to meet cold and altitude ignition requirements so as to maximize igniter life.

FIG 13: EFFECT OF IGNITION ENERGY ON IGNITION PERFORMANCE AND IGNITER DURABILITY



Alternate means of ignition have also been used or are under study. The concept of plasma jet ignition has been studied by various researchers [2]. In this type of igniter, Figure 14, the arc does not occur at the tip of the igniter but is confined in a small cavity. The gases (and liquid fuel) in the cavity are heated by the arc and a pressure rise results. The pressure is allowed to exhaust through an orifice resulting in a jet of energetic plasma which is propelled into the combustor. The concept was developed for automotive applications but can offer advantages to gas turbine designs since it will allow the spark kernel to be projected away from combustor wall, cooling flows into that part of the primary zone most amenable to ignition. The principle can be applied to both high tension and low tension systems.

Emergency power units for special applications can have a requirement for very fast light-up and acceleration at very high altitudes. A one second time-to-light at altitudes up to 15,000 meters with pure airblast fuel injectors has been demonstrated by use of oxygen injection at the fuel injectors.

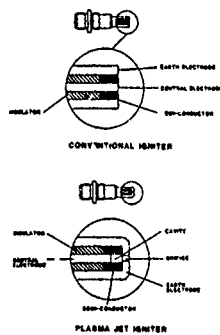
The recent development of solid state LT exciters has improved the efficiency of the energy transfer process so that a given energy can be delivered at the igniter tip with a smaller, lighter, cheaper exciter. This type of device can also offer improved control of spark rate which can be maintained independently of input voltage and ambient temperature. This is particularly important for continuous ignition applications where a low spark rate is desirable. Future developments could allow the adjustment of spark rate or energy to suit ambient or engine condition, diagnostic capability will also be available to warn operator of impending ignition system failure.

FUEL EFFECTS

Small gas turbines, even for aero applications, have to operate with a wide

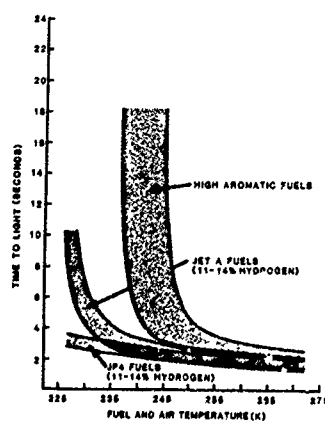
variety of fuels such as Jet A, Jet A1, JP4, aviation gasoline and diesel fuels. These fuels have widely differing properties giving very different atomization and ignition characteristics at low temperatures.

FIG 14: SKETCHES OF CONVENTIONAL SEMICONDUCTOR IGNITER AND PLASMA JET IGNITER



Ignition performance is governed mainly by fuel viscosity and volatility. Decreasing temperature reduces volatility slowing evaporation rates and also increases viscosity deteriorating atomization quality. Data on these effects for a variety of fuels were obtained by P&WC in a research program sponsored by CDND and USAF [3]. Testing was carried out on a PT6A-65 engine at low temperatures with a wide variety of fuels. The effect on time to light is shown in Figure 15 and on time to idle in Figure 16. The results clearly indicate that the more volatile, less viscous fuels like JP4 have better starting characteristics than the high aromatic content fuels.

FIG 15 EFFECT OF FUEL TYPE ON TIME TO LIGHT

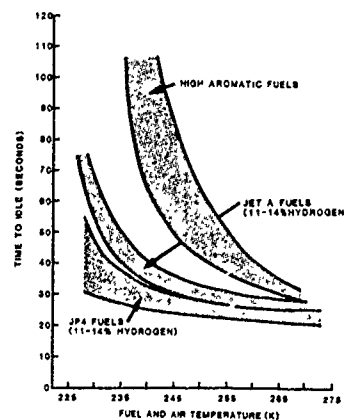


influencing starting performance include number and type of fuel injectors, stoichiometry of the primary zone and the efficiency of the combustor. Sub-idle performance of rotating components also affects starting performance.

The use of electric starters in small engines creates particular challenges due to low cranking speeds under adverse starting conditions, requiring the use of starter/pilot fuel systems and novel scheduling with airblast atomizing fuel systems. Improvements to aerating nozzle designs and use of improved ignition systems are showing good potential to enhance cold weather starting performance. Use of air/oxygen assist can also significantly enhance starting performance especially under high altitude, cold soak conditions.

Some requirements for low emissions may adversely affect cold/altitude starting, requiring the use of more elaborate fuel/ignition systems to achieve required performance. Ability to model transient performance of engines and combustion systems while simulating starting, can enable better understanding of, and improvements to, this very important aspect of engine performance.

FIG 16: EFFECT OF FUEL TYPE ON TIME TO IDLE



CONCLUSIONS

Reliable cold day and altitude start-up of modern aero-gas turbine engines requires careful optimization of combustor internal flows, fuel atomization/placement, ignition source/location and fuel schedule during the starting cycle. Other factors

REFERENCES:

1. Lefebvre, A.H., "Gas Turbine Combustion", McGraw-Hill Book Co.
2. Zhang, J.X., Clements, R.M., Smy, P.R., "An Experimental Investigation of the Effect of a Plasma Jet on a Freely Expanding Methane-Air Flame", *Combustion & Flame*, 50, (1983).
3. Gratton, M., Critchley, I., and Sampath, P., "Alternate Fuels Combustion Research", AFWAL-TR-84-2042, July 1984.

Discussion**1. C. Scott Bartlett, Sverdrup**

Is consideration given to use of gaseous fuel injection or a gaseous fuelled pilot torch for cold start assistance?

Is the primary reason that gaseous fuels are not used due to the complexity of the additional systems required?

Author:

The questioner is right. Although the benefit of gaseous fuels for ignition is well known for static applications it would normally not be considered for commercial aero-applications due to the complexity and logistics of providing and refuelling such a system.

However the idea could be considered for military applications to aid, for example, relighting at very high altitudes. In fact work has been carried out at Pratt and Whitney Canada using oxygen injection through igniters and fuel injectors which demonstrated a significant extension of the relight envelope to high altitudes.

2. D. Hennecke, Technische Hochschule Darmstadt

If I understand correctly you emphasized the importance of smoke emission during start-up. Is this not unimportant compared to smoke emission at full power conditions?

Author:

During my presentation I was referring to high power emissions. Therefore I would agree to this comment.

COLD WEATHER JET ENGINE STARTING STRATEGIES
MADE POSSIBLE BY ENGINE DIGITAL CONTROL SYSTEMS

by

RC WIBBELSMAN
Senior Staff Engineer
General Electric Company Peebles Test Operation
1200 Jaybird Road
Peebles, Ohio 45660
USA

Summary

The subject of automated and adaptive jet engine starting strategy is a complicated subject involving many intricate sets of conflicting requirements, both from the standpoint of the engine environmental situation as well as the engine health situation. In the past, many design compromises had to be made which resulted in limiting the engines ability to achieve 100% starting success, particularly in the "off design" regions. The advent of the computing power of digital controls now make it possible to achieve a major step forward in the control systems ability to cope with the multiplicity of situations confronting the engine starting system designer.

There are many different strategies that could be employed. This paper presents the one used by the GE and CFM Commercial Family of large high bypass ratio turbofan engines. Numerous variations of this basic concept could be employed.

It is hoped that this paper will promote a new vision of what is possible to achieve in the way of:

- Solutions to the present design dilemmas facing the engine designer.
- Better reliability at the environmental extremes.
- More reliable starting of deteriorated engines.
- More reliable starting under extreme emergency situations.
- Make starting more certain under adverse battle damage situation.

We have just begun to scratch the surface. Let us now continue to exploit this concept on the next generation of jet engines.

Table of Contents

1.0	Introduction
1.1	Basis of This Paper
1.2	General Operation
1.3	Manual versus Automatic
2.0	Overview of System and Its Response to Unusual Events
2.1	Ground Start Sequence
2.2	Air Start Sequence
2.3	Arctic Weather Design Considerations
3.0	Stall Sensing and Resequencing
3.1	Ground Start Stall Sensing
3.2	Air Start Stall Sensing
3.3	Resequencing Due to Stall
3.4	Adaptive Strategy for Engines with Repeated Ground Start Stall History
4.0	Light Off Sensing and Resequencing
4.1	Light Off Sensing
4.2	Ground Start Light Off Resequencing
4.3	Arctic Ground Starting Resequencing
4.4	Air Start Light Off Resequencing
5.0	FADEC Scheduling Features
5.1	FADEC Approach
5.2	Normal Ground Start Strategy
5.3	Arctic Ground Start Strategy
5.4	Air Start Strategy
6.0	Starter Usage Strategy During Air Starting

1.0 INTRODUCTION

Full Authority Digital Control Systems are coming into wide use in the large commercial jet engine industry, and are starting to appear in the military engine market. Some of these engines employ automatic start sequence features, which simply automate the conventional hydro-mechanical control concept, while others take advantage of the computing power of the digital approach and incorporate adaptive expert system features. The CFM1 and General Electric large commercial engines, such as the CFM56-5 and CF6-8, fall into this latter category.

This approach is largely being driven by economic considerations because in world-wide operation, aircraft using these engines commonly land in relatively unsupported airports. Under those circumstances, if the engine will not start the passengers must be unloaded, overnight hotel accommodations and meals provided, while another aircraft is ferried in. All of which entail considerable expense and customer dissatisfaction.

Many engines are basically capable of being started under adverse circumstances, but are inhibited by the inherent limitations of the fuel control schedules, i.e., not customized to those specific unusual engine health circumstances. The adaptive system employed on the modern GE engines assure that the engines will start (with some sacrifice in start time) if they are inherently capable of being started.

The adaptive features employed effectively customize the fuel and ignition schedules and sequences so as to match the specifics of a particular engine problem. The design concept was intended to allow the aircraft to remain in service until it could be scheduled into an overhaul facility where the abnormality could be corrected.

These same concepts/features also make the control more adaptable to airstart situations, and more importantly (from the standpoint of this discussion) make the control adaptive to the arctic engine starting environment. All of this was accomplished with sensors previously applied for other reasons.

1.1 Basis of this Paper

Engine starting systems are specifically customized to the characteristics of each engine. Different CFM1 and GE engines employ somewhat different strategies. This paper represents a composite of the different approaches and is not intended to represent any one specific application.

Furthermore, the systems currently in use represent the current phase of the evolutionary nature of this concept. Some of the approaches discussed are not currently in use as they are deemed "not required" at this time, but have been tried/developed, and are known to work, if so required, in response to a specific set of circumstances associated with a particular engine.

1.2 General Operation

The FADEC automated start sequence integrates and automates all of the elements of the start sequence in response to a single command from the pilot.

- | | | |
|---|---|---|
| <ol style="list-style-type: none"> 1. Initiates Starter 2. Initiates Ignition 3. Initiates Fuel 4. Turns Off Ignition 5. Turns Off Starter 6. Programs The Appropriate Fuel Flow 7. Programs The Appropriate Start Bleed | } | Concurrently monitors
all safety instrumen-
tation. |
|---|---|---|

1.3 Manual versus Automatic

The aircraft system allows for both manual and automatic start mode. In the manual mode the pilot must sequence a number of switches, levers, etc., and monitor for proper system operation. This sets up the possibility of pilot error by not sequencing the system properly when in the manual mode, or improperly sequencing when in the automatic mode. Much of the FADEC logic involves the proper sequencing and appropriate action to inappropriate pilot manipulation of the throttle, aircraft fuel shutoff lever, etc.

1.0 INTRODUCTION (cont'd)

- 1.3.1 This paper concentrates on the unique features appropriate for starting engines under environmental and health conditions which presented difficult design conflicts/tradeoffs associated with conventional hydro-mechanical control systems.

2.0 OVERVIEW OF SYSTEM AND ITS RESPONSE TO UNUSUAL EVENTS

The system is intended to be adaptive to various unusual or special situations which are normally not encountered, but if experienced, usually result in an aborted start. It is the intent of these features of the GE FADEC system to circumvent the abnormality and still produce a successful start, although at a small sacrifice to start time.

2.1 General Description Of Ground Start System Sequence

The following presents an overview of the sequence of events and adaptive strategy employed. Details of this logic are described later in this paper.

When a start is initiated the following sequence of events is followed:

1. Starter Initiated
2. Ignition Activated At Appropriate RPM (before fuel admission)
3. Low Starter Assist Check
 - System Checks For Minimum Starter Assist just prior to fuel admission
4. Fuel Initiated At Desired Firing RPM
5. Check For Lightoff
 - Resequence Fuel and Ignition If Lightoff Is Not Detected
6. Check For Stall After Lightoff (and throughout start)
 - Resequence If Stall Detected
7. Check For Fan Rotation Before Reaching Idle
8. Check For Starter Air Pressure Interruption
 - Warn of possible high speed starter re-engagement.
9. Starter Shutoff and Ignition Off at Predetermined RPM.
10. Store In Memory Any Corrective Action
 - If Correction Required On Successive Series Of Starts, Remember Settings And Initiate Following Starts Using Stored Experience

2.2 General Description of Aerial Restart System Sequence

The air restart mode is similar to the ground start mode, but is different in several aspects of its operation.

2.2.1 Starter:

Different modes of operation are employed, ie., with or without starter assist, depending upon core windmilling rpm and other factors ie., such as:

- a. Flight condition
- b. RPM stable or spooling down
- c. Starter crash re-engagement prevention (interlock) if required by starter manufacturer.

2.2.2 Ignition Initiation Point:

Ignition is initiated at any rpm if the start is a windmilling start, but delayed until a predetermined minimum rpm is achieved if assist is employed.

2.0 OVERVIEW OF SYSTEM AND ITS RESPONSE TO UNUSUAL EVENTS (cont'd)

2.2.3 Fuel Initiation Point:

Fuel is initiated at any windmilling RPM if the start does not employ the starter, but is delayed until a minimum firing RPM is achieved if the starter is to be employed. In either case, fuel is never initiated until the ignition is initiated.

2.2.4 Light off detection/resequencing and stall detection/resequencing can be different from ground operation

2.2.5 Automatic fuel shutoff philosophy, in the case of light off failure, and stall recovery sequencing can be different in the air versus on the ground depending upon the airplane manufacturers preference.

2.3 Arctic Cold Weather Design Considerations

The arctic ground starting sequence of events is the same as the normal ground starting sequence, but embody some of the design considerations of air starting as well as ground starting.

2.3.1 Both occur at cold ambient temperatures conditions, i.e., -40 to -60°F.

- Ground starting can occur with both cold and warm fuel depending upon the cold soak time. Air starting rarely encounters extremely cold fuel due to elevated oil cooler temperatures
- This means that fuel viscosity can vary over a wide range and consequently the combustion effects can vary over a 50% to 100% range
- Engines can have radically different thermal conditions depending upon time since shutdown and windmilling time since shutdown.

2.3.2 The following table shows the variety of conditions that could exist at an engine inlet temperature of -65°F:

	FUEL TEMP.	AIR TEMP.	METAL TEMP.	START SITUATION
Ground Start	Very Cold	-65°F	Very Cold	Cold Start
	Mod. Warm	-65°F	Very Cold	Refuel With Warm Fuel After Cold Soak
	Cold	-65°F	Warm	Restart After Aborted Start
	Mod.	-65°F	Warm	Restart After Refueling
Air Start	Warm	-65°F	Mod. Warm	Spool Down Restart
	Mod. Cold	-65°F	Mod. Cold	Extended Windmilling

2.3.3 Engine Thermodynamic Characteristics Scale as classical ζ and ϕ factors, with combustion efficiency being approximately 98%. But, under arctic conditions, combustion characteristics can vary dramatically as a function of fuel viscosity and its effect on fuel nozzle spray pattern. This means that:

- Lightoff fuel requirements can change by 50-100%.
- After lightoff combustion efficiency can vary by 50%.

2.3.4 On some engines compressor stall can vary as a function of compressor metal temperature history.

2.3.5 Oil viscosity increases engine mechanical drag, and disappears as a function of total number of revolutions. This oil viscous drag is not present during air starting, but the effects of aircraft power extraction drag can be substantial during air starting particularly at low engine inlet pressure flight conditions.

3.0 STALL SENSING AND RESEQUENCING

3.1 Stall Sensing

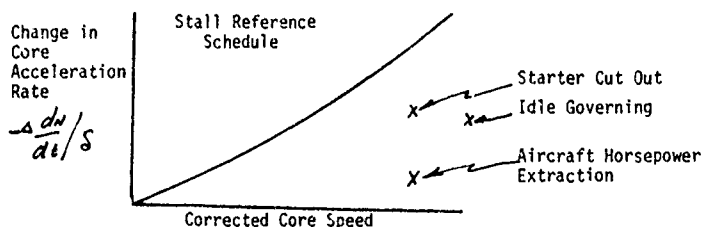
Start range stall is sensed by several means depending upon the stall signature characteristics of the specific engine and depending upon the operating environment (ground versus in-flight).

3.0 STALL SENSING AND RESEQUENCING (cont'd)

3.1.1 Ground Start Stall Sensing

Ground Start Stall Sensing comprises two independent sensing systems, $\Delta \dot{N}/\dot{a}_t$ and a "sliding" EGT limit.

- 3.1.1.1 The $\Delta \dot{N}/\dot{a}_t$ system senses a sudden decrease in core corrected rpm acceleration rate and compares it to a stall reference schedule as a function of corrected core speed.



- Since engine acceleration torque is a "corrected" parameter, the $\Delta \dot{N}/\dot{a}_t$ is biased as a function of engine inlet pressure.
- The key to this concept is to obtain an RPM versus time signal whose noise content is sufficiently low so that a good first and second derivative can be obtained.

In this respect, "many have tried but few have succeeded". The GE FADEC employs a very sophisticated mathematical approach to signal acquisition and processing which makes such an approach possible.

- This approach is applicable if the characteristic of the stall reaction signal is sufficiently strong so as to distinguish between the other events which also produce similar signals, i.e.,

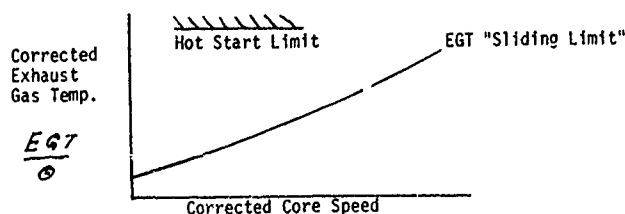
Starter Outout
Aircraft Accessory Load Application
Idle RPM Governor Action

- This concept can detect stall within 0.5 sec. of its occurrence and thus quickly prevent the adverse stress/overtemperature commonly associated with stall.

3.1.1.2 EGT versus core speed as a stall sensing signal.

The system also senses corrected EGT ($\frac{EGT}{\phi}$) and compares it to a schedule of stall EGT versus corrected core RPM ($N_1/\sqrt{\phi}$). (Referred to as the "Sliding EGT" limit).

- This schedule is designed to be higher than that expected during normal starting, but well below the temperature associated with a "hot start".
- The ϕ factor automatically bias the schedule for hot and cold day environmental conditions.
- This reference schedule is further biased to account for any residual EGT caused by previous engine history.



3.0 STALL SENSING AND RESEQUENCING (cont'd)

3.1.1.3 Other alternative approaches to stall sensing which consist of combinations of parameters could be employed during ground and/or air starting conditions where engine idiosyncrasies preclude the sole use of the $\Delta \dot{n}/\dot{n}_0$ or the sliding EGT limit approach. For Example:

- Moderately hot EGT and very slow acceleration rate.
- Low acceleration rate, moderate EGT, and elevated fuel scheduling.

3.2 Air Start Stall Sensing

Air Start Stall Sensing is accomplished differently, depending upon the nature of the stall pinch point.

3.2.1 Lightoff Stall

During air starting lightoff stall, the core RPM can continue to increase due to windmilling assist or due to starter assist. Because of the altitude effect on acceleration rate, the stall signature can be very low thus rendering the $\Delta \dot{n}/\dot{n}_0$ sensor impractical. Likewise, the Sliding EGT, reference schedule (reference paragraph 3.1.1.2) can be relatively low due to the effects of EGT/ ϕ at the cold ambient temperature associated with high altitude, low aircraft machine operation. Thus the sliding EGT limit may also be an inadequate stall indicator.

3.2.1.1 The high residual EGT immediately following an in-flight flameout, coupled with the low EGT reference from the sliding EGT limit, can sometimes produce an erroneous indication of stall. In that case the added intelligence produced by abnormally low core acceleration rate can provide the intelligence required to discern in-flight compressor stall.

3.2.2 "After Light-Off" Type Stall

The sensing of stall after light-off can be accomplished by sensing $\Delta \dot{n}/\dot{n}_0$ as per paragraph 3.1.1.

However, in flight, this is complicated when aircraft power extraction is applied because aircraft power extraction has a much stronger impact on core acceleration at altitude than it does at SLS.

If such is the case, the concept of the sliding EGT limit, biased by the residual EGT, and coupled with low core acceleration rate, is an appropriate indication of stall.

3.3 Stall Recovery Sequencing

3.3.1 Ground Starting Stall Recovery Sequencing

If a ground start stall is encountered, the following sequence is employed:

- o Interrupt the fuel for a short duration in order to break the stall. Continue to apply ignition and starter assist. Core rpm may either continue to accelerate, hang up or decelerate depending upon the relationship between unfired engine pumping torque and starter torque.
- o Lower the WF/PS3 ϕ fuel schedule a pre-determined amount.
- o Re-initiate fuel flow and monitor for light-off:

3.0 STALL SENSING AND RESEQUENCING (cont'd)

3.3 Stall Recovery Sequencing (cont'd)

3.3.1 Ground Starting Stall Recovery Sequencing (cont'd)

- o If the rpm is above normal starter cut out, adhere to the starter crash engagement limits, ie., do not re-engage the starter if RPM > 20%, but allow engine to coast down to the safe starter re-engagement RPM. Then initiate Fuel Flow
- o After light off is sensed, again monitor for stall.
- o If stall is again sensed, interrupt the fuel and further lower the fuel schedule.
- o If required, repeat the stall recovery sequence for a pre-determined maximum number of fuel decrements. If stall persists, abort the start. The pilot can then re-initiate the start sequence.

3.3.1.1 Anti RPM hang-up due to decremented fuel schedule

If stall free acceleration is eventually achieved, engine acceleration with the (stall free) decremented fuel schedule can be sluggish, particularly in the region above starter cut out rpm, or above aircraft load application rpm. If this occurs, the anti-hang up feature is activated which then slowly returns the fuel schedule to its original value.

3.3.1.2 The combination of the stall decrement strategy and the anti-hang up strategy have the effect of reprogramming the fuel schedule so as to "skirt around" an unusual stall "bucket".

3.3.2 Airstart Stall Recovery Sequence

The airstart stall recovery sequence employed can differ due to preference of the airframe manufacturer.

- o One aircraft manufacturer does not automatically resequence for any reason.
 - Their Basic Flight Safety Philosophy is:
 - If a stall is sensed, it is so annunciated to the pilot and requires pilot action to resequence the system.
 - No adaptive fuel reduction features are employed, but fuel enrichment for lean fuel rpm hang-up is available.
- o Another aircraft manufacturer does employ resequencing features due to their philosophy to "Make the System Fully Automatic" and consistent with ground operation.

3.3.2.1 Operational Conflicting Requirement

The following operational situations can be encountered during air starting.

<u>EGT</u>	<u>Accel Rate</u>	<u>Assumed Cause</u>	<u>Corrective Action</u>
Very High	Any	Stall	Resequence
Moderate	Moderate	No Stall	Not Required
Intermediate	Low	Stall	Resequence
Low	Low	Lean Hangup	Raise Fuel Schedule

3.0 STALL SENSING AND RESEQUENCING (cont'd)

3.3.2.2 Air start stall recovery sequencing strategy employed by FADEC is:

After 1st Stall	Interrupt fuel, lower fuel schedule
After 2nd Stall	Repeat first resequence (with additional fuel reduction)
After 3rd Stall	Repeat 3rd stall resequence (no additional fuel reduction)
Successive Stalls	Continue to resequence per 2nd stall

3.3.2.3 Anti-hangup feature in conjunction with stall resequencing

If the fuel decrement successfully clears the stall, and subsequent lean RPM hang-up is encountered, the fuel schedule is slowly increased until such point where sufficient accel rate is established.

3.4 Adaptive Strategy For Engines With A Repeated Ground Start Stall History

Depending upon the preference of the airplane manufacturer, adaptive features can be added which shortens the number of resequencing events required for each start. This feature is intended for use in commercial aircraft until the aircraft can be scheduled into an appropriate overhaul station.

Strategy

Each time an engine is required to be resequenced due to stall, the FADEC Logic.

- a. Determines the number of resequence tries required for success.
- b. Stores this in memory.
- c. When a subsequent start is initiated the number of tries is recalled and then a pre-programmed decision is made about the fuel schedule decrement to start out with.

4.0 LIGHTOFF SENSING

4.1 Light Off Sensing

Several means of sensing lightoff have been employed and are somewhat different between the two "GE" engine programs.

4.1.1 Sense a sudden, almost instantaneous increase in engine acceleration rate.

- Since a sudden, almost instantaneous increase in engine acceleration rate occurs at lightoff, the same $\Delta \dot{n}/\dot{n}_t$ signal used in stall sensing can be employed. This concept is applicable to both ground and air starting which both produce approximately the same signal level.

4.1.2 Sense a significant and sudden increase in EGT.

- Sense a sudden jump in EGT above the residual EGT level. The system therefore determines the residual EGT at the initiation of the start sequence and then looks for significant EGT increases above the residual value.

4.0 LIGHTOFF SENSING (cont'd)

4.2 Light Off Resequencing

4.2.1 Ground System

The GE commercial engines employ dual ignition source for both exciters and ignitors.

- o Normally, for longevity reasons, only one ignitor fires during a given start. The system alternates the excitor and ignitor pair after each successful start.

- o After the fuel is initiated, the light off detector circuit monitors for light-off.

- If light-off is not detected within a predetermined time, the system shuts off the fuel, motors the engine then fires both ignitors.
- The system then re-initiates fuel and monitors for light-off.

- o If failure to detect L/O is again encountered, the fuel off, motor, and fuel on sequence is repeated (using both ignitors).

This sequence is repeated several times depending upon airplane manufacturer preference) after which the system declares a "false start" and the start terminated.

- o Because longer than normal light off delays can routinely occur during air starting and during arctic starting, additional "time to light off" is allowed under these circumstances.

4.2.1.1 The GE Commercial engines do not require additional light off fuel flow to compensate for light off failure. However, other alternatives could easily be applied depending upon, the specific light off characteristics:

- Additional light off fuel flow could be employed on each successive start by:
 - a. Additional incremental step in minimum fuel flow
 - b. Time ramp increase minimum fuel flow after each L/O resequence.

4.3 Cold Ground Starting Light Off Resequencing

- o Experience to date on both commercial engines has shown that the elevated fuel associated with the normal W/P3 scheduling along with the increased allowable light off delay time is adequate when used with the resequence described in paragraph 4.2.1.

- o More sophisticated logic circuits employing incremental increases in light off fuel are programmed into FADEC for future use, but are disarmed at this time. If required at a future date these strategies could be easily activated.

4.4 Air Starting Light Off Resequencing

Light off resequencing can differ between engine programs due to air start light off characteristic differences

- o Currently neither GE engines employ any adaptive air start light off features.

- Since air starting can be an emergency situation, both ignitors are immediately employed.
- Because of the windmilling airflow effect, no fuel purging is required.
- If light off is not detected within 20 seconds, light off failure is annunciated and the system relies on pilot action to resequence.

4.0 LIGHTOFF SENSING (cont'd)

4.4.1 Other adaptive features that could be employed

At extreme flight conditions, air start light off can, on some engines, involve design conflicts between the requirements for elevated light off fuel flow and the subsequent lower fuel required due to the compressor stall characteristics that develop after flame propagation. The ability to detect light off within 0.5 seconds (by the use of the delta acceleration rate sensor) makes possible the resequencing strategy which temporarily raises light off fuel flow until light off is sensed, but then rapidly restores normal min fuel flow.

5.0 FUEL SCHEDULING FEATURES

In the past, the design of fuel scheduling associated with hydro-mechanical control systems has been a compromise between different conflicting circumstances because

$W_p/P_{s3} \phi^n$ versus $N_1/\sqrt{\theta}$ was used as the fuel scheduling and primary stall avoidance parameter.

Since W_p/P_{s3} is not a direct sensor of compressor stall, it is subject to other influences.

- Combustion efficiency variations due to fuel viscosity, altitude pressure, engine metal temperature, etc.
- Varying compressor stall characteristics produced by engine thermal history scenarios.
- Thermodynamic cycle variations due to ram pressure ratio effects (i.e., during air starting).

Unusual combinations of these situations can occur at cold air temperatures, i.e., below -20°F ambient. (reference. Paragraph 2.3.2).

Thus, scheduling W_p/P_{s3} as a function of core rpm and engine inlet temperature is insufficient control intelligence to do the optimum job that is possible with digital controls.

5.1 FADEC General Approach

The computing and scheduling flexibility of the FADEC now makes it possible to do a better job of bringing all of these elements together. Thus promoting a better more reliable system concept, as follows:

1. Design for the normal (or routine) situation encountered during operation in the three major environments.
 - Normal Ground Start
 - Arctic Ground Start
 - Air Starting
2. Use special override features under non-normal circumstances.
3. Where appropriate, or where design conflicts still exists, or where stall risk still exists, use the stall sensing/resequencing, or failed lightoff resequencing and anti-hang up features to override the fuel scheduling features.

Thus, the fuel system becomes very forgiving by adopting the philosophy of scheduling the prime parameter, raising it for additional circumstances, and then if all else fails, using the lightoff/stall resequencing as a final authority override.

5.2 Ground Stall Strategy (normal ambient temp range)

1. Use conventional $W_p/P_{s3} \phi^n$ fuel schedule coupled with a fixed minimum fuel flow as the primary lightoff fuel criteria and during the initial RPM region.
2. Above this RPM use acceleration rate versus corrected core speed as the prime mode.
3. Override the acceleration rate scheduling with the $W_p/P_{s3} \phi^n$ versus $N_1/\sqrt{\theta}$ topping schedule, designed primarily as a stall protection circuit.
4. Design the topping schedule per 60°F day and use normal $S_{AND} \phi$ factors to compensate for ambient pressure and temperature variations.

5.0 FUEL SCHEDULING FEATURES (cont'd)

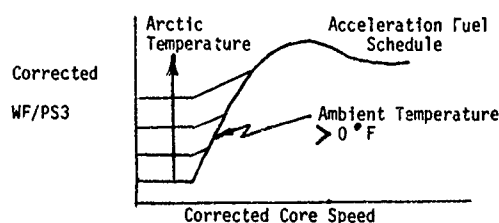
5.2 Ground Stall Strategy (normal ambient temp range) (cont'd)

Bias this W/P_3 schedule downward to compensate for non-normal effects of Engine Thermal History

- Some engines have a depressed compressor stall line when the engine is at an intermediately thermal conditions (i.e., not cold, not hot, but warm).

5.3 Arctic Ground Start Strategy

- 5.3.1 Design the stall protection portion of the fuel scheduling circuit higher at very cold temperature days, i.e., arctic conditions based on the poor combustion efficiency, associated with cold ambient and cold fuel. Assume the engine is thermally stable at cold soak conditions.



- 5.3.2 Provide an additional bias over-ride features so that the base schedule is modified downward to account for the residual engine thermal effects of recent engine running such as:

- Increased combustion efficiency associated with warm fuel produced by a residual of warm oil in the oil cooler.
- Engine Thermal History

The signals associated with establishing the engine thermal condition and oil temperature, and/or fuel temperature are available from other portions of the FADEC system.

- 5.3.3 Increased lightoff fuel flows are usually required, and are subject to the same variety of environmental and operational considerations defined in paragraph 5.0. The details of these requirements are expected to be a function of the specific engine fuel injection system design.

- The GE FADEC systems have been successful with the increased lightoff fuel flow produced by the raised W/P_3 schedule. However, other engines may need additional compensating circuits. (reference, paragraph 5.3.2).
- These compensating circuits can take various forms.
 - Raise minimum fuel flow as a function of fuel temperature, oil cooler temperatures or other indication of fuel viscosity.
 - Ramp increase minimum fuel flow as a function of time (only with very cold fuel conditions).
 - Ramp increase, or time step increase the min. fuel flow but immediately reduce it to a lower level (i.e., within 1/4 - 1/2 second after lightoff so as to be commensurate with stall-free operation.
- There are a variety of other schemes that could be employed depending upon the specific idiosyncrasies of the engine design.

5.0 FUEL SCHEDULING FEATURES (cont'd)

5.3.4 Quite often, the precise combustion efficiency effects of fuel temperature and air temperature are poorly defined. In such situations the following strategy can be adopted:

- Error in the direction of rich fuel scheduling
- If stall is encountered, employ the stall sensing and resequencing feature
- Employ the air start anti-hangup concept if needed.
- Enrich the fuel if the EGT is cool and rpm acceleration rate is slow.

5.4 Air Start Strategy

5.4.1 The same conflicting factors associated with arctic ground starting exist in the air start region, but in different combinations:

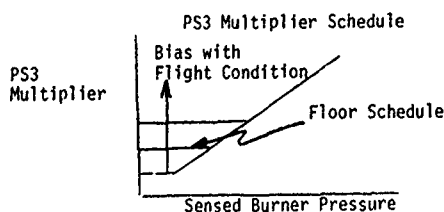
- Combustion efficiency during air starting is usually closer to that associated with normal ground starting than it is to arctic ground starting even though similar engine inlet temperatures are encountered.
- Cold fuel temperature has a greater influence on combustion efficiency than does cold air temperature
- Fuel temperature is determined by oil cooler temperature which is always warm during air starting conditions as contrasted with cold oil during arctic ground starting.
- The fuel schedule design strategy employed is to design for the arctic situation which infers a higher W_f/P_3 , and then provide a bias function which lowers the schedule as a function of a parameter indicative of fuel temperature and/or flight condition.

5.4.2 Lightoff is generally the most stringent constraint during air starting.

- Lightoff fuel flow is generally set by the minimum fuel available at the special flight condition.
- FADEC provides a range of minimum fuel flows as a function of flight condition.
- Min W_f is established by the requirements to achieve proper atomization at the fuel nozzle in order to achieve good light off and flame propagation. Physical min WF can become excessively high corrected fuel due to the effects of engine inlet pressure, thus reducing lightoff stall margin.
- The windmilling effect of aircraft ram pressure ratio (P_2/P_0) has the beneficial effect of raising the apparent corrected fuel flow required for stall and helps compensate for decreased lightoff stall margin.

5.4.2.1 The GE FADEC establishes lightoff fuel flow by the limiting item of one of two features:

- a. Minimum fuel flow scheduled as function of engine flight conditions
- b. Minimum PS3 multiplier floor schedule.
 - The primary control logic schedules $W_f = f(PS3 \times W_f/PS3)$
 - Conventional hydro-mechanical controls schedule a fixed minimum value of the P_3 multiplier circuit called the floor schedule.
 - This same concept is employed by FADEC.



5.2 FUEL SCHEDULING FEATURES (cont'd)

5.4.2.1 (cont'd)

- FADEC provides the capability to manipulate the fuel schedule and thus lightoff fuel flow. The GE commercial engines currently do not require a bias of the fuel schedule, but FADEC is capable of doing so, if required in other applications.

5.4.3 The corrected fuel flow $W_f / \sqrt{\theta}$ required because of lightoff atomization considerations (flame propagation) may be excessive after lightoff due to stall considerations. Because of the availability of the extremely rapid action light-off sensor, it is possible to rapidly reduce lightoff fuel flow after lightoff but before stall is developed. This feature is not currently employed, but available for activation, if required by a specific engine.

5.4.4 Slow acceleration or "RPM hangup" can occur in the air start region due to two factors:

1. Inadequate fuel because of:

- Aircraft power extraction effects
- Inexact knowledge of the required fuel which can occur at flight extremes and/or obscure conditions.

2. Compressor stall

5.4.5 Anti-hang up strategy

5.4.5.1 If slow acceleration is encountered, features can be employed that determine whether the slow acceleration is due to inadequate fuel flow or compressor stall.

5.4.5.2 If the slow acceleration is produced by low fuel flow, the anti-hangup circuit slowly increases fuel flow, overriding the other fuel computations, until a minimum core RPM accel rate is produced.

5.4.5.3 If the rpm hangup is caused by compressor stall, the adaptive stall recovery strategy is activated.

NOTE: This feature has the potential for significantly increasing the unassisted portion of the air start envelope.

6.0 Starter Usage Strategy During Air Starting

Air starting is usually divided into two regions: Windmilling and starter assisted.

- o Starter assist is required when windmilling rpm is less than 10-20% depending upon the engine. If windmilling RPM is low, the starter is activated immediately, but ignition and fuel are delayed until the engine accelerates to a safer firing RPM.
- o If windmilling RPM is greater than 20%, starter assist is not employed.
- o The situation is further complicated by the engines state and the starter energy supply availability when the start is initiated
 - The starter may or may not be available depending upon the status of its energy supply.
 - The engine can be windmilling (stabilized) or spooling down depending how soon after shutdown that the start is initiated.
 - In either case, windmilling versus spool down restart, the FADEC logic does not apply starter assist unless the rpm is below the safe starter engagement RPM.

ACKNOWLEDGMENTS

This author wishes to acknowledge the assistance of Mr. Daniel J. Rundell for his contribution to the "state of the art" of establishing the mathematical approach required to determine the second time derivations of engine rpm and to Mr. Robert L. Mayer, who applied the basic concept to the CF6-80C2 engine, creating several of the strategies described herein, and who is my co-inventor of the patent for this product. In addition the author wishes to acknowledge the efforts of Kevin H. Kast, Jon S. Smith, Scott P. Jolliffe and Tom V. Ny who have worked to refine the initial concept into an operational product.

NOMENCLATURE - List of Symbols

1. Θ Engine inlet total temperature ($^{\circ}\text{F}$) divided by standard SIS temperature (519)
2. ξ Engine inlet pressure (PSIA) divided by standard SIS pressure (14.7)
3. N_c Core RPM
4. N_c/\sqrt{e} Corrected Core RPM
5. $\frac{dN}{dt}$ Core RPM acceleration rate (RPM/SEC)
6. $\Delta \frac{dN}{dt}$ Change in core acceleration rate
7. $\Delta \frac{dN}{dt}/\sqrt{e}$ Corrected change of core acceleration rate
8. EGT Exhaust gas temperature
9. W_f Fuel flow
10. PS_3 Compressor discharge pressure
11. W_f/PS_3^0 Control acceleration fuel schedule parameter

Discussion**1. I. Kurzke, MTU**

How long does it take to modify a control schedule getting all signatures?

Author:

Development units are done immediately under control of the engineering manual application. Production units can modify only quality control, with all of the delays associated.

2. C. Rodgers, Sundstrand Power Systems

What cases of failed starts did you have?

Authors:

None, but we had some hardware problems, not very many considering 600-700 starts a day. We still use the APU and consequently had no battery power problems. We fired at

20% speed, and within some tenth of a second we know whether we had a minimum acceleration rate. If not and if a subsequent stall is encountered we stop the start and fix the APU.

3. H. Saravanamuttoo, Carleton University

You mentioned the need to airstart after extensive time of windmilling, following the shut-down of a second engine. Could you please elaborate on the type of aeroplanes and the cause of incidents?

Author:

On commercial aircraft which employ 2, 3, 4 engines, a flame-out in flight may occur for a wide range of factors. All of them include engine maintenance cost considerations. Thus an engine could be shut down early in the flight for precautional reasons. If an additional engine is shut down later in the flight, particularly for more serious reasons, it may be desirable that the initial engine may have to be restarted after extended windmilling conditions.

COLD START INVESTIGATION OF AN APU WITH ANNULAR COMBUSTOR AND FUEL VAPORIZERS

by

K.H. Collin
Thermodynamics and Performance Department
K. Piel
Consultant
KHD Luftfahrttechnik GmbH
D 6370 Oberursel, Germany

Summary

The paper deals with the combustor of the APU for the "Tornado" fighter aircraft. As this APU has to cope with the narrow space in the fuselage it must be of small size. An annular combustor is favourable as it is short and can be integrated into the envelope of the outer diameter. The fuel vaporizer system is chosen because of its great advantages with combustion.

The paper describes the ignition process which is difficult as no fuel is actually vaporized when the start is initiated. Theoretical background and experimental steps of a development programme are reported. The result was perfect starting of this system down to -40°C and a very high "First Start Reliability" which means no false start leading to several start procedures.

1. Introduction

An APU (Auxiliary Power Unit) is installed in an aircraft to provide secondary energy for one or more of the following tasks.

- On ground an APU has to deliver shaft energy for electrical generators, for hydraulic and fuel systems. In addition it has to deliver bleed air for starting the main engine as well as for air-conditioning.
- As soon as the aircraft is airborne some APU's have to be able to work as standby emergency power sources.
- With the initiation of the landing procedure the APU may again - with some applications in case of emergency it has to - take over all secondary energy in order to relieve the main engine of secondary loads.

Several facts have influence on the operation of an APU. The main aspects are:

- Design of the APU
- Design of the secondary power system of the aircraft
- Operational requirements for the APU
- Requirements for special types of fuel and oil
- Influence of ambient climate conditions and altitude.

Regarding low temperature environment conditions we have to consider two phases of operation of an APU

- Starting the APU even at extreme low temperature conditions
- Running the APU

During the Prototype-Testing of this aircraft, the first phase - starting the APU at low temperature conditions - showed that sometimes two or three start attempts had to be conducted before a successful start was reached. For Production aircraft this was contrary to the user's requirements which stipulated:

- high start reliability which meant no false starts leading to several start procedures: "First start reliability".
- no special preparations before starting like
 - pre-cranking of the rotor
 - pre-heating of the oil
 - pre-pressurization of fuel
- short starting and run up time

For the second phase - running the APU at low temperatures after successful starting - no problems have been experienced: as the air intake of the APU T 312 is located under the body of the "Tornado" aircraft and the opening with the hydraulic operated flap is showing to the ground, there is no danger with ingestion of hail and only small amounts of rain and snow enter the APU. Experience has proved perfect running of the APU. Therefore this Paper deals with the development and experience connected with the first phase of APU operation, i.e. starting at low temperature environments.

2. Auxiliary Power Unit (APU) T 312

2.1 General Description of the APU

The requirements of the secondary power system of the aircraft, which are important for defining start and operation of the APU are:

- small size and weight of the APU
- limited battery capacity in the aircraft
- short starting time for immediate aircraft start
- high starting reliability: "First start reliability"
- same types of fuel and oil as for the aircraft
- immediate delivery of oil with high pressure to a dry friction clutch connecting APU and the gearbox of the aircraft
- no in flight operation required.

For ground operation such as pre- and aft-flight check of the aircraft systems, for stand-by and for starting the main engines via a hydraulic torque converter, the APU delivers the necessary energy as mechanical shaft power. This is transmitted into the gearbox by the clutch which will be automatically engaged as soon as the APU has nearly reached its 100 % speed after start up. To complement these design features the APU T 312 has been defined as a single shaft gas turbine engine. Besides other characteristics, for example the constant output speed, such a single shaft APU has the great advantage of low weight and small size.

Fig.1 shows a cross-section with the main components: A two stage axial-radial compressor, reverse flow annular combustor, two stage turbine, exhaust duct and a planetary type gearing which reduces the output speed to 8.000 rpm. The APU has its own oil pumps, which deliver oil for lubricating the bearings and gearing as well as supply high pressure oil to the clutch. The oil reservoir is in the aircraft mounted gearbox to which the APU is connected. The fuel supply is controlled by a hydraulic governor. The starting sequence as well as overload and overspeed protection are achieved by an integrated Electronic Control Unit.

Dimensions of the APU are: Overall length is 510 mm, including all accessories the diameter is 380 mm. The rated shaft power is 105 kW for continuous running with a 10 % short time contingency power. The ratio of rated power to weight is 2.7. [1]

2.2 Description of the Combustor Design

As the combustor of the APU is of great importance to the starting procedure, it will be depicted here in more detail. The combustor, see Fig.3, is of the reverse flow type. This type allows short engine dimensions. For small gas turbines like the APU T 312 an evenly spray pattern of the fuel cannot be reached with atomizer nozzles since a considerable amount of fuel will be spilled onto the walls of the combustor. Fan sprayers as they were used with some gas turbines may be one solution. At a number of other gas turbine manufacturers greater experience, however, were gained with vaporizer nozzles. Therefore this type of fuel injection was chosen.

Advantages of vaporizer nozzles:

- low fuel pressure system
- excellent combustion because of pre-vaporization of fuel in the vaporizer canes by heat transfer from the primary zone in the combustor
- good maintainability
- low cost

A serious disadvantage, however, exists:

- bad starting at low temperatures and in altitude. The reason for this is poor or even no fuel vaporization at these conditions.

As can be seen in Fig. 2 the dome of the reverse flow annular combustor carries 12 vaporizer nozzles and 3 starter nozzles in 4⁰⁰, 8⁰⁰ and 12⁰⁰ position. The compressor outlet air enters the combustor through bores directly. For film cooling of the walls an air-layer is directed through rows of small holes combined with deflector rings. After an elbow bend of 180 ° the stream of hot gases leaves the combustor and enters into the first turbine nozzle. Fuel is injected into the 12 vaporizer nozzles through thin pipes. During the starting period of the APU ignition is initiated by three ignition nozzles, i.e. one torch igniter in 12⁰⁰ position and two stabilizer nozzles in 4⁰⁰ and 8⁰⁰ position.

A torch igniter is shown in Fig.4. It consists of an atomizing swirl type spray nozzle combined with an electrical high energy spark plug. An oval shielding tube reaches through the turbine housing into the wall of the combustor. The ignition spray nozzle and the igniter plug are assembled on the shielding. A stabilizer nozzle consists of an atomizing swirl type spray nozzle only and is shown in Fig.5. The design is similar to the torch igniter.

3. Theoretical Analysis of Starting

3.1 Balance of Torques

The cold starting condition depends upon the "balance of energies" which prevails during the starting phases.

The balance of torques is described as:

$$\text{Driving Torques} - \text{Drag Torques} = \text{Acceleration Torque}$$

In Fig. 6 and 7 the torques on the turbine shaft versus turbine speed are shown for the early design of the APU with only one ignition nozzle, i.e. a torch igniter at 8⁰⁰ position.

Curve 1 : torque of starter motor
 Curve 2 : turbine torque
 Curve 3 : acceleration torque

Curve 2 is the combination of all drag torques and - after the combustor has lighted - the sustaining torque of the turbine wheels. The acceleration torque, curve 3 reveals a great difference between normal temperatures, +15 °C and lower ones, e.g. -20 °C. At +15 °C ambient temperatures there is sufficient surplus torque for acceleration (0.8 Nm). At -26 °C this surplus torque is already very little (0.1 Nm). At temperatures below -26 °C there will be no acceleration torque, that means a "hanging start".

The elements which influence the balance of the torques are following:

Driving Torques

- Starter motor
 This torque is dependent on the size of the starter motor and capacity and charge of the battery which is aboard the aircraft. Both their sizes, i.e. of starter and battery, are limited by the overall design and weight limits.
- Combustion of fuel
 Tests have shown that a completely "lighted up" combustor will result in a sufficient energy release. However with decreasing temperatures light up procedures of the combustor becomes more and more difficult.

Drag Torques

- Ventilation of compressor and turbine
 These losses cannot be reduced once the basic design has been frozen. All the worse, with decreasing temperatures the ventilation losses of the compressor increases because of higher density and mass flow of the air due to the laws of similarity ($N \propto T$) and ($m \propto T/P$).
- Bearings
 These losses can definitely be reduced by use of ball and roller bearings instead of sleeve bearings. In the APU all bearings with the exception of pump bearings are ball or roller bearings, compared with sleeve bearings their losses raise with increasing viscosity less.
- Sealings
 It was already the intention with the basic design to minimize losses by use of labyrinth-sealings wherever possible. With decreasing temperatures, however, a certain shrinking as well as in other places rubber sealings has been considered.
- Gears
 Here the losses are negligible, with lower temperature they may increase a little because of the oil viscosity.
- Fuel pump
 With the choice of vaporizer nozzles a low pressure fuel system already results in rather small losses.
 Even for spray nozzles like the igniter and stabilizer nozzles the pressure need not be higher, especially as the flow range is limited to the starting phase. The vaporizer system including the igniter and stabilizer nozzles requires only 15 bar pressure compared with approximately 60 bar for a fully swirl type system.
- Oil pumps
 Here the viscosity influence is significant. The losses are proportional to the delivery pressure which increases when flow resistance raises with higher viscosity. Therefore deloading the pressure oil pumps would be helpful.

3.2 Combustion Techniques

3.2.1 General Theories

During the start - especially at low temperatures - the sustaining torque of the combustion energy plays the important roll. The aim must be an immediate ignition and a high efficiency of the combustor.

The ignition of combustors with a vaporizer system is initiated by a torch igniter and sometimes stabilizer nozzles. Combustion efficiency of this type of combustor is influenced by the quality of atomization.

Another influence is the type of fuel. As soon as the torch igniter and stabilizer nozzles are burning the vaporizer nozzles should also start burning. Below a certain temperature the heat for evaporation has to be induced by the torch igniter and stabilizer nozzles.

Another influence of the ambient temperature in connection with the fuel/air ratio of the APU is shown in Fig.8. The turbine speed represents the amount of air delivered from the compressor. Here again the inflammability of fuel depends on the torch igniter and stabilizer nozzles.

3.2.2 Combustion Techniques of APU T 312

Applying the general principles of the ignition theories to the APU T 312 it can be said that reliable starting at low temperatures requires early ignition of all three igniter nozzles to warm up the vaporizer nozzles and inflame there as much fuel as possible. The envelope which allows combustion, however, is limited by local conditions of lean or rich fuel/air ratio. The total fuel flow to the ignition and vaporizer nozzles is scheduled by the fuel control dependent on the CDP (compressor discharge pressure). This fuel flow is shown in Fig. 9. It can be seen that at a CDP up to 1.5 bar a constant quantity of 24 l/hr is scheduled. It shall be noted, that an engine speed is assigned to the compressor discharge pressure 1.5 bar, which depends on the compressor inlet temperature and corresponds to the following values:

Compressor inlet temperature T_0 [°C]	-26	+25
Engine speed N [%]	44	51

The scheduled fuel of 24 l/hr is split by means of a flow/pressure divider within the fuel control unit into 14 l/hr to the ignition nozzles and 10 l/hr to the vaporizer nozzles. Furthermore it has been found by testing that some of the fuel injected through the ignition nozzles is sprayed on the walls of the combustor as can be seen from Fig.10. Calculations have been performed to find out the fuel/air ratio. Only those inlet openings in the combustor which are in the spray area contribute air to the fuel of the ignition nozzles. This air together with the fuel results in a local fuel/air ratio which is dependent on turbine rotor speed. These ratios have been calculated as well as the fuel/air ratio in the vaporizer nozzles. Results are represented in Fig.11. Curve "A" reflects the conditions in the vaporizer nozzles, but this curve does not apply to the first phase of the starting cycle, because the fuel is not vaporized yet. Curves "B" and "C" are related to the ignition fuel nozzles. It shall be noticed, that with insufficient fuel/air mixture, caused by wetting of the combustor walls, the combustible range is reduced by leaning-out.

In summary it can be said that for successful starting it is necessary to reduce the drag torques and to increase the driving torques: Therefore two tasks have to be solved to guarantee at low temperatures reliable starting of this APU with the vaporizer system in the combustor:

- Improvement of good and complete light up of the combustor during the early starting phase.
- Decading the pressure oil pump as long as possible but safeguarding lubrication to the bearings.

Some essential markings have been entered in Fig.11.

- 1) Range, in which the maximum fuel pressure at the ignition fuel nozzles and the nominal fuel flow is reached,
- 2) Maximum cranking speed without ignition
- 3) Switching to fuel control algorithm and end of range in which fuel quantity is constant
- 4) Shut down of ignition fuel nozzles
- 5) Combustion range to be expected at homogeneous fuel/air mixture.
- 6) Cut out of starter motor and electrical ignition

It can be seen from Fig.11 that exceeding a certain speed without a pilot flame has been ignited (because of late fuel supply etc.) the fuel/air mixture fails to be ignited due to leaning-out. So it shall be considered as essential, that either

- the maximum fuel pressure for the ignition nozzles will be reached at low speed, or
- the local fuel/air ratio of the ignition nozzle at 12° position will be increased.

4. Test Results

The tests had to cover the whole operational range of the APU, which are:

Ambient temperatures -40 °C up to +52 °C, Fuel temperatures -40 °C up to +70 °C
(in some cases up to +90 °C)

Type of fuel: AVTUR (Kerosine type, Jet A-1, F 35)

AVTAG (Wide range, JP 4, F 40)

Type of oil: Synthetic lubricating oil, 5 cSt, MIL-L-23699

Main emphasis had been given to testing the starting ability at low temperature environment conditions. As an APU cannot get any easment preceding a start -e.g. pre-cranking- test conditions had to be assessed as realistic as possible. This meant for each start at low temperature that the APU had to be soaked long enough these ended up in rather long cold-soaking-periods, at -40 °C, this were 3 hrs minimum.

On the other hand all design changes or changes in adjustments, e.g. change of fuel setting, had also to be tested at high temperature environment to ensure that no detrimental effect could occur. As an example: influence of different fuel settings in regard to compressor surge or stall.

Besides the above mentioned limitations, for all test procedures and subsequent design changes the basis was defined by the analysis as explained in the preceding chapters.

Low parasite losses, i.e. low drag torques during start up.

Optimization of the combustor, i.e. correct fuel/air ratio for igniter and vaporizer nozzles

In order to give a condensed information two test configurations in the sequence of development will be presented together with their design status.

1. First experimental design with only one igniter nozzle
2. Production standard design with three igniter nozzles

4.1 Optimization of Drag Torques

It was already reported in chapter 3.1 that there could not be a reduction of the drag torques. Except the oil pump torque could be reduced by deloading the oil pressure.

According to the system specification the APU had to deliver an oil flow with a pressure 30 bar in order to serve the pressure for the clutch. This clutch is necessary because a single shaft APU cannot be loaded during the start.

The viscosity of the specified type of oil, MIL-L-23689, increases by a factor of 150 when the temperature decreases from +15 °C to -40 °C. As a result of this the drag increases. Fig. 12 displays the rotor drag lines for both temperatures. The performance of the electric starter motor is nearly constant over this temperature range resulting in steady-state cranking speeds of 3 % at -40 °C and 20 % at +15 °C. Due to the APU control system the fuel does not begin to flow before 8% speed is reached. Therefore additional steps had to be taken to safeguard APU light up with temperatures down to -40 °C. Tests had shown that the oil pressure of 30 bar already builds up at 2 % speed, because the pipes had to fill up. Therefore a device was developed to deload the pump during the starting phase, still ensuring full pressure in time for clutch engagement. During the whole procedure, however, a level of pressure is maintained in order to guarantee the lubrication of the APU. With the modified oil system the oil pump is deloaded during the starting phase by a valve which is electrically switched to "load conditions" at 48 % APU speed. The result will be a greater acceleration torque on the turbine shaft as is shown in Fig. 13 (comparison with Fig. 7). With earlier and complete light up of the combustor the ascending part of curve 2 (Turbine Torque) shifts to the left, curve 2a. The accelerating torque, curve 3 raises to 3a. With this a reliable start and shorter starting time will be reached.

4.2 Optimization of the Combustor

It was explained that reliable starting at low temperatures requires early - i.e. at low APU speed - ignition of all three igniter nozzles. These will then warm up the vaporizer nozzle and inflame the fuel.

Most aggravated conditions were chosen for the tests in order to cover all environmental and operational conditions.

- for cold and normal temperatures lowest battery charge, 1 Volt/35 Amps, i.e. min power supply to the starter motor,
- for high temperature max. battery charge, 1 Volt/70 Amps.
- Fuel pressure head 0,019 bar representing lowest level in aircraft tank.
- Fuel type
 - Jet A-1 for cold and normal temperatures
 - JP4 for high temperatures.

These fuels were selected for the different temperature ranges because of the data of volatility and vapor-pressure. The underlined values in the following table indicate the most adverse properties:

	Begin of volatility	vapor pressure
Jet A-1	<u>+178°</u>	0,04 bar
JP 4	+ 66°	<u>0,64 bar</u>

Jet A-1 has worse condition for starting the engine at cold ambient temperature because there is a large difference in fuel and volatility temperature. JP4 is critical at high ambient temperature because vapour pressure is in the same order of suction pressure of the fuel pump.

For some tests 6 thermocouple-probes had been installed in the combustor as is shown in Fig.14. With this arrangement the light up sequence in the combustor could be well assessed.

Test 1

Test conditions:

Ignition: only torch igniter at 8⁰⁰ position
 Ambient Temperature: -40 °C, 3 hrs soaked
 Fuel: Jet A-1
 Battery: min charge

The test traces, Fig.15 show temperatures of the 6 probes TC_{1...6} and their position in the combustor, average exhaust gas temperature TE and turbine speed N.

Discussion of test result.

The turbine speed raises very slowly: after 25 seconds the speed is only 22 %, although TE is already 900 °C. The temperature indications of the six probes, however, show the actual situation within the combustor. Initial ignition is after 1.5 seconds. Looking at the positions of the torch igniter 8⁰⁰ and the six probes (below right in Fig.15) we see that probes 1, 2 and 3 indicate immediate increase, 1 and 3 stagnate, 2 and 6 climb further on. For probe 1 there is no full inflammation, because the spray angle of the 8⁰⁰ nozzle is too narrow: the vaporizer is not heated up enough.

Probes 1, 3, 4 and 5 are very slow, slowest is 5: it does not reach a temperature increase of 100 °C before 38.5 seconds. This figure has been taken as an indicator: Ignition Delay Time 100°: IDT 100 = 38.5 seconds. The explanation for the increase of TE after 25 seconds can also be clearly explained: fuel is not burning within the combustor but is atomized later on by turbine disks and burns in the exhaust duct where TE probes are positioned. The analysis of this test showed that the initial flame of 8⁰⁰ torch igniter did not heat up the far off side (3, 4, 5) of the combustor, air/fuel ratio of homogenous mixture was very lean. Therefore first start reliability was poor. Once the combustion chamber had warmed up with the first start, the second or third start was 25 seconds.

The conclusion of this test was:

Three igniter nozzles-instead of one equally spaced at 4⁰⁰, 8⁰⁰, 12⁰⁰ with the torch igniter at 12⁰⁰ position because of maintenance reasons

Test 2

Test conditions:

Ignition: 3 starter nozzles
 Ambient Temperature: +10 °C
 Fuel : Jet A-1
 Battery : min charge

This test series was now conducted under normal ambient temperatures to find out the effect of the three igniter nozzles.

The test traces Fig.16 show the temperature indications of the six probes (note different positioning compared with test 1!). The delay time of probe 5: IDT 100 = 11 seconds.

The start up time of 24.5 seconds as well as "First Start Reliability" was still marginal.

The analysis of this test showed that the air/fuel ratio of the igniter nozzles were not sufficient. Therefore a rather wide test series for optimizing these conditions were performed. The result was:

- Increase of the fuel flow to the igniter nozzles
- Change of arrangement of the spray nozzle and the igniter plug of the 12⁰⁰ torch igniter.

The design features were already shown in Fig.4.

Test 3

Test conditions:

Ignition: 3 starter nozzles, optimized flow and optimized arrangement
Ambient Temperature: +15 °C
Fuel: Jet A-1
Battery: min charge

The test traces Fig.17 show much faster ignition and complete light up of the combustor. The delay time, probe 6, is IDT 100 = 6 seconds, start up time is 12.5 seconds. A very important characteristic of this optimized design was, that also at max. dry cranking speed (20 %) ignition was possible.

With this configuration (Test 3) cold and hot chamber tests were performed. Since these tests were "Official Qualification Tests" the APUs were not equipped with the six probes in the combustor. Therefore only the general results can be reported.

Test 4

Test Conditions

	Ambient Temp.	Fuel	Battery	Start time to
			charge	100% speed
Test 4.1	-40 °C	Jet A-1	min	24 seconds
Test 4.2	+70 °C	JP 4	max	12 seconds

Test 4.2 was necessary to proof successful operation at high temperatures. All test results of the complete programme are compiled in Fig.18. First start reliability including all endurance tests was in the range of 98 %. This was achieved mainly to the fact that even with late fuel supply, e.g. because of air bubbles in fuel supply line, the ignition at max. dry cranking speed was successful. With normal fuel conditions the specified max start up time of 30 seconds was also achieved.

5. Conclusion

A combustor with a fuel vaporizer system cannot be started without an auxiliary ignition system because there is no vaporization during the starting phase. With the APU for the "Tornado" fighter aircraft a programme was initiated for a thorough improvement of the start capability at low temperature environment. Theoretical analysis combined with a test programme resulted in successful starts of the APU down to -40 °C. Besides this the user's requirements for "First Start Reliability" could be met.

References

- [1] K Piel: Experience with the KHD APU T312 for a modern Fighter Aircraft, AGARD Conference Proceedings No.324 Engine Handling.

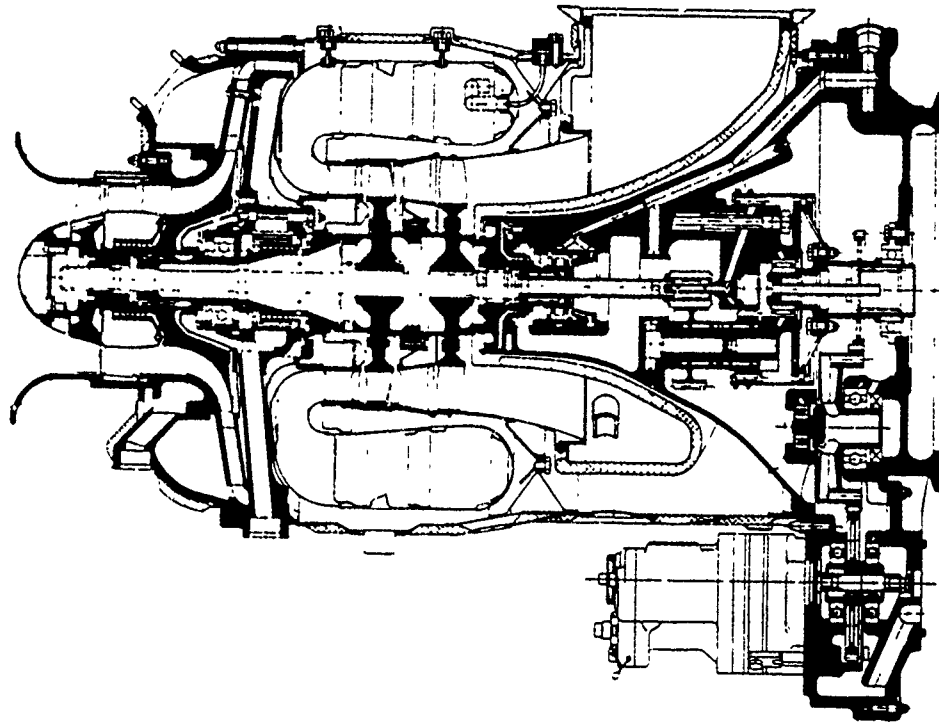


Fig.1 APU T312 Cross section

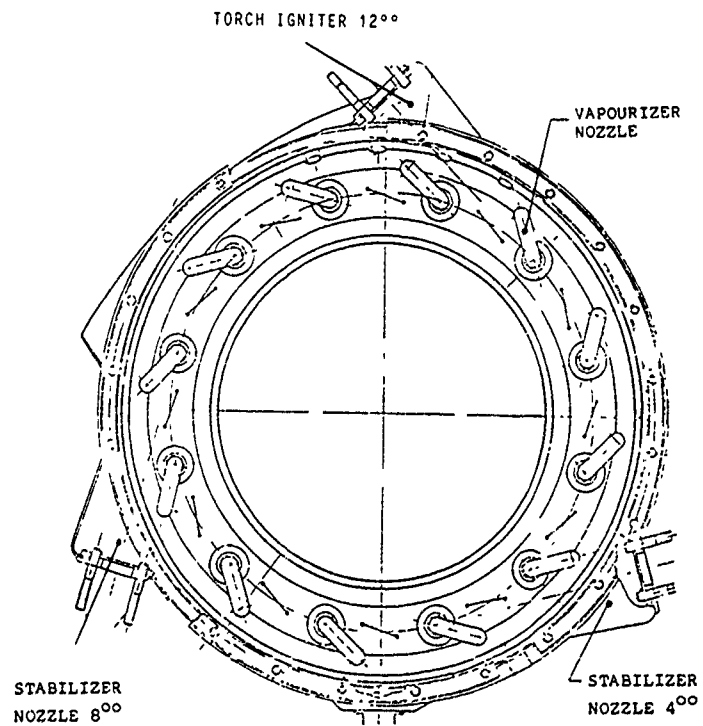


Fig.2 Dome of combustor

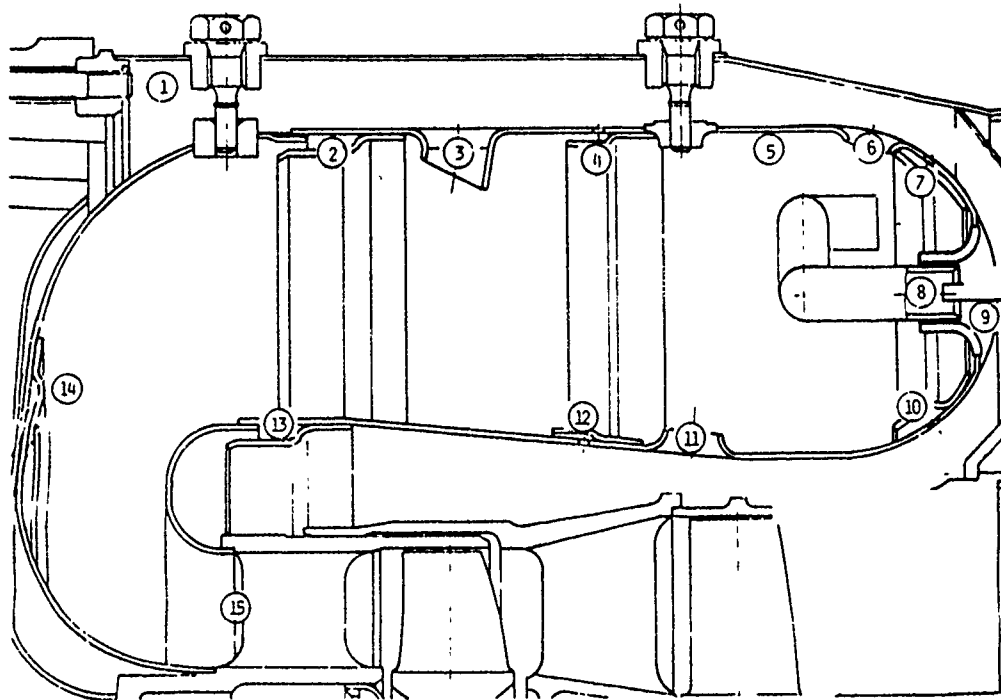


Fig.3 Combustor air flow

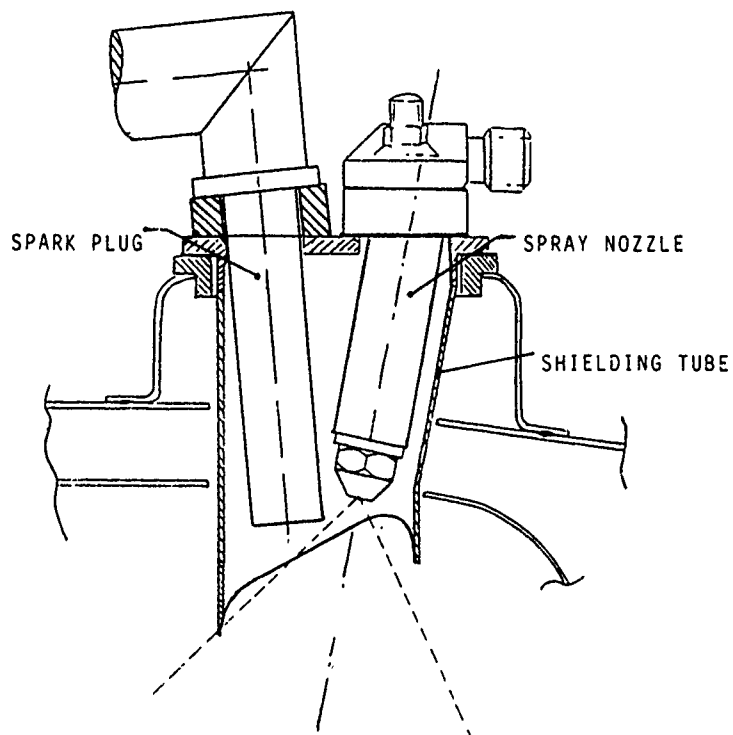


Fig.4 Torch igniter

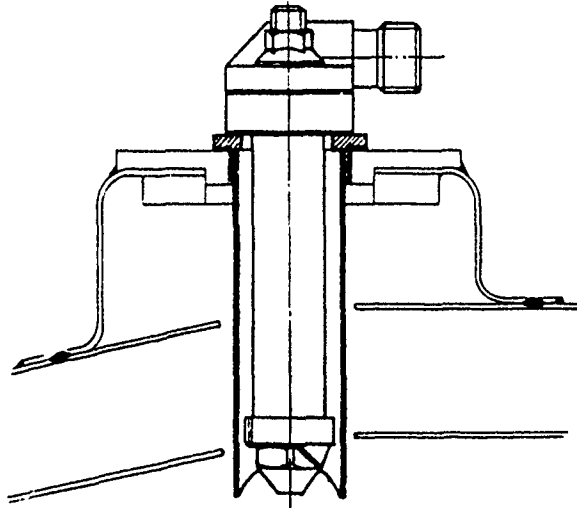


Fig.5 Stabilizer nozzle

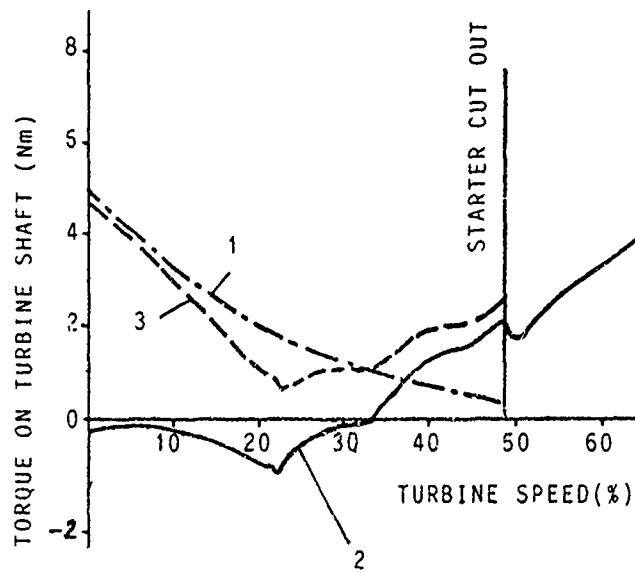


Fig.6 APU Start at 15°C

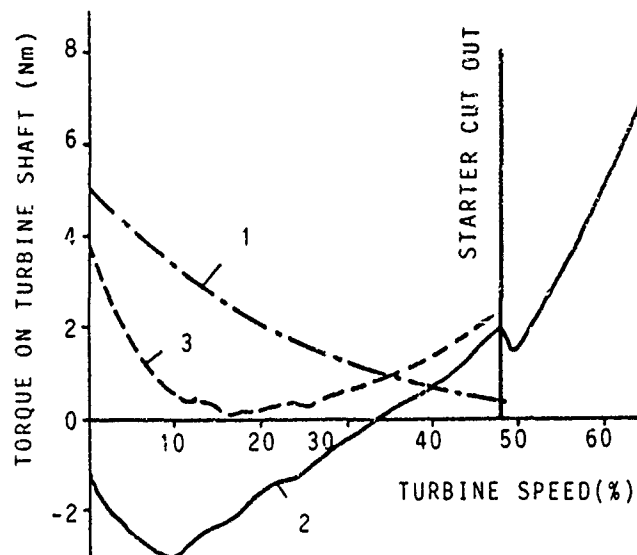
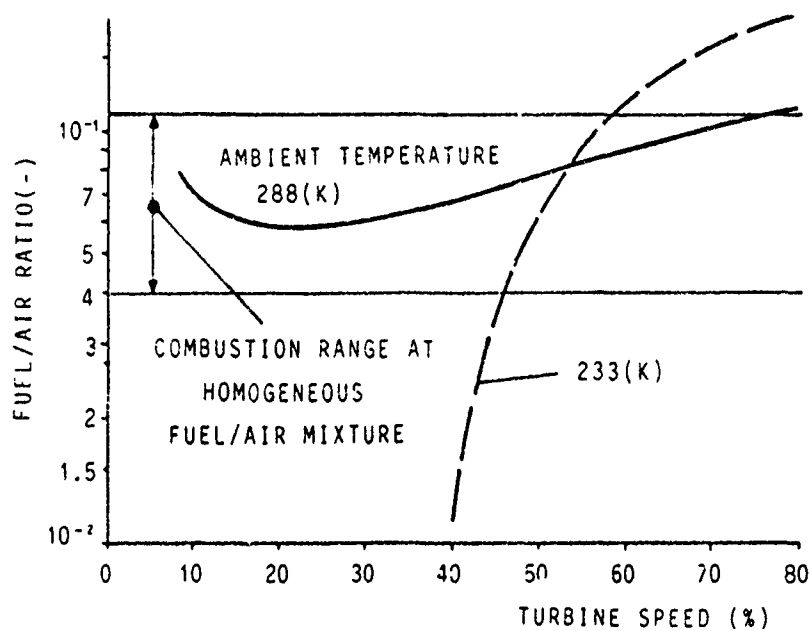
Fig.7 APU Start at -26°C 

Fig.8 Fuel/air ratio at the vaporizer nozzles

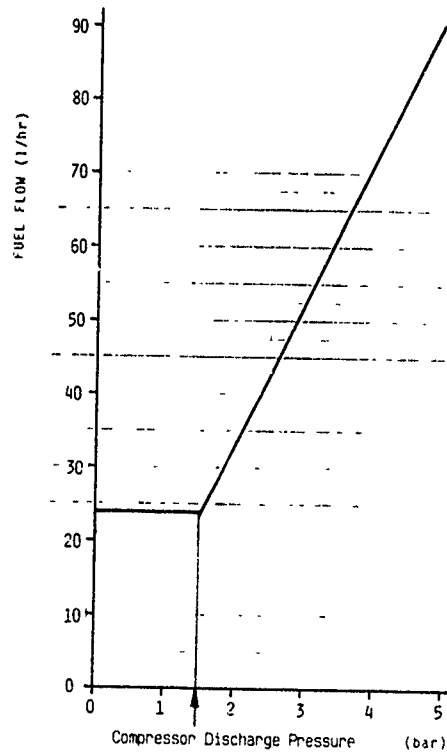
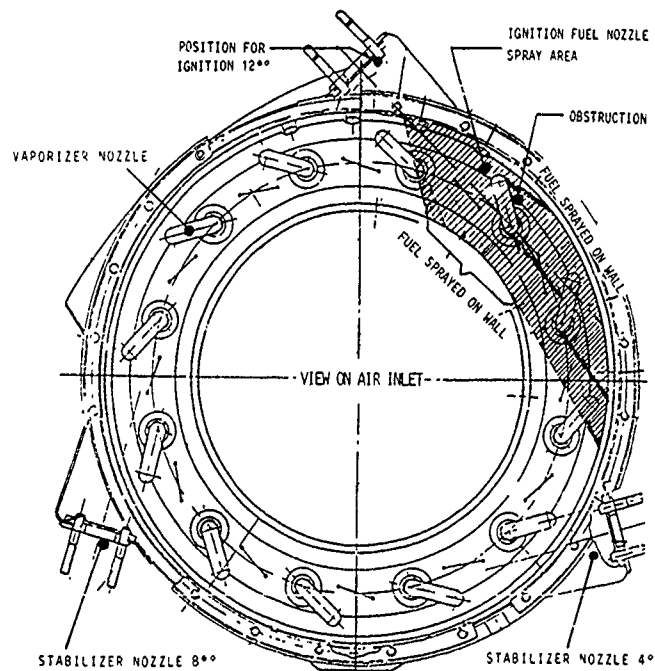


Fig.9 Fuel control schedule

Fig.10 Dome of combustor spray area of
ignition nozzle 12°

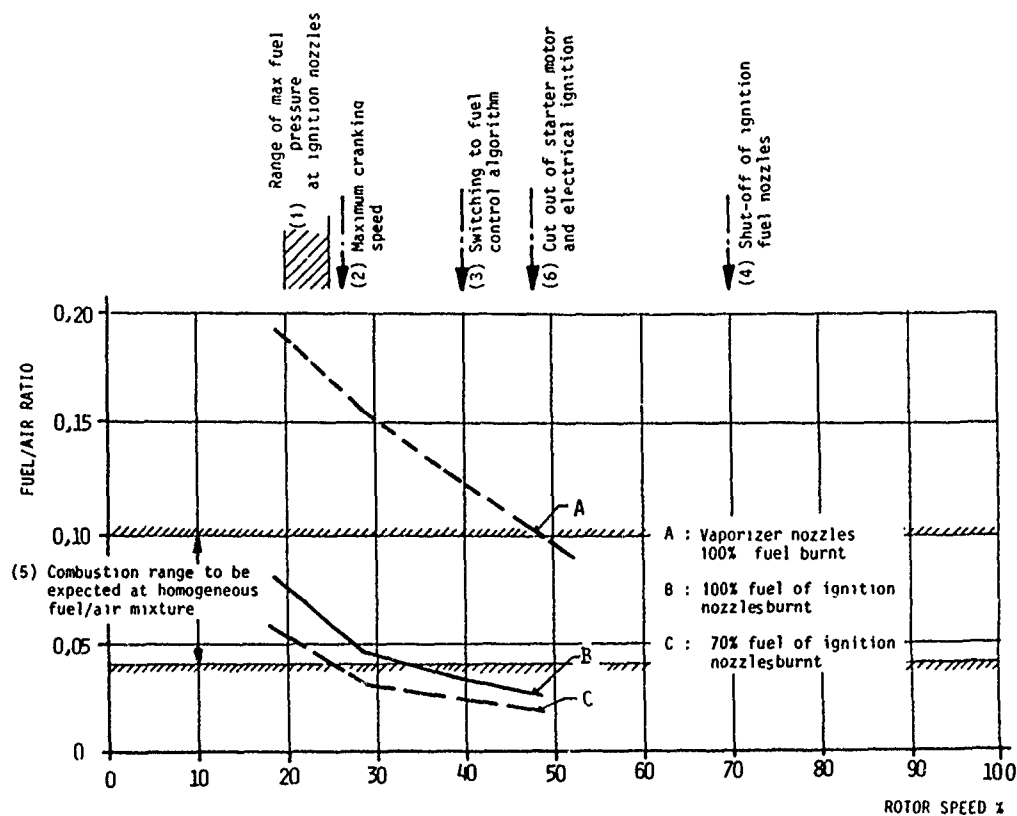


Fig.11 Ignition investigation

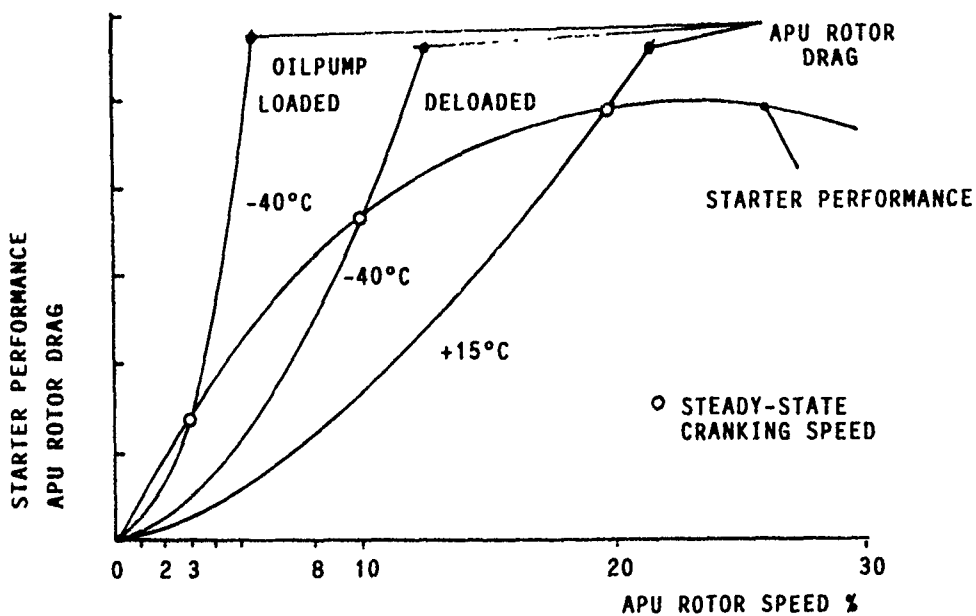


Fig.12 Starter performance and APU rotor drag

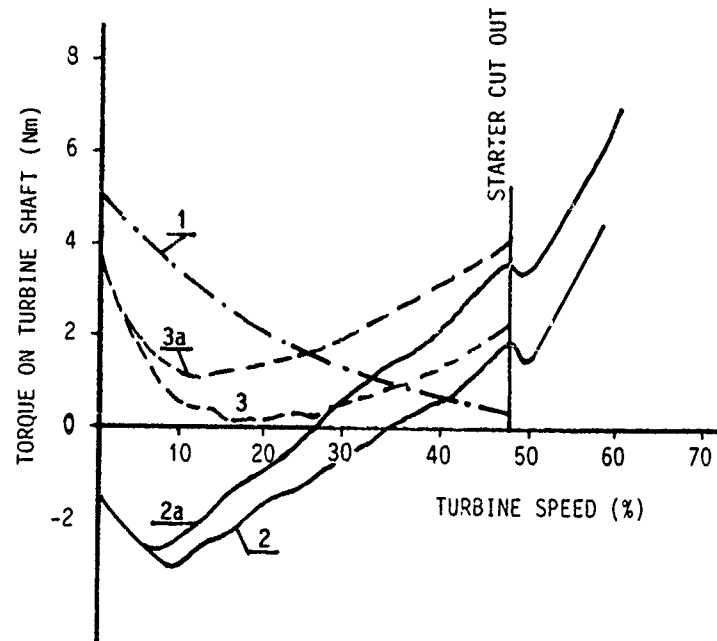


Fig.13 APU Start at -26°C with optimized combustor

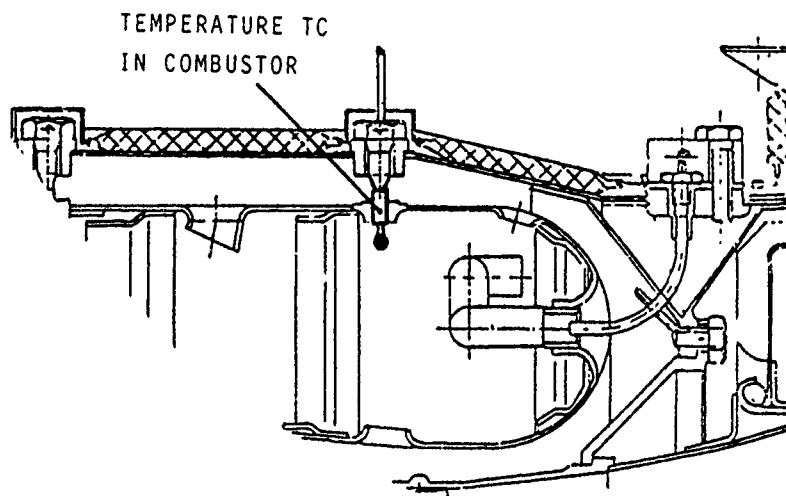


Fig.14 Combustor with six thermocouples

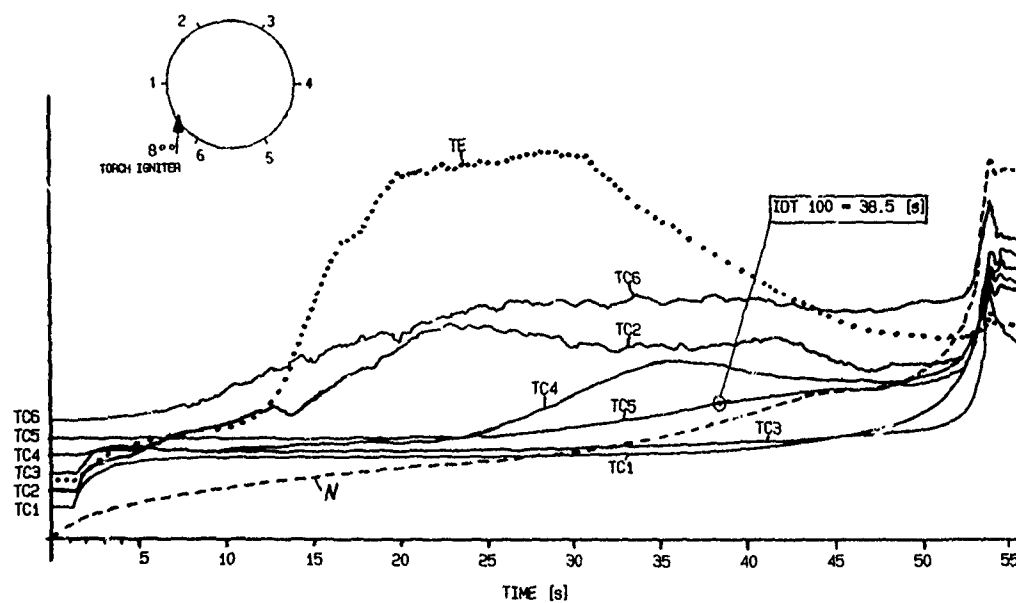


Fig.15 Test 1
Ambient temper. $= -40^{\circ}\text{C}$
Torch igniter 8°C

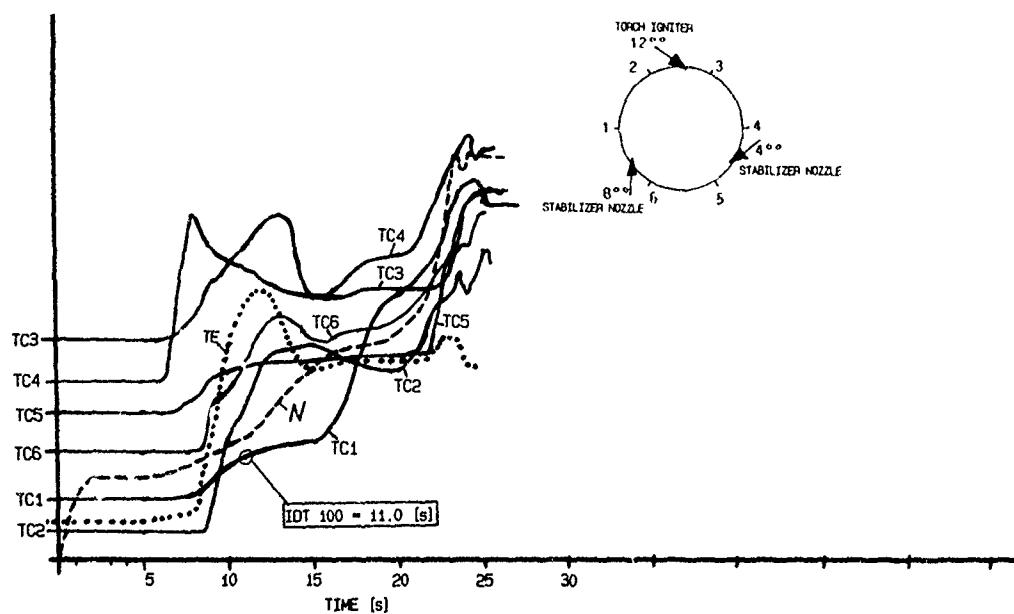


Fig.16 Test 2
Ambient temper. $= +10^{\circ}\text{C}$
Torch igniter 12°C

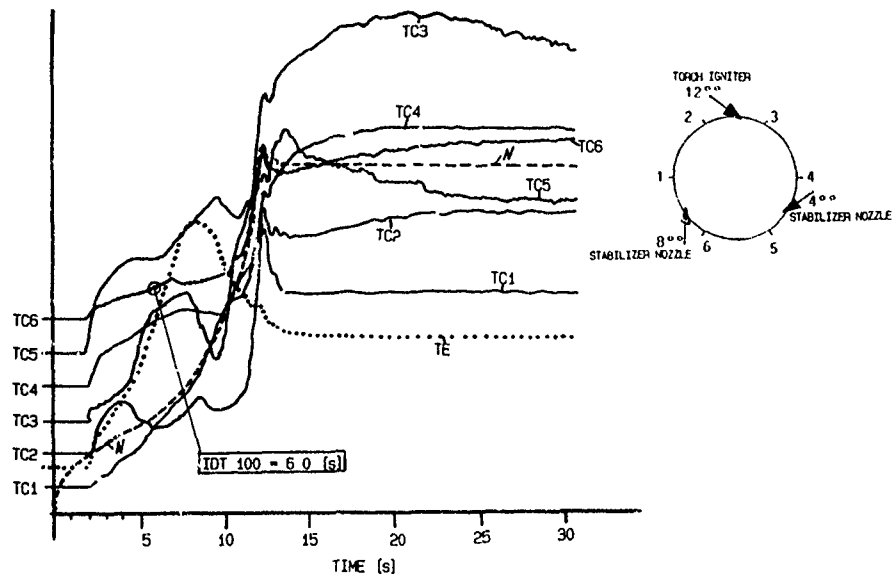


Fig.17 Test 3
Ambient temper = +15 C
Torch igniter 12°

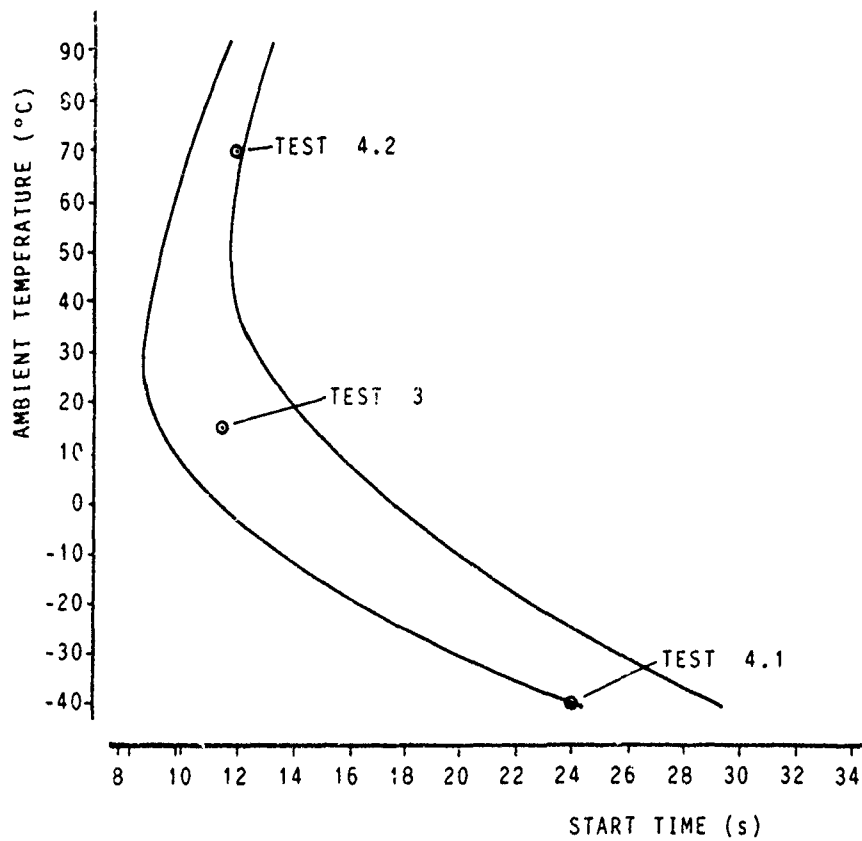


Fig.18 Start time vs temperature

CONTROL SYSTEM DESIGN CONSIDERATIONS FOR STARTING TURBO-ENGINES DURING COLD WEATHER OPERATION

BY

ROBERT R. POLLAK
DEVELOPMENT ENGINEER
PRATT & WHITNEY
GOVERNMENT ENGINE BUSINESS
P. O. BOX 109600
WEST PALM BEACH, FLORIDA 33410-9600
U.S.A.

ABSTRACT

Starting turbo-engines at climatic extremes has always presented challenges to the systems engineer. The wide range of both ambient and engine internal temperatures experienced by many influential variables increase the complexity of the startup process both on the ground and in the air. The content of this paper provides the current status of advanced control methods designed specifically to address combustor ignition and quick, stall-free acceleration to idle. Sensitivity of combustor ignition limits to cold conditions as well as fuel types has been accommodated by both the combustor fuel delivery system and control system design. Specific attention is also given to starting at cold altitude conditions with extremely hot as well as extremely cold internal engine temperatures. Successfully meeting these requirements has been accomplished by designing the control system to automatically monitor external influential variables as well as engine internal parameters both prior to and during the actual startup cycle and using these data to continuously adjust fuel scheduling to obtain optimum startup characteristics.

LIST OF SYMBOLS

N_2 : High Compressor Rotor Speed, Revolutions per minute
 PT_2 : Engine Inlet Face Absolute Total Pressure
 TT_2 : Engine Inlet Face Absolute Total Temperature
 P : Ratio of Engine Inlet Face Absolute Total Temperature to Sea Level Standard Day Temperature
 TQ : Torque
 δ : Ratio of PT_2 to Sea Level Standard Absolute Pressure
 N_2C_2 : Corrected High Compressor Rotor Speed, $N_2/\sqrt{\theta_2}$
 W_F/P_B : Ratio of Combustor Fuel Flow to Combustor Pressure, Mass Flow/Absolute Pressure

W_F/PT_2 : Ratio of Combustor Fuel Flow to Engine Inlet Pressure, Mass Flow/Absolute Pressure
 $FTIT$: Fan Turbine Inlet Temperature
 η_B : Combustion Efficiency Within Main Engine Burner
 $FADEC$: Full Authority Digital Electronic Control
 TQ/δ : Corrected Torque
 TQ_{tot} : Engine Total Aerodynamic Torque
 TQ_{para} : Engine Internal Parasitic Torque
 TQ_{engine} : Engine Torque Available for Acceleration
 TQ_{ext} : Airframe Torque Extracted from Engine
 $TQ_{starter}$: Starter Cranking Torque
 TQ_{accel} : Requested Acceleration Torque (Request)
 TQ_{accel} : Actual Acceleration Torque Sensed (Actual) By the Control
 I_p : Polar Moment of Inertia
Fuels: JP-4, Equivalent to NATO F-40
JP-8, Equivalent to NATO F-34, F-35
JP-5, Equivalent to NATO F-44

INTRODUCTION

The process of ignition that occurs during cold weather conditions within a Turbo-Engine has always presented a challenge to the combustor designer and systems engineer. The multitude of variables that influence the initiation of combustion under these conditions have certainly been encountered by anyone given the challenge to assure ease and consistency of starting.

Surveying any fuel properties reference manual quickly shows that the vapor pressure of the fuel drops dramatically as fuel temperatures approach sub-zero conditions while viscosity similarly increases. With the high viscosity levels encountered, the

process of atomization for any combustor can be significantly altered relative to warm day conditions. The less-desirable fuel droplet distribution together with less available vapor surrounding each droplet minimizes the useful fuel-air ratio to the point that ignition of the mixture is repressed.

Since fuel vapor available for combustion is restricted under extremely cold conditions, introduction of more fuel flow is usually the only alternative available to compensate short of the use of exotic systems such as hypergolic ignition or the use of specially designed fuel injectors that provide locally rich mixtures near the combustor ignitor(s). Further, as the methods used to assure quick, reliable ignition become more complex, the cost of additional hardware designed only to address cold day ignition usually detracts from an engine's posture in the competitive marketplace. As a result, use of the same hardware that provides ignition at warm day temperatures is desirable.

Pratt & Whitney systems engineers have met this challenge through the use of normal control systems that are already bill-of-material while avoiding any fuel or combustion system hardware designed specifically for cold day starting. These full authority electronic control systems are already in use on several engine models and provide the necessary flexibility to accommodate fuel scheduling requirements at all ambient air temperatures.

STARTING PROCESS

Using a multi-spool engine configuration as a typical example, the ease of starting depends on the size of the starting "window" which can be described in terms of the ratio of main combustor fuel flow to main combustor (or burner) pressure, W/P_b . This ratio can be presented as a function of the engine's high pressure compressor rotor speed, or N_2 , as shown on Figure 1.

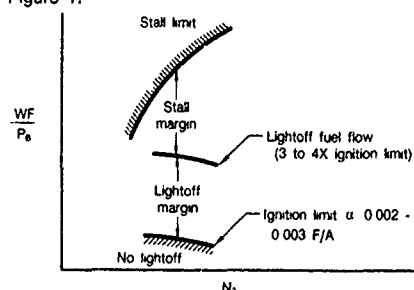


Figure 1. Starting Window Defined by Ignition and Stall

For standard day ambient conditions, the ignition limit should be quite low. The overall fuel-air ratio within F100-Design combustors generally range from 0.002 to 0.003. To provide quick, reliable ignition with typical ignitor systems, the actual level of fuel flow used for lightoff is usually three to four times higher than that actually required to obtain a stable flame.

As the fuel flow for ignition is increased, the resulting pressure due to combustion rises proportionally. The maximum fuel ratio that can be delivered to the combustor is limited by the maximum pressure capability, or stall limit, of the compressor. Similarly, during the actual acceleration process, the stall limit generally varies and is a function of the characteristic shape of the compressor stall line as it varies with rotor speed. Additional variation of this maximum fuel ratio limit is often due to the actual combustion efficiency of the burning process during the start cycle. This variable becomes especially significant during extremely cold ambient temperatures.

The minimum required fuel schedule for acceleration is usually established by the time required to perform the start at given ambient conditions. The level is usually set by the steady-state required-to-run line which includes applied aircraft power extraction and the effect of starter cranking power. The difference between the fuel schedule and the required-to-run line provides the acceleration margin, while the difference between the schedule and the stall limit represents the effective stall margin in terms of fuel ratio units, Figure 2.

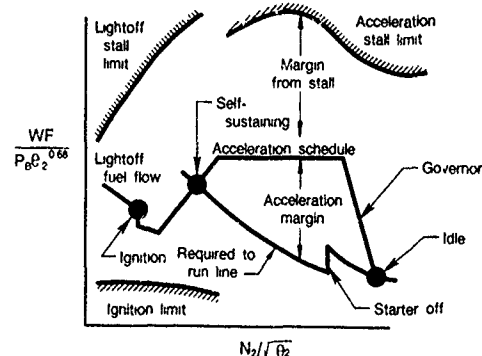


Figure 2. Acceleration Margin Set by Fuel Schedule

Whether the control is hydro-mechanical or fully electronic, the acceleration schedule is usually defined in terms of the already-described W/P_b ratio units or a similar term such as W/P_{t2} (fuel flow ratioed to engine or compressor inlet pressure) scheduled against physical or corrected compressor rotor speed.

Engine testing has verified that the parameter W/P_b presented as $W/P_{t2} \cdot \theta_2^{-1/4}$ against corrected compressor rotor speed, $N_2/\sqrt{\theta_2}$, correlates the stall limit as a single line at different ambient temperatures. While combustion efficiency may vary from ignition to idle, the stall limit remains consistent for a significant range of ambient temperatures, thus providing a consistent relationship between corrected fuel ratio units and corrected rotor speed.

As fuel vapor pressure is reduced with lower ambient temperature, the fuel-air mixture available for ignition

likewise drops. Consequently, more fuel is required to provide sufficient vapor for ignition. The characteristic is manifested as an increase of required fuel ratio units as shown on Figure 3. The amount of increase for a given temperature level is, of course, a function of the fundamental ignition characteristics of the combustor design. Test data under controlled conditions have indicated that the rate of increase of ignition limit is a function of the level of the warm day ignition. If the limit is low, the rate of increase of the limit with temperature reduction is likewise low.

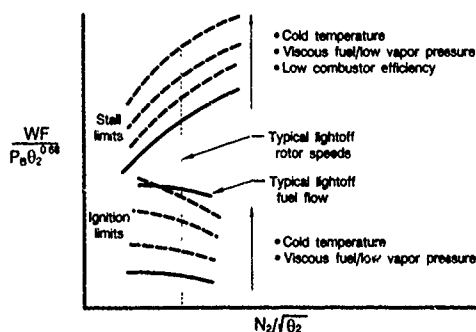


Figure 3. Lightoff Window Influenced by Fuel Characteristics

Depending on the specific design of the combustor, combustion efficiency can drop off significantly at sub-zero temperatures. As a result, the amount of fuel required to drive the compressor into stall likewise increases. If this characteristic is such that the stall limit increases to a greater level than the ignition limit, a useful start window will remain. If the increase of the ignition limit is larger than the stall limit, it is conceivable that the two will intersect, thus relegating the engine to an unstartable condition, Figure 4. This condition, of course, requires a fuel nozzle or combustor redesign, or a compressor with increased stall margin to provide a useful operational window.

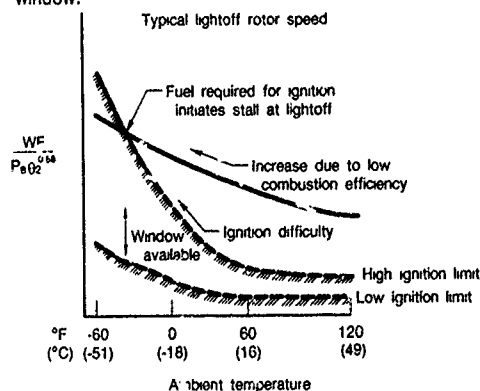


Figure 4. Lightoff Window Varies with Design and Temperature

DESIGN PROCESS

Assuming that a useful starting window exists at all

temperatures, the design task is to provide required fuel flow to initiate a timely lightoff. In the usual case, the fuel flow adequate for warm day ignition is too low for extreme cold day operation. The general technique includes a bias with engine inlet sensed temperature, T_{t2} , or an equivalent compressor inlet temperature behind the fan or low compressor. In any case, as the temperature drops, the fuel schedule is adjusted to provide lightoff flow commensurate with the ambient temperature as shown in Figure 5.

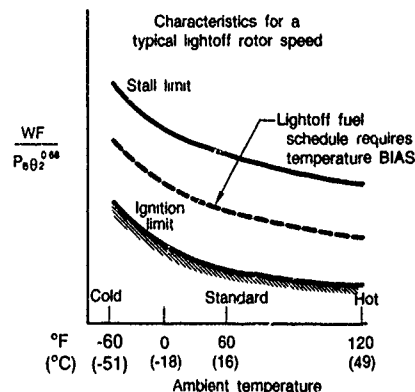


Figure 5. Temperature Bias Used to Optimize Lightoff

As mentioned previously, combustion efficiency can drop significantly as ambient temperature drops. This is especially true at low rotor speeds just after ignition during which low vapor pressure and high viscosity still exist. This low combustion efficiency minimizes energy available for acceleration such that a higher level of fuel flow is required to meet required-to-run operation. Although difficult to measure or calculate, available heat from combustion is dissipated into the surrounding metal thus contributing to the low effective efficiency. As such, the fuel schedules at low rotor speeds must be increased a proportionate amount to maintain acceleration margin, Figure 6.

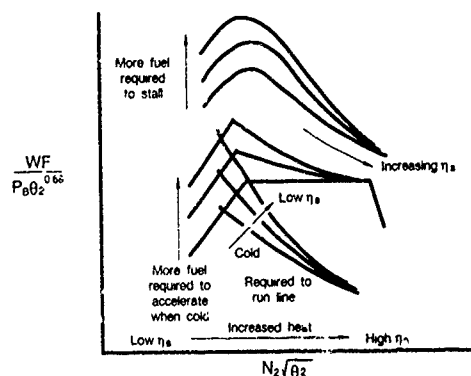


Figure 6. Combustion Efficiency Drives Acceleration Requirements

As the rotor proceeds toward idle, the internal conditions of the engine are rapidly heated to the point that the combustion process becomes more

efficient. Further, less heat is dissipated to internal parts thus releasing more energy for acceleration. Consequently, as rotor speed approaches idle, the initially high fuel schedule required to maintain desirable acceleration is no longer necessary.

Similarly, the amount of fuel required to stall likewise diminishes due to the process of increasing internal temperatures and increased combustion efficiency. As a result of the lower required-to-run line and stall limit, the resulting schedule can be lowered while still meeting acceleration requirements, and must be lowered to avoid stalling the compressor.

The rate of combustion efficiency change during the acceleration to idle is a reasonably consistent process at cold temperatures as long as the engine internal temperature during any given start is initially the same. Difficulty can arise if the combustion efficiency at low rotor speeds is significantly different from one start to another at a given ambient temperature. That is, for a cold-soaked engine or "cold-iron" engine, the efficiency is low, but, for an engine still hot after normal shutdown, or "hot-iron", the efficiency is high. Should available compressor stall margin be sufficiently high to accommodate these differences, no difficulties will occur. However, many high performance compressors may have limited margin to accept these differences. This is true for lightoff fuel flow requirements as well as the acceleration schedule.

ADAPTIVE CONTROL

The now-common Full Authority Digital Electronic Control (FADEC) used on high-technology engines at Pratt & Whitney utilizes internal core engine temperature to schedule lightoff fuel flow to obtain successful ignition during cold day operation with both "cold-iron" and "hot-iron" engine conditions. Shown on Figure 7 is a typical lightoff fuel schedule for an operational engine. Fuel flow is scheduled with control-sensed Fan Turbine Inlet Temperature, or FTIT. During warm day operation the fuel is scheduled at relatively "low" values which provides quick lightoff capability while maintaining adequate stall margin. As ambient temperature and likewise FTIT drop, the scheduled fuel flow is increased to compensate for the more difficult ignition characteristics discussed previously. This technique

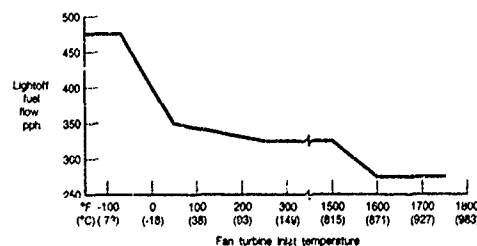


Figure 7. Lightoff Fuel Flow Set by Engine Internal Temperature

has been successfully demonstrated at ambient temperatures as low as -40°F ($^{\circ}\text{C}$) with both JP-4 and JP-8 fuels.

Whenever a start is attempted during a hot-iron condition (an engine with residual heat) the warm FTIT provides the control with the capability to schedule a lower value of lightoff fuel flow to compensate for the higher combustion efficiency that prevails at these conditions even though ambient air temperature is cold. This feature therefore, provides optimum ignition capability at sub-zero air temperatures while assuring maximum compressor stall margin when engine internal temperatures are warm.

Additional lightoff protection is included to address low-grade fuel which may further degrade ignition capability via extra-low vapor pressure or high viscosity. The control monitors the time after fuel is introduced to the fuel manifold and senses whether ignition has taken place. If ignition has not taken place within the prescribed time period which includes expected time to fill and light, the control begins to increase fuel flow in an attempt to establish an acceptable ignition fuel-air ratio, Figure 8. A reasonable limit is included for obvious safety reasons.

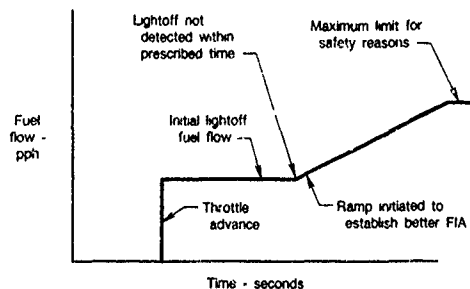


Figure 8. Additional Lightoff Protection Provided for Low-Grade Fuels

As shown in Figure 6, the level of fuel schedule required to accelerate can be significantly higher at cold temperatures during low speed operation due to low combustion efficiency. Since this process is more physical rather than aerodynamic, and the physical process of combustion can change depending on the grade or type of fuel, designing the fuel flow schedule for the acceleration to idle can often be a hit or miss process. The design is further complicated since warm engines must also be started at cold temperature, which will also alter the amount of fuel required to maintain a desired level of acceleration. The FADEC has completely eliminated the need for second-guessing continually changing variables during the starting process.

ACCELERATION PROCESS

The concept of describing turbo-engine starting characteristics in terms of acceleration torque of the high compressor rotor has been fundamental for

years. It accurately describes the power of the engine at a specific speed and relates directly to the aerodynamic capability of compressor and turbine characteristics.

The relative relationship of acceleration torque to compressor operation is shown on Figure 9. The level of torque available for acceleration is proportional to the compressor operating line and the temperature generated within the combustor to provide turbine power. The resulting airflow, pressure, and temperature together with the compressor and turbine efficiency characteristics provide the net excess power for acceleration. As speed increases, airflow and compressor pressure capability increase, and the temperature required to reach this pressure likewise increases, thus increasing net power.

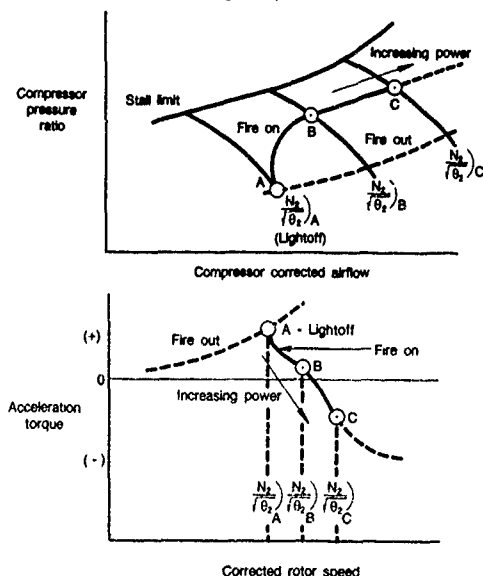


Figure 9. Compressor Fire-on Line Relates to Acceleration Rate

For any given rotor speed, fuel flow can, of course, be increased to the point that the compressor will stall, as shown on Figure 10. At this point on the compressor map, there is a corresponding point of maximum acceleration torque that represents in physical terms the aerodynamic capacity of the engine. These relationships circumvent any variations of combustor efficiency due to fuel grade or internal engine temperatures, such as a hot engine starting on a cold day.

The FADEC on Pratt & Whitney's F100 family of engines has been using this technique successfully for years. The actual allowable level of acceleration torque for any engine model is programmed into the control as Torque/δ and represents the maximum desirable aerodynamic torque available for a start at a given temperature, such as that shown on Figure 11. Corrected torque in terms of Tq/δ is used against

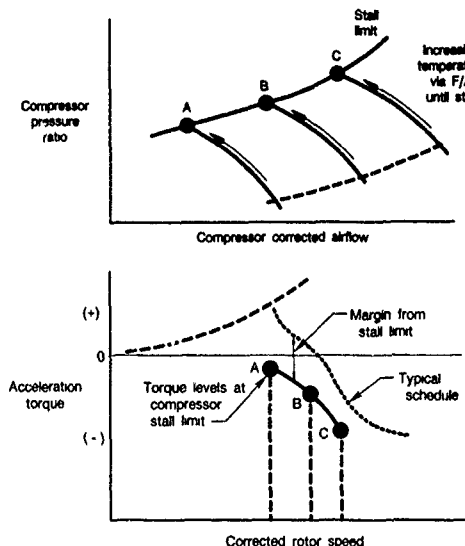


Figure 10. Acceleration Limits Defined by Compressor Stall

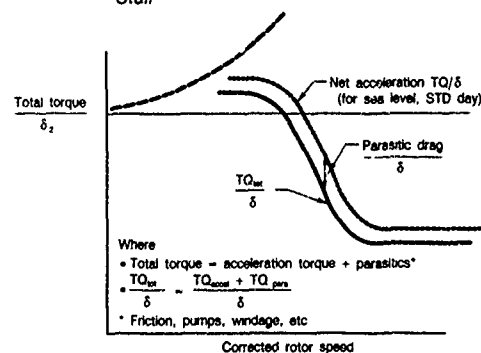


Figure 11. Internal Influences Incorporated Within Control Schedules

corrected high compressor rotor speed, $N2C2$, and represents total engine power which includes net measurable acceleration torque and that absorbed internally within the engine for friction, pumps, windage, etc. This relationship has worked successfully at ambient temperatures ranging from -40°F ($^{\circ}\text{C}$) to over 125°F (52°C).

To construct the physical acceleration characteristics of the engine, the Tq/δ schedule is uncorrected by the following relationships:

$$N2 = N2C2 \cdot \sqrt{\theta_2}$$

$$Tq = Tq/\delta \cdot \delta$$

As part of the overall acceleration rate of the engine, the starter cranking characteristics are also programmed as a function of ambient temperature and pressure altitude (elevation) to represent the starter's contribution to acceleration. Further, the aircraft accessory loads extracted from the engine are also included as shown on Figure 12. The

combination of these three major variables comprises the torque available for acceleration and becomes the actual requested parameter that continuously changes with ambient temperature and pressure conditions.

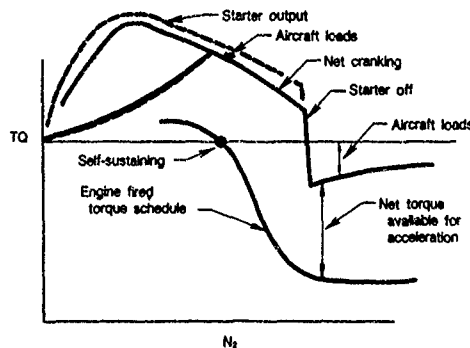


Figure 12. External Influences Define Net Acceleration Capability

The control calculates the desired net acceleration torque from these three variables (including engine parasitic drag) on a continuing basis as a function of N_2 . Figure 13. Rate of change of N_2 with time is sensed by the control and converted to a torque value by way of compressor/turbine moment of inertia. This actual torque is compared to the requested value to provide an error which is used to set the value of fuel flow increase via a gain. The end result is a control system that delivers only the fuel flow required to produce the desired aerodynamic acceleration of an engine rather than scheduling fuel flow on an open-loop basis and obtaining an acceleration rate that can vary significantly with uncontrollable influential variables. With the exception of the initial portion of the start during which the engine is accelerating on open-loop ignition fuel flow, the acceleration times to idle are virtually identical for all engines. Any fuel control hardware tolerances are automatically eliminated since fuel flow is a

closed-loop function described mathematically within the programming of the FADEC.¹ This capability is useful when different types of fuel are used, such as JP-4 and JP-5, especially when fuel type adjustment on the fuel control is not available. While the fuel scheduling used for the two starts will be different, the acceleration rates will be virtually identical together with identical compressor stall margin consumption.

Consequently, as ambient temperature decreases to sub-zero levels, engine acceleration is not altered from the desired, automatically-programmed values. Since fuel flow is continuously-adjusted rather than pre-programmed, the control system adjusts fuel flow to meet the desired start characteristics as influential variables change.

CLIMATIC DEMONSTRATIONS

As mentioned above, all of the F100 family of engines currently in production incorporate the closed-loop control mode which has eliminated the difficulties normally encountered during sub-zero starting. This was successfully demonstrated during climatic testing of an F100-PW-220 in the Climatic Hangar at Elgin Air Force Base in Florida. The entire aircraft was installed within the hangar and tested under temperature extremes of -10°F to -40°F using JP-4 and JP-8 fuels. Each cold test was preceded by at least a 10 hour soak at the specified temperature. The soak time was begun after critical aircraft gearbox and engine oil temperatures had reached ambient temperature. The resulting start times are shown on Figure 14 which demonstrate that the potential start time of an engine is actually faster instead of becoming longer as ambient temperature is lowered.

1. United States Patent No. 4,274,255 and Foreign Patents, R. R. Pollak, "Control For Startup of a Gas Turbine Engine," Assignee: United Technologies Corporation, Hartford Conn.

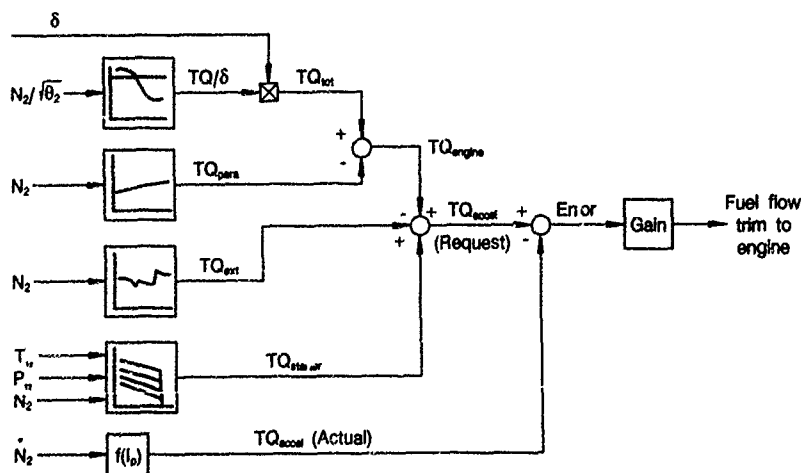


Figure 13. Starting Components Assembled to Control Fuel Flow

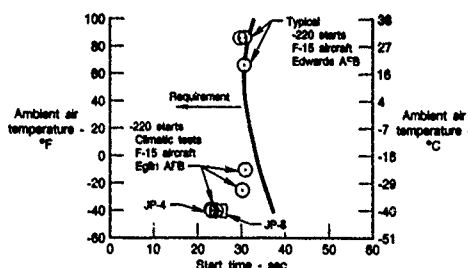


Figure 14. Quick Start Time Capability Provided at Cold Temperatures

The time to obtain ignition was held approximately constant at all ambient temperatures since ignition fuel flow is adjusted as the temperature drops, especially in the sub-zero range. Actual ignition and start times during the test were:

AMBIENT TEMP °F(°C)	FUEL TYPE	IGNITION TIME (seconds)	START TIME, REF. 1 (seconds)
-10 (-23)	JP-4	8	31
-25 (-32)	JP-4	9	30
-40 (-40)	JP-4	7	24
-40 (-40)	JP-4	7	23
-40 (-40)	JP-4	7	23
-40 (-40)	JP-8	8	25

IGNITION TIME is defined between throttle advance to combustor lightoff. START TIME is defined as the total time taken between throttle advance to 95% of idle high compressor/turbine rotor speed, N₂, at the test temperature.

With non-closed-loop controls, longer start times are typical at the colder temperatures and are due either to long ignition times, fuel schedules that should be richer due to poor combustion efficiency, especially with low-grade fuel, or control tolerances which can affect the acceleration capability if too lean.

The consistency of the closed-loop control system can be seen on Figure 15. Start times for 670 F100-PW-220 production engines are compared to the delivery requirement for ambient temperatures that range from 90 °F (32 °C) to about 25 °F (-4 °C). The sample includes 384 F-15 model engines and 286 F-16 model engines. The start time range of the

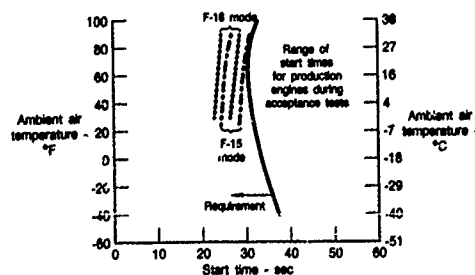


Figure 15. Consistency Provided Through Closed Loop Control

F-15 engines were recorded with the FADEC in the F-15 aircraft mode which uses the power action loads representative of the F-15 aircraft. Similarly, the F-16 engine start times are representative of the loads extracted by the F-16. During field operation, the load schedules are automatically selected by the location of pins in the aircraft-to-engine control cable pin connector for the particular model aircraft. Since the loads are larger for the F-15, the start times are about two seconds longer while the F-16 times are shorter due to the lower levels of extracted loads. This automatic process provides a consistent level of compressor stall margin by keeping the engine power output virtually the same while adjusting the observed net acceleration rate by considering external loads.

More recently, a similar test was conducted on the F100-PW-229 engine in the same climatic test facility. During these tests, the entire aircraft with the engine installed was soaked at the sub-zero temperatures from 11 to 24+ hours after the aircraft central gearbox and engine oil temperatures had reached the desired ambient temperature. Again, the start times at sub-zero temperatures were faster than those demonstrated at standard day conditions as shown on Figure 16.

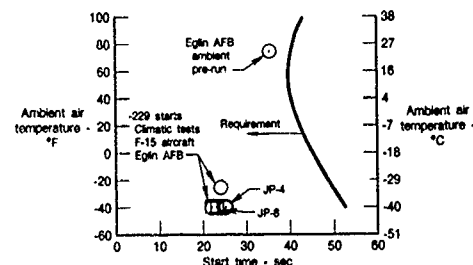


Figure 16. Cold Temperature Capability is a Design Process

Similar to the -220, the times to obtain ignition were held to a minimum by the automatic adjustment of fuel flow by the control as the temperature was reduced. This method again provided reliable and consistent ignition.

AMBIENT TEMP °F(°C)	FUEL TYPE	IGNITION TIME (seconds)	START TIME, REF. 2 (seconds)
+15 (+24)	JP-4	7	35
-10 (-23)	JP-4	8	31
-25 (-32)	JP-4	6	24
-40 (-40)	JP-4	5	25
-40 (-40)	JP-4	3	22
-40 (-40)	JP-4	5	25
-40 (-40)	JP-8	9	22
-40 (-40)	JP-8	4	23
-40 (-40)	JP-8	4	23

AIRSTARTING

The extremes of engine temperatures during starting are found while attempting to start the engine in the

air. Depending on the requirements specified by the customer, procedures can be significantly different from one application to another.

In multi-engine aircraft applications, the classical windmill airstart may be the desired procedure since, for the most part, the time factor for restarting the engine may not be critical. Further, designing for a single procedure offers simplicity and minimizes development costs.

In such cases, the engine is usually in a cold condition due to the relatively long engine-out time at sub-zero engine inlet temperatures. Under these conditions, fuel flows to obtain quick, consistent ignition together with a fuel schedule to provide adequate acceleration can be designed without too much difficulty. In some cases a single fuel flow for lightoff together with a single acceleration schedule, e.g. Wt/Pb, can suffice for all windmill airstart requirements. As mentioned above, at cold temperatures, starting requirements may be met only by rich fuel flow scheduling for both ignition and acceleration. As such, the prescribed procedure must be adhered to in detail to restart the engine during an in-flight shutdown. Should the engine be hot, however, the windmill-designed fuel scheduling will usually be too rich and precipitate compressor stalls.

Requirements for today's generation of military fighter aircraft usually require the engine to be started shortly after the shutdown. Under many conditions for starting, the internally-measured gaspath temperature may be 1300 °F (700 °C) or more at the time a restart is desired. Airstarts attempted under these hot conditions with fuel scheduling designed to produce acceptable windmill recoveries usually stall the compressor. It is clear, then, an alternative approach is desirable.

During combat when a military aircraft engine is shut down for any reason, survivability requirements demand obtaining operational thrust as soon as possible. This requirement is certainly amplified in the case of a single engine aircraft application whether in combat or not. A typical comparison of restart times for a windmill and a quick restart, or spooldown restart, is shown on Figure 17. The amount of time required to perform a windmill start is always

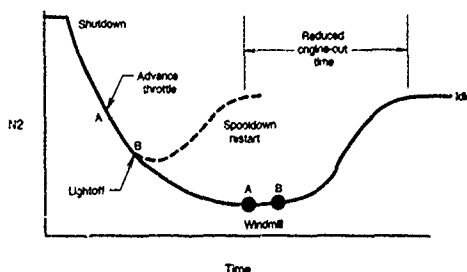


Figure 17. Spooldown Reduces Engine-Out Time

significantly longer and converts into lost altitude for a single engine application. Obviously, if the shutdown event occurs at a low altitude, recovery time is critical.

The same technique used during ground starts that delineates cold vs hot engine conditions is used in the air. Fuel flows for ignition are shown on Figure 18 as a typical schedule that accommodates hot engine conditions at altitude. The schedule uses FTIT as the engine temperature parameter to delineate internal gaspath conditions prior to start initiation. Note that at the upper scale of temperatures, fuel flows are scheduled lean to provide stall-free ignition, while at the colder, sub-zero temperatures that represent windmill conditions, high fuel flows similar to ground starting on cold days are used. This method of scheduling fuel flows provides the capability of starting under any set of engine conditions from cold windmills to extremely hot, quick restarts.

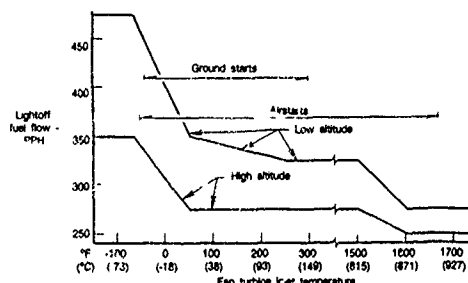


Figure 18. Engine Gaspath Temperature Provides Full Lightoff Capability

The fuel required during acceleration with a hot engine is likewise reduced from that of a windmill. If a schedule is designed to provide stall-free acceleration with a hot engine, it is likely to be insufficient to provide acceleration while in a windmill condition. This is especially true with more viscous fuels such as JP-8 or JP-5.

Using the same closed-loop control techniques during airstarting as is used during ground starting, both hot and cold engine restart capabilities are achievable. An acceleration characteristic that is acceptable for restarting hot engines is available for windmill as well. With the ignition fuel flow design to provide quick lightoff at any temperature, both spooldown and windmill restarts are always available to the customer for any application without concern for unique, mandatory procedures.

If the acceleration torque schedules are designed for the hot engine condition, the pre-programmed safe acceleration rates and necessary fuel flows will be delivered to the control to provide successful restarts for both temperature conditions, and with known, repeatable start times at a given flight condition.

The accuracy of the closed-loop control provides not only consistent airstart characteristics, but a larger airstart envelope. This includes hot as well as cold

engine temperatures at both warm and cold engine inlet air conditions.

With an open-loop control system, hardware tolerances and mechanical wear influence the capability of achieving successful airstarts especially at low airspeeds and reduced rotor speed conditions. While some control units might be able to meet low airspeed requirements, some units, whether too rich or too lean will be unable to accelerate the engine to idle successfully. While it is desirable to initiate the restart as soon as possible at higher rotor speeds, the pilot does not always have this luxury due to aircraft departure, etc. By the time the pilot determines that a restart is required, rotor speeds may have decelerated to extremely low values at which very little compressor stall margin is available.

Under these conditions, accurate scheduling of fuel flow is mandatory if low airspeed recoveries are to be achievable. Maintaining low airspeed during the entire recovery is usually desirable due to more optimum times aloft or glide distances available.

FLIGHT DEMONSTRATIONS

The incorporation of all the requirements mentioned above into one control system was accomplished in Pratt & Whitney's F100-PW-220 used in both the F-15 and F-16 aircraft. Prior to the incorporation of the aforementioned FADEC into the F100 family of engines, the minimum airspeed required to provide 100% reliability for all engine/control combinations was 250 knots indicated airspeed, kts. While some engines had 200 kt. capability with the open-loop control mode, tolerances within the control hardware necessarily required higher airspeed for others.

Engines with the closed-loop control mode within the FADEC now provide consistent airstart capability at 200 kts up to 40,000 feet (12,000 meters) pressure altitude as shown on Figure 19. The procedures used during the flight test included initiating the restarts at compressor rotor speeds that ranged from 25% to 50% of cockpit tachometer reading as well as steady-state windmill conditions. The majority of the starts were initiated after a shutdown from a high power condition in order to place the engine in a condition of minimum available compressor stall margin.

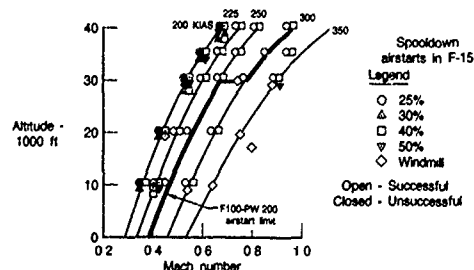


Figure 19. Improved Start Capability with Closed Loop Start System

SUMMARY:

Since the late 1970's, Pratt & Whitney has incorporated the closed-loop starting process in its FADEC engine controls. The design technique of incorporating all the primary parameters that make up the starting process is fundamental to the success of cold-weather starting. Fuel flows for ignition are tailored specifically to the combustor and the desired acceleration characteristics of the engine are built into the control rather than a pre-determined acceleration fuel schedule. The pre-established starter cranking capability and aircraft extraction loads provide all necessary external information for the control to produce successful and consistent starts. The fact that the control senses whether proper acceleration is taking place allows for the complete flexibility of adjusting the level of fuel flow to meet the capabilities of the engine. This design provides on-line instantaneous adjustment to compensate for low-grade, low vapor pressure, or highly viscous fuels as well as sub-zero temperatures. Further, the control is capable of modifying fuel flow delivery to compensate for engine restarts with hot internal temperatures and hot fuel while operating in a sub-zero ambient temperature environment. This is especially desirable during altitude restarts which may include both warm and cold inlet air as well as cold as well as extremely hot gaspath temperatures. With these features, engines can now demonstrate consistency and reliability which assure the customer that special handling and special procedures during sub-zero operation are no longer necessary.

REFERENCES

1. R. Scrivner, United Technologies - Pratt & Whitney, "F100-PW-220 Cold Start Preliminary Data Review," 21 June 1985, Attachment 2.
2. M. J. Pfeiffer, T. J. Norton, J. A. Patterson, United Technologies - Pratt & Whitney, "F100-PW-229 Climatic Laboratory Starting and Acceleration Test Report", 1989, Report Number FR-20490, Table 4, page 43.

Discussion

1. K. Piel, BMW-RR Aeroengines

With reference to figure 19 of the paper, what is the figure of steady-state windmill conditions?

Author:

The windmill limit is defined as the airspeed required to obtain an N2-rpm of 11.4% Tach speed. This is defined as the guarantee rpm required to perform a windmill airstart. In most cases starts can and have been performed at lower rpm.

2. R. Wibbelsman, GE

A/C TP₄ loads can vary dependent on A/C load distribution. This makes rate control schemes more difficult. How do you handle this?

Author:

While power extraction does vary from one engine to another in multiple engine aircraft, the load characteristic programmed into the control represents the worst case conditions. In that way, actually applied loads will always be equal to or less than those used in the control. As such, compressor stall margin is always maintained at the minimum design value or more, thus maximizing reliability.

3. W. Bouwman, Netherlands MOD

Is the worst case also used concerning TQ because of no temperature dependence occurring?

Author:

No temperature bias is included because the effect of cold temperature is less significant for larger engines than in smaller size engines, such as those used for helicopters. However, should a situation exist that the parasites are significant at colder temperatures, the variation of the characteristic can easily be programmed into the FADEC.

COLD START DEVELOPMENT OF MODERN SMALL GAS TURBINE ENGINES AT PRATT & WHITNEY CANADA

by

D.S. Breitman and F.K. Yeung
Pratt & Whitney Canada Inc.
6375 Dixie Road
Mississauga Ontario
Canada L5T 2E7

NOMENCLATURE

N_2 compressor rotational speed
 P_3 compressor delivery pressure
 ΔP pressure drop across combustor
 θ relative temperature ratio T_c/T_{ref}

ABSTRACT

Engine cold start capability is essential for aircraft in Arctic or winter operations. Demonstration of this capability is part of the engine development and certification requirements. Variables such as the combustor design, the ignition system, the fuel nozzle design, the diffuser exit flow characteristics, and the compressor performance at sub-idle conditions all affect the cold start capability of an engine. This paper describes briefly how these factors are usually optimised, and presents an overview of the successful PW305 Engine cold start development (with an electric starter). The PW305 is a new turbofan engine from Pratt & Whitney Canada in the 5000 lb (22.2 kN) thrust range.

INTRODUCTION

The starting cycle of a gas turbine engine is the acceleration of the turbomachinery from 0 to idle speed. The starting procedure generally consists of 3 stages: cranking, ignition, and acceleration to idle. During a typical engine start, many different events are occurring in the compressor, combustor, and turbine, simultaneously and in sequence. Most of these events are inter-related, and sometimes counteract each other. Furthermore, excellent engine starting characteristics may be at the expense of other engine requirements. To ensure relatively healthy engine starts over a full range of operating conditions and environments, considerable development work is necessary to obtain the best possible compromise, taking all of the engine requirements into account.

CRANKING STAGE

In this stage, a starter provides the power to crank the turbomachinery from 0 speed up to a pre-determined light-off speed, at which fuel is introduced into the combustion chamber. The most important consideration for the cranking stage is the selection of the starter.

Selection of Starter

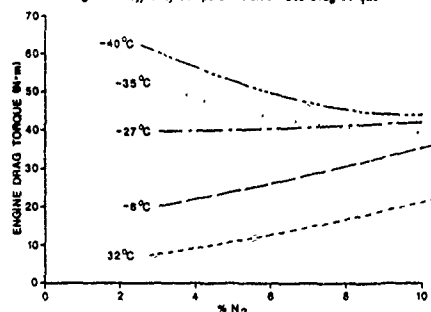
The 2 most common types of starters are air starters and electric starters.

The power of an air starter comes from a turbine which requires high pressure air to drive. The main application for aircraft operations with air starters is to start main engines with

high pressure from the auxiliary power units (APU).

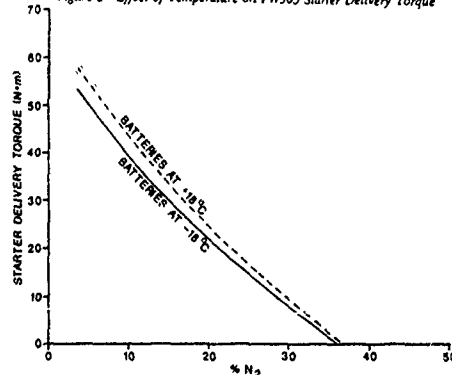
Power to an electric starter is supplied by either batteries or a ground cart. After the engine starts, the starter, drawing power from the engine, will act as a generator to recharge the batteries. This type of starter is usually applied on an APU or in small gas turbine aircraft. The selection of an electric starter requires careful evaluation of the starter/torque/battery match for the application.

Figure 1 Effect of Temperature on PW305 Drag Torque



The main factor affecting the selection of the starter combination is the torque requirement. Figure 1 illustrates how the engine drag torque (at N_2 lower than light-off speed) increases with decreasing temperature. The starter delivery torque (which decreases with decreasing temperature as shown in Figure 2) must be able to overcome this drag at the lowest temperature within the operating range, and must be able to crank the engine beyond the light-off speed.

Figure 2 Effect of Temperature on PW305 Starter Delivery Torque



After the torque requirement is finalised and the starter chosen, the minimum voltage supply for the starter to deliver this torque can be

determined from the starter characteristics. The batteries must be able to provide this necessary voltage.

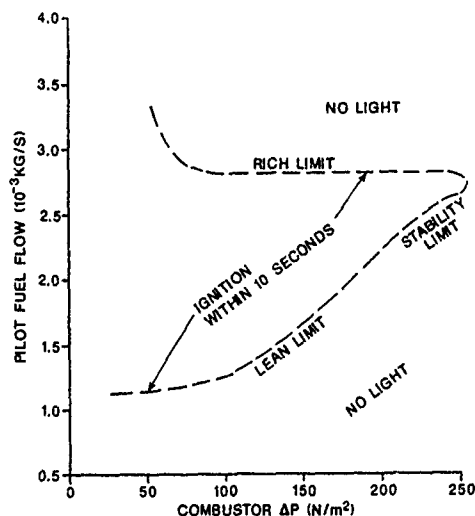
During development of a typical PWC fan engine, the power supply was the electrical simulation of the batteries at the lowest operating temperature. Only when all parameters affecting starting had been optimised were the actual batteries tested to confirm the developed data.

IGNITION STAGE

During cranking, as the engine reaches the light-off speed, fuel is introduced into the combustion chamber and ignition occurs. Fast ignition is desirable in order to avoid fuel pooling at the bottom and unburnt fuel accumulation in the down-stream turbine stages. Hence a long time to light will, very likely, cause torching and damage to the turbine.

Prior to full engine starting tests, the ignition range (ie. optimum fuel/air ratios for ignition) of the combustion system has to be determined throughout the operating range of the engine, including the lowest operating temperature and the most adverse altitude relight conditions. A graphical representation of the ignition range is given in Figure 3. The upper limit is the fuel-rich

Figure 3: Typical PW305 Ignition Range



limit above which the fuel/air ratio is too high for combustion to occur, or that any initial flame will be extinguished by fuel. The lower limit is the fuel-lean limit, below which, either the fuel/air ratio is too low for combustion, or the fuel is

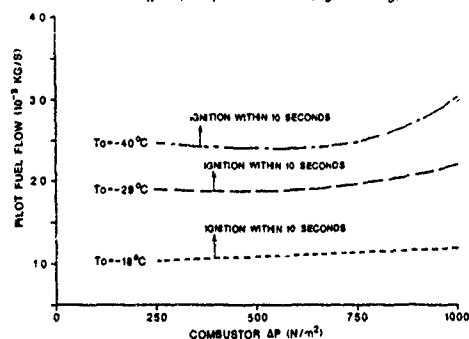
not properly atomised because of the low fuel flow. At combustor ΔP beyond the stability limit the air velocity may be too high for ignition, or for any initial flame to stabilise. The preference is a wide ignition range, which can provide adequate margin to ensure smooth and fast ignition during every start. Obviously, the local flow conditions at the igniters and fuel nozzles are important factors affecting ignition. The optimum combustor and fuel injector configuration, taking all the engine requirements into consideration, must be determined experimentally during development. The other factors that also affect ignition are:

- 1) operating temperatures
- 2) altitude
- 3) ignition fuel flow
- 4) ignition system
- 5) fuel nozzle and igniter locations
- 6) selection of the light-off speed

Operating temperatures

Figure 4 illustrates how the ignition range is affected with decreasing temperature. At lower temperatures increasing fuel viscosity adversely affects fuel atomisation. To compensate, higher fuel flow is necessary to ensure successful ignition.

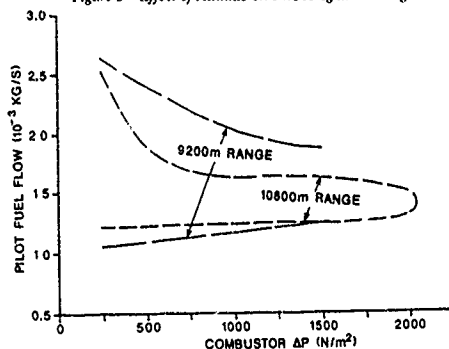
Figure 4: Effect of Temperature on PW305 Ignition Range



Altitude

At altitude, a stalled engine will windmill because of the aircraft's forward speed. This will cause a high pressure drop (ΔP) across the combustor. At higher combustor ΔP 's the stability limit for ignition is reduced (see Figure 5). A wide ignition stability range is essential at altitude where fast relights are expected over a range of aircraft speeds (ie. windmilling and thus combustor ΔP).

Figure 5 Effect of Altitude on PW305 Ignition Range



Ignition fuel flow

The main concern in the fuel system design is fast ignition and light-around. This is essential to provide a good circumferential temperature distribution following ignition, in order to avoid a non-uniform back pressure onto the compressor, which can force it into stall.

After the ignition range is determined for the various operating conditions, the starting fuel flow for each condition can be selected in conjunction with the combustor ΔP (which is determined by the light-off speed). Because of the narrower ignition range at cold temperatures and at altitude, the control on the accuracy of the fuel flow is just as important as the actual amount itself. Otherwise a long time to light will result.

The ignition fuel flow normally consists of a pre-determined amount of "pilot" fuel (from the pressure atomisers) and "main" fuel (from the air-blast nozzles), flowing simultaneously. This is to facilitate a fast light-around to produce a uniform temperature for reasons cited in the previous section.

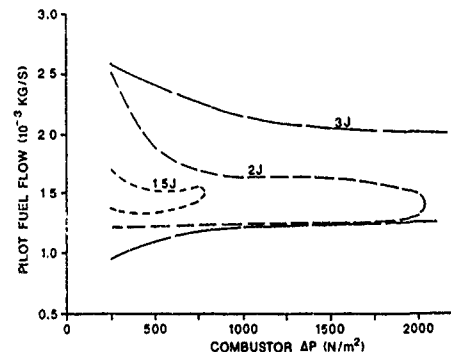
Ignition system

The ignition system consists of an electrical power supply, an exciter box, and usually 2 igniters. The electrical power supply comes from the batteries. The main criteria for igniter selection are durability, low loss (i.e., the ability to transmit the energy from the exciter box to the igniter tip efficiently), and compatibility with the combustor.

The choice of exciter boxes is dependent on the output energy level and the pulse rate. Figure 6 is an illustration that the higher this energy level and/or pulse rate is, the wider the ignition range becomes. The energy level is a more dominant factor. This is very beneficial for low temperature ignition and altitude relight. However, this performance is

achieved mostly at the expense of igniter durability. Therefore, the selected igniter box should have the minimum output energy level and/or pulse rate required to achieve a reasonable ignition range at the lowest temperature and the highest altitude in the operating envelope.

Figure 6 Effect of Exciter Box Energy on PW 305 Ignition Range at Altitude



Although there are usually 2 igniters on an engine, regulations specify that the engine must be able to relight at altitude with 1 igniter only.

Fuel nozzle and igniter locations

The locations of the fuel nozzles and the igniters can significantly affect the ignition range and are determined in relationship to the combustor. In addition to ignition, the other considerations are combustion efficiency, combustor exit temperature profiles, combustion system durability, maintainability, installation and access. After their axial locations are fixed, the circumferential locations of the pilot nozzles and igniters have to be decided carefully.

A pilot nozzle and an igniter must be in the same proximity for ignition. Two of each are required for redundancy. The 2 pilot nozzles may be side-by-side, or they may be separated, depending on the following:

- 1) air-flow around the fuel nozzle/igniter region, including the air swirl
- 2) fuel manifold connections, including the position(s) of the fuel supply
- 3) the intended circumferential fuel flow distribution
- 4) the intended directions of flame propagation after ignition

Selection of light-off speed

The selection of the light-off speed is depen-

dent on the optimum combustion ΔP , the torque demand, and compressor stall characteristics. These requirements are sometimes contradictory, and a careful compromise is necessary.

For a given engine (where the compressor running line has been fixed by the turbine vane size, and the combustor $\Delta P/P_3$ being constant) the absolute combustor ΔP is a function of the compressor corrected speed, $N_2/\sqrt{\theta_0}$. From a plot of the ignition range, it would appear that the optimum combustor ΔP is the lowest possible.

For air-blast nozzles, a higher ΔP generates better fuel atomisation, which is essential for fast light-around after ignition. Since finer fuel droplets require less evaporation energy, good atomisation is even more important at low temperatures, hence this requires a higher ΔP . Fortunately, as the temperature decreases, for a given engine speed (N_2), the corrected speed of the compressor ($N_2/\sqrt{\theta_0}$) is higher than that at normal temperatures, hence a higher compressor delivery pressure P_3 , and a higher combustor ΔP .

As discussed previously, the engine drag torque (at N_2 below the light-off speed) increases with decreasing temperature. With an electrical starter, the delivery torque decreases with decreasing temperature, because of the lower delivery power from the batteries. This delivery torque also decreases with increasing N_2 , as illustrated in Figure 2. This would suggest that a low light-off speed is desirable. The light-off speed must be selected such that the starter delivery torque is always higher than the engine drag over the complete temperature envelope of operation.

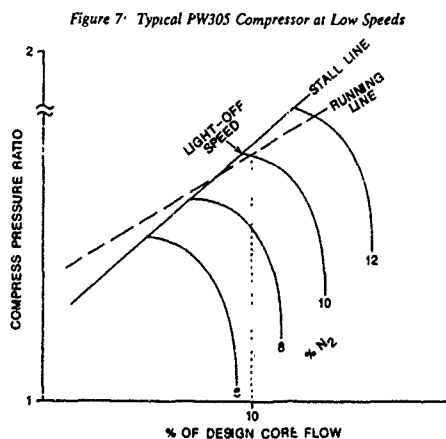


Figure 7 is a sketch of a typical compressor map at very low speeds. Below a certain speed the compressor running line is beyond stall. The compressor stall characteristics add to the engine drag significantly, and may prevent a successful start. At these speeds, a flame in the combustor may simply back pressure it further, forcing it deeper into stall, and increasing the drag torque tremendously. As illustrated in Figure 7, the compressor running line is in the stall-free region above a certain speed. Preferably, the light-off speed should be above this N_2 , otherwise the starter must carry the engine through this regime.

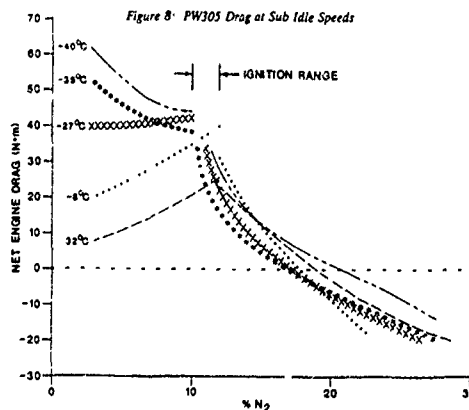
If compressor handling bleed is desirable, the light-off speed should be sufficiently high for this bleed to be effective.

ACCELERATION TO IDLE STAGE

After ignition, a relatively fast and smooth acceleration to idle is desirable. This is controlled by the engine drag, rate of acceleration, fuel schedule, compressor performance, and temperature schedule.

Drag

As discussed previously, the engine net drag (turbine delivery torque - total engine drag) increases with N_2 during the cranking stage. After ignition the turbine extracts power from the combustion gas, hence the net drag starts to fall off. As N_2 increases, the turbine delivery power will exceed the total engine drag at a certain speed, above which the engine self sustains, as illustrated in Figure 8 (the 0-drag line). Normally, the starter motor is applied until the engine speed exceeds this self-sustaining speed.



Rate of acceleration

The control of the engine acceleration rate from ignition to idle speed is very important. Too fast an acceleration can force the compressor into stall, and very likely will result in an unsuccessful start. This will compromise safety for altitude relights. Too slow an acceleration would pro-long the exposure of the turbine stages to the hot combustion gas at sub-idle speeds where cooling is inadequate. This will very likely cause hardware damages. Furthermore, since the engine normally still requires starter assist below the self-sustaining N_2 , very slow acceleration may cause the starter motor to overheat and result in damages.

Figure 9 Effect of Acceleration Rate on Compressor Characteristics

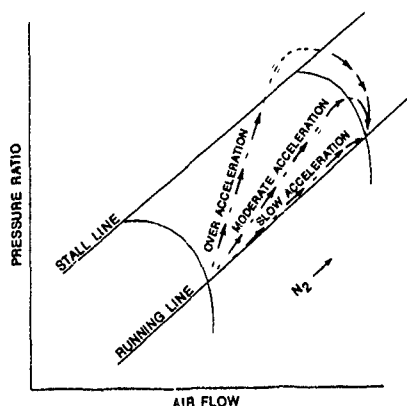


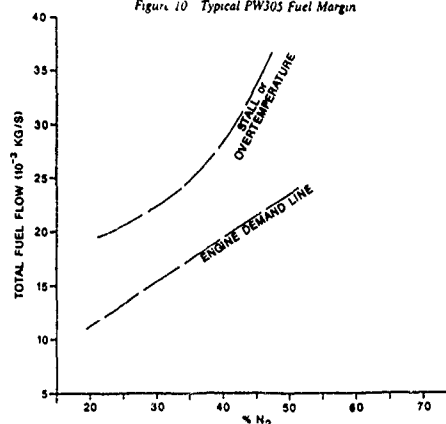
Figure 9 is an illustration of the relationship between the acceleration rate and the compressor characteristics. It is obvious that the preference is a moderately fast acceleration. The main control over this is the fuel schedule.

Fuel schedule

Fuel scheduling provides the most direct control on engine starting. It affects all the other parameters, and therefore has to be set carefully. Prior to the setting of the fuel schedule, the fuel margin as sketched in Figure 10 must be determined experimentally. The upper limit is the over-temperature and stall limit, above which the inter-turbine temperature is exceeded and/or the compressor stalls. The lower limit is the engine "demand line" where the net engine drag = 0, below which the engine cannot self sustain. The minimum difference between the 2 limits is the fuel margin. Since this margin is proportional to the compressor stall margin, it is a very good indica-

tion of the how close the compressor is from stall. It is desirable to have this fuel margin to be as wide as possible. This can be achieved by the improvement of the compressor.

Figure 10 Typical PW305 Fuel Margin



The fuel schedule must be between these 2 limits. A fuel schedule closer to the upper limit corresponds to a fast acceleration, while a schedule closer to the lower limit implies a very slow acceleration. The final schedule should be governed by the selected acceleration rate, which was discussed in the previous section.

The fuel flow on the engine "demand line" at the self-sustaining speed is usually taken as the minimum fuel flow in the starting fuel schedule.

Compressor

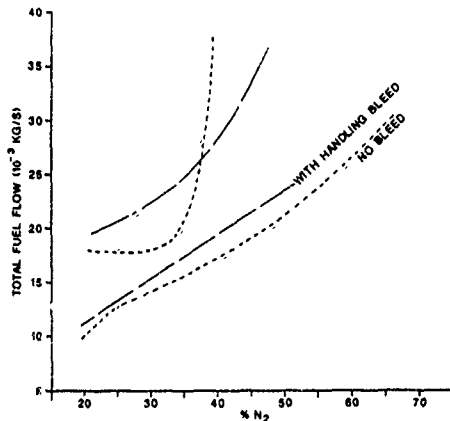
During the start cycle, most of the engine drag is contributed by the high compressor, which in the case of most PWC engines, consists of several axial stages followed by a single centrifugal stage. This drag increases significantly as the compressor is in stall. Therefore it is paramount to eliminate, or at least minimise the extent of the compressor stall. At low sub-idle speeds, stall usually occurs at the first axial stage rotor. At higher speeds, stall is controlled by the diffuser downstream of the centrifugal stage. The speed where the first rotor and diffuser stall lines cross each other depends on the stall margins of these 2 components. The most commonly used method for stall control at these speeds are variable inlet guide vanes, compressor handling bleed, diffuser sizing and alignment.

The variable inlet guide vane (VIGV) consists

of airfoils set at certain angles upstream of the high compressor. Its function is to introduce swirl into the air flow, which delays compressor stall at very low sub-idle speeds. In our experience, the VIGV alone may not be adequate. It is usually employed in conjunction with compressor handling bleed at sub-idle speeds.

The handling bleed is air taken off the compressor gas path through bleed slots. The bleed serves as an air flow sink that helps increase the air flow through the first stages of the compressor, and pulls it away from stall. Figure 11 is an illustration how bleed affects the compressor stall margin, as indicated by the fuel margin. For this bleed to be effective, the light-off speed should be sufficiently high, such that the compressor pressure ratio at the slot is adequate for air to be bled off.

Figure 11 Effect of Handling Bleed on PW305 Compressor Stall Margin



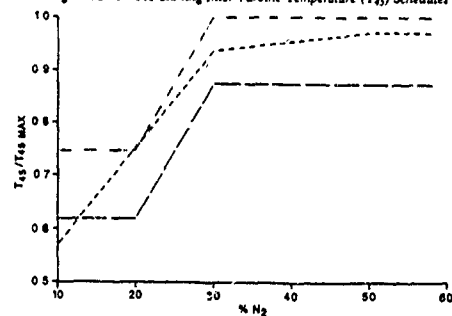
The diffuser throat sizing, while having a significant effect on the sub-idle stall margin, has an even greater effect on performance and stall margin at full speeds. Since this geometry cannot be varied as readily as the VIGV and the handling bleed, it is decided usually with more consideration given to the full speed performance and stall margin.

Temperature schedule

To avoid damages to the turbine stages, inter-turbine temperature limit schedule for sub-idle speeds must be determined. This temperature schedule depends mainly on the amount of cooling available for the turbine stages. At any given speed, this temperature should be sufficiently high for the turbine to extract enough power for reasonably fast acceleration, yet low enough to avoid turbine hardware damages and/or over-acceleration causing

compressor stall. If the "fuel margin" (discussed in the 'Fuel Schedule' section) is very narrow, a carefully controlled temperature schedule can be used to "navigate" through the awkward speed range. This temperature schedule is usually determined experimentally during development, and Figure 12 is an illustration of several schedules that were evaluated during the PW305 development. For a modern PWC fan engine, the start cycle is controlled by a sophisticated electronic engine control system (EEC) to follow a temperature schedule.

Figure 12 PW305 Starting Inter Turbine Temperature (T_{45}) Schedules



OTHER CONSIDERATIONS

During PW305 development all the above parameters were optimised, and successful starts at low temperatures were demonstrated. More tests were conducted in search of improvements, partly to demonstrate safety, and partly to determine ultimate limits.

- 1) More tests at extreme temperatures, even below the operating range, with alternative fuels and oils. The purpose of this was to determine whether the engine starting performance could be improved further with lower viscosity fuel and/or oil.
- 2) Starts conducted with deteriorated batteries to determine the worst conditions these components could be operated at, without compromising safety.
- 3) Starts demonstrated in the test facilities with water saturated fuel at the worst icing conditions.
- 4) Altitude relights at extended operating envelope demonstrated in the test facilities. This was later confirmed in flight tests.
- 5) Successful altitude relights with single igniter and single pilot nozzle beyond the operating envelope demonstrated in the test facilities, and later confirmed in flight tests.

- 6) Starts with deteriorated engine to simulate the hardware conditions after an extended period of operation.

CONCLUDING REMARKS

This has been a brief description on the major parameters affecting starting, the problems that usually arise, and the techniques applied during the development of the PW305 Engine to overcome these problems systematically. Part of this experience may be readily applied to other small gas turbine engines with an electric starter. However, each engine is designed for its own unique application, and hence some of the problems may require considerations on an individual basis.

ACKNOWLEDGEMENT

The authors would like to thank Pratt & Whitney Canada Inc. for the permission to publish this data, and to express special appreciation to Mr. Alan Wheatley (of the PWC Combustion Dept.) and the test crew at the National Research Council for their support during the cold start development.

Discussion

1. C. Meyer, French MOD

Quelles sont les possibilités en cas de redemarrage avorté sur PW 305? Y-a-t-il des procédures et des précautions particulières?

Author:

The starting sequence for the PW 305 both on the ground and in the air is as follows.

- (i) Continuous ignition selected on
- (ii) Thrust lever angle (TLA) selected to idle position
- (iii) Starter motor switch on

As the engine accelerates through 10% N2 (high pressure rotational speed), the electronic engine control automatically introduces fuel. Since the igniters are already on, ignition takes place and the control accelerates the engine to idle.

In the event of an aborted start, at altitude, windmilling will scavenge pooled fuel and the process (i—iii) is repeated. On the ground a motoring cycle must be carried out to ensure scavenging of excess fuel. Then the start procedure is repeated.

This procedure is repeated until a start is successful or it is felt that further investigation of the situation is necessary (burnt out igniter plugs, plugged fuel nozzles, etc)

2. P. Sabla, GEAE

Curve nr. 3 shows delta p off by a factor of 10?

Author:

This is in fact incorrect, scale should read 0—2500.

Design Considerations
based upon

Low Temperature Starting Tests on Military
Aircraft Turbo Engines

by

H.-F. Feig

Wehrtechnische Dienststelle für Luftfahrzeuge (WTD 61)
Flugplatz, 8072 Manching, Germany

SUMMARY

Test experience on engine low temperature starting was obtained in the course of multinational and national trials to assess weapon system performance.

The objective of the trials was to recommend a clearance for the weapon system.

In order to carry out these tests adequately the operational role of the weapon system had to be considered and the operational limits of the engines and associated systems had to be known.

Parameters influencing low temperature start capabilities were reviewed and experience gained from the tests was discussed.

1. INTRODUCTION

Engine start is an interaction of various systems. Consequently, not only the engine has to be considered - of equal importance are the starting system and the capability of monitoring the start process.

The evidence that the solution provided by the contractor complied with the requirements of the Services had to be demonstrated by official tests. Conclusions resulting from these tests are summarized in a recommendation stating the extent to which the weapon system can be operated by the Services.

The assessment of low temperature start performance represents a specific and very important field in the overall testing of the weapon system, since low temperature engine starting has a considerable effect on the value of the weapon system.

- a) The objective of the low temperature engine start test has to be an assessment of whether the technical solution meets the requirements of the Services. This official task can be defined in more detail as follows:
 - checking of the engine and engine starting system standards with regard to performance and characteristics required by the specifications
 - checking the validity and applicability of the operating instructions
 - assessment of the weapon system start up activity from the military operational point of view
 - gathering of information for checking and validating the national weapon system and engine documentation
 - recommending a clearance for Service use.
- b) The mission for which the weapon system was designed together with resulting performance aspects must be considered with regard to their influence on the test programme.

In order to meet operational requirements, each weapon system design - including engine design and starting system design - comprises many technical features which together contribute to a satisfactory weapon system operation. Knowledge of this features is required for the assessment of low temperature engine start capabilities. This information has to be obtained from specifications and design documents and from development test experience available from airframe, engine and system manufacturers.

- c) Operational limits, which must not be exceeded, together with proper interaction of the systems involved, form the technical basis for the assessment of the test results.

2. MILITARY SYSTEMS ENVIRONMENTAL REQUIREMENTS

During the weapon system definition phase environmental requirements and system capabilities were established.

Guidelines for the selection of requirements and the scope of testing necessary are provided by:

- NATO STANDARDISATION AGREEMENTS (STANAG)
- MILITARY STANDARDS
- MILITARY SPECIFICATIONS

List 1 shows an abstract of current documentation relevant to definition and evaluation of system capabilities.

3. TEST ENVIRONMENT

3.1 CLIMATIC CHAMBER TESTING

In order to achieve independence from natural meteorological influences, environment simulation is used. In many cases the environmental systems of test chambers are not capable of delivering the airflow demand of the engine.

Therefore, during start up, outside air is mixed into the test chamber. In general, outside air has a higher temperature and a higher total amount of humidity than the air of the test chamber. This results in a direct fall out of humidity and rapid ice build up on the cold soaked test object.

It must be ensured that the free water content of the air and the ice accretion does not result in any interference with the test objective.

3.2 TESTING IN NATURAL ENVIRONMENT

Complete weapon system testing in a natural environment is the approach desired, sometimes, however, it is the reliability of the weather forecast that is tested!

As shown in Fig: 1, a typical temperature survey of a 94-hour cold start test conducted at WTD 61 airfield during winter 1985 is provided. The lowest temperature reached was -21°C and the highest temperature observed -9°C. Fluctuation of temperature is remarkable in the course of a day.

In order to give an impression of the cool down capability of the natural environment, the frequency distribution of the temperature survey is shown in Fig: 2. The reference soak temperature achieved on aircraft during this test was -14°C.

3.3 COLD SOAK EFFECTIVENESS

A so called "Full Cold Soak" is only completed when all systems affected during the test are cooled down to the same level of temperature. Because of the unequal mass concentration on weapon systems long soak periods were required in order to obtain a balanced temperature. A proper test instrumentation must be installed in order to measure system temperatures.

4. INFLUENCES IN ENGINE COLD START CAPABILITIES

4.1 VISCOUS SHEAR EFFECTS

One of the main influences aggravating engine cold start up are viscous shear effects depending on:

4.1.1 TYPE OF OIL

Modern engines and weapon system designs demand sufficient lubricity and thermal stability under high operating temperatures.

The following oils are used in modern German military systems:

0 - 160 according to UK-Specification
DERD 2497/3

and

0 - 156 according to MIL-L-23699 C Amd 1 or
DERD 2499/1 Amd 2

These oils are of the 5,5 mm²/s Viscosity Class at 100°C. As expressed in Ref: 1, the viscosity of the above mentioned oils increases by a factor of 150 when the temperature is lowered from +15°C to -40°C. This increase in viscosity is the main driver in system drag increase.

The use of oils with a lower base viscosity, which are more suitable for cold operations, is discarded due to the climatic conditions prevalent in Central Europe and because of logistic reasons as:

- restrictions in oil types
- abandonment of oil changing activities necessary for a very short period of the year only.

4.1.2 SYSTEM DESIGN

Geartrains and bearings cause the highest portion in start up drag. A reduction can be achieved by:

4.1.2.1 SEPARATION:

Reducing the number of components operated during cold start up by:

- multi-spool engine design
- use of clutches and freewheels.

4.1.2.2 DELOADING:

- Engine oil pump deloading during start phase
- Accessory hydraulic pump deloading during start phase

4.1.2.3 MINIMIZATION OF GEARTRAIN LOSSES BY

- stacked design of accessories such as fuel and oilpumps
- avoidance of niches and depots where oil can be hidden
- dry sump oil system design and shielding of the geartrain in order to reduce churning losses.

4.1.2.4 ROTOR DRAG REDUCTION

Appropriate clearances/material contraction rates need to be provided in order to avoid brushing or blocking of the rotor. In order to reduce the rotational moment of inertia, separation has to be considered by:

- multi-spool engine design
- use of clutches and freewheels.

In order to reduce the torque demand of the compressor, deloading by use of inlet guide vanes/bleed valves should be considered.

4.2 FUEL AND AIR MANAGEMENT

Matching of all components under consideration of various influences must be ensured in order to enable a reliable light up of the engine. As effects are analysed in detail in Ref: 2, Ref: 3 and Ref: 4, indication of the main subjects is considered to be sufficient in this paper.

4.2.1 TYPE OF FUEL

Introduction of the fuel Nato Code F34(JP8) with a flamepoint of at least +38°C and a destillation range of 130°C to 300°C as a basic engine fuel for German Forces instead of Nato Code F40 (JP4) with a flamepoint of below - 20°C and a destillation range of 50°C to 250°C (Wide cut) aggravated the engine demands in low temperature starting.

4.2.2 SYSTEM DESIGN

Capabilities of cold start up are mainly influenced by

- compressor delivery characteristic
- combustor design
- fuel vapouriser-/atomiser-capabilities
- number and position of starter jets
- start up and acceleration fuel control schedule
- number and position of ignitor plugs
- ignition energy provided by a soaked and loaded battery as power source.

4.3 STARTER ASSISTANCE AND ENGINE RESISTANCE/ASSISTANCE

The most important aim of the overall process called engine start is to enable a reliable and a stable circumferential light up of the combustion chamber.

Ref: 5 describes an annular combustion chamber with a wide fuel/airflow operational range of 10 to 40% of engine speed, for example.

The start window of each individual engine needs to be met by tailoring the engine starter characteristic.

Fig: 3 shows a typical engine resistance/assistance characteristic with a starter characteristic and Fig: 4 typical different engine resistance/assistance characteristics of various engines in cold operation.

Increasing engine speed leads to higher torque demand on the engine up to the light up point when combustion takes place and turbine energy starts to assist the engine run up. At higher speed the resistance reaches zero and a positive torque of the engine commences. The typical speed-torque relation of an engine starter is a descending, linear slope with maximum torque at zero speed. These characteristics are well known from turbines and some types of electrical motors.

Starter size and characteristic must meet the requirements made by:

- maximum drag torque of the engine
- maximum drag torque of the accessories
- start assistance of the engine
- load characteristics of the accessories when hydraulic pumps and generators are getting on line
- rotational moment of inertia of the engine
- rotational moment of inertia of the accessories.

On the basis of the knowledge of the resistance/assistance characteristic and the sum of the rotational moments of all components related to one shaft (for example the power take off shaft), the required starter assistance can be calculated in order to meet the weapon system requirements.

Dependent on weapon system task and environmental range, different start systems are in use.

4.3.1 DIRECT MECHANICAL SYSTEMS

Main engine starts are carried out via one or two shaft APUs, reduction drives, and on some weapon systems by torque convertors.

Because the APU power output characteristic is dependent on air density and fuel control characteristic, power output in cold environment increases and is therefore able to cope with the higher demand of power required.

4.3.2 PNEUMATIC SYSTEMS

4.3.2.1 PRESSURE BOTTLE OPERATED

Provision is made for impingement operation of the turbine or of the compressor wheel, or a separate starter motor is provided. These are the systems often used for small engines. Low temperature performance can only be ensured, when especially extreme care is taken of the water extraction system of the bottle filling compressor. The operating media air is stored under high pressure. Rapid expansion will not be followed by the humid portion of the air. The resulting free water can freeze and can create trouble in pressure control valves, control valves and nozzles.

4.3.2.2 APU OR GROUND CART OPERATED

The power available is substituted by the characteristic mentioned in Para 4.3.1 and an advantage in respect of less run up drag in comparison to direct mechanical drive systems due to the almost gearless design is provided.

4.3.2.3 ELECTRICALLY OPERATED

The main power source is the aircraft battery. Because of the decreasing power output in a cold environment, battery-powered systems can only fulfill the system requirements when the battery is properly sized and service usage allowance and charge factor are taken into consideration. A common factor for service usage allowance is 0.8 and for charge 0.9. In other words, $0.8 \text{ times } 0.9 = 0.72$, which means a battery of 72% capacity shall be considered for sizing and demonstrating system performance.

Because of the limited power available, battery powered starting systems are commonly used only up to the 1500 KW/15 k Newton engine power class.

4.3.2.4 HYDRAULICALLY OPERATED

A high amount of energy can be stored in hydraulic accumulators and recalled even in extreme cold environment. The special effort required is normally applied only when appropriate utility systems are already on board and extreme environmental conditions have to be met.

5. ENGINE STARTING SYSTEM PERFORMANCE ASSESSMENTS

5.1 PNEUMATICALLY AND ELECTRICALLY POWERED

As an denotation of different engine start system capabilities, the respective speed ratios, each calculated from dry crank speed achieved at ISA temperature divided by dry crank speed achieved at -15°C , are shown in Fig: 5.

The WILLIAMS WR 2-6 engine is equipped with a pneumatic starting system.

The KHD T312 and LARZAC 04 engines are equipped with a battery powered electrical starting system.

5.2 DIRECT MECHANICALLY POWERED

As shown in Fig: 6 and already described in Ref: 6, the TORNADO aircraft is equipped with a mechanical secondary power system. For engine starting, APU or main engine power is used to operate a torque converter, the turbine section of which is connected to the main engine power take off shaft. Cold temperature testing revealed a temperature dependency of the torque output as shown in Fig: 7.

The warming up behaviour was investigated. Fig: 8 shows the warming up curve for the left hand and right hand gearbox of the secondary power system respectively. Temperature increase at the end of the curve was caused by torque converter operation. The different warming up behaviour of the gearboxes is mainly caused by the integrated oil system of the right hand gearbox and the APU when hot return oil flow of the APU shortens system warm up. It was determined from test results that in order to fulfil main engine assistance demand, an oil temperature of at least $+30^{\circ}\text{C}$ was required.

A warming up procedure was created and recommended to the Services.

The influence of viscosity in torque converter output torque was eliminated in the meantime by modification action mainly by improving the suction conditions of the scavenge oil pump.

6. ENGINE PROTECTION DURING START UP

As much as engine resistance increases and starter assistance is degraded in cold environment, engine assistance has to take over a higher portion in order to accelerate the engine properly up to idle speed according to the system requirements. That will result in a higher thermal loading during the start phase. In order to protect the engine from thermal overloading special arrangements were built in.

Typical differences in speed and temperature during start up of an engine under ISA and cold conditions are shown in Fig: 9 and Fig: 10.

The protection system has to cope with this wide range of engine parameters. In order to safeguard the engine start under extreme environmental conditions, the following measures were created:

6.1 SCOPE OF PROTECTION

6.1.1 PROTECTION AGAINST TOO LOW STARTER ASSISTANCE

Too low starter assistance can be caused by seizure inside the transmission train or degradation of the power source, as:

- exhausted battery
- exhausted accumulators or air pressure bottles
- flow starvation of the power transmission media.

6.1.2 PROTECTION AGAINST "NO LIGHT UP"

Achieved by minimization of fuel injected in order to avoid overtemperature and to save starter system energy.

6.1.3 PROTECTION AGAINST HUNGSTART

A hungstart is caused mainly by incomplete light up of the combustion chamber or low starter assistance.

6.1.4 PROTECTION AGAINST OVERTEMPERATURE

The necessity has already been mentioned in Para 6.

6.1.5 PROTECTION AGAINST INCORRECT RESTARTING

Proper starter engagement and sufficient drainage time have to be ensured for consecutive engine starts.

6.2 APPLICATION OF ENGINE PROTECTION SYSTEMS

6.2.1 FIRST GENERATION OF ENGINE PROTECTION DURING START

Manual protection is given for early developed systems. Speed and temperature gauges have to be observed by the operating personell according to the operating instructions, and high pressure fuel cock opening/closing and starter shut off have to be initiated manually. Because of the slow beginning and very dynamic behaviour at the end, the outcome of the start, especially in cold operation, depends to a great extent on the skill of the operators.

6.2.2 SECOND GENERATION OF ENGINE PROTECTION DURING START

Combined, automatic and manual protection is provided.

Engine start up operation within the limits is enabled by the use of some threshold values functioning as watchdogs and the assistance of the operator.

Electronic Control Units of discrete or integrated technology were used.

Some typical threshold values which are logically combined in the Electronic Control Units are explained below:

6.2.2.1 PROTECTION AGAINST TOO LOW STARTER ASSISTANCE

This protection is provided by speed observation at the end of the starter only acceleration prior to initial ignition of the engine. Because of the low acceleration customary in cold environment, the threshold value has to be tailored to these conditions.

For example:

6 seconds after start initiation the engine speed must be equal or greater than 8%.

6.2.2.2 PROTECTION AGAINST "NO LIGHT UP"

Such protection is provided by temperature or speed observation of the engine.

6.2.2.2.1 TEMPERATURE OBSERVATION

A temperature threshold value indicates the begin of the light up of the combustion chamber.

For example:

12 seconds after start initiation the exhaust gas temperature must be equal or greater than 150°C.

6.2.2.2.2 SPEED OBSERVATION

A speed threshold value indicates the begin of the light up of the combustion chamber.

For example:

15 seconds after start initiation the engine speed must be equal or greater than 25%.

6.2.2.3 PROTECTION AGAINST HUNGSTART

This protection is provided by engine acceleration or speed observation.

6.2.2.3.1 ACCELERATION OBSERVATION

An acceleration threshold value indicates a minimum acceleration.

For example:

20 seconds after start initiation and up to idle speed the acceleration of the engine must be equal or greater than 0,5% per second.

6.2.2.3.2 SPEED OBSERVATION

A speed threshold value indicates the acceleration above a typical hungstart area.

For example:

20 seconds after start initiation the engine speed must be equal or greater than 40%.

6.2.2.4 PROTECTION AGAINST OVERTEMPERATURE

As shown in Fig. 10 the temperature level is much higher during cold start up of an engine than during all other starts. Because of the very dynamic nature of the engine parameters during the start up, an overtemperature protection has to be provided. In order to meet stringent acceleration requirements, metering of the fuel is scheduled accordingly. This results in a rapid increase of the gas temperature during start up to a high level.

6.2.2.4.1 PROTECTION AGAINST OVERTEMPERATURE BY TEMPERATURE OBSERVATION

6.2.2.4.1.1 TEMPERATURE LIMIT

A temperature threshold value allowing a safe operating range for start up.

For example:

Engine exhaust temperature must be less than 800°C.

6.2.2.4.1.2 TEMPERATURE/TIME LIMIT

A temperature versus time threshold value is built in
For example:

Excursions of the exhaust gas temperature up to 1100°C are allowed for 2 seconds duration.

6.2.2.4.2 PROTECTION AGAINST OVERTEMPERATURE BY ACTIVE CONTROL

6.2.2.4.2.1 BY TEMPERATURE OBSERVATION

The fuel scheduled to the engine is unaffected up to the maximum allowed gas temperature. When the gas temperature threshold is reached, this results in fuel bypassing in order to limit the gas temperature to the maximum allowed. Because of the lower portion of fuel metered to the engine, acceleration is decreased.

6.2.2.4.2.2 TEMPERATURE OR ACCELERATION CLOSED LOOP CONTROL

An exhaust gas temperature or acceleration schedule versus engine speed is provided. The fuel is metered according to this schedule dependent on the environmental conditions. This method demands the greatest effort, ensuring in this way most careful treatment of the engine during starting operation.

6.2.2.5 PROTECTION AGAINST INCORRECT RESTARTING

Threshold values for recycling of a start are built in.

For example:

- For a restart engine speed must be less than 2%.
- For a restart temperature must be less than 150°C.
- Intervals between successive starts must be greater than 2 minutes.

6.2.3 THIRD GENERATION OF ENGINE PROTECTION DURING START

Fully automatic control is provided. After initiation of the start sequence by the operator or programmed start up, observation and protection were performed automatically.

7. CONCLUSION

Tests of Official Test Centres are different to those of the contractor. Test techniques are generally the same but test objectives are different. These are not aimed at research or development, but are addressed to a final product offered to the government for Service use.

Knowledge of the boundaries of engine parameters during cold start up as well as engine observation and protection facilities and their interaction are most important for the planning and conduct of engine cold start tests.

8. RECOMMENDATION

Evaluation of the proper functioning of observation and protection facilities is required. Any interference of the observation and protection system during start up must be displayed to the ground crew for quick correcting action, to enable the aircraft to be returned to flight status as soon as possible.

It should be noted that under cold or ISA conditions speed and exhaust gas temperature build up in substantially different ways. A threshold based observation and protection system should therefore be capable of adapting its threshold values accordingly.

Fully automatic A/C run up systems should be supported by a sub-program capable of at least 3 subsequent engine start attempts. It must be ensured that a reset of the automatic preflight sequence of the airborne system is not required when a failed start occurs.

Minimization of thermoshock loads of the sensitive components of the engine can be achieved by use of advanced observation/protection systems. This method can be applied not only to cold operation but throughout the whole operational range of the weapon system, resulting in increased life. This means that the availability of the system is increased and reduction of cost will be achieved.

REFERENCES

- (1) Piel, K.J.
Experience with the KHD APU T312 for a Modern Fighter Type
AGARD-CP 324; Page 12-1 to 12-15
- (2) Alternative Jet Engine Fuels
AGARD-AR-181-VOL.II
- (3) Combustion Problems in Turbine Engines
AGARD-CP-353
- (4) Combustion and Fuels in Gas Turbine Engines
AGARD-CP-422
- (5) Collin, K.H.;
A Small Annular Combustor of High Power-Density, Wide Operating Range and Low Manufacturing Cost
AGARD-CP-422, Page 42-1 to 42-12
- (6) Hausmann, W.; Pucher, M.; Weber, T.;
Secondary Power System For Fighter Aircraft
Experience Today and Requirements For A Next Generation
AGARD-CP-352, Page 3-1 to 3-15

LIST 1

DOCUMENTATION TO DEFINE AND EVALUATE SYSTEM CAPABILITIES

STANAG 2895	Extreme Climatic Conditions and Derived Conditions For Use In Defining Design/Test Climatic Conditions For NATO Forces Materiel
STANAG 3518	Environmental Test Methods for Aircraft Equipment and Associated Ground Equipment
MIL-STD-210	Climatic Extremes for Military Equipment
MIL-STD-810	Environmental Test Methods And Engineering Guidelines
MIL-E-5007	Engines, Aircraft, Turbojet and Turbofan, General Specification for
MIL-A-87229	Auxiliary Power System, Airborne
MIL-P-85573	Power Unit, Aircraft, Auxiliary, Gas Turbine, General Specification for.

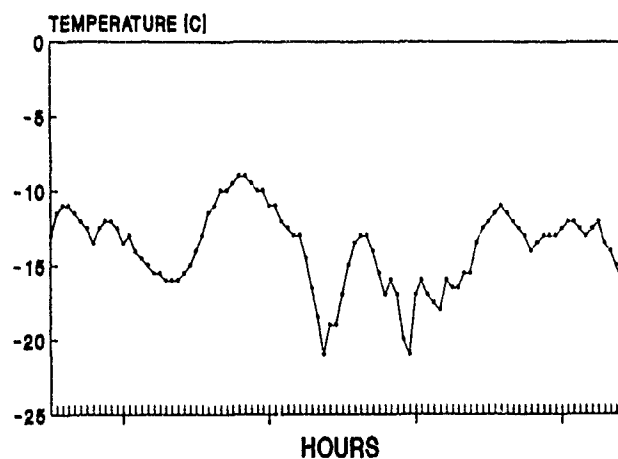


FIGURE 1 94 HOUR COLD SOAK TEST
MANCHING AIRFIELD 11.-15.01.1985

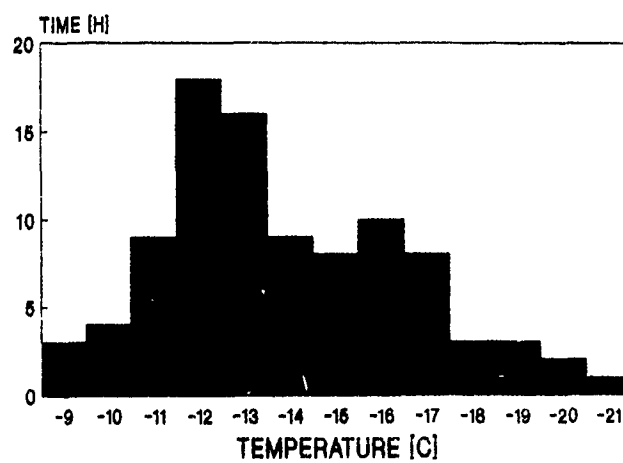


FIGURE 2 TEMPERATURE FREQUENCY DISTRIBUTION

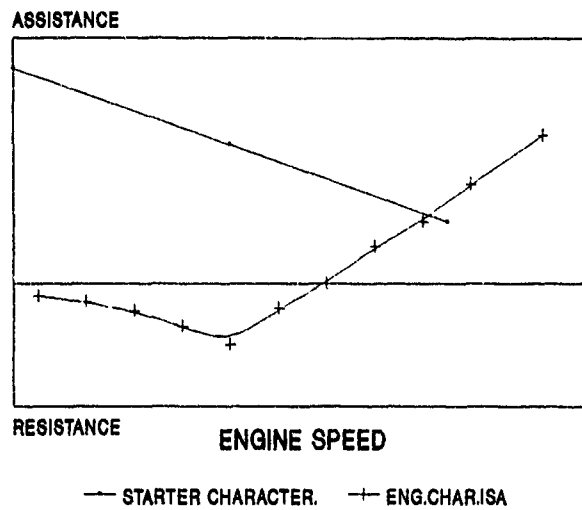


FIGURE 3 TYPICAL ENGINE RESISTANCE/ASSISTANCE AND STARTER CHARACTERISTIC

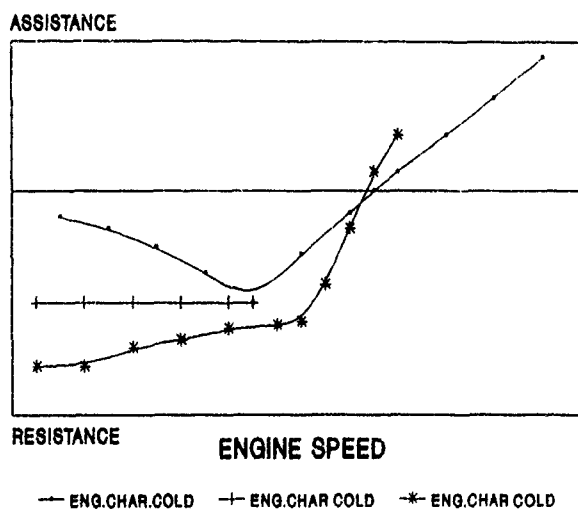


FIGURE 4 TYPICAL ENGINE RESISTANCE/ASSISTANCE CHARACTERISTIC OF DIFFERENT ENGINE DESIGNS IN COLD OPERATION

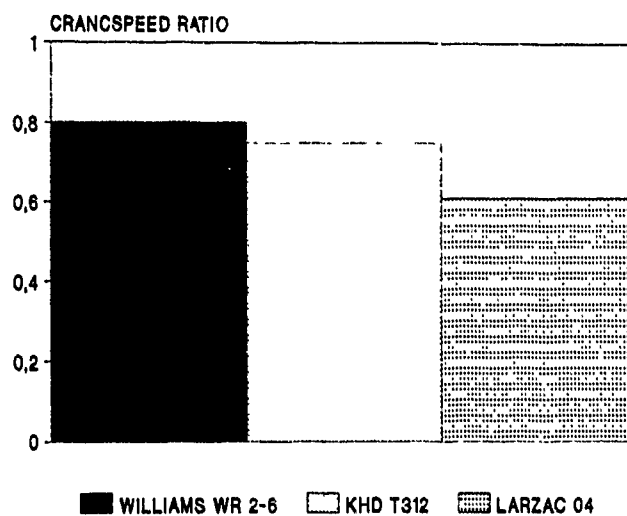


FIGURE 5 CRANKSPEED RATIO ISA/-15°C

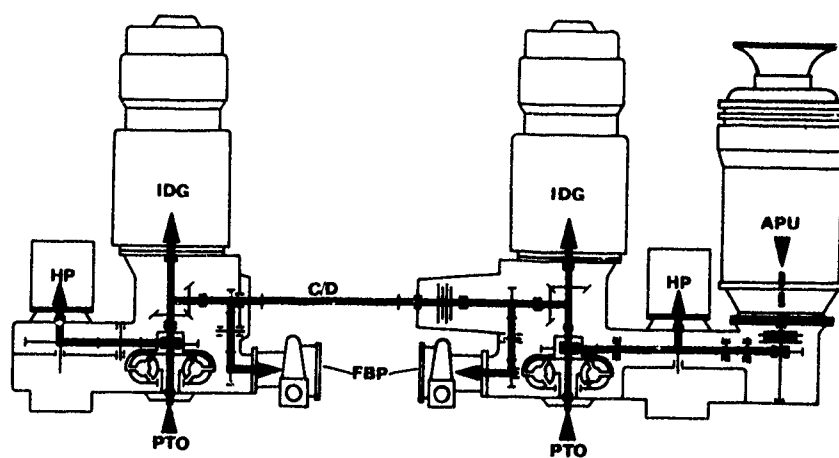


FIGURE 6 DIRECT MECHANICAL DRIVEN
SECONDARY POWER SYSTEM
OF TORNADO AIRCRAFT

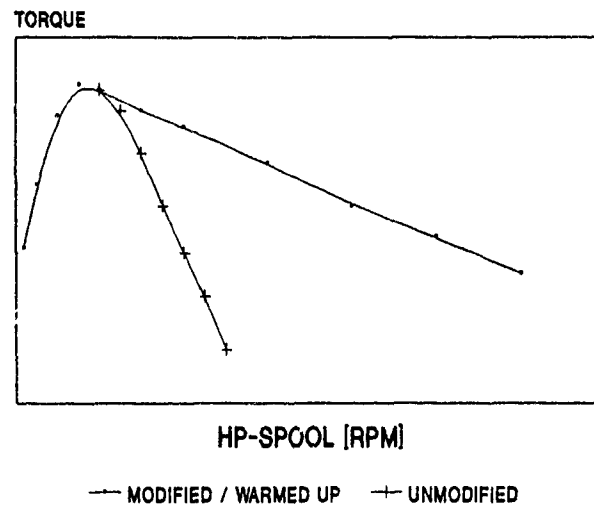


FIGURE 7 TORQUE CONVERTER CHARACTERISTIC

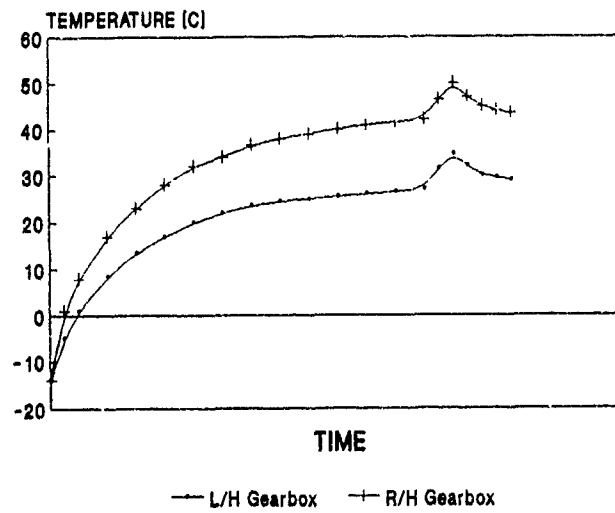


FIGURE 8 GEARBOX WARMING UP CURVE

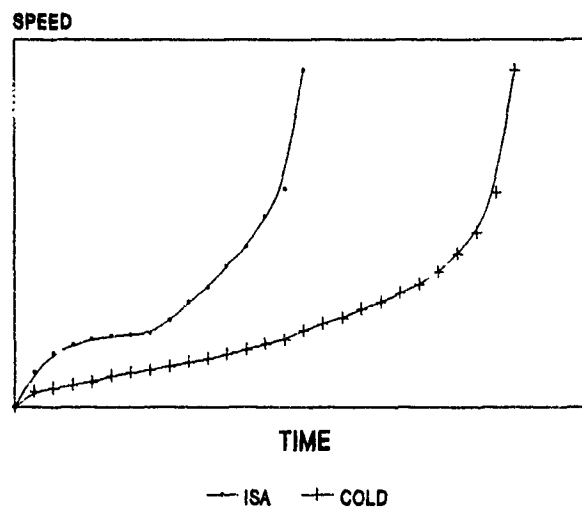


FIGURE 9 TYPICAL ENGINE START
SPEED RELATION

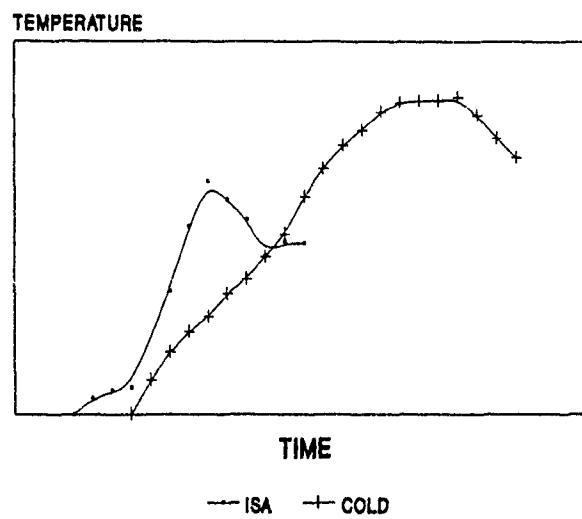


FIGURE 10 TYPICAL ENGINE START
TEMPERATURE RELATION

Discussion

I. C. Meyer, French MCD

Un problème qui se fait généralement en essais de qualification est celui de la dispersion des performances entre matériels d'une même série. Prenez vous en compte cet aspect pour la qualification des capacités de démarrage à basse température?

Author:

Adequate configuration control has to be obtained. The minimum performance is specified and has to be demonstrated. Performance of items of series production has to include the production scatter and has to be above the minimum specified. For demonstrating system performance, for example the battery, the minimum performance required is used.

CLIMATIC CONSIDERATIONS IN THE LIFE CYCLE MANAGEMENT OF THE CF-18 ENGINE

by

Capt. R.W. Cue
Canadian Forces
National Defence Headquarters
Ottawa, Canada, K1A 0K2
Attn: DFTEM 6-3-2

D.E. Muir
GastOPS Ltd.
1011 Polytek Street
Ottawa, Canada, K1J 9J3

SUMMARY

The Canadian Forces have developed an Engine Parts Life Tracking System (EPLTS) to define the scheduled maintenance requirement of CF-18 aircraft engine components. Up to 64 components are tracked by this system, 26 of which are life limited on the basis of eight different Life Usage Indices defined by the engine manufacturer and evaluated during each operational mission by the aircraft's Inflight Engine Condition Monitoring System. Data on the rates of component life consumption collected by the EPLTS during a full 12 month time span have been analyzed. The manner and extent to which seasonal effects might influence these life consumption rates and hence the life cycle management of the engine are presented and discussed.

NOMENCLATURE

ADF - Aircraft Data File	N ₂ - Compressor Rotor Speed
CFB - Canadian Forces Base	N ₂ F - Full N ₂ Cycles
CR - Count Rate	N ₂ P - Partial N ₂ Cycles
EFTC - Equivalent Full Thermal Cycles	OCM - On-Condition Maintenance
EPLTS - Engine Parts Life Tracking System	P ₃ F - Full P ₃ Cycles
EOT - Engine Operating Time	P ₃ P - Partial P ₃ Cycles
ELCF - Equivalent Low Cycle Fatigue	P ₃ - Compressor Delivery Static Pressure
HPC - High Pressure Compressor	PLA - Power Lever Angle
HPT - High Pressure Turbine	RS - Relative Severity
IECMS - Inflight Engine Condition Monitoring System	SRF - Stress Rupture Factor
IRP - Intermediate Rated Power	TAMP - Time at Maximum Power
LCF - Low Cycle Fatigue	TMT - Turbine Metal Temperature
LCMM - Life Cycle Maintenance Manager	T ₁ - Engine Inlet Temperature
LUI - Life Usage Index	t _R - Time to Creep Rupture
LPT - Low Pressure Turbine	ε _C - Creep Strain
MDRM - Maintenance Data Recorder Magazine	dε _C /dt - Creep Strain Rate
MOB - Main Operating Base	

INTRODUCTION

The air element of the Canadian Forces operates 124 CF-18 fighter aircraft from Main Operating Bases located at Cold Lake, Alberta; Bagotville, Quebec; and Baden-Soellingen, West Germany. The operational role of the CF-18 requires that it operate out of bases in various geographical and climatic areas. For the CF-18's Canadian sovereignty and North American Air Defence (NORAD) role, the aircraft operates from far north deployments at Inuvik, Yellowknife, Rankin Inlet and Iqaluit, North West Territories to training deployments at various bases in the southern U.S. The Canadian Forces' NATO commitment has the CF-18 operating out of the European theater. This puts the CF-18 in an operating environment which ranges from the very cold weather in the far north, to the moderate climate of Europe, to the extreme heats of the southern U.S.

The acquisition of the CF-18 by the Canadian Forces has also resulted in a new approach to fighter engine maintenance. Whereas previous engines were overhauled on a fixed time interval basis, the General Electric F404-GE-400 engine is for the most part maintained on an "on-condition" basis. In particular, the life usage of critical components within the engine is continuously evaluated by the aircraft's Inflight Engine Condition Monitoring System (IECMS). A ground-based Engine Parts Life Tracking System (EPLTS) has been developed by the Canadian Forces to record the accumulated life usage, configuration status and maintenance history of these components. The EPLTS also is used to forecast the fallout or removal time for each life component based on historical life usage accumulation rates.

This paper describes the CF-18 IECMS and EPLTS and examines the effects that climatic variations can have on the rates of F404 component life usage accumulation. The influence of these effects on the life cycle management of the engine are also discussed.

BACKGROUND

The CF-18 aircraft is powered by two General Electric F404-GE-400 engines, a low bypass, twin-spool turbofan engine with mixed flow exhaust and afterburning. The F404 is the first engine in the Canadian Forces to be maintained under a formal On-Condition Maintenance (OCM) program. Under this program, engine components are replaced or repaired based upon their condition. For the replacement of life limited parts, "scheduled" maintenance is mandatory when the life limit is reached. For the remaining components, "unscheduled" maintenance is performed when an in-service problem has occurred or when degradation is observed. The OCM maintenance concept therefore requires that an engine condition monitoring capability be developed to monitor and predict component life usage rates and to provide early warning of progressive engine deterioration.

To meet these requirements, each CF-18 is equipped with a fully integrated Inflight Engine Condition Monitoring System which automatically records data on engine life usage, limit exceedances and take-off performance for post-flight analysis. The IECMS logic was developed by General Electric and is implemented as software on one of two aircraft Mission Computers. As the aircraft performs each mission, engine life usage is continuously calculated by the IECMS using eight different Life Usage Indices (LUIs) related to the low cycle fatigue, thermal fatigue and creep damage experienced by the engine components. As such, these LUIs provide a basis for establishing individual component life limits, rather than the general and more conservative life limits applied to older engines. Table 1 presents a brief description of the CF-18 engine LUIs.

In addition to various other aircraft mission data, the running sums of each LUI are stored in the Mission Computer memory and are recorded twice per flight to a removable Maintenance Data Recorder Magazine (MDRM). The gathering and processing of MDRM data is accomplished by a network of ground-based processors as illustrated in Figure 1. Each squadron is equipped with a Ground Data Station which stores a copy of the MDRM contents in an Aircraft Data File (ADF), erases the tape for return to service and provides hard copy reports of specific data records. The ADFs are automatically transferred from each squadron to a central Base Computing Facility and eventually archived onto 9-track tape. Prior to archiving, IECMS data are automatically extracted from each ADF for the EPLTS and other engine application programs.

The Engine Parts Life Tracking System is an application program developed by the Canadian Forces to process and analyze IECMS life usage data and to aid the maintenance decision making process of retiring critical engine components from service before they fail. The EPLTS is a computerized database system which includes a suite of computer programs for: automated usage data entry, interactive entry of maintenance data, validation of maintenance data by configuration and compatibility checks, and interactive data retrieval for reporting purposes. The primary component of the EPLTS is its database, which contains the component part numbers, serial numbers, their relationship to other components and the life usage status of each part. The system tracks by serial number the location and current accumulated LUIs of 24 life-limited and 40 logistically critical components of each F404-GE-400 engine.

The EPLTS also tracks LUI accumulations for each mission flown and, by using historical LUI accumulation rates, the system can forecast life component "fallout" from 1 month to 30+ years. The historical LUI accumulation rates have been found to be dependent on three primary factors:

1. mission-to-mission variations
2. pilot-to-pilot variations
3. climatic variations

Although mission-to-mission and pilot-to-pilot variations are the predominant causes of scatter in the LUI accumulation data, the mean or average accumulation rates of certain LUIs also exhibit significant variations due to climate. As previously noted, the CF-18 operates from main, forward and deployed operating bases whose locations encompass most of North America and Western Europe. The aircraft and its engines therefore experience considerable variations in climatic factors such as ambient temperature, ambient pressure, humidity and air quality. Each of these factors can be expected to influence engine component life usage rates; however, the factor which is by far the most dominant for CF-18 operations is ambient temperature. During winter months the aircraft routinely operates from Cold Lake and Bagotville at ground level ambient temperature conditions of -20 to -30°C. Conversely, during the summer months the ambient temperature at these bases is typically 20 to 30°C.

Engine cycle temperatures (and to a lesser extent rotor speeds) are dependent on engine inlet temperature, T_1 , which, in turn, is a function of ambient temperature, aircraft speed and aircraft altitude. For example, Figures 2(a) and 2(b), representative of the extremes of CF-18 operation, show the estimated T_1 variations over the CF-18 flight envelope on MIL-STD-210A POLAR (-26.5°C) and TROPICAL (32.1°C) days. It is evident from these figures that the engine inlet temperatures experienced on the POLAR day are significantly less than the TROPICAL day temperatures and that T_1 ranges from a maximum of approximately 120°C (TROPICAL day, high speed) to a minimum of -30°C (POLAR day, low speed).

CLIMATIC EFFECTS ON ENGINE LIFE USAGE

The gas path components of a military aero engine are subject to extremely high cyclic stresses which result in a finite life for many of these components. The cyclic stresses arise primarily from the rotor speed, temperature and pressure variations which occur within the engine; thus, engine inlet temperature variations of the magnitude described above can be expected to affect life usage rates, particularly for hot end components whose lives are governed by thermal stresses or hold times at elevated temperatures.

The traditional measure of life used for aero engines is Engine Operating Time (EOT). Experience has shown, however, that EOT is a relatively poor measure of life used for engines subject to variable mission requirements such as fighter engines. To this end, the CF-18 IECMS evaluates a number of Life Usage Indices which provide a more direct measure of the low cycle fatigue, thermal fatigue and creep or stress rupture damage experienced by the engine components. Table 2 identifies the life components of the F404-GE-400 and the LUIs which are used to define their life limits. It is evident that low cycle fatigue due to rotor speed excursions governs most of the component lives; however, the HP turbine blade lives are determined by thermal fatigue cycles and are a significant concern of the engine life cycle managers due to their relatively high cost and short service lives.

The following sections of this paper describe the thermal fatigue, stress rupture and low cycle fatigue life usage algorithms employed by the CF-18 IECMS and the effects that ambient temperature variations will have on the LUI accumulation rates.

a) Thermal Fatigue

Thermal fatigue or stress cycles caused by temperature variations are evaluated by the Equivalent Full Thermal Cycles (EFTC) index. The equation used to assess the relative severity, RS, of each thermal cycle is:

$$RS = 10^{\alpha} \quad (1)$$

$$\text{where: } \alpha = -0.00001058 \text{ TMT}^2 + 0.03076 \text{ TMT} - 19.211 \quad (2)$$

and: TMT = HP turbine trailing edge blade metal temperature (°C)

The HPT trailing edge blade metal temperature is, in turn, determined by the magnitude of a given throttle movement and by the relationship between TMT and T_1 shown in Figure 3. This relationship corresponds to the TMT obtained during a throttle advance to the Intermediate Rated Power (IRP) position. For throttle movements to positions less than IRP, a Power Lever Angle (PLA) correction is applied to the TMT calculation. Above IRP, the engine's temperature limiting system maintains TMT at approximately the relationship shown in Figure 3.

Table 3 summarizes the relative severity of the HPT thermal cycles as predicted by equations (1) and (2). The extreme sensitivity of the EFTC counts to TMT is clearly evident. For example, a cycle to TMT = 960°C is over 20 times more severe than a cycle to 840°C. Figures 4 and 5 present the variations of TMT and EFTC counts with maximum PLA for a single throttle excursion at an altitude of 20,000 ft. and Mach number of 0.8 on both POLAR and TROPICAL days. It is evident from these figures that throttle excursions at the warm inlet conditions result in higher blade metal temperatures and significantly more EFTC counts than on colder days (in this case, by a factor of over 3:1). The sensitivity of EFTC counts to the magnitude of the throttle movement is also apparent. The number of counts rises sharply to a maximum or limiting value at approximately the IRP throttle position. Beyond this position, hot end temperatures are limited by the engine control system as previously noted.

It is evident from Figure 3 that, if the engine's temperature limiting system is functioning properly, the maximum number of EFTC counts for a single throttle excursion is obtained at a T_1 of approximately 76°C and a TMT of 946°C. From equations (1) and (2), this maximum value is 2.6 counts. Considering that the average number of EFTC counts for a given mission is roughly 20 and that the maximum number of EFTC counts per mission can be as high as 150-200, it is evident that the number of throttle excursions is the primary determinant of the EFTC accumulation rates.

b) Stress Rupture

Turbine stress rupture or creep damage is caused by prolonged operations at elevated cycle temperatures. Creep damage is generally measured by the accumulated or time-integrated creep strain, ϵ_c :

$$\epsilon_c = \int (d\epsilon_c/dt) dt \quad (3)$$

where the creep strain rate, $d\epsilon_c/dt$, is assumed constant for a given temperature and stress level. Additionally, the time to creep rupture, t_r , is related to the strain rate by:

$$d\epsilon_c/dt = 1/t_r \quad (4)$$

The IECMS Stress Rupture Factor (SRF) algorithm evaluates a count rate, CR, which is proportional to the creep strain rate using the following equations:

$$CR = e^\alpha \quad (5)$$

$$\text{where: } \alpha = -0.0000321 \text{ TMT}^2 + 0.1038 \text{ TMT} - 78.13 \quad (6)$$

As in the case of the EFTC counts previously described, the stress rupture count rate is a function of the HP turbine blade trailing edge metal temperature which, in turn, is determined by throttle position, engine inlet temperature and altitude. An additional correction is applied to the TMT calculation for SRF if the engine exhaust gas temperature exceeds a reference value.

Table 4 gives the variation of stress rupture count rate with TMT as predicted by equations (5) and (6). It is evident from this table that the SRC rate is also extremely sensitive to turbine blade metal temperature and is therefore likely to be affected by ambient temperature variations. For instance, Figure 4 indicates that the value of TMT will vary between 885°C and 925°C from a POLAR to TROPICAL day at PLA = Intermediate, altitude = 20,000 ft. and Mach No. = 0.8. This would result in the SRC rate on a TROPICAL day being over 6 times the POLAR day rate at these flight conditions.

c) Low Cycle Fatigue

The CF-18 IECMS evaluates full and partial compressor rotor speed, N_2 , cycles to assess the low cycle fatigue (LCF) accumulations for many of the engine's rotating components. The full and partial cycles are defined as follows;

$$\begin{aligned} N_2 \text{ Full (N2F) Cycle: } & 59-92-59\% N_2 \\ N_2 \text{ Partial (N2P) Cycle: } & 76-92-76\% N_2 \end{aligned}$$

where $N_2 = 59\%$ corresponds to the Ground Idle speed of the engine. The N2F and N2P counts are combined by the Engine Parts Life Tracking System to give an Equivalent LCF count;

$$ELCF = N2F + K \cdot N2P \quad (7)$$

where K varies for different components.

The expression for ELCF given in equation (7) appears to be based on a linear LCF damage law, where the value of K is a weighting factor used to assess the damage of a partial cycle relative to a full cycle. Furthermore, since only compressor speed is used to assess LCF, it is implicitly assumed that the fan rotor speed is proportional to N_2 and that the effects of temperature on LCF damage to both the high and low pressure turbines is also proportional N_2 .

Since the effects of cycle temperature are not directly accounted for in the IECMS N2F and N2P algorithms, it is difficult to predict the influence that ambient temperature variations might have on LCF accumulation rates. As shown in Figure 6, which gives the variation of N_2 with T_1 at the IRP throttle position, the engine will operate at lower N_2 speeds on colder days; thus, LCF damage should be less on colder days (as the cyclic stresses are proportional to the square of rotor speed). However, as indicated on the figure, the present LCF threshold of 92% N_2 is set such that only under extremely cold inlet conditions would the number of N2P and N2F counts be affected by ambient temperature.

d) Operational Data Analysis

The effects of ambient temperature variations on F404-GE-400 engine life usage have been investigated using operational data collected by the Engine Parts Life Tracking System over a period of 1 year (1989) from two CF-18 Main Operating Bases: CFB Cold Lake, Alberta and CFB Baden-Soellingen, West Germany. The results of this investigation are presented in tabular form in Tables 5 and 6 and in graphical form in Figures 7 and 8.

Seasonal or ambient temperature dependent variations are clearly evident in the monthly average accumulation rates of EFTC/EOT and SRF/EOT for both bases. In the case of the thermal fatigue cycle accumulations, the average EFTC/EOT rate at CFB Cold Lake ranges from about 7-10 in the winter months to 17-22 in the summer months; or by a factor of roughly 2:1. At CFB Baden-Soellingen, the EFTC/EOT variations are somewhat less pronounced (because ambient temperature variations are more moderate); nevertheless, a seasonal variation is still apparent. The stress rupture damage accumulations also exhibit significant seasonal variations at both Cold Lake (approximately 4:1 variation) and Baden-Soellingen (approximately 3:1 variation). Certain deviations in the monthly or season patterns of the LUI accumulation rates are evident at both bases. These are most likely due to variations in types of missions flown during these months.

At both bases, there is no apparent seasonal variation in the low cycle fatigue accumulation rates, as indicated by the N2P/EOT data. As previously discussed, this result is to be expected because the upper threshold for N2P cycle definition ($N_2 = 92\%$) is likely to be exceeded during major throttle excursions under all but very cold engine inlet conditions.

The average annual LUI accumulation rates for the two bases are compared in Table 7. It is evident that an engine at CFB Cold Lake, which has a substantially lower mean ambient temperature as compared to CFB Baden-Soellingen, will accumulate EFTC counts at approximately 75% of the rate of an engine at CFB Baden-Soellingen. However, engines at both bases appear to accumulate low cycle fatigue and stress rupture damage at approximately the same rate. The similarity of the low cycle fatigue rates indicates that the engines experience similar rates of throttle movement at each base. In view of the colder mean annual temperature at Cold Lake, the SRF results are unexpected. It is possible that the engines at Cold Lake spend comparatively longer periods of time at elevated temperature than those at CFB Baden-Soellingen, even though the rates of throttle movement are similar.

LIFE CYCLE MANAGEMENT CONSIDERATIONS

In order to effectively manage an engine maintenance program, the Life Cycle Maintenance Manager (LCMM) must have an accurate method to forecast the fallout of life-limited parts. Traditional engine maintenance required that an engine be overhauled periodically based on an accumulation of engine hours. The third line Repair and Overhaul contractor would remove life-limited components and return the engine's performance to specification level. Thus, for the maintainers of the engines and the LCMM there was only one component to track and its 'life' was based on aircraft flying time. As the F404 is maintained under an OCM concept, the LCMM must track the life usage of 64 components on each operational engine. In the Canadian Forces, there are some 300 engines which amounts to approximately 19,000 tracked components. Without an EPLTS, a considerable burden would be placed on the LCMM of the F404 engine as each component has its own life limit and each engine accumulates LJIs at a different rate.

The main method of engine repair under an OCM concept is the replacement of modules within the engine. Although OCM requires fewer spare 'engines', it does require a greater number of spares modules be available to repair the engines. The high technology engine components of today with their high cost and complex manufacturing processes have led to delivery times of months or even years. With the long lead times, the LCMM for the F404 fleet must look at the requirements to support F404 maintenance throughout the life of the CF-18 program. One of the primary tasks of the engine LCMM is to identify spare part requirements long enough in advance to place orders which will ensure deliveries when required.

In performing F404 maintenance at the CF-18 Main Operating Bases (MOBs), the engine bay requires an accurate forecast of maintenance workload for up to the next 6 months. The base must know what they need in terms of manpower allocation and spares so that adequate resources are available to ensure engines are repaired and returned to service as soon as possible. The LCMM and the MOBs must know what affects usage accumulation so that micro-management of assets can be carried out to meet the present and short term change outs (less than one year).

There are presently no components on the F404 which are life-limited in terms of SRF counts; as such, the only component fallouts which are affected by ambient temperature variations are the High Pressure Turbine blades (lified by EFTCs). If a base uses a mean annual EFTC rate to project their fallout during the warm months, the blades will be time expired earlier than forecasted. For the MOB, this could mean an additional rotor change out per month. If the MOB doesn't have the spares or the manpower available, delays repairing the engines are encountered. The effect on forecasting is opposite when using the mean annual EFTC rate during the cold months. In this case a forecast could show one more rotor change out per month than would actually occur. Although the reduced workload does not impact operations, it does tie up valuable resources which could be used elsewhere.

Over a period of approximately 1 to 2 years, seasonal variations in the LUI accumulation rates are no longer apparent in the long term life usage rates for a given base; therefore, for long term planning at a particular base, climatic effects are minimal. However, since aircraft are not routinely rotated from base to base, fleetwide planning for the procurement of long lead time spares must take into account the base to base variations in EFTC accumulation rates due to mean annual ambient temperature differences.

CONCLUSION

The predominant climatic factor affecting the life usage of CF-18 engine components is the variation of ambient temperatures resulting from aircraft operations ranging from the extremes of hot and cold weather experienced in North America to the relatively moderate climate of Europe. The influence of ambient temperature variations on CF-18 engine life usage has been investigated by examining the sensitivity of the life usage algorithms employed by the aircraft Inflight Engine Condition Monitoring System to engine inlet temperature variations and by the analysis of operational data collected by the CF-18 Engine Parts Life Tracking System. The results of these investigations indicate the following:

1. Seasonal variations in ambient temperature have a significant effect on the mean monthly accumulation rates of the IECMS thermal fatigue and stress rupture life usage indices. These variations arise from the extreme sensitivity of the IECMS EFTC and SRF algorithms to engine inlet temperature.
2. Ambient temperature variations have little or no effect on the mean monthly accumulation rates of low cycle fatigue counts. The full and partial N_2 cycles computed by the IECMS do not directly assess the effects of cycle temperature levels on the low cycle fatigue of engine components. Furthermore, the upper threshold for the N2F and N2P cycle definitions is set at an N_2 level which is likely to be exceeded during a major throttle excursion under most engine inlet conditions.
3. Significant variations in the mean annual rates of thermal fatigue cycle accumulation can be found between operating bases with significant variations in mean annual temperatures.

In the life cycle management of the F404 engine, the LCMM must take into account the effects of climatic conditions on LUI accumulation rates in order to ensure the accuracy of maintenance forecasts. If there is no significant variation between bases in the mean annual ambient temperature, then the long term management of the engine fleet is not adversely affected by seasonal changes in LUI rates. In the month to month management of the F404 fleet, the LCMM and the personnel at the MOBs must take into account the effects of seasonal mean ambient temperature variations on the LUI accumulation rates in order to ensure that micro-management of assets can be carried out to meet the immediate and short term maintenance requirements.

The conclusions of this paper are based on life usage algorithms developed by General Electric. Although the derivation of these algorithms is proprietary information to General Electric and specific to the F404-GE-400 engine, it is evident that other engines will also experience thermal fatigue, creep and possibly low cycle fatigue damage rates which are also sensitive to ambient temperature variations. It is important therefore that the maintenance managers of these engines take into consideration these climatic effects when forecasting maintenance requirements.

LUI	SYMBOL	DESCRIPTION
1. Full N ₂ RPM Cycles	N2F	- Counts the number of 59-92-59½ N ₂ cycles
2. Partial N ₂ RPM Cycles	N2P	- Counts the number of 76-92-76½ N ₂ cycles
3. Equivalent Full Thermal Cycles	EFTC	- Counts the number of HPT blade metal temperature cycles - Weighted according to the magnitude of the cycle
4. Stress Rupture Factor	SRF	- Temperature-weighted time at temperature count - Rate of count accumulation is dependent on HPT blade metal temperature
5. Time at Max Power	TAMP	- Monitors amount of time spent at PLA ≥ Intermediate
6. Full P _{S3} Cycles	P3F	- Counts the number of 70-407-70 psia P _{S3} excursions - These counts generally occur only at at high speed/low altitude flight conditions
7. Partial P _{S3} Cycles	P3P	- Counts the number of 70-340-70 psia P _{S3} excursions
8. Engine Operating Time	EOT	- Records the total time the engine operates at or above Ground Idle

Table 1 - IECMS Life Usage Index Algorithms

PART	LIFE LIMIT PARAMETER
FAN MODULE	
1. Stage 1 Fan Disk	ELCF*
2. Stage 2 Fan Disk	ELCF
3. Stage 3 Fan Disk	ELCF
4. Fan Blades	ELCF
5. Aft Fan Shaft	ELCF
HPC MODULE	
6. Stage 1-2 Spool	ELCF
7. Front Shaft	ELCF
8. Stage 3 Disk	ELCF
9. Stage 4-7 Spool	ELCF
10. Combustion Casing	P3F
11. Fuel Nozzle Set	ELCF
HPT MODULE	
12. Forward Shaft	ELCF
13. Aft Shaft	ELCF
14. Forward Rotor Seal	ELCF
15. Forward Cooling Plate	ELCF
16. Aft Cooling Plate	ELCF
17. HPT Disk	ELCF
18. HPT Blades	EFTC
19. Fan Drive Shaft Assembly	EOT
20. No. 4 Bearing	
LPT MODULE	
21. Conical Shaft	ELCF
22. Forward Rotor Seal	ELCF
23. LPT Disk	ELCF
24. LPT Blade	EOT

$$* \text{ELCF} = \text{N2F} + \text{K} \cdot \text{N2P}$$

Table 2 - F404-GE-400 Engine Life Limited Parts

<u>TRAILING EDGE BLADE METAL TEMPERATURE, TMT</u>	<u>RELATIVE SEVERITY, RS (Equations (1) and (2))</u>
840 °C	0.15
870 °C	0.35
908 °C	1.00
930 °C	1.75
960 °C	3.67

Table 3 - Relative Severity of F404-GE-400 HPT Blade Thermal Cycles

<u>TRAILING EDGE BLADE METAL TEMPERATURE, TMT (°C)</u>	<u>STRESS RUPTURE COUNT RATE, CR (Equations (5) and (6))</u>
840°C	0.13 10 ⁻⁵
870°C	0.54 10 ⁻⁵
900°C	2.23 10 ⁻⁵
930°C	8.62 10 ⁻⁵
960°C	31.42 10 ⁻⁵

Table 4 - Sensitivity of F404-GE-400 Stress Rupture Count Rate to HP Turbine Blade Metal Temperature

	JAN	FEB	MAR	APR	MAY	JUN	JUL	AUG	SEPT	OCT	NOV	DEC
MEAN GROUND LEVEL TEMP- ERATURE (°C)	-17.6	-13.4	-6.9	3.3	10.4	14.7	17.0	15.6	9.8	4.4	-6.4	-14.2
MEAN THERMAL FATIGUE COUNTS (EFTC/EOT)	11.8	6.9	9.2	15.3	22.6	17.5	17.3	16.5	14.0	14.1	11.3	10.0
MEAN LOW CYCLE FATIGUE COUNTS (N2P/EOT)	5.9	4.9	6.3	6.6	6.1	5.0	5.2	5.3	4.6	5.9	5.8	4.4
MEAN STRESS RUPTURE COUNTS (SRF/EOT)	.09	.05	.07	.14	.25	.23	.25	.24	.20	.15	.10	.11

Table 5 - Seasonal Variations of CF-18 Engine Life Usage Accumulation Rates:
CFB Cold Lake

	JAN	FEB	MAR	APR	MAY	JUN	JUL	AUG	SEPT	OCT	NOV	DEC
MEAN GROUND LEVEL TEMP- ERATURE (°C)	0.6	1.4	8.9	9.7	16.2	17.4	20.7	20.2	16.0	11.6	3.1	3.2
MEAN THERMAL FATIGUE COUNTS (EFTC/EOT)	15.5	12.9	17.2	14.9	20.2	21.4	21.7	23.6	23.9	18.9	16.5	19.9
MEAN LOW CYCLE FATIGUE COUNTS (N2P/EOT)	5.4	5.3	6.0	5.5	6.0	6.6	5.8	6.4	6.5	5.4	5.9	6.2
MEAN STRESS RUPTURE COUNTS (SRF/EOT)	.13	.07	.11	.10	.15	.18	.20	.20	.19	.16	.14	.14

Table 6 - Seasonal Variations of CF-18 Engine Life Usage Accumulation Rates:
CFB Baden-Soellingen

	<u>CFB COLD LAKE</u>	<u>CFB BADEN-SOELLINGEN</u>
MEAN GROUND LEVEL TEMPERATURE (°C)	1.4	10.8
MEAN EFTC/EOT	14.3	19.0
MEAN N2P/EOT	5.6	5.9
MEAN SRF/EOT	0.16	0.15

Table 7 - Average Annual CF-18 Engine Life Usage Accumulation Rates

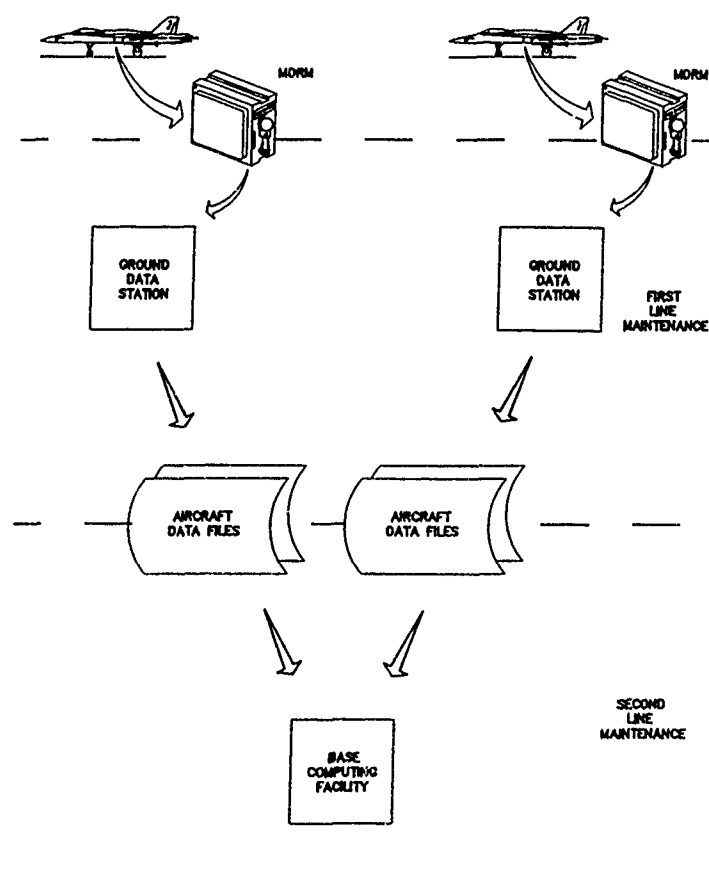


Figure 1 - CF-18 Ground Data Processing

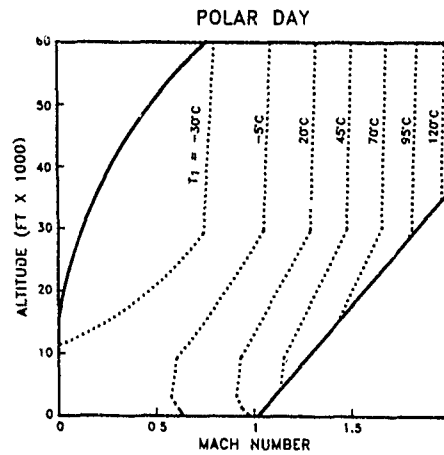


Figure 2(a) - CF-18 Engine Inlet Temperature Variations - POLAR Day

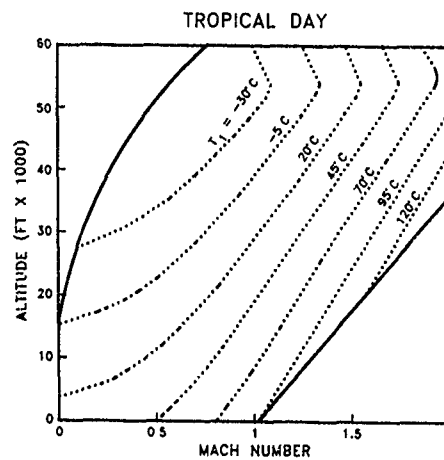


Figure 2(b) - CF-18 Engine Inlet Temperature Variations - TROPICAL Day

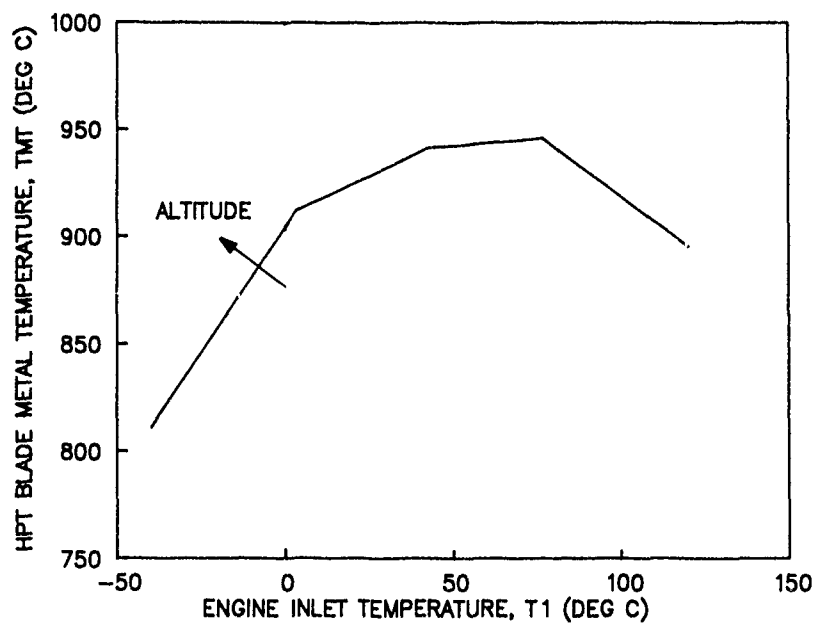


Figure 3 - HP Turbine Blade Trailing Edge Blade Metal Temperature at Intermediate Rated Power

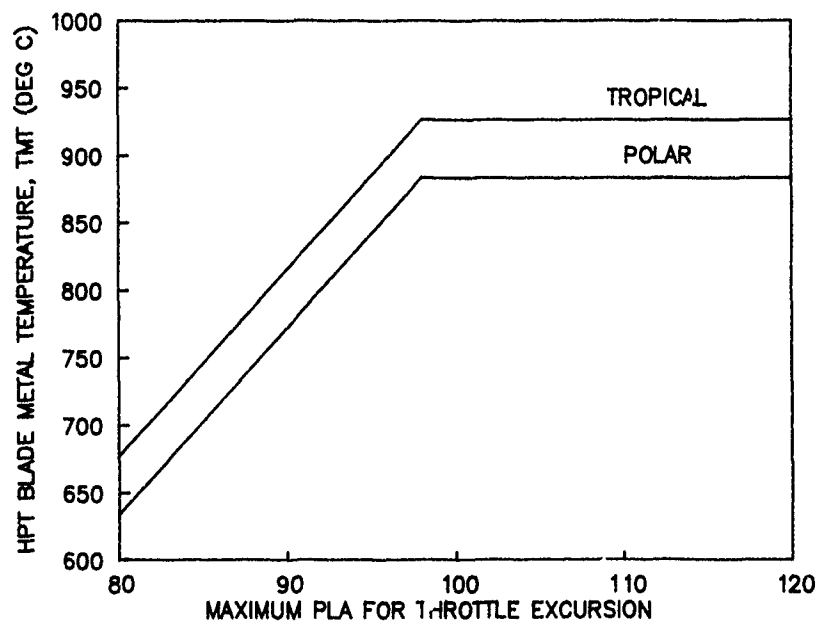


Figure 4 - Variation of HPT Blade Metal Temperature with Power Lever Angle for a Single Throttle Excursion

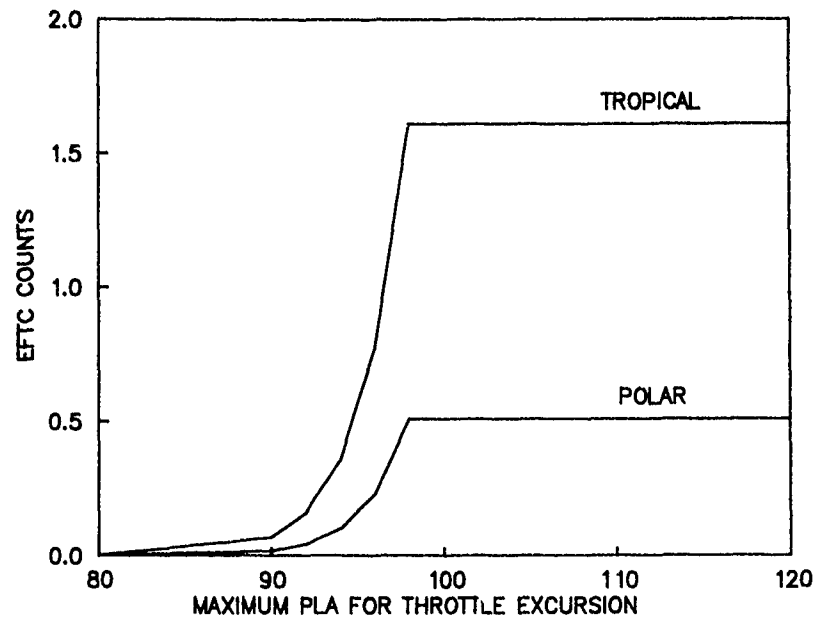


Figure 5 - Variation of EFTC Cycles with Power Lever Angle for a Single Throttle Excursion

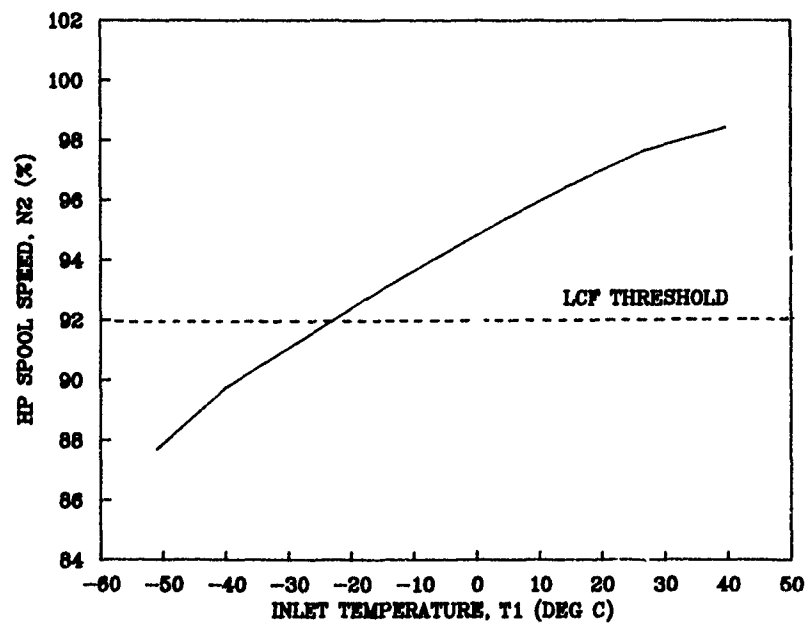


Figure 6 - Variation of Compressor Rotor Speed with Engine Inlet Temperature at Intermediate Rated Power

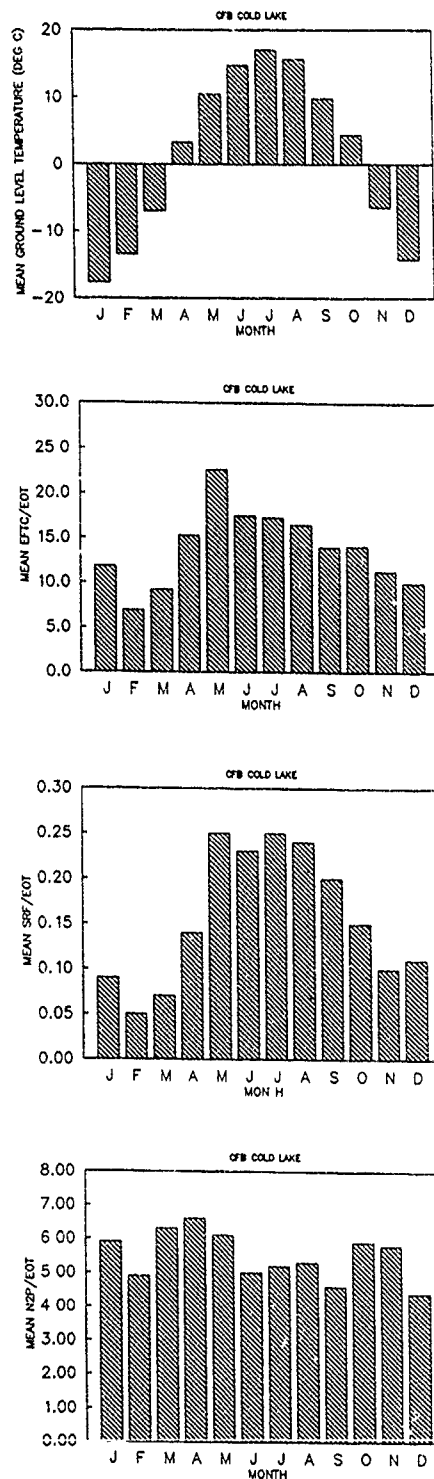


Figure 7 - Mean Monthly Temperatures and Life Usage Accumulation Rates for CFB Cold Lake

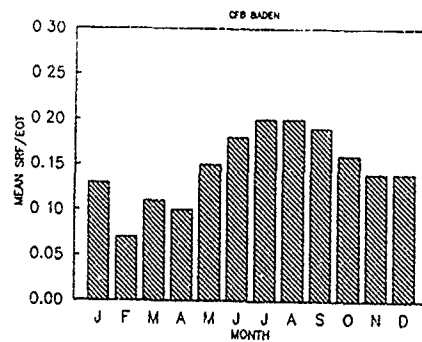
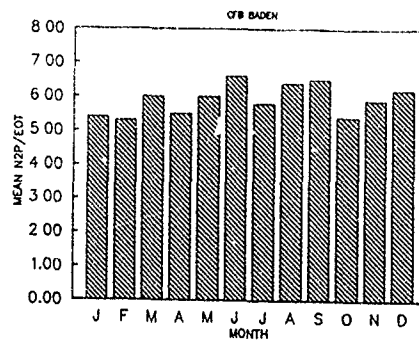
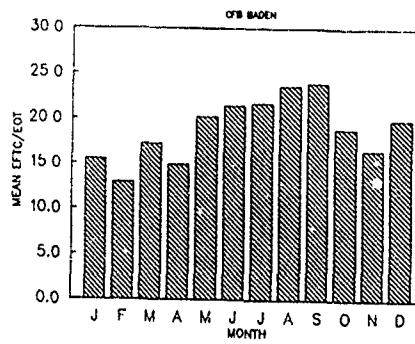
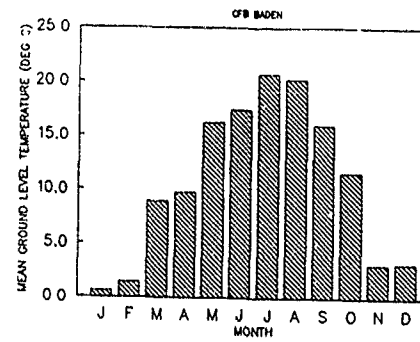


Figure 8 - Mean Monthly Temperatures and Life Usage Accumulation Rates for CFB Baden-Soellingen

Discussion

1. F. Kuiper, MOD Netherlands

The Canadian forces calculate their short term forecast per base. How is the forecasting performed for long term forecasts for the whole fleet? Also average LUTs per base or averages over the entire fleet.

Author:

For short term and long term forecasting at a base, EPLTS

uses historical engine usage data for an individual base. For fleet planning purposes, EPLTS uses average data for the fleet. It depends on the magnitude of the accumulation rate difference. If one date is different by a factor of 1.1/1, then an average between the two should be sufficient for long term planing. If the difference is by a factor of 2 or 3/1, then long term forecast should be done separately (using individual base rates) and then added together.

APPLICATION OF A WATER DROPLET TRAJECTORY PREDICTION CODE TO THE DESIGN OF INLET PARTICLE SEPARATOR ANTI-ICING SYSTEMS

by

D.L.Mann* and Dr S.C.Tan**

*Rolls-Royce plc, Leavesden, Watford WD2 7BZ, United Kingdom

**Cranfield Institute of Technology, Cranfield, Bedford, United Kingdom

ABSTRACT

Over the past five years a dust particle trajectory code has been jointly developed by Rolls-Royce and Cranfield. The paper describes recent work on the code to include an ice accretion prediction model suitable for use as a design aid for a wide variety of gas turbine engine inlets, but particularly for particle separator geometries. The calculation of the local heat transfer coefficient is seen to be critical to the success of the ice accretion prediction. The paper describes the incorporation of a suitable model and shows that a series of validation tests, carried out on a full scale rig, have satisfactorily verified the code. A second series of validation experiments, carried out in an icing facility, further shows the prediction model to be appropriate.

NOMENCLATURE

D_p	Drag coefficient
r_p, θ_p, z_p	Particle's cylindrical coordinate
V_g, V_p	Gas and particle velocity vectors
$V_{rg}, V_{\theta g}, V_{zg}$	Component gas velocities in the cylindrical coordinate system
$V_{rp}, V_{\theta p}, V_{zp}$	Component particle velocities in the cylindrical coordinate system
ρ_p, ρ_g	Particle and gas densities

INTRODUCTION

The susceptibility of rotorcraft to ice accretion problems in icing conditions has been observed almost since the aircraft type first appeared. Rotor blades have been cited as the prime area of concern and much activity has been initiated to investigate the icing phenomena in this area. In particular, the need for suitable predictive tools to ease the burden of necessary design, development and certification testing efforts has produced a number of prediction models, an excellent review of which is contained in Reference 1.

In comparison to the rotor icing problem, the problems of the rotorcraft engine manufacturer may appear to be relatively minor, but with the simultaneous trends towards more aerodynamically efficient (and therefore more damage prone) turbomachinery and the fitting of inertial type inlet particle separators (IPS), the job of engineering a suitable powerplant anti-icing system is becoming more difficult. The advent of the IPS makes anti-icing more difficult due to the fact that internal surface area must inherently increase as the incoming flow is first forced to travel over a bend and is then bifurcated as the flow is split into

engine and scavenge paths (Figure 1). In terms of the engine power performance penalty associated with the fitting of an IPS, the necessary heating energy input may be 80% higher than for a conventional intake duct.

Development of an anti-icing system for such an intake by conventional 'cut and try' methods is expensive, time consuming and will always tend to lead to a design which is energy inefficient in achieving its required performance. Energy efficiency here applies to whatever the chosen anti-icing mechanism is, whether that be by a hot gas engine bleed or by some electrical means. Current state of the art IPS technology gives an anti-icing heating requirement which represents a not insignificant engine power penalty.

This paper describes the development of a predictive anti-icing system design code aimed specifically at reducing the expense and time of development by 'cut and try' methods and, from a power penalty point of view, to reduce current level heating requirements by 50%.

The foundation of the ice accretion prediction model has been software developed during the course of the generation of a particle separator design system (Reference 2,3). The principle components of the model are a Navier-Stokes flow solver, the Moore Elliptic Flow Program (MEFP) (Reference 4), and the joint Rolls-Royce/Cranfield developed particle trajectory prediction program (Reference 5).

Validation of the prediction code to date has comprised two series of rig tests carried out on a full scale IPS. The first set of experiments were aimed specifically at measuring local heat transfer coefficients along the gas passage of the IPS and hence validating the calculation method derived during the course of the work, and the second took place in a Rolls-Royce icing facility and was aimed at validation of the water droplet trajectory/ice-accretion calculation methods.

THEORETICAL MODEL

Flow-field Prediction

MEFP has firmly established itself at the core of the particle separator design package used at Rolls-Royce on the basis of the accuracy of its predictions and its computer c.p.u. efficiency. The code is described in Reference 4 and its use within the particle separator design role is described in Reference 3.

The IPS under consideration during the course of the work described here, being a direct engine mounted device, is near axis-symmetric in form and hence in order to

reduce computation time MEFP was run in its 2D form. Grid generation was fully automated and a typical calculation grid comprised around 4000 node points, as shown in Figure 2.

Water Droplet Trajectory Prediction

The particle equations of motion were derived by assuming the drag force to be the only force of interaction. This assumption is valid if particle density is more than three times greater than that of the surrounding fluid medium (Reference 6). In cylindrical co-ordinates, these equations may be written as follows:-

$$\dot{r}_p = G(V_{rg} - \frac{\partial r_p}{\partial t}) + r_p \dot{\theta}_p^2 \quad (1)$$

$$r_p \dot{\theta}_p = G(V_{\theta g} - r_p \frac{\partial \theta_p}{\partial t}) - 2\dot{r}_p \dot{\theta}_p \quad (2)$$

$$\dot{z}_p = G(V_{zg} - \frac{\partial z_p}{\partial t}) \quad (3)$$

where G is the force of interaction =

$$G = \frac{3\rho_g C_D}{4\rho_p D_p} |(V_g - V_p)|$$

The centrifugal and coriolis acceleration terms are represented by the end terms on the right hand side of equations (1) and (2) respectively. The force of interaction depends on the relative velocity between the particle and the gas flow, and particle size, shape and density. The drag coefficient, C_D , is obtained from the standard drag curve for spherical particles. The trajectory of a particle is calculated by a numerical solution of the three equations of motion obtained through the Kutta-Fehlberg method (Reference 7).

ICE ACCRETION MODEL

The ice accretion model chosen as most suitable for this study has been that developed by Cansdale and Gent (Reference 8). The method is based on the solution of a set of heat balance equations (kinetic heating, convective cooling, etc.) and is used to calculate the rate of ice growth. The water flux distribution is calculated by collecting droplets in a series of 'compartments' located along the IPS wall surfaces. In the model, it has been assumed that water droplets do not rebound upon impact, however, previous experience in icing tests has shown that significant bounce can occur under certain conditions, when sufficient impact energy exists (Reference 9). It is intended that experiments to investigate water droplet restitution ratios will be carried out in the near future to overcome this potential shortfall.

The calculation is primarily dependent on the local heat transfer coefficient (HTC). The method of Jayatilake (Reference 10) has been selected as most suitable to this application.

Whilst it is possible to vary water

droplet size over a wide range of values within the code, for the purposes of this study a size distribution was used comparable with that measured on icing tests carried out to UK Def Stan engine certification requirements (Reference 11), that is, with a mean droplet size of 20 microns.

HEAT TRANSFER COEFFICIENT (HTC) MEASUREMENT TESTS

Experimental Set-Up

The experimental set-up for the HTC measurement tests is illustrated in Figure 3. The rig consists of three detachable sections:-

1. An upstream section which consists of an intake nozzle, followed by a diffuser with an adapter flange at one end.
2. The test section which consists of the IPS inner and outer wall assembly. The two are connected to the upstream section by a 'V' clamp at the flange.
3. The downstream section which consists of the scroll and splitter lip assembly, followed by the scavenge and mainline pipe. The scavenge pipe is joined to the mainline pipe just upstream of the suction fan. A throttle valve is located on the mainline pipe and an ISA 1932 nozzle (for flow metering) is set in the scavenge pipe.

The downstream section was mounted as a permanent feature of the whole rig. The detachable upstream test sections allowed film probes to be 'stuck' to the inner and outer walls with considerable ease.

AERODYNAMIC MEASUREMENT

Wall static pressure tapings were placed along the inner and outer walls of the IPS in positions as shown in Figure 4. The IPS inlet flow rate was monitored by four wall static pressure tapings spaced radially in the inlet nozzle. The scavenge flowrate was metered by an ISA 1932 nozzle. All of the pressure tapings were connected to a scanivalve and recorded with a Druck manometer.

HOT FILM PROBES

The hot film probes specified for the local heat transfer measurements were manufactured in Denmark by DISA and were of the 'glue-on' type (ref: 55R47). These probes are more normally used for skin friction measurements. The probe consists of a polyimide foil substrate (16 x 8mm) on to which a thin nickel film (0.9 x 0.1 x 0.001mm) is deposited. The film ends are joined to two nickel/silver plates or to which a pair of copper wires (0.1mm diameter) are soldered. The resistance of the probe wire usually varies from 10.0 to 18.0 Ohms and lead (copper wire) resistance is usually about 0.2 Ohms.

In order to minimise IPS wall heat conduction effects, the appropriate walls of the IPS had shallow channels cut into the sheetmetal, these channels were then filled with a low conductivity material and

the hot film probes attached, by means of double-sided tape, so as to sit flush with the IPS wall.

HEAT TRANSFER MEASUREMENTS

Copper wires from the probe were soldered to 5m length cable and plugged directly into a constant temperature anemometer. The operation of the anemometer is based on the operation of a Wheatstone bridge with an amplifier which feeds unbalanced signals (caused by the current changes in the sensor) to the sensor in order to maintain a constant wire temperature. A combination of two types of anemometer were used:-

i) 55M system consisting of 55M01 and 55M10 units,

ii) 56C system consisting of 56C01 and 56C17 units.

The construction in both systems are similar but the M-type is more expensive and normally used for high performance measurements.

The heat transfer measurements were carried out with 6 probes connected to 4 M-type and 2 C-type anemometers. The output from the anemometers were connected to an RMS digital voltmeter via a 55D65 scanner. The probe wire temperature is set from the required overheat ratio, α , which is defined as:

$$\alpha = (R_h - R_c)/R_c$$

where R_h and R_c are the hot and cold sensor resistances respectively. The sensor resistance, R is then calculated from

$$R = R_{20} (1 + \alpha_{20} (T - 20))$$

where R_{20} is the sensor resistance at 20.0degC, α_{20} is the temperature coefficient of resistance at 20degC and T is the required sensor temperature. Hence the hot resistance can be calculated as follows:-

$$R_h = (1 + \alpha)R_{20} + R_{cable} + R_L$$

where R_{cable} and R_L are the cable and lead resistances.

The overheat ratio was set and the anemometers were balanced after the probes had been glued onto the IPS wall. Figure 4 shows the location of the probes on the test section. A staggered arrangement was adopted in order to avoid disturbances in the flow caused by the wires (and heat) in the upstream probe from affecting downstream probes.

CALCULATION OF THE LOCAL HTC

The current, I passing through the probe is calculated from Reference 12 as follows:-

$$I = V/(R_c + R + R_{cable})$$

where V is voltage, R and R_{cable} are resistances of the sensor and cable, R_c is the anemometer top resistance, which is given as 50 and 20 Ohm for the M- and C-type systems respectively. The heat transfer to the flow, Q , is calculated

from:-

$$Q = I^2 R - I^2 R(\text{no flow})$$

Therefore, the HTC, h , is given by the formula:-

$$h = Q/(A_{eff}(T_s - T_f))$$

where A_{eff} is the effective heating area of the probe and T_s , T_f are sensor and air temperatures respectively. The effective heating area parameter will be further discussed in a later section.

RESULTS AND DISCUSSION

Figure 5 shows a plot of the predicted velocity vectors in the IPS produced by the MEFP code. The predicted flow recirculation in region A and the stagnation and separation in region B have been previously seen during flow visualisation tests and are hence true phenomena. The wall static pressure readings for the IPS design point flow are shown in Figure 6 alongside the corresponding MEFP prediction. The pressure values have been non-dimensionalised against atmospheric pressure. Agreement is seen to be very good.

The comparison between measured and predicted HTC at the wall locations shown in Figure 4 is plotted in Figure 7. Predicted HTC's come from the Jayatilke model. The results for the inner wall (Figure 7a) shows good agreement except in the region of re-circulating flow, A, where the measured HTC was higher. This difference is to be expected because the turbulence in a re-circulating flow region usually serves to enhance heat transfer rates (Reference 10, 13).

The comparison between experimental and predicted values on the outer wall (Figure 7b) also show good agreement except around the stagnation region, B, just after the maximum diameter point. Again, separation is thought to increase the effective heat transfer in this region.

EFFECTIVE HEATING AREA

The average effective heating area of 0.3mm² employed in the calculation of the local HTC was found by curve fitting of the experimental data. This would give an effective width of the sensor wire as 0.33mm instead of the actual value of 0.1mm, assuming that the heat is conducted into a rectangular area. This, however, is about three times the geometrical area of the sensor wire, which has an actual area of 0.09mm². Many researchers (Reference 14, 15, 16) have encountered the uncertainty of the effective heating area because it depends on the amount of heat conducted into the substrate materials and the immediate flow over the sensor. It is generally recognised as a difficult and time consuming problem, and almost impossible to determine in practice due to the small component sizes involved. Previously, it has been concluded only that the effective heating area is greater than the geometrical area.

Defining a factor, F_a , as the ratio of the effective heating area over the actual geometric area then the work of the above

previous investigators has shown that Fa is greater than unity; thus setting a lower bound value for the factor.

In an attempt to try and locate an upper bound to the factor, a model of the sensor using a conventional heat transfer code was constructed. The effects of heat convection and radiation were ignored and conduction was assumed to be steady state. The non-linear thermal properties of the Kapton material were accounted for. By making these assumptions, a high limit on the effective heating area was able to be calculated. This value was found to be 0.43mm^2 and so $(Fa)_{\text{max}}$ becomes:-

$$(Fa)_{\text{max}} = 0.43/0.09 = 4.78$$

and so, Fa may be said to lie in the range:-

$$1.0 \leq Fa \leq 4.78$$

Curve fitting of the experimental data gave a value of Fa of $0.3/0.09 = 3.33$, which is consistent with the stated band of valid values.

It is intended that the analysis using the heat transfer code will be extended in the near future to include the effects of convection and radiation and hence allow for a more precise justification for the use of the 3.33 value used in the experimental curve fitting exercise.

ICING TUNNEL TESTS

Experimental Set-Up

During the course of IPS certification testing taking place at the icing facility at Rolls-Royce, Hucknall, it was possible to carry out a short series of icing tests with an unheated IPS in order to obtain validation data for the water droplet trajectory prediction part of the ice accretion model.

The Hucknall facility set up is illustrated in Figure 8, which shows the set-up for the IPS work. The facility is a re-circulating, blowing one in which the test section is held within a closed cell. The IPS was full scale and operated at its design point flow conditions. The required flow split into 'engine' and 'scavenge' lines was achieved using a valve at the discharge from the engine section. Super-cooled water droplets were produced from a spray grid upstream of the IPS inlet and droplet size was calibrated to comply with the UK Def Stan (Reference 11) 20 micron mean diameter. The nozzle arrangement to achieve an even distribution of droplets was carried out by trial and error.

The tests were run at -10degC with a water droplet concentration of 0.6g/m^3 . The duration of the trial was established by trial and error to give a satisfactorily measurable ice accretion whilst not significantly altering the flow field within the IPS. A maximum permitted ice accretion depth of 6mm was chosen and this resulted in a test duration of around 10 minutes.

RESULTS AND DISCUSSION

Figure 9 shows predicted water droplet trajectories within the IPS for the test conditions. The distribution of droplets at the inlet was assumed to be uniform from hub to shroud with 155 droplets being launched for each water droplet size. A range of water droplet sizes, compliant with the required 20 micron mean diameter, based on a previously measured characteristic was used. In all, the analysis comprises some 1240 droplet trajectories. Further assumptions made were that the droplets do not bounce and that they do not coalesce.

Figure 10 illustrates the resulting predicted ice accretions on the IPS walls (shown dashed) alongside the measured accretions. The three areas of actual accretion; inlet hub front face, outer wall and splitter lip top surface have all been picked up by the prediction model and generally speaking the agreement in ice shapes is good throughout the IPS.

The main area of discrepancy occurs at the splitter lip accretion where the prediction shows a pronounced 'hill' of ice at the splitter lip stagnation point whereas the tests showed a flat covering of ice. The difference is believed, in part, to be due to the fact that the actual IPS splitter flow - where the flow is turned 180 degrees into the scroll collector system (Figure 1) - was not simulated in the model. It should be stated, though, that if anything, the experimental results at the splitter lip was a surprise in that other tests on different splitter lip shapes have produced the predicted 'hill' of ice at the stagnation point.

Overall, the results would appear to indicate that the theoretical model is an appropriate one.

CONCLUSIONS

The method of heat transfer measurement using hot film sensors has been successfully applied to a helicopter engine IPS intake and has validated a viscous flow prediction code and the Jayatilke HTC model. Discrepancies in areas of re-circulating flow were as expected and have been explained. Tests on an unheated IPS in an icing facility have successfully validated the water droplet trajectory model incorporated into the code.

FUTURE WORK

At the time of writing, the IPS ice accretion studies are on-going. The next stage of work involves the development and validation of a model to predict the heat inputs required through a geometry to prevent the formation of ice. The validation exercise will be done through a second series of icing tunnel tests, this time employing a heated IPS model. It is hoped, subsequently, to design and test a full IPS anti-icing system in order to demonstrate the stated desire to reduce heating requirements over current levels by 50%. With the available evidence, there is no reason to believe that this objective will not be met.

REFERENCES

1. AGARD, 'Rotorcraft Icing - Progress and Potential', AGARD Advisory Report No. 223, September 1986.
2. Tan, S.C., Elder, R.L., Mann, D.L., Thorn R.I., 'Study of Particle Trajectories in a Gas Turbine Intake', Ninth International Symposium on Air Breathing Engines, Athens, September 1989.
3. Mann, D.L., Tan, S.C., 'A Theoretical Approach to Particle Separator Design', Ninth International Symposium on Air Breathing Engines, Athens, September 1989.
4. Moore, J.G., 'An Elliptic Calculation Procedure for 3D Viscous Flow', AGARD Lecture Series No. 140; 3D Computation Techniques Applied to Internal Flows in Propulsion Systems, June 1985.
5. Tan, S.C., 'A Study of Particle Trajectories in a Gas Turbine Intake', PhD Thesis, Cranfield Institute of Technology, Cranfield, Beds, UK, 1988.
6. Rudinger, G., 'Flow of Solid Particles in Gas', AGARD - AG-222, October 1976.
7. Ledermann, W., 'Handbook of Applicable Mathematics, Volume III, John Wiley & Sons.
8. Cansdale, J.T., Gent, R.W., 'Ice Accretion on Aerofoils in Two-dimensional Compressible Flow - A Theoretical Model', RAE Technical Report 82128, 1983.
9. Parker, G.J., Bruen, E., 'The Collision of Drops with Dry and Wet Surfaces in an Air Atmosphere', Proc. Inst. Mech. Eng. (London), 184 (1969-1970), Pt.3G(III), pp57-63.
10. Jayatilleke, C.L.V., 'The Influence of Prandtl Number and Surface Roughness on the Resistance of the Laminar Sub-layer to Momentum and Heat Transfer' Progress in Heat and Mass Transfer, Volume 1, Pergamon Press.
11. UK Military Icing Specification, DEF Stan 00971.
12. DISA, 'Type 55M10, Instruction Manual, DISA 55M System with 55M10 CTA Standard Bridge', DISA Elektronik A/S. DK-2740.
13. Gooray, A.M., Watkins, C.B., Aung, W., 'Numerical Calculation of Turbulent Heat Transfer Downstream of a Rearward Facing Step', Proc. of the 2nd Conference on Numerical Methods in Laminar and Turbulent Flow, Venice, Italy, July 1981.
14. Matthews, J., 'The Theory and Application of Heated Films for the Measurement of Skin Friction', PhD Thesis, Cranfield Institute of Technology, Cranfield, Beds, September 1985.
15. Hodson, H.P., 'Boundary Layer Transition and Separation Nearing the Leading Edge of a High Speed Turbine Blade', ASME 29th International Gas Turbine Conference and Exhibition, Amsterdam, Paper no. 84-GT-179, June 1984.
16. McCroskey, W.J., Durbin, E.J., 'Flow Angle and Shear Stress Measurements Using Heated Films and Wires', ASME Paper 71-WA/FE-17, July 1971.

ACKNOWLEDGEMENTS

The authors would like to express their thanks to colleagues at Rolls-Royce and Cranfield for the invaluable assistance and advice given during the course of this work. Special mention must go to Joan Moore for her advice on the use of MEPP. Finally, thanks are also offered to Rolls-Royce plc and the UK MoD, the two sponsors of this work.

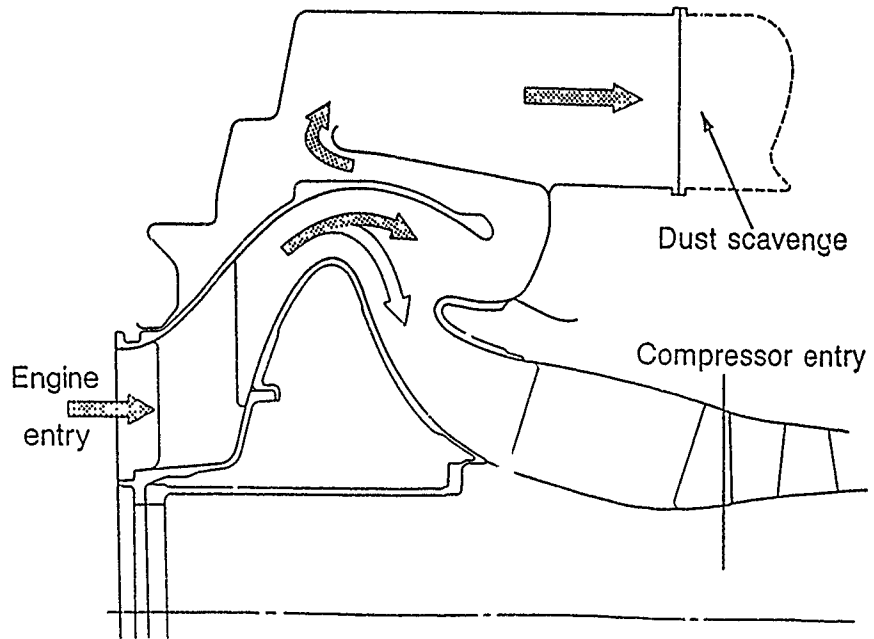
Fig.1 Section T⁺ gh IPS

Fig.2 Typical MEFP Calculation Grid

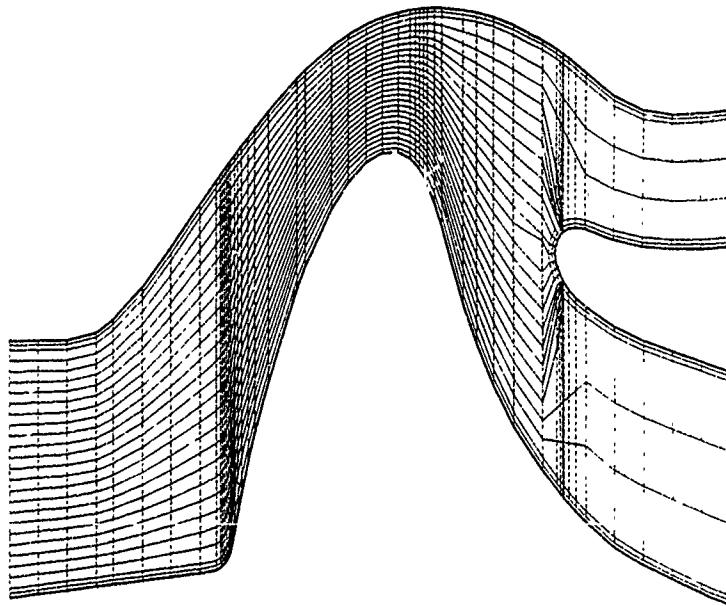


Fig.3 HTC Measurement Rig Set-up

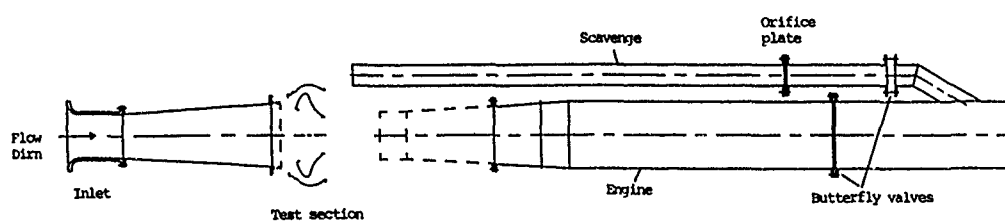


Fig.4 Static Pressure Tapping and Hot Film Probe Positions

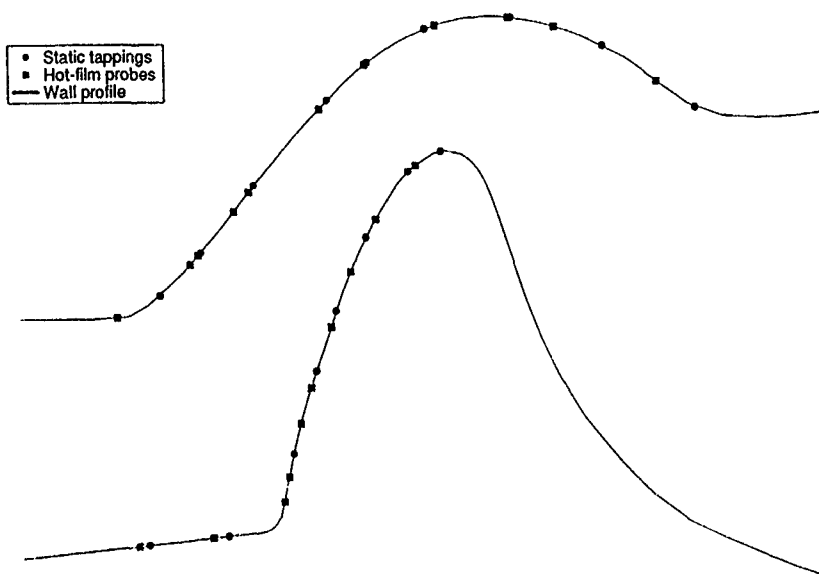


Fig.5 MEFP Predicted Velocity vector plot

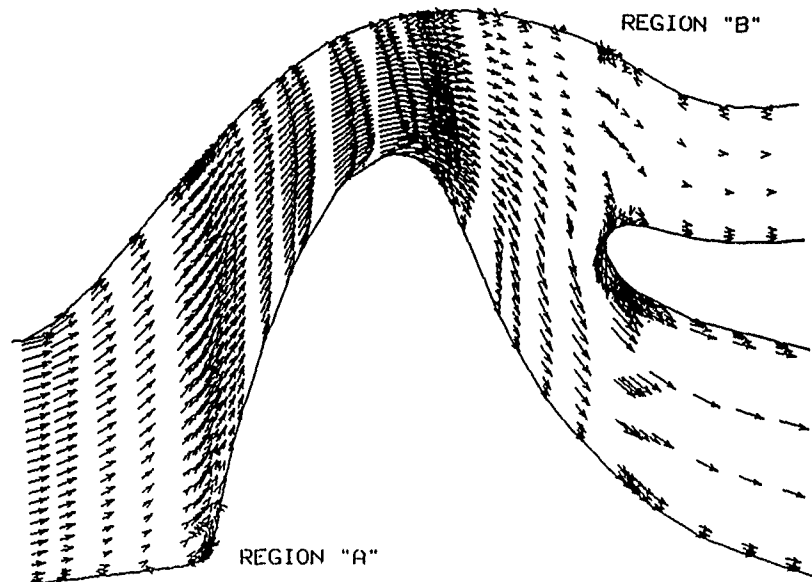


Fig.6 Measured Versus MEFP Predicted Wall Static Pressures

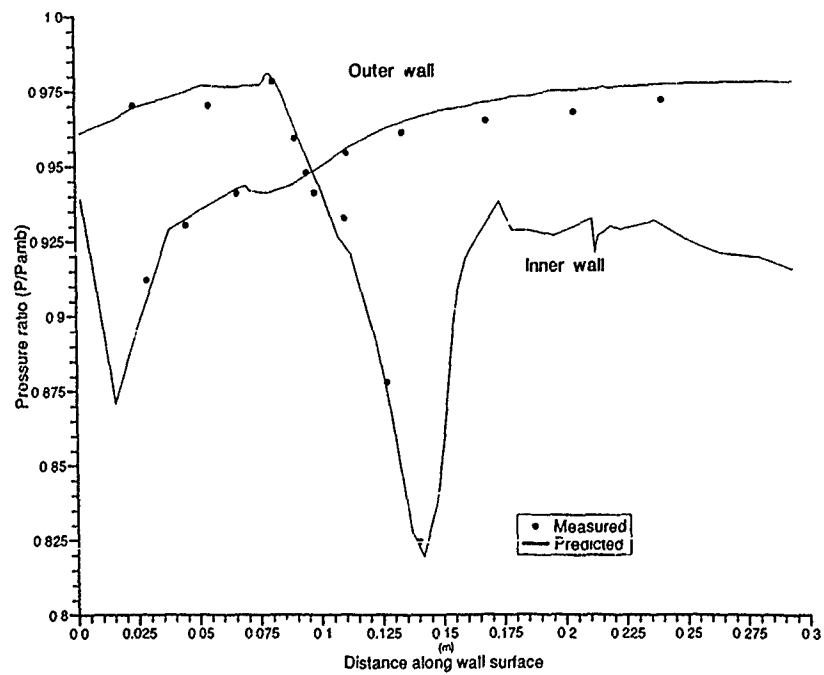


Fig.7 Measured and Predicted Local Heat Transfer Coefficients

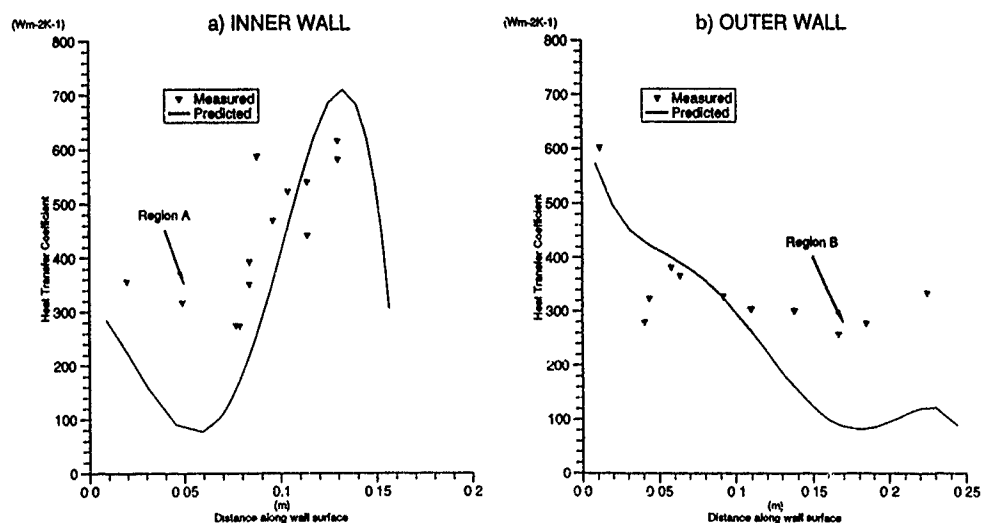


Fig.8 Hucknall Icing Facility

15 IN ICING TUNNEL
DIAGRAMMATIC LAYOUT

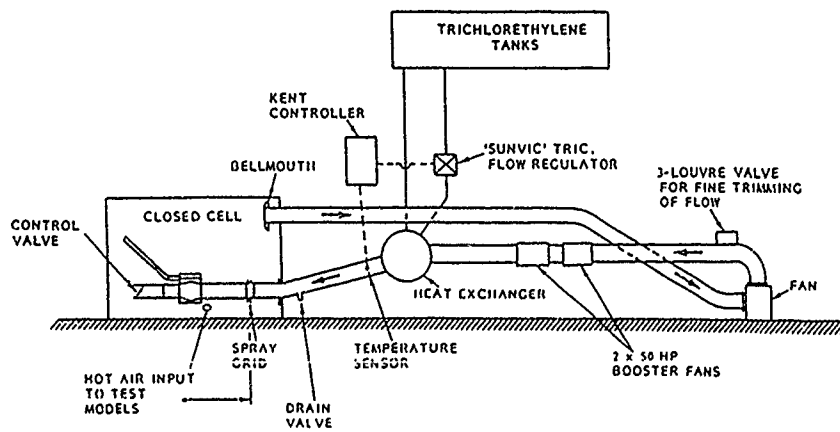


Fig.9 Predicted Water Droplet Trajectories

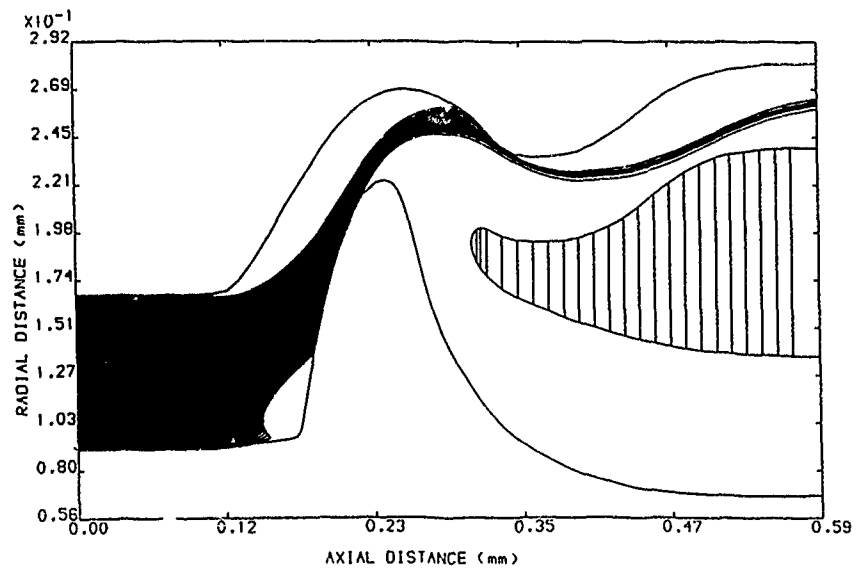
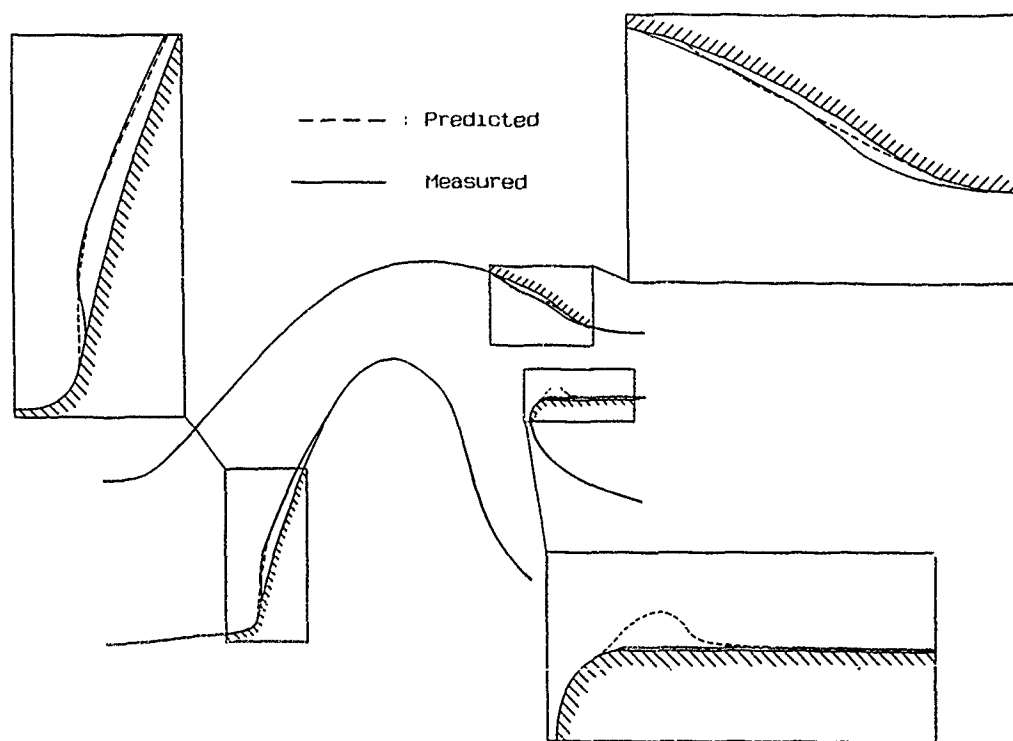


Fig.10 Predicted Versus Measured Ice Accretions



Discussion

1. D. Breitman, Pratt and Whitney Canada

What is the IPS bypass ratio?

Do you analyse particle trajectories that are not parallel to the engine centreline? How sensitive is your design to this?

Author:

At its design point, the IPS of the RTM 322 passes a flow equivalent to around 18% of the core flow through the scavenge system.

A comprehensive run of the trajectory code will consider a wide range of inlet particle velocities, both in terms of direction and speed. This has found to be important in replicating experimental data obtained from a cloud-fed inlet.

Initial particle directions significantly different from that parallel to the engine axis, do exhibit a trend to be less well separated on the RTM 322 IPS. However, for inlet trajectories representative of a cloud-fed dust this effect has been seen to be marginal.

2. G. Bianchini, Allison

Have you validated your predictions with only one configuration of inlet particle separators? Do you feel that the model is flexible enough to be used with other configuration IPS?

Are there any future plans to validate the model with different configurations of IPS?

Author:

The ability of MEEP to calculate heat transfer coefficients has been validated, within Rolls Royce, for a diverse range of engine components. The trajectory code validations have occurred over a range of RTM 322 IPS geometry standards only. A more generalized validation exercise is about to take place during the heated rig tests, where a range of geometries will be evaluated.

The design system is considered to be appropriate to the full range of IPS geometries, both axisymmetric and asymmetric, being considered for the next generation of IPS technology.

3. C. Scott Bartlett, Sverdrup Technology

The droplet trajectory and impingement prediction (figure 9) shows no droplet impingement on the splitter plate, however the following figure (10) shows a prediction of ice accumulation. Would you please comment on this apparent discrepancy?

Author:

Unfortunately, the trajectory prediction done to produce figure 10 did not generate a trajectory plot. The trajectories presented in figure 9 are from an earlier run, performed on an IPS geometry different to that later used on the trajectory validation tests.

4. A. Sutton, BAe

How many data points were collected for the determination of heat transfer coefficients?

What were the conditions of the ice accretion validation test?

Should the impact of water droplet model take into account the runback of the water which is not frozen?

Author:

At each of the heat transfer probe positions, the experimental data capture technique comprised a half hour probe stabilisation period followed by a 30 minute test period, during which time readings were recorded on circa 20 occasions. Thus, a data point on figure 7 describes a mean of the 20 readings taken at a position.

Ice accretion tests were run with the IPS operating at approximately 75 % design point flows, air temperature was -10°C and water droplet concentration 0.6 g/m^3 . Water droplet size was set according to UK Def Stan requirements. The coalescing of water droplets which initiated runback is something which is not currently modelled by the code. Along with water droplets break-up (pre and post impact) and bounce restitution ratios, this is an aspect which is to be the subject of experimental activities in the near future, aimed at generating a programmable model. The motion of single water droplets along the surface is something which the code is already capable of handling.

5. F. Siegmund, Fokker Aircraft

Is it the intention to make a fully evaporative anti-icing system or will the required power be such reduced that only water runs back into the separator?

Author:

Design philosophy, given to current certification requirements, is to prevent any ice formation on gas passage surfaces leading into the engine core passage. The liquid water generated from such a system has not been seen to create a runback problem on the RTM 322 IPS.

Other designs may not exhibit such a characteristic and so care must be taken to ensure that the engine is tolerant to the ingestion of potential large quantities of water, and that the IPS geometry provides the maximum possible water separation efficiency. In the second case this may be achieved by suitable wall profiling in conjunction with other means.

6. R. Toogood, Pratt and Whitney Canada

Could you please elaborate if your accretion analysis incorporates a time-stepping or is it a simple impingement location prediction?

Are you considering a building and a sudden process of ice or do you require completely clean surfaces in the RTM 322 IPS?

Author:

The current accretion model is not time-stepping. An ability to be able to predict ice accretions while continuously accounting for changes being made to HTC's and the flow field is not appropriate for the design of anti-icing systems where the objective is to keep surfaces free from ice, as on the RTM 32. Looking longer term, where controlled shedding devices may become available, then a time-stepping code would have to be considered.

Apologies for the short fall, but the main point of figure 9 was merely to highlight that such plots are produceable and to graphically illustrate the large number of trajectories which are involved in a calculation.

CAPTATION DE GLACE SUR UNE AUBE DE PREROTATION D'ENTREE D'AIR

Par

R. HENRY et D. GUFFOND

O. N. E. R. A, Direction des Etudes de Synthèse
29, Avenue de la Division Leclerc
92320 CHATILLON, France

RESUME

Lorsque les moteurs fonctionnent au ralenti, la protection des aubes directrices de prerotation contre les effets du givre est rendue délicate en raison du calage important des aubes et de la faible énergie disponible. La connaissance de la sévérité du givrage dans ces configurations ainsi que la masse de glace susceptible de se déposer est nécessaire pour optimiser la répartition et l'intensité du flux de chaleur utilisé pour la protection des aubes. La modélisation des trajectoires des gouttes d'eau surfondues, réalisée d'abord dans un champ axisymétrique bidimensionnel, puis sur une nappe de courant à proximité de l'aube, permet de calculer l'étendue et l'intensité de la captation. Un bilan thermodynamique sur la paroi de l'aube permet enfin d'évaluer la forme du givre déposé.

INTRODUCTION

Un des moyens de protéger les aubes de prerotation d'entrée d'air des moteurs contre le givrage consiste à les réchauffer par de l'air prélevé en sortie du compresseur centrifuge (jusqu'à 1,7 % du débit). Cet air chaud circule à l'intérieur des aubes. Lorsque le moteur fonctionne au ralenti, la quantité de chaleur et la température sont plus faibles et donc la protection moins efficace sur certaines parties des aubes.

L'étude de ces phénomènes par la seule voie expérimentale étant très onéreuse, il est intéressant de simuler numériquement la formation de givre sur ces aubes afin de déterminer l'étendue du dépôt, son intensité et sa forme, sans apport de chaleur, dans un premier temps.

La chaîne numérique de calcul bidimensionnel de forme de givre sur profil, développée à l'O.N.E.R.A [1] est adaptée et appliquée à ce cas. Elle est composée de 3 parties distinctes : un calcul aérodynamique donnant le champ de vitesse et pression autour de l'obstacle, un calcul de trajectoires de gouttes d'eau dans l'écoulement aboutissant au coefficient local de captation qui caractérise l'étendue du givrage et, enfin, un bilan thermodynamique à la paroi fournissant l'épaisseur et la forme du dépôt.

L'application de ces différents calculs à la captation sur une aube est présentée dans ce papier ainsi qu'un exemple de résultat obtenu.

CHAÎNE DE CALCUL**1- Champ aérodynamique**

La simulation numérique de l'écoulement dans un étage de turbine a été largement appréhendée par la Direction de l'Energétique à l'O.N.E.R.A. En particulier, un code

tridimensionnel axisymétrique, type Euler compressible [2] calcule le champ aérodynamique dans un étage complet (aubage fixe et mobile). Dans notre cas, seules les données dans l'aubage fixe sont nécessaires. L'écoulement amont ne possède pas de composante de rotation. Utilisant la symétrie de révolution, le champ est déterminé entre deux aubes voisines, dans un repère (R, Z, Θ) (Figure 1).

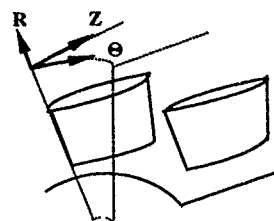


Fig. 1 : Ecoulement entre deux aubes : choix du repère

Le calcul tridimensionnel des trajectoires de gouttes est très coûteux en temps de calcul et n'est pas justifié ici. En effet, on peut distinguer deux zones distinctes dans l'écoulement : la zone située en amont de l'aube, non perturbée par la présence des aubes, et la zone mouillée par les aubes. Dans la première, on peut considérer l'écoulement bidimensionnel axisymétrique dans le plan (Z, R) dans une coupe d'angle Θ constante (Figure 2a). Dans la deuxième, l'écoulement peut être étudié sur une nappe de courant dans le plan $(Z, R \cdot \Theta)$ dans une coupe de rayon R (Figure 2b). Les faibles valeurs de la troisième composante des vitesses dans chacun des cas justifient cette approche.

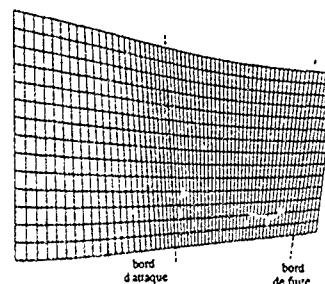


Fig. 2a : Maillage dans le plan (Z, R) à Θ médian.

Les résultats du code aérodynamique sont donc exploités successivement dans deux plans perpendiculaires pour chaque zone de l'écoulement ainsi définie.

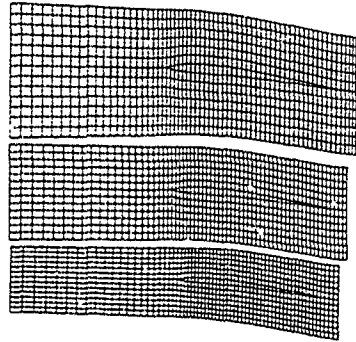


Fig. 2b : Maillage de proximité dans le plan (Z, R, Θ) au niveau : du pied d'aube, du rayon moyen, de la tête d'aube.

Les figures 3a et 3b montrent le champ de vitesse dans ces deux plans dénommés "canal" et "profil - aube", situés chacun dans une coupe médiane dans la 3^e dimension. On peut noter que les lignes de courant sont très peu déviées par les aubes. Le choix du maillage conduit à une imprécision de calcul au niveau du bord d'attaque de l'aube : en effet, un "becquet" doit être ajouté à l'avant du profil (Figure 4). C'est un des inconvénients de ce code.

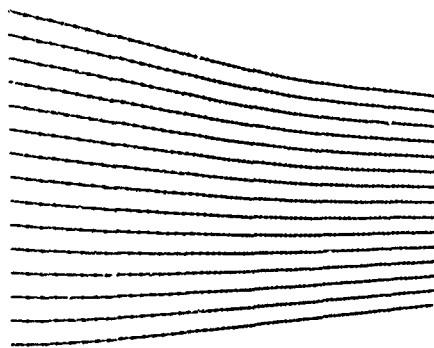


Fig. 3a : champ de vitesse dans le plan "canal" (Z, R) à Θ médian

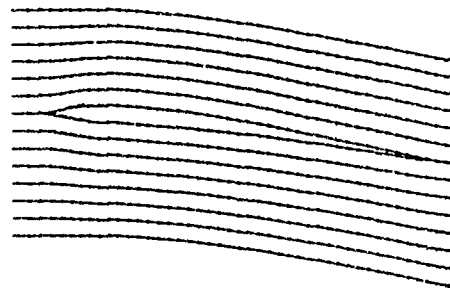


Fig. 3b : champ de vitesse dans le plan "profil-aube" (Z, R, Θ) à R médian

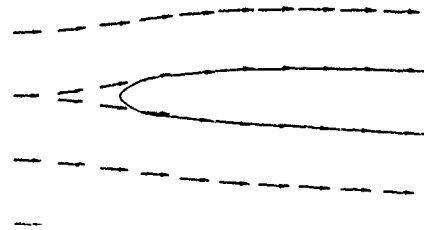


Fig. 4 : Approximation au bord d'attaque

2 - Calcul des trajectoires des gouttes d'eau

Equations générales

Les équations de l'écoulement diphasique sont appliquées avec les hypothèses suivantes :

- l'écoulement n'est pas modifié par la présence des gouttes (faible nombre).
- les gouttes sont parfaitement sphériques
- la goutte n'est soumise qu'à la force de trainée.

Le bilan de force appliqué à une goutte s'écrit :

$$F_t = M_g \frac{dV_g}{dt} \quad (1)$$

avec : F_g = force de trainée
 M_g = masse de la goutte
 V_g = vitesse de la goutte
 t = temps

En exprimant la force de trainée en fonction du coefficient de trainée, (1) s'écrit :

$$\frac{dV_g}{dt} = \frac{3}{4} \frac{\rho_a}{\rho_g} \frac{V_r^2}{R_g} C_t \quad (2)$$

avec : ρ_a = masse volumique de l'air
 ρ_g = masse volumique de la goutte
 $V_r = V_a - V_g$
 R_g = rayon de la goutte
 $C_t = f(Re)$ Coefficient de trainée fonction du nombre de Reynolds de la goutte

Le calcul des trajectoires est effectué de manière explicite [1] : à partir de la vitesse de la goutte à l'instant t , on calcule l'accélération (2) et en la supposant constant pendant dt , on intègre (2) et déduit la vitesse de la goutte à l'instant $t+dt$ ainsi que sa position jusqu'à l'impact sur l'obstacle.

Les figures 5a et 5b montrent les trajectoires dans les deux plans définis précédemment : dans le plan "canal", le calcul met en évidence un léger resserrement des trajectoires ; dans le plan "profil-aube", situé dans une coupe médiane de rayon, les gouttes sont peu déviées et suivent les lignes de courant. La zone d'impact s'étend à l'intrados jusqu'au bord de fuite.

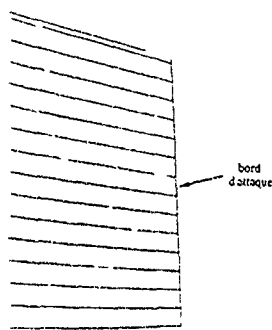


Fig. 5a : Resserrement des trajectoires dans le plan "canal". Mach amont = 0,33. Diamètre médian = 20 μ m

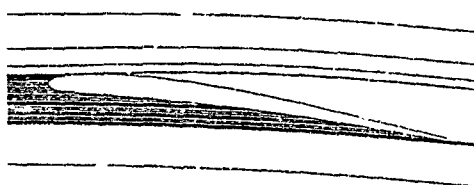


Fig. 5b : Trajectoires autour de l'aube. Rayon médian.

Coefficient local de captation

D'une manière générale, le coefficient local de captation, noté β , est le rapport, en suivant un tube de courant défini par deux trajectoires voisines, de la densité de flux massique d'eau \dot{m}_i impactant localement, à la densité de flux massique rencontrée par une surface perpendiculaire à l'écoulement à l'infini amont \dot{m}_∞ (Fig. 6).

$$\beta = \frac{\dot{m}_i}{\dot{m}_\infty} \quad (3)$$

En écrivant la conservation du débit massique entre deux trajectoires voisines, (3) s'écrit dans un plan :

$$\beta = \frac{dy_\infty}{ds} \quad (4)$$

avec : y_∞ = ordonnée de la goutte à l'infini amont,
 s = abscisse curviligne de l'impact sur le profil.

On obtient donc β en calculant la dérivée de la fonction reliant, pour chaque goutte, l'ordonnée à l'infini amont à sa position d'impact sur le profil. Le calcul de trajectoires dans le plan "canal" permet donc le calcul d'un premier coefficient local de captation β_c sur le bord d'attaque de l'aube, en fonction du rayon. Caractérisant l'effet de resserrement des gouttes à leur arrivée sur le profil, il s'agit en fait d'un coefficient de surconcentration dont les valeurs peuvent être supérieures à 1.

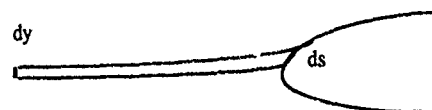


Fig. 6 : Coefficient local de captation

La courbe représentant la position à l'origine en fonction de l'abscisse curviligne d'impact par rapport au pied de pale est reportée sur la Figure 7, pour un nombre de trajectoires variant de 10 à 30.

La dérivée de cette fonction donne les valeurs de β_c aux différents points d'impact. Une fonction de cubic-spline interpole les valeurs en fonction du rayon et calcule en particulier le facteur de surconcentration aux rayons correspondants aux différents plans de coupe du calcul dans le plan "profil-aube" (Figure 8).

En raison de l'interpolation de la dérivée, les valeurs varient en fonction du nombre de trajectoires choisi. Cependant, les oscillations sont gommées pour un calcul effectué avec la valeur moyenne de 15 trajectoires, couramment utilisée. On constate que la captation est nulle au niveau du pied de l'aube, ainsi qu'au sommet et que les valeurs décroissent, pour des rayons croissants.

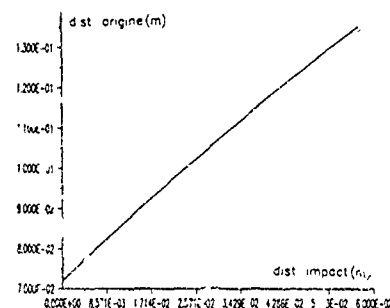


Fig. 7 : Positions initiales des gouttes à l'origine en fonction de leur position d'impact sur le bord d'attaque dans le plan "canal".

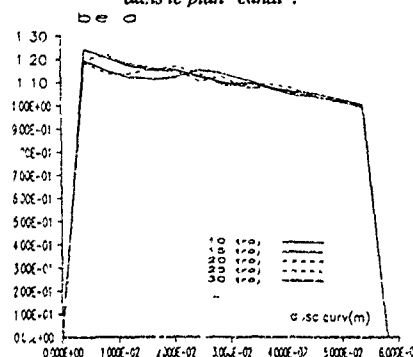


Fig. 8 : Coefficients locaux de surconcentration β_c dans le plan "canal". Influence du nombre de trajectoires.

De la même manière, dans chaque plan "profil-aube", situé à une coupe de rayon différente, on peut calculer des coefficients locaux de captation sur le profil de l'aube (β_i). La position à l'origine est représentée en fonction de l'abscisse curviligne d'impact sur la Figure 9, dans une coupe de rayon médian; l'abscisse 0 correspond ici au bord d'attaque. La courbe croît fortement à partir de ce point : la captation sera maximale. La figure 10 montre les valeurs de β_i correspondantes, pour différents nombres de trajectoires. La valeur est faible à l'intrados, maximale au bord d'attaque et devient nulle à l'extrados. Les oscillations sont minimales pour un nombre de trajectoires égal à 20.

Finalement, on peut définir dans chaque coupe de rayon, un coefficient local de captation global β égal au produit des coefficients β_i et β_c .

$$\beta = \beta_c \cdot \beta_i \quad (5)$$

Ce coefficient prend en compte à la fois la déviation des gouttes par le profil dans le plan "profil-aube" et le resserrement des gouttes dans le plan "canal".

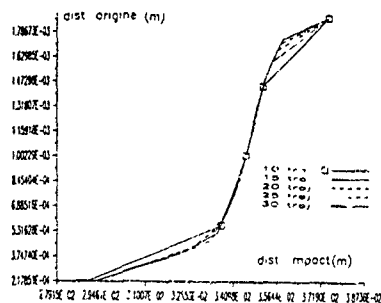


Fig 9 . Positions initiale des gouttes à l'origine en fonction de leur position d'impact sur l'aube dans une coupe de rayon médian

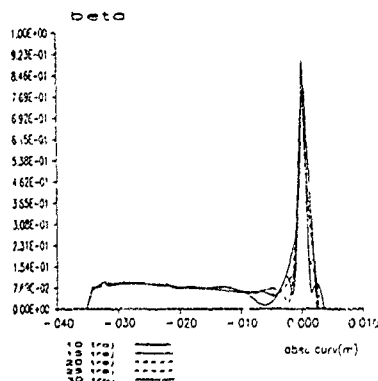


Fig. 10 : Coefficient local de captation β_i autour de l'aube. Influence du nombre de trajectoires.

Les valeurs de β sont représentées en fonction de l'abscisse curviligne pour trois coupes de rayon situées: au pied de l'aube, à mi-hauteur et au sommet (Figure 11). L'origine est située au point d'arrêt. La corde étant différente pour chacune des coupes, la captation débute à l'intrados à des abscisses différentes. Les valeurs sont faibles à l'intrados ($\approx 0,1$) et augmentent fortement au voisinage du bord d'attaque pour atteindre des valeurs supérieures à 1 en raison du facteur de surconcentration. La captation est nulle sur l'extrados.

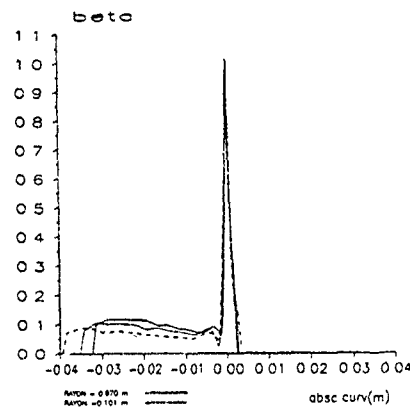


Fig. 11 : Coefficient local de captation global β en fonction de l'abscisse curviligne, pour des rayons : de pied d'aube, médian, et de tête d'aube.

3 - Bilan thermodynamique

Le bilan thermodynamique permet d'évaluer la forme du dépôt de glace en déterminant la fraction d'eau captée qui se congèle et la température de la paroi.

Lorsque cette dernière est nettement inférieure à 0°C , la congélation est quasi instantanée ; la forme se développe autour des points de fort coefficient de captation.

Par contre, autour de 0°C , une fraction d'eau ruisselle de part et d'autre du point d'arrêt et se congèle en aval ; le dépôt s'étend pour donner une forme dite "en corne".

La surface de l'aube est découpée en facettes supposées isolées entre elles et n'échangeant de la chaleur qu'avec l'extérieur. Les échanges thermiques sont liés à la captation d'eau surfondue, à la convection et aux changements de phase eau/glace. Deux bilans sont donc établis en surface : un bilan massique et un bilan thermique [1].

Bilan massique

Chaque facette est susceptible de recevoir de l'eau

provenant de la captation (\dot{m}_j) et du ruissellement de

l'élément précédent (\dot{m}_{rS}). Une partie s'évapore (\dot{m}_{vS}),

une fraction se congèle (\dot{m}_g) et une autre ruisselle vers la facette suivante (\dot{m}_{rs}) (Figure 12).

La conservation du bilan de masse donne :

$$\dot{m}_i + \frac{\dot{m}'_{rs}}{\Delta s} = \frac{\dot{m}_{rs}}{\Delta s} + \dot{m}_{v/s} + \dot{m}_g \quad (6)$$

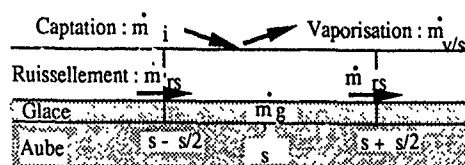


Fig 12 : Bilan massique au niveau de la paroi

Bilan thermique

De la même manière, un bilan thermique est effectué sur chaque facette. On peut distinguer les pertes et les gains (Figure 13). Dans le cas d'une température de paroi négative, les pertes proviennent :

- de la convection (\dot{q}_a)
- de l'évaporation/sublimation ($\dot{q}_{v/s}$)
- du réchauffement de l'eau d'impact (\dot{q}_i)

Les gains proviennent :

- de la chaleur latente de congélation (\dot{q}_g)
- du refroidissement de la glace (\dot{q}_f)
- du refroidissement de l'eau de ruissellement (\dot{q}_r)
- de l'énergie cinétique des gouttes (\dot{q}_u)

Le signe de certains termes peut être inversé selon les configurations.

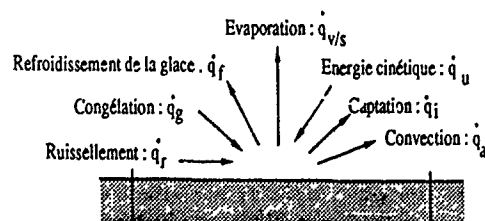


Fig. 13 : Bilan thermique à la paroi

Le coefficient d'échange par convection est déterminé à partir d'un calcul de couche limite avec rugosité de paroi (Figure 14).

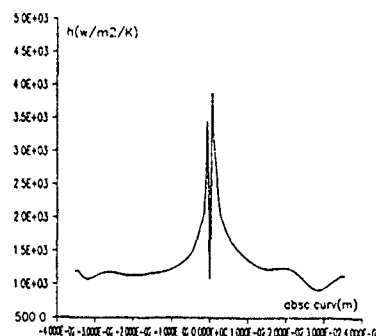


Fig. 14 : Coefficient d'échange par convection

Sur chaque facette, on suppose le bilan en équilibre :

$$\sum_{j=1}^7 \dot{q}_j = 0 \quad (7)$$

On détermine de manière itérative la température de paroi et la fraction d'eau qui se congèle, afin que les deux équations de bilan (6) et (7) soient vérifiées. Ce calcul suppose les échanges instantanés et ne prend pas en compte les échanges par conduction dans la glace et la paroi.

Enfin, on en déduit un taux de croissance et donc, une forme de glace à un instant donné.

A ce stade, un nouveau calcul du champ aérodynamique prenant en compte les perturbations induites par le dépôt de glace est généralement effectué. Ce n'est pas possible ici dans la mesure où le maillage utilisé dans le calcul aérodynamique ne permet pas de modification au bord d'attaque. La forme obtenue constitue donc une première évaluation.

RESULTATS ET DISCUSSION

Plusieurs simulations sont effectuées à partir du même champ aérodynamique correspondant à un nombre de MACH d'environ 0,3 en amont de l'aube et à un calage des aubes nul, c'est à dire à un fonctionnement en régime avec volets ouverts.

Dans un premier temps, on fait varier la température d'arrêt de -15 °C à +3 °C pour une teneur en eau liquide moyenne de 0,6 g/m³, un diamètre volumique médian de gouttes de 20 µm ; la durée de captation est de 60 secondes. Les résultats sont examinés dans une coupe de rayon médiane et représentés sur deux aubes voisines.

Influence de la température

Pour les températures de -15 et -10 °C (Figures 15 et 16), la glace recouvre essentiellement le bord d'attaque, atteignant une épaisseur de 3 mm environ. Alors qu'une fine couche (<1 mm) recouvre l'intrados, l'extrados reste propre.

A partir de -5 °C (Figure 17), la forme se modifie : elle s'aplatit au bord d'attaque pour évoluer vers une forme

"en corne" à 0 °C (Figure 18). Le point d'arrêt n'est plus recouvert mais l'eau se congèle de part et d'autre. La largeur de la forme atteint 7 mm. Elle reste confinée autour du bord d'attaque.

La glace est encore présente pour des températures d'arrêt légèrement positives car les températures sont toujours négatives à l'intrados et à l'extrados (Figure 19 et 20). Une épaisseur relativement importante subsiste au début de l'extrados et l'eau ruisselant sur l'intrados se congèle plus loin vers le bord de fuite. En résumé, on constate une évolution importante des formes avec la température.

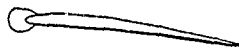


Fig. 15: - 60 s de captation - $lwc = 0,6 \text{ g/m}^3$
- $dmv = 20 \mu\text{m}$ - $tar = -15 \text{ °C}$ - Rayon médian

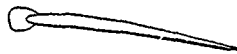


Fig. 16: - 60 s de captation - $lwc = 0,6 \text{ g/m}^3$
- $dmv = 20 \mu\text{m}$ - $tar = -10 \text{ °C}$ - Rayon médian

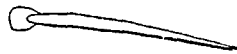


Fig. 17: - 60 s de captation - $lwc = 0,6 \text{ g/m}^3$
- $dmv = 20 \mu\text{m}$ - $tar = -5 \text{ °C}$ - Rayon médian

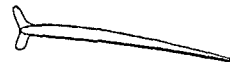
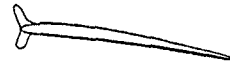
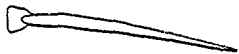


Fig. 18: - 60 s de captation - $lwc = 0,6 \text{ g/m}^3$
- $dmv = 20 \mu\text{m}$ - $tar = 0 \text{ °C}$ - Rayon médian

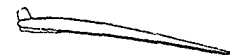
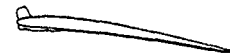


Fig. 19: - 60 s de captation - $lwc = 0,6 \text{ g/m}^3$
- $dmv = 20 \mu\text{m}$ - $tar = +2 \text{ °C}$ - Rayon médian

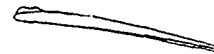
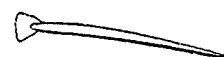


Fig. 20: - 60 s de captation - $lwc = 0,6 \text{ g/m}^3$
- $dmv = 20 \mu\text{m}$ - $tar = +3 \text{ °C}$ - Rayon médian

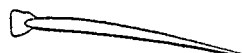


Influence de la section de l'aube

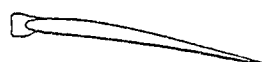
Le code permet d'effectuer les calculs de forme dans chacune des 15 coupes de rayon définies dans le code aérodynamique, du pied d'aube à la tête. D'une manière générale, le calcul de trajectoires a montré qu'aucune goutte n'impactait sur les extrémités ; les limites de la zone captation sont donc situées en retrait d'environ 4 mm par rapport au sommet et à la base. Entre ces deux limites, la comparaison des formes pour trois coupes différentes ne révèle pas de différence notable (Figure 21). La forme n'évolue que très peu avec le rayon de l'aube.



- Pied d'aube -



- Rayon médian -



- Tête d'aube -

Fig. 21: - 60 s de captation - $lwc = 0,6 \text{ g/m}^3$
- $dmv = 20 \mu\text{m}$ - $tar = -5^\circ\text{C}$ -

Influence de la teneur en eau liquide et de la taille des gouttes

Une simulation à 0°C avec une teneur en eau liquide de 1 g/m^3 montre, comme on pouvait s'y attendre, que la quantité de glace est plus importante que dans le cas à $0,6 \text{ g/m}^3$. Par contre, la forme reste inchangée (Figure 22). La sévérité du givrage augmente avec la teneur en eau liquide. L'influence de la taille des gouttes se révèle négligeable. Ceci est en contradiction avec les résultats obtenus sur profil d'avion mais s'explique par les fortes valeurs du coefficient d'inertie en raison des très faibles dimensions de l'aube.

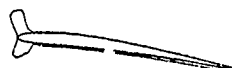


Fig. 22: - 60 s de captation - $lwc = 1 \text{ g/m}^3$
- $dmv = 20 \mu\text{m}$ - $tar = 0^\circ\text{C}$ - Rayon médian -

En résumé, l'application du code à une configuration précise et une étude non exhaustive de paramètres mettent en évidence la présence de givre, essentiellement autour du bord d'attaque. Pour un champ de vitesse identique, la prépondérance du paramètre température est confirmée : elle influence largement sur la forme du dépôt de glace dans une section donnée. Par contre, la forme paraît peu évoluer

avec le rayon : l'épaisseur est identique de la base au sommet de l'aube.

L'influence du calage des aubes n'a pu être étudiée car sa modification nécessite un nouveau calcul aérodynamique à partir de nouvelles données de profil. Selon l'exemple traité ici, l'application de cette chaîne de calcul à une configuration de fort calage (60°) permettra une meilleure localisation des dépôts de givre.

CONCLUSION

La chaîne numérique de calcul de forme de givre sur profil développée à l'O.N.E.R.A a été modifiée et adaptée au cas de captation sur un aubage de prérotation d'entrée d'air de moteur. Le champ aérodynamique tridimensionnel est exploité successivement dans les deux plans perpendiculaires (Z,R) et (Z,θ) afin de déterminer les coefficients locaux de captation dans ces deux dimensions. Un bilan thermodynamique est ensuite effectué dans une section de l'aube et la forme de glace évaluée.

Une simulation est effectuée dans une configuration de calage nul (volets ouverts). En général, la zone de captation maximale est située autour du bord d'attaque dont il conviendra donc de privilégier la protection. L'intrados est recouvert d'une mince couche de glace, alors que l'extrados n'est pas atteint.

Les quantités apparaissent insuffisantes pour conduire à une obstruction par recouvrement de plusieurs aubes voisines. Toutefois, on retrouve l'évolution classique des formes qui tendent à s'élargir lorsque la température augmente et avoisine 0°C . Le rôle prépondérant de la température est ici confirmé.

La simulation de configurations différentes, en particulier avec un calage important peut être réalisée avec ce code. Elle permettra de mieux appréhender les problèmes de protection contre le givrage rencontrés dans ces conditions.

REFERENCES

- [1] D. GUFFOND O.N.E.R.A - France
Captation de glace par une surface non protégée au cours d'un vol en conditions givrantes. Recherches et établissement d'une méthode de calcul - 1981 - R T n° 3/5146 SY
- [2] J. P. VEUILLLOT et G. MEAUZE O.N.E.R.A
A 3D Euler Method for Internal Transonic Flows Computation With a Multi-Domain Approach AGARD/PEP - Lecture Series n° 140, Paris, 13 - 14 Juin 1985
- [3] L. BRUNET
Conception et discussion d'un modèle de formation du givre sur des obstacles variés. 1985 - Thèse de doctorat - Université de CLERMONT 2 - France

Discussion

1. K. Broichhausen, MTU

My question is also directed to the authors of paper 16. Both codes, the Moore code and the Veuillot code, work either with cusps or have some problems in the stagnation zone. On the other hand, the icing effects are concentrated near the leading edge. Could you please comment on this?

Author:

That is the problem of the flow field calculation. These codes were not developed for this application. The main purpose of the codes is to know the flow field at the exit of a stage. ONERA/energetic direction is developing a new code with a mesh. I will take this problem into account.

2. S. Riley, Rolls Royce

How does the heat transfer coefficient at the ice surface warm transiently and how is the time stepping achieved?

Author:

The transfer coefficient is calculated with an integral boundary layer code. The calculation is done on the blade roughness and introduced by an equivalent sand height roughness. Transition appears with a critical Reynolds number. The boundary layer is not re-calculated. The calculations are steady, and we calculate an ice growth rate.

3. A. Sutton, BAe

Is there any possibility of using this code on rotor blades as well as on stator vanes?

Author:

No, this code cannot be used on rotor blades. In this case, the problem is a really 3-D flow field code one. Droplet trajectory codes are not developed with effect of girator.

4. E. Brook, Rolls Royce

Does the code re-calculate the flow field to take account of the accretion?

Author:

No, in this application the flow field is not re-calculated. The approximations at the leading edge do not permit it. The final ice shape is not important. The main question is to determine the areas of accretion.

5. P. Sabla, GEAC

What inclement weather corrosion does 0.6 g/m^3 drop represent?

Author:

These conditions represent the standard conditions of LWC and DVM by FAR 25 law (Appendix C). Other conditions can be simulated. Accretion increase with the LUC, but there is a weak effect of the DMV because of the value of the inertial coefficient.

DEVELOPMENT OF AN ANTI-ICING SYSTEM FOR THE T800-LHT-800 TURBOSHAFT ENGINE

by

Gary V. Bianchini

Allison Gas Turbine Division, General Motors Corporation

P.O. Box 420

Indianapolis, Indiana USA 46206-0420

ABSTRACT

The T800-LHT-800 is a modern technology 1200 hp (900 kW) class turboshaft engine developed for the U.S. Army's LH helicopter and various civil applications. One of its significant features is an integral inlet particle separator (IPS). The presence of an IPS significantly complicates development of an anti-icing system for protection against the hazards associated with ice formation during operation in environmental icing conditions.

Characteristically, inlet particle separators expose large areas to the incoming air, with the potential for widespread impingement of supercooled cloud droplets and resulting accretion of ice. Thermal anti-icing of such an inlet system, with the limited amount of compressor bleed air available, presented a significant design challenge, which has been addressed through three design iterations, an engine test involving a thermal survey of the protected surfaces, and an engine test in environmental icing conditions. A second thermal survey test and a final environmental icing test, which will satisfy military and civil certification requirements, will be run on the resulting system late in 1990.

The anti-icing system that has evolved from this series of designs and tests is simple and light weight, imposes a performance penalty of less than 5% in power and specific fuel consumption, and protects against harmful formations of ice throughout the envelope defined by the Military and the Federal Aviation Administration (FAA). In addition, the system provides protection for the vulnerable surfaces of the IPS scavenge system so that separation capability is available to aid in preventing core ingestion of ice shed by the air vehicle.

This paper describes the T800 engine, discusses the anti-icing system requirements, design evolution, and validation testing, and presents the final anti-icing system configuration resulting from the development effort.

PROGRAM DESCRIPTION

The T800-LHT-800 engine is under development for the U.S. Army's LH helicopter and has significant potential for commercial application. The Army's development program was structured as an effort for two competing

partnerships through the Preliminary Flight Rating (PFR) phase with competitive procurement from the winning partners following the Qualification Testing (QT) phase.

Following the PFR contract award, the Light Helicopter Turbine Engine Company (LHTEC), a partnership between Allison Gas Turbine Division of General Motors Corporation and Garrett Engine Division of Allied Signal/Signal Aerospace Company, began a 3-year development program competition. LHTEC won the downselect and is currently in the QT phase of the program. Following the completion of QT, scheduled for 1991, Allison and Garrett will compete for the T800 Government procurement. Both LHTEC partners will, however, be awarded a minimum order in each production lot to ensure their continued competitiveness.

In parallel with the LH application engine development, other engine applications have been explored. Commercial ventures including T800 installation in an Agusta A129 and Westland Lynx are currently being pursued. In conjunction with the U.S. Coast Guard, the Army has issued a T800 contract modification providing for a proof of concept flight demonstration for an Aerospatiale HH65 aircraft re-engined with T800 propulsion units.

ENGINE DESCRIPTION

The T800-LHT-800 engine is a 1200 hp (900 kW) class, modular design, 310 pound (141 kg), turboshaft engine. The engine's core consists of a dual-stage centrifugal compressor, an annular flow combustor, two-stage gas generator turbine, air cooled with the exception of the second-stage blade, and a two-stage front drive power turbine. The engine was initially designed for the U.S. Army which required a high level of maintainability and battle field hazard resistance. The engine features a dual channel full authority digital electronic control, which utilizes a Mil Standard 1553 bus. Other outstanding features of the engine include attitude capability to 120 degrees noseup, 90 degrees nosedown, and 45 degree roll; 6 minutes loss of oil capability; and an engine-mounted IPS. The engine is shown in Figure 1.

INLET PARTICLE SEPARATOR

The engine IPS consists of an inner dome, which forms the inner flow path, and the IPS casing assembly, which forms the outer flow path and also contains the flow splitter, scavenge vanes, and scavenge scroll. An engine-mounted blower, which is driven by the accessory gearbox, pulls air through the IPS system to create the aerodynamic separation. The flow path of the IPS forms a 'Y' with one leg leading to the inlet of the compressor and the second leg connecting to the IPS scavenge system. This flow path shape coupled with the aerodynamic separation helps protect the engine core from foreign object ingestion. Foreign material in the engine inlet is separated and pulled through the IPS and discharged overboard. The IPS creates a large surface area exposed to incoming airflow, which is a characteristic of particle separating systems. The scavenge vanes and the scroll account for a significant portion of the surface area.

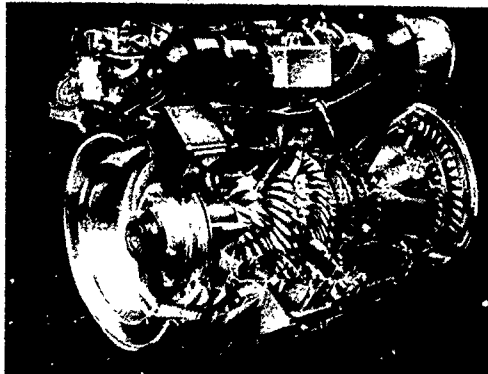


Figure 1. T800-LHT-800 turboshaft engine.

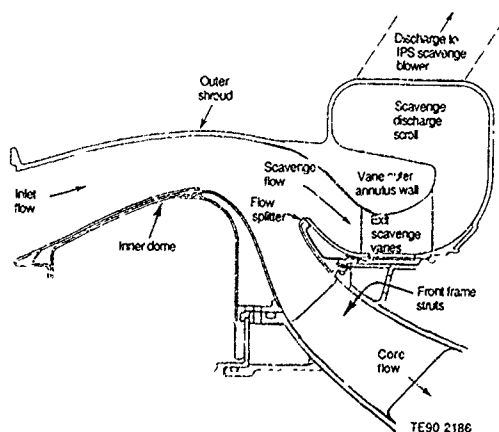


Figure 2. Inlet particle separator system.

The IPS system is illustrated in Figure 2.

The IPS has been developed from detailed flow analysis and over 100 hours of both aerodynamic and sand ingestion rig testing. The IPS system sand ingestion separation efficiency has been demonstrated on both the rig and engine to be 86% with AC coarse and 96% with Mil-C Spec sand. Additionally, foreign object damage (FOD) ingestion tolerance, by either separation or foreign object retention, has been demonstrated on the rig.

Although the IPS system has a demonstrated high separation efficiency, the large surface area, inherent to IPS design, results in the potential of widespread super-cooled water impingement on the flow-path surface, and the subsequent ice accretion while operating in environmental icing conditions. This, coupled with the budgeting of anti-icing energy source to reduce performance impact, created a significant anti-icing system design challenge.

ANTI-ICING SYSTEM REQUIREMENTS

The engine anti-icing system was designed to satisfy both the Military and FAA anti-icing requirements. The T800 Engine System Specification (military) requirements state that the engine's anti-icing system shall prevent ice accretion on all core flow-path surfaces of the front frame and all flow path surfaces of the inner dome. On the IPS casing assembly, all the flow-path surfaces upstream of the scavenge vanes 20% chord point (Figure 3) must be ice free, except light frosting will be allowed on the outer shroud upstream of its point of maximum diameter. These areas are shown in Figure 3. Additionally, ice accretion or shedding on surfaces other than the described areas shall not: cause damage to any engine components, cause IPS scavenge flow degradation greater than 10% at 10 minutes in the icing condition, cause airflow disturbances that excite harmonic compressor frequencies, cause secondary damage due to reduced clearances between rotating and stationary components, result in stall or surge, adversely affect the power setting parameters, or cause engine flameout.

The engine performance loss associated with operating in icing conditions with the anti-icing activated cannot exceed 5% loss in delivered power available at all conditions above Maximum Continuous power and 5% increase in SFC at all conditions above 50% Maximum Continuous power. Engine transient response must be demonstrated to be within specification limits while operating in icing conditions.

The icing conditions that are required to be tested by the Engine System Specification represent a ground fog point (at idle only), a 23° F (-5° C) condition, and a -4° F (-15° C) condition. Water content, drop diameters, and exposure times at each of these conditions are shown in Table 1.

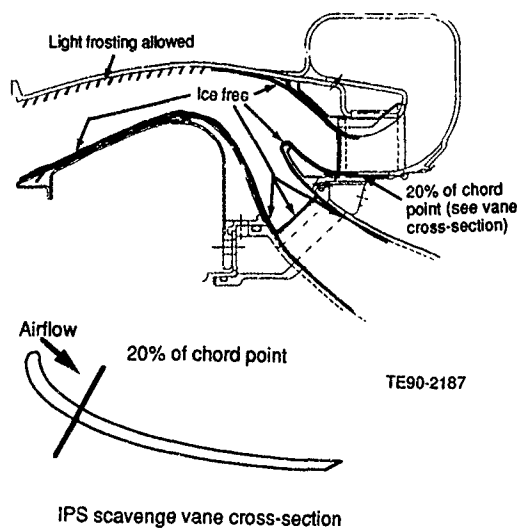


Figure 3. Required ice free surfaces.

The military requirements preclude the use of engine oil as the primary anti-icing energy source. During the icing test, it is required that the engine inlet oil temperature be maintained at or below the minimum oil thermostat setting. Also, the ground fog icing condition (Table 1, condition 3) must be run with the engine inlet oil temperature maintained at or below the engine inlet air temperature, 23° F (-5° C), for a 60 minute duration of cloud exposure. These requirements ensure that any oil heat transfer effects are minimized.

Table 1. Military icing test points.

	Conditions		
	1	2	3
Engine inlet total temp-- °F (°C)	-4 (-20)	+23 (-5)	+23 (-5)
Mean effective drop diameter--microns	20	20	30
Liquid water content -- g/m ³	1.0	2.0	0.4
Exposure time -- minutes	10	10	60

The FAA imposes anti-ice system requirements very similar to the military, with some exceptions. The icing test conditions specified, as shown in Table 2, differ from the test conditions specified by the military. This is insignificant to the design criteria because the anti-icing system is designed to prohibit ice accretion during any icing condition encountered within the engine operating and icing envelopes, shown in Figures 4 and 5.

The FAA also requires that the engine operate in an icing environment without anti-icing activated for 1

minute, immediately followed by anti-ice actuation. The engine anti-ice system is manually activated, so this requirement simulates the probable delay in anti-icing system actuation since an encounter with an icing condition may not be immediately recognized by a pilot.

Table 2. FAA icing test points.

	Conditions		
	1	2	3
Engine inlet total temp-- °F (°C)	-4 (-20)	+23 (-5)	+29 (-2)
Mean effective drop diameter--microns	15	25	40
Liquid water content -- g/m ³	1.0	2.0	0.6
Exposure time -- minutes	10	10	30

The FAA, similar to the military, requires the engine operate in the particular icing condition with anti-ice actuated for 10 minutes, except the FAA also requires that the engine continue to run in the icing conditions until any ice accretion has stabilized. This is a significant requirement for engines with inlet particle separators, since ice formation in the IPS scavenge flow path is allowable, and due to the large surface area inherent to an IPS, almost unavoidable.

Other requirements, not specifically documented in the specification, are self imposed to ensure the anti-icing system is reliable, simple, light weight, maintainable, and easily producible.

INITIAL ANTI-ICING SYSTEM DESIGN APPROACH AND RATIONALE FOR REDESIGN

Several anti-icing concepts were evaluated. The selection criteria of the anti-icing system included consideration of satisfying the Military Specification and FAA requirements, cost, weight, reliability, maintainability, and producibility.

The initial anti-icing system concept was to anti-ice only the inner dome and front frame flow path. Using this criteria, several schemes were proposed and evaluated, including compressor discharge air anti-icing, engine oil anti-icing, and compressor interstage anti-icing, the one chosen for the T800.

During the engine development program, the IPS splitter nose was extended to increase sand separation efficiency (Figure 6). This resulted in the need to actively anti-ice the flow splitter, instead of relying solely on heat

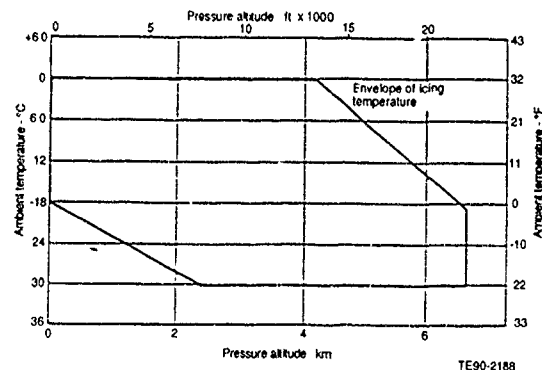
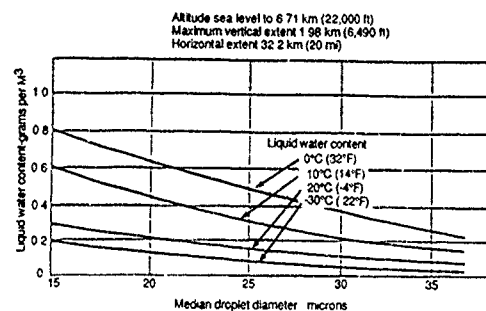


Figure 4. Continuous icing envelope.

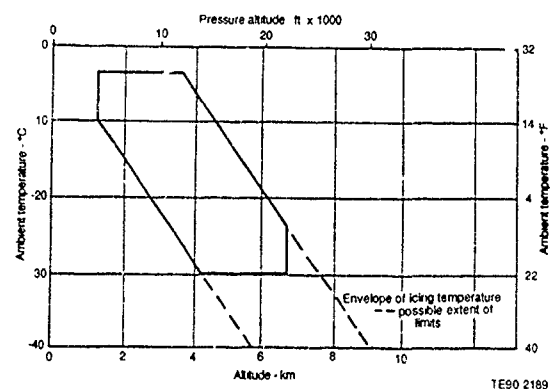
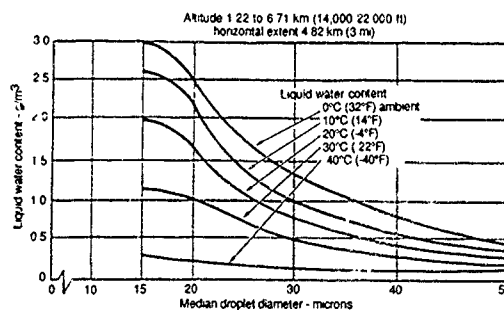


Figure 5. Intermittent maximum icing conditions.

conduction from the front frame. Since this forced an anti-icing system redesign, and in order to further reduce risk, it was decided to also actively anti-ice the IPS outer flow path and the scavenge vanes. The anti-iced engine flow paths of the initial design and the redesign are compared and illustrated in Figure 6.

Using the redesign concept, four anti-icing schemes were evaluated. An air and electrical system (Figure 7) was studied. The air would anti-ice the IPS flow splitter, front frame, and inner dome, and electrical heaters would anti-ice the IPS outer flow path and scavenge vane leading edges. The electrical heater power could be provided by the engine driven PMA, which would require a 50% increase in output capability. This scheme was rejected due to cost, weight, and maintainability concerns.

The second concept consisted of integrating the power turbine buffer air with the anti-ice system. Buffer air is supplied from compressor interstage to the rear support to cool the power turbine wheels. This anti-icing concept would use compressor interstage air to anti-ice the inner dome and IPS flow splitter, flow path, and scavenge vanes. The portion of the air used in the IPS would exit the IPS casing assembly then be routed to the

power turbine support for wheel cooling. This is schematically shown in Figure 8. This concept was rejected because at several flight conditions the flow circuit pressure drop reduced power turbine cooling airflow excessively. Also, the size and weight of the plumbing resulted in weight and maintainability penalties.

The third concept evaluated was a compressor interstage dual pass system. The anti-ice air would be delivered from compressor interstage to the front frame struts. The air would then pass through the struts and to the leading edge of the inner dome. Then it would flow aft along the inner dome flow path surface, then through the IPS flow splitter, outer flow path, and scavenge vanes. This concept as shown in Figure 9, was rejected because a significant increase in strut and inner dome passage area would be required to accommodate the increased total flow. This would impose cost and weight penalties.

The fourth concept investigated, shown in Figure 10, was chosen for the PFR configuration of the T800. It is a compressor interstage split flow system. The anti-icing air is delivered from compressor interstage to the front frame. The air then passes forward thru five tunnels in the front frame to the struts. The airflow splits at this point. Part of

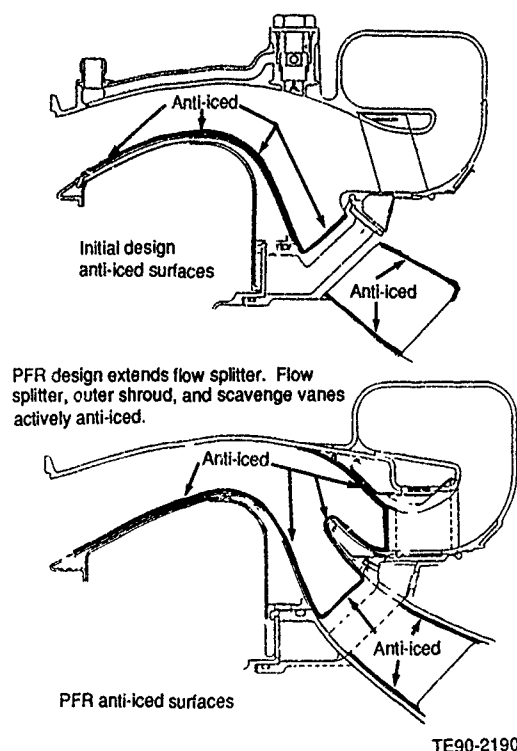


Figure 6. PFR anti-iced surfaces.

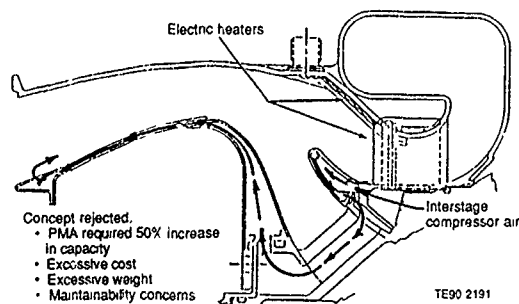


Figure 7. Air/electric anti-ice system concept.

the air is directed through the struts, anti-icing the struts leading edges, to the inner dome. This portion of the air then flows forward near the flow path surface of the inner dome and exits through slots at the front edge of the dome, then mixing with inlet air. The other portion of the air is directed to the IPS flow splitter then through the scavenge vanes and along a portion of the IPS outer flow path before exiting into the IPS scroll. This system was chosen because it best fit the selection criteria, and imposed the least impact on hardware changes from the original design.

Once the anti-icing design concept was established, several analytical tools such as computer-aided design

(CAD), heat transfer analysis, flow system analysis, and engine performance analysis were utilized during the design. The design point of the system was established, using these analytical tools, as -4°F (-20°C), static, sea level. All power conditions were considered. Heat transfer analysis was used to determine the required anti-ice air temperature and flow rates to provide flow path surface temperatures at a sufficient level to retard any ice formation of the super cooled water droplets impinging on flow-path surfaces. The analysis accounted for heat transfer due to conduction, convection, and evaporation. The analysis also predicted and accounted for anti-ice air heat loss due to delivery losses through the anti-ice valve and delivery tube. Engine performance loss is directly related to the amount of compressor interstage air used for anti-icing. This coerces the heat transfer analysis to accurately predict the anti-icing airflow rates required. Flow analysis was used to determine anti-ice passage size to ensure the proper airflow rates. Using the heat transfer analysis predictions of anti-ice air temperature, the flow analysis accounted for pressure losses to determine the metering orifice sizes. Engine performance analysis was used to predict engine power loss and SFC increase due to anti-ice bleed extraction.

The analytical tools were integrated to provide a basis for the design. It was determined, based on engine performance predictions that a variable anti-ice flow rate was required, to ensure minimal engine performance loss impact. Compressor interstage air temperature increases with engine power level, so more anti-icing energy is available in the air at high power than at idle. Therefore, less flow is required at the higher power to obtain acceptable anti-icing.

The anti-ice flow is controlled by a self modulating, engine mounted valve. The valve is schematically illustrated in Figure 11. The anti-icing valve is an integral part of the engine's acceleration bleed valve which is located on the bottom the engine. It is mounted onto an engine housing which has slots to access the compressor interstage area. The anti-ice valve consists of an electrically actuated solenoid, a pressure switch, and a piston and modulating spring. The anti-ice valve is fail safe,

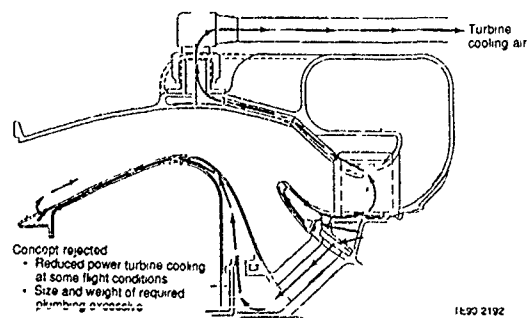


Figure 8. Buffer air anti-icing system concept.

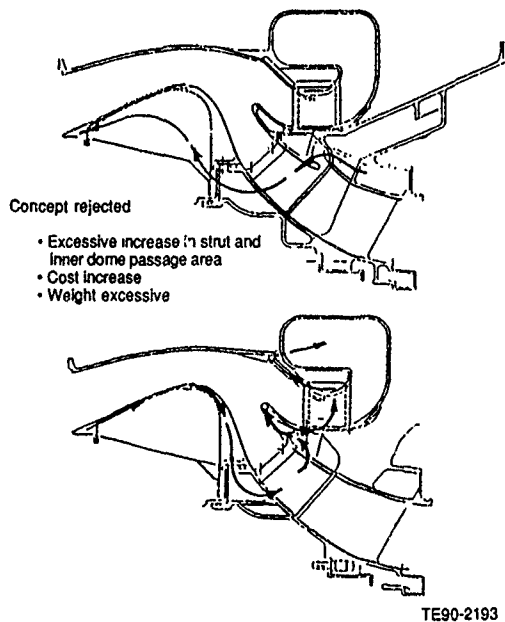


Figure 9. Dual pass anti-ice system concept.

requiring power to actuate the solenoid and turn anti-ice off. When anti-ice is selected off, the solenoid becomes powered and allows compressor discharge air to enter the valve's piston. The pressure of the air acts against the

lower pressure of compressor interstage air and a spring causing the valve to close, disallowing airflow through the valve. When anti-ice is selected on, the solenoid is unpowered and blocks compressor discharge air from entering the piston. This, in turn, allows compressor interstage air pressure to act against the spring and modulate the valve. Compressor interstage air pressure, similar to temperature, decreases as engine power level decreases. The lower interstage pressure results in increasing valve area, as seen in Figure 11. A pressure switch senses pressure in the anti-ice flow circuit and provides a cockpit indication of anti-ice actuation.

INITIAL THERMAL SURVEY TEST AND PRELIMINARY ENVIRONMENTAL ICING TEST

The anti-ice system design was supported with several analytical tools; however, due to the complexity of the flow circuit and heat transfer effects, and to demonstrate the system as required by specification, hardware flow tests and two test programs were performed.

The flow tests were designed to verify the part fabrication and design integrity by ensuring that the engine hardware was capable of flowing the design flow rates. Flow tests were run on the anti icing valve, the inner dome, the front frame, the IPS casing assembly, and the entire assembled anti-icing circuit.

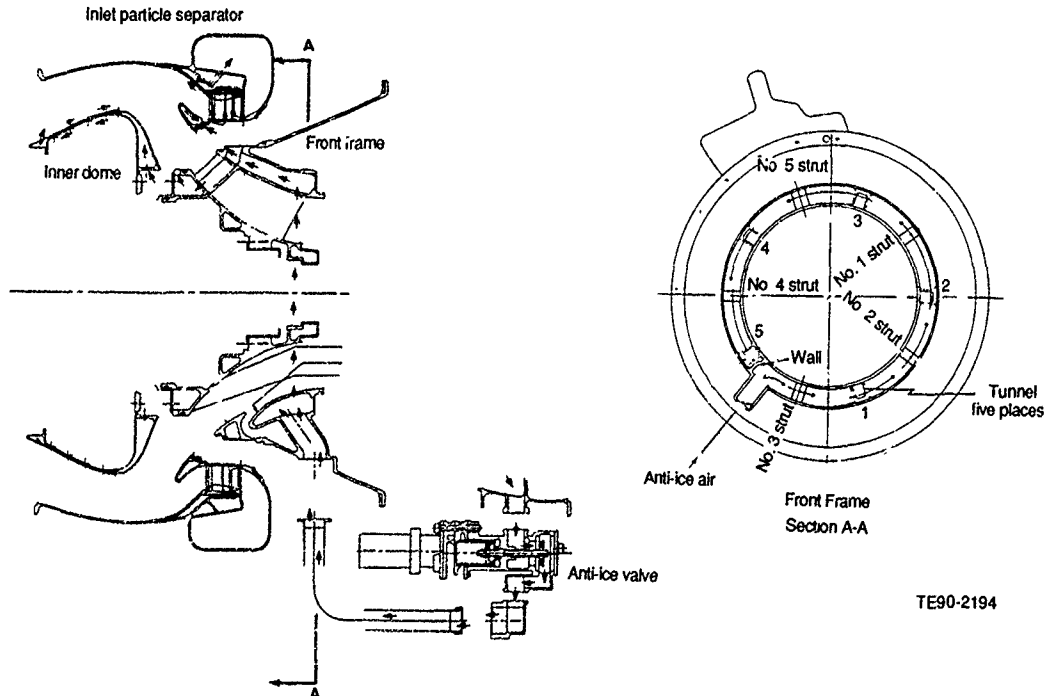


Figure 10. PFR configuration anti-icing system.

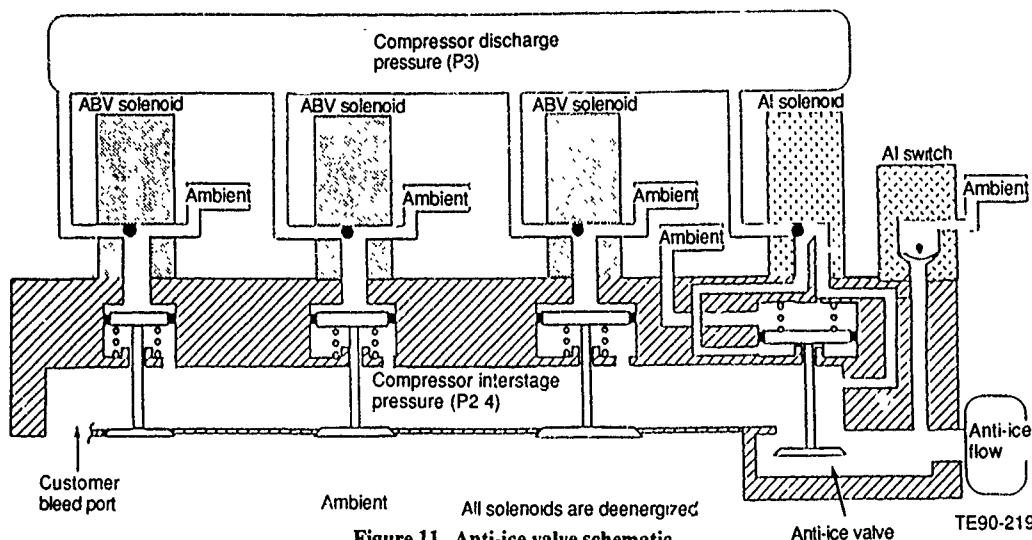


Figure 11. Anti-ice valve schematic.

The first test program run was an anti-ice thermal survey. Thermocouples were installed at various circumferential and axial locations of all anti-iced surfaces. Figure 12 illustrates the location of thermocouple placement. The thermocouples were imbedded in the flow-path surface to reduce convection errors and provide a true surface temperature. The engine was then run throughout the power range with dry inlet air at 23° F (-5° C) and -4° F (-20° C), since these are demonstration points required by the specification. Early in the test it was found that the anti-ice flow rate was lower than predicted values. The valve was modified to obtain higher flow rates and thus provide meaningful temperature data.

The temperature data revealed that the surface temperatures were lower than expected, as shown in Figures 13 and 14. Review of the test data showed a significant temperature drop, about 100° F (56° C) more than expected, from the anti-icing valve inlet to the aft manifold.

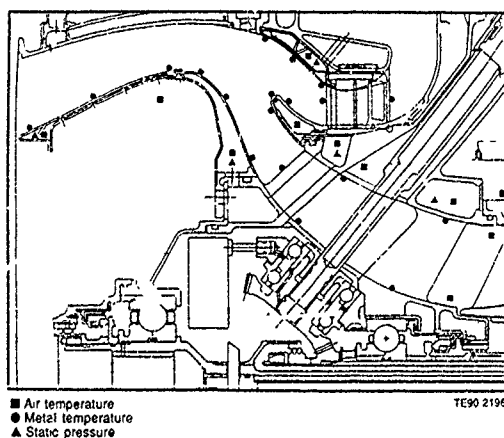


Figure 12. PFR anti-ice thermal survey instrumentation.

fold in the front frame, resulting in lower temperatures of the anti-icing air in both the front frame, inner dome, and the IPS casing flow circuit.

Heat transfer analysis, used to model the test data and provide possible solutions, focused in the aft manifold area. As the air enters the aft manifold from the delivery tube, it is forced to flow circumferentially in one direction by a blockage wall in the manifold (Figure 10, Section A-A), thus ensuring that the air is distributed evenly. The analysis verified that removal of the blockage could result in less temperature drop. Furthermore if the wall had a properly sized opening, acceptable flow distribution could occur. Later in the engine development program, prior to the QT phase, the front frame was redesigned and the aft manifold was completely eliminated. This will be discussed, in detail, in a later section.

The temperature data from the the most severe condition, -4° F (-20° C) inlet temperature, revealed that all surface temperatures were above freezing except for the IPS outer flow path and the leading and trailing edges of the scavenge vanes.

The thermal data provided a preliminary evaluation of the anti-icing system effectiveness, however a preliminary icing test was required to determine flow-path response to icing conditions and to further evaluate engine performance loss due to anti-icing operation. The test unit was configured as a gas generator, (power turbine removed), during the icing test in order to simplify the test equipment adaptation of the icing spray system through elimination of the load absorption system. This did not compromise the test objectives because the entire anti-icing system was intact. Engine performance during these icing runs was synthesized baser on actual performance data from this same engine prior to removal of the power turbine.

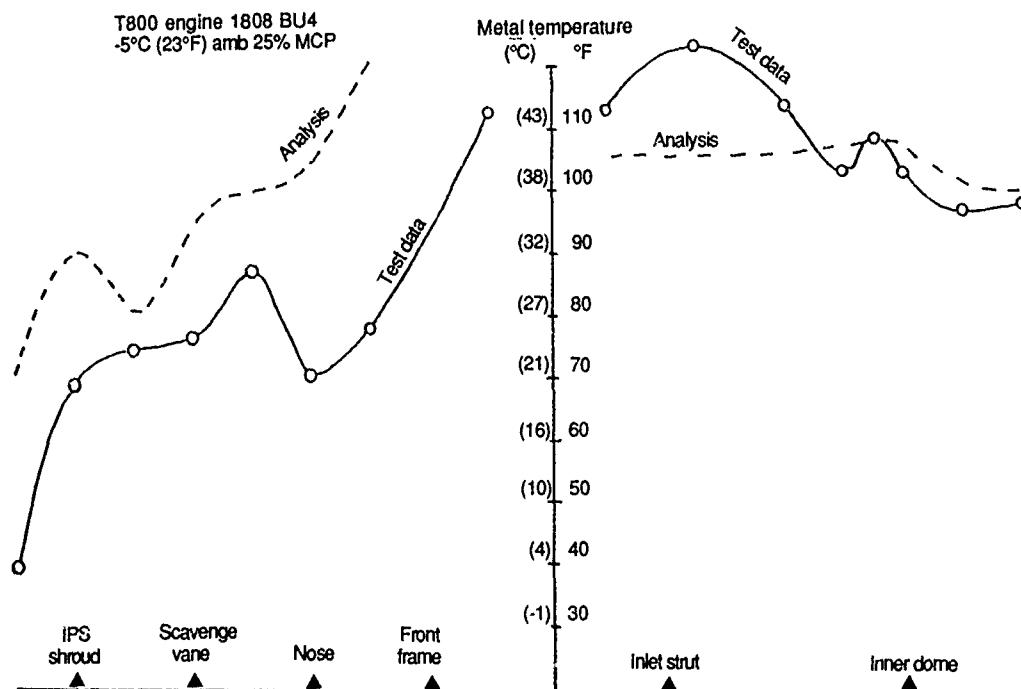


Figure 13. PFR thermal survey data; 23°F, 25% MCP.

TE90-2197

The test stand was converted from an altitude test facility to an icing simulation test stand for this test. Spraying Systems 1/4J-1A nozzles were used to produce the water spray. The variable conditions were set by changing the nozzle water flow rate and the atomizing air pressure. Each test condition (cloud liquid water content and droplet diameter) also required that the number of spray nozzles be varied because of the limited operating range of water flow and atomizing air pressure of each nozzle. The uniformity of the icing spray, which if not correct could significantly bias test results, was established by collecting ice on a screen located at the end of the engine supply air duct. After nozzle radial location was varied to optimize spray uniformity, the spray system was calibrated using laser probes. The calibration not only identified the required water flow and air pressure set points for each operating condition, but also established sensitivity to variations of these parameters.

Internal on-line video recording of a front frame strut, the IPS flow splitter, and an IPS scavenge vane was provided from borescopes mounted in the IPS casing assembly. This on-line monitoring was used as a diagnostic tool and as a safety feature, to ensure engine damage due to ice build up and shedding was avoided during the test. The borescope system was designed and implemented due to the inability to visually inspect and document the 'Y' shaped engine inlet flow path, as can be seen in Figure 2. The video monitoring system design criteria were very demanding. The borescopes tips were installed flush with the engine flow-path surface and

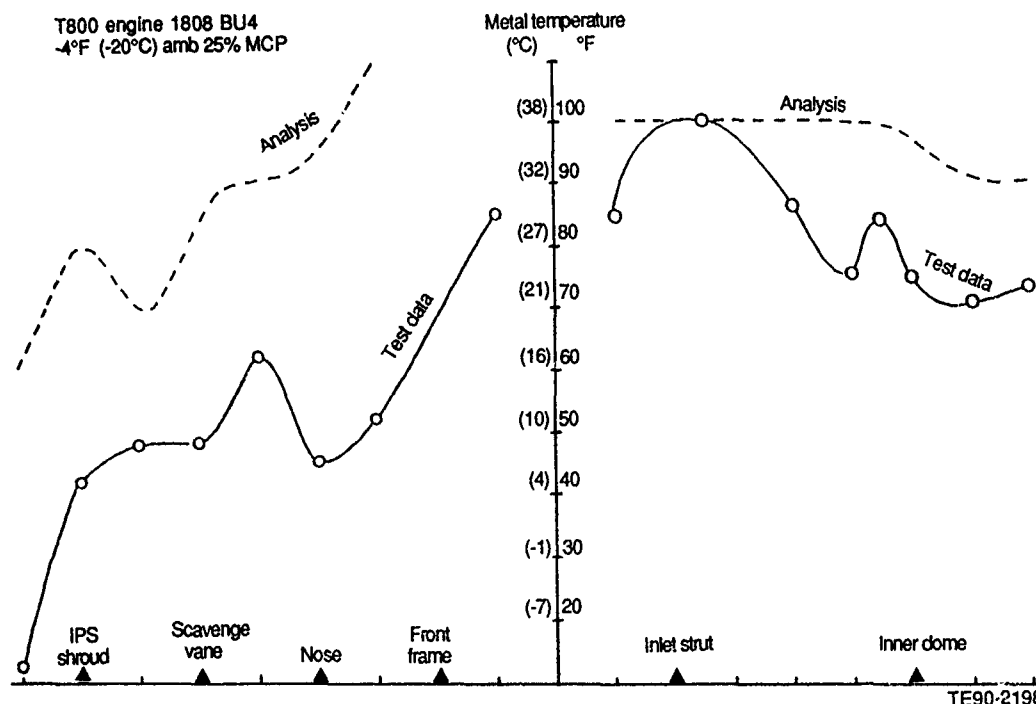
required a sophisticated deicing and defogging system. Additionally, the borescopes and support equipment were mounted to the engine and had to survive the engine and icing environment.

Additional documentation of flow-path surfaces was obtained with videotaped borescope inspections immediately following the icing runs and still photographs of the engine inlet. Cold airflow was maintained during these post-test inspections to prevent any ice melting for the duration of the inspections (usually 20 minute duration).

The simulated icing conditions that the engine was exposed to conformed to the Military requirements delineated by Table 1. They were:

- (1) 23°F (-5°C) inlet temperature, 2.0 g/m³ liquid water content, 20 micron drop diameter
- (2) -4°F (-20°C) inlet temperature, 1.0 g/m³ liquid water content, 20 micron drop diameter
- (3) 23°F (-5°C) inlet temperature, 0.4 g/m³ liquid water content, 30 micron drop diameter, idle only

The test points run during the icing test were extensive. Power points from idle to maximum power were run with simulated conditions (1) and (2). The engine was exposed to the icing condition for a 10 minute duration. After 5 minutes of exposure a rapid acceleration to maximum followed by a rapid deceleration to the test point was run to demonstrate transient response. Immediately following the full 10 minute exposure period, the



engine was shutdown and the post test inspections were performed.

Condition (3) was run for a 60 minute duration at idle only. During this period engine oil was maintained at 23° F (-5° C), to eliminate any heat transfer effects from engine oil.

Anti-icing flow rates were adjusted by means of an external valve, throughout the test, to optimize the required anti-ice flow rates to prevent ice formation. This data proved to be invaluable during the system redesign for the QT configuration (reference next section).

Performance data were obtained while the engine was operating in icing conditions. Direct measurement of output power was not possible since the test article was configured as a gas generator. The dry air performance data obtained previously on the complete engine was used in conjunction with the gas generator performance data to synthesize output power determination. The performance data was ultimately used to establish the performance degradation, output power loss and SFC increase, associated with operating in an icing condition with anti-ice activated.

The test results of the icing simulation points revealed some ice formation along the IPS outer flow path, forward of the anti-iced surface, and on the pressure surface of the IPS scavenge vanes. The engine's core flow path remained free of any ice accretion during all points.

The output power loss and SFC increase, resulting from anti-ice operation in icing conditions were both within the specification limits.

Additional development work was performed to determine if the engine could operate in the icing condition until ice accretion stabilized, as required by the FAA specification. Ice formation in the IPS scavenge vanes continued to build but did not significantly reduce the scavenge flow of the IPS. However, the ice buildup on the IPS outer flow path caused test point termination prior to accretion stabilization.

It had already been determined prior to the conduction of this PFR preliminary icing test that the QT version of the IPS casing assembly would have scavenge vanes constructed of aluminum instead of stainless steel, as in the PFR version. This design change was made primarily to reduce engine weight but it offered a benefit to the anti-icing system due to increased heat transfer characteristics of aluminum. An early configuration IPS casing with aluminum vanes was available near the end of the preliminary icing test. This IPS casing assembly was installed on the engine and evaluated in simulated icing conditions. The ice accretion on the scavenge vanes was significantly reduced with this IPS casing assembly, without making any other system modifications.

The thermal survey and the preliminary icing tests were not intended to be qualification tests but rather to

identify areas of the anti-icing system that needed further enhancement. Both of these tests were very effective in providing this data.

ANTI-ICING SYSTEM REDESIGN BASED ON TEST RESULTS

Following completion of the engine PFR development program, LHTEC was awarded the follow-on contract for QT development (and engine production). Several engine hardware redesigns were initiated to address problems encountered in the PFR phase as well as to enhance engine reliability, producibility, and decrease weight and cost. Part of this redesign was focused on the anti-icing system. The test results from the anti-ice thermal survey and the preliminary icing test were very valuable in highlighting the areas of the anti-icing system that required design changes. The original anti-icing concept of the compressor interstage dual bypass system was maintained; however, the anti-ice flow circuit was modified to increase the anti-icing system effectiveness.

The front frame was modified significantly by relocating the oil supply and scavenge passages. This change was made primarily due to a compressor modification, however it allowed beneficial rerouting of the anti-ice airflow. As discussed previously, the anti-ice air temperature decreased significantly in the aft tunnel of the front frame anti-icing air manifold. Relocating the oil tubes allowed this manifold to be eliminated, thus theoretically reducing a large portion of the 100° F (56° C) temperature drop. With the new design, schematically shown in Figure 15, the anti-ice air enters the front frame from the delivery tube and flows directly to the forward manifold.

Both the PFR thermal survey temperature data and the preliminary icing test verified that the inner dome and front frame strut surface temperatures were at a level well

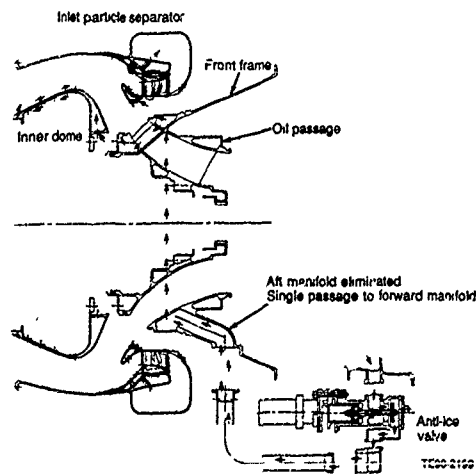


Figure 15. QT anti-icing system.

above that required to inhibit ice accretion. This coupled with the icing problems in the IPS outer flow path and scavenge vane areas led logically to a redistribution of the anti-ice flow rate splits. It was imperative to maintain the same level of total anti-icing flow rate to ensure minimal engine performance loss penalties. Therefore, the flowrate in the front frame/inner dome anti-ice flow circuit was reduced 10% by decreasing the size of the inner dome anti-icing inlet holes, which meter the flow. The redistribution, coupled with slight modifications to anti-ice flow orifices and passages in the IPS casing assembly, increased the anti-icing flow to the IPS by 10%, thus the overall anti-ice flow rate was unchanged.

In addition to the increase in anti-icing flow to the IPS flow splitter and IPS scavenge area, other IPS casing assembly changes were also implemented. The anti-icing flow circuit on the outer flow path was extended forward, as shown in Figure 16. This change addressed the outer shroud ice formation problem encountered in the icing test. The anti-ice holes in the scavenge vanes were modified to provide more uniform heat transfer to the vane surface. As planned near the end of the PFR phase, the vane material was changed from steel to aluminum to reduce weight. This increased the heat transfer characteristics of the vanes.

The anti-icing valve was redesigned to provide the anti-ice flow rate changes determined from the preliminary icing test. As part of the initial development test the anti-ice flowrates were controlled with an external valve to provide variability not available in the engine valve. This flow data defined the design flow rates for the QT anti-icing valve.

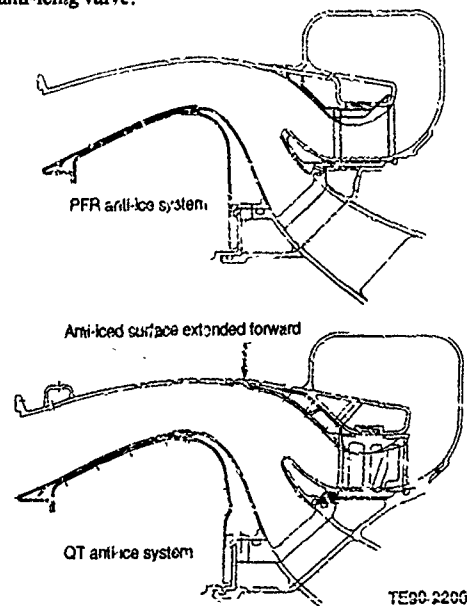


Figure 16. IPS outer flow path anti-icing design change.

The modifications made to the engine anti-icing circuit addressed all of the concerns resulting from the thermal survey and icing test. These changes did not impose major setbacks to engine hardware fabrication schedules because they were coordinated with hardware changes which enhanced the other features of the engine (reliability, cost, weight, producibility). The modifications, made on the basis of the development data, provided a high degree of assurance that the effectiveness of the anti-icing system would be increased to a level that both the Military and the FAA certification tests could be successfully completed, including the extended exposure requirement of the FAA.

VALIDATION OF REDESIGN BY THERMAL SURVEY TEST

The QT anti-icing system will be validated with hardware flow tests and a second thermal survey of the protected surfaces, scheduled to be performed in 1990.

The anti-icing circuits of the redesigned inner dome, front frame, and IPS casing assembly, and anti-icing valve will be flowed to verify design flow capacity. The parts will then be instrumented to allow anti-icing air temperature and flow path surface temperature measurement during engine calibrations, which will be run with variable inlet temperatures.

Instrumentation during the thermal survey test will be very similar to that used during the PFR development phase thermal test, except for slight changes to thermocouple location based on experience and design differences. Figure 17 illustrates the location of the instrumentation. As before, the thermocouple sensing tips will be imbedded in the surface to provide a true surface temperature indication unaffected by convection. The size of the thermocouple wire used during this test will be minimized

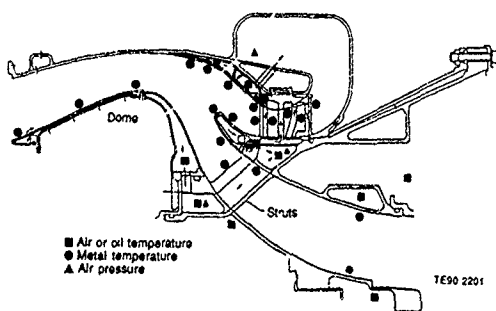


Figure 17. QT thermal survey instrumentation.

to virtually eliminate any blockage since the leads will be routed through some of the anti-icing flow passages. In order to allow access, the thermocouples located on the IPS scavenge vanes are installed during the basic IPS casing fabrication process.

Thermocouples will also be located near the shroud of the IPS scavenge vanes. The purpose of this instrumentation is to ensure that the epoxy used during the IPS casing manufacturing process remains below the allowable temperature limit during the hot day anti-ice failed condition.

The engine will be operated throughout the power range with dry air (no icing cloud) at each of the following conditions; 59°F (15°C), 40°F (4.4°C), -4°F (-20°C), and 131°F (55°C). Each of these conditions will be run with and without anti-ice actuated and with customer bleed extraction. The source of the customer bleed air, like the anti-ice air source, is compressor interstage. Bleed extraction provides a more challenging condition for anti-icing system operation, due to the increase in temperature and pressure loss occurring when a higher flow rate is delivered.

Following the completion of the dry air runs, the 40°F (4.4°C) inlet temperature run will be repeated while simulating an icing cloud at the engine inlet. The 40°F (4.4°C) inlet temperature was chosen to eliminate the complex test equipment provisions required to prevent ice formation in water supply lines and the spray nozzles that would occur with below freezing inlet temperatures.

The purpose of this water injection test is to provide data so the heat transfer analysis model can be further enhanced, and then extrapolated, to provide confidence in actual icing conditions. Slight variations between the PFR thermal survey test results and the PFR preliminary icing test results occurred because the location of the icing cloud water droplets on engine flow-path surfaces could not be accurately predicted. The water significantly affects the heat transfer characteristics of the surface, therefore determining its location and quantity becomes a critical part of the analysis. Predicting the location of the water droplets is challenging due to the complex engine airflow and aerodynamic separation.

Surface temperature variations between the dry air run and the simulated icing cloud run will provide the temperature data required to accurately predict the location and quantity of the water droplets on flow-path surfaces. Following this, the heat transfer model can be used with a high level of confidence to predict surface temperatures during icing condition operation.

The thermal survey test is intended to provide data so that the heat transfer model can be enhanced. Ultimately, the thermal survey testing will provide a high level of

confidence that the anti-icing system can provide acceptable engine icing protection throughout the icing envelope prior to running the final environmental icing test.

FINAL ENVIRONMENTAL ICING TEST

The QT environmental icing test will take place late in 1990 at the Naval Air Propulsion Center (NAPC) in Trenton, New Jersey. The test will be identical to the icing test performed in the PFR phase except the test article will be configured as an engine instead of a gas generator.

NAPC has performed several icing tests on various engines, including the Allison T406. NAPC's facility, equipment availability, and experienced personnel made their test site very attractive. LHTEC has the capabilities to perform the test but the cost associated with a one time setup were not an acceptable option to the NAPC test site.

The preliminary work completed on the engine's anti-icing system provides LHTEC with confidence that the engine will successfully complete the icing test. It is planned that the testing completed at NAPC will be approved by the U.S. Army as completion of the required demonstration of the anti-icing system. LHTEC will also build on the test program to include additional test points that will satisfy the FAA requirements.

SUMMARY

The T800-LHT-800 engine anti-icing requirements imposed a design challenge due to the presence of an integral inlet particle separator (IPS). Characteristically, inlet particle separator systems expose a large areas to

incoming area and provide potential for ice accretion. This challenge was met by designing and developing an anti-icing system that exceeds all military and FAA requirements.

The anti-icing system design evolved from the initial concept to the final configuration through the use of analytical tools, a thermal survey test, and an environmental icing test. It has undergone three design iterations, which were integrated with other modifications as the engine matured, so as to reduce schedule and cost impact. The system utilizes compressor interstage air as the energy source and delivers the air through a dual bypass arrangement. The airflow rate is regulated by a self modulating valve to prevent excess air delivery at higher engine powers and thereby minimize performance loss associated with the use of the anti-icing system.

Effectiveness of the system has been repeatedly demonstrated with analytical and actual test results during various test programs. Final verification of the system will result from a second thermal survey. Military and FAA flight certification of the system will be obtained through a final environmental icing acceptance test at the Naval Air Propulsion Center in Trenton, New Jersey, scheduled to be performed late in 1990.

The anti-icing system is effective, meeting all requirements. It is light weight, low cost, reliable, easily maintained, and provides the pilot with engine icing protection by activation of a single switch. The anti-icing system development, as well as the T800 engine development, represents many thousands of hours of dedicated work from LHTEC personnel to providing a state-of-the-art helicopter engine that meets or exceeds all requirements and design goals.

Discussion

1. R. Wibbelsman, GE

Have you checked the surge margin under the conditions of anti-icing or STD inlet temperature?

Author:

The engine surge margin has been completely characterized under all operating conditions, including operation with anti-ice on.

2. R. Toogood, Pratt and Whitney Canada

What is the IPS bypass/core airflow ratio?

Have you determined that the change from steel to aluminium for the IPS turbo shafts will maintain adequate erosion capability?

Did you consider an IPS design, which did not include turning vanes in the scavenge duct?

Author:

The IPS scavenge flow is in excess of 20% of the engine inlet flow.

We have run the IPS with aluminium scavenge vanes on the sand ingestion rig to evaluate erosion of the aluminium. The result of this test showed no significant erosion.

To the best of knowledge, a design without turning vanes was not considered.

3. A. Spirkel, MTU

How much anti-icing air flow is used at high power ratings?

Author:

Approximately 2.5 % of the engine core flow is the quantity of anti-icing air used at idle, about half of this amount at maximum power.

4. W. Alwang, Pratt and Whitney

Did the laser probe measure both particle size distribution and density distribution?

Was it a commercially available probe?

Author:

Yes, the laser probes measured both particle size distribution and density distribution. The probes used were called a Fowaro scattering spectrometer probe (FSSP) and an optical array probe (OAP). These probes are commercially available.

5. D. Mann, Rolls Royce

Have you made any separation efficiency measurements on water droplets?

How important do you believe is the water/ice separation efficiency to the configuration of the anti-icing system?

Author:

We have not made water droplet separation efficiency measurements.

I believe that water separation efficiency is very critical to the anti-icing system. I do not think that increased water separation efficiency is critical to anti-icing system design, but rather, identifying the location of the water droplets is the critical aspect relating to anti-icing design.

6. W. Rearson, Naval Air Propulsion Center

Besides PFR icing, the engine was configured as a gas generator. How was the performance deterioration determined in this configuration?

Author:

Prior to the removal of the power turbine (configuration of gas generator) the engine performance was characterized. Power turbine inlet total pressure and inlet temperature was measured during this. When the engine was run as a gas generator, the power turbine inlet pressure measurement and power turbine inlet temperature measurement were used to compare the complete engine data. Therefore, gas generator performance loss was determined by analyzing and comparing the gas generator and complete engine performance data.

ENGINE ICING CRITICALITY ASSESSMENT

by
E. Brook
Rolls-Royce plc
PO Box 31
Derby DE2 8BJ
United Kingdom

SUMMARY

Assessment of an engine design for icing risk is important at both the design stage and for development and certification testing. Icing must be included with aerodynamic and noise constraints during the design phase to minimise the risk of design change during development, and the compromise tested must be tested at the extremes of the atmospheric icing, and aircraft and engine operating envelopes most appropriate to the particular components. This paper addresses the type of assessment necessary illustrated mainly by reference to high bypass ratio turbofans.

The approach to identifying critical conditions is presented and areas where research can provide basic data for the development of design methods are discussed.

1. INTRODUCTION

In evolutionary engine design where relatively small changes distinguish engine types, it is easy to ignore icing as a design constraint and accept that the modest changes will not cause problems when tested in icing conditions for certification, or in service. However, icing constraints are often directly opposed to other design considerations, such as noise, and anti-icing use is a performance penalty. It is therefore necessary to review modifications for effects on icing at an early stage, most of this review being by comparison with existing satisfactory designs.

Revolutionary designs lead to a requirement for more analytical techniques. These must combine experience from past engine testing with research for basic data acquisition to establish methods that may allow extrapolation beyond the range of existing designs.

Assessment of engine designs at an early stage can also identify evidence to be obtained during development testing to validate analyses.

At a later stage in the engine development process, the engine must be assessed against the Certifying Authorities' requirements to determine the details of the icing testing for engine certification.

2. BASIS FOR ASSESSMENT

The assessment must bring together the details of the engine design, the aircraft flight envelope and engine operating envelope with the atmospheric icing envelopes defined by the Certifying Authorities.

The design must then be assessed to identify areas of concern for production of

unacceptable performance loss or engine damage. The assessment can be carried out by breaking down the engine into areas according to type of risk. Figure 1 illustrates the areas of concern on a high bypass ratio turbofan. Each area is considered in detail in the following sections.

3. NON-ROTATING COMPONENTS UPSTREAM OF THE FIRST ROTOR3.1 Intakes

The engine intake is often treated as part of the aircraft rather than the engine. Aerodynamic considerations determine the shape, but anti-icing considerations are one of the factors affecting structure and materials. Much data is already available and analytical techniques are used routinely, confirmed by testing on the aircraft. I do not propose to cover intake anti-icing design in this paper, however, ice shedding following delayed selection of nose cowl anti-icing, or caused by incomplete anti-icing, can directly affect the design of the first rotor stage due to potential damage. Therefore, collection of ice and size of ice shed is an engine design consideration that must be considered, along with other debris ingestion questions, when designing compressor blading.

3.2 Intake Ducting

For the modern pod mounted high bypass ratio engine, intake ducting is minimal and offers no surfaces for collection of ice. However, this is not true for all, and shaped inlet ducting (Fig. 2) such as used on turboprops and on some tail mounted engines, or where inlet particle separators are used to prevent grit and debris entering the engine can offer surfaces on which ice collection is likely.

Prediction of requirements for anti-icing and identification of areas of concern requires detailed flow prediction programmes for three-dimensional flow more complex than those necessary for intake lip anti-icing design.

Heated surfaces within a shaped intake must be assessed against propensity to accumulate ice in ice crystal conditions where surface temperature and local airflow velocity are directly relevant. Consideration must also be given to drainage to prevent ice forming whilst the aircraft is parked that could be sucked into the engine on start-up.

3.3 Instrumentation

Pressure and temperature probes for engine control or for measurement of thrust mounted in the engine intake are normally continuously anti-iced on modern engines. The adequacy of this anti-icing needs to be

addressed on the engine as local flow effects can produce areas of enriched water content within the intake, although detailed testing of the isolated probe in icing conditions will have been carried out by the supplier. Prediction of water droplet behaviour around the intake lip can be used to assess the acceptability of the probe immersion.

Modern temperature and pressure probes are usually electrically anti-iced to minimise their performance penalty. For these the critical icing conditions are likely to be maximum engine power conditions at minimum altitude and either at minimum temperatures, if heat removal is dominated by the airflow, or at about 0°C total inlet temperature, where water input is maximum due to the nature of the atmospheric icing envelopes, if heat removal is dominated by the requirement to evaporate the supercooled water droplets caught by the probe surfaces.

On some older engines hot air anti-iced probes are used and critical conditions then depend on the hot air supply.

The design of the probe anti-icing system should be such as to prevent any ice forming on the probe either by heating the whole probe body, or by providing full evaporation of all water caught by the probe on the critical areas. Probe designs that are not fully anti-iced must be assessed against the damage that could be caused by shedding of the maximum size of ice particle.

3.4 Inlet Guide Vanes and Nose Cones

Figure 3 illustrates an engine with non-rotating engine hardware immediately upstream of the first rotor stage. This type of hardware must be anti-iced, and because of the danger of damage caused by ice shedding and the distortion caused by blockage the inlet guide vanes at least should be continuously anti-iced. Critical conditions will depend on the type of anti-icing used, whether it is independent of engine power, like electrical heating, or dependent such as the use of engine oil or hot air.

4. THE FIRST ROTOR STAGE

All surfaces ahead of the first rotor stage are potential sources of ice debris that could damage the aerofoils or casing linings of the first, and subsequent, rotating stages. This type of damage can be minimised by appropriate application of anti-icing or de-icing, i.e. prevention of ice accumulation or removal of ice before an unacceptable quantity has accumulated. Once into the rotating stages it becomes virtually impossible to provide anti-icing and it is, therefore, necessary to appraise the design for its propensity to accumulate ice and the likely consequences of the accumulation. It is then necessary to determine how this ice will shed and consider the design of the surfaces against which it will impact.

4.1 The Nose Cone

There is one further part that it may be possible, and desirable to anti-ice at

least partly, the rotating nose cone or spinner. With no anti-icing ice must accumulate on this and the low centrifugal forces acting close to the engine centre-line may allow an excessive accumulation before melting or out-of-balance forces cause shedding.

There are two approaches to nose cone design; either accept the shape determined by compressor intake flow design and design an anti-icing system adequate to prevent ice build-up, or determine the shape of nose cone that minimises ice build-up and ensure that this is established as the basis for design. Departures from this ideal design, which may still not require any deliberate anti-icing, can then be assessed provided data on ice catch and ice shedding is available, similar to that used on fan blades discussed in Section 4.2.

If the methods to assess the design are not available, specific testing of a new design may be necessary once criteria for acceptability, e.g., maximum ice build-up in weight or thickness, have been established. As a last resort, engine testing in icing conditions will establish the acceptability of a particular design, at a cost.

The critical conditions for ice build-up on a spinner are likely to be extended exposure at minimum temperature conditions such as occur during hold as this produces the strongest ice bonding, and is therefore likely to accumulate more ice than higher liquid water contents at higher temperatures which will shed earlier.

For aircraft that normally cruise at lower altitudes, within the continuous maximum icing envelopes, higher engine powers may give rise to a worse situation due to the higher energy imparted to the shed ice.

A further aspect to be considered in spinner designs is the possibility of asymmetric ice accumulation. Uneven gaps around fairings can give rise to ice accumulations sufficient to give unacceptable out-of-balance and, hence, engine vibration. Spinner drainage must also be addressed for the same reasons.

4.2 The Fan

Ice cannot be prevented from accumulating on the fan blades, the first rotating stage in a high bypass ratio engine. Assessment of an engine design, therefore, reduces to prediction of the quantity of ice that will accumulate before shedding, how this ice will shed, where the ice debris will go and how to prevent this ice debris causing damage.

Current fan designs are unlikely to suffer from unacceptable performance loss due to flow passage blockage by ice, but it cannot be ignored for revolutionary designs if blade spacing is significantly reduced, especially at the blade root where distortion generated would directly affect the core engine.

Ice accumulation on fan blades is a function of the fan blade relative air temperatures. This leads to a maximum radius above which ice cannot adhere for a

given set of ambient conditions and rotational speed, and a gradation in ice bond strength to the blade surface decreasing as radius increases.

This bond strength is an important parameter if analysis techniques are to be established to predict ice shedding from fan blades, and also nose cones or any other surface.

The energy of the ice debris can then be considered for design of the fan track liner and casing panels downstream, and prediction of worst case scenarios for engine icing testing for certification. For example, is the maximum accumulation of ice occurring during extended exposure at low power conditions likely to produce more damage than the limited accumulation at high power conditions where much of the fan blade will be ice free? For the low power condition ice shedding during engine acceleration must also be considered.

In most current high bypass ratio engine designs it is not possible for ice shed from the fan blades to enter the core engine. Reduction in fan blade trailing edge to core engine inlet spacing may permit ice to shed into the core engine. This could cause core engine damage, or power loss due to compressor surge or flame-out. Methods to predict ice trajectory once released from the blade surface are, therefore, necessary for design assessment.

5. ENGINE COMPONENTS DOWNSTREAM OF THE FIRST ROTOR STAGE

The assessment of the components downstream of the first rotor stage in icing conditions is fundamentally different from components considered in Sections 3 and 4 as the temperature and pressure rise through the first, and subsequent, compressor stage alters the envelope of icing conditions. Engine power becomes a major factor in the exposure of components to icing. At high engine powers in flight ambient conditions with supercooled water droplets present may never exist combined with temperatures downstream of the first rotor stage at which ice can accumulate.

Ice catch on the fan blades and nose cone is also an important parameter in predicting the liquid water contents in the airflow that must be considered. Therefore, it is not usually necessary to anti-ice components downstream of the first rotor stage, and it is often impossible to provide anti-icing on the aerodynamically determined components due to their size or the problems of supply of hot air or electrical power.

However, there are a number of areas of particular concern that should be considered at the design phase and addressed during engine certification icing testing.

5.1 Engine Section Stators

The engine section stators are the first set of components within the core engine. Ice accumulation on these can cause core engine inlet blockage, leading to distortion and compressor surge. Shedding

of excessive quantities of ice can cause surge or flame-out as well as damage to rotor and stator blades or rotor path liners.

Methods to predict ice accumulation and shedding from stator vane sets based on ice catch and bond strength data may be possible, although prediction of the aerodynamic forces responsible for shedding, given the highly three-dimensional form of the flow, especially after ice has started to accumulate and is causing local blockage dependent on ice shape, is extremely difficult. It is also necessary to consider the interaction between ice on adjacent vanes as ice structures bridging between vanes are strong and do not rely on bond strength to the individual vanes to prevent shedding, but require a failure within the ice structure.

Stator vane spacings that permit ice to bridge between vanes, given the icing conditions that actually occur within the engine, and realistic exposure times are unlikely to be acceptable due to blockage, and hence compressor inlet distortion.

Empirical data is needed to permit assessment of the propensity for unacceptable ice accumulation on stator vane sets as a function of vane spacing, stagger angle and temperature, as reduced spacings are often favoured for noise reduction reasons.

Temperature is an important parameter as the ice form and quantity is dependent on the temperature of formation. Icing conditions giving worst blockage need to be identified for certification testing. Highest air temperatures give the least aerodynamic ice forms, but also the weakest ice a compromise temperature must, therefore, be identified.

Ice catch on surfaces is also important in identifying realistic airflow water contents to be considered once the fan blades have removed a proportion of the atmospheric liquid water content.

5.2 Fan Bypass Stream Outlet Guide Vanes

Ice accumulation on fan outlet guide vanes follows the same basic rules as that on engine section stators but is usually less critical as spacings are usually wider and there are no components downstream that can be affected by either the blockage generated distortion or the ice that is shed. However, excessive blockage can give rise to pressure loss through the outlet guide vanes or loss in aerodynamic efficiency leading to excessive swirl in the bypass stream airflow, giving reduced engine thrust if not compensated for by the engine control system.

An assessment of the envelope of engine thrust, aircraft operating conditions and atmospheric conditions in which icing can occur downstream of the first rotor stage is, therefore, important.

5.3 Intercompressor Ducting

Intercompressor ducting usually has a very limited envelope when icing may occur depending on the number of stages in the

upstream compressors. For ducting with major changes in direction of flow, such as high radius ratio swan-necked ducts, consideration must be given to accumulation of ice during encounters with ice crystals, which can occur at much lower ambient temperatures than supercooled water droplets. The effect of local duct surface temperatures due to passage of engine services such as oil pipes must be considered as this can give rise to surfaces heated to the correct temperatures for ice crystals to melt initially and provide adhesion to the surface if aerodynamic forces are not sufficient to prevent it.

Experimental data on ice crystal accumulation as a function of surface temperature and local velocity is necessary for detailed prediction.

5.4 Depth of Penetration of Icing

Assessment of the depth into the core engine that icing conditions can occur at all normal operating conditions, needs to be carried out. Although the liquid water content is reduced at each stage by ice accumulation, icing penetration into high pressure compressor stages where spacings and vane sizes become smaller must at least be considered and, if outside the range of current experience, development testing should be recommended to reduce the risk of failure during identified worst case conditions tested during certification icing tests.

Consideration of icing of bleed ports is also necessary if blockage could cause compressor surge.

5.5 Instrumentation

Core engine instrumentation must also be considered relative to depth of penetration of icing. Blockage of pressure probes or incorrect reading of thermocouples due to ice can affect engine control such as bleed valve and variable guide vane operation.

Instrumentation most likely to be affected by icing is that in the bypass duct. Pressure rakes used to determine engine thrust should be anti-iced if it is necessary to guarantee their proper operation in all icing conditions. Where engine pressure ratio is used as the major control parameter for the engine it is preferable to avoid danger of inaccuracy in icing conditions by using hot stream rakes only.

For instrumentation icing and maximum depth of penetration the critical engine conditions will be minimum power, when compressor temperature rises are minimum, combined with minimum flight speed.

6. CONCLUSIONS

For both assessment of engine design to reduce risk and for identification of conditions that should be addressed during certification testing in icing conditions the engine and intake design must be considered in stages according to the parameters affecting icing, and the following question answered:

- o How much ice will accumulate during an icing encounter?
- o What effect will the accumulation have on the component and those downstream of it?
- o How will the ice be removed?
- o Where will the ice go once it is removed and what subsequent effect can this debris have?

Collection of data of either fundamental ice properties, such as ice bond strengths, or component specific data, such as ice catch on surfaces and stator vane passage blockage, are important to permit these questions to be answered.

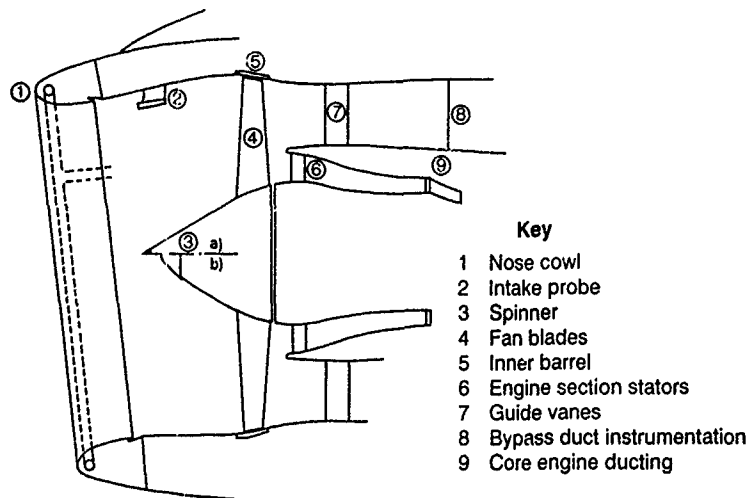


Figure 1. Engine and nacelle icing considerations

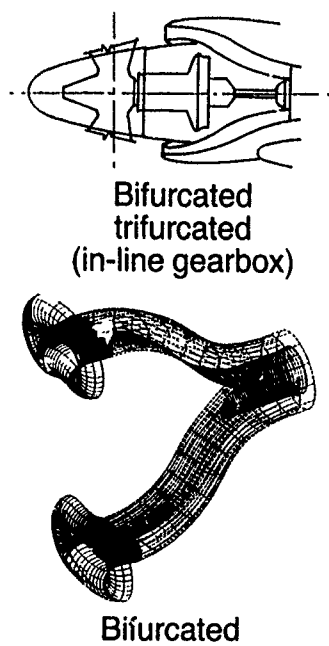


Figure 2. Example of convoluted
intake duct

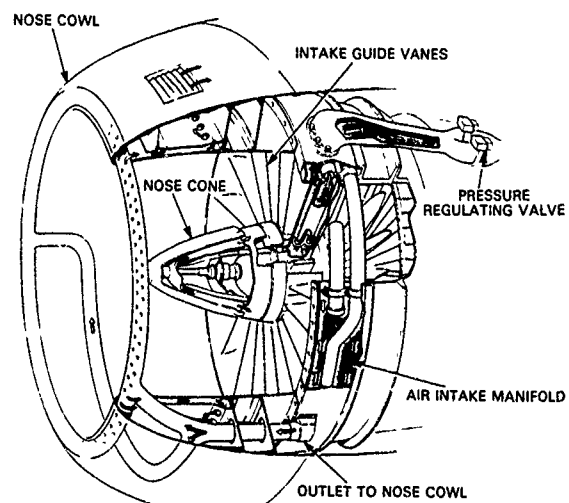


Figure 3. Anti-iced inlet guide vanes and nose cone

Discussion

1. M. Holmes, RAE

To what extent are altitude test facilities used by Rolls Royce for icing qualification tests compared with flight tests behind an aircraft carrying water droplet spray equipment?

Author:

RR use altitude test facilities for engine icing tests extensively and consider an altitude test facility the best way of performing engine icing tests. Aircraft icing tests are only contemplated where problems occur during flight testing or where the certifying authorities of the airframe constructor insist. However, in the future, the limited size of the altitude test facilities available may force a change as engine size increases.

2. W. Grabe, NRC Ottawa

Have you estimated energy requirements for anti-or de-icing the Contrafan nacelle lip on account of its larger diameter? Suggested is not to reject the cyclic de-icing which is done now quite successfully, providing accretions are not allowed to grow too large?

Author:

Engines like the contrafan, which has both a large diameter fan cowl and a gas generator cowl ahead of the aft mounted fan, plus struts and inlet guide vanes which require protection from icing, puts a demand on core compressor blade flow for full anti-icing which is unacceptable. I do not know the exact numbers but they are such that the bleed demand would give an unacceptable effect on gas generator operation. The same applies to many of the designs currently being proposed for ultra-high bypass ratio engines, and alternatively anti-or de-icing of engine inlets must be considered, such as electro-impulse de-icing. However, any de-icing method gives an additional problem in that the engine must then be proved to be capable of accepting the regular inputs of the ice debris generated. This should not be an insuperable problem but it increases the erosion problems already generated by rain and hail.

3. A. Sutton, BAe

What amount of blockage have you found with ice accretion on the fan blades?

Author:

We have not measured the ice blockage on the fan blades

except indirectly through the change in the engine as the ice accumulates. It should be noted that no loss in thrust occurs as the ice accumulates since the engine is usually controlled to an overall pressure ratio which means a direct measurement of engine thrust.

4. D. Way, RAE

Which of the icing problems that you have described is most troublesome, in the sense that it is least amenable to protection or experimental model testing early in the engine development programme?

Author:

The worst problem recently has been icing of engine section stators. Engine section stator designs have been giving reduced gaps and increased blade numbers for noise reasons, and ice building on these can lead to problems due to the pressure loss through the blockage, or flow distortion, or ice shedding into the core. This can produce compressor stall or surge and combustion extinction. Without testing of the full engine the interaction between core inlet icing and the operation of the core compressor is very difficult to predict, especially as problems are likely to occur at descent idle powers.

If problems occur during engine testing the only solution is to apply some restrictions on engine operation in icing conditions which is undesirable.

5. M. Holmes, RAE

You suggested that your icing assessment and prediction methods were aimed at minimizing or even eliminating the need for expensive testing. Do you believe you will ever reach that goal, and what evidence have you obtained so far which gives you (and the airworthiness authorities) such confidence?

Author:

The assessment and prediction methods have arrived at eliminating expensive testing, but they have also arrived at ensuring that the testing carried out is the most effective one. Having identified areas of risk relative to operation in icing this is accepted by the airworthiness authorities already as evidence in adjusting test conditions or eliminating test requirements. The evidence of the success of the approach is in the excellent operation record of Rolls Royce engines in service both in term of safety and in-service behaviour with icing.

ICE INGESTION EXPERIENCE ON A SMALL TURBOPROP ENGINE

L.W. Blair, R.L. Miller, D.J. Tapparo
General Electric Aircraft Engines
1000 Western Avenue, Lynn, Massachusetts 01910

Introduction

Premise

Modern high technology turbine aircraft engines often employ high rotor speed compressors with thin advanced blading designs to achieve better performance. The engine designer is faced with a tradeoff between optimum compressor performance and on-wing durability. During the engine/aircraft development stage, certain assumptions are made regarding the icing environment and the testing required to confirm compatibility with it. Often the true impact of the design trade-off is not realized until the engine is exposed to its service environment.

Despite successful engine test cell and aircraft natural icing certification tests, in 1984 General Electric Aircraft Engines Company began to experience an unacceptable level of foreign object damage (FOD) caused by ingested ice with its CT7-5/-7 family of turboprop engines.

Purpose

The purpose of this paper is:

- (1) to address the issue of Stage 1 compressor rotor blade ice FOD in the CT7 engine,
- (2) to explain the methods and techniques used in assessing the icing environment,
- (3) to explain the lessons learned from test and analysis, and
- (4) to define the final resolution of the compressor maintenance problem which simultaneously created accelerated performance deterioration for the engine.

The paper is divided into two parts, the first dealing with the airframe icing environment and its impact on the engine inlet system, and the second concentrating on the design improvement and durability testing of the Stage 1 compressor blade.

PART I

Basic Engine Design

The CT7 turboprop engine is a free-turbine modular design derivative of the T700 turboshaft engine. It employs a five-stage variable stator axial and single stage centrifugal compressor with a combined pressure ratio of 18:1.

The compressor operates behind an integral inertial particle separator (IPS). The separator system, shown in Figures I-1A and I-1B, is integrated into the power unit oil cooling system and provides airflow to cool the electronic engine control. Originally designed as a sand separator for the military helicopter environment, the system incorpo-

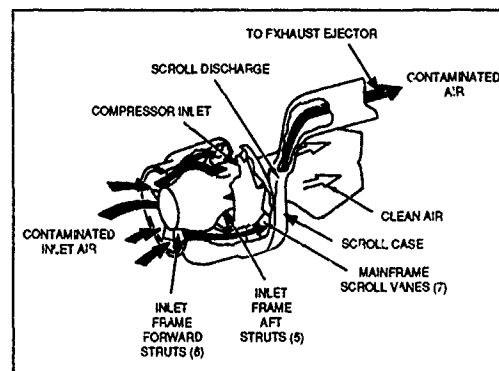


Figure I-1A Engine Inlet Flow Diagram

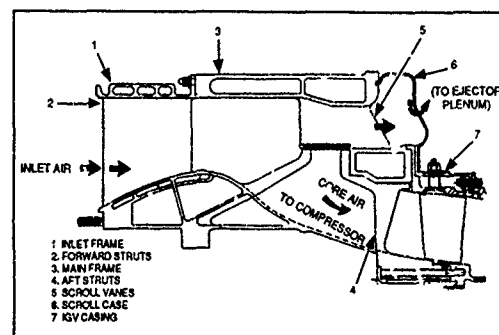


Figure I-1B Inlet Frame, Mainframe, IGV Casing Assembly

rated swirl and deswirl vanes to optimize efficiency. It has since been changed from a swirl concept to a straight axial bypass to reduce pressure loss and improve performance.

Inlet and Installed Icing Environment

The airframe-provided inlet design is a conventional S-duct with a throat area optimized to aircraft specifications. An inlet protection device (IPD) is incorporated to meet bird ingestion certification requirements.

Responsibility for inlet aerodynamics was assumed by the engine manufacturer. The airframer assumed responsibility for the mechanical design, structural integrity, anti-icing, test and procurement.

Other areas forward of the engine, which are subject to the icing environment are shown in Figure I-2. Propeller spinners on both applications are parabolic profile and unheated (neither anti-iced nor de-iced). Original ice-shed trajectory analyses showed no ingestion into either inlet design. Later analytical refinements reversed this finding for accumulations on the spinner nose. The two propellers used, were each 4-bladed with de-icing provided in alternating pairs. Propeller cuffs have been observed to accrete ice which was not shed with blade de-icing. In the upper inlet highlight-to-spinner boundary layer diverter area, one inlet, which is integral with the forward nacelle cowl, incorporates anti-icing. The other inlet, which moves relative to the forward nacelle cowl, is not anti-iced in this area. Both diverters have been observed to accrete ice.

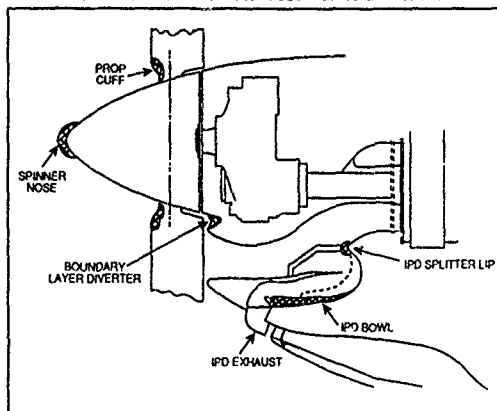


Figure I-2 Installation Ice Accretion

Certification Testing

The CT7 turboprop was successfully certified according to the requirements of FAR 33.67, FAR 25 Appendix C, and Advisory Circular 20-73 in January of 1983, at the General Electric Test Facility, Evendale, Ohio. Test conditions are shown in Table I-1. The Evendale facility is a sea level test cell capable of providing a controlled icing cloud from a free jet pipe 30 inches in diameter at a maximum velocity of 88 knots. Testing was conducted using an anti-iced bellmouth. No installation specific inlet testing was required or performed. During all phases of testing, engine surfaces remained ice-free and no discernible ice ingestion, causing either Stage 1 blade damage or parameter fluctuation, occurred.

Inlet ducts for both installations were certified at the inlet manufacturer's facility. This facility is a closed tunnel capable of simulating airspeed up to 195 knots and full Appendix C icing conditions to -30° C. No engine hardware was included in this testing.

ENGINE ICING CERTIFICATION TEST CONDITIONS (REF AC 20-73)

ENVIRONMENTAL ICING TEST CONDITIONS			
Condition Number	1	2	3
Atmospheric Temperature °F	29	23	-4
Liquid Water Content (minimum), gram/meter ³	0.3	2.0	1.0
Mean Effective Drop Diameter, microns	40	25	15
Icing Condition Power Settings	Ground Idle	Flight Idle 50% Max Cont 75% Max Cont Takeoff	Flight Idle 50% Max Cont 75% Max Cont Takeoff
Duration at each of the power settings specified above, (minutes)	30	10	10

Table I-1

Inlet testing indicated fairly good results, however, the duct was not ice-free, as required by the engine manufacturer. Accretions up to 50 grams on the inlet to IPD splitter were noted. Testing was conducted under the conditions shown in Table I-2. Since both inlet and installation were subjected to significant natural icing certification flight tests, and not a single ice FOD event was observed, the CT7 entered revenue service in 1984. By the end of that year however, the ice FOD rate was 1.2/1000 EFH and considered unacceptable.

CONDITION	AIRSPEED (KTS)	TAMB (°C)	LIQUID WATER CONTENT (g/m ³)		DROP DIA (MICRONS)
			MAX CONTINUOUS	INTERMITTENT	
1.	195	-10	0.6	2.2	20
2.	195	-20	0.3	1.7	20

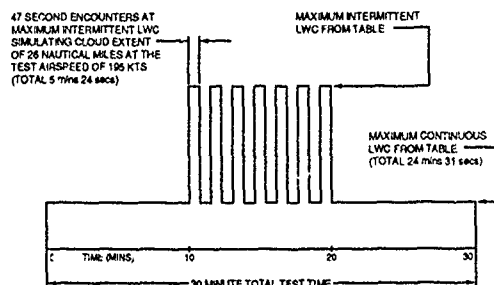


Table I-2 Flight Icing Encounter Pattern for Test Conditions 1 & 2

Engine Inlet System Development

Follow-on Icing Tests

From 1984 to 1988, six additional inlet tests and two engine tests were conducted to troubleshoot actual or suspected anomalies that might have caused ice FOD. Several of these tests were conducted on the initial prototype design. Later tests on production ducts revealed additional problems that required further optimization and proof tests.

Inlet component tests were run at the GE Evendale facility late in 1984 in an attempt to find a correlation between the engine certification testing conditions and those for the inlet at the inlet manufacturer's facility.

Because the GE open facility has limited viewing of the test specimen, a technique was developed to allow real-time remote viewing and recording through the inlet duct wall during the icing test. This technique proved useful in subsequent tests for viewing both of the IPD and engine face areas (See Figures I-3A and I-3B).

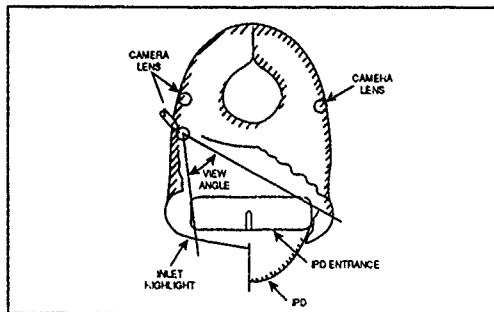


Figure I-3A

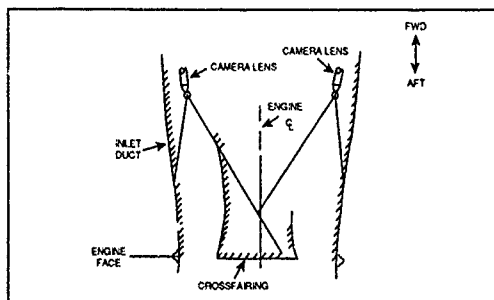


Figure I-3B

The icing was still apparent and a second test, paralleling the Evendale engine test conditions, was conducted in January 1985 at the inlet manufacturer's facility. Improvements made as a result of that testing were proof tested there later that year.

Although the ice FOD rate seemed to be coming down as additional fleet hours were accumulated (See Figure I-4), operators, particularly in the wet and cold winter climates (Sweden, Switzerland and Midwest U.S.), were still experiencing engine performance loss, associated with compressor blade maintenance and causing some premature engine removals. In addition reports of increased maintenance being required to keep the IPD from filling up with ice prompted more testing.

Late in 1985, at GE's outdoor crosswind test facility in Peebles, Ohio, an inlet icing test was conducted using an entire SAAB 340 aircraft (See Figure I-5). The aircraft was tied down in front of a bank of 15 fans. These fans created an icing cloud that enveloped the entire propeller and spinner in the right-hand installation. However, the fans only provided 60 knots of ram airspeed. The underlying

intent of the test was to see if propeller effects had any impact on ice accretion within the duct. While no new inlet ice was found, ice accumulated on both spinner nose (700 g max) and prop blade cuffs (20-30 g). These new sources prompted new analysis and efforts, described later, to reduce these potential threats.

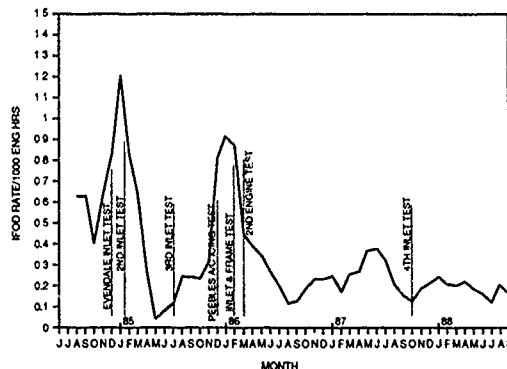


Figure I-4 Engine Ice FOD Rate 3 Month Rolling Average



Figure I-5 Outdoor Crosswind Test Facility

Ground tests in heavy blowing snow were conducted in Cincinnati, Ohio and Erie, Pennsylvania in the same time period. These tests consisted of 30 minutes at ground idle followed by accel-to-takeoff power. No ingestion events occurred. Upon shutdown of the engines, little or no ice was found in the IPD, yielding no correlation to the field reports.

It was clear that the missing ingredient was airspeed and it was the inlet manufacturer's facility that was capable of testing airspeed along with ice crystals (simulated snow) and slush-like environments. Because the engine inlet and separator frame has a large frontal area of low velocity, like the IPD, a combined inlet and engine frame test was proposed in February 1986. The inlet facility, however, was not capable of running a CT7 engine. As a result, the test rig consisted of the inlet duct, inlet and separator frames, and the engine accessory gearbox, fitted with starter generator and IPS scroll casing (See Figure I-6).

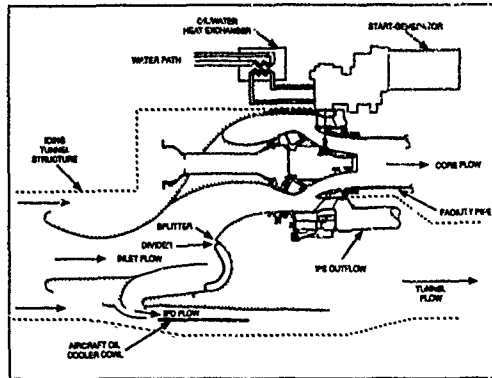


Figure I-6 Inlet/Frame Test Setup

Externally heated oil was supplied to the gear box and circulated by motoring on the starter generator. This provided engine frame anti-icing for those surfaces normally protected by oil temperature. Hot air was generated externally to anti-ice those engine surfaces which rely on bleed air. Skin temperatures obtained from a simultaneous engine anti-icing test at Evendale were maintained to simulate anti-iced engine heat rejection.

In addition to the ice crystal and mixed conditions, the standard test liquid water content (LWC) was factored up. This accounted for the additional water impingement created by the aircraft normal cruise speed of 260 knots vs the tunnel maximum speed of 195 knots. Three things were learned: (1) the engine frames did not ice or pack slush, (2) the IPD required additional flow-through ventilation to reduce packing of slush and aerodynamically assure that the slush would not enter the engine, and (3) the factored LWC put additional load on the inlet anti-icing system requiring further improvements. One of these improvements was a heated IPD exhaust chute.

During the above-mentioned second engine test at Evendale, this time with aircraft inlet installed, a single FOD event was observed. Using the inlet video cameras, the event was traced to ice build-up inside the inlet temperature sensor duct, from runback along the inlet frame. As the ice built up in the sensor duct, it gradually was sucked out by the compressor. A reworkable fix, demonstrated later in this test, was implemented immediately across the fleet and in production.

As duct improvements were gradually incorporated into the fleet the ice FOD rate stabilized at about 0.2/1000 EFH. This, however, was still an unacceptable performance and maintenance penalty for the small commercial operator. As a result, a target goal of .075/1000 EFH was established. While further inlet improvements continued to be addressed, the possibilities of ice FOD coming from additional sources, and measures needed to deal with these possibilities, were explored.

Other Approaches to Ice FOD Reduction

Turboprop spinner icing experience was reviewed and a conical spinner design was service evaluated in an effort to reduce accretions and thereby alter trajectories. There had been success in the past on turboprop applications for such designs; Figure I-7 depicts the turboprop test results upon which the turboprop service evaluation was based. The results of this survey yielded no improvement. Spinner coating experience was examined with no obvious benefit uncovered. A program to anti-ice the spinner nose was carefully reviewed, however, a shortfall of aircraft electrical power eventually ruled out such a program, as well as any potential for increased de-icing of propeller blades/cuffs.

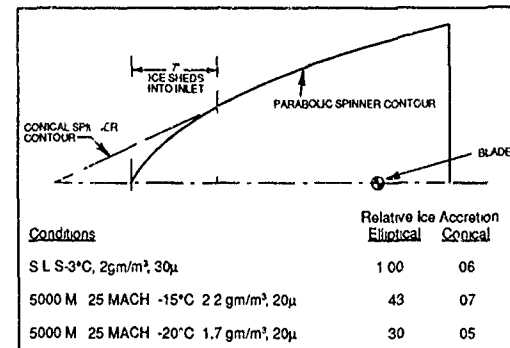


Figure I-7 Spinner Ice Elimination/Reduction

Simultaneous to these source reduction/elimination efforts, GE embarked on an extensive program to evaluate and improve the effectiveness of the engine separator system for target size pieces of ice. Trajectory analyses, using the standard axis-symmetric model of the separator, were conducted for varying degrees of adverse particle preconditioning imposed by the turboprop S-duct. Baseline cases were correlated with factory test results for 3 gram pieces of ice (.75 inch dia).

Several flowpath modifications were analyzed for efficiency improvement and the most promising was selected for model testing (See Figures I-8A through I-8D). Modified inlet and separator hardware model testing was conducted in the GE Lynn component facility, using separator scavenge flows confirmed from flight test measurements. The mixed test results (see Figure I-9) showed no consistent net improvement in ice protection. It was concluded that the range of inlet duct exit trajectories is too broad to achieve substantial IPS performance gains within the confines of a compatible installation. While gains may be realized for a given preconditioned trajectory, a comparable loss is likely for another trajectory of equal probability. While inlet separators are effective in minimizing the number of damaging objects reaching the compressor, they are at best statistical devices which cannot be 100 percent effective. When faced with a steady input of instantaneous damage-producing objects (as opposed to a time dependent

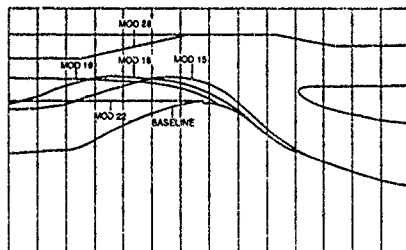


Figure I-8A

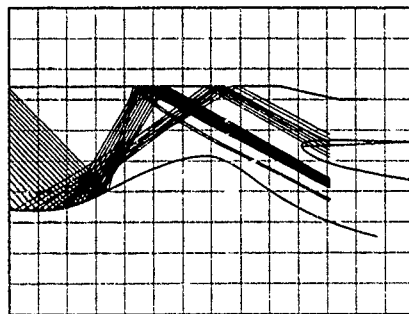


Figure I-8B

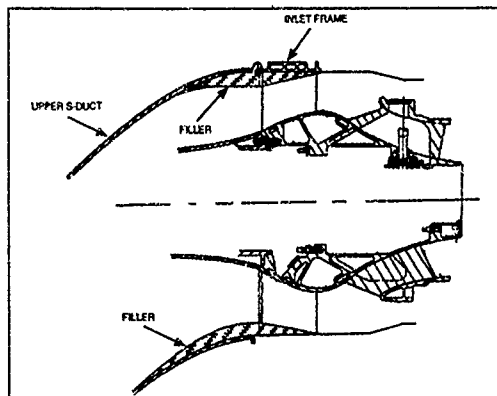


Figure I-8C

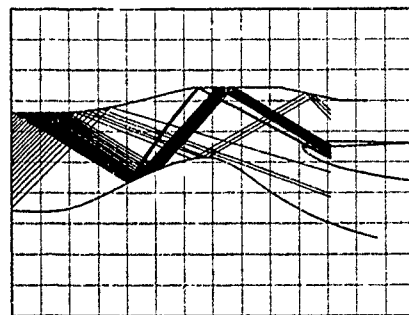


Figure I-8D

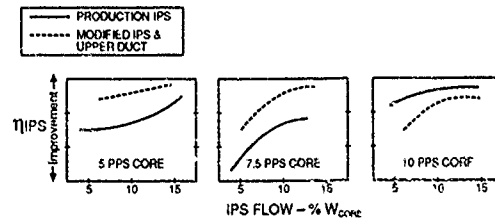


Figure I-9 Separation Efficiencies with Production Inlet

erosion process), separation efficiency improvements may be misleading. At this point, attention was turned to the Stage 1 compressor blades themselves.

Engine Inlet System Development Conclusions

- 1) To ensure a consistency in the application of icing test requirements, the aircraft inlet and engine should be tested together in the most severe environment available. This environment should include ice crystals and mixed conditions.
- 2) Successful operation in natural icing tests may not be sufficient to preclude in service icing problems.
- 3) Follow-up icing testing of the final Production inlet design is required to ensure proper implementation of prototype test results.
- 4) During the initial installation design phase, the complete inlet/propeller/spinner icing environment should be assessed as a system to ensure optimum distribution of anti-icing energy.

Part II

Ice FOD-Resistant Compressor Blade Development

Stage 1 Compressor Blade Clipping

Even with improved inlet ducts, the ice FOD rate requiring maintenance action for CT7-5 powered aircraft was about .20/1000 EFH; still beyond customer expectations. The FOD appeared as a curled stage 1 blade tip as shown in Figure II-1, and it caused an audible compressor whine and loss in engine temperature margin. The maintenance action required removal of an axial compressor casing half for access to the damaged stage 1 compressor blade(s); clipping the deformed blade material and a similar portion from an opposite blade to maintain rotor balance, and hand benching a leading edge on the clipped airfoils.



Figure II-1

This action eliminated the compressor whine but did not fully restore the engine's original performance level because the material removal adversely impacted compressor efficiency and airflow.

Test Set-up

A key part of developing a more rugged compressor blade was to determine the degree of the ice FOD which could result in Stage 1 blade damage. A rig was designed with a row of inlet guide vanes (IGV) ahead of the Stage 1 blisk driven by a high speed spindle at engine speeds (See Figure II-3). Due to the possibility of FOD wedging action between the blade and casing, a shroud over the blades was used to simulate the casing. A pneumatic gun was used to propel the FOD objects at various velocities up to 400 ft/sec (120 m/sec). The ice FOD tests however, were conducted at 85 - 90 ft/sec (27 m/sec), the highest possible velocities determined for ingested ice objects released during flight. It is possible that ice chunks impacting on the inlet S-duct could enter the compressor inlet at slower speeds, but the impact of these objects was considered less severe than the test simulation. The approximate ice velocity was calculated by equating the acceleration of a spherical ice mass to the drag of free stream flow using a drag coefficient of 0.55. Figure II-2 shows the calculated velocity at the Stage 1 blade as a function of ice ball size.

The ice objects used for the test were spherical in shape because the initial small right cylinders tumbled,

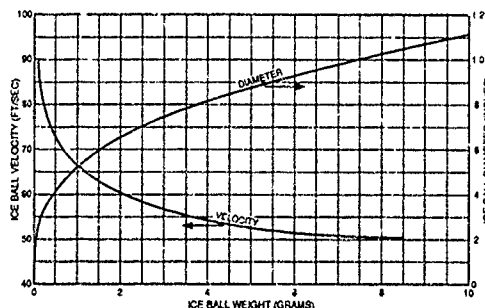


Figure II-2 Ice Ball Parameters at IGV Inlet

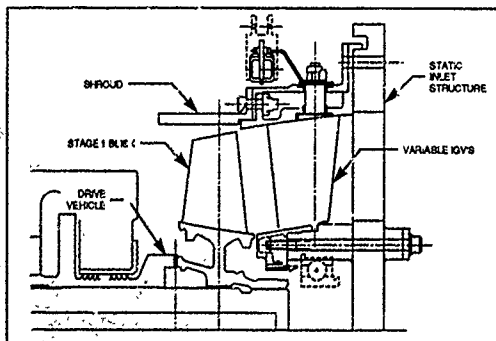


Figure II-3 Component Test Setup

causing erratic flight and inconsistent impact areas. The ice balls were targetted to pass cleanly between the IGV's and impact the blades as close as possible to the tip without contacting the shroud. A speed trap measured the object velocity just before entering the inlet casing. The largest ice chunk would be the circumferential space between the inlet guide vanes (about 1-inch at the casing) and would permit an 8 gram sphere to pass through when the vanes were fully open (i.e., axial at casing O.D.).

The test events were recorded with a high speed camera system at 22,000 frames/second. This provided insight on the impact phenomenon and verified the impact area of the objects. High speed video (2500 frames/second), which had the advantage of instant replay to monitor testing, was used to verify the impact area and ice velocity. The test speed was 42,000 RPM, a typical altitude cruise speed at which most ice FOD events occur.

Results

The initial blisk testing was done on a CT7-5 blade. It was found that a 2.8 gram ice object caused initial bending, and a 4.5 gram ice object caused a single event blade tip curl similar to field damage (See Figure II-1). Smaller chunks of ice (i.e. 3 grams) can cause a blade curl from successive hits. Successive hits occur on a particular blade because it is bent forward of the plane of the other blades. The testing also determined the vulnerability of a blade which is adjacent to a clipped blade. A clipped blade allows more ice penetration prior to impact by the adjacent blade. This causes full tip curls from smaller ice objects. This correlated with field observations where compressors with clipped blades had higher rates of maintenance action after the first clip. The high speed photography also revealed that a large ice object can impact and bend a blade on its initial hit and then, due to a heavier impact on the protruding blade, cause a full curl on the next revolution. Large ice chunks (5 to 8 grams) were also fired at the pitch sections causing minor bulging. This was not typical of observed field damage. Therefore, it was concluded that the damaging ice objects were traveling along the outer casing wall and impacting in the blade tip area.

A sample of operator ice FOD data was evaluated to determine the extent and frequency of the blade curls (See Figure II-4). The data included the bend radius, since it is the amount of material removed prior to benching a new leading edge radius. About 75% of the events required a clip of 0.3 inches along the blade tip chord and 0.8 inches down the leading edge.

It was judged that a cutback of .25 inches along the tip and .65 inches down the leading edge along with a reshape of the leading edge to improve the aerodynamics would eliminate most of the problem associated with tip curls. Furthermore, a swept leading edge would present a more aerodynamic shape to minimize performance loss. This was called the "smart clip" (See Figure II-5) and is subject of a pending patent application. This "smart clip" was

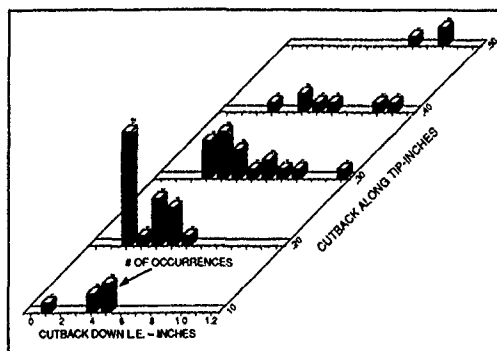


Figure II-4 Operator Ice FOD Data

evaluated in the test rig in steps of .12, .18, and .25 inches of tip cutback. The test results in Table II-1 show that the .25 inch cutback eliminates any damage that could be caused by an 8 gram iceball passing between the inlet guide vanes at 85 ft/sec. Although these larger objects travel more slowly when accelerating in an engine inlet, these tests were conservative because they held velocity constant at the upper limit of smaller objects.

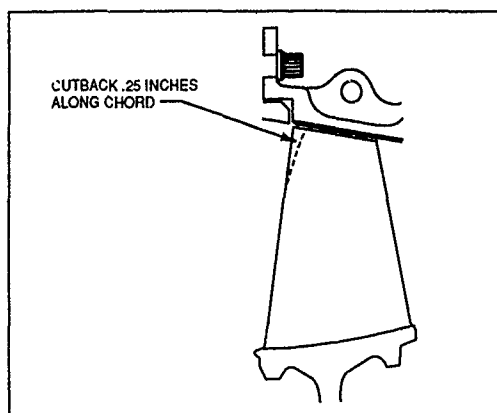


Figure II-5 "Smart Clip" Stage 1 Blisk

A significant reduction in the baseline blisk damage resistance was observed for a blade positioned next to a clipped blade. The results show that the initial damage threshold was reduced by objects from 2.8 to 1.5 grams. This is also where major curl damage was reduced by objects from 4.5 to 2.8 grams. Also, the .25 inch cutback showed initial damage occurring at 6.5 grams weight, whereas a uniformly cutback blisk was above 8 grams (See Table II-1).

TABLE II-1 TEST RIG ICEBALL FOD SUMMARY

Blisk Configuration	Object which Initiates Damage grams	Object which Causes Extensive Damage or Tip Curl grams
CT7-5A		
Baseline	2.8	4.5
.12 Cutback	>4	5
.18 Cutback	6	>6
.25 Cutback	>8	>8
Baseline CT7-5A next to Field Clip	1.5	2.8
CT7-5A .25 Cutback next to Field Clip	6.5	>6.5
CT7-9 Cutback	>8	>8

Test Conditions:

Rotor Speed 42,000 rpm
Ice Ball Velocity 85 ft/sec
Impact Area @ Blade Tip

Initial blade cutbacks were carried out at the operator's shop or during on-wing maintenance that required access to the compressor. After the "smart" blade cutback, virtually all ice FOD problems were eliminated with that engine. As the field engine population increased in cutback compliance, corresponding reductions in maintenance action occurred (See Figure II-6). As of December 1989, the rate has been reduced by over 30 times to less than .005/1000 EFH with 98% compliance. The performance effect of the "smart clip" has been small particularly when carried out with other compressor refurbishment which, in itself, offsets the cutback Stage 1 blade performance loss.

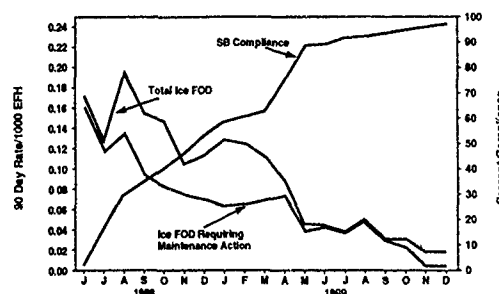


Figure II-6 CT7-5 Turboprop Ice FOD Reduction From "Smart Clip" Compliance

Additional ice testing and further review of the high speed films was done to understand whether blade leading edge thickness or sweep back geometry was influential in improving ice FOD resistance of the "smart clip" blade. Blade leading edge shapes of the test hardware were photographed, measured and correlated with the test results. This follow-on investigation which included tests of swept back blades with thin leading edges showed that good correlation could be obtained between damage resistance and thickness measured .04 inches back from the leading edge at a location 0.5 inches down from the blade tip. Figure II-7 is a plot of ice ball size and leading edge thickness showing a

line of demarcation between damaged and undamaged airfoils. For this plot, damage was assumed to be any detectable plastic deformation of the blade leading edge. This plot points out the sensitivity of the damage resistance to blade leading edge thickness.

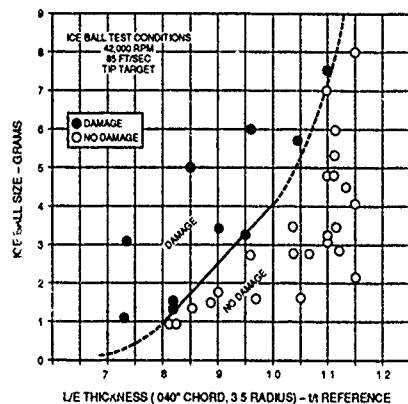


Figure II-7 FOD Resistance Correlates Well With L.E. Thickness

The blade leading edge thickness is felt to be critical since damage is initiated at this location. More dramatic blade curling occurs later due to the increased exposure of the blade because of the forward deformation of the leading edge. The high speed films show the ice ball is shattered by the initial blade impact which causes a significant load on the leading edge. However, blade curling is caused by the high loads imposed on the blade as it accelerates the ingested mass of ice up to wheel speed. The measurement location of .04 inches from the leading edge is somewhat arbitrary but does provide a quantitative measure of the lead edge bluntness where the initial ice impact occurs. Figure II-8 shows enlargements of the leading edge shape of two airfoils and how the relative thickness at .04 inches characterizes the leading edge shape. Velocities of the ice ball and blade are such that the ice is ingested at a rate of approximately .07 inches per blade at 80 feet per second. This adds further justification to a thickness measurement near the leading edge.

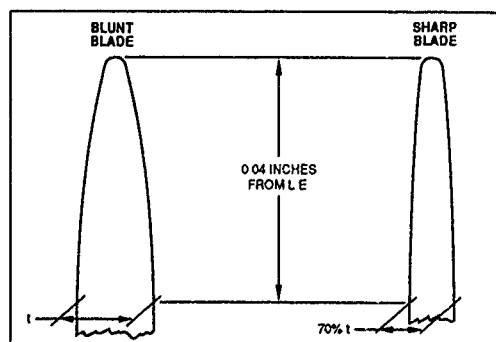


Figure II-8 Thickness at 0.04 Inches From L.E. Characterizes L.E. Bluntness

This investigation has demonstrated the importance of leading edge thickness in preventing ice damage to blades. It allows the engineer to design the best aerodynamic blade configuration including leading edge contour and assure good ice damage capability by controlling the leading edge thickness. This assumes that the remainder of the airfoil has sufficient strength to accelerate the ingested ice particles up to wheel speed without deformation.

Ice FOD-Resistant Compressor Blade Development

Conclusions

- 1) Blade leading edge thickness is the most important parameter for resisting ice FOD damage.
- 2) A full tip curl can be caused by a single large ice object, or by a succession of smaller objects which, initially, only partially deform the airfoil.
- 3) Airfoils which protrude forward of the plane of the other blades are likely to be hit repeatedly and more severely. Similarly, airfoils following more deeply cutback blades are more vulnerable to damage caused by deeper ice penetration prior to impact.
- 4) Increased ice velocity and size increase blade damage. However, larger particles accelerate slower and have lower velocity at blade impact.
- 5) As a rule to durability, the stage 1 compressor blades should be capable of withstanding impact from any piece of ice that can pass between the inlet guide vanes.
- 6) Cutback modification to the leading edge of the CT7-5 Stage 1 blade has an ice FOD resistance that will eliminate most field damage.

Discussion

1. H. Saravanamuttoo, Carleton University

Could you please indicate how many compressor blades were subject to damage in a typical FOD incident, and could you give some quantitative idea of the penalties in compressor efficiency or engine temperature margin?

Author:

Most ice-fod events involved a single blade which resulted in an audible whine from the compressor and a 5-10 degree C shift upward in T5 temperature at constant torque. The repair, which clipped off the bent blade material and a similar amount from the opposite blade, costs about 1 point in compressor efficiency and about 6 C in temperature margin.

2. D. Mann, Rolls Royce

Did you at any stage operate your trajectory code in a reverse mode, in an attempt to assess where the FO could have come from, upstream of the damaged parts of the compressor blades?

It appears from figure I-8A that during the course of assessment of different designs, no consideration of changes to the splitter lip was made, despite the fact that this is an area which has a significant effect on separation efficiency. Could you comment on this?

Author:

This is an interesting suggestion but we did not evaluate this approach. We suspect the ice objects are much slower than the air stream and they tend to slide along the outside walls. The tests with cameras viewing the inlet duct demonstrated this behaviour.

Splitter lip changes were too extensive for consideration as a field fix. Major redesign certification programmes would be needed to implement those kind of changes.

3. R. Jones, Boeing Arnprior Canada

What is the mechanism by which the cut back on the leading edge of the blades prevent fod from one inch pieces of ice?

Author:

The cut back increases the leading edge thickness resulting in a stronger blade. Figure II-7 illustrates that only modest increases in thickness are required.

4. M. Holmes, RAE

What lessons were learned as a result of the CT7-5 ice fod problems in service on repeat of qualification of future engines?

Author:

First, compressors should be capable of handling ice objects large enough to pass cleanly between the inlet guide vanes. Second, ice accretion in the inlet system must be negligible or limited to sizes easily handled by the compressor blades. This issue of qualification (certification) often focusses on the safety of flight issue which was not the problem for CT7. Our problem was unscheduled maintenance from ice-fod and I do not think these kinds of issues are easily demonstrated in an engine qualification programme.

5. C. Scott Bartlett, Sverdrup Technologies

Would you please comment on considerations given to the type of the ice used during your ice ingestion tests and if you feel there is a difference in damage due to ingestion at different types of ice?

Author:

We felt that ice near freezing would be less brittle and may cause larger energy transfer to the blade because it is less likely to scatter upon impact. Therefore, we allowed the ice to warm up slightly before test so that there was some liquid on the surface of the iceball.

FUELS AND OILS AS FACTORS IN THE OPERATION OF AERO GAS TURBINE ENGINES AT LOW TEMPERATURES

by

G L Batchelor

Eng 2a

Procurement Executive, Ministry of Defence
St Giles Court, 1-13 St Giles High Street
London WC2H 8LD
United Kingdom

Two factors strongly influence the low temperature behaviour of aero gas turbine fuels and oils. They are Viscosity, and State or phase change - i.e. whether the material is liquid or solid. In fact the question is whether solids are, or are not, present because, although the whole may cease to flow at some designated temperature, the lighter components of hydrocarbon and other organic mixtures are likely to be liquids under all natural circumstances. Terms such as Freezing Point, Pour Point, and the like, will be familiar enough. This presentation examines the chemical and physical realities underlying such parameters and considers their impact on aero gas turbine engine performance. For the purposes of this paper fuels and oils will be treated quite separately.

Part I: FUELS

FUEL TYPES

All ordinary aviation turbine fuels are variants of kerosine. The Wide-Cut fuel F-40, or JP4, is kerosine plus naphtha. The current European Theatre primary fuel F-34, or JP-8, is Kerosine per se. The naval High Flash fuel F-44, or JP-5, is a slightly higher boiling kerosine cut which can, on occasion, satisfy either F-34 or F-44 requirements. Such differences may be manifest in fuel low temperature behaviour.

FUEL COMPOSITION

From the low temperature performance aspect there is need to take account only of those organic compound classes present in "bulk" proportions; i.e. whose percentage contribution will be at least five, and will likely be numbered in tens. Namely:-

Paraffins (normal and iso)

Naphthenes (or cyclo paraffins)

Aromatics (single ring)

but only such members of each class as are allowed by the boiling range of any given fuel.

Two trace components have significant

impact. They are water itself, and the fuel system icing inhibitor (FSII) added to all military fuels to combat any free water forming in those aircraft not equipped with engine fuel filter heaters.

Water is present in solution in all fuel at equilibrium concentrations of the order tens of parts per million. FSII is added at tenths of a percent by volume.

The water occurring naturally should not be confused with that which may arise through contamination of the fuel supply. The latter is a logistic concern not to be addressed here.

FUEL COMPOSITION EFFECTS

(A) Phase Change

WATER. Apart from the fact that its equilibrium solubility varies marginally with hydrocarbon class, water will behave almost independently of fuel type. When in solution, water is no problem. But it is a low temperature performance issue due to the simple natural fact that from about 0°C and on downwards the dissolved water will crystallise out as ice. Although that process is virtually complete at -30°C, the ice crystals tend to remain in suspension. Those which do reach the tank walls form an ice film and are thereby inactivated until that film melts. Another wholly natural

source of water is precipitation out of the aircraft fuel tank ullage air.

The function of the FSII is that of an "anti-freeze" which so modifies water:fuel partitioning as to obviate the blockage of engine filters by ice. There is a popular misconception that FSII operates on the Freezing Point (see below) of the fuel itself. IT DOES NOT.

So much for water.

HYDROCARBONS Generally speaking, the heavier members of a given series can be regarded as being dissolved in the lighter ones. Certainly it is the heaviest which crystallise first on cooling. Adding to the lighter end of a fuel cut (if that be an option) allows greater flexibility at the other end. This is well demonstrated by wide-cut fuel which has a Freezing Point 10 degrees or more below that of a kerosine but has the higher final boiling point.

Straight chain normal paraffins are the really "waxy" types which most readily and distinctly crystallise out. The phenomenon becomes increasingly less definitive as the molecular pattern compacts through branched structures to saturated rings. There are also inter-specie effects.

Normal fuels being always comprised of mixtures, the low temperature behaviour of any particular fuel will be a function of the balance of its components. A mixture of two fuels of differing composition will not necessarily average the properties of the two individuals. This is not a practical concern except for the rare event of both being at the specification margins.

(B) Viscosity

So long as they remain wholly liquid, most fuels are fully Newtonian in their flow. That is true for the more paraffinic examples even to below their Freezing Points. But this is open to some question with the extremely cyclo-paraffinic types yielded by modern hydrocracking processes .. a point to which I shall return later.

THE FUEL PARAMETERS

FREEZING POINT Best known of all the fuel low temperature parameters, Freezing Point addresses the transition between a fuel being wholly liquid and there being solid hydrocarbons present. Thermodynamics dictate that both the first appearance of crystals on cooling, and their final disappearance upon warming, shall take place at different temperatures. The definition of Freezing Point centres on disappearance; it marks the lowest temperature at which

the fuel will be wholly liquid in terms of its hydrocarbon make up.

FLOW POINT Flow Point addresses the threshold of flow. Under the title "Pour Point", it is a common enough parameter for oils and diesel fuels. In the context of jet fuel it has specific meaning.

When fuel temperature continues to fall below the Freezing Point, more and more hydrocarbons crystallise out until a point is reached at which the solids form a stable matrix. Precisely at that point the still liquid components remain fully mobile but very soon thereafter even they become entrapped in the growing matrix, and the fuel then becomes a *de facto* solid.

The jet fuel criterion of flow concerns the ability of the crystal matrix to collapse at its unsupported edges under its own weight such that the two phase mush can still flow of its own volition to the aircraft tank backing pump; thereafter, any mechanical work on the fuel ensures that the phase balance cannot again worsen.

Flow Point has attracted attention from time to time (chiefly at times of perceived fuel shortage) but has yet to attain practical significance.

Without there having been cause for full consensus on the issue, Flow Point has thus far been defined in terms of recoverable fuel under designated test conditions.

VISCOSITY In an aviation fuel context the parameter is the kinematic variety.

MEASUREMENT

FREEZING POINT Determination entails cooling a fuel sample in glass apparatus at a controlled rate to just beyond the point of hydrocarbon crystal formation. Normally this is readily distinguishable from the ice crystal haze mentioned above. The fuel is then allowed to warm until the last hydrocarbon crystal melts. This procedure is repeated until the temperatures of appearance and disappearance differ by no more than some prescribed amount.

With normally paraffinic fuels all is straightforward and operator experience is not critical. When, as with some of the newer cyclo-paraffinic fuel varieties, the transition points are difficult to observe, and temperature differentials cannot be met, subjectivity increases markedly.

ALTERNATIVES TO FREEZING POINT The fact that Freezing Point determination is labour intensive, coupled with the fact of its increasing element of subjectivity, has driven a search for automation. Any automatic equipment capable of truly replicating the Freezing Point has thus far

proven to be extremely sophisticated. But there are now several simpler, portable, devices capable of indicating the Freezing Point, or something closely related to it.

The importance of these does not lie in their specification potential but in the possibilities they offer for greater operational flexibility. At present, although Freezing Points are frequently well within specification, the absence of an actual value at the point of refuelling means that aircraft flight plan must presume a value at the specification limit. A "plane-side" Freezing Point capability would be a considerable operational boon.

FLOW POINT The only test method thus far formally published is that developed by the UK Institute of Petroleum in the late 1950s when it was thought that there might be insufficient fuel of low enough Freezing Point to meet the requirements of the then dawning inter-continental commercial jet aircraft traffic. It entails a vertically cylindrical test vessel at whose bottom end is a conical valve capable of sudden release such as to allow the fuel to flow - if it can.

OPERATIONAL and PERFORMANCE IMPACT

(A) Phase Change

FREEZING POINT The parameter is often seen as being an airframe concern inasmuch that any resultant constraints applied to aircraft routing arise essentially out of the relationship between meteorologically projected fuel tank temperatures and understood fuel Freezing Points.

But, in the final analysis, it all comes back to the engine. There seems to be a universally accepted stipulation to the effect that fuel shall be delivered by the airframe to the engine three degrees above the Freezing Point - the latter again taken as being at the specification limit.

Such a rule presumably purports to ensure single phase flow regardless of the precision of the Freezing Point test method employed (of which aspect more anon).

FLOW POINT The parameter, as it has so far has been defined, is perhaps a little pessimistic in that vibration, coupled with attitudinal g forces, will very probably keep a crystal matrix unstable below the temperature indicated by static laboratory testing.

However, the blithe assumption that ordinary aircraft might somehow be able to utilize semi-frozen fuel (thus giving the

parameter viability) is far from being valid.

(B) Viscosity

Because it is a design criterion that fuel viscosity shall not exceed 12 cSt at any functional point in the engine system, the parameter is not generally seen as a performance or operational consideration other than when the aforesaid criterion is, for some reason, not met. Certainly there have been spectacular instances of starting difficulties with kerosine fuels under unusually cold conditions.

Certain hydromechanical devices apart, viscosity at the burner spray or atomiser is the main concern.

SPECIFICATION

It is quite usual to think of fuels in terms of their specified Freezing Points: viz ..

-40 [°C] for Jet-A; -47 for Jet-A1
and JP-8; -58 [-72°F] for JP-4: etc.

However, the purpose of this short section is to briefly review the manner in which specifications address the low temperature requirements.

(A) Phase Change

FREEZING POINT Although its definition is centred on crystal disappearance, the latter is only the indirect basis of limits set by fuel specifications.

The reality is best illustrated by the outcome of the lengthy ASTM debate which attended the lowering of the Jet-A1 limit from -50°C to -47°C in response to the fuel supply crises of the late 1970s. After due consideration of data from the airlines and from Boeing's studies of its 747 aircraft, the consensus finally settled at minus 47 on the basis that ...

The best overall number for in-flight minimum fuel temperature was -43°C.
ADD the 3° margin for the engine.
ADD 1 more for good measure!

It might appear, in the light of the data entailed, that there is over-caution here. But, the data is only as good as the measurements made in those aircraft tanks wherein measurement was possible.

Caution is not misplaced. The protagonists of specification change are usually looking only at the fuel side of the equation. One hears tell of "difficulty" in getting fuel

out of wing tip tanks in cases where the operators have sailed close to the Freezing Point wind.

FOR SO LONG AS AERO GAS TURBINE FUEL SYSTEMS ARE TO BE DESIGNED FOR SINGLE PHASE HYDROCARBON FLOW ONLY, THEN SO LONG WILL FREEZING POINT REMAIN THE KEY FUEL LOW TEMPERATURE PARAMETER.

FLOW POINT There is little that can be said, in a specification context, of a fuel parameter that has yet to be specified.

(B) Viscosity

Although the 12 cSt hardware limit is independent of temperature, a specification must stipulate a temperature of testing.

This will preferably be some convenient laboratory norm. For aviation kerosine that turns out to be -20°C whereat an 8 cSt maximum satisfies the operational need.

Wide-cut fuel is, by its very nature, well inside the viscosity mark; but, even were that not so, its volatility would put routine measurement beyond reach.

HARDWARE DESIGN IMPLICATIONS

(A) Airframe

The aircraft fuel system must respect Flow Point in order to deliver fuel at all, and respect Freezing Point in order to deliver fuel of acceptable quality.

Warming a just flowing fuel mush to an engine-acceptable condition has to entail aircraft fuel tank heating .. *with the necessary heat deriving ultimately from the engine.*

Boeing, and others, have carried out numerous paper studies - often with seeming enthusiasm. But the outcome, be it initial installation or retrofit, always carries so many, and such varied, penalties that I am forced to the view that such action would be set in train only by the most traumatic of fuel eventualities.

(B) Engine

On the engine side, there are far less traumatic options which can, and perhaps should, be looked at in the shorter term as a safeguard against any future fuel supply eventualities.

Again I sub-divide into already noted categories; but I discount Flow Point as even a medium term recourse.

FREEZING POINT This is certainly a simple and convenient parameter but must we remain forever locked-in to the concept of nil solid hydrocarbons? Cannot engine systems handle just a few?

Admittedly that begs the question of defining a "few" but let fuel specification writers worry on that score for the moment.

From a hardware aspect the solution to such a problem may already be to hand. It may simply be a matter of the batting order for the fuel system's components. Are they always in optimum sequence? Once an engine is running heat is plentiful. Indeed, a current concern is the limiting capacity of fuel as a heat sink.

If the heat exchanger can be as far upstream as possible, then only at start-up would there be need for auxiliary energy to raise the incoming fuel through a probably very small temperature increment.

Test methods coming under the heading **ALTERNATIVES TO FREEZING POINT** may well offer a route to definition of acceptable solid hydrocarbon levels - they may even have on-line potential.

FRESH STUDY

VISCOSITY may be deserving of detailed reappraisal in the aero engine context.

Hitherto, we have been accustomed to fuels whose flow has remained consistently Newtonian albeit that their Freezing Points have been relatively high. Now we see hydro-cracked fuels whose Freezing Points, though hard to measure, are very low.

Is enough known about these liquids at those temperatures? Might their reluctance to crystallise be accompanied by some form of nucleation in solution? Do perceived viscosity temperature relationships hold for them? Above all, how might any such aberrant behaviour impact on combustor performance?

In recommending this as an area ripe for study I would point out that, to be meaningful, such studies would entail the most careful fuel modelling.

PART II : ENGINE OILS

Aviation fuels come directly from naturally available resources. They are subjected only to the minimum of processing and/or additive treatment essential to ensure specification compliance. The oil situation is very different. Petroleum based mineral gas turbine oils today form a minority category; they will not be addressed here. The majority of current oils are "synthetic" in that their primary constituents are synthesised from raw materials of animal or vegetable origin. Such oils are in fact *designed* with specific user engine types view. Their successful manufacture is as much an art as it is a science.

OIL TYPES

Aero gas turbine synthetic oils are mostly categorised by notional viscosities at 40°C .. viz:

3 cSt eg .. Nato O-148, or O-150

5 cSt eg .. Nato O-156, or O-160

7½cSt eg .. Nato O149

Multiple designations under a single category arise out of differing national qualification processes or out of differing performance levels (O-160 has a higher load bearing capability than O-156).

There is no specific categorisation with respect to low temperature performance. It is, of course, easier to achieve a desired low temperature capability with a thinner oil. Oil viscosity is as much an engine design parameter as it is an oil one albeit that some engines can use oils of differing viscosities.

OIL COMPOSITION

A synthetic aero gas turbine oil is usually characterized by the type of ester making up the bulk of oil volume and thereby giving the product its underlying fluidity and elasto-hydrodynamic quality.

To this base will be added various additives whose purpose(s) will be to confer, or enhance, specific properties of the finished lubricant.

ESTERS are the reaction products of alcohols and organic acids. They can be looked upon as falling into three classes:-

(1) [The first on the scene] Long chain acids coupled with relatively simpler alcohols .. generally termed di-basic acid esters - eg di-octyl sebacate, or its azelaic or adipic counterparts.

Thereafter come complex alcohols coupled

with shorter chain acids - principally esters based on ..

(2) Tri-methylol-propane (TMP)

or,

(3) Penta-erythritol (PE)

The two last named allow a measure of product tailoring through variation of the esterifying acid or acid mix.

ADDITIVES

These regulate thermal and oxidative stability, load bearing capability, hydrolytic stability, corrosivity, foaming, and so forth, *but not*, it should be noted, low temperature performance per se.

The low temperature concern is that additives, particularly any which happen to be at the threshold of true solution, might precipitate irreversibly - especially when exposed to prolonged soak.

This is as much a problem between oils as it is one within an oil.

PHASE SEPARATION and VISCOSITY

That final comment re additives said virtually all that there is to tell about low temperature phase separation in oils.

VISCOSITY is the key. And the key is to engine starting.

I exclude from this discussion circumstances in which aircraft heating, or other external aids to starting, are a recognised part of an operational scenario.

Given such exclusion, interest centres on starting torque engendered by the oil.

That will be primarily an engine design parameter but consequential oil design will depend also on the lower operating temperature envisaged for the user aircraft.

Such limits typically vary between -25°C and -54°C.

The real problem with attaining appropriate low temperature viscosity is that of matching this particular need with the parallel one of having sufficient viscosity at normal running temperatures.

In fact, as a dominant factor, the oil low temperature requirement has but brief duration. Once the engine is up and running, oil quickly takes on the crucial rôle of a heat transfer medium.

OIL COMPOSITION EFFECTS

It is not really realistic to set out to examine composition as an option vis-a-vis oil low temperature performance. Such are the conflicts with the high temperature imperatives, and such is the increasing weight given to the latter, that there is little option other than compromise at the low end.

Certain advanced engine systems (using specialised lubricants) have resorted to oil dilution .. itself a fairly venerable dodge in the piston engine world! Others allow for higher than normal viscosity (at low temperature) in relatively conventional oil types.

A sometimes necessary reverse compromise (from a lubricant design standpoint) is constraint on additive addition where an otherwise optimum treatment level might result in unacceptable low temperature characteristics.

It is a not unreasonable generalisation to state that , for any given oil type, whilst it may be possible to move the range band of high to low temperature capability up or down the temperature scale, it is very difficult to widen that band.

SPECIFICATION and MEASUREMENT

The only quantified oil low temperature parameters are Viscosity and Pour Point.

VISCOSITY is measured in the conventional manner. Specification limits have generally been predicated to a functional kinematic viscosity of 13,000 cSt at -40°C. However, as implied above, high temperature performance demands are forcing a re-think and numbers such as 14,000 cSt at -20°C are being mooted for some impending aircraft projects.

POUR POINT is an empirical observation of the limiting temperature at which an oil just flows of its own volition. The specification limit is usually -60°C. It is a batch quality control and is also used in screening new products.

At the type approval stage it is usual also to confirm low temperature homogeneity empirically in the laboratory.

OIL PRODUCTION

The raw materials for synthetic aero engine oils derive from natural renewable resources. They are, therefore, subject to climatic and other environmental vagaries.

Moreover, aviation is only a minor user of them and in no position to dictate the shape of the market in any fundamental way.

As a consequence, oil suppliers prefer to have a range of optional compositions approved for any product, albeit that some options may be superior others in the final analysis.

ENGINE DESIGN and OPERATIONAL CONSIDERATIONS

In the matter of oil superiority there very definitely are "Horses for Courses".

Not all oils perform equally well in all the engines for which they are notionally suited.

Different engines do not rank the same oils in a single order. Indeed, different parts of the same engine may rank a given oil set differently. And this even more true when the ranking is done with regard to differing oil performance parameters.

There is, therefore, a need perhaps to rank the parameters. We might observe at once that the exigencies of aircraft performance seem already to have ranked the oil high temperature requirement above the low.

That being so, there is need to examine the low temperature requirement itself.

After start-up it involves a very small part of the flight envelope other than for those APUs and other accessories which may be exposed to static cold soak on long flights; they might be allowed to windmill, or be started-up periodically, to maintain their readiness.

Furthermore, low temperature starting occupies only a small part of the total operational envelope; one ponders the extent to which it should be allowed to predicate overall oil design?

FUTURE OIL DEVELOPMENTS

The viability of alternative "chemistries" for the lubrication of aero gas turbines in the broad inventory is a subject of current and on-going interest and review.

Discussion

1. P. Sabla, GEAE

Should surface tension be considered as a controllable parameter to enhance the atomization at low temperatures?

Author:

An additive approach would be viewed with caution as it carried unacceptable penalties in other directions. The desirable first step is a deeper understanding of the relationship between physical effects, such as atomization and fuel composition.

2. M. Holmes, RAE

What is the fuel property that most limits the low temperature operation of turbo engines? Is this a serious limitation and, if so, does your organization have any programmes to find a solution?

Author:

At the moment freezing point, in the future perhaps also viscosity, as the aircraft criteria are presently defined, are absolute limitations (go/no go). The fuel man can offer little service. Any solution open to him must necessarily limit fuel availability or increased fuel price or both. Limits can be altered only with the consent of the aircraft design side. The fuel side does attempt to maintain a data base for current and foreseeable fuels. Perhaps that needs to be reconsidered with design options for the eventuality of a fuel availability shortfall.

3. F. Garnier, SNECMA

Pour les turboréacteurs, on a parlé aujourd'hui des huiles de 3 et 5 cst, 5 jusqu'à -40 C, au dessous mais on parle aussi maintenant de plus en plus de nouvelles huiles de 4 cst. Que seraient les avantages de ces nouvelles huiles par rapport aux autres, auront-elles les mêmes comportements?

Author:

These standard viscosity classifications are predicated to +40 C. I doubt that a 4 cst oil would necessarily offer improved low temperature performance above 5 cst unless specifically designed with such an end in view.

4. D. Way, RAE

At long distance aircraft, the ranges are becoming longer and longer, and the danger of the fuel coming to lower temperature increases. Is this a concern?

Author:

It does on transatlantic flight with slower aircraft. With normal aircraft, it is somewhat compensated by aerodynamic heating. The problem increases with tip tanks with a smaller volume to surface ratio and a thin skin. For extremely long distances there must be a compromise between the commercial and the technical interest.

THE EFFECT OF FUEL PROPERTIES AND ATOMIZATION ON LOW TEMPERATURE IGNITION IN GAS TURBINE COMBUSTORS

by

D.W. Naegeli, L.G. Dodge and C.A. Moses
Southwest Research Institute
6220 Culebra Road
San Antonio, Texas 78228
U.S.A.

ABSTRACT

Experiments were conducted in a T63 engine combustor to gain a better understanding of the role played by volatility and atomization in low temperature ignition. Eight test fuels were used, some of which were specially blended to vary either viscosity or volatility while holding the other constant. Six atomizers were used to vary the fuel spray characteristics, and average drop sizes, represented by Sauter mean diameter (SMD), were measured. Air temperatures were varied from 239 to 310K. Ignition comparisons were made by the minimum fuel-air ratios necessary to achieve ignition. Significant results included: 1) viscosity, which determined atomization characteristics, was more important than volatility in the ignition process; 2) ignition depended more on achieving a critical drop size than on reaching the lean-limit fuel-air ratio; and 3) fuel temperature was found to be more important than air temperature for low-temperature ignition, an effect due principally to viscosity and atomization rather than evaporation. A practical implication is that fuel heating would give a much greater improvement in cold-start performance than heating the combustor inlet air.

NOMENCLATURE

V_f	reference velocity
F/A	fuel-air ratio
SMD	Sauter mean diameter, micrometers
μ	kinematic viscosity, cSt
σ	surface tension, dynes/cm
FN	flow number, $\text{kg/s} - \sqrt{\text{Pa}}$
w_f	mass flow rate, g/s
R^2	coefficient of determination
Rosin-Rammler Parameters for:	
R	cumulative volume fraction of spray
D	droplet diameter
X	droplet size parameter
N	width of distribution

INTRODUCTION

The fuel quality/availability ratio has become complex in recent years because of the uncertainty in the supply of petroleum. Alternatives, such as synfuels, tend to have different boiling point distributions and increased viscosities when compared with their petroleum equivalents. This trend toward reduced volatility and increased viscosity could cause degradation of low temperature ignition, altitude relight, and flame stabilization in gas turbine engines.

Several aspects of the ignition process in gas turbine engines are not clearly understood. Combustor rig tests have been effectively used to demonstrate the effects of varying fuel properties on ignition and flame stabilization.⁽¹⁻¹¹⁾ Analytical models have been developed to correlate⁽¹²⁻¹⁷⁾ data from several combustors. However, the modeling efforts have been seriously hindered by the absence of information on the effects of fuel volatility, and atomization.

It has been found⁽¹⁸⁾ that ignition models are quite sensitive to the drop-size distribution in the fuel spray, characterized by the Sauter mean diameter (SMD), but this sensitivity has not been properly measured in the combustor data available to date. Previous studies⁽¹³⁻¹⁵⁾ have employed correlations that were based on measurements of SMD in sprays from atomizers that were similar, but not sensitive to the subtle differences in the design of the actual fuel atomizers used in gas turbine combustors. The purpose of the present study was to provide a clearer definition of which fuel property, *viscosity or volatility*, plays the more important role in the ignition process.

EXPERIMENTAL FACILITIES AND METHODS

General Description - This work was performed in the combustor facility of the Belvoir

Fuels and Lubricants Research Facility (BFLRF) at Southwest Research Institute (SwRI). The combustor facility was specially designed to study fuel-related problems in the operation of gas turbine engines. The air supply system provides a clean, smooth flow of air to the combustion test cell with mass flow rates up to 1.1 kg/s, pressure to 1620 kPa (16 atm), and temperatures from 239K (-30°F) to 1089K (1500°F) (unvitiated). For cold start ignition tests, the combustor inlet air is cooled by injecting liquid nitrogen and gaseous oxygen through a manifold placed upstream of the combustor. This system is capable of lowering the temperature of the burner inlet air supply to -34°C (-30°F) for the mass flow rates (0.09 to 0.27 kg/s or 0.2 to 0.6 lb/s) used in the T63 combustor ignition tests. Turbine flowmeters and strain-gage pressure transducers are used to measure flow properties of the air and fuel. Thermocouples are referenced to a 338.5K (150.0°F) oven. Data reduction may be performed on-line with test summaries available immediately; these summaries provide average flow data as well as standard deviations (typically less than 1 percent of average value) of inlet temperature and pressure, exhaust temperature, flow rates of fuel and air, emissions data, and combustion efficiencies. Further detail on the facilities and procedures described below may be found in Reference 19.

T63 Combustor Rig - The combustor used in this study was fabricated from T63 engine hardware. This combustor has been used in previous programs to study the fuel effects on ignition, combustion stability, combustion efficiency, exhaust pattern factor, radiation, and smoke. Figure 1 is a schematic of the combustor rig showing the locations of the fuel atomizer, igniter, and

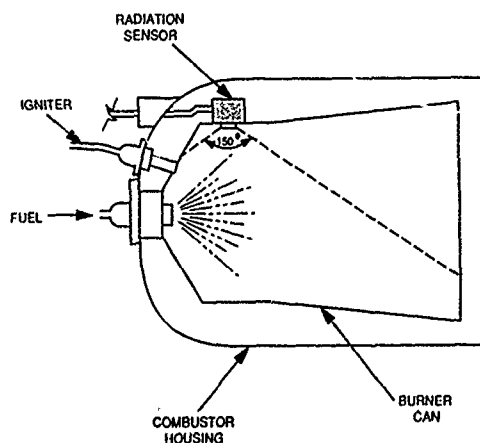


Figure 1. T63 combustor

the radiation sensor used to detect the onset of a visible flame in the ignition measurements.

The T63 combustor employs an igniter that produces sparks at a rate of 8 per second with energies of about 0.87 joules, and a dual-orifice pressure-swirl atomizer. The primary orifice is used principally for the atomization of fuel in the ignition process. The secondary orifice supplies the bulk of the fuel but does not engage until the fuel flow rate is above that required for ignition. To further examine the effects of atomization on ignition, an adapter was constructed to allow use of single-orifice, Delavan pressure-swirl atomizers with flow capacities ranging from approximately 15 to 30 liters/hr (4 to 8 gal./hr) at a differential fuel pressure of 689 kPa (100 psid).

Test Fuels - The test fuels described in TABLE 1 were chosen for the ignition study because of

TABLE 1. Fuel Properties

Fuel No.	Fuel Description	Specific Gravity at 15.6°/15.6°C	Vis at 0°C (cSt)	Surface Tension at 25°C (dynes/cm)	10% Boil off Temp(°C)
1	JP-8	0.8236	2.51	27.18	169.4
2	JP-4	0.7519	1.22	24.29	98.0
3	JP-5	0.8080	3.48	27.02	189.2
4	NDF/25% Gasoline	0.8265	3.61	27.01	112.2
5	NDF/70% Gasoline	0.7839	1.32	24.01	36.1
6	NDF	0.8484	7.85	28.79	209.9
7	Methanol	0.7913	1.03	22.44	65.0
8	Gasoline	0.7555	0.90	21.89	16.6

their broad range of viscosities, and volatilities. To independently study the effects of viscosity and volatility on the ignition process, Fuel 4 was blended with a viscosity equal to that of JP-5 and a front end boiling point distribution similar to JP-4. Fuel 5 was blended with a viscosity equal to that of JP-4 and a front end boiling point distribution similar to gasoline. The viscosities of gasoline and methanol are essentially the same, but their 10 percent boil-off temperatures and heats of vaporization are very dissimilar.

Droplet Size Measurement - Atomization is a crucial factor in the ignition of fuel sprays in gas turbine engines. Ignition failure occurs with diminished atomization quality because of the decreased fuel surface area available for evaporation and the increased spark energy required for droplet evaporation. For a given engine design

poor atomization is caused, for the most part, by increased fuel viscosity; consequently, higher viscosity fuels and lower fuel temperatures lead to higher fuel/air ratio requirements for ignition. It is a general rule that when fuel viscosities exceed 12 cSt combined with lower burner inlet air temperatures, the probability of ignition in gas turbine engines is greatly reduced at any fuel-air ratio.

To better understand the ignition test results in the T63 combustor, droplet-size measurements were made on hollow cone sprays produced by the atomizers described in TABLE 2.

Table 2. Fuel Atomizers			
Description	Flow Capacity* @ 689 kPa (g/s)	Flow Number* (kg/s-√Pa)	Cone Angle (degrees)
Factory T63 Dual Orifice Pressure Swirl	5.93**	7.14×10^{-6}	---
Delavan Simplex Pressure Swirl	3.18	3.83×10^{-6}	90
Delavan Simplex Pressure Swirl	4.01	4.83×10^{-6}	90
Delavan Simplex Pressure Swirl	5.13	6.18×10^{-6}	90
Delavan Simplex Pressure Swirl	5.88	7.08×10^{-6}	90
Delavan Simplex Pressure Swirl	7.00	8.43×10^{-6}	90
* Capacity and flow number for JP-5			
**Primary nozzle on!			

The standard T63 atomizer is a dual-orifice nozzle that uses a flow divider valve internal to the nozzle body to determine the fuel flow split between the primary and secondary nozzles. At low flow rates, such as those used in ignition, the valve completely restricts the flow of fuel through the secondary nozzle. As a result, the droplet-size measurements were made only on sprays originating from the primary nozzle.

The standard T63 atomizer is also equipped with passages to carry burner inlet air through the nozzle to prevent deposit buildup on the nozzle face exposed to combustion gases. However, the airflow was also found to affect atomization and, therefore, had to be accounted for in the droplet-size measurement. To simulate this airflow, a special manifold was designed to allow the separate flows of fuel and air through the atomizer.

The Delavan atomizers were single-orifice pressure-swirl (simplex) nozzles differing only in flow rate capacity. Compared to the standard T63 atomizer, the droplet-size measurements in sprays from the Delavan atomizers were relatively straight forward.

The test fluids and test conditions used in the atomization measurements are given in TABLE 3.

Table 3. Test Fluids for T63 Ignition/Atomization Study to Generate the Correlation of Sauter Mean Diameter (SMD) with Fuel Properties and Flow Conditions

Fluid	Test Temp (K)	Kinematic Viscosity at Test Temp (cSt)	Surface Tension at Test Temp (dynes/cm)	Density at Test Temp (g/mL)
JP-4	298	0.85	23.9	0.746
JP-5	298	2.02	26.6	0.801
NDF	298	3.77	28.4	0.841
HMGO	298	9.8	31.1	0.868
HMGO (cold)	274	29	33.3	0.884

The first three of these fluids, JP-4, JP-5, and NDF are test fuels described in TABLE 1; HMGO is a heavy marine gas oil selected because of its relatively high viscosity. The flow rates ranged from 1 to 7 g/s depending on the atomizer and fuel combination examined.

Drop-size data were obtained with a Malvern Model 2200 particle sizer based on the diffraction angle produced by drops when illuminated by a collimated beam of mono-chromatic, coherent light from a HeNe laser. A 300-mm focal length $f/7.3$ lens was used to collect the scattered light. The laser beam diameter was 9 mm with a Gaussian intensity distribution truncated at the edge by the 9-mm aperture. Data were recorded at an axial distance of 38.1 mm (1.5 in.) downstream of the nozzle tip.

Two procedures were necessary to ensure the proper calibration of the particle sizing instrument. The drop-size distribution is computed from the relative scattered light intensity measured at different scattering angles by a set of 30 annular ring photodiodes.

For an ideal optical and electronic system and uniform responsivity between photodiodes, the signal intensity may be used to compute the drop-size distribution without resorting to exter-

nal calibration standards. Tests at this laboratory have shown that the nonidealities of the system are negligible except for the detector responsivities that must be determined for each instrument in order to get accurate results. The first procedure⁽²⁰⁾ was used specifically to assure proper calibration of the particle sizing instrument.

The second procedure⁽²¹⁾ was necessary to correct for multiple light scattering off droplets in very dense fuel sprays obtained at the higher fuel flow rates. This procedure was used in only a few instances to correct the data recorded when dense sprays were encountered.

All tests were performed at atmospheric conditions in a test chamber of square cross-section 30 cm on a side and 76 cm long, with air pulled through the chamber at a velocity of about 2.1 m/s by an explosion-proof exhaust fan. A set of twisted metal screens in the exhaust duct removed the fuel mist from the air before exhausting to the atmosphere.

All spray data were reduced assuming a Rosin-Rammler drop-size distribution, which is specified by two parameters X and N , defined by,

$$R = \exp(-(D/X)^N) \quad (1)$$

where R is the cumulative volume (or mass) fraction of the spray contained in drops whose diameters are larger than D ; X is a size parameter and N indicates the width of the distribution. Large values of N imply narrow distributions and vice versa. Fuel sprays were characterized by an "average" size based on the volume-area mean diameter, more commonly called the Sauter mean diameter (SMD), which may be computed from the Rosin-Rammler parameters.⁽²²⁾

RESULTS AND DISCUSSION

The purpose of this study was to gain a more basic understanding of the ignition process in gas turbine combustors. The results of this work are presented as two parts. The first part describes the droplet-size measurements in the sprays of the six atomizers used in the ignition measurements and the correlation of SMD's with atomizer flow conditions and fuel properties. In the second part, the actual ignition measurements are presented; also, the effects of combustor flow conditions, fuel properties, and SMD's on the limiting fuel-air ratio are examined. Con-

clusions are drawn concerning the relative roles of atomization and evaporation on low temperature ignition in gas turbine engines and the potential use of fuel heating as an effective starting aid.

Droplet-Size Results - Ignition in gas turbine engines is strongly dependent on fuel atomization because it is the droplet size that determines the rate of fuel vaporization. The Sauter mean diameter (SMD) of the spray at the spark-gap depends on the atomizer, fuel properties, and the flow conditions within the combustor. The SMD's were measured in fuel sprays produced by the standard T63 dual-orifice pressure-swirl atomizer and five Delavan simplex atomizers at several flow rates using five test fluids (see TABLE 3). The measurements were made along the centerline of the spray about 38 mm from the nozzle tip. The SMD obtained by this approach was an average through the spray centerline; no account was taken of the radial drop-size distribution in the spray. Figure 2 shows the effect of the fuel

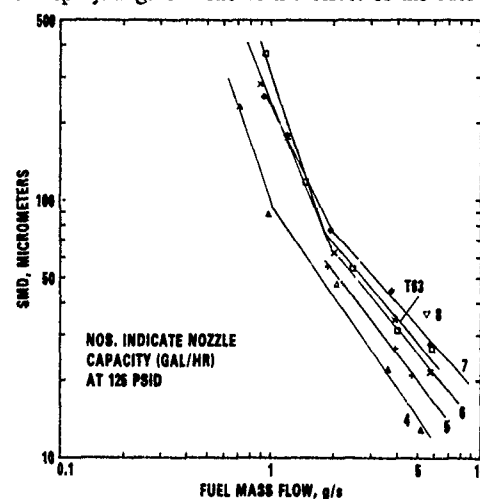


Figure 2. Effect of fuel flow rate and atomizer capacity on SMD for JP-5 fuel

flow rate on the SMD for all the atomizers examined. Clearly, the results show that the capacity of the atomizer has a significant effect on the flow rate required to achieve a desired SMD. It is found that for a given fuel flow rate, the measured SMD decreases in almost direct proportion as the capacity (or flow number) of the atomizer is reduced.

The break in the curves at low fuel flow rates shown in Fig. 2 is probably due to the Weber number effect observed by Simmons and Har-

ding.⁽²³⁾ The Weber number, We , is the ratio of inertial forces to the surface tension forces. The SMD is much more dependent on flow rate when $We < 1$, i.e., at lower flow rates.

This effect was not important in the present study because the minimum fuel flow rates for ignition always occurred at $We < 1$.

Figure 3 shows the effect of fuel type on the

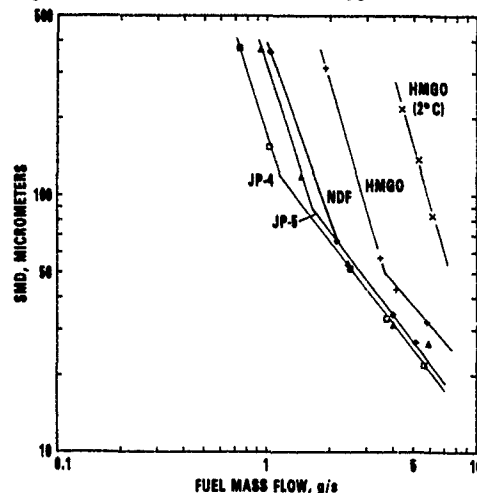


Figure 3. Effect of fuel flow rate and fuel type on SMD produced by the standard T63 atomizer

SMD's measured in sprays produced by the T63 atomizer. The results show that fuel properties have a significant effect on the SMD/mass flow rate correlations. The fuel effect is most pronounced for HMGO at ambient temperature and 274K. Otherwise, the JP-4, JP-5, and NDF fuels tested in the high mass flow rate regime ($We > 1$) gave very similar SMD's. Basically, the effects on SMD's measured in sprays from the Delavan simplex atomizers were similar to those found for the T63 atomizer. However, the fuel effects on SMD appeared to be more pronounced in sprays produced by the Delavan atomizers. This fuel effect was especially apparent among the JP-4, JP-5, and NDF fuel sprays generated at the higher mass flow rates that were used in the actual ignition studies. Considering the fuel properties in TABLE 3, it is apparent that the relatively high SMD's determined for HMGO are most probably attributed to increased viscosity.

Atomization Correlations - The five Delavan simplex atomizers with different flow capacities performed similarly, with the larger capacity noz-

zles producing larger drop sizes at equivalent conditions. The average drop size as represented by the Sauter mean diameter (SMD) could be correlated with the fuel nozzle capacity (flow number), the fuel flow rate, and the fuel viscosity and surface tension as follows:

$$SMD = 4.052 FN^{1.18} \mu^{0.212} \sigma^{0.457} w_f^{-1.16} \quad (2)$$

In correlating the SMD data from the T63 atomizer, it was necessary to account for the airflow directed across the nozzle face used to reduce carbon deposition. This airflow was considered because it had a significant effect on the atomization process. The ignition tests in the T63 combustor were performed at three airflows, 91, 182, and 273 g/s. SMD's were measured with air pressure drops across the T63 nozzle corresponding to combustor airflows of 91 and 273 g/s; the atomization at the intermediate airflow was assumed to be an average of the two extremes. The SMD correlation at the 91 g/s airflow condition for the T63 atomizer was,

$$SMD = 112.6 \mu^{0.399} w_f^{-1.21} \quad (3)$$

and at the 273 g/s airflow condition,

$$SMD = 99.7 \mu^{0.334} w_f^{-1.09} \quad (4)$$

Equations 2 through 4 were used to calculate SMD's of fuel sprays at the ignition limits and to ascertain the effects of atomization on the ignition process in the T63 gas turbine combustor.

Low temperature ignition experiments were conducted at several operating conditions in a T63 combustor rig; TABLE 4 shows the range of test conditions used. To simulate a sea-level start, pressures were kept close to one atmosphere. Burner inlet temperatures were varied from ambient to -34°C (-29.2°F). The mass flow rate of air was varied to change the reference velocity in the combustor. Fuel temperature was varied in order to examine the effects of viscosity, surface tension, and the SMD of the spray

Table 4. Combustor Operating Conditions for Ignition

Pressure, kPa	103 to 124
Burner Inlet Temperature, $^\circ\text{C}$	25, 10, 0, -24, -34
Fuel Temperature, $^\circ\text{C}$	0 to 30
Mass Flow Rate of Air, kg/s	0.09, 0.18, 0.27
Reference Velocity, m/s	5, 11, 16

on the limiting fuel-air ratio for ignition. Fuel temperature was varied both as a result of the variation of inlet temperature, and independently of inlet temperature by using an ice bath. Fuel temperature was monitored by a thermocouple inserted into the fuel line and located at the entrance to the atomizer.

The ignition limits of the test fuels were measured in terms of the overall fuel-air ratio required to achieve ignition at a given set of operating conditions. These tests were performed by first establishing the desired air flow conditions in the combustor. The igniter was turned on, and the fuel flow was started at a flow rate below the ignition limit. The fuel flow was gradually increased, using a motorized valve until ignition occurred. At the point of ignition, the motor turning the fuel valve was stopped, and the minimum fuel flow rate for ignition was recorded.

Most of the ignition measurements were made on Fuels 1 through 6 in TABLE 1. Limited data were obtained on methanol and gasoline. Figure 4 shows the effect of reference velocity on the

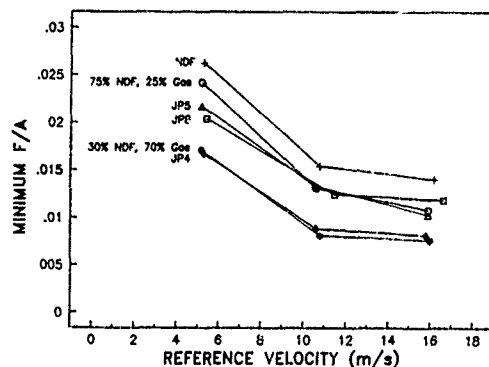


Figure 4. Effect of reference velocity and fuel type on minimum fuel-air ratio for ignition with the standard T63 atomizer

minimum fuel-air ratios for ignition of Fuels 1 through 6 at a fuel and burner inlet temperatures of 300K using the standard T63 dual-orifice atomizer. Similar results were obtained using the Delavan simplex atomizers. It was found that the minimum fuel-air ratio for ignition decreased as the reference velocity was raised. This decrease is explained in part by the fact that the mass flow rate of fuel delivered to the atomizer must increase to maintain the fuel-air ratio when the mass flow rate of air through the combustor is raised. When the fuel flow rate is increased, the SMD of the fuel spray decreases and the

fuel evaporates more rapidly. As a result, the minimum fuel-air ratio for ignition is expected to decrease as the SMD of the fuel spray is lowered.

The fuel effects on the minimum fuel-air ratio for ignition are very apparent in Fig. 4. Fuels such as NDF with high viscosity and low volatility require a higher minimum fuel-air ratio for ignition than the more volatile and less viscous fuels such as JP-4. Fuels with similar viscosities such as JP-8, JP-5, and NDF/25-percent gasoline have similar minimum fuel-air ratios for ignition. It is important to note that Fuel 4, NDF/25-percent gasoline, was blended with the same viscosity as JP-5, but with a front-end volatility ($T_{10\%}$) similar to JP-4. Fuel 5, NDF/70 percent gasoline, was blended with the same viscosity as JP-4, but similar front-end volatility to gasoline. By inspection of Fig. 4 it is apparent that Fuel 4, NDF/25-percent gasoline, has a minimum fuel-air ratio for ignition similar to JP-5. Also, Fuel 5, NDF/70-percent gasoline, has a minimum fuel-air ratio for ignition similar to JP-4. The gasoline data are not presented, but its minimum fuel-air ratio, in fact, falls significantly below that of JP-4. *These results show that fuels of equal viscosity require similar minimum fuel-air ratios for ignition, and that viscosity appears to be more significant than volatility in the ignition process.*

Figures 5 and 6 show correlations of the minimum fuel-air ratio for ignition with viscosity

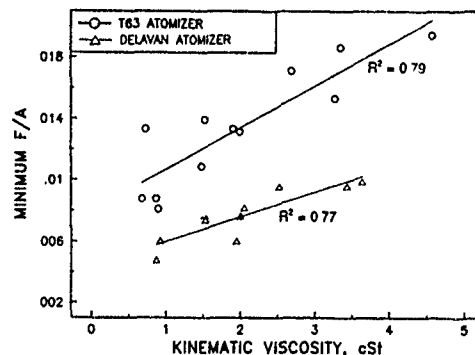


Figure 5. Correlation of minimum fuel-air ratio for ignition with viscosity for the standard T63 atomizer and the 15 liter/hr Delavan simplex atomizer

and 10 percent boil-off temperature, respectively. These data were obtained with the standard T63 dual orifice atomizer and the 15 liter/hr Delavan atomizer. *The results clearly show that the mini-*

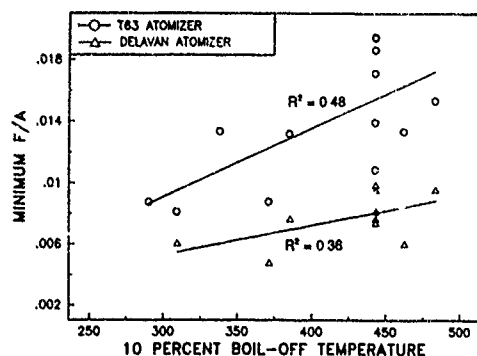


Figure 6. Correlation of minimum fuel-air ratio for ignition with volatility (10 percent pt) for the standard T63 atomizer and the 15 liter/hr Delavan simplex atomizer

minimum fuel-air ratio correlates more favorably with viscosity than front-end volatility.

The effects of atomization on the minimum fuel-air ratio for ignition have been apparent in the results discussed above. Figure 7 shows the effect of atomizer flow number on the minimum fuel-air ratio for ignition. The data were measured using JP-5, a burner inlet temperature of 300K, and reference velocities of 5, 11, and 16 m/s. The six points on each line represent the six atomizers examined. If ignition depended only on achieving a critical fuel-air ratio, there would be little or no dependence on atomizer flow number. The fact that the minimum fuel-air ratio for ignition increases with atomizer flow number means that the average drop size of the spray must be less than some critical value if ignition is to be successful. For the higher capacity atomizers, this critical SMD is reached at a higher fuel flow rate than for the lower capacity atomizers.

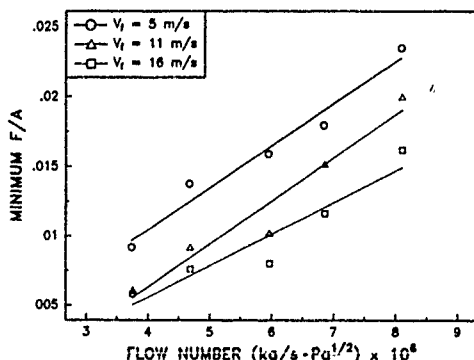


Figure 7. Effect of atomizer flow number on the minimum fuel-air ratio for ignition, JP-5 fuel; data obtained at reference velocities of 5, 11, and 16 m/s

If indeed a critical SMD is the important criteria for ignition, then it should be relatively independent of the flow number of the atomizer. Figure 8 shows the dependence of the SMD at the mini-

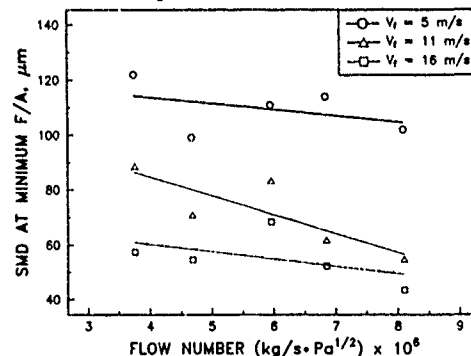


Figure 8. Effect of atomizer flow number on the SMD at minimum fuel-air ratio for ignition of JP-5; data obtained at reference velocities of 5, 11, and 16 m/s

imum fuel-air ratio for ignition versus the atomizer flow number for JP-5 fuel at three reference velocities. The SMD's were calculated from Eqns. 2 through 4. At the 5 m/s condition in Fig. 8, the SMD's ranged from 99 to 122, a factor of 1.2 while in Fig. 7, the corresponding fuel-air ratio at ignition varied by a factor of 2.6 over the range of flow numbers. At 11 m/s and 16 m/s, the respective SMD's ranged from 56 to 88, a factor of 1.6, and 43 to 69, a factor of 1.6 whereas the corresponding fuel-air ratios at ignition varied by 3.2 and 2.7.

In previous combustor studies, the effect of the burner inlet air temperature on ignition has been difficult to discern because of the effect of fuel temperature. In the present study, the effect of fuel temperature was accounted for in the viscosity and surface tension terms of the SMD correlations. Figures 9 and 10 show the effect of burner inlet air temperature on the required SMD at the minimum fuel-air ratio for ignition. These data were obtained with test fuels listed in TABLE 1 using the respective T63 dual orifice and 15 liter/hr Delavan simplex atomizers with a reference velocity through the combustor of 11 m/s. The trend lines through the data indicate that smaller SMD's are necessary for ignition when air temperatures are reduced. The SMD's required for the more volatile fuels such as JP-4 appear to vary more strongly with air temperature than the less volatile fuels like JP-8 and JP-5. In fact, the SMD's required for the less volatile fuels are relatively independent of

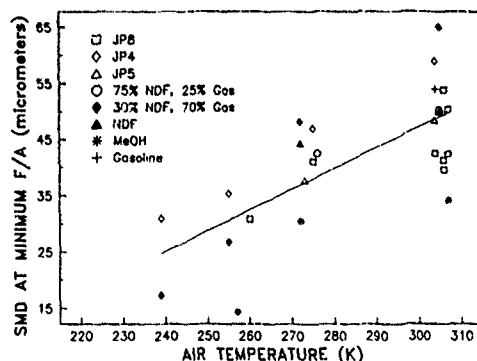


Figure 9. Effect of inlet air temperature and fuel type on SMD required for ignition using standard T63 atomizer and reference velocity of 11 m/s

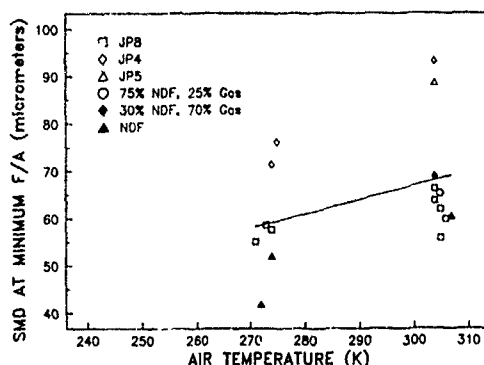


Figure 10. Effect of inlet air temperature and fuel type on SMD required for ignition using 15 liter/hr Delavan simplex atomizer and reference velocity of 11 m/s

the burner inlet temperature. It is also important to note that the NDF/25-percent gasoline fuel blend which had a viscosity close to JP-5, but a volatility similar to JP-4, seemed to require SMD's for ignition nearer to that required by JP-5, JP-8 and NDF. These observations tend to favor fuel viscosity over volatility and suggest that fuel vaporization depends, for the most part, on droplet size.

It should be noted that during engine start up, there is very little compression of the air so that the burner inlet air temperature is essentially the ambient temperature. Thus the significance of these results is that at lower temperatures, changes in the air temperature will not have a significant effect on the ignition characteristics of low-volatility fuels such as JP-8 and JP-5. It is more important to reduce the SMD of the fuel spray. This is because the evaporation of the fuel is caused by the spark energy, not the

air temperature, and also because smaller drops will be more easily carried to the igniter by the airflow and will evaporate more readily.

To reduce the SMD of the spray, it is necessary only to heat the fuel to reduce the viscosity. This can be seen in Eqns. 2, 3 and 4. Figure 11 shows the effects of fuel temperature on viscosity for several aviation fuels.⁽²⁴⁾ In Fig. 10, the ignition characteristics at an air temperature of 273K (0°C) for JP-8 can be improved to that at 305K (32°C) by reducing the SMD by the ratio of the minimum SMD requirement or about 8 percent. Using Eqn. 3, this would mean a viscosity reduction of about 33 percent. From Fig. 11, reducing the viscosity from 2.5 cSt to 1.7 cSt would mean heating the fuel from 0°C to 18°C. This concept would be expected to be applicable to full scale engines starting in cold air, but in general the amount of heating would be different for each engine design. For new aircraft, a fuel tank heater would greatly improve the starting characteristics of cold weather aircraft. To avoid the cost of retrofitting existing aircraft, perhaps loading the aircraft with "warm" fuel, e.g., room temperature, 25°C, just prior to starting would suffice; for quick response time though, a small heater in the fuel tank that the engine draws from would be better. It should also be noted that these results refer only to combustor ignition; there may be other low temperature effects on engine and gear box lubricants that further inhibit engine starting.

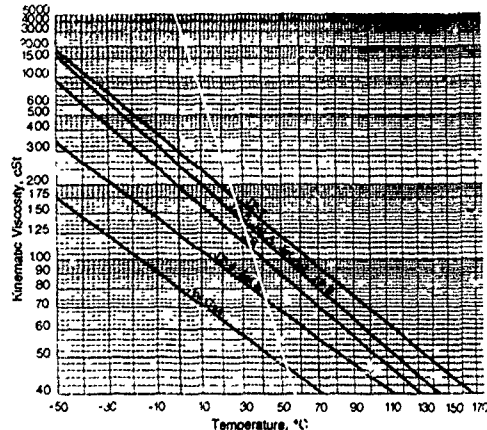


Figure 11. Typical dependencies of viscosity on temperature for aircraft fuels

CONCLUSIONS

Extensive experiments were carried out in a T63 gas turbine combustor to determine which fuel

property, *viscosity or volatility*, is the most critical in low temperature ignition in gas turbine engines.

Ignition depended more strongly on achieving a critical average drop size (SMD) than on reaching the lean-limit fuel-air ratio. Fuel viscosity, which determines atomization characteristics, was found to be more important than volatility in the ignition process. The importance of viscosity was particularly apparent in the less volatile fuels such as JP-5 or JP-8. Volatility effects were most apparent in JP-4 and fuels containing gasoline. Low temperature ignition performance appeared to depend more so on the effect of fuel temperature, i.e., the fuel viscosity, rather than the burner inlet air temperature. This observation has the important practical implication that heating the fuel or using a lower viscosity fuel would be a much more efficient way to improve low-temperature ignition than heating the inlet air, a guideline particularly suited to combustors employing pressure-swirl atomizers for ignition.

REFERENCES

1. Moses, C.A., "Studies of Fuel Volatility Effects on Turbine Combustor Performance," Presented at the 1975 Joint Central/Western States Section Spring Meeting of the Combustion Institute, San Antonio, Texas.
2. Gleason, C.C., et al., "Evaluation of Fuel Character Effects on F101 Engine Combustion System," Final Technical Report AFAPL-TR-79-1018, CEEDO-TR-79-07 (June 1979).
3. Vogel, R.E. and D.L. Troth, "Fuel Character Effects on Current High Pressure Ratio, Can-type Turbine Combustion Systems," Final Technical Report AFAPL-TR-79-2072, ESL-TR-79-29 (April 1980).
4. Oller, T.L., et al., "Fuel Mainburner/Turbine Effects," Final Technical Report AFWAL-TR-81-2100 (May 1982).
5. Gleason, C.C., et al., "Evaluation of Fuel Character Effects on J79 Engine Combustion System," Final Technical Report AFAPL-TR-79-2015, CEEDO-TR-79-06 (June 1979).
6. Gleason, C.C., et al., "Evaluation of Fuel Character Effects on J79 Smokeless Combustor," Final Technical Report AFWAL-TR-80-2092, ESL-TR-80-46 (November 1980).
7. Reider, S.B., Vogel, R.E. and Weaver, W.E., "Effect of Fuel Composition on Navy Aircraft Engine Hot Section Components," Report No. DDAEDR11135 (September 1982).
8. Beal, G.W., "Effect of Fuel Composition on Navy Aircraft Engine Hot Section Components," Report No. PWA/GPD/FR-16456 (August 1982).
9. Rutter, S.D., "Effect of Fuel Composition on T53L13B Hot Section Components," Report No. D12-6-032-83 (March 1983).
10. Rutter, S.D., "Effects of Fuel Composition on Navy Aircraft Engine Hot Section Components, Lot II-Component Test," G.E. draft report prepared under Contract No. N00140-79-C-0483.
11. Ball, I., Graham, M., Robinson, K., Davis, N., "T76 Alternative Fuels Final Report," Garrett Turbine Engine Company, Report No. 21-4744 (August 1983).
12. Ballal, D.R. and Lefebvre, A.H., "A General Model of Spark Ignition for Gaseous and Liquid Fuel-Air Mixtures," 18th Symposium (International) on Combustion, The Combustion Institute, Pittsburgh, pp. 1737-46 (1981).
13. Peters, J.E. and Mellor, A.M., "A Spark Ignition Model for Liquid Fuel Sprays Applied to Gas Turbine Engines," *Journal of Energy*, 6 (4), p. 272 (1982).
14. Peters, J.E. and Mellor, A.H., "Characteristic Time Ignition Model Extended to an Annular Gas Turbine Combustor," *Journal of Energy*, 6 (6), p. 439 (1982).
15. Peters, J.E. and Mellor, A.H., "An Ignition Model for Quiescent Fuel Sprays," *Combustion and Flame*, (38), p. 65 (1980).
16. Derr, W.S. and Mellor, A.H., "Characteristic Times for Lean Blowoff in Turbine Combustors," Presented at the Fall Meeting of the Western States Section/The Combustion Institute (1986).
17. Naegeli, D.W., Moses, C.A., and Mellor, A.H., "Preliminary Correlation of Fuel Effects on Ignitability for Gas Turbine Engines," ASME 83-JPGC-GT-8.
18. Moses, C.A., et al., "An Alternate Test Pro-

cedure to Qualify Fuels for Navy Aircraft, Phase II Final Report, Appendix D. Ignition and Altitude Relight," SwRI-5932-3, NAPC-PE-145C (August 1984).

19. Naegeli, D.W., Dodge, L.G. and Moses, C.A., "Effects of Fuel Properties and Atomization on Ignition in a T63 Gas Turbine Combustor," Interim Report BFLRF No. 235, December 1987.

20. Dodge, L.G., "Calibration of the Malvern Particle Sizer," *Applied Optics*, 23, p. 2415 (1984).

21. Felton, P.G., Hamidi, A.A., and Aigal, A.K., "Multiple Scattering Effects on Particle Sizing by Laser Diffraction," Report No. 413HIC (August 1984).

22. Allen, T., *Particle Size Measurement*, 3rd Ed. Chapman and Hall, New York, p. 139 (1981).

23. Simmons, H.C. and Harding, C.F., "Some Effects of Using Water as a Test Fluid in Fuel Nozzle Spray Analysis," ASME 80-GT-90 (1980).

24. Handbook of Aviation Fuel Properties, CRC Document No. 50, p. 34, Coordinating Research Council, Atlanta, Georgia (1983).

ACKNOWLEDGEMENTS

This work was performed by the Belvoir Fuels and Lubricants Research Facility (BFLRF) located at Southwest Research Institute (SwRI), San Antonio, Texas under Contract Nos. DAAK70-85-C-0007 and DAAK70-87-0043 with the U.S. Army Belvoir Research, Development and Engineering Center (Belvoir RDE Center). Funding was provided by the Naval Air Propulsion Center (NAPC) through a Military Interdepartmental Purchase Requisition, and also in part with funds from the SwRI Fuels and Lubricants Research Division.

Mr. P.A. Karpovich was the principal NAPC staff member providing Program direction. Mr. F.W. Schackel of Belvoir RDE Center (STRBE-VF) served as the Contracting Officer's representative; and Mr. M.E. LePera, Chief of Fuels and Lubricants Research Division (STRBE-VF), served as the project technical monitor.

Messrs. R.C. Haufier and M.G. Ryan conducted the experimental measurements. Ms. S.J. Hoover and Ms. L.A. Pierce performed the manuscript preparation with the editorial assistance of Mr. J.W. Pryor and Ms. C.G. Wallace. Mr. S.J. Lestz provided assistance in contract management.

Discussion

1. R. Pollak, Pratt and Whitney

Have you examined the effect of small quantities of lower viscosity/higher volatility fuels, say JP5, mixed into more viscous/low volatility fuels, say JP4, to obtain better ignition characteristics at cold temperatures?

Author:

We have conducted experiments such as this several times over the years including the results reported here where two of the test fuels were blends of gasoline in diesel fuel to tailor the viscosity and volatility properties. In earliest studies (at ambient air temperatures) we used blends of pentane with both Jet-A and diesel fuel. In all cases, the addition of the lighter materials improved the ignition characteristics of the combustor. We have not, however, conducted a thorough study of the type you mentioned in the sense of developing a fuel sensitivity model for low-temperature ignition. The significance of the more recent studies, of which the work reported here was a part, is that we can now do these combustor experiments at low temperatures and make detailed measurements of atomization, air-fuel ratio and velocities at the spark gap, and spark energy to isolate the fuel variables.

2. P. Kotsiopoulos, Hellenic Air Force Academy

I would like to know if you have any comments to make about the effect of the change of fuel composition, for instance from JP4 to JP8, on the hot engine components as a result of the change of the viscosity — provided that the mass flow rate is kept constant by adjusting the fuel control system.

Have you observed any phenomena like carbon particle formation at the hot parts etc?

Author:

Fuel effects on hot-section durability are due to increases in the flame radiation or changes in temperature distributions, i.e. hot streaks. The major differences between JP4 and JP8 which could cause these problems are lower hydrogen content and higher viscosity. Lower hydrogen content increases the soot formation and flame radiation in the primary zone leading to higher liner temperatures. This soot can also deposit on the liner surfaces or atomizer face and disturb the flow pattern leading to hot spots. Higher viscosity means larger drops in the fuels spray and could mean inadequate air-fuel mixing or even impingement on the liner. Such problems are generally eliminated in the design of the combustor and most combustors are designed to operate satisfactorily on both fuels; however, it is possible that in an older, perhaps marginally designed combustor, a change from JP4 to JP8 could result in inadequate air-fuel mixing and/or create an increase in deposit formation in isolated areas and lead to durability problems. In the combustor studies conducted by the US Air Force, there were no hot section durability problems identified due to a change from JP4 to JP8.

GIVRAGE DES CIRCUITS DE CARBURANT DES TURBORREACTEURS

par

Francis GARNIER

Ingénieur expert en systèmes d'huile

SNECMA

Direction technique

Centre d'essais de Villaroche

77550 MOISSY-CRAMAYEL (FRANCE)

RESUME

Sur les avions civils, il n'est pas de pratique courante d'ajouter d'additifs anti-givre dans le carburant. Il s'ensuit aux très basses températures des risques de dépôts de givre dans certains composants des circuits moteur à partir de l'eau inéluctablement contenue dans le carburant.

Ce phénomène de givrage peut affecter tous les moteurs à la fois au moment du décollage, entraîner des perturbations importantes touchant leur pilotabilité, pouvant même aller jusqu'à leur extinction.

Pour éviter le givrage, la solution la plus simple est de réchauffer suffisamment le carburant avant son entrée dans les composants sensibles pour qu'il soit toujours à température positive; la difficulté étant de connaître avec suffisamment de précision la quantité de calories disponibles sur le circuit d'huile dans les conditions extrêmes froides dès le début des études de développement d'un nouveau moteur.

Nous avons donc été amenés à développer, mettre au point et valider un modèle mathématique capable de déterminer les équilibres thermiques huile/carburant dans tout le domaine d'exploitation du moteur.

A partir des analyses effectuées grâce à ce modèle, il a été possible de définir une solution simple qui, sans rien changer à l'équilibre du circuit d'huile, a permis de réchauffer suffisamment les circuits d'asservissement.

Au cours de cet exposé, nous décrivons ce modèle, les principales analyses effectuées, l'installation d'essai et les résultats obtenus en conditions extrêmes de givrage qui montrent que la solution retenue avec réchauffeur huile-carburant des servomécanismes permet un fonctionnement correct jusqu'à - 45 °C au lieu de - 30 °C pour des conditions identiques sur le circuit d'huile.

PREAMBULE

Le carburant consommé par les moteurs d'un avion est stocké dans un système de réservoirs situés dans les ailes et la partie centrale du fuselage de l'avion. Après un système de transferts entre réservoirs, il est pompé dans une "nourrice" et acheminé vers les moteurs. Pour des raisons de sécurité, pollution de l'environnement en particulier, ce carburant est très souvent stocké sur les aéroports dans des cuves non enterrées. En conséquence, par temps froid, on peut considérer que le carburant pompé vers le moteur est à la température ambiante qui peut atteindre, dans certains pays, des valeurs excessivement basses. Malgré toutes les précautions prises par les compagnies pétrolières qui assurent l'avitaillement des avions, de l'eau peut subsister dans le carburant sous forme dissoute et libre.

Aux températures négatives, l'eau libre se trouve en suspension sous forme de micro-paillettes de glace qui seront pompées avec le carburant. Ces cristaux de glace peuvent obturer les circuits carburant: les filtres, mais aussi et surtout les systèmes de régulation qui dosent le carburant à injecter dans la chambre de combustion ou qui commandent la position des vannes de décharge et des stators à calage variable. Il peut s'ensuivre de graves perturbations pouvant affecter la pilotabilité du moteur et conduire, à la limite, à l'extinction des moteurs. Des moteurs, en effet, car le phénomène de givrage peut les affecter tous à la fois puisque la cause est commune.

Si on montre par les calculs que la condition la plus critique est celle du régime de décollage, on comprend alors la gravité de situation que peut engendrer le phénomène de givrage des circuits carburant. Si en exploitation militaire, le problème est résolu par l'adjonction au carburant de produits anti-givre, cette pratique n'existe généralement pas en exploitation commerciale. Il revient donc au motoriste la charge de définir et d'installer sur le moteur un système permettant d'éviter le phénomène de givrage ou, pour le moins, d'éviter ses conséquences.

Nous vous proposons au cours de cet exposé de présenter :

En 1^{ère} partie :

- les diverses solutions qui avaient été imaginées lors de la conception du CFM56 et plus particulièrement celle qui a été retenue
- les analyses et les calculs qui ont permis d'aboutir à ce choix

En 2^{ème} partie :

- les moyens d'essais mis en oeuvre
- les essais de validation effectués au banc de simulation

En 3^{ème} partie :

- une actualisation

1^{ère} PARTIE - L'ANALYSE

1 - LE CIRCUIT CARBURANT DE BASE

Il comprend, pour ce qui nous intéresse :

- les réservoirs de carburant (partie avion)
- la pompe basse pression du moteur (pompe B.P.)
- un filtre qui protège la pompe haute pression à engrenage (pompe H.P.)
- la régulation du moteur
- la chambre de combustion avec ses injecteurs
- un échangeur de chaleur destiné à refroidir l'huile de lubrification du moteur

2 - ELEMENTS DU CIRCUIT POUVANT ETRE AFFECTES PAR LE GIVRAGE

En conditions givrantes, les cristaux de glace véhiculés par le carburant peuvent affecter le fonctionnement de certains organes du circuit carburant.

2-1 ECHANGEUR HUILE CARBURANT

Bien que l'huile du moteur soit chaude, les tubes et les plaques frontales de l'échangeur peuvent être à température négative, favorisant l'accrochage et l'accumulation des cristaux de glace. Il va s'ensuivre une diminution de la section libre pour le passage du carburant et consécutivement une augmentation de la perte de charge de l'échangeur; la limite étant l'obstruction totale. A partir d'une certaine valeur, le clapet de dérivation va s'ouvrir, pouvant à la limite dériver tout le carburant. La réduction du débit carburant dans la matrice conduit à une augmentation de la température de l'huile, des plaques frontales et des tubes. Le dégivrage de la matrice va s'opérer progressivement jusqu'à refermeture du clapet. Ce phénomène d'ouverture fermeture peut s'opérer plusieurs fois mais sans jamais perturber réellement le fonctionnement correct du moteur, si les systèmes en aval peuvent accepter du givre, bien sûr.

2.2 FILTRE

Les premières manifestations du phénomène de givrage se produisent sur le filtre à carburant à cause des températures de paroi plus basses d'une part et des sections de passage unitaires plus faibles d'autre part. Dans les cas de colmatage extrême par le givre, le moteur peut être amené à fonctionner clapet ouvert, c'est à dire sans filtration, pendant une durée importante du vol; le moteur fonctionnant néanmoins correctement, seule la durée de vie de la pompe H.P. risque d'être affectée.

2.3 REGULATEUR

Les servomécanismes du régulateur qui dosent le carburant et fixent la position des systèmes à géométrie variable (VSV et VBV) constituent la partie du moteur qui peut entraîner des conséquences graves en cas de givrage. En effet, le colmatage de ces organes peut conduire à des perturbations importantes sur le fonctionnement du moteur: délai d'obtention important voire non obtention du taux de poussée affiché par le pilote à la manette des gaz; ces perturbations pouvant aller jusqu'à l'extinction du moteur, situation particulièrement grave puisque, comme nous allons le voir, la condition la plus critique se situe à pleine puissance du moteur, c'est à dire au régime de décollage et de montée donc à très basse altitude. Les analyses ont donc porté plus particulièrement sur cette partie du circuit carburant.

3 - LES REGLEMENTS

Les règlements demandent que le moteur soit capable de fonctionner correctement dans tout le domaine d'utilisation pour lequel il est conçu avec du carburant initialement saturé d'eau à 27°C (80°F) et ayant au moins 0,75 cm³ d'eau libre ajoutée par US gallon de carburant (200PPM) et refroidi jusqu'à la condition la plus critique du point de vue givrage pouvant être rencontrée en exploitation.

4 - ANALYSE

En l'absence d'additifs anti-givre ajoutés au carburant ou de systèmes capables d'enlever tous les cristaux de glace pouvant être contenus dans le carburant, la première solution qui vient à l'esprit est de réchauffer suffisamment les circuits pour que, dans la condition de vol la plus sévère, les pièces et le carburant lui-même soient à température positive. En effet, il ne suffit pas que le fluide soit à température positive pour éviter tout problème lié au givrage : les cristaux de glace qui n'ont pas eu le temps de fondre peuvent adhérer aux pièces à température négative et obturer les circuits; la température des pièces dépendant des échanges thermiques avec le carburant d'une part et avec l'air de l'environnement (nacelle) d'autre part. Il est clair que la condition la plus critique se rencontrera lors de fonctionnements aux températures les plus basses spécifiées.

Les études ont porté plus particulièrement sur les cas de vol suivants :

- décollage, maxi continu et maxi montée en ISA -124°F (Tamb=-54°C)
- maxi montée et maxi continu depuis le sol jusqu'à une altitude de 35000 ft en atmosphère extrême froide.

Pour mener à bien ces études, un modèle de calcul comportant plusieurs modules a été créé et validé sur des résultats d'essais provenant des moteurs en développement.

Le modèle complet comprend les modules suivants :

- le "module technologie" dans lequel sont introduites toutes les données géométriques permettant de décrire le moteur :
 - . géométrie des roulements, des pignons
 - . surfaces d'échange des enceintes-huile
 - . définition géométrique des joints à labyrinthe
 - . description des rotors susceptibles d'entraîner de l'air ou de l'huile en rotation
 - . diamètre et longueur des tuyauteries
 - . circulation des fluides au sein du moteur
 - . liaisons mécaniques entre le moteur proprement dit et ses équipements
- le "module thermodynamique" permettant d'introduire les données du cycle pour les points que l'on désire calculer :
 - . vitesse de rotation des corps
 - . températures, pressions et débits à des points caractéristiques des flux primaires et secondaires
- le "module circuit d'huile", le plus important, contient les méthodes de calcul. C'est lui qui calcule la puissance calorifique recueillie par l'huile qu'il délivre sous la forme d'une courbe
- le "module circuit carburant", il contient la technologie et les méthodes de calcul propres au circuit carburant. C'est lui qui calcule l'équilibre et délivre les températures
- le "module échangeur" fait l'interface entre les modules "circuit huile" et "circuit carburant" et contient les champs d'efficacité des échangeurs provenant d'essais ou d'analyses; c'est à dire l'efficacité thermique en fonction des débits et des températures

4.1 DETERMINATION DE LA PUISSANCE CALORIFIQUE DISPONIBLE DANS L'HUILE PAR LE MODELE "CIRCUIT D'HUILE"

Pour une condition de vol et un fonctionnement moteur donné, la puissance calorifique W_h rejetée par le moteur sur le circuit d'huile ne dépend plus que de la Température d'Huile à l'Entrée du Moteur. Le rôle du module "circuit d'huile" est donc de déterminer les courbes $W_h = f(THEM)$ pour tous les cas de vol étudiés. La puissance totale recueillie par l'huile est la somme de toutes les puissances élémentaires rejetées par les composants du moteur en contact avec l'huile. Ces puissances sont calculées analytiquement et non pas par une identification avec des résultats obtenus sur le moteur lui-même.

Elle proviennent :

- des roulements des lignés d'arbres; c'est la plus grande part : environ 60% au plein gaz, jusqu'à 90% au ralenti.
- des pignons et engrenages
- des échanges de chaleur entre les enceintes-huile et leur environnement (convection + rayonnement + conduction au travers des supports de palier)
- de l'air de pressurisation introduit dans les enceintes au travers des joints à labyrinthes
- des centrifugations d'huile créées par les rotors contenus dans les enceintes
- des puissances mécaniques nécessaires à l'entraînement en rotation du groupe de lubrification (circuit fermé)
- du frottement de l'air sur les parties tournantes situées dans les enceintes : friction sur le voile des engrenages, friction entre rotor

- et stator dans les labyrinthes, ...
- des échanges de chaleur, principalement par convection, entre les équipements et l'air nacelle : réservoir d'huile, boîte d'engrenages, tuyauteries, pompes à huile, ...
- des échanges de chaleur par convection et rayonnement entre les tuyauteries dans la traversée des parties chaudes du moteur : traversées des bras du carter d'échappement par exemple

Ce module, le plus compliqué, comporte environ 1400 lignes d'écriture en FORTRAN

4.2 DETERMINATION DU NIVEAU D'EQUILIBRE THERMIQUE ENTRE L'HUILE ET LE CARBURANT PAR LE MODULE "CIRCUIT CARBURANT"

La puissance calorifique recueillie par l'huile est transmise au carburant par les échangeurs de chaleur. Selon leur efficacité thermique, cette transmission se fera à des niveaux plus ou moins élevés sur chacun des circuits :

- * efficacité élevée : - niveau bas sur l'huile
- niveau élevé sur le carburant
- * efficacité faible : - niveau élevé sur l'huile
- niveau bas sur le carburant

Comme le module précédent, ce module comporte un sous-programme permettant de calculer les puissances calorifiques générées au sein du circuit carburant lui-même par les pompes basse pression et haute pression, la recirculation de carburant dans la boucle par dégradation de l'énergie de pression, les diverses pertes de charge jusqu'aux injecteurs. Par ailleurs, il prend en compte les échanges thermiques entre les composants du circuit et l'air nacelle.

Enfin, comme nous l'avons déjà vu, il détermine l'équilibre par application du premier principe de la thermodynamique.

4.3 VALIDATION DU MODELE

Avant d'entreprendre des calculs pour déterminer les températures susceptibles d'être atteintes en extrême froid, il convient de valider les résultats produits par le modèle composé des deux principaux modules décrits plus haut, dans un domaine de fonctionnement exploré en essai le plus large possible, de façon à faire varier tous les paramètres influents sur une plage la plus large possible. Car, il est bien évident que si les conditions de basses températures peuvent être reproduites en essai partiel sur le circuit carburant, elles ne peuvent l'être sur un moteur complet en fonctionnement, particulièrement au régime du plein gaz.

4.3.1 MODULE "CIRCUIT D'HUILE"

Pour ce faire, lors du développement du CFM56-2, les circuits d'huile et de carburant du moteur 004 ont été fortement instrumentés et un programme d'essai spécifique a été réalisé.

Un aménagement des circuits au niveau des échangeurs de chaleur a été nécessaire de façon à explorer une plage de température d'huile plus large que celle rencontrée normalement au banc sol :

- . adjonction sur le circuit d'huile d'échangeurs supplémentaires huile/eau et huile/azote liquide de façon à abaisser la température d'huile à l'entrée du moteur aussi près que possible des températures précalculées par le modèle lors d'un fonctionnement stabilisé au sol sur avion en extrême froid.
- . adjonction d'un système de vannage, sur le circuit de manière à dériver de l'échangeur tout ou partie de l'huile de manière à obtenir des températures d'huile élevées.

Ces essais ont permis d'obtenir un nombre important de résultats couvrant toutes les vitesses de rotation possibles sur une plage de températures d'huile à l'entrée du moteur variant de 20 à 120 °C. L'effet des prélèvements d'air et mécanique a également été quantifié.

C'est à partir de ces champs de valeurs que le "module circuit d'huile" a été vérifié et validé. Il est bien évident que de nombreuses retouches ont dû être effectuées.

En particulier, il s'est avéré que les puissances calorifiques obtenues sur moteur aux faibles températures d'huile étaient plus faibles que celles obtenues par le calcul; ceci provenant principalement du choix des exposants sur le terme de viscosité dans la méthode utilisée initialement pour le calcul des puissances calorifiques générées par les roulements.

D'autre part, des aménagements ont dû être apportés en ce qui concerne la détermination des puissances calorifiques générées par barattage de l'huile dans les enceintes confinées ou l'effet de la pression dans ces mêmes enceintes : effet

du frottement de l'air sur les rotors. Une boîte d'engrenages fonctionnant avec une pression interne de 1,5 bar absolu dissipera plus de puissance qu'à 0,5 bar absolu.

L'effet des ventilations externes au moteur a dû également être affiné pour tenir compte de l'environnement : moteur au banc sol sans nacelle ou moteur avionné avec des nacelles de types de ventilation différents.

Les corrélations calculs/essais obtenues in fine sont les suivantes :

• au banc sol sur le moteur 004/4

La comparaison des puissances met en évidence l'excellent accord calculs-essais pour tout le champ régimes-températures exploré au banc. L'écart quadratique moyen est de 6 % ce qui se traduirait au sol par un écart maximum de 2 °C sur le niveau d'équilibre des températures

• en vol

* sur banc volant "Caravelle". Moteur 006/2.

* sur avion YC15 avec le moteur 003/2.

Le but de ces recoupements était de s'assurer que les effets de moteur, d'altitude et de ventilation nacelle (effet du mach de vol) étaient correctement restitués.

4.3.2 MODULE "ECHANGEURS DE CHALEUR"

Dans sa version finale, ont été introduits dans ce module les résultats d'essai obtenus au banc partiel, par simulation des conditions réelles de températures d'huile et de carburant à l'entrée des échangeurs pour respecter les effets de REYNOLDS, d'épaisseur de couche limite

4.3.3 MODULE "CIRCUIT CARBURANT"

Le même processus que 4.3.2 a été appliqué, c'est à dire des champs de performances provenant des essais partiels réalisés sur les pompes H.P. et B.P. et le circuit carburant au complet mais dépourvu de calories provenant du moteur et transmises par les échangeurs.

4.3.4 MODELE COMPLET

Chaque module ayant été préalablement testé et validé séparément, il ne pouvait subsister que des problèmes d'interface entre les modules; c'est à dire des problèmes d'écriture informatique mais nullement de simulation mathématique des systèmes ou des phénomènes physiques.

La précision finale, en terme de température est meilleure que 6 °C.

A la suite de quoi le modèle a été déclaré validé et applicable à la détermination des températures d'équilibre en particulier en extrême froid.

5 - SPECIFICATIONS

Un moteur d'avion doit être capable de fonctionner correctement sur une plage très étendue de température ambiante : depuis - 55 °C jusqu'à + 55 °C environ au sol; le carburant, comme nous l'avons vu, étant également supposé être à cette température à l'entrée du moteur. On conçoit que les systèmes de refroidissement d'huile/réchauffage de carburant ne pourront être qu'un compromis pour satisfaire les valeurs des températures limites souhaitées sur chacun des circuits. D'où la nécessité de spécifier ces valeurs, qui peuvent résulter pour certaines des propriétés physiques des fluides et pour d'autres de considérations fonctionnelles inhérentes au moteur lui-même : expérience acquise, essais partiels, analyses ...

Il est ainsi apparu nécessaire après analyse :

- que le débit de carburant qui traverse les asservissements soit réchauffé suffisamment de manière que la température du fluide soit toujours supérieure à 10°C et non pas 0 °C afin de tenir compte des effets de convection autour du régulateur d'une part et d'échanges thermiques à l'intérieur du régulateur entre le carburant principal froid (< 0 °C) et le carburant chaud des asservissements d'autre part (cas du réchauffage du débit d'asservissement)
- que les températures extrêmes pouvant être atteintes sur les circuits d'huile restent à l'intérieur des limites acquises par l'expérience, tant à froid qu'à chaud; ce qui a pour effet, dans les cas qui nous intéressent, de limiter le prélèvement de puissance sur le circuit d'huile
- que les températures maximales dans le circuit carburant restent, en atmosphère chaude, inférieures à certaines valeurs pour éviter tout problème de cavitation des pompes, de "vapor-lock" ou de cokéfaction.

Par ailleurs, il était demandé que les circuits soient les plus simples possibles. En particulier, il était conseillé d'éviter tout système de vanne thermostatique ou commandé par calculateur. En un mot, éviter toute géométrie variable.

6 - DETERMINATION DES TEMPERATURES D'EQUILIBRE EN CONDITIONS EXTREMES FROIDES

Le modèle établi et validé comme nous l'avons vu, va nous permettre maintenant de simuler les conditions extrêmes froides en introduisant dans le "module thermo-dynamique" les conditions aux limites représentatives des cas que l'on veut étudier; valeurs déterminées en amont par un autre modèle.

Dans les conditions de températures au sol ISA - 124 °F ($T_{amb} = -54$ °C) et nombre de Mach de vol sévère du point de vue ventilation autour du moteur, la puissance calorifique recueillie par le circuit d'huile du moteur dépend du niveau de poussée demandé par le pilote. C'est cette puissance qui va d'abord être utilisée pour réchauffer le carburant et les pièces, car elle est gratuite. Elle ne dépend pas du système de réchauffage de carburant que l'on va être amené à adopter : un ou plusieurs échangeurs, huile/carburant, huile/air, air/carburant ou autre, ainsi que nous l'avons déjà souligné au paragraphe 4.1. Elle ne sera donc calculée qu'une seule fois par le "module huile"; ce qui a l'avantage d'éviter des itérations entre ce module et le "module carburant" et d'accroître la vitesse de calcul.

6.1 EQUILIBRE OBTENU SUR LE CIRCUIT DE BASE (SANS RECHAUFFEUR)

Ce circuit est le plus simple. Hélas, s'il est satisfaisant dans la plupart des cas, il ne l'est pas à froid. La température de 10 °C minimum à l'entrée des servomécanismes est loin d'être satisfaite.

Dans la condition de décollage extrême froid ($T_{amb} = -54$ °C), la température du fluide à l'entrée des servomécanismes atteint 0 °C pour une température du carburant de -30 °C à l'entrée du moteur. Pour satisfaire la condition des +10 °C, il ne faudrait pas que la température du carburant pompé soit inférieure à -15 °C. Ceci montre tout simplement l'incapacité du moteur à réchauffer suffisamment tout le carburant qu'il consomme. L'énergie calorifique provenant du circuit d'huile et du circuit carburant (laminages, rendement des pompes) ne permet d'échauffer toute la masse consommée que de 25 °C à 30 °C (-15 °C \rightarrow +10 °C et -30 °C \rightarrow 0 °C); la différence de 5 °C provenant de la pente négative de la puissance calorifique délivrée par le moteur en fonction du niveau d'équilibre THEM.

Pour satisfaire la condition des 10 °C, il faudrait apporter au carburant consommé environ 3 fois plus de puissance que le moteur n'en dispose. Les solutions consistant à apporter ce manque de chaleur par des systèmes électriques ou par prélèvement d'air chaud sur le compresseur (échangeur air/huile ou air/carburant) ont été envisagées, étudiées, puis abandonnées pour des raisons diverses: complexité, sécurité, fiabilité, masse, performance du moteur, etc...

Des considérations précédentes, il ressort que la voie à suivre pour protéger le circuit carburant contre le givrage, en utilisant la seule puissance thermique disponible sur le circuit d'huile, est la suivante :

- réchauffer suffisamment le débit carburant qui traverse les asservissements du régulateur (débit 4 fois plus faible que celui consommé) de manière à ce que la température du fluide soit supérieure à 10 °C
- compléter le refroidissement de l'huile jusqu'aux niveaux de température désirés par un refroidisseur adapté situé en lieu et place de celui qui existe dans le circuit de base
- démontrer par des essais partiels que la partie du régulateur non suffisamment réchauffée est capable de fonctionner correctement pendant des temps très longs en condition givrante

C'est cette solution qui a été également utilisée avec succès par notre partenaire GENERAL ELECTRIC sur ses moteurs CF6-50 et CF6-80.

6.2 EQUILIBRE OBTENU SUR LE CIRCUIT AVEC UN RECHAUFFEUR DES SERVOMECHANISMES

Tout d'abord, de très nombreux calculs ont été nécessaires pour définir le meilleur couple (refroidisseur d'huile, réchauffeur des servomécanismes) du point de vue de leurs efficacités respectives, et du choix de leur emplacement dans les circuits. Mais aussi pour s'assurer que, dans tous les domaines d'exploitation possibles du moteur, les températures d'huile et de carburant ne dépassaient pas les limites fixées : effet des régimes de rotation, de l'altitude, des conditions ambiantes, froides mais aussi chaudes, des diverses phases de vol, des prélèvements, de l'état du moteur et de ses équipements (influence du débit d'huile délivré par la pompe d'alimentation, d'une erreur sur l'estimation de la puissance rejetée sur l'huile, du débit d'asservissement, de la nature des fluides utilisés : huile type I ou type II, carburant JETA, JP4, etc ...).

Hormis pour la température du carburant à l'entrée des servomécanismes, cette optimisation a permis de rendre le niveau général d'équilibre pratiquement insensible à la présence ou non du réchauffeur des servomécanismes. C'est à dire que la présence du réchauffeur n'abaisse et n'échauffe que de 1 à 2 °C le niveau des températures d'huile et de carburant à l'injection dans la chambre de combustion.

Les évolutions des températures calculées en fonction de la température du carburant TCa à l'entrée du moteur font apparaître :

- un classement des températures inverse de celui de l'énergie calorifique recueillie par le circuit d'huile. Ceci provient du fait que, dans la condition décollage par exemple, le débit carburant consommé a relativement plus augmenté que l'énergie recueillie par l'huile : plus le taux de poussée du moteur est élevé, plus les niveaux d'équilibre thermique des circuits sont bas
- en extrême froid un rehaussement de la température du carburant des servomécanismes de 25 °C par rapport à celle à l'entrée du régulateur et un niveau d'équilibre qui se situe autour de 10 °C. Rappelons qu'en l'absence de réchauffeur de carburant des servomécanismes, la température à l'entrée de ceux-ci serait celle à l'entrée du régulateur.

7 - CONCLUSION DES ETUDES

Les nombreuses analyses effectuées ont montré qu'en condition extrême froide, le circuit d'huile du moteur n'est pas capable de réchauffer tout seul la totalité du carburant consommé jusqu'à un niveau de température tel que toute cause de givrage puisse être évitée sur la totalité des équipements mouillés par le carburant.

Si pour certains, le givrage ne peut entraîner que des dysfonctionnements locaux n'affectant pas la marche normale du moteur, pour le régulateur et ses asservissements, on peut être confronté à des ennuis graves affectant la pilotabilité même du moteur, pouvant aller à la limite jusqu'à son extinction par mauvais dosage du carburant ou mauvais contrôle de la position des staturs variables. La recherche d'une solution simple nous a conduit à réchauffer séparément les servomécanismes, partie la plus sensible, jusqu'à un niveau de températures évitant tout risque de givrage et le circuit principal du régulateur jusqu'au maximum possible autorisé par le circuit d'huile du moteur; la température dans le régulateur restant cependant fortement négative en extrême froid.

Le domaine de fonctionnement correct de ce concept ne pouvait qu'être exploré et validé par des essais partiels reproduisant le plus fidèlement possible les conditions de givrage susceptibles d'être rencontrées en exploitation. C'est l'objet de la deuxième partie.

2^{ème} PARTIE - LES ESSAIS EN CONDITIONS GIVRANTES

Les essais de simulation ont été effectués au Centre d'Essais des Propulseurs (CEPr) de SACLAY (FRANCE), centre disposant de moyens d'essai et d'investigation très importants mis à la disposition des constructeurs de moteurs aéronautiques mais aussi des avionneurs, en particulier pour ce qui concerne les simulations de vol en altitude.

1 - GENERALITES SUR LES CONDITIONS DE SIMULATION

Des analyses présentées en première partie, il ressort que les conditions de décollage sont les plus critiques et couvrent par leur sévérité tous les autres cas de vol possibles. En conséquence, nous nous sommes attachés à faire subir au circuit carburant complet les conditions qu'il pourrait être à même de rencontrer sur avion dans des conditions de températures extrêmes : Décollage $Z = 0$, $M = 0.6$, $ISA = -124$ °F.

1.1 TENEUR EN EAU

Nous avons déjà vu que les règlements demandent que la teneur en eau libre ne soit pas inférieure à 200 PPM au cours des essais; le carburant à 27 °C ayant été préalablement saturé en eau dissoute. Ce qui, compte tenu des courbes de solubilité de l'eau dans le carburant, conduit à un rapport en masse de 0.0078 % d'eau dissoute dans le carburant, soit environ 100 PPM en volume.

Dans la réalité sur avion, cette eau dissoute peut se libérer totalement grâce à l'abaissement de la pression avec l'altitude. En définitive, le carburant peut contenir, à la limite, jusqu'à 300 PPM d'eau libre : cas d'un avion long courrier décollant d'un pays chaud et humide (zones équatoriales) et contraint de redécoller en fin de mission suite à un atterrissage avorté. En conséquence, l'ensemble des essais a été effectué avec une quantité d'eau en volume équivalente à 300 PPM au moins d'eau libre.

1.2 PUISSANCE CALORIFIQUE

Un paramètre très important à simuler est la loi de puissance calorifique transférée par les échangeurs, du circuit d'huile moteur au circuit carburant: loi qui n'est pas constante mais, comme nous l'avons vu en première partie, décroissante quand la température d'huile à l'alimentation du moteur augmente. Le débit d'huile étant constant et fixé, le plus simple était de restituer par un système de régulation la différence de température (sortie moteur - entrée moteur) en fonction de la température entrée moteur.

1.3 ENVIRONNEMENT

On s'est efforcé de recréer autour des équipements, les conditions aérothermiques les plus défavorables susceptibles d'être rencontrées sur avion : respect de la température ambiante et du coefficient d'échange par convection. Ce qui a nécessité d'installer tous les matériels en essai dans une enceinte climatique calorifugée.

1.4 TEMPERATURE CARBURANT

De façon à déterminer les limites de fonctionnement correct des systèmes, des essais de 5 en 5 degrés ont été effectués depuis - 25 °C jusque vers - 50 °C.

1.5 DUREE DE CHAQUE PHASE D'ESSAIS

La majorité des essais a été effectuée pendant des durées continues de 60 et 90 minutes en conditions extrêmes de givrage.

1.6 CONFIGURATIONS

- 2 configurations ont été testées :
- sans réchauffeur des servomécanismes
 - avec réchauffeur des servomécanismes

1.7 FLUIDES

* CARBURANT

Pour tous les essais, le carburant utilisé était du TR-0 (JET A1) sans additif anti glace. Il répondait à la norme AIR 3405/C.

* HUILE

L'huile utilisée sur le circuit des échangeurs était de l'huile synthétique répondant aux exigences de la norme AIR 3514 (type I).

2 - MATERIELS EN ESSAI

La configuration d'essai était en tout point identique au montage des circuits carburant et huile du moteur (équipements, diamètres de canalisation, boucles d'asservissement...). Les écarts par rapport aux modèles définitifs ne portaient que sur l'aspect physique extérieur, dus aux modes de fabrication, mais ne remettaient pas en question leur fonction. Par ailleurs, les liaisons mécaniques et hydrauliques étaient identiques à celles utilisées sur moteur.

3 - INSTALLATION D'ESSAI

La définition, la réalisation et la mise au point de cette installation ont été effectuées par le CEPr de SACLAY sur la base des spécifications d'essai émises par la SNECMA.

Elle se composait des parties principales suivantes :

- * un circuit carburant
- * un circuit d'huile
- * un circuit d'air régulé
- * une enceinte climatique
- * un dispositif d'entraînement mécanique

3.1 LE CIRCUIT CARBURANT

Parmi les différentes procédures d'essais de givrage appliquées au CEPr sur les circuits de carburant et leur composants, c'est celle du "refroidissement préalable et d'ingestion d'eau proportionnelle" qui a été retenue, car elle permet de réaliser des dosages précis et des essais de longue durée : plus de 9 heures dans notre cas.

Dans ce type d'essais, une des difficultés vient du fait que le débit d'eau à injecter dans le carburant est souvent faible : quelques litres par heure.

En conséquence, on crée 2 circuits :

- * Le circuit principal constitué d'un réservoir de grande capacité contenant le carburant nécessaire à l'exécution de l'essai, refroidi à la température demandée et envoyé vers les matériels à tester.
- * Un circuit secondaire comportant un réservoir d'eau et un réservoir de carburant. Il permet d'obtenir un mélange eau + carburant à la température ambiante. Ce mélange est introduit dans le circuit principal par un injecteur qui délivre un débit correspondant à la concentration souhaitée.

Cinq fonctions doivent être assurées :

- * réserve de carburant froid et sec
- * injection d'eau
- * récupération du carburant contaminé par l'eau
- * rinçage des circuits au carburant sec
- * séchage du carburant

3.1.1 RESERVE DE CARBURANT FROID ET SEC

Le carburant d'essai préalablement "séché" par un filtre coalesceur était stocké dans deux réservoirs de 4,5 m³ chacun, communiquant en leur point bas. Lors de la préparation du carburant froid, ils étaient raccordés en circuit fermé, successivement sur deux refroidisseurs :

- * l'un utilisé pour refroidir jusqu'à - 35 °C, constitué par un groupe moto compresseur à fréon capable de compenser un apport thermique de 75 kw à -35 °C.
 - * l'autre, utilisé pour descendre au dessous de - 35 °C, constitué par une installation à évaporation d'azote liquide, capable de compenser un apport thermique de 10 kw aux plus basses températures des essais.
- Ce carburant froid et sec filtré à 50 µm, était acheminé aux matériels en essai par une pompe capable de 5 m³/h sous 2,5 bars relatifs; la pression et le débit étant réglables par un système de vannage.

3.1.2 INJECTION D'EAU

Le mélange, à raison de 20 % d'eau et 80 % de carburant, était préparé automatiquement par pompage, filtration, et réglage des débits dans deux réservoirs à température ambiante :

- * un réservoir d'eau déminéralisée de 0,1 m³
- * un réservoir de carburant de 0,4 m³

Après régulation et mesure du débit, la partie de ce mélange correspondant à la concentration recherchée est injectée dans la veine de carburant froid; l'excédent étant renvoyé dans un réservoir de récupération de 0,5 m³.

L'injecteur, soumis extérieurement aux basses températures du carburant froid, était pourvu d'un dispositif de réchauffage à huile chaude pour éviter la formation de glace et l'obstruction. A l'endroit de l'injection, la veine était transparente pour permettre de regarder l'état de l'injecteur lui-même mais aussi la formation des palettes de glace dans le courant froid. La pulvérisation de produits anti-givre sur la paroi externe de la veine était fréquente pour améliorer la visualisation.

3.1.3 RECUPERATION DU CARBURANT CONTAMINE PAR L'EAU

A la sortie du circuit carburant moteur en essai, le carburant froid, chargé de particules de glace, était dirigé vers un réservoir d'une capacité de 11 m³ pour stockage temporaire avant traitement.

3.1.4 RINCAGE DES CIRCUITS AU CARBURANT SEC

Juste après chaque phase d'essai en conditions givrantes, les circuits en essai étaient alimentés avec du carburant sec à température ambiante provenant d'un réservoir de 0,72 m³. Après chaque passage dans le circuit du moteur, le carburant était déchargé de son eau par passage dans le filtre coalesceur avant de retourner au réservoir.

3.1.5 SECHAGE DU CARBURANT D'ESSAI

De même que précédemment pour le rinçage des circuits, l'opération de séchage du carburant avait lieu après chaque essai.

Elle s'effectuait en 2 phases :

- * Première phase
Réchauffage du carburant stocké dans le réservoir de 11 m³ par circulation en circuit fermé.
- * Deuxième phase
Transvasement du carburant du réservoir de 11 m³ dans les deux réservoirs de 4,5 m³ après passage au travers du filtre coalesceur chargé de séparer l'eau libre du carburant. Des analyses effectuées suivant la méthode de KARL-FISCHER à l'aval du filtre coalesceur permettaient de contrôler la teneur résiduelle en eau libre. Elle se situait aux environs de 80 PPM.

3.2 LE CIRCUIT D'HUILE

Ainsi que nous l'avons déjà signalé au paragraphe 1.2, ce circuit était chargé de restituer exactement les conditions des transferts de chaleur du circuit d'huile moteur vers le circuit carburant.

Il se composait des principaux éléments suivants :

- * Un circuit comprenant : un réservoir, un vase d'expansion, une pompe de circulation.
- * Un dispositif de chauffage de l'huile.
- * Un circuit véhiculant l'huile chaude vers les échangeurs du circuit carburant en essai comprenant : une pompe volumétrique, un système de vannage pour restituer le débit et la pression d'huile que l'on aurait sur moteur.

Il convient d'apporter quelques précisions sur le dispositif de chauffage. Il était constitué par :

- * un ensemble de 4 groupes de résistances électriques immergés dans le réservoir d'huile et dont la puissance totale était de 60 kw (6+12+18+24).
- * un ensemble de régulation de température à partir d'une sonde (thermo-couple) constitué par un régulateur à modulation de temps du type Proportionnel - Intégral

De plus, afin de simuler au mieux l'évolution de la puissance transférée au carburant par l'huile moteur du fait d'un colmatage éventuel par le givre de l'échangeur principal, un boîtier de régulation de la chute de température d'huile à travers l'échangeur, donc la puissance transférée au carburant, avait été intercalé dans le circuit principal de régulation de cette température. La loi de régulation était représentative du cas de fonctionnement simulé; la constante de temps choisie (2 min à 63% de l'échelon) correspondant à celle du moteur CFM56 en ce qui concerne les phénomènes de réjection de puissance dans l'huile.

3.3 SIMULATION DE LA PRESSION-COMPRESSEUR

L'indication de la pression statique sortie compresseur H.P. "PS3" au régulateur était recréée par une batterie de 2 bouteilles d'air comprimé à 200 bars équipées chacune d'un détendeur 200 - 40 bars.

Cet air détendu alimentait un régulateur de pression permettant l'ajustement et le maintien de la pression à la valeur fixée par le programme d'essais.

3.4 L'ENCEINTE CLIMATIQUE

L'ensemble de régulation, comprenant les pompes, le filtre, les échangeurs et le régulateur lui-même, était installé dans un caisson climatique, à l'exclusion du moteur hydraulique d'entraînement des V.B.V. et du vérin de commande des stators variables du compresseur H.P. qui étaient situés à l'extérieur du caisson.

Cette enceinte confectionnée, à l'aide de panneaux isolants en laine de verre était refroidie par un évaporateur à azote liquide alimenté par un réservoir de 0,6 m³ de N₂.

L'homogénéité de température dans l'enceinte était assurée par un ventilateur brassant continuellement l'ambiance; la vitesse autour des équipements était représentative de celle obtenue sur avion.

La régulation de la température à l'intérieur du caisson était assurée par l'ouverture et la fermeture d'une électrovanne assurant l'alimentation en N₂ liquide et commandée à partir d'une sonde de température et d'un régulateur.

3.5 LE DISPOSITIF D'ENTRAÎNEMENT MECANIQUE

Le dispositif d'entraînement du régulateur et de ses pompes était composé par les deux éléments essentiels suivant :

- un moteur électrique à courant continu à vitesse variable d'une puissance nominale de 195 kW, capable d'une vitesse maximale de 3000 tr/min.
- un multiplicateur de vitesse de rapport 1 à 3 muni de son système de lubrification et dont l'arbre de sortie était accouplé à celui du régulateur.

L'alimentation du moteur et le réglage de sa vitesse de rotation étaient assurés par un générateur électrique statique à thyristors.

4 - INSTRUMENTATION

L'instrumentation permettait de vérifier à tout moment des essais les conditions de simulation et de déterminer le comportement des matériels.

Hormis les paramètres nécessaires à la conduite des essais, le système permettait l'acquisition d'une cinquantaine de valeurs dont certaines visualisées sur écran et table traçante en temps réel.

Citons les plus importantes :

- les débits de carburant, d'eau injectée, d'huile
- les pressions d'injection, sortie pompe B.P. et H.P., entrée et sortie réchauffeur

- les pertes de charge du filtre carburant, des échangeurs
- les températures de fluide :
 - * carburant : entrée pompe B.P., entrée et sortie échangeurs, sortie régulateur
 - * huile : entrée du réchauffeur de carburant, sortie du refroidisseur d'huile
 - * à l'intérieur du caisson climatique
- les températures de masse : pompe carburant, régulateur, échangeurs.

5 - PROCÉDURES D'ESSAI

Des procédures de mise en route, d'arrêt et de reconditionnement de l'installation avaient été établies et affinées lors des essais préliminaires qui s'étaient déroulés du 26 OCTOBRE au 21 DECEMBRE 1977 pour optimiser et figer les nombreuses manipulations afin de rendre les divers essais parfaitement comparatifs entre-eux.

6 - CRITERES DE REUSSITE

Ces essais qui étaient effectués dans le cadre de la certification du moteur avaient pour but :

- de démontrer que le circuit carburant était capable de fonctionner sans interruption
- de réguler correctement le débit carburant dans les conditions de givrage susceptibles d'être rencontrées dans le domaine de vol prévu
- de déterminer la durée pendant laquelle ces fonctions étaient assurées correctement.

En conséquence, le comportement du circuit carburant devait être analysé, en régime permanent, en terme de la stabilité de certains paramètres de régulation : en particulier

- . débit carburant injecté
 - . position des vannes de décharge (VBV) et des staturs variables (VSV),
- paramètres qui servaient de référence pour justifier la réussite de l'essai et la conformité des circuits vis à vis des règlements.

Bien que n'intervenant pas directement sur le fonctionnement du moteur lui-même, le comportement de l'échangeur principal et du réchauffeur était noté pour chaque point d'essai, tant du point de vue thermique qu'hydraulique.

7 - RESULTATS DES ESSAIS ET ANALYSE

7.1 CONFIGURATION SANS RECHAUFFEUR DE CARBURANT DES SERVOMECHANISMES

Le montage était donc celui du circuit carburant de base comprenant essentiellement en suivant le sens de l'écoulement :

- . la pompe basse pression recevant le carburant froid à la température TCa et à la pression PCa
- . l'échangeur huile/carburant
- . le filtre à carburant
- . la pompe haute pression
- . le régulateur et ses servomécanismes
- . le circuit d'injection
- . la boucle de recirculation

4 essais ont été effectués en condition décollage avec des températures de carburant à l'entrée de la pompe basse pression suivantes : - 25 °C, - 30 °C, - 35 °C, - 40 °C pendant des durées de 35 min pour les deux premières températures et 60 min pour les deux autres.

Comportement des circuits

Deux comportements sont apparus suivant la température de carburant à l'entrée des équipements :

- . température supérieure à 0 °C (TCa ≥ - 30 °C) : tous les circuits fonctionnaient correctement, les paramètres restaient stables au niveau des valeurs initiales
- . températures négatives à l'entrée des équipements (TCa < -30 °C) : le filtre à carburant était le premier équipement à subir les effets du givrage. La perte de charge de l'élément filtrant commençant à croître 1 à 2 minutes après le début de l'essai d'injection d'eau et le colmatage total entraînant l'ouverture du by-pass, intervenant après 8 à 10 minutes. A noter cependant, que plus la température était basse, plus l'augmentation de la perte de charge était lente. Ceci peut s'expliquer par la consistance et la structure de la glace : des cristaux mous s'agglutinant plus facilement que des cristaux durs.

En ce qui concerne l'injection du débit carburant dans la chambre et les systèmes d'asservissement (VBV, VSV), on notait un fonctionnement correct pendant au moins huit minutes. Au delà, apparaissaient des variations de débit du carburant injecté de ± 10 % environ autour de la valeur nominale, pouvant devenir au bout d'une dizaine de minutes suffisamment significatives pour affecter le fonctionnement du moteur. Les cristaux s'accumulant, il s'ensuivait

des instabilités de plus en plus importantes affectant les pressions d'asservissement des stators variables (VSV) et des vannes de décharge (VBV). Par exemple, l'essai à - 40 °C a été arrêté 38 minutes après l'injection d'eau: la variation des paramètres était telle qu'il n'était plus possible d'exploiter les enregistrements. Des battements de 40 bars ont été relevés sur la pression d'injection du carburant dans la chambre. A noter que dans tous les cas, l'échangeur principal a toujours fonctionné correctement, sa perte de charge n'ayant d'ailleurs que très peu varié : + 15 % au maximum.

Ces essais ont montré clairement que la pilotabilité du moteur est affectée très rapidement dès lors que les températures du carburant à l'entrée du régulateur et des servomécanismes deviennent négatives.

7.2 CONFIGURATION AVEC RECHAUFFEUR DES SERVOMECHANISMES

Dans cette configuration, un échangeur de chaleur réchauffe le carburant des systèmes d'asservissement prélevé à la sortie de la pompe HP et dont le débit est environ 1/4 du débit consommé; ce réchauffage étant effectué par la totalité du débit d'huile à la température de sortie du moteur. Pour le reste, le circuit est le même que le circuit de base. 4 essais ont également été effectués en condition décollage, soit pour des températures de - 25 °C, - 30 °C, - 35 °C, - 45 °C et des durées de 90 minutes.

Comportement des circuits

Mise à part l'ouverture du clapet de dérivation du filtre pour les points à - 30 °C, - 35 °C, - 45 °C, quelques minutes après l'injection d'eau, ce qui traduit un comportement identique à 7.1, les systèmes de régulation sont peu affectés par la présence de glace dans le carburant. Le débit carburant injecté et la position des servomécanismes (VBV + VSV) sont restés stables pendant les 90 minutes de l'essai, excepté pour TCa = - 45 °C où à 88 minutes exactement un accroissement de 10 % du débit carburant injecté est apparu. Puis le débit est resté stable à sa nouvelle valeur jusqu'à la 94^{ème} minute, moment où est apparu un deuxième accroissement de près de 40 %; l'essai ayant été arrêté à la 96^{ème} minute par suite de l'épuisement de la réserve destinée à l'essai.

Ceci montre que :

- des temps de fonctionnement forts longs peuvent être nécessaires avant que n'apparaissent les premiers symptômes dus au givrage et qu'il convient en conséquence d'être prudent en la matière quant aux extrapolations.
- le système proposé a ses limites comme nous le pensions au cours de l'analyse puisque le carburant le long du circuit d'injection est toujours resté à température négative.

A noter qu'en ce qui concerne l'échangeur principal, il a été relevé des colmatages de la matrice, conduisant à l'ouverture du clapet de dérivation, puis à décolmatage pour TCa = -45 °C comme attendu par l'analyse, suite au réchauffage des plaques frontales par l'huile. Mais ce décolmatage ne s'est pas produit à des températures moins froides; ce qui traduit encore l'effet de la structure de la glace sur les phénomènes d'agglutination des cristaux et d'obstruction qui s'ensuivent.

Pendant toute la durée de ces essais, les pertes de charge du réchauffeur du carburant des servomécanismes sont restées stables aux valeurs d'origine traduisant qu'il n'y a jamais eu d'accumulation de glace; les températures de paroi étant toujours à température positive.

8 - CONCLUSION DES ESSAIS

Les principaux enseignements (ou confirmations) qui découlent des essais effectués en conditions givrantes du 18 Janvier au 30 Mars 1978, sur des circuits carburant typiques de la famille des moteurs CFM56, fonctionnant avec du carburant contenant de l'eau dans les proportions définies par les règlements, soit 300 PPM en volume (300 à 380 PPM lors des essais), sont les suivants :

- * Le fonctionnement correct est assuré sans restriction de durée due à la présence de l'eau, dès lors que la température du carburant à l'entrée du régulateur est supérieure à 0 °C, ceci malgré le colmatage éventuel du filtre principal.
- * Pour des températures de carburant inférieures à 0 °C au régulateur, le fonctionnement correct du circuit carburant n'a pu être assuré que pendant des durées limitées dont les valeurs dépendent des niveaux de température à l'entrée de la pompe BP et également du taux de poussée délivré par le moteur.
- * Le premier phénomène anormal rencontré après 8 à 10 minutes de fonctionnement est une variation périodique du débit carburant, délivré à la chambre, autour de sa valeur nominale, ce phénomène restant stable dans le temps.

- * Le deuxième phénomène est une obstruction du circuit des servomécanismes du régulateur conduisant à une dérive des paramètres essentiels au fonctionnement du moteur : position des vannes de décharge et des stators variables, contrôle du débit carburant consommé ; ce second phénomène apparaissait 10 à 35 minutes après fonctionnement en conditions givrantes.

Cette limite de fonctionnement correct, sans limitation d'aucune sorte sur les conditions moteur, est atteinte avec le circuit de base du CFM56, non équipé de réchauffeur du carburant des servomécanismes, lorsque la température du carburant à l'entrée de la pompe BP descend à - 30 °C.

Cette limite est repoussée à - 45 °C par l'adjonction d'un petit échangeur huile/carburant dont le rôle est de réchauffer le carburant qui circule dans les servomécanismes plus sensibles aux effets du givrage que le circuit principal du régulateur; la puissance calorifique extraite du circuit d'huile étant sensiblement la même dans les deux cas.

Ainsi que nous l'avons déjà vu, des fonctionnements au dessous de - 30 °C sans réchauffeur conduiraient assez rapidement à une impilotabilité du moteur; de même, dans les mêmes conditions moteur, des fonctionnements au dessous de - 45 °C conduiraient aux mêmes anomalies avec des circuits équipés de réchauffeur, et des systèmes annexes seraient nécessaires pour "descendre" plus bas. Cependant, jusqu'à ce jour, aucun avionneur, aucune compagnie aérienne n'est demandeur, une température de - 45 °C n'étant vraisemblablement pas du pratique courante !

3^{ème} PARTIE - ACTUALISATION

Les études présentées précédemment datent de l'époque de la définition et du développement des premiers CFM56. Elles sont donc vieilles de 15 ans aujourd'hui. Les essais décrits en deuxième partie datent de 1977-1978.

Qu'en est-il aujourd'hui ?

- * les systèmes définis à l'époque se sont-ils révélés satisfaisant au cours de ces presque 10 années d'exploitation des CFM56 ?
- * Quelles sont les tendances actuelles ?

1 - EXPERIENCE ACQUISE

1.1 EN ESSAI EN VRAIE GRANDEUR SUR AVION

Au début de l'utilisation des CFM56-2B sur les avions ravitailleurs KC135R, l'USAF a effectué à EGLIN (FLORIDE) des essais climatiques sur un avion équipé de ses 4 CFM56-2B. L'avion était installé dans un hangar à l'intérieur duquel la température avait été abaissée et maintenue à des niveaux compris entre - 29 et - 51 °C, pendant des durées suffisamment longues, de façon que l'ensemble avion + moteurs ait eu le temps de se mettre à la température ambiante du hangar.

Tous les essais effectués montrèrent un fonctionnement correct des moteurs lors des démarrages et des quelques minutes effectuées au ralenti; les durées de fonctionnement ne pouvant qu'être courtes puisque l'éjection des gaz se faisait dans le hangar. On ne connaît pas la quantité d'eau que pouvait contenir le carburant.

Cet essai est relaté car c'est le seul cas, à notre connaissance, où des CFM56 ont fonctionné à si basse température au sol.

1.2 EN EXPLOITATION

Contrairement à ce que l'on peut penser, il n'est pas aisé pour un motoriste de connaître quelles ont été les conditions les plus sévères que ses moteurs ont pu rencontrer en exploitation ... tout du moins quand ils ont fonctionné sans faire parler d'eux !

Après 20 millions d'heures de vol cumulées par tous les moteurs, nous n'avons jamais eu de plaintes concernant un moteur qui aurait eu des troubles de fonctionnement suite à un givrage présumé du circuit carburant; certains de ces moteurs opérant pourtant en zones réputées très froides à certaines périodes de l'année ou ayant rencontré en altitude des couches plus froides que les - 56,5 °C de l'atmosphère standard valables au dessus de 11 km.

Mais il faut dire aussi que du carburant à - 45 °C au sol doit être fort peu fréquent et qu'en vol, il faudrait voler plus de 5,5 heures à M = 0.8, au régime de décollage en ISA - 15 °C (Tamb = - 71 °C) et avec 30 J PPM d'eau dans le carburant pour qu'il y ait une probabilité que les premiers signes de givrage apparaissent (cf 2^{ème} partie). On peut donc en conclure que la solution couvrant des conditions jusqu'à - 45 °C est satisfaisante.

2 - NOUVEAUX CONCEPTS DE CIRCUIT CARBURANT

Sur certains moteurs, pour améliorer la consommation spécifique du moteur installé, le refroidissement du circuit d'huile des alternateurs de l'avion est assuré par le circuit carburant. Ce concept permet d'éviter l'échangeur situé derrière la soufflante, échangeur volumineux qui crée des pertes de charge et des hétérogénéités de débit dans l'écoulement secondaire; ce qui se paie par une surconsommation.

Sur les CFM56-5A qui propulsent les AIRBUS A320, un échangeur huile-IDG/carburant est installé dans la boucle carburant du moteur.

Une vanne thermo-commandée associée à un circuit de retour carburant aux réservoirs de l'avion permet d'obtenir un débit de refroidissement supérieur au débit de carburant consommé par le moteur, particulièrement aux bas régimes pour lesquels la consommation est insuffisante pour assurer le refroidissement et du moteur et de son alternateur avion sans entraîner des sur-températures sur les circuits. Aux régimes de décollage, cette vanne est en position fermée pour des questions de sécurité mais aussi parce que la consommation élevée le permet, même aux conditions les plus chaudes.

La puissance calorifique, qui provient du refroidissement d'un alternateur délivrant une puissance électrique de 60 kVa, représente environ la moitié de celle générée au plein gaz par le circuit de lubrification d'un CFM56.

L'alternateur est alors un merveilleux réchauffeur de carburant ... tout du moins pour les conditions froides. Dans les mêmes conditions que celles des essais décrits en 2^{ème} partie, le réchauffage de la totalité du débit consommé est de l'ordre de 10 °C, au régime de décollage en ISA - 124 °F (Tamb = - 54 °C). Ce qui signifie que sans réchauffeur des servomécanismes les phénomènes de givrage ne se manifesteraient que vers - 40 °C et vers - 55 °C avec un réchauffeur des servomécanismes.

Par ailleurs, si l'on tient compte que la consommation spécifique des moteurs d'aujourd'hui est plus faible que ceux conçus il y a 15 ans, on est en droit de penser à la suppression du réchauffeur des servomécanismes.

La seule difficulté est que si une panne intervient sur l'alternateur et que le pilote soit contraint de le débrayer mécaniquement, on ne saurait plus tenir que - 30 °C environ puisque l'on est ramené au circuit de base ... pour lequel il avait fallu un réchauffeur. Seules des études fines permettent de statuer.

3 - 'NOUVEAUX MODELES' MATHEMATIQUES

Au fil des années, le modèle décrit en première partie a eu plusieurs descendants.

D'abord pour satisfaire la demande des avionneurs (BOEING, AIRBUS INDUSTRIE) qui avaient besoin de modèles mathématiques moteur pour :

- * aider à la certification de l'aéronef (extrapolation aux conditions chaudes et froides)
- * mieux restituer dans les simulateurs de vol les indications pilotes provenant des circuits huile et carburant.

Mais aussi pour nous, afin de mieux approcher la réalité des phénomènes physiques. Le modèle, qui au départ ne calculait que des températures en régime stationnaire, a pu assez rapidement effectuer des calculs en régime thermique instationnaire.

Aujourd'hui, pour les études sur CFM56-5C destiné à l'avion A340, le modèle est capable de calculer les températures des circuits huile/carburant du moteur mais aussi du circuit d'huile de l'alternateur le long d'une mission complète, tout en évaluant la température du carburant délivré par l'avion aux moteurs, avec et sans recirculation de carburant dans ces réservoirs. En un mot, la simulation est complète.

Ainsi, on peut suivre par le calcul l'évolution des températures du carburant lors de vol en conditions extrêmes froides au niveau de l'entrée du régulateur et des servomécanismes, comparer les valeurs mais aussi les durées par rapport aux essais de certification décrits en 2^{ème} partie et déterminer les marges de sécurité en terme de givrage.

Les études effectuées avec de tels modèles permettent d'optimiser encore plus finement les solutions technologiques et conduisent à des gains en masse et en coût.

4 - PIEGES A GIVRE

Nous avons résolu les problèmes de givrage des circuits carburant moteur qui se sont posés à nous en réchauffant suffisamment le carburant pour faire fondre les cristaux de glace. Mais nous ne serions pas complets si nous ne parlions pas des systèmes basés sur la captation des cristaux. De tels systèmes sont utilisés avec succès sur certains moteurs d'hélicoptères tels que le "MAKILA" qui équipe le SA331 SUPER PUMA.

Comme les essais l'ont montré (cf 2^{ème} partie) le plus simple des systèmes passifs pourrait être un filtre à carburant. Mais pour assurer des durées de fonctionnement suffisamment longues, l'encombrement risquerait d'être prohibitif car la forme plissée

s'avère inadéquate, la glace faisant des pontets entre les plis; très rapidement le filtre ne travaille plus que sur sa périphérie.

En conséquence, les systèmes sont plus compliqués et ressemblent plutôt, pour certains, à un échangeur de chaleur sans tubes, dans lequel ne subsistent que les chicanes. La captation se faisant d'abord sur les premières chicanes, puis sur la deuxième et ainsi de suite. Ces systèmes simples dans leur principe, demandent une longue mise au point faite à base d'essais pour déterminer l'agencement interne qui confèrent l'autonomie la plus longue.

Si ces systèmes sont séduisants dans leur principe puisqu'ils ne nécessitent pas d'énergie, ils ont cependant quelques inconvénients :

- leur autonomie est limitée
- les débits de carburant à traiter doivent rester faibles sous peine d'encombrement important
- la captation peut ne pas être totale
- enfin, à l'arrêt du moteur, il faut dégivrer le système et drainer l'eau de fusion de la glace.

Tous ces inconvénients font que de tels dispositifs sont difficilement utilisables sur les turboréacteurs des avions commerciaux.

5 - CONCLUSION

Pour les moteurs de la classe des 100 kNewtons de poussée et au delà, il semble que la meilleure solution, pour éviter les conséquences dues au givrage, soit celle qui consiste à réchauffer suffisamment la partie du carburant qui circule dans les organes les plus sensibles par un petit réchauffeur huile/carburant.

L'énergie disponible sur le circuit d'huile doit permettre de couvrir de façon satisfaisante les conditions les plus sévères. Sur les moteurs très récents, compte tenu de l'amélioration de leur consommation spécifique, des vitesses de rotation de plus en plus élevées, de l'environnement de plus en plus chaud autour des enceintes paliers de par l'augmentation des taux de compression, voire de la prise en charge du refroidissement des alternateurs par le circuit carburant moteur, un "circuit de base" consistant à réchauffer tout le débit consommé pourrait être envisageable jusqu'à des températures de - 40 °C environ.

L'expérience montre que, pour éviter les phénomènes de givrage, il suffit que la température du carburant à l'entrée des organes sensibles soit très légèrement au dessus du point de congélation de l'eau; les cristaux de glace ayant peu d'inertie thermique d'une part, étant donné leur faible masse, et d'autre part, la température de peau des circuits en contact avec le carburant étant très proche de la température du fluide en raison du rapport des coefficients d'échange entre le carburant et l'air qui environne les équipements.

Néanmoins, si, au sein d'un même équipement sensible, une circulation de carburant froid jouxte une circulation de carburant chaud, les coefficients d'échange par convection risquant d'être du même ordre de grandeur, une analyse thermique devra être effectuée pour s'assurer que la température des parois n'est pas négative sur le circuit chaud.

Cependant, étant donné les situations extrêmement graves que peut entraîner le givrage des circuits de carburant, des essais recréant au plus près les conditions de fonctionnement sur moteur en situation extrême de givrage doivent être effectués sur les circuits de la définition finale pendant des durées suffisamment longues pour s'affranchir de tout risque.

Discussion

1. R. Jacques, Ecole Royale Militaire

La puissance calorifique dégagée est uniquement fonction de la température d'entrée de l'huile. N'y a-t-il des lors anciens autre paramètre que la viscosité d'huile fonction de la température, qui influence ce transfert de chaleur?

Author:

Pour une condition de fonctionnement donnée, la courbe est unique la puissance calorifique recueillie par l'huile ne dépend plus en fait que de la viscosité de l'huile, soit de la température pour une huile donnée, ce qui était le cas dans l'exposé.

Fig. 1 **STOCKAGE TYPE DU CARBURANT
EN EXPLOITATION CIVILE**

TEXTE : préambule

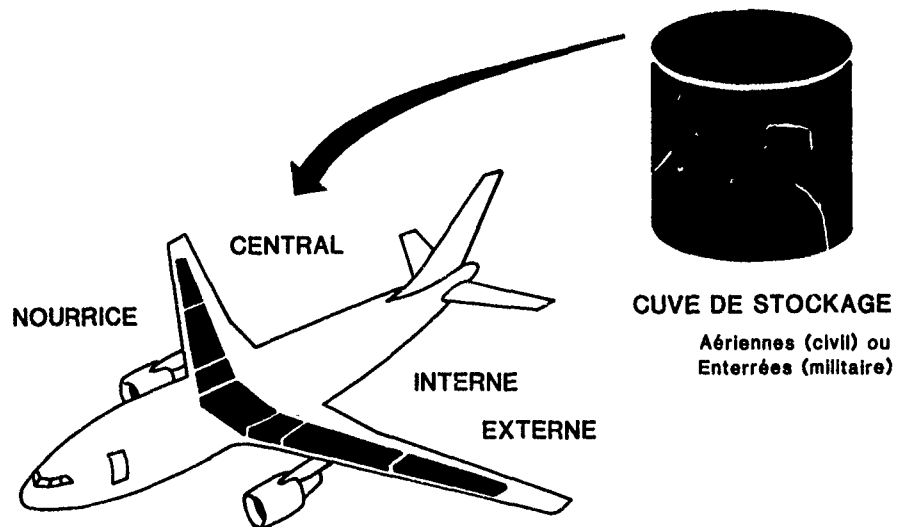


Fig. 2 **SYSTEME CARBURANT DE BASE**

TEXTE : paragraphe 1
1ère partie

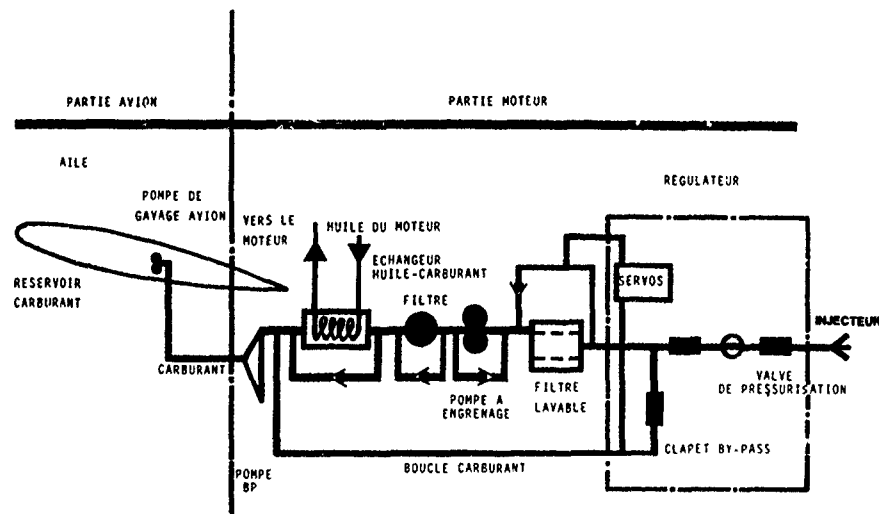


Fig. 3 LE MODELE DE CALCUL

TEXTE : paragraphe 4 - 1ère partie

Paramètres du cycle
thermodynamique →

THERMODYNAMIQUE

TECHNOLOGIE

Données définissant la
géométrie du moteur.

CIRCUIT D'HUILE

Calcul de la puissance
calorifique recueillie
par l'huile.Les Différents
Modules

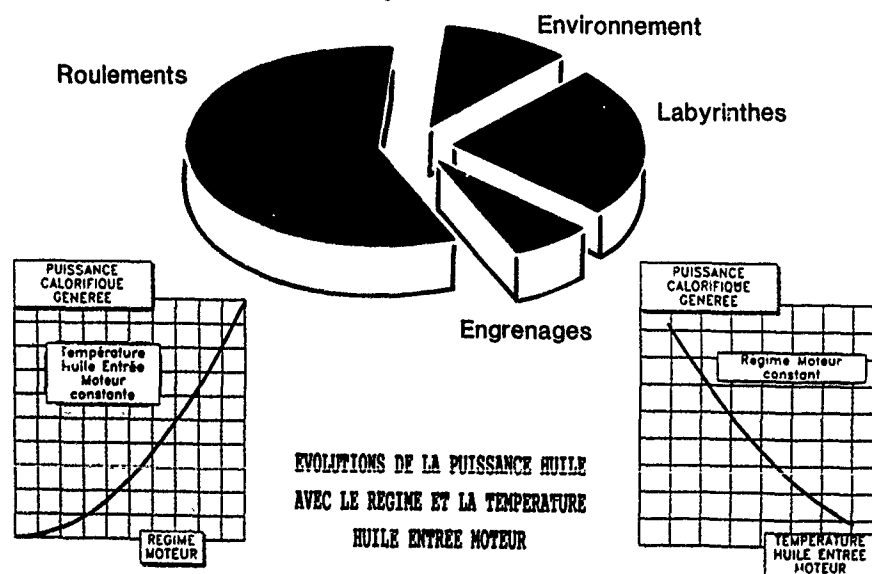
ECHANGEURS

CIRCUIT CARBURANT

RESULTATS

Fig. 4 ORIGINE DE LA PUISSANCE CALORIFIQUE
RECUEILLIE PAR L'HUILE

TEXTE : paragraphe 4.1 - 1ère partie



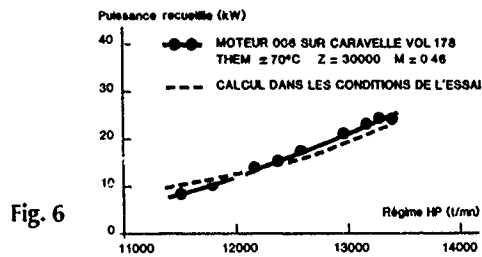


Fig. 6

MODULE "CIRCUIT D'HUILE"

TEXTE : paragraphe 4.3.1
1ère partie

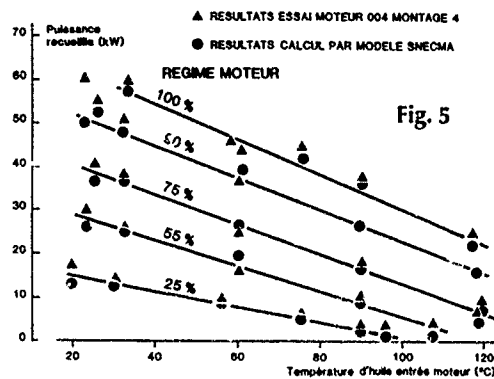


Fig. 5

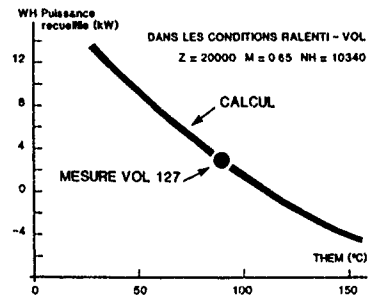


Fig. 7

Fig. 8 PUISSANCE CALORIFIQUE DISPONIBLE SUR LE CIRCUIT D'HUILE

TEXTE : paragraphe 6 - 1ère partie

CONDITIONS : Z=0
M=0.6 ISA-124°F

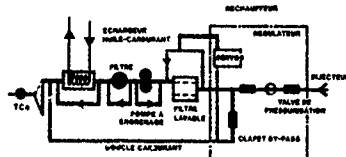
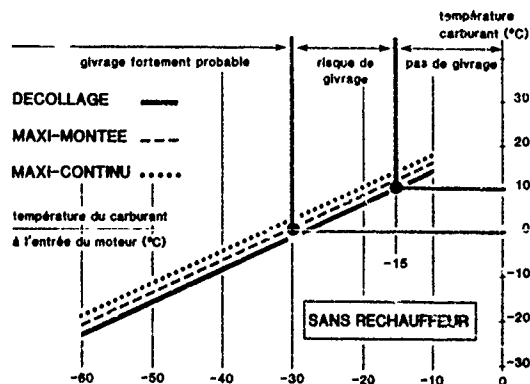
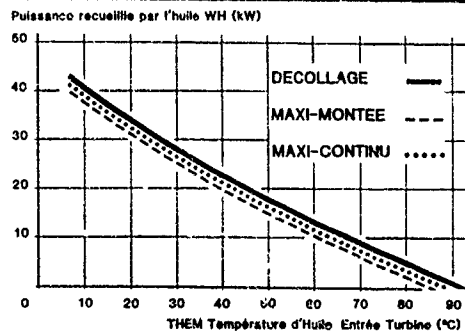


Fig. 9 TEMPÉRATURES DU CARBURANT A L'ENTRÉE DES SERVOMECHANISMES

TEXTE : paragraphe 6.1 - 1ère partie

CONDITIONS : Z=0 M=0.6
ISA-124°F (Tamb = -54°C)





TEXTE : paragraphe 3.1.1
2ème partie

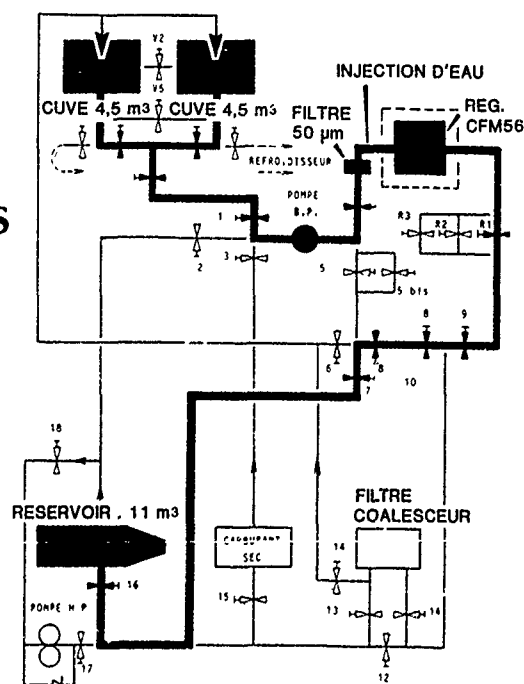


Fig. 12

DISPOSITIF DES ESSAIS DE GIVRAGE

INJECTION D'EAU

TEXTE : paragraphe 3.1.2
2^{ème} partie

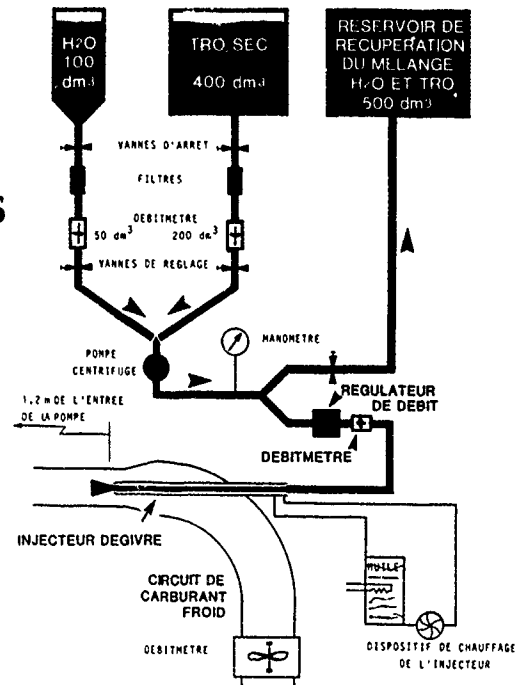


Fig. 13

DISPOSITIF DES ESSAIS DE GIVRAGE

RINCAGE DES CIRCUITS

TEXTE : paragraphe 3.1.4
2^{ème} partie

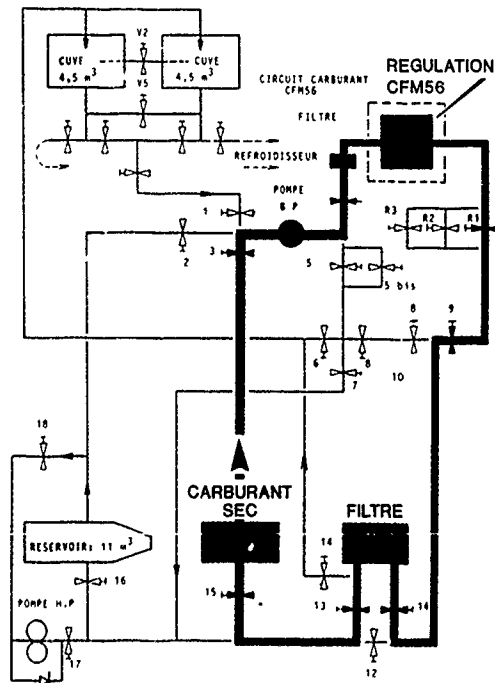


Fig. 14

DISPOSITIF DES ESSAIS DE GIVRAGE

"SECHAGE" DU CARBURANT D'ESSAI

TEXTE : paragraphe 3.1.5
2ème partie

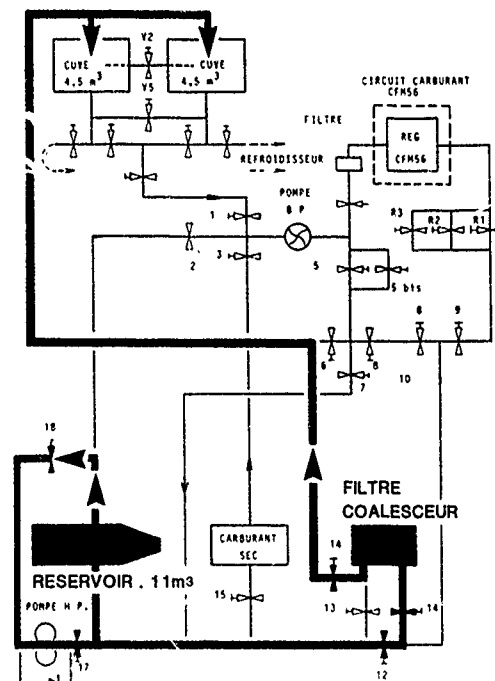


Fig. 15

DISPOSITIF DES ESSAIS DE GIVRAGE

CIRCUIT D'HUILE ET DE REGULATION DE TEMPERATURE

TEXTE : paragraphe 3.2
2ème partie

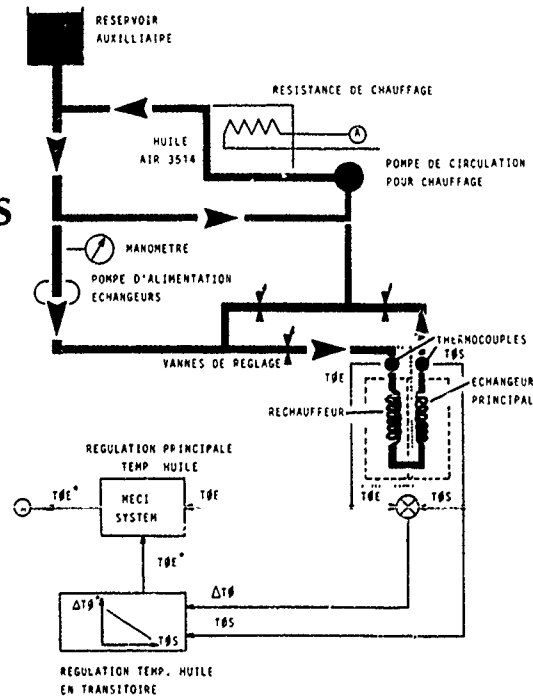


Fig.16
**DISPOSITIF
DES ESSAIS
DE GIVRAGE**

**ENCEINTE
CLIMATIQUE**

TEXTE : paragraphe 3.4
2^{ème} partie

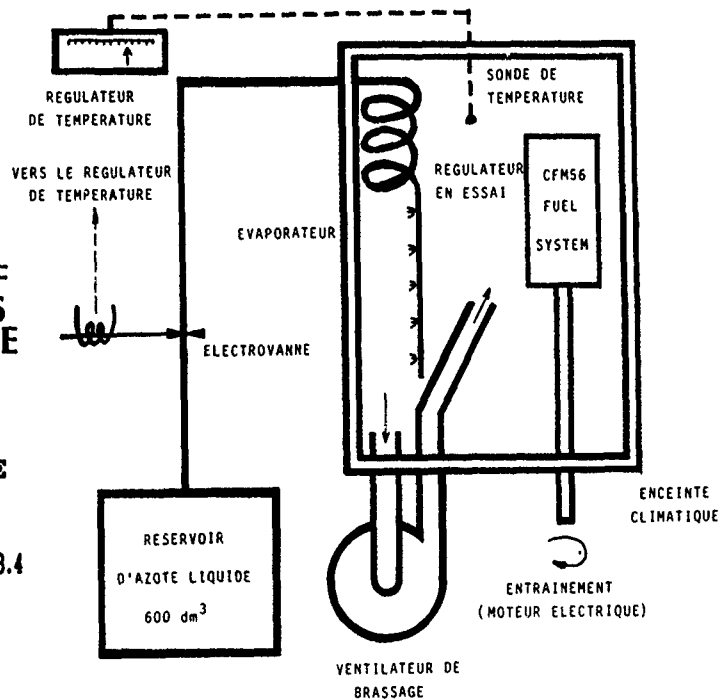
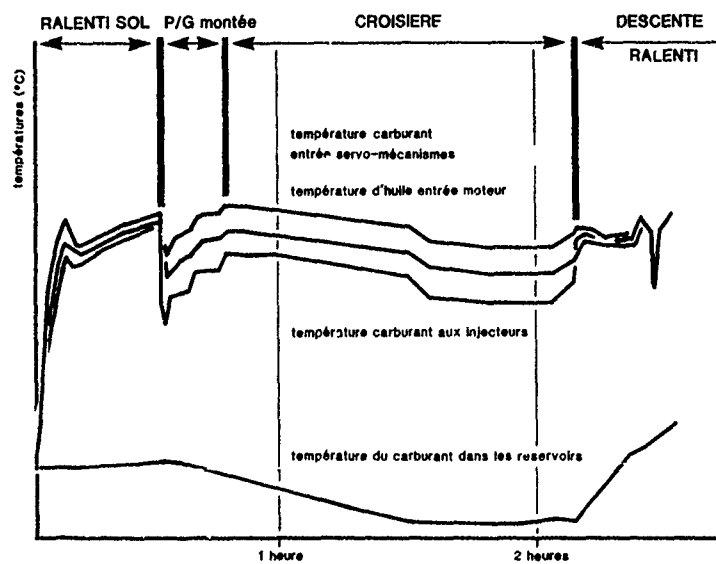


Fig. 17 **NOUVEAUX MODELES MATHÉMATIQUES
EXEMPLE DE CALCULS EFFECTUES POUR CFM56-5C**

TEXTE : paragraphe 3 - 3^{ème} partie



THE INFLUENCE OF FUEL CHARACTERISTICS ON HETEROGENEOUS FLAME PROPAGATION

M.F. Bardon, J.E.D. Gauthier and V.K. Rao
Department of Mechanical Engineering
Royal Military College of Canada
Kingston, Ontario K7K 5L0
Canada

ABSTRACT

This paper describes a theoretical study of flame propagation through mixtures of fuel vapour, droplets and air under conditions representative of cold starting in gas turbines. It combines two previously developed models - one for heterogeneous flame propagation and the other for describing the complex evaporative behaviour of real fuel blends. Both models have been validated against experimental data, and the combined model incorporates the effects of pressure, temperature, droplet diameter, turbulence intensity, delivered equivalence ratio, fuel prevaporization, and fuel type on flame propagation. Differences in the combustion performance of Jet A1, JP 4 and two single component reference fuels are compared. Conclusions are drawn regarding the use of pure compounds to represent real fuel blends, and the relative importance of various engine conditions and spray parameters on combustion.

LIST OF SYMBOLS

a_i, b_i, c_i, d_i	= coefficients for volatility equations (Appendix B)
B	= mass transfer number
c_p, \bar{c}_p	= specific heat and average specific heat at constant pressure
C_1, C_2	= Clausius-Clapeyron constants
C_1, C_2, C_3	= droplet size distribution constants (Appendix C)
C_s	= shape factor in equation (4)
D_c	= characteristic dimension in equation (4)
D	= droplet diameter
E	= activation energy
f_1, f_2	= temperature independent functions of Ω
H_v	= latent heat of vaporization of the fuel at boiling point
ΔH	= enthalpy of vaporization
k	= thermal conductivity
K	= proportionality constant (in equation (A-7))
M	= molecular weight
MDD	= mean droplet diameter
MSD	= mean surface diameter
MMD	= mean mass diameter
P	= pressure
P_i	= Legendre polynomials (Appendix B)
R	= universal gas constant
Re_D	= Reynolds number based on droplet diameter
S	= shifted variable in polynomials (Appendix B)
S	= burning velocity of heterogeneous burning velocity
SMD	= Sauter mean diameter
t	= characteristic time for droplet vaporization inside the flame front
T, T_F	= temperature and flame temperature respectively
u'	= turbulence intensity
δ	= flame front thickness
λ_b	= vaporization (burning) constant
ϕ	= equivalence ratio
ρ	= density
Ω	= mass fraction of fuel vapour, i.e. ratio of fuel vapour to total fuel
Subscripts	
a	= air
d	= droplet condition inside the flame front or just after the flame front
δ	= representative condition inside the flame front
eff	= effective condition inside the flame front due to evaporated fuel
ev	= at droplet evaporating temperature condition

fl	= liquid fuel
g	= gas phase
L	= laminar condition
$mean$	= mean value (between reactants and products of combustion)
mf	= multicomponent fuel
o	= condition in the reactants just ahead of the flame front
r	= (of all the) reactants
sat	= saturated conditions
$surf$	= droplet surface condition
T	= turbulent condition
v	= fully prevaporized, i.e. gaseous condition

INTRODUCTION

Flame propagation into heterogeneous mixtures of fuel droplets, fuel vapour and air has received only limited attention and is of great interest in many practical applications, including gas turbine main combustors. Mathematical models which predict the effect on combustion of changes in chemical, physical or aerodynamic properties of a heterogeneous mixture provide valuable insight into the relative importance of various parameters and can thereby aid in the design of future combustion systems. In particular, the need for a better understanding of both the qualitative and quantitative effects of fuel properties on flame propagation motivates this work. Appropriate design strategies require a thorough understanding of the interaction between fundamental fuel characteristics and combustion behaviour.

Ultimately, a complete understanding of the many subprocesses (fuel droplet trajectories, evaporation, mixing, reaction rate, turbulence, etc.) involved in heterogeneous flame propagation would allow a comprehensive computer model to be developed. Preliminary versions of such "exact" models have been proposed (e.g. Aggarwal and Sirignano, [1] and Swithenbank et al, [2]). The most common approach in this type of numerical model is to solve a set of governing differential equations using some finite difference scheme. This approach is clearly necessary in the long run, since it is the only means to completely model the physics of the problem. However, existing work is still rather embryonic, and arguably, is still too complex and uncertain for use in most practical analyses. There is therefore an ongoing requirement for simpler more tractable phenomenological models. Such models are developed using basic thermal considerations [3, 4, 5, 6, 7], considering flame propagation to be controlled by the interaction between droplet evaporation rate and heat transfer ahead of the flame. The work reported in this paper uses this latter approach.

A flame propagation model has been developed which uses the general style of Ballal and Lefebvre [6] but is applicable to both rich and lean mixtures and includes a more realistic treatment of the augmentation of vapour in the gas phase by evaporation and its contribution to flame propagation [8]. It is applicable to monosized and polysized droplet distributions and accounts for the effects of changes in pressure, temperature, droplet diameter, overall equivalence ratio and fuel type on the heterogeneous burning velocity. The basis of the model is the hypothesis that flame propagation through heterogeneous mixtures is controlled by the total amount of fuel which becomes available in vapour form as droplets pass through the flame front. This is the aggregate of vapour initially present in the mixture plus that formed by partial or complete droplet vaporization during flame passage. Relations were developed to evaluate the effective equivalence ratio of the gas phase inside the flame front. Predicted flame speeds agree satisfactorily with published results [8]. The model is therefore considered to be useful in helping to elucidate the influence of fundamental fuel properties on combustion in reciprocating engines, gas

turbines and other devices employing fuel sprays.

In its initial form, the model, like other existing flame propagation models, was limited to single component fuels or at best, rather unrealistic binary mixtures. On the other hand, real fuels are composed of hundreds of components. This makes their volatility behaviour quite complex. Unlike a single component fuel, the vapour pressure of a mixture depends not only upon its temperature but also upon how much has already evaporated. For example, the vapour pressure of JP-4 decreases by an order of magnitude as it evaporates at constant temperature. Light volatile components produce high vapour pressures initially when most of the fuel is still liquid, but less volatile compounds remain behind, and the vapour pressure drops continuously as evaporation proceeds.

Recent work by two of the present authors [9,10,11,12] has resulted in the development of simple mathematical models for multicomponent hydrocarbon fuels. These allow real fuel volatility variations to be predicted with reasonable accuracy and the computational procedures are simple enough to be included as subcomponents of larger analyses.

The aim of the work presented in this paper was to incorporate the multicomponent fuel equations into the heterogeneous flame propagation computational procedures, then use the refined model to investigate the effect that these real fuel characteristics would have on flame propagation compared to single component idealizations. Of particular interest are the effects of real fuel properties on combustion behaviour during cold starting and idling in a gas turbine.

HETEROGENEOUS FLAME PROPAGATION MODEL

Consider a reference frame fixed with respect to a plane flame of thickness δ into which a heterogeneous mixture flows at velocity S , as shown in Figure 1. The heterogeneous burning velocity is assumed to be equal to that of a homogeneous mixture of equivalence ratio equal to that of the total gaseous mixture available for chemical reaction inside the flame front. To apply this model, it is therefore necessary to calculate the effective equivalence ratio of the gas phase ϕ_{eff} including both the vapour initially present, plus the fuel which vaporizes from the droplets passing through the flame front. The heterogeneous burning velocity is then equal to the burning velocity of a homogeneous air/fuel mixture having this overall equivalence ratio.

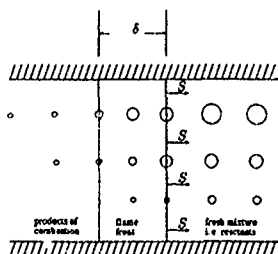


Figure 1: Diagram of plane flame front propagation

The principal assumptions inherent in the calculation procedures used in the model are as follows:

- Transient droplet heat-up is not included - the quasi-steady treatment of the well-known "d² law" is used;
- individual droplet envelope flames or relay transfer are not explicitly included; in effect, all mixing and non-uniform flame spread effects are lumped by the averaging inherent in the concept of effective equivalence ratio;
- buoyancy and droplet acceleration through the flame zone are neglected;
- turbulence effects are accounted for using empirically derived relations.

A summary of the details of the model is included as Appendix A. Figure 2 shows a comparison between the predictions of the model for iso-octane, a single component fuel, and measured flame speeds. The agreement is considered to be satisfactory. The trends predicted by the model have also shown to be correct under a wide range of other conditions. [8]

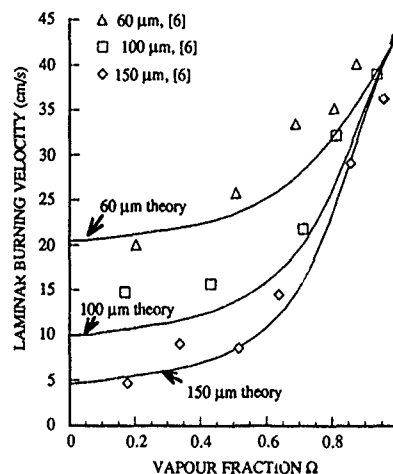


Figure 2. Comparison of Predicted and Measured Laminar Flame Speed for Iso-Octane Sprays [8]

MULTICOMPONENT FUEL VOLATILITY MODEL

The simplest functional relationship for the vapour pressure of a pure component is the Clausius-Clapeyron equation:

$$P_{sat} = C_1 \exp(-C_2/T) \quad (1)$$

where:

- P_{sat} = equilibrium saturation pressure
- T = absolute temperature
- C_1, C_2 = constants for a given pure substance

The basis of the method outlined in references [9] - [12] is the assumption that real multicomponent behaviour can be described by treating C_1 and C_2 as functions of the extent of vaporization, defined by the vapour fraction Ω . This latter is the mass fraction of fuel in the form of vapour,

$$\Omega = \frac{\text{mass of fuel in the vapour phase}}{\text{total fuel mass}} \quad (2)$$

The basic vapour pressure equation of the multicomponent fuel is therefore written as

$$P_{mf,sat} = f_1 \exp(-f_2/T) \quad (3)$$

where f_1 and f_2 are temperature independent functions of Ω alone, for any particular fuel. The technique uses the ASTM distillation data [13] and specific gravity to predict the variations of f_1 and f_2 as well as those of the mean vapour phase molecular weight M_{mf} , and enthalpy of vaporization ΔH with the vapour fraction Ω . The relationship between each of these four quantities and the vapour fraction is expressed by a polynomial equation. Appendix B gives further details.

Figure 3 shows a comparison between vapour pressures predicted by the model and those measured experimentally for JP-4. The results are satisfactory; the volatility model is therefore considered adequate for use in analysing real fuel behaviour in combustion systems.

In this study, the turbulent burning velocity was determined for a wide variety of conditions using different fuels. Results for the case of very rich cold starting conditions in a spark ignition engine have been reported elsewhere [14]. In this paper, the model is used to study conditions relevant to cold starting of gas turbines. The fuels studied are JP-4, JET A1, and two single component reference fuels, n-nonane and

n-decane. The coefficients used for the volatility model for these fuels are included in Appendix B.

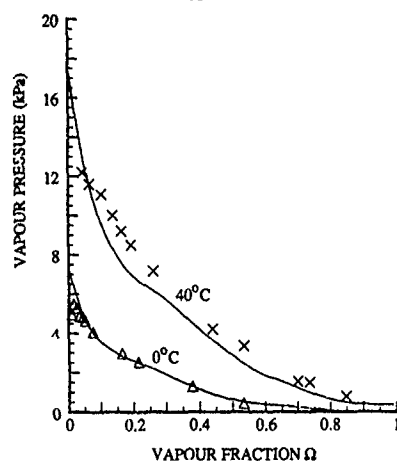


Figure 3. Measured and Predicted Vapour Pressure of JP 4

GENERAL INFLUENCE OF MULTICOMPONENT FUELS

Annex C gives details of the conditions assumed to be representative in the calculations presented in this paper. Figure 4 shows the flame propagation speed calculated for conditions typical of idle conditions in the combustor. These are the same as given in Appendix C except that pressure ratio at idle is taken to be 2. In order to compare combustion behaviour independent of prevaporization, these results assume a fixed quantity of vapour (0 or 25%) for all fuels.

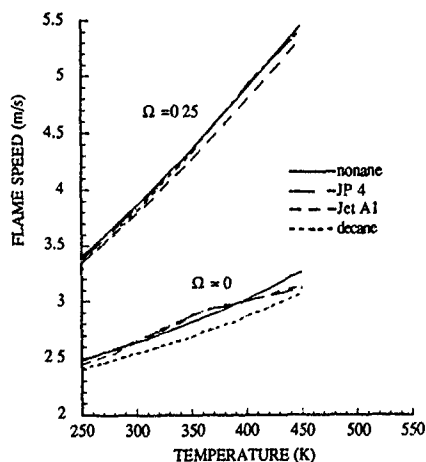


Figure 4. The Influence of Fuel Type and Prevaporization on Flame Speed for Fixed Reactant Conditions.

The effect of temperature on flame propagation is clear in Figure 4. Flame speed increases some 60% over the temperature range shown. Likewise, the extent of prevaporization is very important as seen by comparing flame speeds with no pre-existing vapour ($\Omega=0$) and those when 25% of the fuel is vaporized before entering the flame zone. However, there is very little difference between the fuels at any given temperature and value of Ω . This is perhaps surprising since the differences in volatility characteristics might be expected to lead to significantly different combustion behaviour. The reasons for this become easier to understand if droplet evaporation and combustion are considered more closely. Using the classical quasi-steady droplet equation [15] for a single 100 μm droplet in an infinite stagnant medium, computations were performed to show the effect of variable fuel volatility. In addition to the usual

approximations, droplet internal mixing was assumed to be sufficient to maintain the liquid composition uniform throughout. Thus vapour pressure at the surface drops in the manner shown in Figure 3 as evaporation proceeds.

Figure 5 compares JP-4 and n-nonane evaporating at an ambient temperature of 25°C, whereas Figure 6 shows the same fuels when burning surrounded by the spherical flame shell of the simple classical model. The results have been plotted as the ratio of diameter squared so as to better illustrate the multicomponent effects. The slope of this curve is the so-called evaporation or combustion constant of the d^2 law. Therefore, any single component fuel would give a straight line.

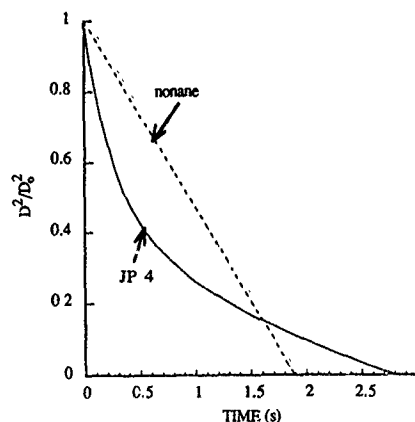


Figure 5. Evaporation Histories of JP 4 and Nonane Droplets (Initial Diameter = 100 μm , Ambient Temperature = 25°C)

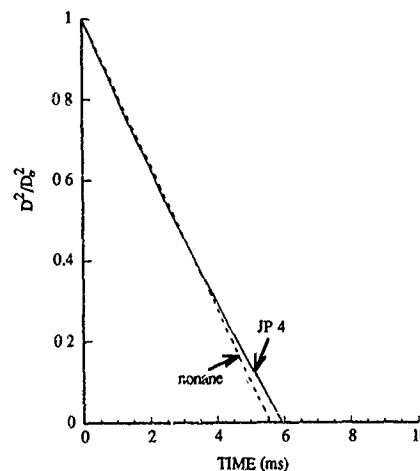


Figure 6. Evaporation Histories of Burning JP 4 and Nonane Droplets (Initial Droplet Diameter = 100 μm)

Figure 5 shows that the initial JP-4 evaporation rate is faster than that of nonane and its final rate is slower. This reflects its high vapour pressure when vapour fraction is low and the decreasing vapour pressure as evaporation proceeds. The difference at 25°C is considerable. On the other hand, Figure 6 shows that under combustion conditions, when surrounding temperature is very high, the differences are virtually negligible. Less than complete internal mixing within the droplet would decrease the multicomponent effect still further. This explains why flame propagation is but little influenced by variable volatility compared to a representative pure fuel of similar average volatility. On the other hand, vaporization prior to combustion would be significantly influenced by the volatility characteristics of real multicomponent fuels. As seen in Figure 4, prevaporization

exerts a very significant influence on flame propagation. It is here rather than in the combustion itself that the effects are important.

The conclusion is thus that it is in the conditions leading up to combustion that differences in fuel characteristics are significant for middle distillates such as the fuels studied here. The similarity of the flame speeds for the different fuels seen in Figure 4 is thus due to the fact that prevaporization was taken to be the same for all fuels.

RESULTS FOR GAS TURBINE STARTING CONDITIONS

Appendix C lists the conditions taken to be representative of the combustor under cold starting conditions. Droplets are injected at an initial diameter, partially evaporate during a short period before entering the combustion zone and then burn at a rate determined by, among other things, the reduced droplet size and the vapour present due to prevaporization.

The model predicts flame speed. The question is then how to relate this to the starting performance of a real engine. The models developed here could be used as subcomponents of larger cold starting models of varying degrees of complexity. For purposes of comparison in this paper, a simple and accepted means of relating fundamental flame speed to some recognized operational parameter was needed. For this purpose, the blow-out velocity was selected because there is a straightforward way of relating it to flame speed without entraining other moot considerations which would cloud the issue. The relation of Ballal and Lefebvre [16] was used:

$$U_{BO} = \frac{C_p D_s^2}{\alpha_s} \quad (4)$$

In order to ensure that the model gave physically realistic predictions of blow-out velocity, comparisons with published experimental data were made. Figure 7 shows a comparison between the measured blow-out velocity of nonane as presented by DeZubay [17] and the predictions of the model. These values are for complete prevaporization, and are seen to agree satisfactorily. No data were found in the open literature to permit a direct comparison for a heterogeneous case, but the present model compares favourably to the theoretical prediction of Ballal and Lefebvre [16]. In fact, the model presented here offers an advantage over that of Ballal and Lefebvre in that it correctly predicts the well-known observation that droplets below a certain size behave as if the fuel were completely evaporated. Having validated the model to the extent possible, it was then used to investigate the relative importance of various parameters.

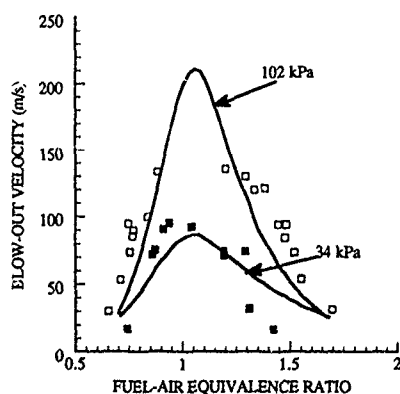


Figure 7 Comparison of Blow-Out Velocity Predictions with Data of DeZubay [17]

Figure 8 shows the blow-out velocity for the assumed cold starting conditions listed in Appendix C. The effect of a higher pressure ratio is to increase combustion chamber temperature, with concomitant effects upon evaporation and flame speed.

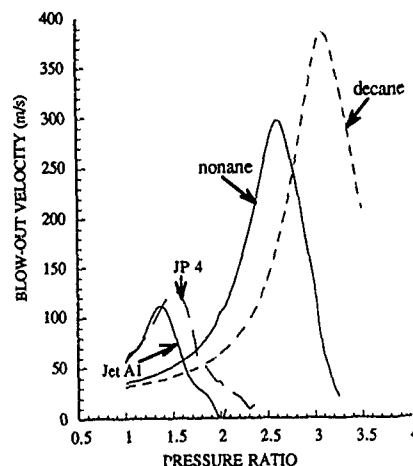


Figure 8 Effect of Fuel Type and Pressure Ratio on Blow-Out Velocity (Initial Diameter = 100 μ m, Ambient Temperature = 20°C)

In addition to the obvious major impact of pressure ratio (hence cranking speed) on combustion, there are several other noteworthy observations which can be made from this figure. The first striking feature is how different the single component fuels behave compared to the real blends. It is clear that, under some conditions at least, the use of pure compounds to represent JP-4 or Jet-A1 leads to very unrepresentative results. The disparity can be attributed to the different prevaporization occurring with the fuels during the flight of the droplets from injector to flame zone. The poor simulation of the real fuels by pure compounds of similar overall properties is in marked contrast to the earlier observation that, all other conditions including prevaporization being equal, flame propagation is virtually identical for all four fuels.

A second observation from Figure 8 is that there is a maximum blow-out velocity occurring at some pressure ratio. Further increases in pressure ratio (and thus in chamber temperature) reduce blow-out speed. This is due to the rich overall mixture (equivalence ratio of 3.3) and relatively small droplet size (100 μ m) used in these calculations. For such conditions, excessive pressure rise results in a chamber temperature so high that evaporation to local values well beyond stoichiometric occurs and the flame is slowed or extinguished altogether. The practical likelihood of such an occurrence seems small under cold starting conditions, but designers might need to take the possibility into account when systems designed for good cold starting are started at warm ambient temperatures with high cranking speeds and better atomization.

A final observation from Figure 8 is that the differences between JP-4 and JET A1 are insignificant in the range of pressure ratios up to the peaks. These latter are slightly different and occur at somewhat different pressure ratios, but are again close enough that differences are probably not of great practical significance. This apparent indifference to the volatility advantage of the wide-cut JP-4 can probably be attributed to the combination of favourable spray size, very rich mixture and high ambient temperature (20°C) used in this particular calculation. Under cold starting conditions, coarser sprays and lower volatility would accentuate the differences between wide-cut and high flash point fuels, leading to significantly better vaporization with the latter.

Figure 9 represents similar conditions to those of Figure 8, except that droplet size is assumed to be 350 μ m instead of 100 μ m and ambient temperature is reduced to -40°C. It again shows that the pure fuels are poor representatives for the blends; however, this time, there are no peaks within this range of pressure ratio. For these less favourable conditions, the JP-4 shows its better volatility; for a given

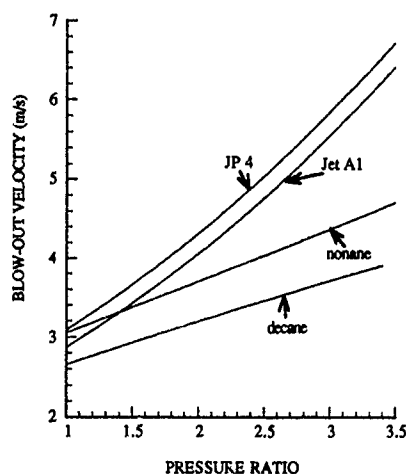


Figure 9 Effect of Fuel Type and Pressure Ratio on Blow-Out Velocity (Initial Diameter = 350 μm , Ambient Temperature = -40°C)

blow-out velocity (i.e. a given combustion performance) the pressure ratio must be higher for the lower volatility JET A. This would correspond to somewhat poorer cold starting and idling performance in the case of a real engine.

In view of the unsuitability of the single component fuels to adequately represent the real fuel blends when vaporization is involved, the remaining discussion will concentrate on the two real fuels. Figure 10 shows the effect of temperature and mean droplet size (SMD) on combustion performance. The particular conditions used in the calculation again lead to curves which show peak combustion performance at some optimum mean droplet size. Lower ambient temperature decreases blow-out velocity substantially, and also requires smaller droplets to attain best results. At a mean diameter of 125 μm , blow-out velocity at 20°C is some 60% higher than at 0°C . In reality, droplet size would be expected to become coarser at lower temperatures due to increased liquid viscosity, aggravating the disparity still further.

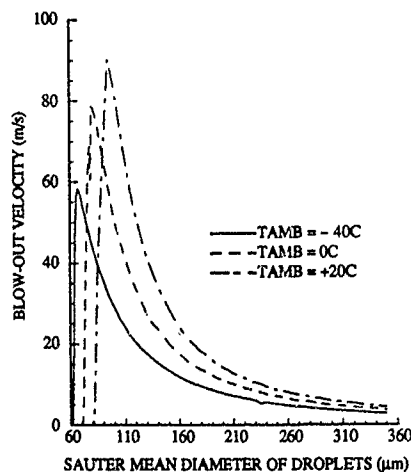


Figure 10 Effect of Temperature and Droplet Size on Jet A1 Combustion

Figure 11 shows the change in optimum droplet size as ambient temperature is varied. The advantage of JP-4 at low temperatures is clear in that droplets need not be as small as for Jet A1. However, the difference is not great for the rather short evaporation time arbitrarily selected for these calculations. The two curves cross at higher temperature because JP-4 droplets evaporate too quickly for the rich local equivalence ratio used for the calculations. For either fuel, the effect of ambient temperature

is quite substantial.

Figure 12 shows the importance of the droplet size distribution on blow-out velocity. The spray having the greatest range of sizes, and hence many small droplets, shows the highest blow-out velocity at low temperatures. By comparison, a monosized spray has greatly inferior performance. The effect again, is due to the change in prevaporization. A relatively small mass fraction of small droplets can markedly improve evaporation rate.

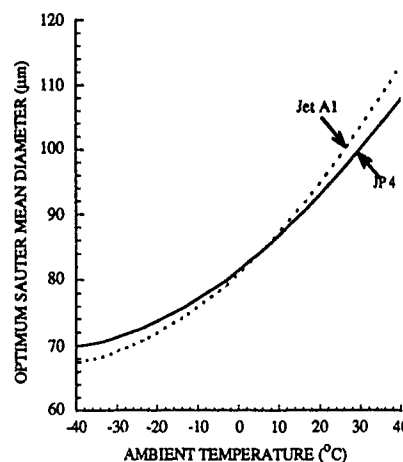


Figure 11 Effect of Ambient Temperature on Optimum Droplet Size

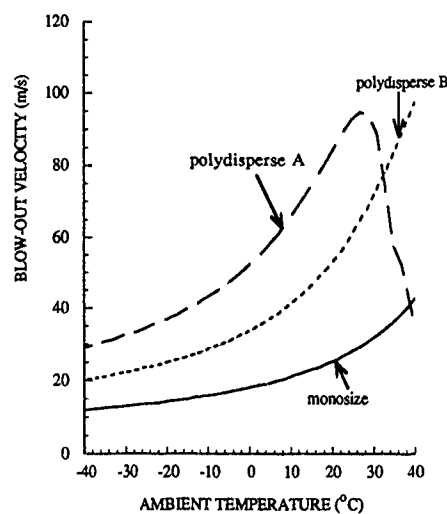


Figure 12 Effect of Droplet Size Distribution on Jet A1 Combustion (SMD=100 μm)

CONCLUSIONS

1. The flame propagation model with multicomponent fuel properties accounted for can shed useful light on combustion behaviour. A simple example has been presented here; but the multicomponent fuel model and the flame propagation model could also be utilized individually or in combination as components of more complex gas turbine combustion analyses. For instance, they could be used to help evaluate the evaporation occurring from individual droplets and to calculate the combustion rate at different locations within the combustor.

2. Single component idealizations are quite satisfactory for many combustion and flame propagation calculations; however, when prevaporization is important, such as under cold starting conditions, real fuel behaviour is badly represented by single component approximations. Multicomponent volatility behaviour can critically influence the conditions leading up to combustion.
3. The extent of prevaporization can exert a dominant effect on flame propagation; therefore accurate representation of this process is essential to any model. Multicomponent effects must be accounted for.
4. For the particular conditions studied here, the differences between JP-4 and Jet A1 are relatively slight. However, detailed modelling of particular cases would be expected to show much greater impact of the more volatile JP-4. The equations presented here for vapour pressure can readily be used for such studies.
5. The effect of mean droplet size, size distribution, cranking speed (via pressure ratio), ambient temperature and fuel type have been studied for an arbitrary set of conditions intended to represent cold starting in a gas turbine. Particular conclusions relevant to this case have been drawn and may offer some qualitative guidance. However, actual behaviour is very sensitive to the values of parameters assumed (eg. turbulence intensity). These results should therefore be considered as merely an illustration of the type of computations which can be performed with the flame propagation and volatility models.

REFERENCES

1. Aggarwal, S.K. and Sirignano, W.A., "Numerical Modeling of One-Dimensional Enclosed Homogeneous and Heterogeneous Deflagrations," *Comput. Fluids*, Vol.12, No.2, 1984, pp.145-158.
2. Swithenbank, J., Turan, A., Felton, P.G., "Three-Dimensional Two-Phase Mathematical Modelling of Gas Turbine Combustors," *Gas Turbine Combustor Design Problems*, Lefebvre, A.H., ed., Hemisphere, Washington, D.C., 1980, pp.249-314.
3. Polymeropoulos, C.E., "Flame Propagation in Aerosols of Fuel Droplets, Fuel Vapor and Air," *Combust. Sci. Technol.*, Vol.9, 1974, pp.197-207.
4. Polymeropoulos, C.E., "Flame Propagation in Aerosols of Fuel Droplets, Fuel Vapor and Air," *Combust. Sci. Technol.*, Vol.40, 1984, pp.217-232.
5. Mizutani, Y. and Ogasawara, M., "Laminar Flame Propagation in Droplet Suspension of Liquid Fuel," *Int. J. Heat Mass Transfer*, Vol.8, 1965, pp.921-935.
6. Ballal, D.R. and Lefebvre, A.H., "Flame Propagation in Heterogeneous Mixtures of Fuel Droplets, Fuel Vapor and Air," *Eighteenth Symp. (Int.) Combust.*, The Combustion Institute, Pittsburgh, 1981, pp.321-328.
7. Myers, G.D. and Lefebvre, A.H., "Flame Propagation in Heterogeneous Mixtures of Fuel Droplets and Air," *Combust. Flame*, Vol.66, 1986, pp.193-210.
8. Gauthier, J.E.D. and Bardon, M.F., "Laminar Flame Propagation in Mixtures of Fuel Droplets, Fuel Vapour and Air," *J. Inst. of Energy*, Vol. LXII, No.451, Jun 1989, pp.83-88.
9. Bardon, M.F. and Rao, V.K., "Calculation of Gasoline Volatility," *J. Inst. of Energy*, Vol.57, 1984, pp.343-348.
10. Rao, V.K. and Bardon, M.F., "Estimating the Molecular Weight of Petroleum Fractions," *Ind. Eng. Chem., Process Des. Dev.*, Vol.27, No.2, April 1985.
11. Bardon, M.F., Rao, V.K., Vaivads, R. and Evans, M.J.B., "Measured and Predicted Effect of the Extent of the Evaporation on Gasoline Vapour Pressure," *J. Inst. of Energy*, Vol.65, No.441, December 1986.
12. Bardon, M.F., Nicks, G.W., Rao, V.K. and Vaivads, R., "A Vapour Pressure Model for Methanol/Gasoline M85 Blends," SAE Paper #870366 presented at the International Congress and Exhibition, Detroit, Feb.23-27, 1987.
13. "Distillation of gasoline, naphtha, kerosine and similar petroleum products," Test D86, American Society for Testing and Materials, Philadelphia, 1978.
14. Bardon, M.F., Gauthier, J.E.D. and Rao, V.K., "Flame Propagation through Sprays of Multi-Component Fuel," *J. Inst. of Energy*, Vol. LXIII, No.405, Jun 1990, pp.53-60.
15. Kanury, A.M., *Introduction to Combustion Phenomena*, Gordon and Breach, New York, 1977.
16. Ballal, D.R. and Lefebvre, A.H., "Some Fundamental Aspects of Flame Stabilization," *Fifth International Symposium on Airbreathing Engines*, Feb. 1981.
17. DeZubay, E.A., "Characteristics of Disk-Controlled Flame," *Aero. Digest*, Vol.61, Nov. V, Jul. 1950, pp.94-96, 102-104.
18. Williams, F.A., *Combustion Theory*, 2nd ed., Benjamin/Cummings, Menlo Park, California, 1985.
19. Hubbard, G.L., Denny, V.E. and Mills, A.F., "Droplet Evaporation: Effects of Transients and Variable Properties," *Int. J. Heat Mass Transfer*, Vol.18, 1975, pp.1003-1008.
20. Gordon, S. and McBride, B.J., "Computer Program for Calculation of Complex Chemical Equilibrium Compositions, Rocket Performance, Incident and Reflected Shocks, and Chapman-Joulet Detonations," NASA, SP-273, March 1976.
21. Fenn, J.B. and Calcote, H.F., "Activation Energies in High Temperature Combustion," *Fourth Symp. (Int.) Combust.*, Williams and Wilkins, Baltimore, 1953, pp.231-239.
22. Gauthier, J.E.D., *Flame Propagation in Mixtures of Fuel Droplets, Fuel Vapour and Air*, thesis submitted to the Royal Military College of Canada, Kingston, Ontario 1987.
23. Raju, M.S. and Sirignano, W.A., "Multicomponent Spray Computations in a Modified Centerbody Combustor," *J. Prop. and Power*, Vol.6, No.2, March-April, 1990.
24. Lefebvre, A.H., *Gas Turbine Combustion*, McGraw-Hill, New York, 1983.
25. Andrews, G.E., Bradley, D. and Lwakabamba, S.B., "Turbulence and Turbulent Flame Propagation - A Critical Appraisal," *Combust. Flame*, Vol.24, 1975, pp.285-304.

APPENDIX A

FLAME PROPAGATION MODEL

A.1 Overall Model

Since the amount of fuel vapour in the fresh mixture is known, the main task is to find a procedure to calculate the amount of fuel which vaporizes from the liquid droplets passing through the flame front. The time t for any mixture to pass through the flame front is given by the ratio of the flame front thickness to the burning velocity:

$$t = \frac{\delta}{S} \quad (\text{A-1})$$

As stated above, the droplet diameter D_d , while passing through the flame front, decreases according to the " d^2 law"

$$D_d^2 = D_{d0}^2 - \lambda_b t \quad (\text{A-2})$$

Under steady conditions, the rate of heat transfer to the reactants from the flame is balanced by the rate of heat liberation in the flame [15,18]. From this, an expression can be found [8] to derive the effective equivalence ratio available in the flame front. This is simply the sum of original fuel vapour present plus that produced by the partial evaporation occurring as droplets pass through the flame front.

$$\phi_{eff} = \phi_r \left(1 - (1 - \Omega) \left[1 - \frac{\lambda_b k_g}{(D_{d0} S_L)^2 \rho_s \overline{c}_{pg}} \right]^{1.5} \right) \quad (\text{A-3})$$

In accordance with the model hypothesis, the heterogeneous burning velocity is equal to that of a homogeneous mixture of equivalence ratio equal to ϕ_{eff} . Note that the laminar heterogeneous burning velocity S_L is a function of ϕ_{eff} but that ϕ_{eff} is itself a function of S_L via equation (A-3). This open form solution means that the value of S_L (hence of ϕ_{eff}) must be found using an iterative method.

Gas phase properties are calculated using conventional mixture procedures and component properties. The calculation of specific heat as functions of temperature is done with third degree polynomials. Following the approach used by other workers [4,6], the representative gas properties inside the flame front are assumed to be those of air at the arithmetic mean of the reactant and flame temperatures. The mean specific heat of the gas phase in the reactants is also approximated by the value at the arithmetic mean of the reactants and flame temperature.

The 1/3 rule of Hubbard and Mills [19] is used to calculate the appropriate reference temperature for single droplet evaporation. The flame temperature is taken as the adiabatic flame temperature calculated using the NASA Chemical Equilibrium program [20].

A.2 Burning Constant λ_b

The burning constant for use in the " d^2 law" is found from

$$\lambda_b = \frac{8k_{a,v} \ell_n(1+B)}{\rho_f t c_{p,a,v}} \quad (A-4)$$

where the droplet transfer number is approximated by:

$$B = \frac{c_{p,a,v}(T_{mean} - T_{surf})}{H_v + c_{p,f}(T_{surf} - T_f)} \quad (A-5)$$

The droplet surface temperature is assumed equal to the boiling temperature of the liquid at the instantaneous value of Ω . The effect of turbulence on droplet evaporation rate is accounted for using a conventional correlation of the form

$$\lambda_{bT} = \lambda_{bL}(1 + 0.3Re\beta^{0.5}) \quad (A-6)$$

where the Reynolds number is based on droplet diameter and turbulence intensity. Reference [8] provides further details as well as a description of how droplet size distribution is accounted for.

A.3 Homogeneous Burning Velocity

A.3.1 Laminar

The calculation of the laminar homogeneous burning velocity S_{L_v} is done using the modified Semenov equation [21]:

$$S_{L_v} = \sqrt{K \frac{T_o^2 T_F^2}{(T_F - T_o)^3}} e^{(E/RT_F)} \quad (A-7)$$

The value of K is calculated using the known conditions of maximum homogeneous laminar burning velocity at normal ambient conditions. The effects of temperature and pressure are accounted for with power law expressions using the method proposed by Gauthier and Bardon [8] to evaluate the exponents.

A.3.2 Turbulent

Reference [22] describes the technique used to compute turbulent burning velocity, given the laminar flame speed. The equation used was of the form:

$$S_{T_v} = S_{L_v} + C_T u' \quad (A-8)$$

where $C_T = 0.453 + 4.467/(1+u'/S_{L_v})$ (A-9)

This latter equation is based on empirical data for turbulent combustion under conditions similar to those in gas turbines [22].

APPENDIX B

FUEL VOLATILITY MODEL

In the present program, the functions f_1 and f_2 in equation (3) were derived in accordance with an improved version of the procedure described in references [9]-[12]. The functions f_1 , f_2 and M_{mf_v} and ΔH are expressed by shifted Legendre polynomials:

$$\begin{aligned} f_1 &= a_1 P_1 + a_2 P_2 + \dots + a_n P_n \\ f_2 &= b_1 P_1 + b_2 P_2 + \dots + b_n P_n \end{aligned} \quad (B-1)$$

$$M_{mf_v} = c_1 P_1 + c_2 P_2 + \dots$$

$$\Delta H = d_1 P_1 + d_2 P_2 + \dots$$

The degrees of the least-squares polynomials required to adequately approximate the functions f_1 , f_2 , M_{mf_v} and ΔH vary from case to case; they are determined largely by the shape of the ASTM distillation curve of the fuel. A curve whose slope changes considerably as the distillation progresses, results in functions that require a larger number of terms in the polynomial approximations, particularly the two functions f_1 and f_2 . In the present case, a fourth-order polynomial was used to represent the functions for. The first five Legendre polynomials are:

$$\begin{aligned} P_1 &= 1 \\ P_2 &= S \\ P_3 &= (3S^2 - 1)/2 \\ P_4 &= (5S^3 - 3S)/2 \\ P_5 &= (35S^4 - 30S^2 + 3)/8 \end{aligned} \quad (B-2)$$

where $S = 1 - 2\Omega$

Tables B-1 and B-2 give the values of the coefficients used for JP-4 and Jet A1 respectively.

Table B-1: JP-4 Coefficients for use with Equation (B-1)

	f_1	f_2	M_{mf_v}	ΔH
1	.29160E+07	.43807E+04	.11030E+03	.36421E+05
2	-.53703E+06	-.69283E+03	-.14869E+02	-.57603E+04
3	.14320E+06	.10733E+03	-.12463E+00	.89241E+03
4	-.35832E+05	-.24750E+02	-.15587E+01	-.20586E+03
5	-.49269E+05	-.79834E+02	-.91133E+00	-.66367E+03

Values in this table give pressure in kPa and enthalpy in J/mol.

Table B-2: Jet A1 Coefficients for use with Equation (B-1)

	f_1	f_2	M_{mf_v}	ΔH
1	.36596E+07	.52342E+04	.17337E+03	.43518E+05
2	-.50351E+06	-.45246E+03	-.14785E+02	-.37616E+04
3	.14903E+05	-.24603E+02	-.10524E+01	-.20456E+03
4	.88803E+04	.12795E+02	-.85762E+00	.10640E+03
5	-.27068E+05	-.29642E+02	-.10516E+01	-.24662E+03

For the single component fuels, the Clausius-Clapeyron Equation (1) was used

Table B-3. Coefficients for Equation (1) for Pure Fuels

	C_1	C_2
n-nonane	1.573E+08	5166.5
n-decane	1.5672E+08	5455.54

Figures B.1 to B.3 compare Jet A1 and n-decane at three temperatures. It is clear that the single component fuel does not reflect the true vapour pressure behaviour at any given temperature; furthermore, it does not even represent a reasonable mean value except over a very limited temperature range.

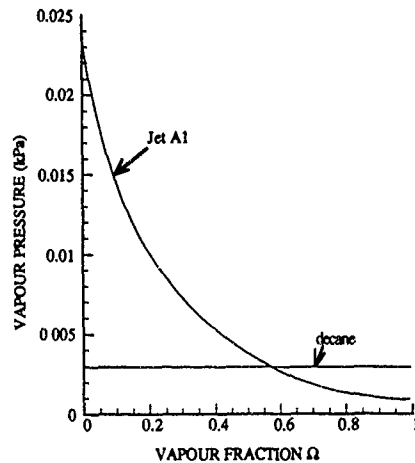


Figure B1 Vapour Pressure of Jet A1 and Decane at -20°C

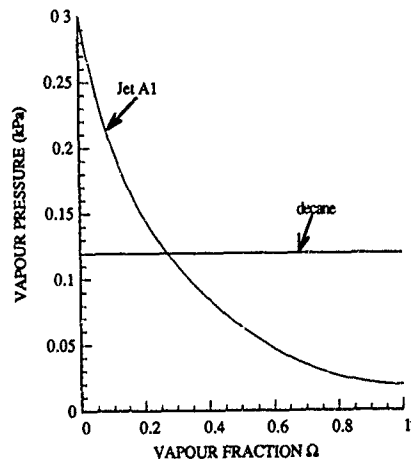


Figure B2 Vapour Pressure of Jet A1 and Decane at +20°C

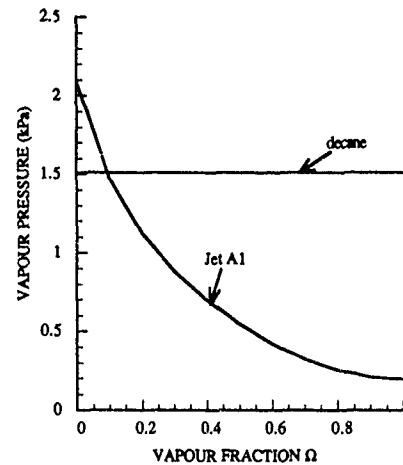


Figure B3 Vapour Pressure of Jet A1 and Decane at +60°C

APPENDIX C

Data Used to Represent Typical Cold Starting Conditions in a Gas Turbine

Ambient Pressure:	101 kPa
Ambient Temperature:	20°C except where explicitly varied.
Pressure ratio at start-up:	1.2
Sauter Mean Diameter of Droplets produced by the fuel injector:	100 μm [23,24]
Turbulence intensity:	350 cm/s [25]
Local fuel air equivalence ratio in flame zone:	3.3 [23]
Blow-out velocity coefficients (equation (4)):	$C_s = 1.33$ [16] $D_c = 0.01$ m [16]

Time available for droplet evaporation before reaching the flame: 0.007 s [23]

The coefficients C_1 - C_3 describing the droplet size distribution are as described by Lefebvre [24]:

$$C_1 = \text{MSD/SMD} \quad C_2 = \text{MDD/SMD} \quad C_3 = \text{MMD/SMD}$$

Default values used:

$$C_1 = 0.31 \quad C_2 = 0.21 \quad C_3 = 0.46 \quad [6]$$

For comparison purposes, a second polydisperse spray is also used in Figure 12, referred to as "Polydisperse B" using the following values:

$$C_1 = 0.84 \quad C_2 = 0.73 \quad C_3 = 0.89 \quad [23]$$

Discussion

I. C. Moses, Southwest Research Institute

There are two major theories in the mechanism of droplet evaporation with multicomponent fuels. At one extreme, the interior of the drop is well mixed. This allows for light components to be continuously brought to the surface, and thus the fuel effectively destills as you have discussed. At the other extreme, there is no mixing and the droplet evaporates much as an onion skin with all components, light and heavy, effectively evaporating at the same time. Have you investigated these two possibilities to see which provides the better agreement?

Author:

Our work so far has been exclusively on the case of droplets which are well mixed internally. This is due to the use of equilibrium vapor pressure, and implies that droplet evaporation and diffusion outwards is slow with respect to internal diffusion. This is one of the two limiting cases, the other being the case with no internal mixing or onion-skin evaporation. The latter is more nearly the case for heavy viscous fuels and very short residence times. The case in the cold combustor is probably closer to the equilibrium limit but we have not verified it experimentally. For the present circumstances many of the conclusions would in any case be unchanged. The relatively similar performance of JP4 and JET A1 for example, would be unaffected by which limiting model we used in the calculations presented here.

THE DEVELOPMENT OF A COMPUTATIONAL MODEL TO PREDICT LOW TEMPERATURE FUEL FLOW PHENOMENA

R. A. Kamin and C. J. Nowack
Naval Air Propulsion Center
Trenton, NJ 08628 USA

B. A. Olmstead
Boeing Military Airplanes
Seattle, Wa 98124 USA

SUMMARY

Fuel availability studies indicated that the relaxation of the F-44 freeze point specification could greatly increase the yield of F-44 per barrel of crude. A thorough analysis was initiated to ensure that the higher freeze point fuel would not form solid wax precipitates during low temperature operations that could impact aircraft mission performance. In order to evaluate the effects of a potential change in the freeze point specification over the entire inventory of United States Naval aircraft, a general three dimensional computational fluid dynamics code, PHOENICS 84, was modified for use. Inputs into the code include tank geometry (cylindrical, rectangular or body fitted), mission profile (outside air temperatures or altitude, airspeed and time on station), and fuel properties (specific heat, thermal conductivity, viscosity, freeze point, etc.). Outputs from the model include fuel cooldown and holdup (unpumpable frozen fuel) as a function of time and position in the tank. The accuracy of the code was verified by experimental data obtained during flight and simulator testing of instrumented tanks.

NOMENCLATURE

A	Area
C	Numerical Constant
C ₁	Empirical Turbulence Model Coefficient
C ₂	Empirical Turbulence Model Coefficient
C ₃	Empirical Turbulence Model Coefficient
C _p	Specific Heat
C _t	Empirical Turbulence Model Coefficient
g	Acceleration of Gravity
h	Sensible Heat
H	Enthalpy
i, j, k	Subscripts Denoting Cartesian Coordinate Directions
K	Turbulent Kinetic Energy
K'	Permeability
L	Total Latent Heat
P	Pressure
q'	Numerical Constant
Re _t	Turbulent Reynolds Number ($K^2 \rho / \mu$)
S _B	Buoyancy Source Term
S _L	Latent Heat Source Term
S	Darcy Source Term
t	Time
T	Temperature
\vec{U}	Velocity Vector
U	Cartesian Space Velocity
u, v, w	Velocity in x, y, z Directions
x, y, z	Cartesian Space Coordinates
β	Coefficient of Thermal Expansion
ϵ	Rate of Turbulent Kinetic Energy
λ	Porosity
k	Thermal Conductivity
ρ	Density
σ_t	Turbulent Prandtl Number
σ_K	Prandtl-Schmidt Number for Turbulent Dissipation Rate
σ_ϵ	Prandtl-Schmidt Number for Turbulent Kinetic Energy
μ	Dynamic Viscosity
μ_t	Turbulent Viscosity ($\rho K^2 / \epsilon$)
ν	Kinematic Viscosity
θ	Angular Coordinate

INTRODUCTION

F-44, due to its unique requirements of a high flash point ($60^{\circ}\text{C}/140^{\circ}\text{F}$) and low freeze point ($-46^{\circ}\text{C}/-51^{\circ}\text{F}$), is a specialty product which accounts for only a small fraction, less than 1%, of total refinery production. Therefore, to make the production of F-44 profitable to the refinery, it is produced at a premium cost to the United States Navy. In addition, the increasing commercial demand for the refinery distillate stream combined with the increased use of heavier, high sulfur, lower yielding crudes creates the potential for shortfalls in the production of F-44. The U.S. Navy, in response to these potential fuel shortages, has given a high priority to investigating methods of increasing the availability of F-44. Various studies^{1,2} have shown that the two most critical properties affecting the yield of F-44 per barrel of crude are the flash point and the freeze point. Since the flash point specification is set more as a shipboard safety than an aviation requirement and cannot be lowered, the relaxation of the freeze point specification is the most logical and cost effective method to increasing F-44 yield. By relaxing the current $-46^{\circ}\text{C}/(-51^{\circ}\text{F})$ freeze point specification to the commercial Jet A specification of $-40^{\circ}\text{C}/(-40^{\circ}\text{F})$, it is possible to obtain a 10% to 75% increase², depending on crude source, in the maximum theoretical yield of F-44 per barrel of crude.

However, before the specification change can be made, its potential impact on aircraft performance must be evaluated. This investigation is necessary because of the concern that the higher freeze point fuel may form solid wax precipitates during extreme low temperature operations. These precipitates may cause plugging of filters or blockage of fuel tank transfer lines that could severely restrict flow to the engine.

The ideal method for assessing the impact of higher freeze point fuels would be to measure the fuel temperatures within the tank of each aircraft during extreme low temperature operations. This, however, would have required an extensive number of tests that would be extremely costly and time consuming. Therefore, the only practical cost effective method by which to approach this problem was to develop a mathematical computer model, verified by experimental results, to predict fuel temperature and holdup (portion of unusable fuel due to freezing) during a mission.

MODEL DEVELOPMENT

The turbulent, unsteady boundary conditions and the extremely high Rayleigh numbers (10^{12}) encountered during a flight make the modeling of fuel cooldown and holdup within a tank a difficult and complex analytical problem. Although a one dimensional model³ has been developed to predict fuel temperatures in thin wing tanks, many aircraft fuel tanks must be modeled in two or three dimensions in order to give accurate results. Prior to initiating the development of the two and three dimensional model, a literature search was performed to determine if any existing multidimensional computational fluid dynamics (CFD) codes were available that could be modified to handle this problem. After an extensive review of CFD codes, the general purpose PHOENICS 84 (Parabolic, Hyperbolic or Elliptical Numerical-Integration Code Series) code was determined as the best available code to solve this problem. The PHOENICS 84 code is a centralized, versatile system capable of performing a large number of fluid-flow, heat transfer and chemical reaction calculations simultaneously⁴. The code consists of an inaccessible proprietary core program, called Earth, which contains the theoretical, problem solving algorithms. The Earth code obtains the specific information necessary to define and solve each problem from two user accessible programs, called Satellite and Ground respectively.

An extensive effort was initiated to develop the specific user input routines for Satellite and Ground that would be necessary to allow the source code, Earth, to both accurately and cost effectively predict fuel temperature and holdup. Major areas of development included 1. Optimum grid selection for both rectangular and cylindrical geometries, 2. Turbulence modeling, 3. Phase change modeling, and 4. Expert system development.

Grid Selection

The optimum computational grids were developed based on the criteria that they produce well-converged, stable and accurate solutions at as low a computational cost as possible. For both rectangular and cylindrical geometries, the grids developed were finely divided at the walls and the bottom of the tank where the steepest temperature gradients occur and became increasingly coarser as they approached the center of the tank. The computational costs were further reduced for the two dimensional simulations by assuming symmetry within the tank, i.e. at the vertical centerline $\partial v_x / \partial \theta = 0$ and $\partial T / \partial \theta = 0$, and only modeling half the tank. This assumption, which cut the computational time in half, was verified by experimental testing to be accurate⁵. Finally, a grid refinement sensitivity study was performed to determine the most cost effective grids, Figure 1, which would give accurate, well-converged solutions⁵.

Turbulence Model

The convective flow in aircraft fuel tanks, caused by the temperature gradient between the bulk fuel and outside air temperature, has been calculated to be in the transitional or turbulent regime, Rayleigh number $> 10^6$. The failure to account for the increased mixing of the fuel due to these convective flows could cause significant

error in the calculation of the local heat transfer coefficients. This error could result in the prediction of fuel cooling and holdup rates which were low. The initial approach to account for these turbulence effects was to calculate the local turbulent viscosity by using the K- ϵ 2-equation turbulence model⁶. The K- ϵ model was chosen because of its demonstrated success in calculating two dimensional steady state heat transfer in turbulent buoyant flows^{7,8}. The equations were modified to include buoyancy terms to account for turbulent kinetic energy generation and destruction due to buoyancy⁹. The resulting K- ϵ equations formed were

$$\rho \frac{DK}{Dt} = \frac{\partial}{\partial x_j} \left(\left(\frac{\mu_t}{\sigma_K} + \mu \right) \frac{\partial K}{\partial x_j} \right) + \mu_t \frac{\partial U_i}{\partial x_j} \left(\frac{\partial U_i}{\partial x_j} + \frac{\partial U_j}{\partial x_i} \right) - \frac{\mu_t}{\sigma_\epsilon} (g_j \frac{\partial \rho}{\partial x_j}) - \epsilon \quad (1)$$

$$\rho \frac{D\epsilon}{Dt} = \frac{\partial}{\partial x_j} \left(\left(\frac{\mu_t}{\sigma_\epsilon} + \mu \right) \frac{\partial \epsilon}{\partial x_j} \right) + C_1 \frac{\epsilon}{K} \mu_t \frac{\partial U_i}{\partial x_j} \left(\frac{\partial U_i}{\partial x_j} + \frac{\partial U_j}{\partial x_i} \right) - C_2 \frac{\epsilon \mu_t}{\rho K \sigma_\epsilon} (g_j \frac{\partial \rho}{\partial x_j}) - C_3 \frac{\epsilon^2}{K} \rho \quad (2)$$

The coefficients in equations (1) and (2) are set to constant values in the high Reynolds number turbulence model. However, to account for the low Reynolds number occurring in the turbulent natural convection, two of the coefficients, C_2 and C_3 , were set instead to functions of the turbulent Reynolds number, Re_t . The coefficients¹⁰ used in the modified K- ϵ model were

$$C_2 = 0.09 \exp[-2.5 / (1 + \frac{Re_t}{50})] \quad (3)$$

$$C_1 = 1.44$$

$$C_3 = 1.92 [1.0 - 0.3 \exp(-Re_t^2)] \quad (4)$$

$$C_2 = 1.44$$

$$\sigma_K = 1.0$$

$$\sigma_\epsilon = 1.3$$

These modifications were found to further enhance the accuracy of the model.

Fuel Freezing/Thawing Model

A fixed grid porous cell model was selected to simulate the freezing/thawing of the fuel within the tank¹¹. This model assumes that the crystalline-liquid, two phase region will behave as a porous medium and that Darcy's law

$$\vec{u} = - \frac{K'}{\mu} \text{grad } P \quad (5)$$

will govern the flow. Therefore, when the fuel in a specific cell is entirely in the liquid phase, $K' = \infty$, and when the fuel is completely in the solid phase, $K' = 0$.

The Darcy source terms, S_x , S_y and S_z , used to simulate the flow behavior in the two phase flow regions are defined as

$$S_x = -Au, S_y = -Av \text{ and } S_z = -Aw$$

where,

$$A = -C(1-\lambda)^2 / (\lambda^3 + q') \quad (6)$$

and increases in a nonlinear manner from zero to a large value as the local, solid fraction increases from 0 (liquid) to 1 (solid). The values of C and q' were set to 1.6×10^3 and .001 respectively. These values, based on previous work¹², were set to ensure that 1. C would be sufficiently small enough to allow flow in the two phase region which contained only small percentages of solid fractions and 2. The limiting value of A ($-C/q'$) would be large enough to suppress the velocities in the cells containing large percentages of solid.

The Darcy source terms are added to the right hand side of the momentum equations as follows:

u - momentum:

$$\frac{\partial(\rho u)}{\partial t} + \text{div}((\rho \vec{u})u) = \text{div}(\mu \text{grad } u) - \frac{\partial P}{\partial x} + S_x \quad (7)$$

v - momentum:

$$\frac{\partial(\rho v)}{\partial t} + \text{div}((\rho \vec{u})v) - \text{div}(\mu \text{ grad } v) - \frac{\partial P}{\partial y} + S_y + S_s \quad (8)$$

w - momentum:

$$\frac{\partial(\rho w)}{\partial t} + \text{div}((\rho \vec{u})w) - \text{div}(\mu \text{ grad } w) - \frac{\partial P}{\partial z} + S_z + S_s \quad (9)$$

where $u = u_i + v_j + w_k$

In the totally liquid cell, these source terms equal zero and, therefore, make no contribution. As a greater portion of the cell becomes solid, the size of the source terms increases until it becomes very large and suppresses all the velocities.

Another essential portion of the freezing model for convection/diffusion heat transfer phase change is the energy equation. This equation includes the latent heat source term, S_L , as follows:

$$\frac{\partial(\rho h)}{\partial t} + \text{div}(\rho \vec{u}h) - \text{div} \frac{K' \text{ grad } h}{C_p} - S_L \quad (10)$$

In this model the phase change is accomplished through enthalpy, defined as the sum of sensible and latent heats

$$H = h + \Delta H \quad (11)$$

The main advantage of this method is that there are no explicit heat transfer conditions to be satisfied as the phase change occurs, and the tracking of the phase change is therefore not required. With this method, the source term in the energy equation becomes

$$S_L = \frac{\partial(\rho \Delta H)}{\partial t} + \text{grad}(\rho \vec{u} \Delta H) \quad (12)$$

For a mixture of a large number of different components, as is found in aviation fuel, ΔH is a function of temperature¹³ constrained by the limits of

$$0 \leq \Delta H \leq L$$

where L , the total latent heat, is defined below the freeze point as

$$L = \int_t^{t'} C_p(T) dt \quad (13)$$

Although this temperature dependence is nonlinear, a simplified linear relationship was used as a first approximation. Therefore, at any temperature, the value of ΔH has the following physical interpretation:

Liquid fraction = $\Delta H/L$
Solid fraction = $1 - \Delta H/L$.

Additional details on solving the phase change equations using the PHOENICS 84 code are reported in reference 11.

A 2-D simulation with and without the use of the fuel freezing model was performed to determine the effects of the freezing model on the prediction of fuel temperatures. The results showed that the use of the model had little or no effect on the bulk fuel temperatures predicted. However, the simulation using the fuel freezing model predicted temperatures for the fuel located in the bottom of the tank 1°C to 3°C (2°F to 6°F) lower than the simulation not using the model. Upon comparison with the experimental results, Figure 2, the temperatures predicted by the simulation using the fuel freezing model agreed more closely than those predicted by the simulation that did not use the model¹⁴.

The most important piece of data needed to determine whether a higher freeze point aviation fuel can be used is fuel holdup. However, this property is extremely difficult to model accurately. The difficulty in this prediction is due to a number of reasons. First, small differences in temperature around the freeze point can result in a large

difference in fuel holdup. Therefore, if the temperatures predicted are only a few degrees Centigrade off from the actual values, they may have a large effect on the predicted holdup. Secondly, since less than 10% of the fuel actually solidifies and this wax-like matrix can prevent the flow of the remaining bulk liquid fuel, holdup results tend to be somewhat random and may vary from test to test. This variability, shown in duplicate tests to differ by as much as 30%¹⁵, cannot currently be theoretically modeled.

The fuel freezing model uses an empirical holdup correlation, derived from results obtained using the Shell Thornton cold flow tester, to determine the fraction of holdup at any given temperature. The cold flow tester consists of two distinct chambers separated by a poppet valve. One hundred milliliters of fuel is placed in the upper chamber, and the fuel is cooled to the specific test temperature. Upon reaching the specified temperature, the poppet valve is opened, and the liquid fuel is allowed to flow to the lower chamber. The valve is then closed and the amount of fuel remaining in the upper chamber is measured. The percentage of fuel remaining in the upper chamber is the holdup fraction of the fuel. Each fuel is tested over a wide range of temperatures below its freeze point and a graph of holdup versus temperature is developed (Figure 3). This information, accessed through the Ground routine of the PHOENICS 84 code, is used to predict the percentage of solid and liquid fuel for each grid cell.

Expert System Development

Due to the size and the complexity of the programming involved, the development of a user-friendly, menu driven format was necessary to avoid as much potential operator error as possible. The subroutines of the model were assembled to operate in a menu driven step-wise format, graphically depicted in Figure 4. After the user selects the type of aircraft and mission to be modeled, the external temperature exposures for the desired mission are determined by either of two methods. The temperature data may be selected by 1. Tracking the mission through an extensive database of recorded atmospheric temperatures obtained from approximately fifteen years of worldwide atmospheric measurements or 2. User defined requirements such as those measured during a test or defined in literature (e.g. MIL-STD-210B, Climatic Extremes For Military Equipment). Next, the geometry of the tank to be modeled is selected. Since optimum grid sizes for both rectangular and cylindrical geometries have been developed and installed in the program, the user simply has to input the dimensions of the tank and the amount of fuel desired.

The user then selects how the external boundary conditions should be defined. The two choices available are 1. Actually deriving the conditions from experimental tank skin measurements or 2. Calculating the temperatures based on environmental conditions (e.g. air temperatures and airspeed). The user is then asked to input the specific fuel properties (e.g. C_p , K , B , μ , ρ , ΔH and Shell holdup tester data) for the fuel to be simulated. These properties are mostly temperature sensitive and, therefore, must be defined as a function of temperature. A subroutine was written for the Ground portion of the PHOENICS 84 code to input the property data into the Earth code. Although the same properties were used for every simulation, the user does have the option to input specific property values.

Finally, the user selects the type of data, e.g. temperature data, holdup data, etc., and location in the tank from which the data is desired.

MODEL VERIFICATION

The computational model was verified in both two and three dimensions by a number of experimental tests. Model simulations were run for rectangular and cylindrical geometries using data obtained from both laboratory simulator and flight tests.

TWO DIMENSIONAL MODEL

Thick Wing Rectangular Tank

The results from a 1981 NASA flight test of an L-1011 aircraft¹⁸ were used to verify the model. This research aircraft contained an instrumented vertical thermocouple rake in the center of the approximately 22' deep outboard tank. For the simulation, the tank was assumed to be full of Jet A and the recorded top and bottom skin temperatures were used as the boundary conditions. The predicted temperatures for the bulk fuel located in the center of the tank were within 1°C to 3°C (2°F to 6°F) of the measured values (Figure 5). The predicted values for the fuel located in the bottom of the tank, thermocouple located approximately 1/4' from the bottom, were consistently 2°C to 5°C (4°F to 10°F) colder than the experimental values. Since the temperatures for the entire simulation remained above the fuel's freeze point, no frozen fuel was predicted.

Thin Wing Rectangular Tank

The thin wing rectangular tank verification was performed utilizing test data recorded in a wing tank simulator⁵. The wing tank simulator consisted of a 20 gallon rectangular tank instrumented with a vertical thermocouple rake. Jet A fuel having a -46°C (-51°F) freeze point temperature was used. Initial fuel temperature for the simulation was -42°C (-44°F). The top and bottom skin temperatures were used as the

boundary test conditions and held at approximately -50°C (-58°F) for the entire 280 minute test.

The predicted temperatures for the bulk fuel were within approximately 1°C (2°F) of the experimental results (Figure 6). However, the predicted value of 30% fuel holdup did not agree with the 70% holdup value that was measured experimentally. Potential reasons for the large difference between the calculated and measured values were discussed in a prior section.

Cylindrical Geometry

The cylindrical geometry model was verified using the experimental results obtained in a NAFPC wind tunnel test of an instrumented 150 gallon FPU-3A external tank¹⁷. The tank, Figure 7, contained two rakes of thermocouples, one placed in the front (Station 32) and the other in the rear (Station 108) of the tank. The tank contained approximately 122.5 gallons of JP-5 leaving approximately 2.5 inches of ullage space at the top. Two separate simulations were performed. The first simulation utilized the measured wall temperatures recorded during the test as the boundary conditions, while the second calculated the tank wall temperatures from the external air temperatures and velocities measured during the test.

The predicted temperatures for the calculated wall temperature boundary condition case showed excellent agreement (Figure 8) with the experimental results measured by the thermocouple located in the center of the tank (bulk fuel). The predicted temperatures for the measured wall temperature boundary condition case, however, were approximately 3°C to 5°C (6°F to 10°F) cooler than the bulk fuel. This may be attributed to the fact that temperature measurements were taken at only four points on the tank's skin (at 0, 90, 180, 270 degree intervals) and the remaining temperatures along the circumference of the skin were determined by linear interpolation. If the interpolated temperatures were in error then the boundary conditions used in the simulation would be in error, thereby causing the difference in the predicted bulk fuel temperatures. However, the measured wall temperature boundary condition simulation predicted fuel temperatures for the fuel located .25 inches from the bottom of the tank in excellent agreement with the experimental values, while the calculated wall temperature boundary condition case predicted values approximately 2°C to 5°C (4°F to 10°F) above the experimental results¹¹ (Figure 9).

The holdup measured upon draining the tank at the completion of the test was 15%. This compared to the predicted values of 11% for the measured wall temperature boundary condition case and 5% for the calculated wall temperature boundary condition case. Considering the inherent uncertainty in both the measurement and calculation of holdup, the agreement between the calculated value obtained in the simulation using the measured wall temperatures as the boundary condition and the actual holdup value was quite good.

THREE DIMENSIONAL MODEL

Flight Test

A flight test of the 150 gallon instrumented FPU-3A tank mounted on an A-6 aircraft was used to verify the model. The 3D model was needed for this simulation because the inclination of the tank during flight caused the formation of three dimensional temperature gradients which could not be accounted for by two dimensional modeling. The tank skin temperatures measured during the flight were used as the boundary conditions for the simulation. The tank contained 125 gallons of F-44 and had an initial fuel temperature of 11°C (52°F).

The predicted temperatures for the fuel located at the bottom of the tank were approximately 2°C to 5°C (4°F to 10°F) above the measured temperatures for the front thermocouple and 1°C to 3°C (2°F to 5°F) below the measurements taken at the rear of the tank¹¹ (Figure 10). However, the ability of the 3-D model to accurately predict the temperature difference between the front and the rear of the tank demonstrated its importance in accurately modeling actual fuel behavior occurring during low temperature missions.

CONCLUSION

The model was demonstrated to accurately predict, in both two and three dimensions, fuel temperature profiles at temperatures both above and below the fuel's freeze point. This model, verified for both rectangular and cylindrical geometries, is capable of predicting fuel cooling for any anticipated aircraft mission. In addition, the model can also be used, with minor modifications, to predict the heating of the fuel within the tank, making it a valuable tool in investigating fuel behavior during supersonic flight.

Although the accuracy of the fuel holdup prediction was not as good as that of fuel temperature, general approximations were able to be made. This prediction was based on an empirical correlation derived from Shell Thornton Cold Flow Tester data because holdup was shown to be a somewhat random phenomena containing an inherent degree of variability that could not be accounted for theoretically. Since holdup is such an extremely important piece of information, additional simulator studies are being

performed to develop the improved empirical correlations needed to w the model to make better holdup calculations.

The model is currently being used to predict the effects of higher freeze point fuels on naval aircraft mission performance. The results of this study will be used to determine if the F-44 freeze point specification can be safely relaxed to the commercial Jet A specification, thereby increasing the potential yield of F-44 per barrel of crude.

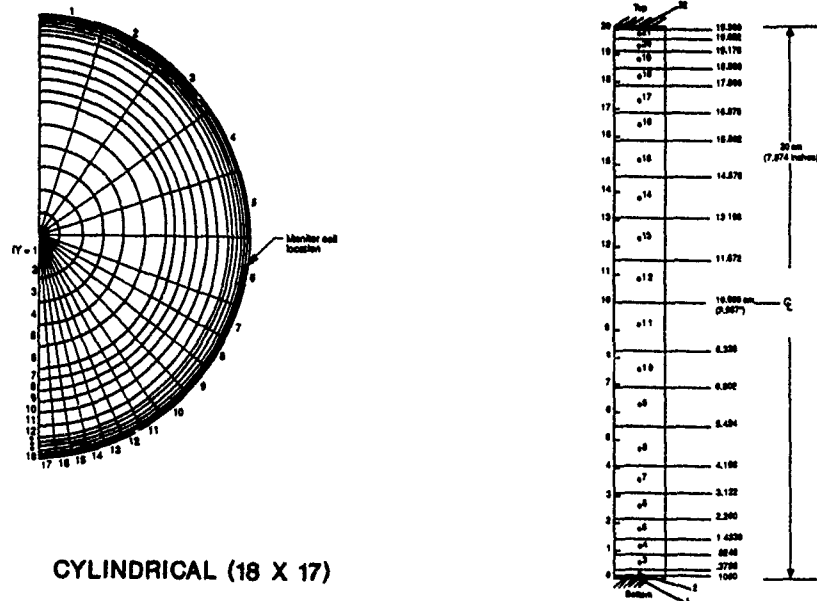
REFERENCES

1. Lieberman, W., and Taylor, W.F., "Effect of Refinery Variables on the Properties and Composition of JP-5," RL.2PE80, June 1980
2. Varga, G.M., Lieberman, W., and Avella Jr., A.J., "The Effects of Crude Oil and Processing on JP-5 Composition and Properties", NAPC-PE-121C, July 1985.
3. McConnell, P.M., Desmarais, L.A., and Tolle, F.F., "Heat Transfer in Airplane Fuel Tanks at Low Temperatures," ASME paper 83-HT-102.
4. Spalding, D.B., "A General Purpose Computer Program for Multi-Dimensional One and Two Phase Flow," Mathematics and Computers in Simulations, North Holland Press, Vol XXIII, 1981.
5. McConnell, P.M., "Development and Use of a Fuel Tank Fluids Characteristics Mathematics Model - Phase I," NAPC-PE-142C, January 1987.
6. Launder, B.E. and Spalding, D.B., "The Numerical Computation of Turbulent Flows," Computer Methods in Applied Mechanics and Engineering, Vol 3, 1974, pp. 269-289.
7. Markatos, N.C. and Pericleous, K.A., "Laminar and Turbulent Natural Convection In An Enclosed Cavity," International Journal of Heat and Mass Transfer, Vol. 27, No. 5, 1984, pp 755-772.
8. Humphrey, J.A.C., Sherman, F.S. and To, W.M., "Numerical Simulation of Buoyant Turbulent Flow," SAND85-8180, August 1985.
9. Rodi, W., Turbulence Models and Their Applications In Hydraulics - A State-of-the-Art, Institut Fur Hydromechanik, 2nd Ed, February 1984, pp. 27-31.
10. Olmstead, B.A. and Kamin, R.A., "Numerical Analysis of Turbulent Natural Convection in Airplane Fuel Tanks," To be published.
11. Vollar, V. and Prakash, P., "A Fixed Grid Numerical Methodology For Phase Change Problem Involving Mushy Region and Convection In the Melt", PDR/CHAM/NA9, July 1986.
12. Domanus, H.M. and Sha, W.T., "Solidification with Natural Convection," April 1988.
13. Mehta, H.K., and Armstrong, R.S., "Detailed Studies of Aviation Fuel Flowability," NASA CR-174938, June 1985.
14. McConnell, P.M., "Development and Use of a Fuel Tanks Fluids Characteristics Mathematics Model, NAPC-PE-177C, October 1988.
15. Desmarais, L.A., and Tolle, F.F., "Fuel Freeze Point Investigations," AFWAL-TR-84-2409, July 1984.
16. Svehla, R., "In Flight Atmospheric and Fuel Tank Temperature Measurements," NASA Conference Publication CP2307, 1984.
17. Kamin, R.A. and McConnell, P.M., "Impact of Higher Freeze Point Fuels on Naval Aircraft Operations," ASME paper 86-GT-262, June 1986.

ACKNOWLEDGMENT

This program was sponsored by the Energy and Natural Resources Office of the United States Office of Naval Research.

The authors wish to acknowledge P.M. McConnell and A.F. Grenich of Boeing Military Airplanes and L.L. Byrd of the Naval Weapons Center for their support and efforts in this program.



CYLINDRICAL (18 X 17)

RECTANGULAR (20 X 22)

FIGURE 1

OPTIMUM GRIDS FOR TWO DIMENSIONAL SIMULATIONS

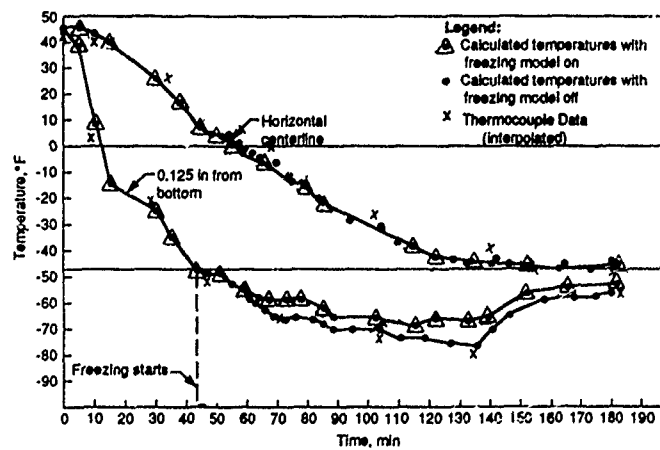


FIGURE 2 EFFECT OF FREEZING MODEL ON FUEL
TEMPERATURE CALCULATIONS

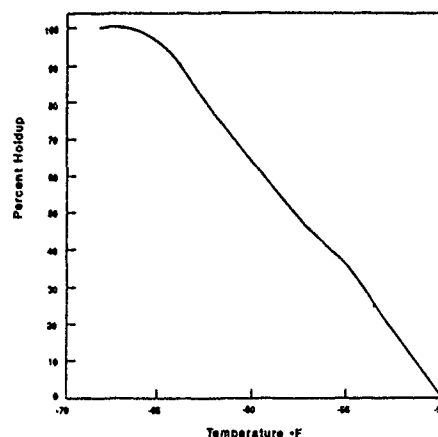


FIGURE 3
FUEL HOLDUP CURVE BASED ON SHELL THORNTON TESTER DATA

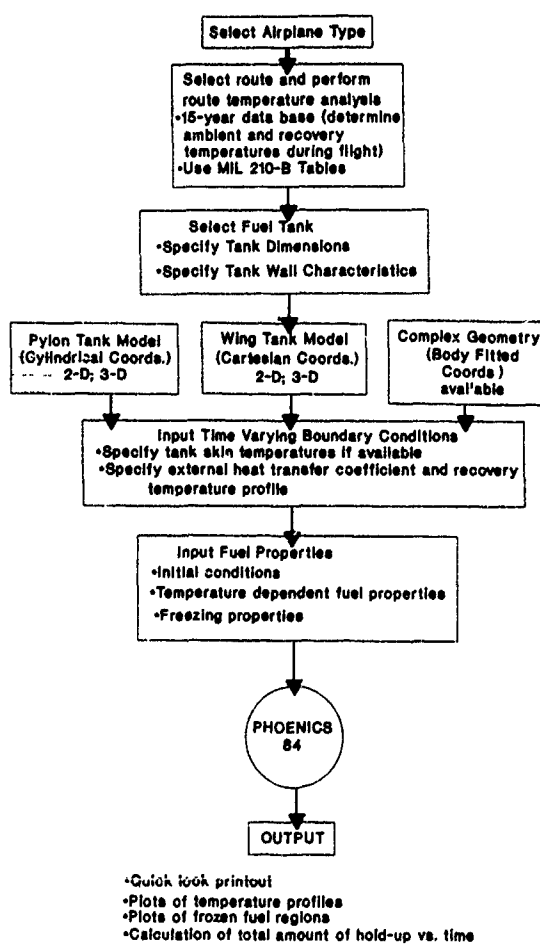


FIGURE 4
FLOW DIAGRAM ON APPROACH TO USE COMPUTER MODEL

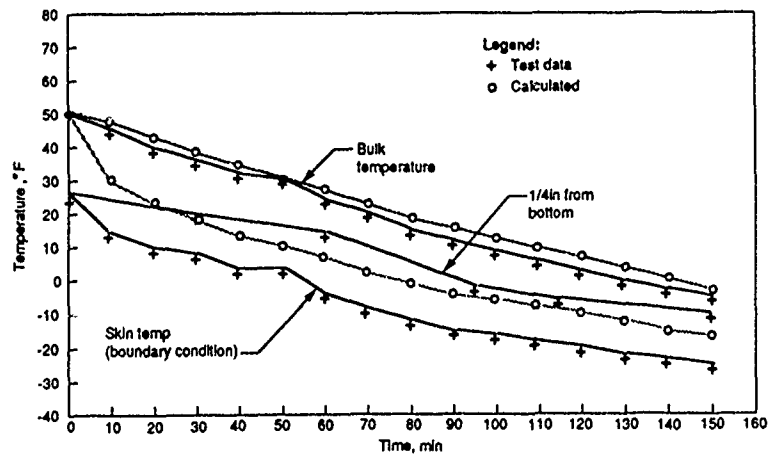


FIGURE 5
COMPARISON OF CALCULATED AND MEASURED
FUEL TEMPERATURES FOR THICK
WING RECTANGULAR TANK TEST

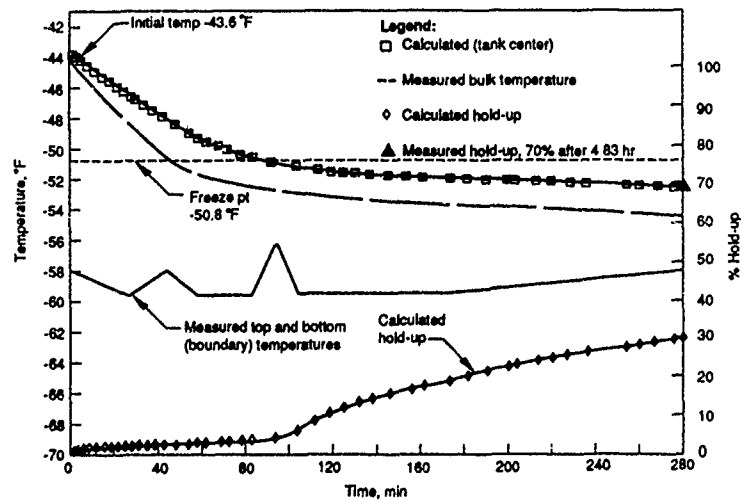


FIGURE 6
COMPARISON OF CALCULATED AND MEASURED
FUEL TEMPERATURES FOR THIN WING
RECTANGULAR TANK TEST

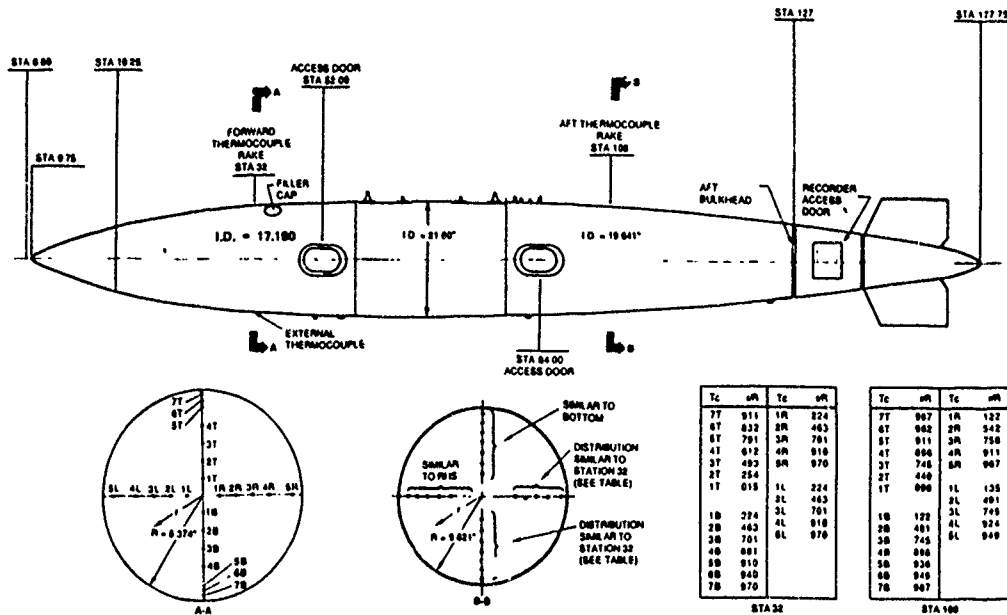


FIGURE 7
150 GALLON FPU-3A INSTRUMENTED
FUEL TANK

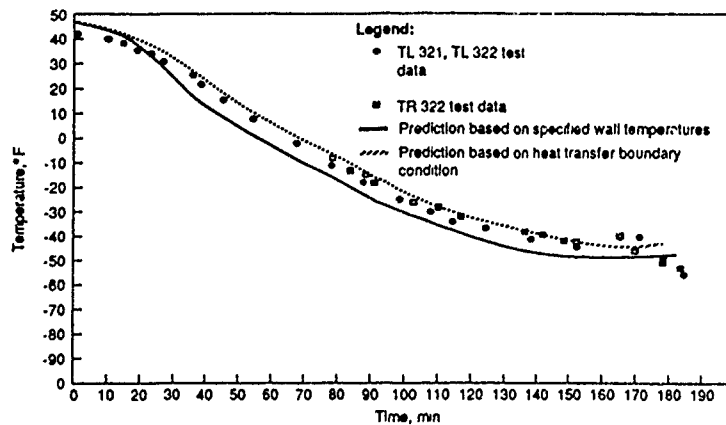


FIGURE 8
COMPARISON OF CALCULATED AND MEASURED
BULK FUEL TEMPERATURES FOR FPU-3A
WIND TUNNEL TEST

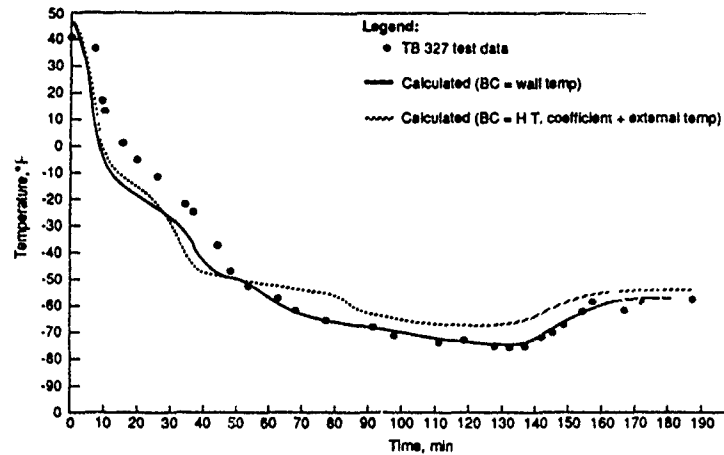
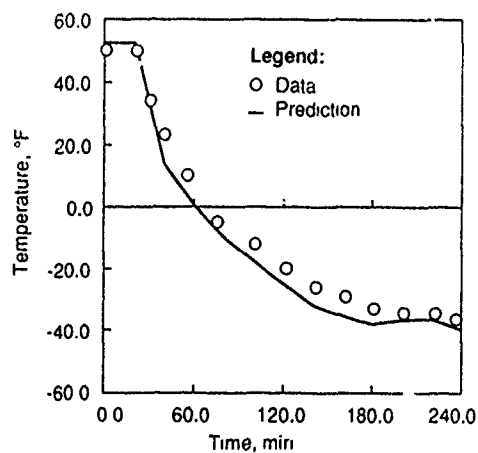
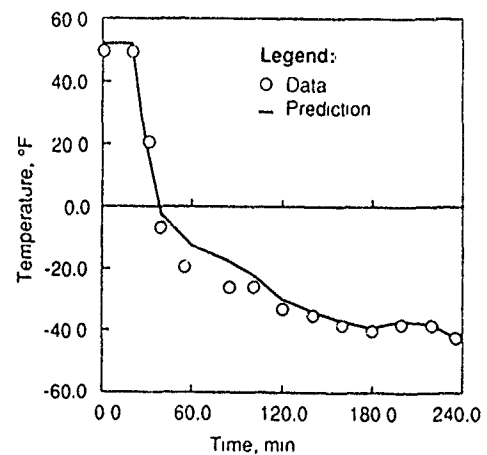


FIGURE 9

COMPARISON OF CALCULATED AND MEASURED
FUEL TEMPERATURES (BOTTOM OF THE TANK)
FOR FPU-3A WIND TUNNEL TEST



STATION 32



STATION 108

FIGURE 10

COMPARISON OF THREE DIMENSIONAL
MODEL CALCULATED FUEL TEMPERATURES
WITH VALUES MEASURED DURING
FPU-3A FLIGHT TEST

Discussion

1. C. Scott Bartlett, Sverdrup Technologies

Do you foresee any instances where the additional cost of a 3-D solution over a 2-D one will be justified?

Author:

The 3-D model, although much more costly to operate, other than the 2-D model would be justified if the benefits of its results would be of a higher value than the associated costs of the model

2. D. Hennecke, Technische Hochschule Darmstadt

How did you determine the internal heat transfer coefficients for the wind tunnel and flight conditions?

Author:

The external heat transfer coefficients were calculated by the computer model using a general flat plate correlation. Additional information regarding the specifics of the correlation can be found in reference 5 of the paper

3. R. Jacques, Ecole Royale Militaire

Your calculations are done for a steady flight and given temperature gradients in the fuel tank. Does air turbulence or aircraft manoeuvring (roll or steep bank angles) not disturb completely the temperature distribution in the tank?

Author:

Although tank vibration, air turbulence and flight manoeuvres will cause fuel sloshing and movement in the tank, previous work performed by the Boeing airplane company has shown that these effects are relatively minor and have little effect on the fuel cooling profiles or hold-up within the tank.

4. L. Richards, BAe

Were you able to check that the position at the four hold-up was in agreement with the predicted position?

Author:

No, because the cylindrical tank was bill-of-material hardware. Access to view the internal freezing patterns was impossible. However, the total amount of fuel hold-up, unpumpable frozen fuel, was measured during wind tunnel testing and compared to predicted results. The work is going on in the NAPC low temperature fuel flow facility, which has optical access to determine the frozen fuel locations

ENVIRONMENTAL ICING TESTING AT THE NAVAL AIR PROPULSION CENTER

by

William H. Reardon and Vito J. Truglio
Naval Air Propulsion Center
P. O. Box 7176
Trenton, New Jersey 08628-0176
U.S.A.

SUMMARY

A comprehensive Environmental Icing Simulation System has been developed by the Naval Air Propulsion Center. This system has accommodated the testing of ducted and free stream mounted engines and free stream mounted aircraft inlets.

Three areas are discussed in detail in this paper:

1. Navy specification icing test procedures, success criteria and rationale for the requirements;
2. The overall capabilities of the NAPC icing facilities in terms of critical icing cloud parameters such as liquid water content, mean effective droplet diameter, humidity and inlet air temperature; and how the icing environment is established, calibrated prior to test and verified during testing along with historical experience and lessons learned;
3. NAPC test experience in Navy qualification programs for the T406, T700 and F404, as well as demonstration and development test programs performed with the TOMAHAWK Cruise Missile inlet and the F-14A aircraft inlet duct.

Navy Specification Requirements

The Navy General Specifications MIL-E-005007E (turbofan/turbojet) and MIL-E-008593E (turboshaft/turboprop) (reference 1) are the baseline documents from which Navy engine model specifications are built. They require that turbine engine anti-icing systems allow the engine to operate satisfactorily under the meteorological conditions as defined in Table I, with not more than 5.0% total loss in thrust or shaft horsepower (SHP) available and no more than 5.0% total increase in specific fuel consumption (SFC) at all operating conditions above 50% maximum continuous power (MCP) setting. For operation at less than 50% MCP, 95% of the desired power above 50% MCP must be obtained within specification acceleration times. No permanent performance deterioration is permitted after the meteorological conditions have been removed. The engine anti-icing system must also prevent accumulation of ice on any engine part exposed to the gas path while operating in icing conditions. The total loss in performance of 5% includes the effect of operation in the icing environment plus the effects of operation of the engine anti-icing system. The baseline for determining engine performance loss is established by operating the engine with no customer bleed air or power extraction under the inlet temperature conditions of Table I with air between 80 - 100% relative humidity (RH) and zero liquid water content (LWC). Delivered power losses and fuel consumption increases are determined by comparison of engine performance when operating in the icing conditions defined in Table I with the baseline values. The test consists of two parts:

- a. Part A contains two runs at each of six power settings under the three conditions of Table I, Part 1. At each power setting the engine is operated for a minimum of 10 minutes. During each period the engine is rapidly accelerated to intermediate power to demonstrate transient response.
- b. Part B contains a one-hour run at idle, followed by an acceleration to maximum power, under the conditions of Table I, Part 2.

Rationale for Specification Requirements (Reference 2)

Generally, some form of anti-icing system is incorporated into the engine design to provide warm compressor bleed air to those surfaces susceptible to ice build up. Shedding of ice into the gas path can result in flameout, stall, surge, and engine failure. Ice build up that chokes off the engine inlet can result in performance deterioration and/or turbine overtemperature due to air starvation, and control schedule changes caused by engine sensor malfunction due to icing.

Measurement of performance degradation is intended to be based on power loss at a particular throttle setting. This has also been interpreted to mean that the 5% power loss should be based on the intermediate power level setting, because this is the highest available power condition. Another interpretation is commonly used in the turboshaft engine community, where most of the engines tested are operating on an external torque limiter at the Table I cold inlet conditions. This interpretation contends that shaft power which degrades with the initiation of anti-icing and the icing cloud can usually be recovered by increasing the throttle (power lever, collective pitch, etc.) until a temperature, torque, fuel flow or speed limiter is reached. This is justified since power is recovered if power is still available, up to

operational limiters, with the protection against excessive degradation reflected in the associated values of SFC. One assumption here is that the correlation between calculated and measured turbine temperature does not shift during test. Deviations in the 5% power loss requirement have been granted in the past, based on the engine bleed requirements necessary to prevent ice accumulation. The transient power requirements for power levels below 50% MCP were incorporated to confirm that and power loss at low power is not only recoverable, but does not prevent the engine from accelerating to high power levels. Transient performance within 125% of specification allowable transient times for power changes is required while operating in the icing environment.

Part I testing is performed to determine the engine anti-icing capability throughout its entire operating range. The specification icing test requirements which were derived from National Advisory Committee on Aeronautics (NACA) Technical Notes 1855 and 2569 are based on data gathered from stratiform clouds (usually prevalent at 3,000-6,000 feet) which have a low to moderate LWC, and cumuliform clouds which occur from 4,000-24,000 feet and have a moderate to high LWC. In the case of stratiform clouds, depicted in Figure 1A, the levels of LWC in the cloud form are normally less than the 1 gram per cubic meter (gm/m³) test requirement, while icing encounters in cumuliform clouds (Figure 1B) tend to be relatively short in duration (approximately 1 minute). The icing test conditions of the specification are fairly consistent with the encounters in cumuliform clouds, but the engine is required to operate there for a much greater period of time. Although conservative, the Navy specification test requirement seems to adequately verify an engine anti-icing system capability, as service experience shows a relatively good record with a low number of icing incidents related to the engine anti-icing system.

Part II testing of one hour at ground idle in the Table I, Part 2 icing environment is very similar to the Federal Aviation Regulations (FAR) Part 33.68, Category B test requirement for civil certification which requires a similar condition run for 30 minutes. It is intended to simulate engine operation, on the ground, in a freezing rain or icing environment while waiting for takeoff clearance. The ensuing acceleration to maximum power simulates the takeoff roll.

Earlier versions of the Navy specification required altitude in addition to sea level icing tests. Altitude tests were deleted from the specification, in part due to the high cost associated with performance of this test in an altitude chamber. Technically, the sea level icing conditions represent the most severe requirements for the engine anti-icing system. This was justified by comparing various engine anti-icing system energy outputs, to icing cloud energy input, at combinations of engine power level, and inlet flight and meteorological conditions. Low engine power, low Mach number, cold inlet conditions (idle, static) produce the lowest compressor bleed anti-icing system energy. Sea level icing conditions provide the highest engine total mass flow yielding greater total liquid flow. Combining high liquid flow with longer dwell times encountered at low airspeed, the greatest difference in energy or most severe requirement for the engine anti-icing system is created.

Allison used specification sea level icing tests in the development of the model 501 and 250 engines based on studies made using data from flight tests at 3,700 to 19,000 feet. During the FAA Aircraft Icing Symposium of April 1969, Allison indicated that an anti-icing system designed to meet the military specification requirements at sea level would result in a configuration which was satisfactory at altitude, and in the meteorological conditions encountered in flight operations (reference 3). At the same symposium, airline operational experience in icing conditions showed that the most potentially serious icing problem in the jet engine airplane was engine icing on the ground, standing in line, waiting for take off clearance. In addition, experience showed that jets had somewhat less of a problem once airborne, as the high rate of climb allowed them to exit the icing environment quickly (reference 4). It should be recognized that icing conditions can be encountered at high altitudes, although encounters above 22,000 feet are rare.

Test Facilities

Engine icing tests have been conducted at NAPC for the past 30 years. During this period the facilities which have been developed to perform these tests have grown in number as has the expertise to provide a reliable environmental icing system for testing engines.

There are four small engine test cells which have sea level as well as altitude capability. The maximum total airflow for icing tests in these cells is 50 pounds/second (lb/sec). There are 5 large engine cells, 2 sea level and 3 altitude, with a maximum air flow of 300 lb/sec. As mentioned, altitude icing requirements have not been part of the Navy military specification in recent years; however, altitude icing tests have been performed at NAPC in the past. NAPC icing test history includes: (1) Turbojets; J32, J79, (2) Turbofans; T41, TF30, TF34, F404, (3) Turbofans; T55, T700, T56, T406 and (4) the F107 engine/TOMAHAWK Cruise Missile inlet combination and the F-14A aircraft inlet. Currently, icing calibration installations are being prepared for the T800, F110 and F412 engines.

There are two basic icing inlet configurations utilized at NAPC which are depicted in Figure 2, the direct connect and free jet. Large engines with mass flows greater

than 40 lb/sec are directly connected and small engines with mass flows less than 40 lb/sec are generally configured as a free jet. The F-14A inlet test required a free jet configuration despite requiring mass flows greater than 300 lb/sec.

Cloud Simulation

Simulation of cloud conditions is accomplished with a spray system consisting of horizontally mounted bars shown in Figure 3. Each bar has openings which accept either a plug or nozzle, allowing for pattern adjustment. Metered and controlled air and water to the nozzles is introduced into individual manifolds to which each spray bar is connected.

The nozzle, an aspirating type similar to a design developed by the National Aviation and Space Administration (NASA) is shown isometrically in Figure 4. Water is forced through a hypodermic size tube and aspirated at its exit by mixing with a pressurized air source. Liquid water droplets are generated when the mixture exits an orifice. The air is heated to prevent icing of the nozzles. Flow of both water and air are remotely controlled, independently, which provides for the setting of LWC and drop diameter. In the direct connect configuration, nozzle water and air flow must be adjusted as engine air flow changes. In the free jet configuration, a constant duct airflow can be maintained, therefore a constant nozzle setting can be held for a given LWC and drop diameter regardless of engine power changes. The nozzle water is potable water which is demineralized and filtered. Nozzle air is also filtered as well as dried. It is important to minimize the entrained particulates which can seed the supercooled liquid water droplets causing them to freeze and form ice crystals. Saturation of inlet air is accomplished independently by injecting steam through a nozzle located in a plenum upstream of the water spray system.

Calibration Techniques

Full scale calibrations are conducted prior to icing tests primarily because of variations that exist from test to test, such as engine air flow range and inlet configuration differences, test cell dissimilarities or modified icing requirements. Figure 5 shows the typical inlet arrangements for a full scale calibration and engine test.

The primary objective of a calibration is to set up the entire icing simulation installation without the test article. Generation of LWC and drop diameter are verified quantitatively and qualitatively as required by the specification prior to the actual test. Inlet air temperature is measured using thermocouples located upstream of the spray bars. Pressure is measured with a steam-heated free stream total pressure rake and wall static taps in the duct downstream of the spray bars. Generally this probe is only used during calibrations. It is correlated with a total pressure probe located upstream of the spray bars for setting flow conditions during test. In the direct connect arrangement there is a reducer duct which can be heated to prevent ice build up, however nozzle patterns are adjusted to minimize the amount of accretion on the reducer surface. Humidity is measured during both the calibration and test with a thermally-cycled photocell type dew point sensor. Saturation is verified visually. Droplet size is controlled by proportioning measured water flow and air flow to the nozzles. During pre test calibrations this relationship is confirmed using a forward scattering spectrometer probe (FSSP) which is traversed across the exit of the inlet duct where the test article interface would be located. This probe is a laser optical instrument which measures and counts droplets according to the amount of energy scattered when the droplets pass through a focal point in the laser beam. LWC is generated by introducing a metered amount of water flow proportioned to a given amount of measured inlet air flow. A single rotating cylinder introduced into the duct near its exit provides an independent means to measure and calculate LWC which can be compared to the metered quantity. The cylinder is housed outside the duct in a supercooled chamber. It is remotely immersed in the air stream for a set time interval and retracted back into the chamber. The ice weight is measured after the cylinder is removed from the chamber. From the ice weight, exposure time and duct velocity, LWC can be calculated and compared to the metered quantity using the following equation (reference 5):

$$\frac{\pi}{2\sqrt{\pi}} \left[\sqrt{\frac{rW}{\pi L}} + r^2 + r \right]$$

Where:

V = Specific Volume of Ice
 η = Catch Efficiency of Cylinder
 T = Exposure Time
 W = Weight of Ice
 L = Length of Cylinder
 r = Radius of Cylinder

This cylinder is used both during calibrations and tests to verify that the droplets are supercooled liquid and that evaporation or crystallization has not occurred. Ice distribution is checked during calibrations by positioning a 2 inch by 2 inch mesh screen at the test article inlet plane. The ice accretion is measured and the nozzle pattern adjusted as required.

Capabilities

The icing capabilities at NAPC can best be summarized as shown in Figures 6A and 6B. Total inlet temperature and LWC are shown as a function of inlet airflow. The minimum temperature obtainable is -50°F at 40 lb/sec and $+32^{\circ}\text{F}$ at 310 lb/sec. The icing cloud simulation capacity is comprised of two envelopes which differentiate between free jet and direct connect LWC capacities. Nozzle water and air flow limitations are the constraining parameters that establish the LWC and droplet diameter boundaries.

NAPC Experience

Producing a consistent icing cloud simulation in terms of LWC and droplet diameter is the most important consideration in the development of an environmental simulation system for the performance of icing tests. This is due to the fact that the stability of the water droplets produced for such a system is highly sensitive to the surroundings. The supercooled droplets are susceptible to evaporation when the inlet air is not saturated and freeze-out (ice crystallization) when particulates are present. Furthermore there are uncertainties involved with any method available to measure and validate LWC rendering it difficult to detect freeze-out or evaporation.

Considerable effort has been made at NAPC to provide the best possible icing simulation system (reference 6). To minimize freeze-out the nozzle water supply is demineralized and filtered to one micron. Nozzle air is also filtered and dried. Inlet air is not filtered; however, there have been tests in the past substantiating that the amount of particulates in the supply are minimal.

There have been many attempts made to measure LWC accurately. Currently the FSSP has been used to accurately count and measure droplet diameter reliably. Also in order to increase its usefulness, a program was developed to calculate LWC from droplet count data acquired. However, the calculations have proven to be unrepeatable and unreliable. A major shortcoming is that the probe can not distinguish discretely between water droplets and ice crystals.

The method found to be most reliable in terms of verifying LWC has been the single rotating cylinder. There are inaccuracies inherent in this method but it is the only way presently known where freeze-out can be detected since frozen droplets will not accrete on the cylinder. In the near term, efforts are on-going to investigate the feasibility of an alternative to the FSSP, the phase/doppler particle analyzer. This is a non-intrusive instrument which is capable of measuring droplet size and velocity through a volume defined by the intersection of two laser beams. The probe could possibly be installed external to the inlet, thereby allowing for use during engine testing. However, it is not anticipated that freeze-out detection could be possible using this instrument.

NAPC Icing Test Experience

1. T406-AD-400 Turboshaft Engine

The Allison Gas Turbines Division (AGTD) T406-AD-400 turboshaft engine, designed to power the V-22 tiltrotor aircraft, was tested to the Allison Model Specification 937 Environmental Icing Test requirements during its Low Production Qualification (LPQ) phase. Model Specification 937 was derived from Mil-E-8593E and was approved by the Navy. It contains success criteria of no more than 5% SHP loss and 6.5% SFC increase in the icing environment.

In the first test attempt (reference 7), the engine anti-icing system was found to be deficient at low power conditions: At Table I, Part 1 condition; -4°F , $1\text{gm}/\text{m}^3$, below approx 50% MCP (1100 pound-feet (lb-ft)) unacceptable ice formed on the engine inlet guide vanes (IGV's). At Table I, Part 1 condition; $+23^{\circ}\text{F}$, $2\text{gm}/\text{m}^3$, unacceptable ice formed on the IGV's below approximately 400 lb-ft torque. At the Table I, Part 2 condition, the lowest torque at which the engine had adequate anti-icing capability for a one hour period of operation was 450 lb-ft. Below that, unacceptable ice formed on the IGV's. The engine did however, meet performance degradation requirements of 5% SHP and 6.5% SFC when measured at constant Power Demand Signal (PDS).

Allison in-house investigation of the engine anti-icing system post test (reference 8), revealed that the engine IGV anti icing airflow supply was deficient. This flow is supplied via external plumbing from the fourteenth stage compressor discharge to the engine inlet housing, where it is internally manifolded to the individual guide vanes through vane tip ports. Flow checks by Allison confirmed that only 1/2 the design flow rate was passing through the vanes. In addition several areas of system overboard leakage were identified at anti-icing supply tube to engine case mating points and around guide vane bushings. Heat transfer modeling with these inputs predicted local areas of the IGV at the hub and blade tip which could be susceptible to icing. These results were consistent with the ice accretions seen during the initial test at NAPC, where on video monitors the ice accretions were seen accumulating from the hub area outward radially along the leading edge of the IGV's.

A retest of the T406-AD-400 was performed with a modified IGV anti-icing flow

scheme, incorporating reworked IGV hub and tip exit holes and better sealing of the anti-icing flow path. In the retest, the engine anti-icing system prevented ice accumulation in the engine gas path at all three specification icing conditions. Losses in shaft horsepower related to operation of the anti-icing system in the icing environment exceeded the specification limit of 5% at the +23°F and -4°F meteorological conditions of Table I when compared at constant power demand signal (PDS), constant gas generator speed (NG) or constant measured gas temperature (MGT) above 50% MCP. In all cases, at and above 50% MCP, power loss was recoverable throughout the range of environmental icing test conditions with an increase in PDS while remaining within engine temperature and speed limits. This was attributable to engine torque limiting being in effect. The V-22 propeller gearbox torque limit is 2150 pound-feet, which is below the engine maximum power output capability at the Table I test conditions. The increases in SFC in the icing environment when compared at constant SHP were within the Model Spec 937 limit of 6.5% at all conditions. For this test program the NAPC recommendation was to accept the engine as having met the icing requirements of Model Spec 937 for the V-22 installation. This would require granting a waiver for SHP loss associated with operation of the engine anti-icing system in the icing environment. Presented in Tables IIA and IIB, is the T406-AD-400 engine performance as run in the retest of the environmental icing test.

2. T700-GE-700 Turboshaft Engine (reference 9)

The anti-icing system of the T700-GE-700 engine contains an integral inlet particle separator (IPS), which adds extensive flowpath surfaces beyond conventional engine configurations. Anti-icing of the T700 IPS, IGV's and engine front frame is accomplished with a combined system of continuous hot engine oil and modulated axial compressor bleed air. A valve varies the bleed air with corrected compressor speed through a variable compressor vane actuator linkage.

Testing was conducted in a freestream environment with a specially fabricated engine bellmouth and bulletnose assembly. The bellmouth and bulletnose were designed to be anti-iced by a facility hot air supply. In addition, engine power absorption was accomplished by means of a high speed waterbrake enclosed in the bulletnose.

No ice accumulations were observed on the engine inlet surfaces (IGV's, struts, front frame) during the testing. Post test observations revealed that small amounts of ice had accumulated on the inside diameter of the IPS scroll cover assembly. This served to explain light puffs of smoke which were observed exiting the IPS blower during icing testing. This ice did not damage the IPS blower. Engine performance changes due to the operation of the anti-icing system and operation in the icing environment are shown in Tables IIIA and IIIB. The T700-GE-700 Engine Model Specification DARCOM-CP-2222-02000C which is an Army approved derivative of MIL-E-008593E, allowed up to 9% SHP loss and 7% increase in SFC under Table I conditions. Where levels of SHP exceeded these values during test, it was shown that up to intermediate rated power (IRP), a percentage of the lost power was recoverable. For testing at the -4°F icing conditions, additional power loss was observed once the icing spray was introduced, which was greater than the loss seen with only engine anti-icing systems on. These power losses were suspect due to inconsistency with the +23°F results. Cycle analysis and other GE turboshaft engine icing test experience indicated that losses in performance at icing temperatures for wet operation should be no worse than for dry operation. The T406 test showed a similar inconsistency at the -4°F icing conditions. One explanation could be the difference in the energy required to vaporize the super cooled droplets at -4°F versus the energy required to vaporize the droplets at +23°F, combined with the difference in the axial location in the compressor where that change of state occurs, could effect overall engine performance depending on the contribution of each stage of compression to the overall efficiency of the compressor.

Transient performance between ground idle and IRP with customer bleed and anti-icing activated showed no indications of stall or instability. Standard procedure for documenting transient times in a turboshaft installation with a free turbine, where a waterbrake is used for power absorption, is based on the change in gas generator speed (NG) equivalent to that required to achieve 95% of the overall power change. This method most nearly reflects the transient response capability of the engine independent of the power absorber inertia and dynamics. The NG speed associated with the starting and finishing points of the transient excursion are defined by steady state operation at these points.

3. F404-GE-400 Turbofan Engine (reference 10)

The F404-GE-400 Engine Environmental Icing Test was conducted at NAPC in accordance with GE Model Specification CP45K0008, which allowed losses of up to 10% in thrust and up to a 10% increase in SFC while operating in the icing environment. The test requirements were modified by the Navy to expedite the program. Only the flight idle and IRP power settings were retained. It was felt that if the engine could satisfactorily anti-ice at these conditions, it could anti-ice at any power in between.

The installation was a direct connect inlet arrangement, where the 60-inch diameter facility air supply duct transitioned to 28-inch diameter at the engine inlet. The transition section was jacketed so it could be heated to prevent ice formation on the internal surfaces. The initial setup contained a labyrinth seal to allow a floating

thrust bed and associated force measurement, however, it was removed when it was found to be a source of ice buildup. This necessitated locking of the thrust stand because the axial displacement allowed by the labyrinth seal had been eliminated.

In order to prevent ice formation in the engine inlet duct from the inlet rakes, they were removed prior to the icing test. Without the inlet rakes and the labyrinth seal, the engine thrust could not be measured directly during icing runs, and was obtained by comparison of parameters to precalibration values. In this case, the relationship of gross thrust to engine pressure ratio (EPR) obtained during the precalibration was used to determine engine net thrust, as a function of the 'engine pumping pressure ratio' (low pressure turbine discharge pressure / engine inlet pressure). The engine inlet total pressure and total temperature during the precalibrations were based on temperature and pressure measurement rakes mounted in the inlet duct. After these rakes were removed for the icing tests, the engine inlet temperature was assumed equal to the average of four thermocouples (TC's) located upstream of the water spray bars. These TC's had agreed within 1 F of the engine inlet temperature based on the engine inlet rakes. After the pressure rakes in the inlet duct were removed, the engine inlet pressure was assumed equal to the pressure in the 60-inch plenum located upstream of the spraybars. By using this pressure together with the wall static pressures in the 28-inch duct, a corrected airflow was calculated which was within 2% of the airflow during precalibration.

The results of the test showed no significant ice buildup on the engine at any of the three environmental icing conditions tested. As shown in Table IV, the anti-icing bleed air caused thrust losses of approximately 4-7% at constant measured turbine temperatures. No additional significant performance loss was noticed while operating in the icing conditions. Increases in SFC at constant thrust at IRP were well within the 10% allowable limit.

4. F107-WR-400 Turbofan Engine with a TOMAHAWK Missile Inlet

The Navy Specification requirements have also been tailored to address specific installations. The F107-WR-400 engine was designed to power the TOMAHAWK Cruise Missile. Neither the engine nor the missile inlet was anti-iced in this installation. As a demonstration, the specification test was tailored to provide a representative icing environment for the engine/missile inlet combination (reference 11).

An F107-WR-400 engine installed behind the TOMAHAWK missile inlet was mounted in the freestream configuration. All testing was performed at Sea Level, Mach 0.65 freestream conditions with an inlet air total temperature of +23°F. Three icing runs were performed, consisting of two one-minute runs and one five-minute run. The desired liquid water content was 1.0 gm/m³ and the mean effective droplet diameter (MEDD) was 20 microns.

The engine was run at cruise power for one minute with half the desired liquid water content (0.5 gm/m³). The only ice accumulation on the engine hardware was a 1/16-inch buildup on the center of the spinner located forward of the 1st stage fan. The TOMAHAWK inlet duct had a rough accretion of ice on the inside lower half of the forward 3/4 of its length at an average thickness of 1/16 inch. The inlet lip had a 1/8-inch build up on its circumference. The engine had ingested an 8-inch long section without damage. A second one-minute run at 1.0 gm/m³ yielded build up at similar locations at about double the thickness, indicating the rate of buildup was proportional to LWC. A five-minute run was attempted, during which, ice continuously built up and broke off the inlet lip. Engine stall occurred at 2:50 into the run, after a section of ice from the outboard side of the inlet lip was ingested. Engine inlet housing vibrations were high during the final two minutes of the run. Inspection of the engine on shutdown, revealed the only ice formation on engine hardware was a 1/16-inch buildup on the center of the spinner. On closer inspection, five 1st stage fan blade tips were found bent over.

Review of the transient data revealed that during each of the icing runs, the first minute was characterized by an increase in fan speed (N1), thrust and compressor discharge pressure (CDP). This was due to the mass flow increase introduced by the icing environment through the engine. Following, was a drop in fuel flow, thrust and CDP due to inlet blockage from ice buildup and corresponding duct pressure drop. These parameters cycled as ice broke off the inlet. The inlet pressure loss also affected speed match of the engine. After 2:50 and 4:20 of the icing run, N1 increased for a given gas generator speed (N2) at constant inlet temperature. Those stated times appear to be when the two incidents of ice ingestion and damage occurred. N1 is higher for a given N2 due to reduced efficiency of the damaged fan blades. Engine thrust also decreased continuously during the test from inlet pressure loss. Because of the accumulation of ice on the engine installation hardware, engine thrust could not be determined from meter readings during the icing runs due to the increased drag force. Engine thrust loss was determined by comparison of engine parameters during the icing run with those obtained in the pretest performance calibrations. Figure 7 is a representation of the thrust loss seen throughout the five minute run.

The severity of the icing environment in this demonstration may be evaluated as

follows: The missile traveling at Mach 0.65 will travel about 7.5 miles in one minute. To maintain the missile inlet below freezing (+23°F) at Mach 0.65 flight condition, the equivalent ambient temperature is -15°F. Cumuliform clouds at -15°F do not exist below 12,000 feet altitude. In addition, this cloud form is typically less than an average of 3 miles long if its LWC is 1 gm/m³. Which would relate to a cloud dwell time for the missile of less than 30 seconds. Stratiform clouds exist at very low altitudes and at -15°F, their LWC is typically less than 0.2 gm/m³. Stratiform clouds with this LWC have an average horizontal extent of 20 miles which would equate to approximately 3 minutes duration in that environment.

5. F-14A Aircraft Inlet Icing Test

In another developmental effort, NACP utilized the specification icing conditions to investigate a fleet problem encountered by the F-14A aircraft. The program was initiated because of several reports of F-14A aircraft engines experiencing foreign object damage (FOD) from ice ingestion (reference 12). From information available after one of these icing incidents, the aircraft had been operating for approximately 30 minutes in what was perceived as icing conditions at 8,000-10,000 feet at 250 knots (0.4Mn). The aircraft descended and made a normal carrier approach and landing. F-14A engine icing FOD was reported to have occurred in some incidents during the carrier approach and in others on carrier arrestment. Ice was found on the rear wall of the bleed/bypass cavity in an F-14A aircraft that did not experience ice damage.

Prior to the NACP test there had been essentially no previous testing conducted to determine how the bleed/bypass system functions in flight. Questions regarding the percentage of total inlet duct airflow that is bled, and whether the bleed/bypass system functions as an auxiliary inlet in flight were unanswered. Grumman Aircraft Corp. estimated that approximately 10% of the air entering the inlet duct exits through the bleed/bypass door.

The F14-A aircraft engine inlet duct (Figure 8) is a variable geometry inlet used to decelerate free stream air in flight to provide even subsonic airflow to the engine throughout the aircraft flight envelope. The inlet has a two dimensional, four-shock, external compression system with horizontally oriented ramps. It has a three degree initial fixed ramp and three automatically controlled variable compression ramps which are programmed to vary with Mach number. The compression ramp boundary layer is bled through a throat bleed slot and dumped overboard through the bleed/bypass door.

The objective of this program was to attempt to duplicate the ice formations that had been observed in flight aircraft and recommend possible solutions to the icing problem. The program was later expanded to include actual testing of the proposed heating blanket fixes. With limited facilities available for the icing installation, the test was run at sea level and reduced Mach number conditions. Due to airflow limitations, air was permitted to flow into and across the top and bottom of the inlet duct only. Air was allowed to flow across the top of the inlet duct in an attempt to simulate the inflight airflow conditions around the bleed/bypass door, which affects the airflow rate and direction of airflow through the bleed /bypass cavity. Simulating the airflow patterns in and around the F-14A inlet duct in the area of the bleed/bypass system is critical, since the rate and pattern of ice accretion in that area is dependent on this airflow pattern. A controlling factor in the ice build up in the bleed/bypass system cavity and on the leading edge of the #3 ramp is the amount of air that is bled by the bleed/bypass system; the ice build up is directly related to this airflow rate. Conditioned plant air was allowed to flow over the bottom of the duct to prevent distortion of the airflow to the engine from the inlet lower lip. Testing was conducted using plant air and a TF30-P-408 engine as a 'workhorse pump' behind the inlet in an attempt to create a realistic simulation of the airflow patterns of the inlet duct.

The port engine inlet duct from an F-14A aircraft was installed in the test cell and partially inserted into a 72-inch diameter plant facility duct. Aluminum closure plates installed between the facility duct and the F-14A duct were used to block airflow past the sides of the inlet. Aerodynamic surveys showed that the bleed/bypass functioned solely as a bleed for testing with the ramps in the stowed position. The bleed/bypass system with the Numoer (#1) and #2 ramps lowered functioned as a bleed for the lower engine power settings, but as engine power increased, the bleed/bypass airflow decreased until the flow reversed. After the point of flow reversal was reached, the bleed/bypass functioned as an auxiliary inlet.

At the icing condition of +23°F inlet temperature, 2 gm/m³ LWC and 15 microns droplet diameter, with the #1 and #2 ramps stowed (low Mach condition), heavy ice accumulated on the #3 ramp leading edge and the inlet duct tie rod. Testing with the ramps lowered (high Mach condition), showed essentially no ice formation in the bleed/bypass cavity. Some ice formed on the lower corner of the #3 ramp leading edge and lower (engine gas path exposed) surface. In both cases there was also significant ice build up on the lower lip of the F-14A inlet. Testing was then performed with the ramps in the stowed position to determine where shed ice from the #3 ramp leading edge would collect. After achieving the ice buildup, the facility air was warmed rapidly, after which the engine was shut down. Examination of video tape of this event showed that #3 ramp leading edge ice had broken away and lodged in the cavity above the #3 ramp. Also found in the cavity was ice which had accumulated on the hydraulic ramp

actuator.

This test demonstrated that the ice found in the bleed/bypass cavity of flight aircraft was most likely caused by ice breaking from the #3 ramp leading edge. The large amounts of ice reported in the bleed/bypass cavity of flight aircraft could be the result of flying through a series of icing and non-icing conditions, whereby ice may repeatedly form on the #3 ramp and break off collecting in the bleed/bypass cavity. This theory is supported by some of the icing incidents reported which stated that the ice found in the bleed/bypass cavity appeared to be composed of several layers.

References:

1. Naval Air Propulsion Center, Military Specifications Mil-E-008593A, 13 Oct 1975 and Mil-E-005007E, Apr 1983.
2. Naval Air Propulsion Center, NAPC-E-79003B/1, Mil-E-005007D Requirements Rationale, 10 Feb 1981.
3. G. Bianchini, Allison Division of General Motors, "Small Gas Turbine engines and Inlet Icing Protection", Aircraft Icing Protection Symposium, FAA, April 1969.
4. P.A. Soderlund, Northwest Airlines, "Airline Operational Experience in Icing Environment", Aircraft Icing Protection Symposium, FAA, April 1969.
5. C. K. Rush and R. L. Wardlaw, National Aeronautical Establishment Canada Report, "Icing Measurements With a Single Rotating Cylinder", LR-206, 1957.
6. V. J. Truglio, Naval Air Propulsion Center, NAPC-OP-94, "Sea Level Icing Rig Calibrations for Small Engine Tests," October 1976.
7. Allison Gas Turbines Division, T406-AD-400 Quarterly Progress Report, 27 April 1989.
8. W. H. Reardon, Naval Air Propulsion Center, NAPC Ltr Ser PE21/E419, T406-AD-400 Environmental Icing Test Results, 2 June 1989.
9. S. H. Green, General Electric Co., Report R76AEG031, T700-GE-700 Engine Qualification-Anti-icing Test, 30 April 1976.
10. R. R. Thaler, Naval Air Propulsion Center, NAPC-LR-78-23, F107-WR-400 Ice Ingestion and Icing Environment Tests of 15 Nov 1978, PE62:RRT-cjs, Ser E850, 30 Nov 1978.
11. R. L. Magnussen and K. P. Halbert, General Electric Co., Report R79AEG1026, F404-GE-400 Qualification Test Phase - Environmental Icing Test, Oct 1979.
12. M. K. Fall, Naval Air Propulsion Center, NAPC-PE-83, Icing Tests of the F-14A Aircraft Engine Inlet Duct and Evaluation of Proposed Icing Fixes, Jan 1983.

TABLE I
SEA LEVEL ANTI-ICING CONDITIONS
(MIL-E-005007E (AS))

	PART 1			PART 2
Engine Inlet Total Temperature	-4°F (-20°C) ±1°	+15°F (-10°C) ±1° (1)	+23°F (-5°C) ±1°	23°F (-5°C) ±1°
Velocity	0 to 60 knots	0 to 60 knots	0 to 60 knots	0 to 60 knots
Altitude	0 to 500 ft	0 to 500 ft	0 to 500 ft	0 to 500 ft
Mean Effective Drop Diameter	20 microns	20 microns	20 microns	30 microns
Liquid Water Content (Continuous)	1 gm/m ³ ±0.25 gm/m ³	2 gm/m ³ ±0.25 gm/m ³	2 gm/m ³ ±0.25 gm/m ³	0.4 gm/m ³ ±0.1 gm/m ³

(1) This condition is deleted for non-fan engines.

TABLE IIA
T406-AD-400 ENVIRONMENTAL ICING TEST II
TEST RESULTS
SEA LEVEL / +23°F / 2 gm/m³ LWC

POWER ¹ SETTING	ENGINE A/I	ENGINE BLD	ICING SPRAY	SHF (HP)	SFC (LB/HR/HP)	MGT (°F)	SHF % LOSS	SFC % INC
IRP	OFF	OFF	OFF	6070	.435	1385	----	----
	ON	OFF	OFF	5875	.448	1432	-3.2	+3.7
	ON	ON	OFF	5810	.450	1445	-4.3	+4.2
	ON	ON	ON	5743	.452	1437	-5.4	+4.6
MCP	OFF	OFF	OFF	5120	.453		----	----
	ON	OFF	OFF	4968	.467		-3.0	+3.1
	ON	ON	OFF	4844	.471		-5.4	+4.0
	ON	ON	ON	4846	.470		-5.4	+3.9
PART POWER	OFF	OFF	OFF	4607	.462		----	----
	ON	OFF	OFF	4465	.476		-3.1	+3.0
	ON	ON	OFF	4410	.479		-4.3	+3.7
	ON	ON	ON	4410	.479		-4.3	+3.7
PART POWER	OFF	OFF	OFF	3852	.480		----	----
	ON	OFF	OFF	3731	.498		-3.1	+3.3
	ON	ON	OFF	3728	.498		-3.2	+3.8
	ON	ON	ON	3728	.498		-3.2	+3.8
PART POWER	OFF	OFF	OFF	3112	.500		----	----
	ON	OFF	OFF	3023	.517		-2.9	+3.4
	ON	ON	OFF	3009	.520		-3.3	+4.0
	ON	ON	ON	2998	.525		-3.7	+5.0

¹ ALL POWER SETTINGS ARE CONSTANT POWER DEMAND SIGNAL (PDS)

² MEASURED GAS TEMPERATURE (MGT) LIMIT = 1540°F

TABLE IIB

T406-AD-400 ENVIRONMENTAL ICING TEST I
TEST RESULTS
SEA LEVEL / -4°F / 1 gm/m² LWC

POWER ^a SETTING	ENGINE A/I	ENGINE BLD	ICING SPRAY	SHF (HP)	SFC (LB/HR/HP)	MGT (°F)	SHF % LOSS	SFC % INC
IRP	OFF	OFF	OFF	6070	.429	1335	----	----
	ON	OFF	OFF	5778	.444	1376	-4.8	+3.5
	ON	ON	OFF	5742	.447	1385	-5.4	+4.2
	ON	ON	ON	5513	.453	1372 ^a	-9.1	+5.6
MCP	OFF	OFF	OFF	5237	.449		----	----
	ON	OFF	OFF	5059	.464		-3.4	+3.3
	ON	ON	OFF	5003	.467		-4.5	+4.0
	ON	ON	ON	4780	.475		-8.7	+5.8
PART POWER	OFF	OFF	OFF	4652	.454		----	----
	ON	OFF	OFF	4535	.467		-2.5	+2.9
	ON	ON	OFF	4473	.470		-3.8	+3.5
	ON	ON	ON	4353	.477		-8.4	+5.1
PART POWER	OFF	OFF	OFF	4188	.463		----	----
	ON	OFF	OFF	4103	.476		-2.1	+2.8
	ON	ON	OFF	4045	.478		-3.4	+3.2
	ON	ON	ON	3947	.483		-5.8	+4.3
PART POWER	OFF	OFF	OFF	3655	.485		----	----
	ON	OFF	OFF	3607	.498		-1.6	+2.7
	ON	ON	OFF	3559	.500		-2.9	+3.1
	ON	ON	ON	3482	.503		-5.0	+3.7

^a ALL POWER SETTINGS ARE CONSTANT POWER DEMAND SIGNAL (PDS)

^a MEASURED GAS TEMPERATURE (MGT) LIMIT = 1540°F

TABLE IIIA

T700-GE-700 ENVIRONMENTAL ICING TEST
TEST RESULTS
(G.E. R76AEG031)
SEA LEVEL / +23°F / 2 gm/m² LWC
CUSTOMER BLEED = 0%

AS RUN DATA								
POWER RATING	A/I VALVE	ICING SPRAY	T4.5H (°F)	SHF (HP)	SFC (LB/HR/HP)	SHF LOSS	SHF % LOSS	SFC % INC
IRP	OFF	OFF	1544	1550	.487	----	----	----
	ON	OFF	1544	1410	.508	140	9.0	4.3
	ON	ON	1544	1410	.506	140	9.0	3.9
MCP	OFF	OFF	1432	1380	.491	----	----	----
	ON	OFF	1432	1168	.525	212	15.4	6.9
	ON	ON	1432	1168	.525	212	15.4	6.9
PART POWER	OFF	OFF	1350	1200	.501	----	----	----
	ON	OFF	1355	1200	.521			4.0
	ON	ON	1445	1200	.521			4.0
PART POWER	OFF	OFF	1269	1000	.526	----	----	----
	ON	OFF	1377	1000	.551			4.7
	ON	ON	1377	1000	.551			4.7
PART POWER	OFF	OFF	1197	800	.572	----	----	----
	ON	OFF	1315	800	.600			4.9
	ON	ON	1310	800	.600			4.9
PART POWER	OFF	OFF	1130	600	.640	----	----	----
	ON	OFF	1251	600	.687			7.3
	ON	ON	1233	600	.687			7.3

TABLE III

**T700-GE-700 ENVIRONMENTAL ICING TEST
TEST RESULTS
(G.E. R76AEG031)
SEA LEVEL / -4°F / 1 gm/m³ LWC
CUSTOMER BLEED = 0%**

POWER RATING	A/I VALVE	ICING SPRAY	AS RUN DATA					
			T4.5H (°F)	SHP (HP)	SFC (LB/HR/HP)	SHP LOSS	SHP % LOSS	SFC % INC
IRP ¹	OFF	OFF	1501	1641	.485	----	----	----
	ON	OFF	1530	1527	.497	114	6.9	2.5
	ON	ON	1530 ²	1547	.502	114	6.9	3.5
MCP	OFF	OFF	1432	1546	.486	----	----	----
	ON	OFF	1432	1363	.503	177	11.5	3.5
	ON	ON	1432 ²	1363	.505	177	11.5	3.9
PART POWER	OFF	OFF	1270	1200	.502	----	----	----
	ON	OFF	1359	1200	.516			2.8
	ON	ON	1359 ²	1200	.520			3.6
PART POWER	OFF	OFF	1195	1000	.525	----	----	----
	ON	OFF	1288	1000	.543			3.4
	ON	ON	1288 ²	1000	.548			4.4
PART POWER	OFF	OFF	1123	800	.566	----	----	----
	ON	OFF	1225	800	.593			4.8
	ON	ON	1225 ²	800	.598			5.7
PART POWER	OFF	OFF	1047	600	.642	----	----	----
	ON	OFF	1155	600	.670			4.4
	ON	ON	1155 ²	600	.670			4.4

¹ AT IRP (DRY) THE ENGINE WAS RUN TO A CORRECTED SPEED LIMIT
NG/ = 103%

² AS MEASURED, DATA IS SUSPECT. DATA SHOWN IS ESTIMATED.

TABLE IV

**F404-GE-400 ENVIRONMENTAL ICING TEST
TEST RESULTS
(G.E. R79AEG1026)
PERFORMANCE LOSSES DURING ICING CONDITIONS**

ENGINE INLET TEMPERATURE	23°F	15°F	-4°F
LIQUID WATER CONTENT	2 gm/m ³	2 gm/m ³	1 gm/m ³
POWER SETTING	IRP	IRP	FN=7500 LBS. (XNH=14,500 RPM)
THRUST LOSS (LBS.) AT CONSTANT T5H	480 TO 770	500	560
ALLOWABLE (10%) THRUST LOSS (LBS.)	1150	1160	750
SFC LOSS (%) AT CONSTANT THRUST	1.5 TO 3.7	2.6	1.9 TO 2.3
ALLOWABLE SFC LOSS (%)	10	10	10

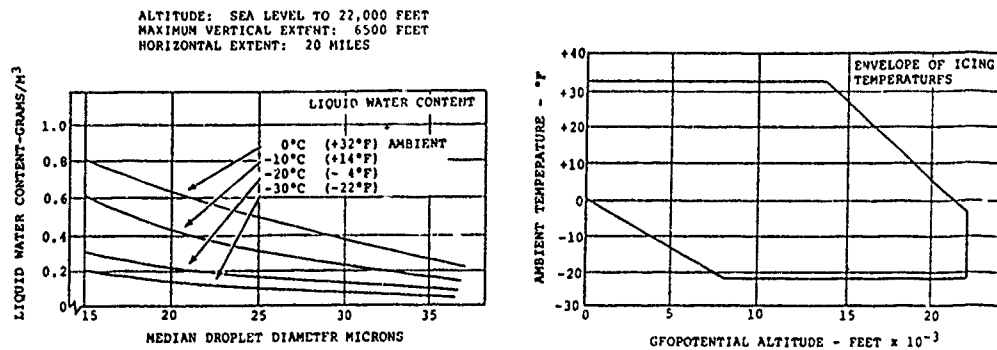


FIGURE 1A : CONTINUOUS MAXIMUM ICING CONDITIONS
 (MIL-E-005007E (AS); MIL-E-008593E (AS); FAR 25, APP. C)

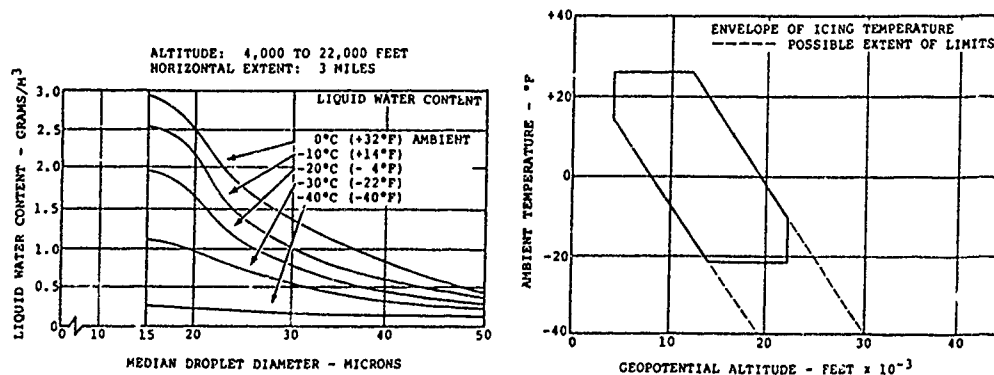
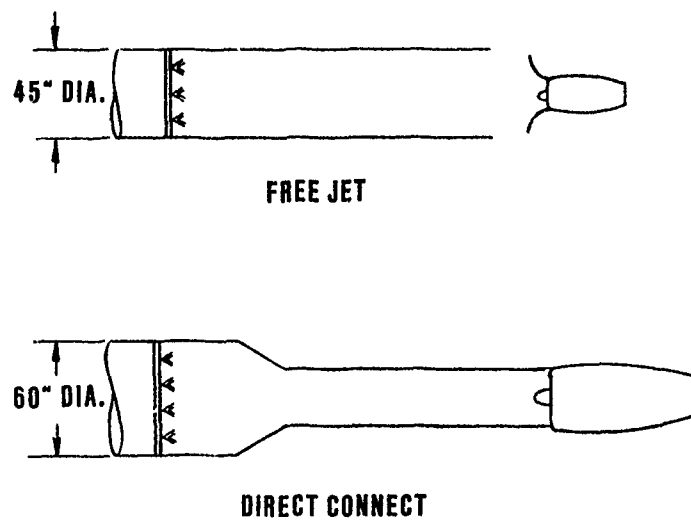
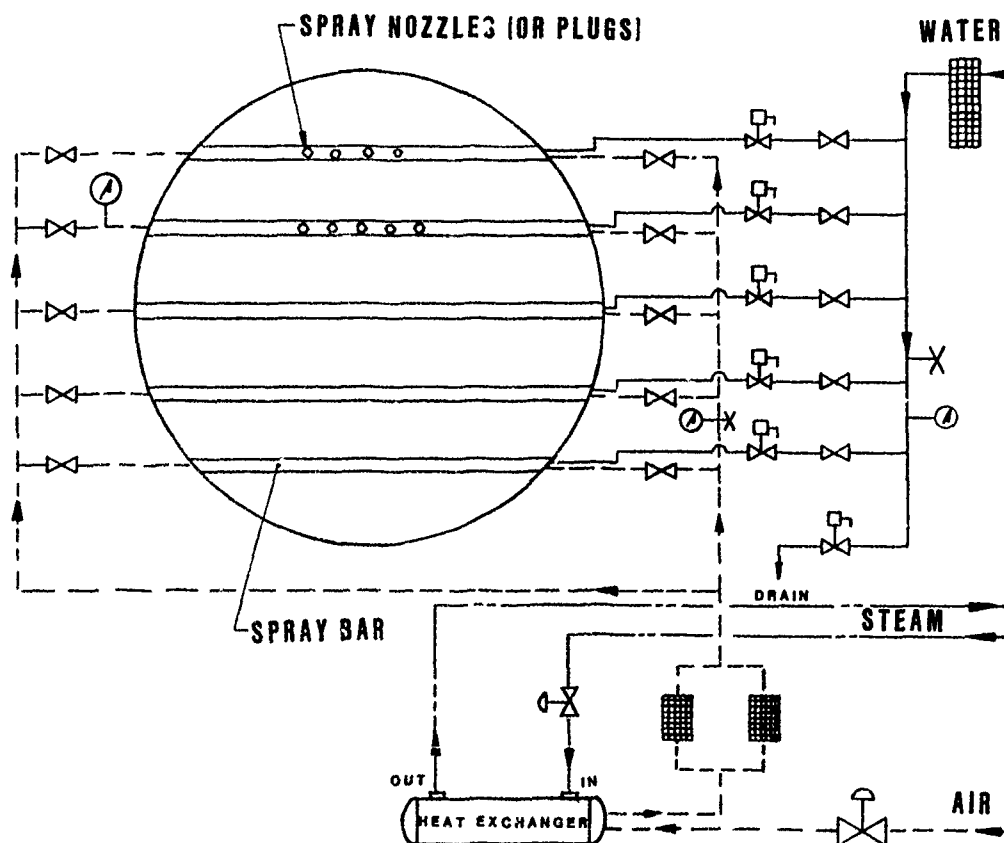


FIGURE 1B : INTERMITTENT MAXIMUM ICING CONDITIONS
 (MIL-E-005007E (AS); MIL-E-008593E (AS); FAR 25, APP. C)

FIGURE 1: ICING CLOUDS

**FIGURE 2: ICING INLET CONFIGURATIONS****FIGURE 3: ICING SPRAY BAR SCHEMATIC**

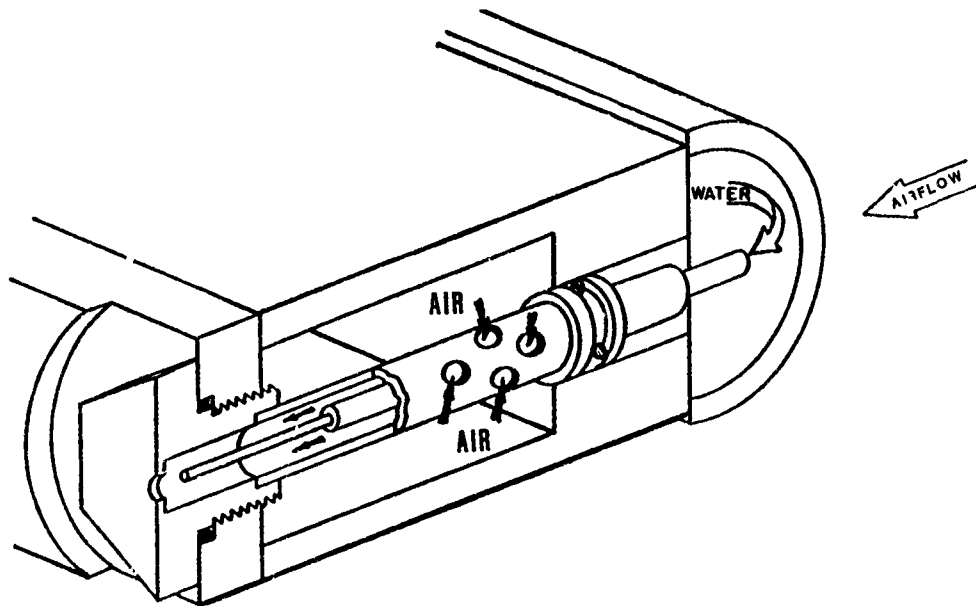


FIGURE 4: ICING SPRAY BAR AND NOZZLE

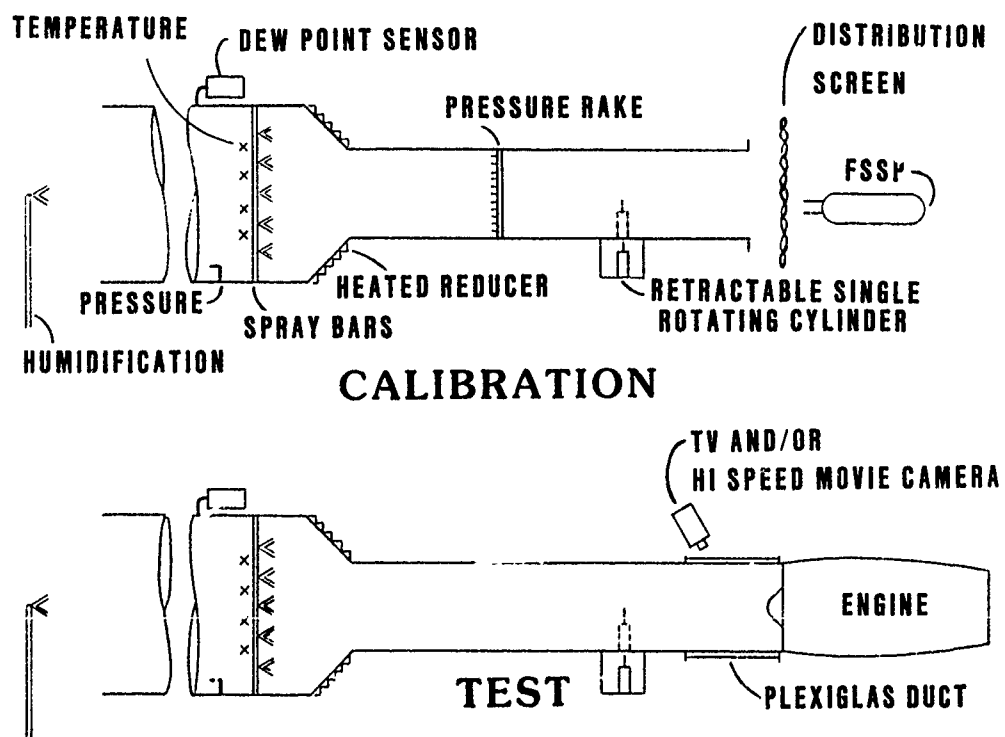
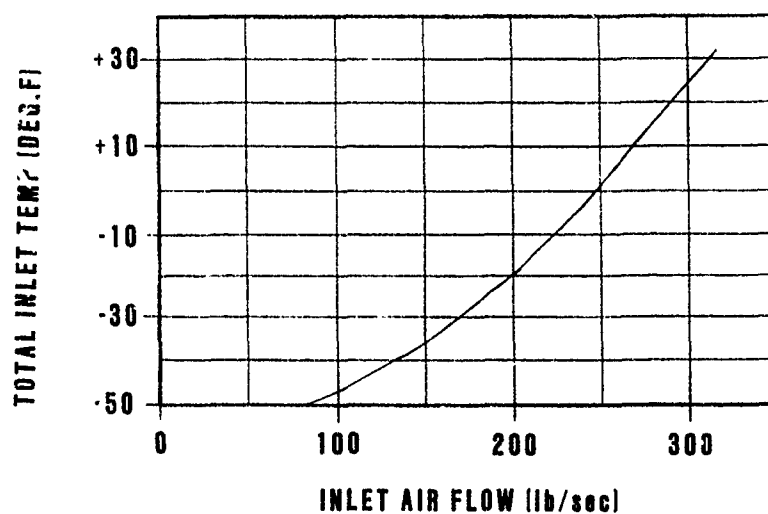
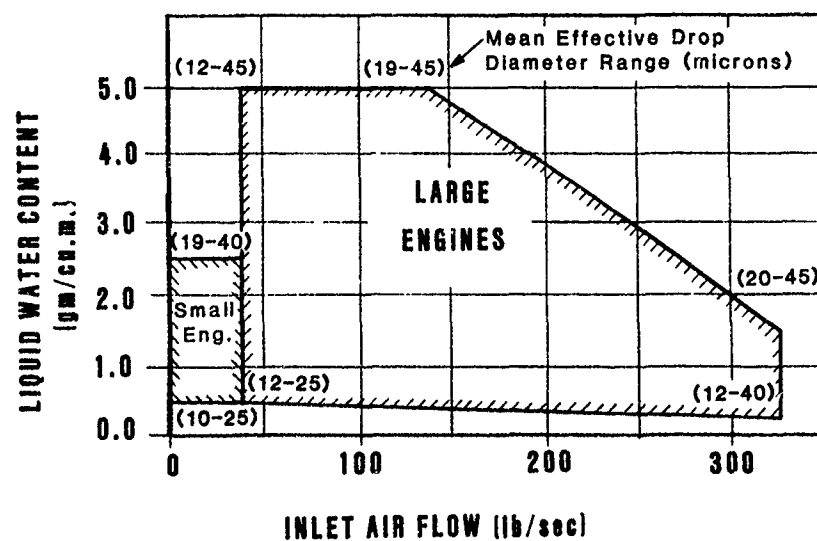


FIGURE 5: TYPICAL CALIBRATION/TEST ARRANGEMENTS



a. INLET TEMPERATURE CAPACITY



b. ICING CLOUD SIMULATION CAPACITY

FIGURE 6: NAPC ICING CAPABILITIES

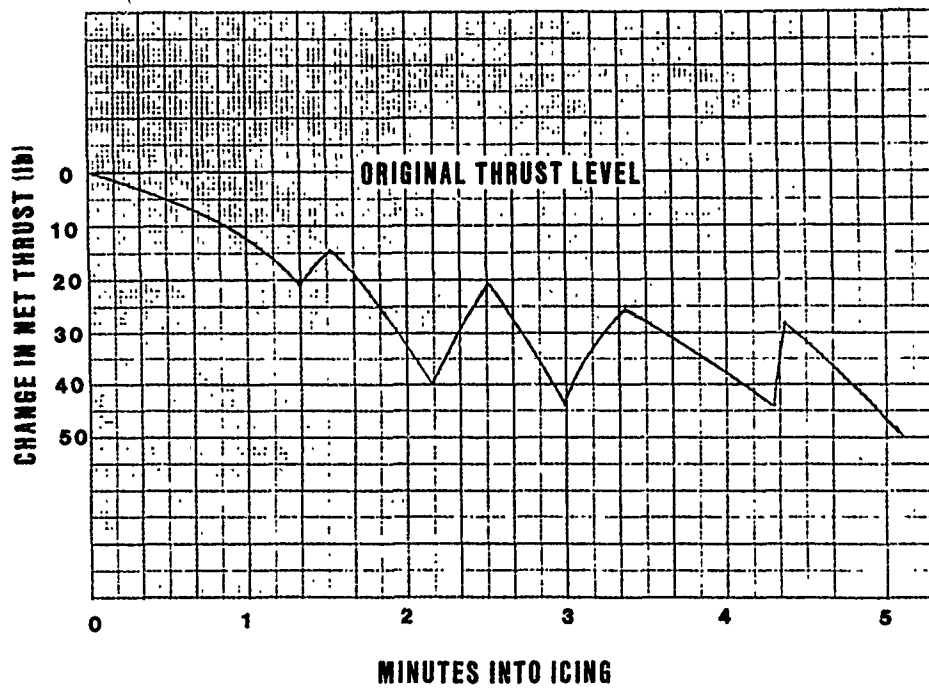


FIGURE 7: NET THRUST LOSS DURING ICING

F107-WR-400 ICING TEST WITH TOMAHAWK INLET

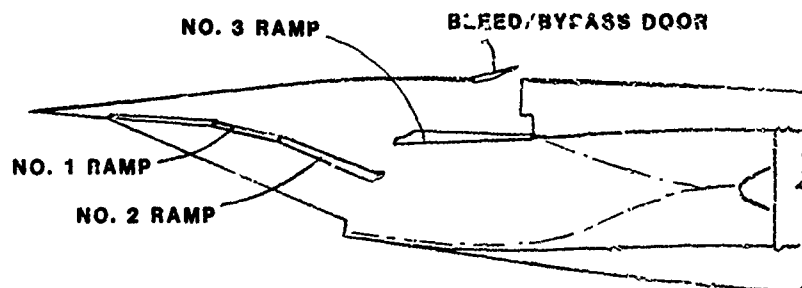
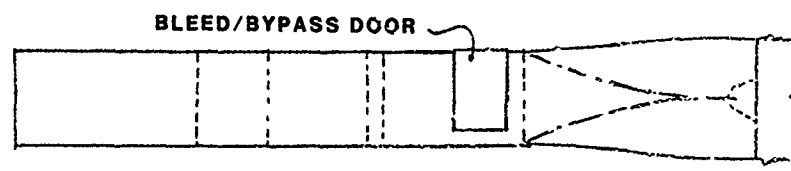
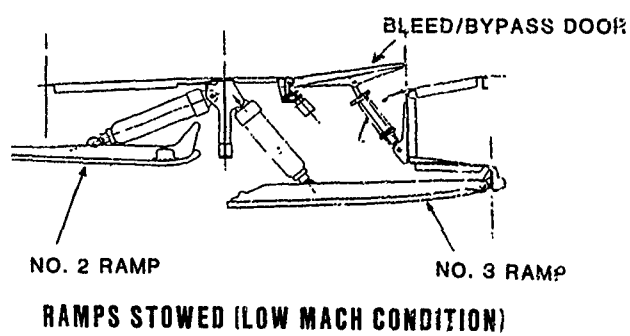
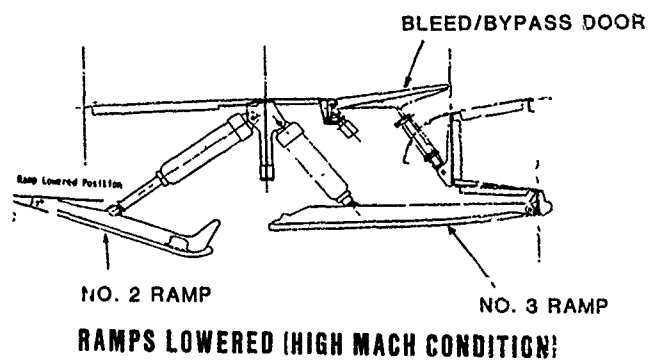


FIGURE 8: F14A AIRCRAFT ENGINE INLET DUCT

Discussion

1. G. Bianchini, Allison Gas Turbine

During the T 700 icing test, you used a heated bullet nose connected to the engine inlet. Have you performed any evaluation to investigate the heat conduction effects of the bullet nose on the engine anti-ice surfaces?

How do you control humidity? Please comment on any problems encountered with the humidity control system.

Author:

Prior to the T 700 icing test an extensive icing consideration was performed with the facility, whenever there were temperature profiles at the plane of the engine inlet. No heat transfer calculations were performed to determine conduction heating. However, during the total environmental icing test, a similar facility heated inlet system was used. During this test, the FAA ice ingestion condition was performed at both specification kind conditions, throughout the engine power range. This test required the operation of the engine anti-icing system for one minute to determine the worst accretion. The facility system was on for the entire test period. The results show that ice accreted on the engine gas path surface uniformly. From these results we concluded that the facility system had no adverse effect on the meteorological conditions exposed to the engine.

Steam was the medium used to humidify the air supply. It was controlled via a close loop electro/pneumatic control system which used line pressure as a feedback signal. Problems encountered with the control of humidity had essentially been related to consistency of the of the thermally heated photo cell sensors' ability to provide accurate point temperature measurements.

2. W. Alwang, Pratt and Whitney

How did you calibrate the collection efficiency of the rotating cylinder?

Author:

Reference 5 of this paper is a report in which NAPC measured LWC using a single rotating cylinder. In this report there is a plot of collection efficiency versus velocity for average drop diameters and given cylinder diameters. The average drop diameter is determined from the FSSP laser probe applied to this plot along with measured duct velocities to determine the collection efficiency.

3. C. Scott Bartlett, Sverdrup Technologies

Would you please comment on the work performed to ensure that the aerodynamic flow field fidelity is maintained for your subsonic free jet test installations?

Author:

For the subsonic free jet icing installations, NAPC had used

both a traversing pitot and static pressure probe and anemometers as well as a profile pressure rake 1-2 diameters upstream of the engine interface plane to quantify the aerodynamic flow field fidelity during the calibrations

4. M. Holmes, RAE

Does your organisation advise on anti-icing methods as well as performing icing evaluation tests?

Have you any evidence which shows that ice accretion on engines/rigs measured in ground-based facilities agrees with flight behaviour?

Author:

The Naval Air Propulsion Center serves the US naval aviator through the Naval Air Systems Command. We provide the navy with technical advice pertaining to all engine and component systems. Examination of engine anti-icing systems represents one facet of the support.

The F 14 A inlet cone test was an example of a fleet problem which was effectively simulated in our icing facility. However, we normally test according to the requirements of the military specification as highlighted in the paper.

5. V. Garratt, RAE

Is the median droplet size mentioned the same as the mean effective diameter also mentioned? If it is so, how is it defined?

What is the droplet size spectrum about the median?

Author:

For all intents and purposes the median droplet diameter is the same as the mean effective droplet diameter because generally the distribution obtained from the FSSP laser probe is a normal one. However, it is the mean that is calculated. The probe counts the droplets in 3 μm diameter increments and the diameters averaged.

For a 20 μm average droplet diameter, the droplet measured ranged from 3-50 μm .

6. P. Derouet, SNECMA

Est-ce que les appareils que vous utilisez aujourd'hui pour mesurer et régler les paramètres de givrage (diamètre goutte, quantité d'eau) donnent les mêmes résultats que ceux utilisés dans les années 1950 pour établir les normes des nuages givrants?

The probe which is used by NAPC today to measure the icing parameters of droplet size and relative moisture content is designed to be an airborne cloud measurement instrument. The results which have been gained from this probe through in-flight measurements are representative of the engine requirements for specification of intermittent and continuous maximum icing conditions. Airborne test results for droplet diameters show that they are within the average level of data scatter

ICING RESEARCH RELATED TO ENGINE ICING CHARACTERISTICS

by

S.J. Riley B.Tech MSc
P.O. Box 31, Rolls-Royce plc
Moor Lane, Derby DE2 8BJ
United Kingdom

SUMMARY

Physical properties and characteristics of ice formed by accretion have been investigated experimentally to provide a database relevant to civil turbofan engine and powerplant surfaces. This paper summarises part of that work, relating to unheated surfaces, including observations of ice accretion on various bodies over a range of conditions and measurement of the adhesive strength of ice samples.

NOMENCLATURE

g acceleration due to gravity
h height of manometer liquid
p static pressure
P dynamic (total) pressure
V air velocity
 ρ_a air density
 ρ_l manometer liquid density

INTRODUCTION

Ice accretion on airframe leading edges and forward-facing surfaces has been of increasing concern during recent years, since it can degrade aerodynamic performance and represent a potential source of ingestion damage, thus causing a hazard to the safe progress of the aircraft. The solution of the problem as a safety issue is not straightforward, since any anti-icing or de-icing provision represents an engine performance penalty which must be balanced against powerplant performance deficit that may occur without icing protection. Such performance deficits could be generated by drag of iced surfaces or by mechanical deformation of compressor blading caused by major ice shedding. It is desirable to determine firstly which surfaces require protection and secondly the level of protection necessary to optimise the balance between real and potential performance loss. In order to acquire a database to enable such assessments to be efficiently and accurately carried out, Rolls-Royce has investigated icing phenomena and ice protection systems appropriate to civil turbofan engine and powerplant surfaces (Figure 1) by means of several experimental research packages. This paper summarises part of that work, relating to ice properties and formation on unheated surfaces. The following experimental investigations are discussed:

- o calibration of the icing wind tunnel used, for a range of simulated ambient parameters
- o macroscopic and microscopic observations of ice formed by accretion at various conditions

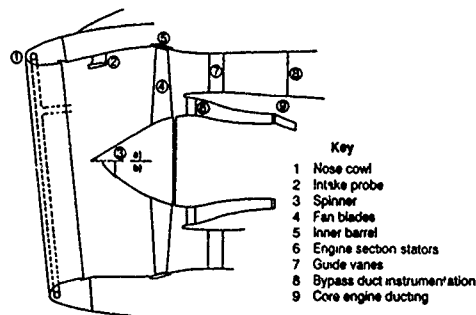


FIGURE 1 Engine and nacelle icing considerations

- o ice accretion on static vane sets
- o ice accretion on an engine intake leading edge
- o ice/water formations at a total temperature of $+2^\circ\text{C}$
- o adhesive strength of ice samples on a moving collector.

Further research on ice shedding characteristics, sublimation, insulation effects and flowfield changes (drag) due to the presence of ice would be useful to develop understanding of the physics.

CALIBRATION OF ICING WIND TUNNEL

For all the studies covered in this paper, a blow diameter sea level wind tunnel based at Rolls-Royce Hucknall was used. The tunnel is fitted with water spray nozzles which can produce a supercooled water cloud of controllable droplet size and total liquid water input to simulate an atmospheric icing cloud. The tunnel airflow and water spray beyond the tunnel exit plane, in the region of the test piece working section, were investigated by recording the air temperature, air pressure (velocity) and liquid water content distributions at four planes downstream of the tunnel fitted with a 280 mm (11 inch) reducing nozzle. Figure 2 is a diagram of the test configuration and measurement planes. The pressure and temperature profiles were investigated by means of pitot and thermocouple rakes, Figure 3. The pressure rake comprised 25 pitot rakes spaced one inch apart centre to centre interspersed by six probe type static tappings along a horizontal bar. The 25 thermocouples on the temperature rake were also spaced one inch apart along a supporting bar. The rakes were moved in the vertical plane by means of a motor, and their position indicated on a scale on the test cell viewing window by a pointer on the end of the pressure rake.

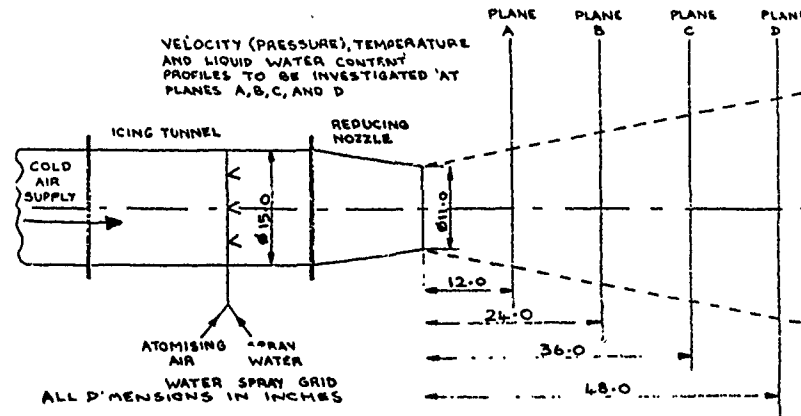


FIGURE 2 Icing tunnel calibration measurement planes

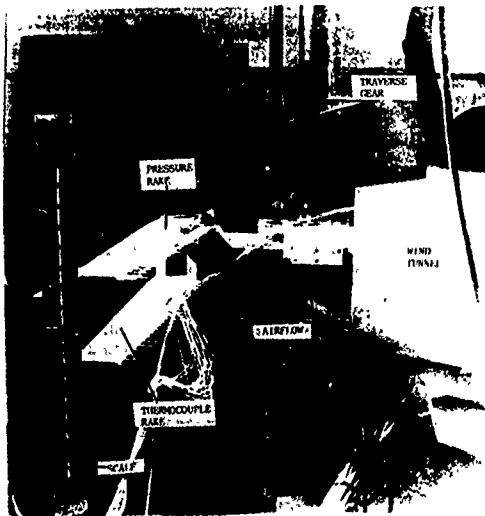


FIGURE 3 Instrumentation rakes mounted downstream of wind tunnel

Readings were taken at one inch intervals from below the tunnel upwards to avoid back-lash in the traverse screw thread and advancing mechanism. The vertical extent of measurements was chosen to encompass significant pressure and temperature gradients, with outermost readings approaching ambient conditions in the test cell.

Readings were taken at nominal air velocities of 61 and 122 m/s (200 and 400 fps) at the four measurement planes for total tunnel air temperatures of 0°C, -15°C and -30°C (pressure readings were taken at 0°C only since the differences observed at plane A for 0°C and -15°C were negligible). Sample rake positions were retested at intervals to check experimental repeatability and note the

effect of varying ambient conditions. Repeatability was good in the high velocity core. The outermost temperatures varied with time according to test cell conditions, but variation during a given scan was negligible. Sufficient time was allowed for stabilisation at each test point.

A contour plotting program was used to plot results as contour maps for each test condition at each measurement plane. Figure 4 shows the resultant pressure contours at 0°C in terms of pressure heads (inches of water) to 12 inches either side of the centreline. The geometric centre-point of the tunnel is marked +. The pressures plotted on Figure 4 are related to velocities via a simplified Bernoulli's equation:-

$$P - p = \frac{1}{2} \rho a V^2$$

$$\text{and } P - p = \rho l g h$$

$$\text{hence } V = \sqrt{2 \frac{\rho l g h}{\rho a}}$$

Figure 5 shows sample temperature contours in degrees centigrade to 12 inches either side of the centreline. Inspection of Figures 4 and 5 shows that the flow remains in a core formation up to at least 1.2 m from the nozzle exit plane, and the temperature of this core flow approaches the nominal air temperature. The size of the core diminishes with downstream distance. The circular nature of the pressure contours indicates that the flow produced is axisymmetric, but the flow is distributed about a point offset from the geometric centrepoint. This is due to the proximity of the test cell wall (to the left of plots Figures 4 and 5 as viewed) and floor. Calculations suggest that the actual velocity of the core flow exceeds the nominal tunnel velocity. As distance from the exit plane increases the size of this 'high velocity' core diminishes. For a given nominal velocity, the local air velocity more than 150 mm (6 inches) radially from the centre of flow is not significantly changed with downstream distance, i.e. velocity and temperature gradients are greatest near to the nozzle.

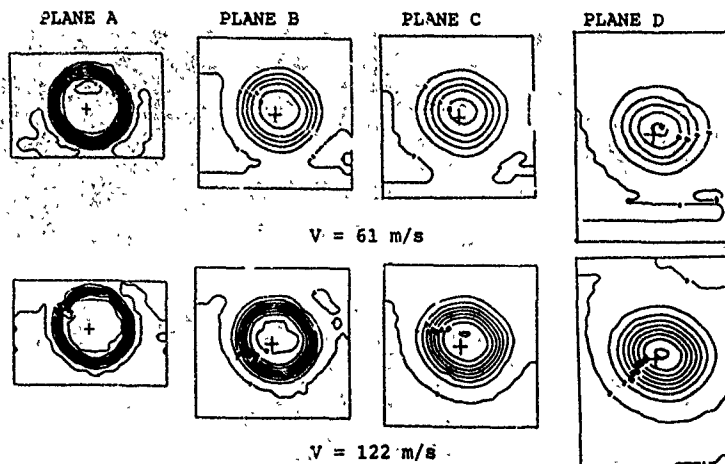


FIGURE 4 Pressure profiles

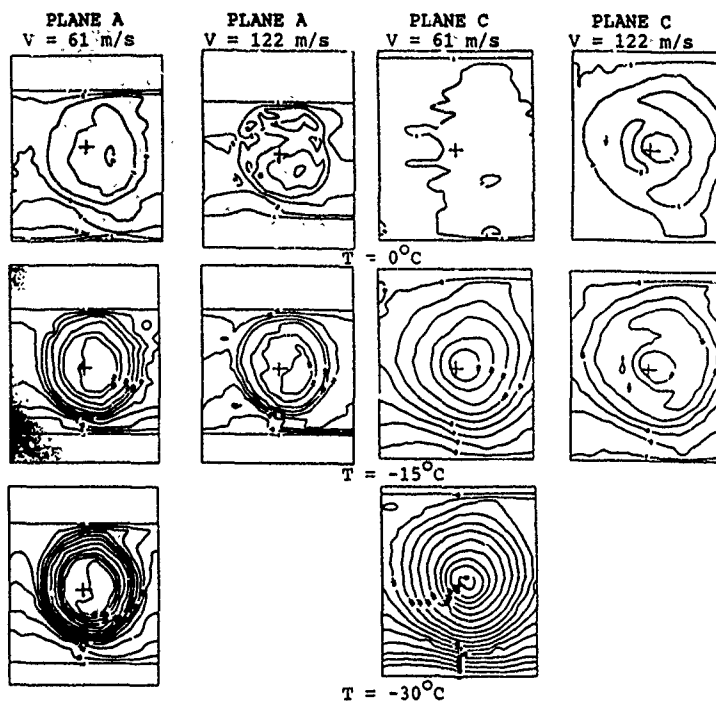


FIGURE 5 Temperature profiles

Research was carried out in the Hucknall facility to determine the effects of certain variables on ice accreted at -10°C on a steel tubing grid. Air velocities tested were 61 m/s and 122 m/s at the wind tunnel exit plane. For corresponding test conditions, it was found that the higher tunnel airspeed produced more brittle ice,

which shed more easily and was generally more opaque. The contact area with the grid was less for the higher speed and the classic forward-facing horned formation was better defined, this being more apparent with increased water input. Figure 6 shows sample photographs of ice accretions, and Figure 7 shows the difference in cross section at various test conditions.

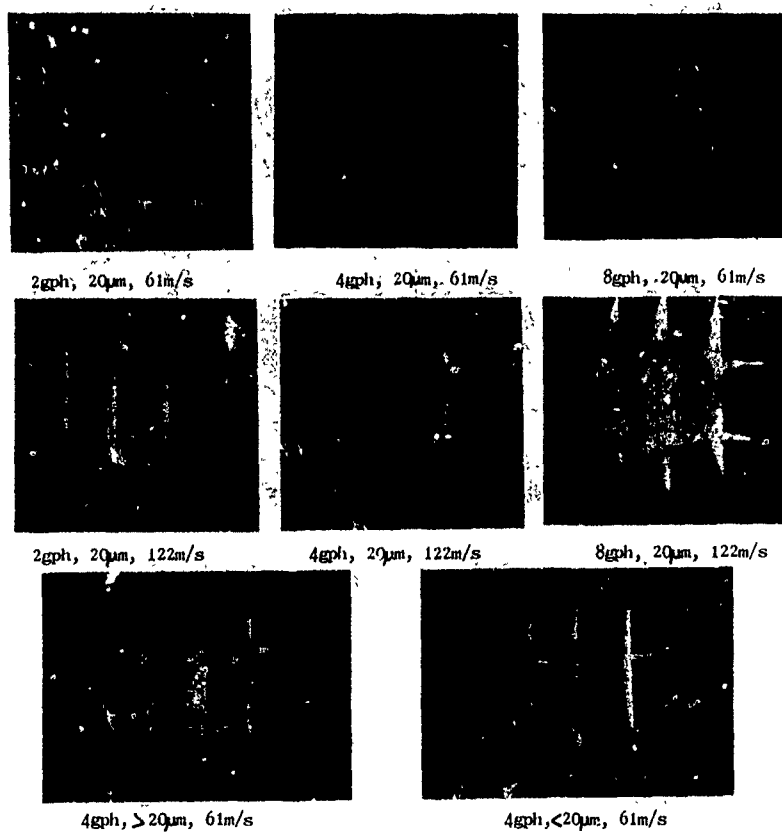


Figure 6 Ice accretions on grid after 5 minutes at -10°C

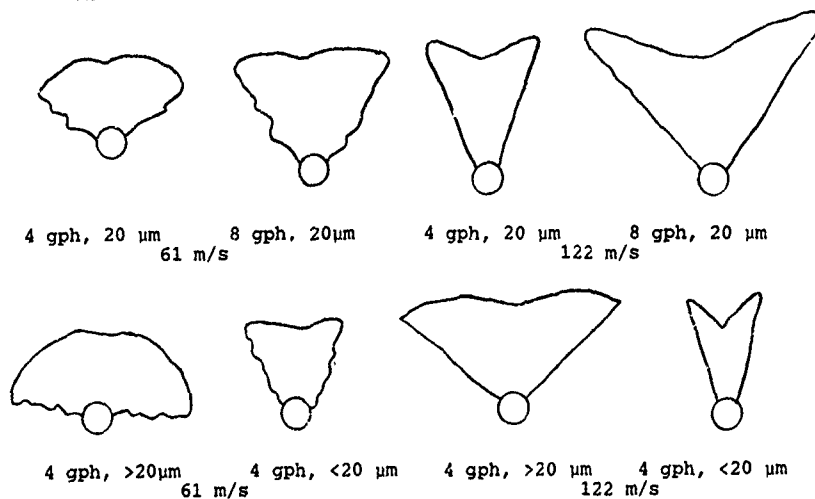


FIGURE 7 Profiles of grid ice accretions after 5 minutes at -10°C

As water input increased, i.e. simulated cloud liquid water content increased, the amount of accreted ice increased proportionately. However, a reduction in liquid water content associated with an increased exposure time to the icing condition had a similar effect to increasing velocity in that the resultant ice was more brittle, shed more easily,

was more opaque and featured a reduced contact area and better defined horned formation. The ice formed on the collection grid was removed and weighed after each test, and it was found that for a given total water input, a lower water flow rate resulted in a greater quantity of ice due to the different transportation and heat transfer phenomena at the surface of the accreting ice.

Experimental evidence showed that a reduction in water droplet size had a similar effect on ice type as an increase in airspeed or reduction in liquid water content, producing more brittle, opaque ice which shed more easily.

Ice formed at different temperatures displays different characteristics. There are two categories of ice normally quoted; rime ice and glaze ice. Rime ice forms at low temperatures, is smooth, opaque and tends to follow the shape of the surface on which it is building. Glaze ice forms at temperatures approaching 0°C , is clearer and comprises forward facing 'feathers' of ice which give the classic horned shape. In the case of a point attachment this type of ice forms a rosette growing forwards and sideways. Examination of results discussed above shows a tendency towards glaze ice characteristics rather than rime for an increase in airspeed, reduction in droplet size or reduction in liquid water content. At the intermediate test total air temperature of -10°C , it will be noted that either type of ice or a combination may form, dependant upon ambient conditions. Glaze ice is generally a greater problem in respect of aero-engine intakes since cloud liquid water content is greater at higher temperatures and the glaze ice shape will have a larger effect on drag and damage potential if the ice is released. However, glaze ice tends to be more brittle with a smaller contact area and is more readily shed. The only deviation from transition between rime and glaze ice noticed during the experimental investigations was an increase in opacity rather than an increase in clarity. The physical formation characteristics distinguishing the two ice types are as follows: the major influencing factor is the freezing fraction; the proportion of the impinging supercooled water droplets which freeze instantaneously on impact. For pure rime ice the freezing fraction is 1.0, the resultant ice being opaque. At low freezing fractions there is some water flow along the surface prior to freezing, forming clear glaze ice. The post-impact

water flux gives rise to the horned or rosette type growth of glaze ice. The associated increased frontal area and transient local heat and mass transfer coefficient distributions escalates the deviation from the original collector surface shape.

The size and location of a test piece should be chosen to lie within the reasonably uniform core flow. However, the presence of a model will deviate the flow thus effectively increasing the size of this core, and heat transfer phenomena at the model surface will influence the effective local air temperature e.g. viscous heating.

MACROSCOPIC AND MICROSCOPIC OBSERVATIONS OF ACCRETED ICE

The appearance, net quantity, shape, distribution, relative location, physical properties and shedding propensity of ice formed by accretion are a function of ambient conditions at the time of formation, characteristics of the

collecting surface and surroundings, and any external forces prevailing. The variables contributing to a given icing condition include air temperature (static and total), air velocity, cloud liquid water content, water droplet size and distribution, cloud extent (time in icing) and altitude. The pertinent collecting surface characteristics may be considered to be rotational speed, heat input, shape, material and surface finish. As an initial step towards understanding the physics and mechanics of the aforementioned phenomena, ice was formed on a stainless steel collector mounted downstream of the Rolls-Royce Hucknall 15 inch icing wind tunnel for a range of airspeeds, air temperatures, liquid water contents and droplet sizes. The samples were observed manually, photographed in close-up using a Hasselblad camera plus bellows, and photographed through a microscope using a Leitz camera attachment plus light box.

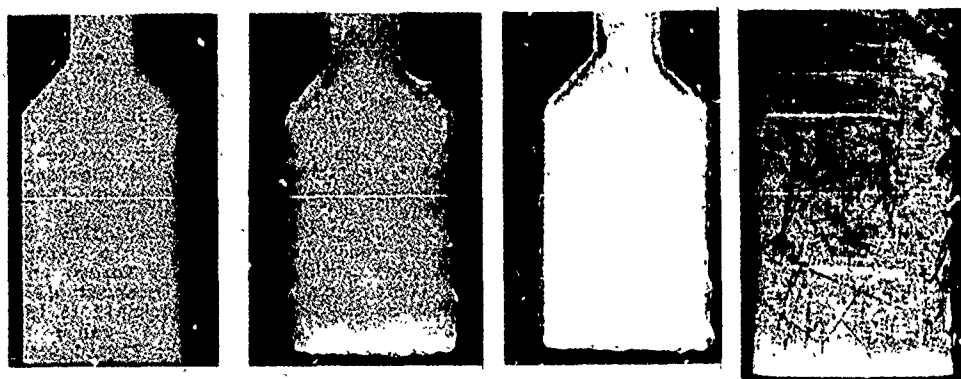
The collector was cleaned prior to each test, and the tunnel run prior to the introduction of supercooled water to allow temperature and airspeed to stabilise. Ice was collected for one minute at each test condition. Samples were collected over ranges of airspeed 30 to 122 m/s (100 to 400 fps), total air temperatures 0 to -30°C and water flow from 2.5 to 10.1 g/s (2 to 8 gph). Most tests were at a nominal water droplet size of $20\mu\text{m}$, but some tests were repeated at smaller and larger droplet sizes.

Following manual and close-up photographic observation, each sample was removed for microscopic observation at 100 times magnification. It was not possible to make microscopic observations of ice formed at 0°C due to rapid melting. The wind tunnel was completely run down to avoid vibration which could be transmitted to the microscope. There would have been little advantage in setting the microscope arrangement up in the test cell, since the main contributory factor to increased melting was the light source, and condensation would have been a problem.

Sample close-up photographs are given as Figures 8 and 9.

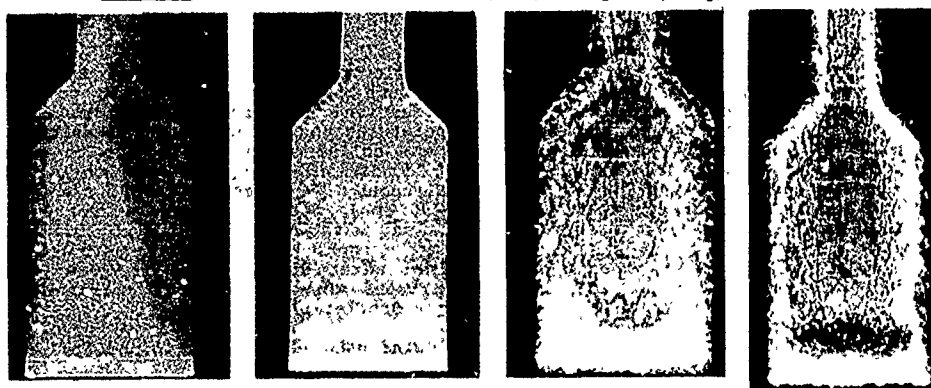
Figures 10 and 11 show microscopic photographs corresponding to Figures 8 and 9.

As temperature increased, the surface structure of the ice became more uniform. No indication of the infrastructure could be gained due partly to melting and partly to inadequate magnification. Surface observations only could be made with equipment available. As airspeed increases, water droplet Reynolds number and inertia parameter (Bowden) increases. These changes have opposing effects on collection efficiency, limiting the net effect on ice accretion. From results it was seen that as airspeed increased the ice became more opaque and brittle. This observation was consistent with those made during the calibration research described earlier. As water input increased the amount of accreted ice increased proportionately. However, as previous research has shown, a reduction in liquid



-30°C -20°C -10°C 0°C

FIGURE 8 Ice formations at 30 m/s, 20µm droplets, 5 g/s water



-20°C -15°C -5°C 0°C

FIGURE 9 Ice formations at 91 m/s, 20 µm droplets, 5 g/s water

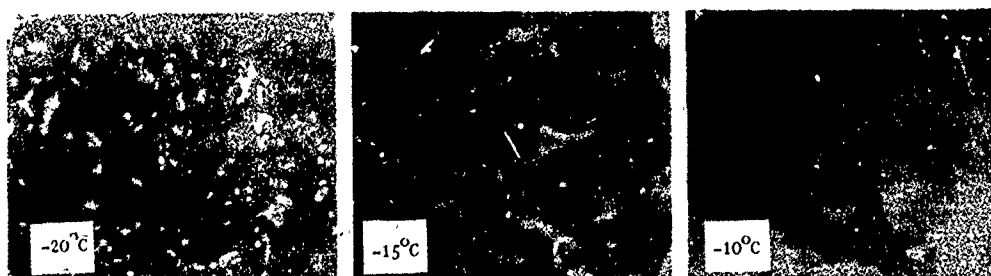


FIGURE 10 Microscope results at 30 m/s, 20 µm droplets, 5 g/s

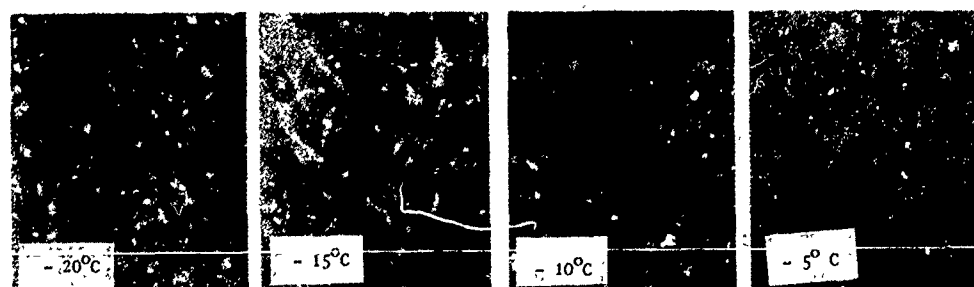


FIGURE 11 Microscope results at 91 m/s, 20 µm droplets, 5 g/s

water content associated with increased exposure to give an equivalent total water input had a similar effect to increasing velocity in that the resultant ice was more brittle, more easily shed, more opaque and features a reduced contact area and better defined horned formation. For a given total water input, reduced liquid water content resulted in a greater quantity of ice. Similarly, a given quantity of water input at a higher velocity gave a greater ice accretion; this was also an effective reduction in liquid water content since volumetric flow through the wind tunnel was increased. Water droplet size affected ice collection efficiency (quantity) and the type of ice formed, although the effect was much less than that of other parameters. At low air temperatures, rime ice is formed and at temperatures approaching 0°C glaze ice forms. The horned formation is less apparent for a flat collector, peripheral ice growth providing the best indicator. Results clearly showed the transition from rime to glaze ice characteristics as temperature increased. At intermediate temperatures, either type of ice or a combination formed on the unheated collector. Examination of experimental results also showed that the tendency towards rime or glaze-type ice is affected by airspeed, droplet size and liquid water content. Microscopic observations indicated an associated surface area and roughness change consistent with the foregoing discussion, i.e. as temperature increases freezing fraction is reduced and the droplets spread laterally on impact before freezing, giving the more open texture.

These investigations concluded that:

- o The physical and mechanical properties of ice formed by accretion are a function of formation conditions.
- o The effects of altitude, rotational speed, vibration, heat input, material type and surface finish may also influence ice properties, and these phenomena should be investigated.
- o Alternative techniques for microscopic observations should be investigated.

ICE ACCRETION ON STATIC VANE SETS

Excessive core engine blockage due to icing of engine section stators can be detrimental to engine performance, giving a reduced flow area, increased pressure loss and consequent power loss and must be avoided. However, it is desirable to maximise the number of fan outlet guide vanes and compressor inlet guide vanes for optimised noise suppression. Therefore model static vane sets of 19.1, 25.4, 38.1 and 55.9 mm (0.75, 1.0, 1.5 and 2.2 in) spacing were subjected to icing conditions in the Hucknall 15 inch icing wind tunnel to investigate the phenomena involved. The effects of fan swirl and relative angle of the vanes to the flow were also investigated. Each set of stainless steel

vanes was contained in wooden ducting with a perspex viewing panel. The vanes were of constant profile, representing approximately the mid section of typical inlet guide vanes. The trailing edge of each vane was thickened to enable fitment of locating pins. Tests were conducted:

- (A) with the 25 mm vane set in-line at 0° vane incidence
- (B) with all vane sets at 23° to (A) and 0° vane incidence, to simulate fan swirl
- (C) as configuration (I) with the 38 mm vanes skewed ±20°.

Prior to icing tests, the velocity profiles upstream of the vane sets were checked using a traversing pitot rake comprising 27 tappings connected to water manometers. The profiles were found to be uniform over the majority of the test section, with negligible wall effects. The rake was removed during icing tests and replaced by a sealing plug in the ducting lower wall. Pre-test ice distribution checks indicated satisfactory water (ice) distributions, even with one spray nozzle operating only for low water input conditions. Each test build was also checked for leaks. The tunnel air temperature was allowed to stabilise at the desired velocity before supercooled water was introduced at each test condition. Results were recorded at one-minute intervals or as appropriate via static pressure tappings connected to water or mercury manometers according to the magnitude of pressure drops across the model. Still photographs were taken remotely during each test and video monitoring was used, selected tests being recorded. Times of major ice sheds were noted.

Tests were 30 minutes long unless either ice blockage rendered it impossible to maintain conditions or an ice accretion and shedding cycle had been established. The highest scheduled airspeed of 137 m/s (450 fps) could not be achieved due to

blockage by the vanes themselves, and 119 m/s (392 fps) was used as the practical maximum. For most builds temperatures of -15°C, -6°C and -2°C at 61 m/s (200 fps) and 91 m/s (300 fps) air velocity and 0.15 g/m³ and 0.3 g/m³ liquid water content were tested, although intermediate temperatures, the higher velocity and a wider range of liquid water content (0.1 to 0.6 g/m³) were tested for 25 mm and 38 mm angled vane sets. The swivelling vanes were tested at incidences of -20° (almost parallel to the airflow), -10°, 0° (datum), 10° and 20°. The latter caused maximum blockage by the vanes, limiting achievable tunnel air velocity. In all tests the nominal water droplet size was 20µm.

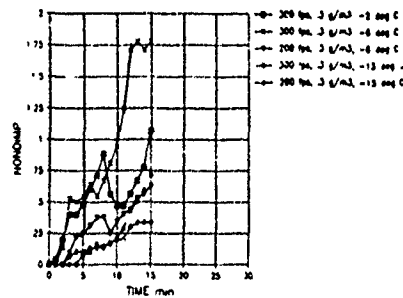
To make comparisons easier, results have been plotted non-dimensionally in the form

$$\text{NONDIMP} = \frac{\Delta P - \Delta P_o}{\Delta P_o} \text{ where } \Delta P = \text{measured pressure drop} \text{ and } \Delta P_o = \text{initial } \Delta P$$

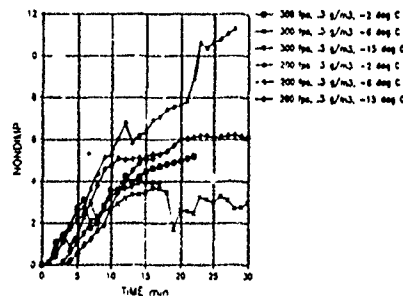
Figure 12 shows results at 0.3 g/m^3 for all spacings angled to the flow and Figure 13 shows results for in-line and swivelling vane sets.

Observations showed that ice formed at -2°C grew forwards and laterally (glaze ice) and as temperature of formation reduced, frontal area reduced (rime-type ice). In general ΔP increased with temperature, reflecting the different ice types, but blockage was not necessarily greater at higher temperatures since shedding propensity also increased. For similar reasons it did not necessarily follow that an increase in airspeed (and associated increase in water input for a given liquid water content) caused increased blockage. Having noted that shedding was a major contributory factor in net ice accretion/blockage, shed ice must pass between the blades to be completely removed. For closely spaced vanes, ice often wedged between the vane

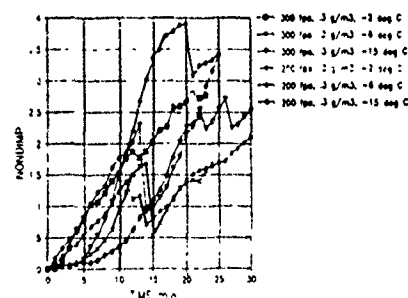
from which it had been shed and an adjacent vane, providing a further accretion surface to exacerbate the build-up. Initial pressure drop across the vane sets varied considerably with vane spacing and angle relative to the airflow, but it must be assumed that this 'blockage' due to the vanes is acceptable for the particular application. In many tests, for closely spaced vanes and low temperatures, the pressure drop across the vane set decreased slightly before increasing. This was apparently due to slight streamlining of the blade, caused by the initial (rime) ice formation. From inspection of Figure 12 it may be seen that blockages of 19 mm, 25 mm and 38 mm spaced vanes were of the same order and that 56 mm vanes were much less susceptible to blockage. From a comparison of Figures 12 and 13, no conclusion can be drawn concerning the benefit or otherwise of the presence of swirl due to the fan. Figure 13 shows that the amount of skew on the vanes



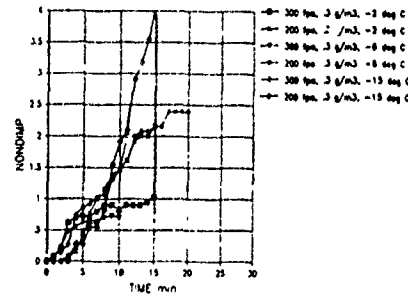
55.9 mm spacing



25.4 mm spacing

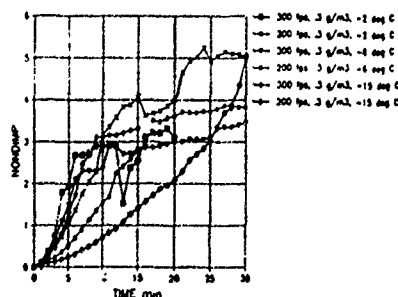


38.1 mm spacing

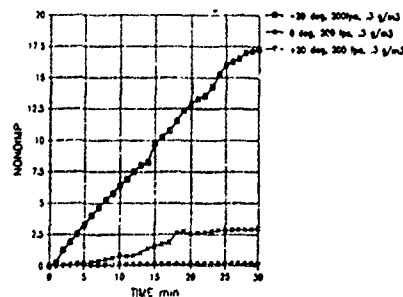


19.1 mm spacing

FIGURE 12 Non-dimensionalised pressures for angled vane sets



25.4 mm in-line



swivelling

FIGURE 13 Non-dimensionalised results for in-line and swivelling vane sets

affected blockage greatly. This was because oblique vanes relative to the airflow themselves represent a large blockage, so additional blockage due to ice is low as a percentage of the initial value. In all cases it was noted that ice on the leading edges tended to 'shield' pressure surfaces, and any ice located there shed and did not rebuild unless the leading edge ice shed. This is not apparent of fan blades, where the relative pressure surface area is large, leading edges thin and the blades are presented obliquely to the flow at their hubs. The pressure levels at which shedding occurred increased throughout a given test. This is thought to be due to initial sheds removing the weaker ice, leaving the stronger ice as a base for new accretion. Once the initial more frequent shedding was complete, the shedding appeared to occur in a cyclic fashion unless build-up was such that the ice could not shed because it had nowhere to move to, e.g. ice bridging adjacent vanes formed a firm accretion base and blocked the corresponding passageway.

The investigations concluded that:

- o Closely spaced vanes are more prone to blockage, and ice bridging, but initial pressure drops were similar.
- o Blockage is highly dependant on shedding propensity. At conditions tested, significant blockages occurred.
- o Vane angle relative to the flow was significant mainly due to initial ΔP . Fan swirl had no quantifiable effect.

The data acquired must be considered in conjunction with icing tolerance characteristics of a particular engine, e.g. surge margin, impact resistance, ingestion capability (damage potential) and detail geometry.

ICE ACCRETION ON ENGINE INLETS

Limited sea level testing has been carried out on unheated full-scale two-dimensional turbofan inlet section models to check water (ice) catch prior to anti-icing system tests. The ice formed displayed characteristics consistent with those discussed earlier, and ice shape and quantity were consistent with Bowden. Ice formations were also similar to those noted during observations of ice accreted in flight for delayed selection of nose cowl anti-icing. Some photographs of runback ice (un-evaporated water running back from a heated surface and freezing on a downstream unheated surface) in the icing tunnel and in flight. This ice takes the form of rivulets due to surface tension effects. Figure 14 shows a typical example.



FIGURE 14 Typical runback ice

ICE/WATER FORMATIONS AT +2°C

The purpose of these tests was to observe the interactive phenomena of ice and water on a typical turbofan intake surface and to determine the effect of controlled parameter changes on ice formation. At temperatures around 0°C there is an intermediate situation whereby both ice and running water exist on the surface. Prediction of the physics, mechanics and hydrodynamics of this phase is a complicated heat and mass transfer balance.

A full-scale two-dimensional section of a typical aero engine intake was mounted downstream of the Rolls-Royce Hucknall 15 inch icing wind tunnel and enclosed in ducting, the walls of which were shaped to simulate the airflow distribution for a typical descent flight condition. The model was fitted with a mock-up section of anti-icing system, comprising a length of 'piccolo' pipe featuring three rows of holes such that air jets impinged on the intake model internal surface. A tunnel total air temperature of +2°C and water droplet volume median diameter of 20µm were used throughout testing. Ice and water formations and behaviour on the intake section highlight region and inner surface were observed for a range of tunnel air velocities of 26 to 82 m/s (50 to 160 kts) and water flows of 1.9 to 10.1 g/s (1.5 to 8 gph) with no internal airflow. Selected tests were repeated with ambient air fed to the model anti-icing system. Still photographs and video were used to record observations. The spread of test conditions was intended to cover the range from full evaporation to total phase change in the intake highlight region within the limits of the plant and aircraft operating ambient conditions to which the test points corresponded. Velocity was allowed to stabilise and soak down so the entire model and the air inside it were at +2°C prior to each test. After the water flow was introduced, the test duration was such that conditions were stable.

Generally, flowing water on the cowl surface tended to limit ice formation. At the lowest velocity of 26 m/s virtually no ice formed, at 64 m/s ice build up was observed, less so at higher water flows, at 82 m/s no more ice built up for a given water flow and at 103 m/s the ice quantity was reduced. The addition of air into the mock-up anti-icing system at 11 to 13°C did not change the water flow patterns, but ice accretion was severely limited

compared with no flow. An increase in airspeed at a given water flow rate (reducing liquid water content) affected the type of ice formed but not the volume accreted prior to major shedding i.e. a critical mass was reached. This is also true up to a point of increasing water input, beyond which the increased water flow limits ice formation, i.e. washing away ice formed. Theoretically, more ice would be expected to form as airspeed increased since this effectively reduces the static air temperature, hence the reason for no ice formation at the lowest airspeed, when the static air temperature was positive. For higher airspeeds static air temperature was negative.

Water rivulets observed were a result of surface tension effects. Rivulets were seen upstream of the anti-icing air exhaust slot and were therefore not the result of effects afforded by the slot itself or the air issuing from it.

The presence of ice on the highlight of the intake affected airflow around the model, confirmed by the almost concurrent shedding of nose ice and surface ice. The ice acts as an insulator as indicated by a thermocouple inside the model. In some instances surface ice slid in a downstream direction, indicating that the interface had melted. In all cases ice build up and shedding followed a well defined cycle, the cycling times being fairly constant and a function of airspeed and water input, and possibly partly due to the effective air velocity change arising from increased ducting blockage with ice present relative to the bare model.

This qualitative testing indicated that, near the freezing point, the net coverage of an aerofoil by ice and/or water is the result of the interaction of several effects. Additionally, ice accretion is self limiting owing to insulation effects and flow pattern alterations due to shape changes. Water flow patterns and

quantities are dominated by evaporation and surface tension effects, but the presence of ice modifies water flow patterns. These phenomena produce a transient situation at the surface, but the process is cyclic. The observations made were considered in the development of analytical models of icing behaviour, and assisted in the interpretation of full scale aircraft and engine tests in ice forming conditions.

ADHESIVE STRENGTH OF ICE FORMED BY ACCRETION

Net ice accretion, as discussed previously, is a function of ice collection and shedding propensity, which in turn is related to ice mass, forces acting upon it, shear strength of the ice and the adhesive bond strength at the ice/surface interface. Experimental investigations were carried out to determine the bond strength of ice built up on rotating collectors mounted downstream of an annular nozzle attached to the Hucknall 15 inch icing wind tunnel. The ice mass resulted in a centrifugal shedding force which was recorded by strain gauges on the collector arm front and back faces. Figure 15 shows the rig schematically.

Two 25 mm (1.0 in) square titanium collectors were mounted at a radius of 275 mm (10.8 in), adjustable from normal to the tunnel airflow to 30° rotation. The collector surfaces were degreased and grit blasted to a consistent and recognised standard. The tunnel airspeed, drive motor rotational speed and collector angle were arranged such that the impingement velocity was always normal to the collector face.

When ice formed on the collector with the rig spinning, the forces on the arm were:

- (i) centrifugal force (CF) due to the collector mass

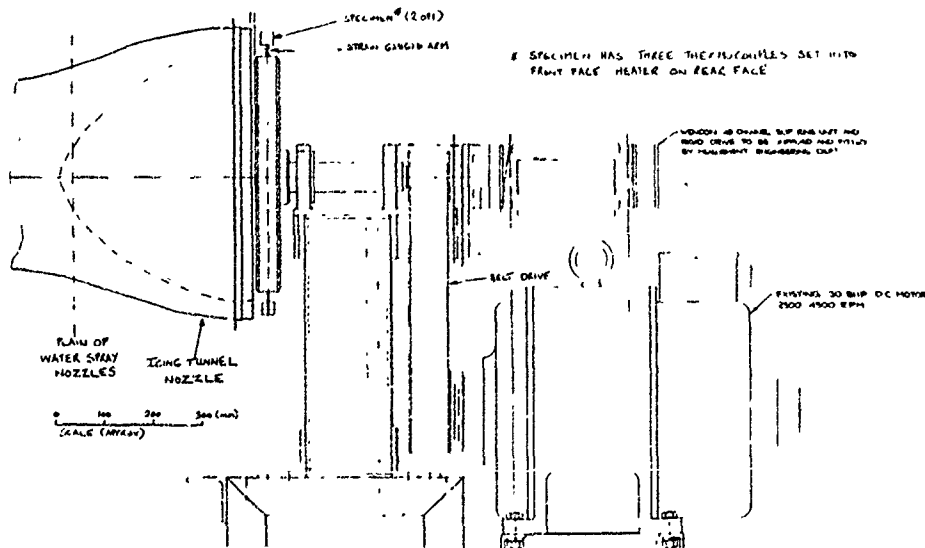


FIGURE 15 Ice adhesion rig

- (ii) centrifugal force due to the ice mass
- (iii) moment due to the collector/ice CF offset from the arm centreline
- (iv) moment due to aerodynamic forces on the collector (probably small compared with (i) to (iii)).

This combination of forces resulted in a net tensile force on the forward face of the collector and a compressive force on the rear face. When ice shed, the resolved force was reduced and the resultant change in strain was used to calculate the force which caused the shedding and hence the shear strength of the bond and ice. It should be noted that results would be affected to some degree by the presence of the strain gauges themselves. The strain gauge data and thermocouple readings were continuously monitored via a U/V chart recorder. A slip ring unit was used to transmit measurements from the rotating shaft to the recorder. Strobe-triggered video cameras were used for observation of the icing process, and a still camera was used to record the condition of the ice fracture surface immediately after shedding.

Pre-test checks on velocity (pressure) and water distributions showed that velocity was even over the area swept by the collectors, and water distribution was even after modifications to the grid. A deflector plate was added to avoid ice accretion on the arms and bridging to provide possible strengthening. A large number of tests were carried out at each condition to establish statistical credibility because of high scatter due to variations in accretion and shedding times (and hence ice mass) and experimental errors, although accretion and shedding were essentially cyclic. Most tests were for 1.0 g/m^3 liquid water content, $20 \mu\text{m}$ droplets and a clean surface with impingement velocities normal to the collectors of 61 to 213 m/s (200 to 700 fps) and temperatures of -2 to -20°C (note that for a 30° collector angle the normal impingement velocities were twice the tunnel airspeeds). Additional tests were carried out to investigate the effects of liquid water content (0.5 to 2.5 g/m^3), droplet size (15 to $30 \mu\text{m}$), impingement angle (30 and 35°), surface preparation (clean and

greased) and coatings (PTFE and GRP). After the first ice shed of a given test, the surface nature of the base on which subsequent ice built would not be as pre-test, so most tests comprised more than one shed, until ice shed from the tunnel walls affected the results.

Numerical values of average and maximum shear strength were calculated from strain gauge readings. Figure 16 shows these results against temperature for the bulk of tests. The mean values shown may be lower than the true mean in some cases owing to the inclusion of results from partial ice sheds not recognised as such. The maximum shear strength values are dependant on the number of tests at a condition.

It has been suggested that, because the centre of mass of the ice sample was offset from the shear face, the ice would tend to peel rather than shed in pure shear. This was limited by not allowing the ice sample thickness to exceed 12 mm (0.5 in), but there is no evidence to support or dismiss the hypothesis that the shedding mechanism was either entirely peeling or initiated by peeling.

The size and shape of the ice collectors were not representative of a fan blade section or other rotating engine component. There are two scaling effects; firstly the aerodynamic forces increase as the size of the accretion surface is reduced owing to the relative proportions of the ice and 'clean' surrounding surface and secondly ice gains strength from adjacent ice. The shape of the surface affects the aerodynamic characteristics and ice collection efficiency.

The mechanism by which ice sheds (adhesive/cohesive failure) is determined by the fracture mechanics involved, and no attempt was made to study the nature of the adhesive bond between the ice and the metal surface. It was noted, however, that failure tended to be cohesive, i.e. failure occurred within the ice, at lower total air temperatures. At higher temperatures adhesive failure occurred, i.e. the bond between the ice and the metal surface was broken. The transition occurred between -5 and -10°C air temperature, which also corresponds with the transition between rime and glaze ice. The ice type and failure mechanism did not

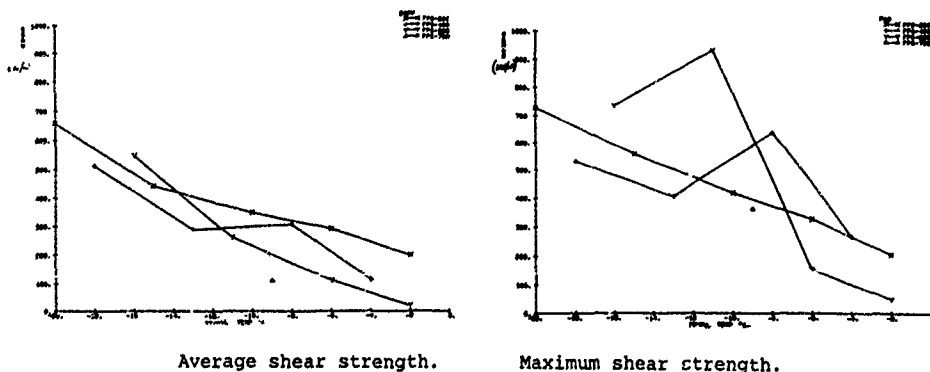


FIGURE 16 Adhesive strength results

appear to significantly affect results except that an increase in gradient of the strength-temperature curves was noticeable at lower temperatures. Figure 16 indicates that shear strength increased as air temperature at formation reduced, approximately linearly. The impact speed had a significant effect on shear strength, higher accretion velocities producing lower strength ice, probably due to increased aerodynamic forces, reduced capability for trapped air to escape, increased droplet spread prior to freezing and changes in water flow characteristics at the ice surface. A reduction in droplet diameter apparently increased shear strength, which is in opposition to the findings of calibration tests described earlier. This has been attributed to the flat collector versus the smaller contact area grid. A 5° change in impingement angle did not have any quantifiable effect on shear strength, but this is a relatively small change. A 'greased' surface gave lower adhesion. A PTFE coating reduced shear strength and GRP reduced it further. Liquid water content variation had no significant effect on strength.

The results of investigations were used to validate a fan blade ice accretion and shedding model. For predictive purposes, the averaged data showed that strength decreases with total air temperature increase at a rate of $-30 \text{ kN/m}^2/\text{C}$ and the maximum shear strength falls at a rate of $-85 \text{ kN/m}^2/\text{C}$.

CONCLUSIONS

The following conclusions may be drawn from the work covered.

- o The research summarised in this paper has provided a significant quantity of data which has improved knowledge and understanding of phenomena associated with ice formed by accretion.
- o Further investigations are required in order to provide a more comprehensive understanding of the physics involved.
- o The data available has been used in the design, development and in-service phases of turbofan installations.

REFERENCES

- 1 Bowden et al 'Engineering summary of airframe icing technical data', TR ADS-4, March 1964.

Discussion

1. V. Truglio, Naval Air Propulsion Center

Regarding your icing test rig, is there any compensation necessary in the generation of liquid droplets due to what seems like relatively short time between the nozzles and tunnel exit plane? Also is there any consideration to humidity effects?

Author:

Investigations (theoretical and experimental) were carried out to determine a minimum distance downstream of the spray grid. A model had to be placed to ensure that the droplets were as required. A limitation is the physical length of the test cell, but the rig is being refitted with this criterion as a design feature.

Humidity has been measured but is not a problem due to the tunnel configuration, with heat exchangers drained upstream of the control room and the fact that the entire room soaks down to the test temperature.

MODELISATION NUMERIQUE DE L'EVOLUTION D'UN NUAGE DE GOUTTELETTES D'EAU EN SURFUSION DANS UN CAISSON GIVRANT

CREISMEAS paul et
D.G.A.
C.E.Pr. Saclay
91481 ORSAY-CEDEX

COURQUET Joel
O.N.E.R.A./C.E.R.T.
2 Avenue Edouard BELIN b.p. 4025
31055 TOULOUSE-CEDEX

RESUME

Depuis peu, le C.E.Pr. a développé pour ses besoins d'essais en givrage un outil de calcul qui lui permet de prédire l'évolution de gouttelettes d'eau en surfusion dans un écoulement d'air froid.

Ce code, baptisé M.A.G.I.C. (Modélisation et Analyse du Givrage en Caisson) a des qualités de robustesse et de souplesse d'emploi que l'on attend d'un code industriel.

Afin de confronter les résultats numériques obtenus par M.A.G.I.C. avec des mesures physiques, une analyse a été menée en prenant pour référence des résultats de granulométrie sur un spray de gouttelettes dans une soufflerie de laboratoire.

Le résultat de la confrontation s'est avéré très satisfaisant.

ABSTRACT

Since a few time C.E.Pr. has developed a computation tool for its own icing tests needs.

This tool allowed the prediction of supercooled droplets evolution in a cold air flow.

This program is named M.A.G.I.C. and has qualities of stability and adaptability expected for an industrial program.

In order to compare numerical results from M.A.G.I.C. to physical measurements, an analysis based on granulometry measurement concerning droplets inside a laboratory wind tunnel is performed.

The results of the comparison are very acceptable.

1-INTRODUCTION

Lors de la certification aéronautique de matériels volants en vol givrant simulé, il est indispensable de respecter les normes de simulations édictées par l'organisme certificateur [1].

Ces normes permettent de calculer les différents paramètres nécessaires à l'exécution des essais de givrage [2], et en particulier le diamètre volumique médian du nuage givrant.

Dans un caisson de givrage, l'injection se fait en prémélange et en amont de la maquette dans un souci d'homogénéité. Cependant, la distance séparant la naissance du nuage et l'impact sur la maquette étant de l'ordre de 4 à 5 m, il peut se produire une modification du D.V.M. du nuage par effet d'évaporation.

Il est alors utile de disposer d'un outil prédictif qui puisse quantifier une telle évolution. Pour ce faire, il devient nécessaire de modéliser le plus complètement possible les échanges thermiques entre la phase liquide et la phase gazeuse, en prenant en compte l'hygrométrie.

Le code numérique M.A.G.I.C. (Modélisation et Analyse du Givrage en Caisson) a été conçu dans ce but au C.E.Pr..

Etant données les incertitudes qui pèsent sur les différents coefficients d'échange liquide/vapeur, il s'est avéré nécessaire de confronter les résultats numériques à des résultats expérimentaux.

A notre connaissance, il n'existe pas dans la littérature de résultats de mesure expérimentaux d'évolution de diamètre de gouttelettes d'eau, faisant intervenir l'hygrométrie.

Cette constatation nous a amené à concevoir un montage expérimental et à réaliser une série de mesures portant sur le spectre de diamètre d'un nuage et sur le diamètre volumique médian.

Les résultats de ces mesures ont pu être directement comparés à ceux des calculs numériques du code M.A.G.I.C., et la comparaison s'est avérée très satisfaisante.

Après avoir présenté les principales caractéristiques du code M.A.G.I.C., nous confrontons les résultats de calcul sur la mise en vitesse de gouttelettes à quelques résultats issus de la bibliographie.

Dans le paragraphe suivant, nous introduisons l'environnement expérimental qui a permis les mesures, et nous comparons ces résultats à ceux de M.A.G.I.C..

2-PRESENTATION DU CODE M.A.G.I.C. (Modélisation et Analyse du Givrage en Caisson)

Le code M.A.G.I.C. a été conçu pour prédire l'évolution des différentes classes de diamètre qui composent un nuage de gouttelettes.

Les champs aérodynamique, thermique et hygrométrique étant donnés, on utilise une approche Lagrangienne pour déterminer la position de chaque classe de gouttelettes. Celles-ci peuvent être sous 3 états possibles:

- . liquide (eau)
- . Solide (glace)
- . liquide+Solide (mélange eau/glace).

Seule la phase liquide fait l'objet d'une étude comparative dans cette publication.

A chaque pas de temps, on calcule par interpolation linéaire les caractéristiques aérodynamiques, thermiques et hygrométriques au voisinage des gouttelettes.

On suppose que la phase liquide, de par son évaporation ne modifie pas ces caractéristiques de l'air.

On résout alors explicitement les trois bilans suivant:

Bilan de masse:

$$\frac{D(M)}{Dt} = Kx \cdot (P_i D^2) \cdot M_v \quad (1)$$

avec

- .Kx: coefficient d'échange de matière eau/air
- .Mv : Masse molaire de vapeur
- .Pi D² : surface d'échange eau/air
- .xvs : fraction de vapeur saturante
- .xv : fraction molaire de vapeur dans le flux

La fraction molaire de vapeur est donnée par l'expression suivante:

$$xv = Hr Pvs / P$$

- .Hr : hygrométrie au voisinage de la goutte
- .Pvs : pression de vapeur saturante au voisinage de la goutte
- .P : pression statique au voisinage de la goutte

Le coefficient d'échange Kx se calcule de la manière suivante:

$$Kx = \frac{\mu}{d Sc M_v} f$$

avec

$$f = 2 + 0.216 \left(\frac{Sc}{1/3} \right)^{1/3} \left(\frac{Re}{1/2} \right)^{1/2} \quad \text{pour } (Sc^{1/3} Re^{1/2}) < 1.4259$$

$$f = 1.56 + 0.616 \left(\frac{Sc}{1/3} \right)^{1/3} \left(\frac{Re}{1/2} \right)^{1/2} \quad \text{pour } (Sc^{1/3} Re^{1/2}) > 1.4259$$

Sc : nombre de Schmidt défini par:

$$Sc = \frac{\mu}{\rho_g D_{if}}$$

Dif : diffusivité massique de la vapeur dans l'air entre -40 C et 40 C en m² s⁻¹

Bilan de quantité de mouvement:

Le bilan de quantité de mouvement s'écrit:

$$\frac{D(MV)}{Dt} = F$$

Au cours de leur parcours, les gouttes subissent l'influence de différents efforts qui s'exercent sur elle.

Ces efforts sont dus:

- . à la trainée
- . à la pression engendrée par le champ d'accélération de l'aérodynamique
- . à la poussée d'Archimède
- . à la force de Basset qui tient compte de l'histoire du mouvement de la goutte.

En général, seules les forces de trainée sont prises en compte: l'ensemble des autres efforts étant négligeable dans le cas où la masse volumique de la particule est plus de 100 fois supérieure à celle de l'air.

Le bilan de quantité de mouvement se met sous la forme:

$$\frac{D(MV)}{Dt} = \left(\frac{1}{2} \rho_a C_x \frac{V^3}{d} \right) (V_g - V) \quad (2)$$

Le coefficient de trainée est calculé par:

$$C_x = (24/Re) (1 + 0.15 Re^{0.687})$$

Re : Reynolds associé à la goutte

$$Re = \frac{\rho_g (V_g - V) d}{\mu}$$

bilan d'énergie

$$\frac{D(Ts)}{Dt} = \frac{H}{M} \frac{D(M)}{Dt} + \frac{Cpl}{M} \frac{D(M)}{Dt} \quad (3)$$

- . m : masse de la goutte
- . D : Diamètre de la goutte
- . Ts : Température de surface de la goutte
- . H : Enthalpie massique
- . Cpl: Capacité calorifique de la goutte liquide
- . Tg : Température du gaz porteur
- . Hv-Hl: chaleur latente de vaporisation

3- LE CALCUL DES LOIS DE TRAÎNÉE DANS LE CODE M.A.GI.C.

3-1 expression du coefficient de traînée

Une expression générale du coefficient de traînée peut se mettre sous la forme [2]:

$$Cx = f(Re, We, Sc, Pr, B)$$

Re : nombre de Reynolds qui caractérise le régime de la goutte.

We : nombre de Weber qui identifie l'influence de la déformation de la goutte.

Sc et **Pr** : respectivement nombre de Schmidt et nombre de Prandtl qui caractérise les échanges massiques par convection ou diffusion, ainsi que les échanges thermiques au voisinage de la gouttelette, dans le film de vapeur qui l'entoure.

B : nombre de Spalding qui caractérise l'intensité du flux massique.

Compte tenu de la difficulté de trouver de telles corrélations, on suppose que $Cx = f(Re)$, et malgré cette simplification, de nombreuses lois existent [3], [4], [5], [6].

Nous en donnons quelque exemples:

$$Cx = 24/Re \quad \text{loi de Stokes}$$

$$Cx = (24/Re) (1 + Re^{2/3}/6) \quad [5]$$

$$Cx = (28/Re^{0.85}) + 0.48 \quad [8]$$

$$Cx = 24/Re \quad \text{pour } Re < 0.48 \quad [6]$$

$$Cx = 27/Re^{0.84} \quad Re \quad [0.48; 78] \quad [6]$$

$$Cx = 0.271 Re^{0.217} \quad \text{pour } Re > 78 \quad [6]$$

$$Cx = 0.32 + 24/Re + 4.4/Re \quad [3]$$

M.A.GI.C.

$$Cx = (24/Re) (1 + 0.15 Re^{0.687})$$

Les différentes formulations sont représentées sous formes de courbes sur la figure 3-2-1.

On constate la bonne concordance existant entre les courbes, exception faite de celle correspondant à la loi de Stokes, qui se détache nettement des autres et qui sous estime la force de traînée.

3-2 confrontation avec des résultats de la bibliographie

Nous avons sélectionné deux publications [7], [9] qui nous permettent de situer les résultats obtenus par M.A.GI.C. par rapport à des résultats de calculs et à des résultats de mesure.

Nous présentons dans les figures 3-2-2 et 3-2-3 une comparaison entre la mise en vitesse des gouttes calculée par M.A.GI.C., avec celles données par les références [7].

Les conditions initiales sont présentées dans le tableau suivant:

vitesse de l'air (m/s)	100
vitesse initiale des gouttes (m/s)	0

On observe que l'allure des courbes est conservée, mais M.A.GI.C. a tendance à sous estimer nettement la mise en vitesse des gouttes par rapport aux résultats de [7].

Il reste délicat d'avancer une cause, la loi de mise en vitesse des gouttes dans [7] n'étant pas précisée.

La discussion précédente s'est portée sur des résultats de calculs: la référence [9] va nous permettre une comparaison avec des mesures expérimentales par anémométrie laser.

Les conditions initiales sont les suivantes:

vitesse de l'air (m/s)	48
vitesse initiale des gouttes (m/s)	0
température de l'air (K)	amb
taille des gouttes (μm)	38.8
	48.8
	58.8

Nous présentons les comparaisons entre l'expérience et le calcul par M.A.GI.C. sur les figures 3-2-4 pour chaque diamètre de goutte énoncé dans le tableau ci-dessus.

La comparaison s'avère satisfaisante, l'allure des courbes obtenues par le calcul suit assez bien les résultats expérimentaux.

Cependant, on notera que dans ce cas M.A.GI.C. a une tendance à surestimer la mise en vitesse des gouttelettes par rapport à l'expérience.

3-3 synthèse

La loi de calcul de la

trainée aérodynamique des gouttes utilisée dans M.A.G.I.C. nous permet de soutenir une comparaison avec des résultats issus de mesures [9].

Mais cette confrontation semble montrer que l'on peut s'attendre à une surestimation de la mise en vitesse des gouttelettes de la part de M.A.G.I.C..

4- CONFRONTATION PREDICTIONS/MESURES SUR L'EVOLUTION D'UN NUAGE DE GOUTTELETTES.

4-1 conditions expérimentales de mesure de granulométrie

Pour disposer d'un outil numérique capable de prédire l'évolution des différentes classes de diamètres de gouttes composant un nuage, il est nécessaire de formuler une modélisation des échanges thermiques entre les phases liquides et gazeuses qui soit satisfaisante.

L'évolution du diamètre d'une gouttelette composant le nuage est fonction de nombreux facteurs. Nous pouvons citer par exemple, la température de la gouttelette, celle du fluide porteur ou encore la quantité de vapeur d'eau dans l'écoulement, quantité qui est mesurée par l'hygrométrie.

L'expérience qualitative acquise au C.E.Pr. dans les bancs de simulation de vols givrants a tendance à montrer que sur les distances d'utilisation du nuage givrants, (4 à 5 m), l'hygrométrie a une influence prépondérante sur l'évaporation des gouttes.

Notre recherche dans la littérature pour collecter des résultats de mesures portant sur l'évolution de diamètres de gouttes en fonction de l'hygrométrie s'est avérée vaine.

Une campagne de mesures a donc été réalisée à l'I.A.T. de St CYR, sous contrat C.E.Pr. [10], dont l'un des buts était de mettre en évidence l'aspect échange thermique gouttelettes/air par l'intermédiaire de mesures granulométriques.

Afin de mettre en évidence cet aspect transfert thermique sans que d'autres paramètres viennent perturber les mesures, celle-ci ont été réalisées dans les conditions suivantes:

* Le champ de vitesse de la phase gazeuse a été choisi uniforme et très peu turbulent.

* Une première mesure de granulométrie est réalisée à une distance de l'injecteur pneumatique ou les gouttes formant

le spray ont terminé leur régime de mise en vitesse.

* Une deuxième mesure de granulométrie est réalisée à une distance suffisante pour qu'il y ait évolution notable du diamètre des gouttes, mais que l'effet de la pesanteur puisse être considéré comme négligeable.

4-1-1 conditions aérodynamiques

les conditions aérodynamiques sont résumées dans le tableau ci-dessous.

vitesse de l'écoulement	13.5
m/s	
hygrométrie	33
%	8
	38.2
taux de turbulence	1
%	
distance de l'injecteur	
m	
mesure 1	0.25
mesure 2	1.95

Les mesures ont eu lieu dans la soufflerie S2 de l'I.A.T. de St CYR qui n'est pas équipée d'un système de contrôle de l'hygrométrie.

Il s'ensuit que l'hygrométrie mesurée est celle qui a été imposées par les conditions météorologiques pendant toute la durée de la campagne de mesures.

4-1-3 conditions d'injection et granulométrie à l'abscisse x=0.25 m

Le spray sur lequel a été réalisée les mesures de granulométrie a été obtenu à l'aide d'un injecteur pneumatique du C.E.Pr. [10] et figure 4-1-3-1.

Les mesures de granulométrie proprement dites - répartition massique des gouttelettes en classes de diamètres et Diamètre Volumique Médian - sont issues de mesures par "MALVERN".

Les différents D.V.M. mesurés dans le nuage sont réalisés par variation de la perte de charge du circuit d'air d'alimentation de l'injecteur pneumatique.

Le tableau suivant résume les différentes valeurs de la perte de charge - ΔP - et les D.V.M. correspondant.

Durant toute la campagne de

mesure, le débit d'eau de l'injecteur est constant à une valeur de 4 l/h, valeur qui correspond à un point de fonctionnement courant en essai de givrage.

perte de charge (Bar)	D.V.M. (μ m)
0.67	17.72
0.46	23.68
0.29	31.32
0.20	38.63

Ces quatre valeurs de D.V.M. couvrent la gamme de diamètres qui est demandée en essai de givrage [1].

4-2 Conditions du calcul pour M.A.G.I.C.

Les conditions aérodynamiques prises pour M.A.G.I.C sont celles reproduites au cours de la campagne de mesure dans la soufflerie de l'I.A.T. [10].

On suppose qu'à l'abscisse de la première mesure de granulométrie ($x=0.25$ m), les gouttelettes ont fini leur phase de mise en vitesse: en conséquence, la vitesse initiale des gouttelettes dans M.A.G.I.C. est celle de l'aérodynamique.

Les conditions aérodynamiques sont prises constantes au cours du temps à une valeur de 37%.

La répartition massique en classe de diamètres correspond à celle mesurée dans la soufflerie à l'abscisse $x=0.25$ m, et est donnée dans les tableaux de la figure 4-2-1.

4-3 comparaison résultats numériques/mesures expérimentales

La confrontation des mesures et du calcul se fait pour une abscisse de $x=1.95$ m.

Nous présentons une synthèse portant d'une part sur une comparaison classes par classes et d'autre part sur le comportement global du spray, identifié par son D.V.M..

4-3-1 comparaison classes par classes

Nous présentons sur les figures 4-3-1-1 à 4-3-1-4 une comparaison graphique entre les résultats expérimentaux et le calcul.

On constate une grande cohérence entre calcul et expérience. Cependant, M.A.G.I.C. sous estime l'évolution des

classes de diamètre supérieur à 50 μ m.

4-3-2 comparaison entre D.V.M.

Les résultats sont portés sur la figure 4-3-2-1.

On note une bonne coïncidence pour des D.V.M. supérieur à 20 μ m.

En revanche M.A.G.I.C. semble sous estimer l'évolution des très faibles D.V.M..

4-4 étude numérique de l'influence de l'hygrométrie

Du point de vue expérimental, la mesure de l'hygrométrie reste toujours soumise à une grande incertitude.

C'est pourquoi il nous a paru intéressant d'évaluer, d'une façon purement numérique l'influence de ce paramètre sur l'évolution du D.V.M. d'un spray.

Les conditions du paragraphe 4-2 ont été reprises à l'exception de l'hygrométrie.

Les résultats sont présentés sur les courbes de la figure 4-4-1 pour les valeurs d'hygrométrie suivantes : 20%, 30%, 40%, 50%, 60%.

Cela souligne l'importance de l'hygrométrie dans la prédiction de l'évolution d'un nuage givrant.

Ce phénomène est particulièrement sensible dans le cas de faibles D.V.M..

5- CONCLUSION

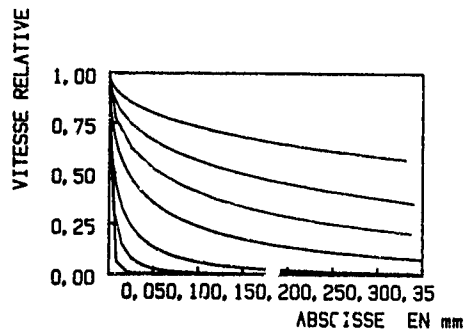
L'ensemble des lois d'échanges thermiques et dynamiques de M.A.G.I.C. permet d'obtenir sur des mélanges eau/air des résultats réalistes.

Lors de campagne de certification de matériel aéronautique en vol simulé givrant, le C.E.Pr. est tenu de respecter des conditions de D.V.M. de plus en plus précises.

Il est désormais possible, à l'aide de M.A.G.I.C. d'évaluer l'écart de D.V.M. entre l'injection et la maquette en essai, donc d'apporter d'éventuelles corrections sur les paramètres d'injection pour obtenir le D.V.M. nominal.

D'autre part, par cette approche lagrangienne, il est envisageable de déterminer le comportement dynamique des différentes classes de gouttes au voisinage d'un obstacle.

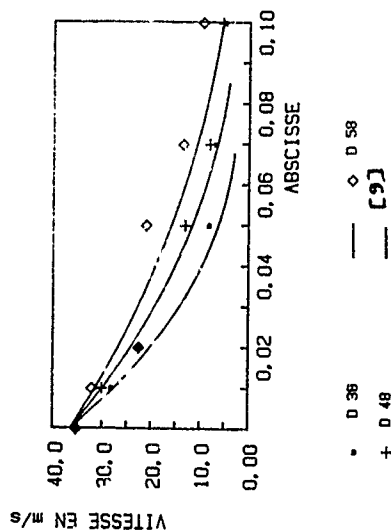
Cela permet d'évaluer le D.V.M. réel impactant sur la maquette.



loi de mise en vitesse d'après
M.A.G.I.C.

figure 3-2-3

figures 3-2-2 et 3-2-3: mise
en vitesse pour des gouttes de
diamètre 5, 10, 20, 50, 100,
500 μm.



loi de mise en vitesse
comparaison expérience [9] / calcul
figure 3-2-4

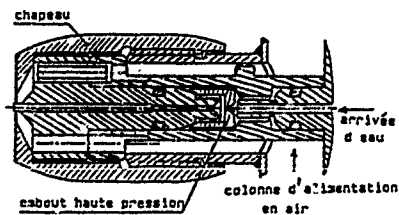


schéma d'un injecteur pneumatique
figure 4-1-3-1

Cas n° 41	Cas n° 42	Cas n° 43	Cas n° 44
19.8	7	4.7	3.5
2.5	5.3	2.4	1.5
4.3	5.2	3.4	1.3
13.5	9.8	4	2.5
14.4	9	7.8	5.8
15.3	15.3	8.9	5.4
18.6	22.3	14.7	9.2
7.4	14.2	17.1	15.9
2.4	11.2	19.2	16.8
0	0	15.8	19.4
0	0	1.5	14.5
0	0	0	3.7
0	0	0	0
0	0	0	0
0.7	0.7	0.7	0.1

Vitesse air: 13.5 m/s Hygro: 37% débit eau: 1/1/h

tableau 4-2-1

répartition des diamètres mesurée et calculée

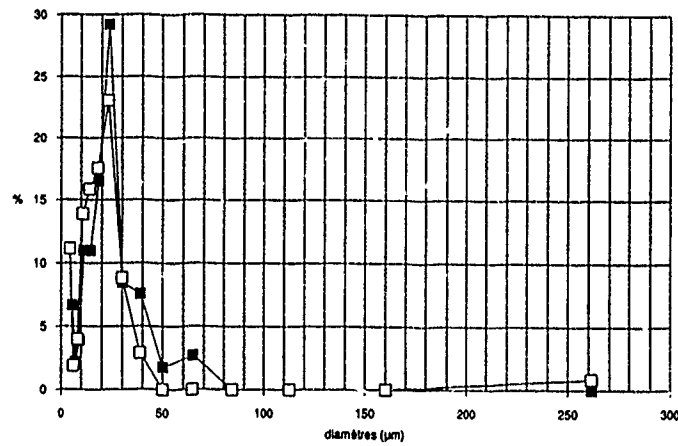


figure 4-3-1-1 cas 41

répartition des diamètres mesurée et calculée

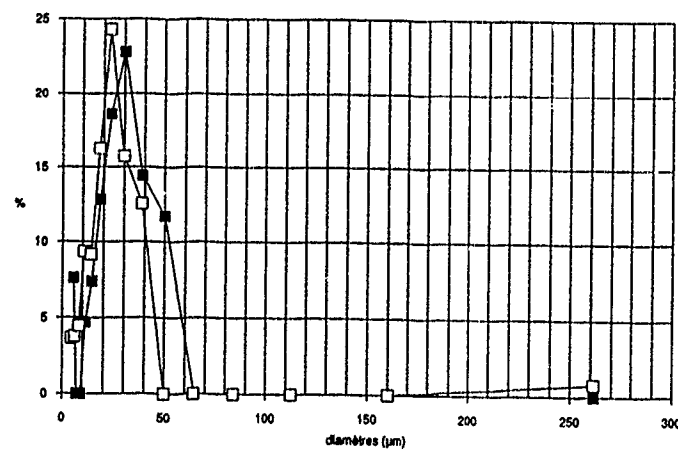


figure 4-3-1-2 cas 42

répartition des diamètres mesurée et calculée

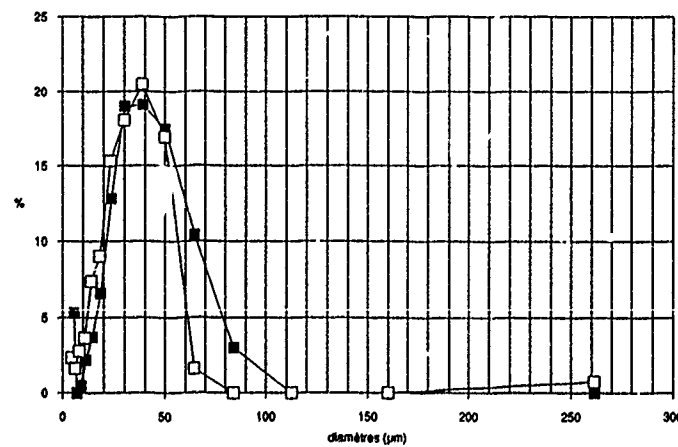


figure 4-3-1-3 cas 43

répartition des diamètres mesurés et calculés

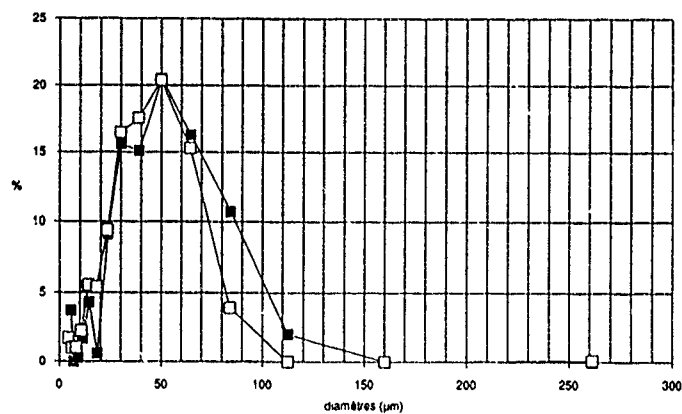


figure 4-3-1-4 cas 44

évolution du D.V.M.

D.V.M. (µm)	13.6	17.5	25.5	33.8
D.V.M. (µm)	17.7	22.7	31.3	38.6
D.V.M. (µm)	13.8	21.5	31.2	38.9
D.V.M. (µm)	2.9	2.2	0.1	-0.4
erreur relative (%)	16.38%	9.28%	0.32%	-1.04%

tableau 4-3-2-1

influence de l'hygrométrie sur le diamètre

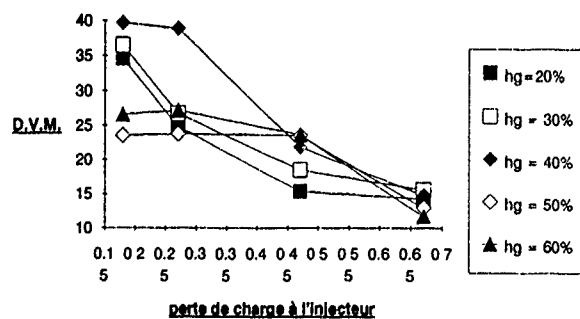


figure 4-4-1

Discussion

1. M. Mulero, INTA

Did you compare the results of your model with other models for similar application?

Author:

Typical for the MAGIC code is the use of hygrometric parameters. In the literature we did not find any code of this kind.

2. T. Sutton, BAe

Is there any typical explanation in your table 4.3.2.1 why the error is least at a medium diameter?

Author:

I cannot give you a very clear answer. There are two possibilities. First, small diameter droplets do not evaporate but behave like solids. MAGIC would assume that they do evaporate. Second, I do not know what the validity and precision of the measurements done by Moven with small MVDs was.

ICING TEST CAPABILITIES FOR AIRCRAFT PROPULSION SYSTEMS AT THE ARNOLD ENGINEERING DEVELOPMENT CENTER

C. Scott Bartlett, J. Richard Moore, and Norman S. Weinberg
Sverdrup Technology, Inc., AEDC Group
and
Ted D. Garretson, U. S. Air Force
Arnold Engineering Development Center
Arnold Air Force Base, TN 37389 (USA)

SUMMARY

Icing test capabilities for full-scale turbine engine propulsion systems have been developed in the Engine Test Facility (ETF) at the Arnold Engineering Development Center (AEDC). The current capability to simulate natural in-flight icing environments includes knowledge and control of the principal factors that govern the mechanics and thermodynamics of icing, namely, water droplet size distribution, liquid water content, cloud temperature, pressure, and propulsion system airflow rates. The AEDC facilities provide the capability to conduct evaluation tests in either the direct-connect or free-jet mode.

The methods and hardware used to inject liquid spray into a cold airstream to simulate in-flight icing conditions are discussed. The spray manifold systems and spray injection nozzles currently in use at AEDC are described. The methods used to operate and control the cloud generation systems are given. Pulsed-laser and pinhole viewing techniques used to view rotating engine hardware in freeze-frame, and low-light cameras coupled with fiber-optics used to penetrate to the inner recess of inlet system to observe real-time transient icing processes on surfaces susceptible to icing are described. Test experiences in both direct and free-jet connect icing testing are addressed.

Recent ice accretion scaling techniques and test results, and developments and observations in cloud liquid water content and droplet sizing are briefly discussed. Uses of real-time ice accretion detectors for facility calibration and test article ice accretion rate monitoring are addressed.

BACKGROUND

The formation of ice on aircraft propulsion system surfaces occurs during flight through

clouds of supercooled water droplets. Ice accretion on these surfaces always results in a degradation of performance and operational safety. Icing tests can be conducted in an altitude facility and cover a wide range of Mach numbers, pressure altitudes, and inlet conditions without regard to the prevailing outside weather conditions. Further, the variables which define an icing cloud can be accurately controlled and monitored during tests in altitude test facilities. The use of the altitude icing test facility has become an acceptable approach for evaluation and qualification of aerospace systems for flight into icing conditions. Icing test facilities have been developed at the AEDC/ETF which provide the capability to simulate icing environments for a wide range of aircraft propulsion systems and components.

INTRODUCTION

Aircraft engine icing test facilities have been developed at AEDC/ETF to simulate natural atmospheric icing conditions. The facilities have been used to conduct icing tests for military and commercial and domestic and international customers. The current capability to provide icing environments for engine testing includes the knowledge and control of the principal factors that govern the mechanics and thermodynamics of icing, namely, water droplet size distribution, liquid water content, cloud temperature, humidity, pressure, and airflow. The AEDC facilities provide the capability of simulating the free-stream icing conditions in either the free-jet or direct-connect testing modes as illustrated in Figs. 1 and 2, respectively. The direct-connect testing mode is typically used to conduct engine icing tests. The free-jet testing mode is used to conduct engine, inlet/engine combination, component, sensor, and external surface (wing, empennage, etc.) icing tests.

* The research reported herein was performed by the Arnold Engineering Development Center (AEDC), Air Force Systems Command. Work and analysis for this research were done by personnel of the Air Force and personnel of Sverdrup Technology, Inc., AEDC Group, operating contractor of the AEDC propulsion test facilities. Further reproduction is authorized to satisfy needs of the U. S. Government.

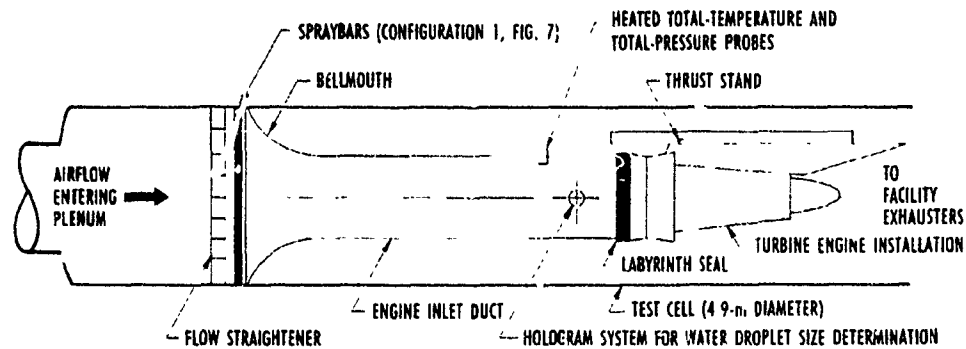


Fig. 1. A direct-connect propulsion engine altitude icing test cell configuration.

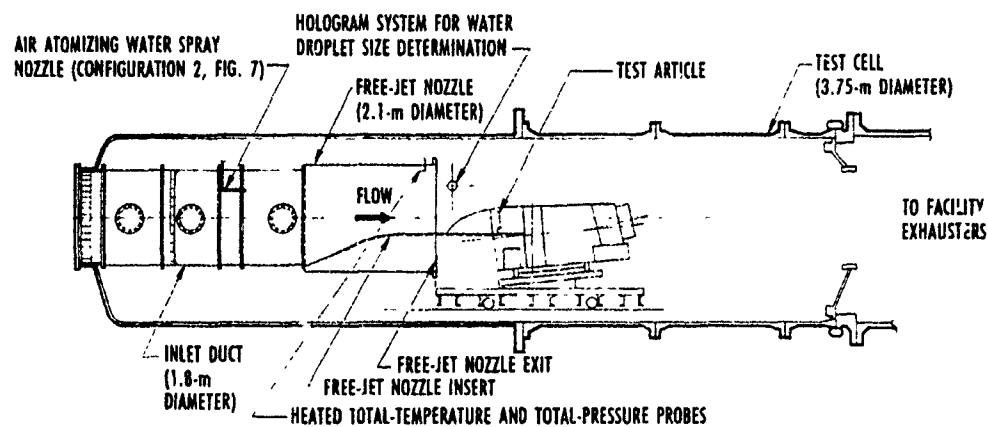
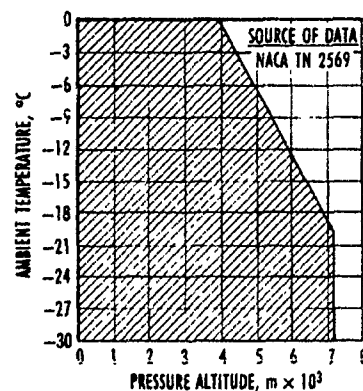


Fig. 2. A free-jet propulsion engine altitude icing test cell configuration.

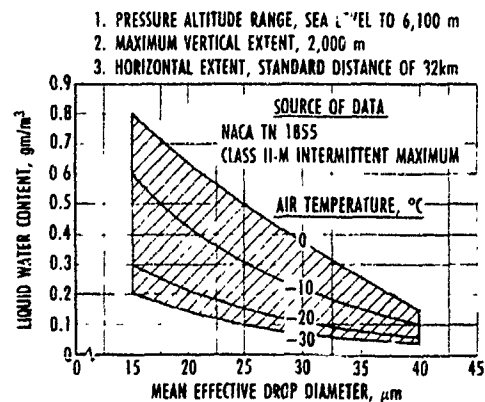
The natural icing conditions that are typically simulated during testing are well known and documented in the "Airworthiness Standards," Ref. 1. A summary of the icing conditions is presented graphically in Fig. 3. These airworthiness standards pertain specifically to icing on external aerodynamic surfaces and not to engine performance under icing conditions. Standard icing condi-

tions that have been used for the purpose of testing turbojet and turbofan engines for military applications are given in Table 1, Ref. 2.

The icing conditions that exist at the engine face during actual flight are seldom identical to those that exist in the freestream. The air entering

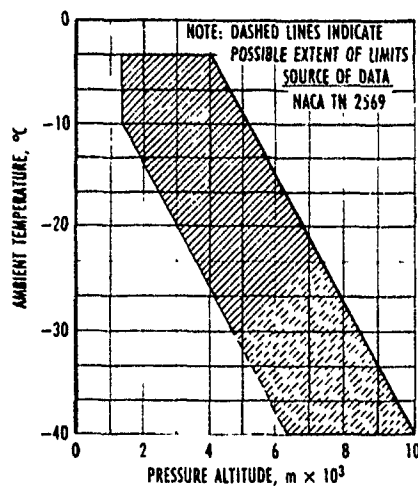


a. Ambient temperature versus ambient pressure, stratiform clouds

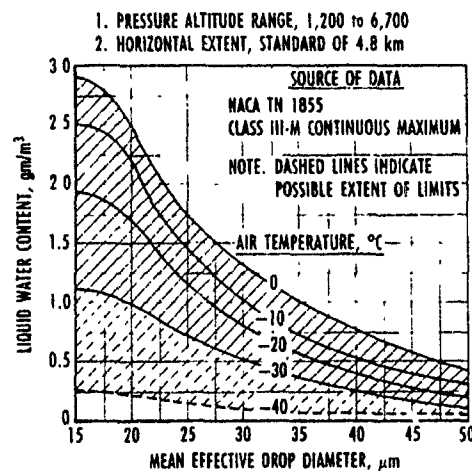


b. Liquid water content versus mean effective drop diameter, stratiform clouds

Fig. 3. Cloud icing conditions (from Ref. 1).



c. Ambient temperature versus ambient pressure, cumuliiform clouds



d. Liquid water content versus mean effective drop diameter, cumuliiform clouds

Fig. 3. Concluded.

Table 1. Icing Conditions Specified in the Military Specifications for Turbojet and Turbofan Testing (MIL-E-5007D)

I. Sea-Level Anti-Icing Conditions

Attribute	Condition I	Condition II
Liquid Water Content	1 gm/m^3	2 gm/m^3
Atmospheric Air Temperature	-20°C (-4°F)	-5°C (+23°F)
Flight Velocity	Static	Static
Altitude	Sea Level	Sea Level
Mean Effective Drop Diameter	15 μm	25 μm

II. Altitude Anti-Icing Conditions

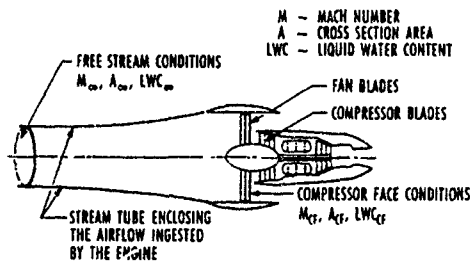
Attribute	Condition I	Condition II
Liquid Water Content	0.5 gm/m^3	0.5 gm/m^3
Atmospheric Air Temperature	-20°C (-4°F)	-20°C (-4°F)
Flight Velocity (Mach No.)	0.32	0.71
Altitude	6,100 m (20,000 ft)	6,100 m (20,000 ft)
Mean Effective Drop Diameter	15 μm	15 μm

the inlet/engine has generally either been accelerated or decelerated from freestream according to the flight and inlet Mach number match or capture, as illustrated in Fig. 4, Ref. 3. The level of airflow acceleration or deceleration is a function of the inlet capture ratio as determined from both the flight Mach number and the inlet Mach number. Therefore, the inlet/engine icing conditions can be quite different from the free-stream conditions. For free-jet icing testing, the free-stream stagnation conditions can be set in the plenum chamber and the cloud will adjust itself to enter the propulsion system in a manner closely duplicating natural flight. In the direct-connect mode of testing, the proper stagnation conditions must be set to account for any losses in the installed configuration, and the liquid water content must be adjusted according to the inlet capture condition to be simulated. The change in

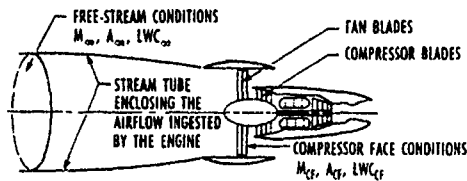
liquid water content required to simulate different inlet capture ratios can be estimated (Ref. 4). A typical plot of the required direct-connect engine face liquid water content ratio to the free stream liquid water content is shown in Fig. 5 (Ref. 5).

FACILITY PERFORMANCE CAPABILITIES

The facility performance capabilities currently available for icing environment simulation are summarized in Fig. 6. The meteorological icing conditions, Fig. 3, are completely within the direct-connect testing capabilities of the AEDC/ETF for engines requiring up to approximately 340 kg/sec maximum sea-level airflow. Engines requiring sea-level airflows greater than 340 kg/sec can be tested at increasingly higher altitudes. Many icing problems occur at reduced power settings, hence meaningful icing tests can be conducted on



a. Inlet Mach number less than flight Mach number, $LWC_\infty < LWC_{CF}$



b. Inlet Mach number greater than flight Mach number, $LWC_{CF} < LWC_\infty$

Fig. 4. Schematic showing possible stream tube configuration for turbofan icing conditions (from Ref. 3).

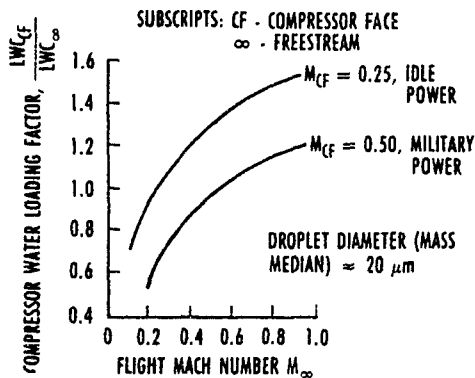
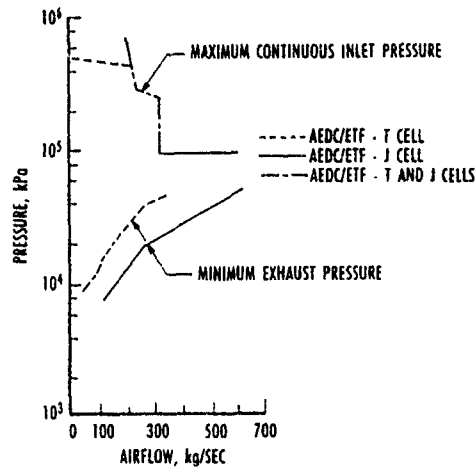
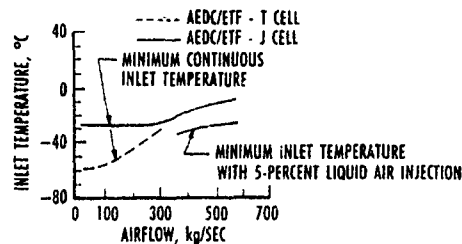


Fig. 5. Compressor liquid water content loading factor for two compressor face Mach numbers.

engines with maximum airflow requirements greater than the facility capability. As indicated in Fig. 6, the low-temperature portion of the meteorological conditions can be achieved with the addition of liquid air to the inlet air; however, this technique has not been required at AEDC for icing tests. The facility performance capabilities for free-jet testing are identical to those shown in Fig. 6. However, the size of the engines that can be tested in a free-jet mode is significantly reduced since substantial airflow must spill around the engine to ensure adequate flight flow-field simulation. The future addition of an icing capability to the new ETF C-side test cells, with larger conditioned airflow capacity, will expand the AEDC icing test capability.



a. Air supply and exhaust capability



b. Estimated inlet air temperature capability

Fig. 6. Facility performance capability.

Spray nozzle manifolds are used to provide the water droplets for the icing cloud. Typical spray manifolds used at AEDC/ETF are shown in Fig. 7. The water spray nozzles are commercially available, two-fluid atomizers. AEDC currently has an inventory of ten different air atomizing spray nozzles, each offering a unique range of droplet size and water flow rate. The number and position of the spray nozzles can be varied within the manifold to provide a uniform icing spray distribution at the test section. As illustrated in Figs. 1 and 2, the icing spray manifold is typically located in the test cell plenum chamber upstream of the test section. This arrangement allows the spray manifold the flexibility to be adapted to different propulsion system installations without major modifications. Both the air and demineralized water, delivered through an all stainless steel plumbing, pump, and storage system, and furnished to the spray manifold, are filtered and heated to temperatures near 100°C to prevent freezing in the spray nozzles during testing (Ref. 6).

The liquid water content of the cloud represents the amount of liquid water in the atmosphere and is typically expressed in terms of grams of liquid water per cubic meter of air. The liquid water content of clouds varies greatly with cloud type and atmospheric conditions. The

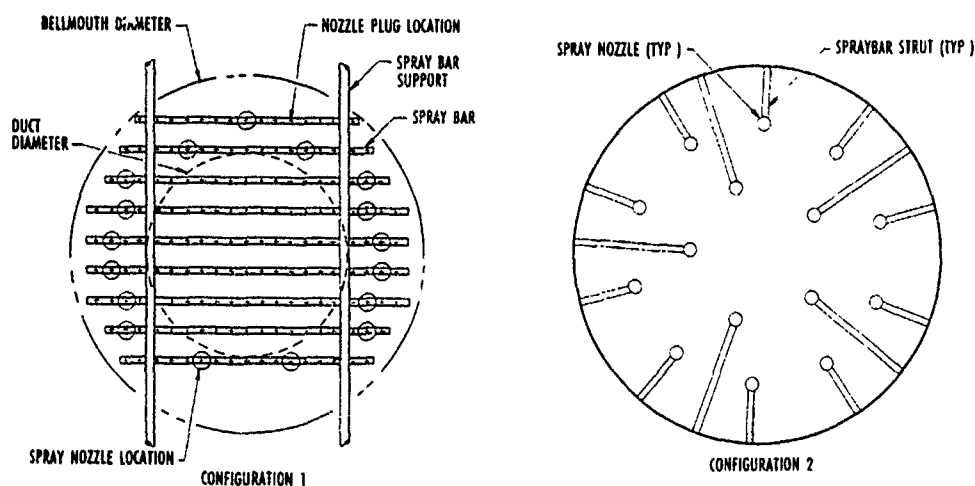


Fig. 7. Water spray manifold systems.

droplet size spectrum is generally characterized by the droplet mass median diameter. The mass median diameter represents the droplet size for which half of the total water mass is contained above and below that diameter. The liquid water content and droplet size are controlled by varying the water flow rate and atomizing air pressure to the spray manifold. The size and number of the spray nozzles selected can be tailored to a particular engine installation. Liquid water contents up to above 3.9 grams per cubic meter have been obtained at AEDC with spray nozzles calibrated for mass median droplet diameter from 15 to 35 microns, demonstrating the ability to cover a broad range of expected natural icing conditions.

An extensive computational fluid dynamics (CFD) capability exists at AEDC/ETF (Ref. 7). A full three-dimensional Navier-Stokes flow-field solver is used to evaluate the aerodynamic fidelity of icing test installations, and its use is especially important to ensure the natural flight flow field is adequately simulated during free-jet icing tests. A full three-dimensional, two-phase flow code is available to help predict droplet trajectories during icing testing. This code is used in spray nozzle positioning to ensure the most uniform spray cloud possible is available during testing.

Icing Test Techniques at AEDC/ETF

The technique used at AEDC/ETF to produce an icing cloud is to inject a continuous stream of water droplets into a cold airstream directed at the engine. Injection of the water spray is accomplished in the low-velocity region of the test cell upstream of the test-cell bellmouth. The injected water droplets are accelerated to near the air speed by aerodynamic forces, and through heat and mass transfer, the droplets reach the air temperature in a supercooled liquid state (Ref. 3).

The amount of spray water injected into the flow field to obtain the specified liquid water content is analytically determined. The liquid water content is specified as a test condition and the amount of water evaporated as the cloud travels from injection to the test section of the test cell is determined analytically from a mathematical model (Ref. 3). By measuring the airflow and injected water flow rate precisely, the desired liquid water content at the test section is accurately set and maintained.

The uniformity of the icing cloud is gauged for each unique installation by evaluating the uniformity of ice accreted on a calibration grid positioned in the test section prior to test article installation. This time-honored technique has been automated at AEDC by application of piezoelectric transducers operating in the ultrasonic frequency range (Ref. 8). An array of the "ultrasonic" transducers is integrated into a calibration grid, and the thickness of ice accreted on the transducer is calculated from the signal received by a dedicated signal processing system remotely located from the test cell. This automation of the calibration grid technique for cloud uniformity assessment greatly reduces time expended for icing test preparation.

The spray nozzles used in the spray manifold system are calibrated to determine the water droplet size production and the control parameters necessary to obtain the specified droplet size. The calibration data are obtained in the AEDC/ETF icing research test cell, R1D. Researchers collect droplet size and size spectrum data with a laser-based imaging technique. Calibration data currently exist for ten different air atomizing spray nozzles capable of meeting a wide range of specified conditions.

The operation of the water spray system is essentially the same for all icing tests. The test apparatus used to make the clouds for either direct-connect or free-jet testing has been standardized. A standard icing cloud simulation computer program exists to provide the necessary control measurements and system stability to meet icing cloud test requirements. The control program is designed to: establish defined clouds in the test cell free-stream airflow; rapidly control the cloud liquid water content, altitude (pressure), Mach number, and duration; execute controlled changes for multi-level cloud requirements; and terminate clouds as rapidly as possible.

The cloud simulation program provides automated sequence of required events that include pre-cloud system preparation, cloud initiation, cloud duration control, cloud termination, and post-cloud system shutdown/ preparation for the follow-on cloud. For the pre-cloud system preparation, during the time the prescribed test cell free-stream air test conditions are being established, water is recirculated to a water reservoir. The required conditions (water and high-pressure atomizing air flow rates, temperatures, and manifold pressures) to admit flow into the spray bars are set. Once the free-stream air and spray system conditions are set, water recirculation is terminated, the water spray bar supply valves are opened, and water flows into the spray bars. The water system drain valves (located at the end of the water spray bars opposite the water supply valves) remain open for the first 10 sec of water flow to provide a more rapid purge of air from the spray bars. During this purge, there is essentially no flow of water out of the spray nozzles. When the water drain valves are closed, water is injected into the airstream

rapidly and uniformly. A sequence of controlled events occurs to properly establish the desired icing cloud target set points in a reasonably short time. During the duration of the icing cloud, the cloud simulation program maintains the desired liquid water content and mass median droplet diameter by automatic control of the water and atomizing airflow rates through flow control valves. After the specified cloud duration, the cloud is terminated rapidly by closing the water spray bar supply valves, opening the water system drain valves, and allowing water to recirculate to the water tank. The icing simulation program, for control flexibility, can extend or abort an icing cloud on command.

Many state-of-the-art video techniques have been successfully used to view ice accumulations during icing tests of aeropropulsion systems at the AEDC/ETF. In most cases, low-light-level black-and-white charge-coupled device (CCD) cameras adapted to a pinhole lens arrangement have been used to view ice accumulations on engine front frame struts, inlet guide vanes, spinners, and first-stage fan blades.

Viewing of stationary structures such as engine inlet front frames and structures buried out of normal view within the inlet has been accomplished by installing a pinhole lens in the inlet ducting. The typical lens used will provide a 50-deg field of view. Two such lens installed 180-deg opposed will provide near full coverage of the inlet face. The pinhole lens is installed as shown in Fig. 8. A hole of approximately 4 cm in diameter in the inlet duct is required for the installation. This small hole minimizes the effect of the viewing system on the inlet flow field. The actual assembly is flush with the duct wall. The lens

assembly is designed to accept a dry gaseous nitrogen purge to keep it clean and free of moisture.

The engine inlet is lighted by fiber-optic cables coupled to variable intensity light sources installed external to the test cell. Fiber-optic cables are installed, as shown in Fig. 8, using a fiber-optic light guide threaded into the inlet duct. A hole of approximately 2 cm in diameter in the duct is required. Four light sources normally provide sufficient coverage

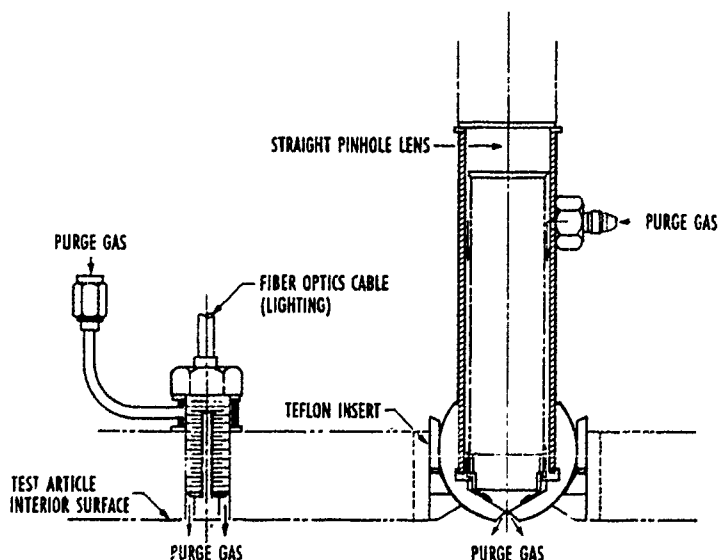


Fig. 8. Typical pinhole lens and fiber optics lighting system.

for inlet ducts in the 1-m-diam class. The variable intensity light source is useful in adjusting the light level for maximum performance from the low-light-level cameras. A dry gaseous nitrogen purge keeps the optics clean and moisture free.

Successful viewing of ice accumulation on rotating fan blades has been accomplished by using a laser system as a light source (Fig. 9). Laser light is routed to the engine inlet through a single coherent fiber-optic cable which can be attached to the inlet duct in the same manner as described above. Coherent fibers are used to minimize the light loss within the cable itself. The fiber-optic cable ends in a lens assembly designed to spread the beam to the proper dimensions at the inlet face. The laser light system provides a frequency-controlled light source which can be synchronized with the rotational speed of the fan to provide stop-action viewing of ice accumulation and evidence of shedding on individual fan blades. With proper camera alignment, focusing, and careful mismatch of light source and fan speed synchronization, views through the rotating fan blades to the accumulations on the stator assemblies just downstream of the fan have been obtained.

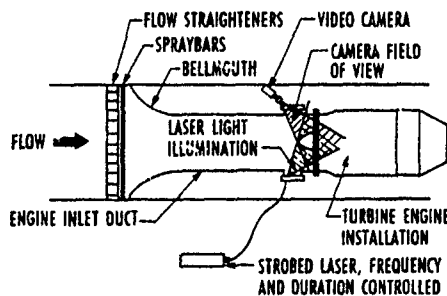


Fig. 9. Typical strobed laser viewing system schematic.

The piezo-electric ultrasonic ice thickness transducers mentioned earlier can be flush mounted to provide an ice accretion thickness measuring system for many test articles. The measuring system provides the capability to measure ice thickness and growth rate in near real time. A hot wax technique is routinely used to produce wax molds to document complete ice accretion shape and surface characteristics. This documentation is beneficial for post-test analysis of the ice accretions.

A continuing icing test technology development program is

conducted at AEDC to provide the technology advancements necessary to improve the ability to perform aerospace propulsion system icing tests. As a part of the icing test technology development program, an icing research test cell was constructed in 1975. The cell, Test Cell R-1D, was modified in 1986 to provide a larger free-jet nozzle area. The cell can be used in either a 30.5-cm or 46-cm-diam free-jet mode. The test cell, also capable of direct-connect icing testing, matches many of the features of the larger AEDC icing test cells and provides a capability to simulate icing environments similar to the larger test cells.

The ultrasonic ice thickness measurement technique is one of the recent developments resulting from the continuing icing test technique technology development program at AEDC. Other current areas under technology development include ice scaling methods, real-time nonintrusive cloud liquid water content uniformity measurement, and icing cloud simulation requirements.

The work in icing scaling is being conducted, in concert with other U.S. Government agencies, to ease the restrictive nature of the scaling laws currently used at AEDC. Figure 10 illustrates successful scaling results obtained at AEDC (Ref. 9).

The cloud liquid water content uniformity measurement effort is aimed at developing electro-optical diagnostics to replace the piezo-electric transducer-equipped calibration grids. The current approach under consideration is to use a fluorescent dye in the water, excite the droplets with a light source, and correlate the liquid water content uniformity with the uniformity of the intensity of light scattered by the water droplets.

The work in icing cloud simulation is directed towards gaining an understanding of the influence

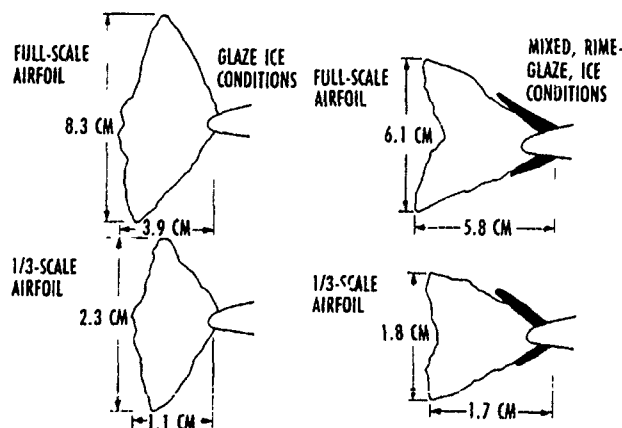


Fig. 10. Ice shape scaling results, test article size, full and 1/3-scale (from Ref. 9).

of icing parameter uncertainties in the validity of icing test results. The efforts to date are reported in Ref. 10. The work indicates which icing condition uncertainties are most influential in altering test results. A typical result of the work, shown in Fig. 11, illustrates the impact of droplet sizing uncertainty on ice accretion test results.

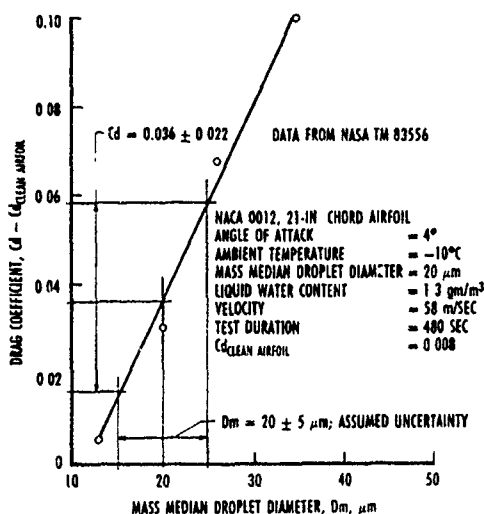


Fig. 11. Effect of uncertainty of mass median droplet diameter on the iced airfoil drag coefficient uncertainty.

SUMMARY

The icing test capabilities available at AEDC/ETF have been successfully used during the evaluation of many aircraft propulsion systems and components. Many tests have been conducted in both the free-jet and direct-connect test modes. The testing has been conducted for inlet systems, engines, and external flow surfaces such as full-scale cockpit, empennage, and wing sections. Icing evaluations have been conducted at AEDC during various stages of aircraft propulsion system developmental programs over a wide range of conditions as shown below:

- Free jet
 - Bell helicopter inlet/engine
 - ALCM
 - GLCM
 - Various full scale inlets
 - Inlet guide vane sectors
 - Icing sensors
 - Full scale components
 - Direct Connect
 - F110
 - F101
 - TF39
 - F109
- Range Tested at
AEDC
Mach: 0.1 → 0.8
Alt: SL → 9 km
Temp: -29 → 5°C
Size: 0.5 → 2.4 m
diam
DM: 15 → 35 μm
LWC: 0.2 → 3.9
gm/m³

The AEDC/ETF icing test facilities allow test, evaluation, and qualification of full flight systems as well as subsystems or components. The capability to expose subsystems or components to icing conditions is particularly important in the system design process, since it allows design concepts to be evaluated prior to committing resources to full system development. The AEDC icing research test cell (R-1D) described earlier is particularly well suited for subsystem or component design evaluation. Because of its small size, it can be operated more economically than the larger test cells. Once component or subsystem icing evaluations are complete, AEDC/ETF icing facilities are capable of conducting full-scale engine/inlet compatibility icing tests.

Altitude test facilities such as those at AEDC offer a safe and economical method for environmental icing testing. In these facilities, control over the pertinent flow variables such as temperature, pressure, liquid water content, droplet size, and Mach number can readily be achieved. The icing clouds produced in the icing test cells closely simulate those found in nature. Many successful icing evaluations have been conducted at AEDC, and an experience base exists to conduct accurate and closely controlled icing tests.

REFERENCES

1. "Airworthiness Standards: Transport Category Airplanes: Appendix C." Federal Aviation Regulations, Part 25, Federal Aviation Administration.
2. Military Specifications for Turbojet and Turbofan Testing. MIL-E-5007D, 1973.
3. Willbanks, C. E. and Schulz, R. J., "Analytical Study of Icing Simulation for Turbine Engines in Altitude Test Cells." AEDC-TR-73-144 (AD-770069), November 1973.
4. Pfeifer, G. D. and Maier, G. P., "Engineering Summary of Power Plant Icing Technical Data." FAA-RD-77-76, July 1977.
5. Bartlett, C. S., "Icing Scaling Considerations for Aircraft Engine Testing." AIAA-88-0202, January 1988.
6. Marek, C. J. and Bartlett, C. S., "Stability Relationship for Water Droplet Crystallization with the NASA Lewis Icing Spray Nozzle." AIAA-88-0289, January 1988.
7. Phares, W. J., Cooper, G. K., Swafford, T. W., and Jones, R. R., "Application of Computational Fluid Dynamics to Test Facility and

Experiment Design." AIAA-86-1733, June 1986.

8. Hansman, R. J. and Kirby, M. S., "Real Time Measurement of Ice Growth During Simulated and Natural Icing Conditions Using Ultrasonic Pulse-Echo Techniques." AIAA-86-0910
9. Ruff, G. A., "Analysis and Verification of the Icing Scaling Equations, Volume I." AEDC-TR-85-30 (AD-A162226), November 1985.
10. Bartlett, C. S. and Foster, R. G., "The Effect of Experimental Uncertainties on Icing Test Results." AIAA-90-0665.

Discussion

1. W. Grabe, NRC Ottawa

To what atomizer air pressure do you work?
How do you determine atomizer air temperatures and water temperatures required?

Author:

We do not currently have a water spray injection system necessary to conduct icing tests in the largest of the propulsion test cells at AEDC, the C1 and the C2 (Aeropropulsion System Test Facility, ASTF) test cells. Some planning has already been done in consideration of adding an icing test capability to these test cells. The facility is designed to test the air breathing systems capable of generating 90,000+ pounds of thrust. The ability to test specific engines at specific icing conditions would require an analysis and a feasibility assessment.

2. M. Holmes, RAE

Have you any experience of conducting icing tests in the ASTF at Tullahoma and if these facilities have the capability to test the new generation of civil fan engines, producing up to 90,000 lb thrust at take off, which demand a very high air flow at low altitude conditions?

Author:

The water spray nozzles at AEDC are operated at typical atomizing air pressures of 100 and up to 150 psia. Studies have been conducted to determine the lower level of temperature of the atomizing air necessary to prevent freezing of the droplet as they exit the spray nozzle. These studies are documented and referenced (ref 6, Marek and Bartlett) in the paper. Typically at AEDC, the water is heated to about 180-200 F. This is as warm as we can comfortably heat the water to prevent boiling in the spray system and yet keep the spray nozzles warm enough to prevent ice deposits from forming at the water discharge.

3. V. Garratt, RAE

Do you apply any corrections for the modification of a) the LWC, and b) the droplet spectrum by impingement of the droplets on the bell mouth entry? The larger droplets will tend to hit and coalesce. The incidents of these larger droplets would slightly affect the ice accretion.

Author:

During the test cell preparations for icing testing, efforts are taken to position the water spray nozzles so that impingement of water on the bell mouth is eliminated. There are two reasons for it. One is the unknown effect impingement would have on the liquid water content and droplet diameter spectrum. The other is that droplet impingement might form ice accretions on the bell mouth that are potentially damaging to the test article. Since the amount of impingement and its effect on liquid water content and droplet diameter spectrum are unknown and efforts are taken to eliminate droplet impingement, no corrections are applied during testing.

4. K. Piel, BMW - RR Aeroengines

Are there any results available of comparisons between testing at AEDC and actual aircraft icing conditions, e.g. on slave engines etc?

Author:

Comparisons between icing tests results obtained in ground test facilities and results obtained in other ground test facilities or results obtained in natural or artificial flight have been carried out. The comparisons range from close agreement to poor to unacceptable agreement. The agreement issue is a continuing problem within the icing community and is currently best explained as a result of uncertainty associated with the absolute values of the icing conditions. There are no published comparisons between AEDC and flight icing tests.

5. P. Derouet, SNECMA

At the station of the spray bars, the water is heated to 100 C. Taking into account the distance between spray bars and the test engine, do you think that the droplets have sufficient time to reach the temperature of the air flow? Have you done calculations?

Author:

The spray droplets do have sufficient time to reach thermal equilibrium with the air. Calculations are carried out for each icing test installation to ensure that there is sufficient droplet residence time. Details of the calculation procedure and mathematical model are described in a report by Schulz and Willbanks, ref. 3 of this paper.

ICING TEST PROGRAMMES AND TECHNIQUES

E Carr
Project Chief Engineer
Aero Gas Turbines and Fuel Injectors
Combustion Technology Centre
Aero and Industrial Technology Ltd
Burnley, Lancashire, England

D Woodhouse
Senior Project Engineer
Combustion Technology Centre
Aero and Industrial Technology Ltd
Burnley, Lancashire, England

ABSTRACT

An Altitude Test Facility with a main chamber 4m diameter x 12m long and capable of providing air flows up to 5kg/s and simulating altitudes up to 15km, is operated at Burnley in the UK by Aero and Industrial Technology Limited (AIT).

This paper details the capability of the facility, describes the type of work carried out and reviews the experience obtained on icing programmes since the plant was commissioned in 1953.

Examples of the procedures used to establish the susceptibility of equipment to icing are given and cover the use of scale models, the evaluation of probes and the testing of complete helicopter engine intakes.

INTRODUCTION

In the early 1950's Joseph Lucas (Gas Turbine Equipment) Limited built a high altitude test plant at Burnley in the UK on behalf of the then British Ministry of Supply. Over the years this plant has had a high level of utilisation and continuing programmes of refurbishment and updating and is now wholly owned by AIT Limited and operated on a normal commercial basis. At its inception the plant was primarily intended for the examination of aero gas turbine combustion stability and relight problems but in practice it has been used for a much wider range of programmes.

The main advantages of the plant are its low running costs, its flexibility and the rapidity with which test points can be achieved. As a result the plant is very cost effective for the evaluation of the light-up performance of large aero engine combustion systems, the full range performance assessment of smaller gas turbine engines and also the testing of ancillary equipment required to operate at altitude or cold day conditions. The facility is a CAA approved test house.

PLANT DESIGN AND OPERATION

The configuration and operation of the plant is described below, following the path taken by the air flow through the main plant equipment. Figure 1 shows the main plant items schematically and Figure 2 an isometric cut away drawing, also showing the main plant items. Figure 3 shows a view of the end of the main test chamber with the

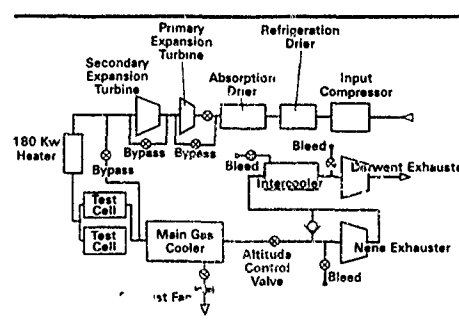


FIG 1 AIR FLOW PATH THROUGH FACILITY

access door removed and an engine being installed.

Air is drawn into the plant by a seven stage compressor fitted with interstage and after cooling. It then passes through refrigeration and absorption driers to reduce the dew point. At this stage the air is essentially dry at 480 kPa and +10 C and it then flows through two loaded expansion turbines to reduce the temperature to -80 C. The air then passes through a trim heater to one of the two test areas i.e. the engine test cell or the rig test cell.

On leaving the test area in use the air passes through a large gas cooler to the altitude control valves and it is the setting of the latter which chiefly controls the test pressure. The air is then drawn from the plant by two exhausters. As will be seen from Figure 1 various bypass lines, bleed lines and antisurge valves are fitted so that it is possible to use or bypass one or both of the expansion turbines and use one or both of the exhausters as required. The second exhaust blower has a substantially larger capacity than the first, hence if the test pressure is in the range 90kPa to 38kPa it is possible to induce additional air directly from atmosphere i.e. bypassing the input compressor and the expansion turbines.

PLANT CAPABILITY

Air Flow, Pressure and Temperature

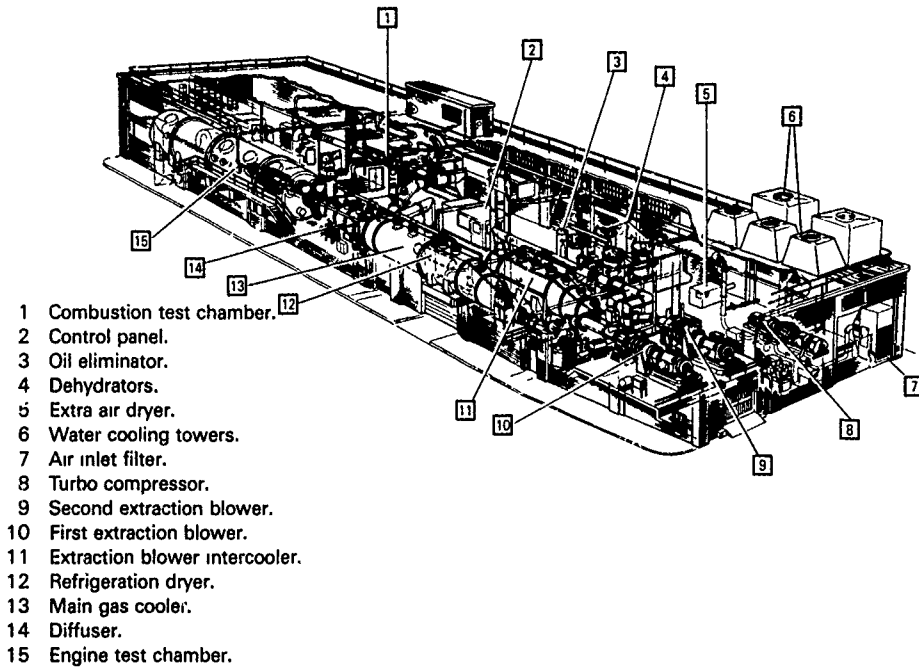


FIG2 "CUT AWAY" VIEW SHOWING MAIN PLANT COMPONENTS



FIG3 INSTALLATION OF ENGINE INTO TEST CELL

An air flow of up to 5,7 kg/s can be supplied at pressures down to 38 kPa (i.e. corresponding to an altitude of 7620m). Over the pressure range 38 kPa to 13 kPa (7620m to 15240m) the maximum air flow is 3,4 kg/s.

The basic plant will supply the air at temperatures in the range -65 C to +75 C over the air flow/pressure range quoted above. Higher air supply temperatures are provided if required by installing additional heaters.

Rapid changes of air pressure and temperature can be achieved

Typically
100 kPa to 46 kPa in 165 seconds
46 kPa to 100 kPa in 60 seconds

+40 C to -54 C in 13,3 minutes
-33 C to +38 C in 8,5 minutes

Rapid decompression tests can be simulated by specially constructed test rigs.

ENGINE TEST CELL DIMENSIONS

The engine test cell is 12,2 m long by 4m diameter giving a normal working space 7,9m long by 1,8m diameter. Entry is through a 2,6m diameter door with a 3000 kg capacity crane runway

RIG TEST CELL DIMENSIONS

An open test cell is available which will accommodate test rigs requiring low pressure air supplies (e.g. combustion system test rigs). This cell is 8,23m long x 3,66m wide x 6,1m high. An additional small sub-atmospheric test chamber is available which can be installed in the rig test cell and this chamber is 2,4m long by 1,5m diameter.

SERVICES

A comprehensive range of services is available and includes

Provision for the supply of a range of fuel types at temperatures controlled between -50 C and +100 C.

Electrical supplies at all of the normal industrial and aircraft voltages and frequencies.

Air humidity control.

Equipment for ice accretion and water ingestion testing.

Computerised data logging.

Colour video observation and recording.

Gas analysis to EPA standards.

Fuel injector cleaning and or calibration.

Workshop facilities for equipment manufacture and repair

An in-house probe build and calibration department referenced to NPL standards.

TYPICAL WORK PROGRAMMES

Typical work programmes carried out in the two test areas are:-

ENGINE TEST CELL

Engine Calibration e.g.

Altitude Light-up characteristics.
Altitude performance measurement (bhp or thrust).
Engine starting assessment following prolonged temperature soak
Intake Icing Tests.
Probe Icing.
Foreign body ingestion.
Water ingestion.
Intake filter evaluation.
Decompression Testing.
Evaluation of anti-icing equipment
Auxiliary power unit (APU) performance and starting

RIG TEST CELL

Combustion Chamber Evaluation e.g.

Determination of ignition and stability limits
Evaluation of light round characteristics.
Combustion efficiency testing.
Reheat system evaluation (Scale models).

Portable Altitude Chamber e.g.

Engine and APU starting assessment following prolonged temperature soak.
Combustion chamber ignition and stability testing with ability to view flame propagation.

REQUIREMENTS FOR ICING TESTING

To carry out effective icing tests it is necessary to reproduce the correct conditions, i.e., air velocity, air pressure, air temperature, water content and water droplet size and to test for predetermined times. The requirements are set out, in the Joint Airworthiness Requirements (JAR) and the Federal Aviation Regulations (FAR) which specify the conditions applying under various flight regimes and the minimum satisfactory performance requirements. Copies of graphs taken from FAR 25 Appendix C showing the requirements for intermittent and continuous maximum icing conditions are reproduced in Figures 4,5,6 and 7.

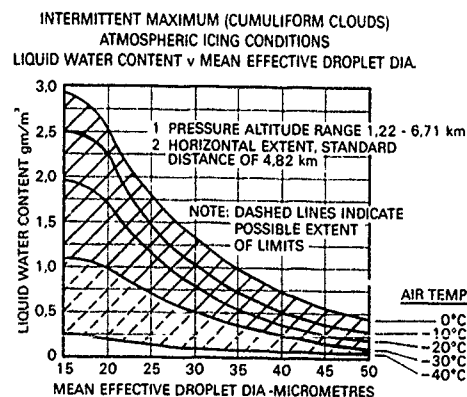


FIG 4

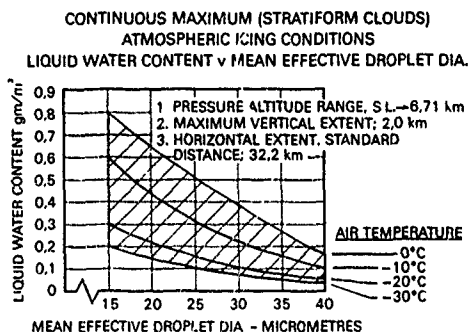


FIG 5

INTERMITTENT MAXIMUM (CUMULIFORM CLOUDS)
ATMOSPHERIC ICING CONDITIONS
AMBIENT TEMPERATURE v PRESSURE ALTITUDE

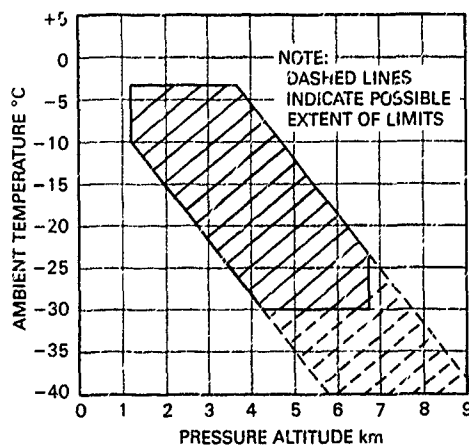


FIG 6

CONTINUOUS MAXIMUM (STRATIFORM CLOUDS)
ATMOSPHERIC ICING CONDITIONS
AMBIENT TEMPERATURE v PRESSURE ALT.

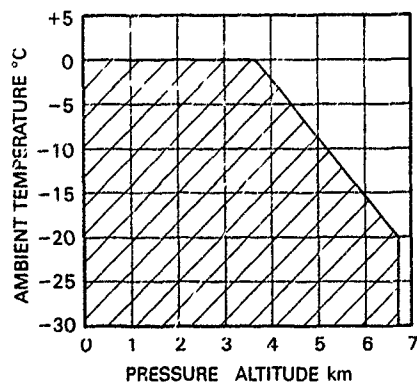


FIG 7

In addition there can be a requirement for testing to establish the effect of ice formations becoming dislodged. This can be determined by either allowing the ice to form and shed by the process applying in service or by forming blocks of ice in refrigerators and injecting pieces of a known size into the item to be tested. Hailstones can also be produced and injected into the test item by means of a specially designed gun.

ICING TEST EQUIPMENT

The parameters specific to or of particular importance when conducting icing tests are air humidity, water droplet size and air/water approach conditions

It is essential that the humidity of the air supplied is closely controlled, if it is too low any ice formation can be ablated and if it is too high additional ice will form. It is normal practice to control the humidity in the range 90% to 100%. In the AIT plant the required humidity is obtained by injecting steam into the upstream air supply ducting.

The required water droplet size is obtained by injecting water through air blast atomisers into the air fed to the test equipment. Seven atomiser nozzles are available (see Figure 8) and all of the nozzles or a selected few can be used as required. It is possible to control the water flow to each nozzle separately and to adjust the atomising air pressure to control both the water distribution and the quality of atomisation. Until recently the droplet size achieved was established using an oiled slide technique for the measurement and counting of the droplets. Recently Laser Equipment (Malvern Type 2600C) has been installed for water droplet measurement. This equipment determines the droplet size by establishing the extent of the light scattered from a laser light beam.



FIG 8 WATER SPRAY INJECTORS

The correct air flow conditions at approach to the equipment on test are obtained by using specially shaped and sized ducts and controlling the flow and condition of the air supplied from the main plant. The final check before commencing a new test programme is usually to fit a grid into the air/water supply duct immediately upstream of the equipment on test and to check that the required ice distribution is obtained i.e. either uniform or biased as required.

ICING TECHNIQUES

It follows from the foregoing that the techniques for icing testing are as follows:-

1. Build a suitable test configuration
2. Set up the required operating conditions.
3. Test for the time required to prove compliance with the specification whilst observing any ice build and taking measurements to determine any change of air flow or pressure loss.
4. Shut down quickly following the test and record the extent of any ice formed.

ICING TEST PROGRAMMES

Examples of the icing test programmes carried out are given in the following subsections.

HELICOPTER INTAKE TESTING

Tests have been carried out to determine if ice formed and became dislodged in a helicopter engine intake. The programme was carried out in two parts (a) using the intake alone and (b) with the intake feeding an operating engine.

In the first series of tests it was possible to explore a wide range of conditions without risk of damaging the engine and also with the facility to collect and examine any ice obtained. In the second series of tests it was possible to confirm that a satisfactory configuration had been obtained and to prove that it fulfilled the type test requirements.

Figure 9 shows the configuration of the set-up used for intake testing and Figure 10 shows the arrangement used for engine testing with the correct aircraft intake fitted. The main features of the test rigs are (a) the air supply ducting provided specifically for the test programme to achieve the correct velocity conditions at approach to the intake, (b) the facility for catching any ice becoming detached during the tests on the intake only, (c) design features permitting quick access to the parts subject to icing and observation of ice build-up during testing

Figure 11 shows icing on a wire mesh grid fitted across an aircraft intake to check the water distribution. In this case the highest water concentration was required towards the outboard side of the passage and it was confirmed by the test. Figure 12 shows icing on the outer lip of the same aircraft intake after the subsequent performance test with the intake grid removed.

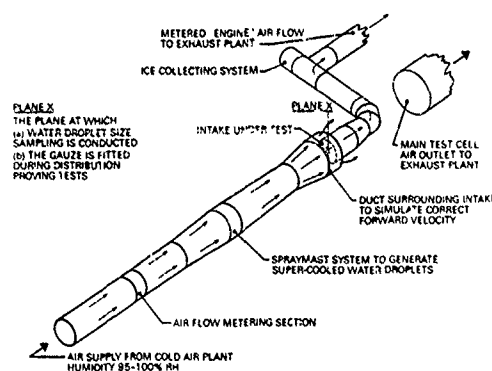


FIG 9 TYPICAL CONFIGURATION FOR INTAKE ICING TESTS

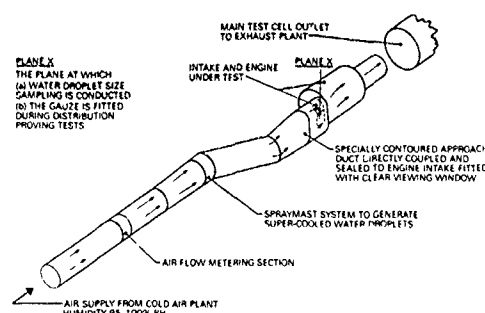


FIG 10 TYPICAL CONFIGURATION FOR ENGINE AND INTAKE ICING TESTS

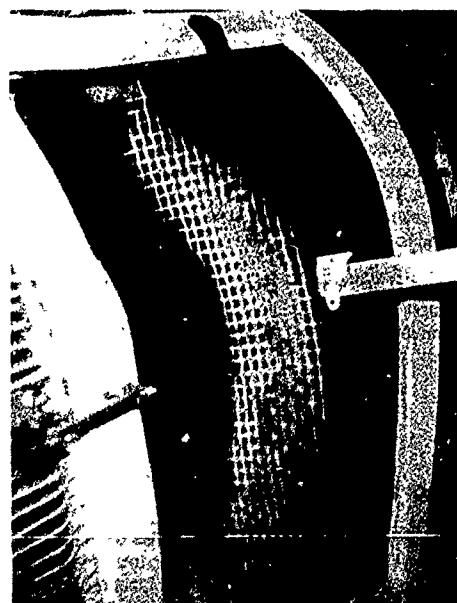


FIG 11 DISTRIBUTION TEST



FIG 12 INTAKE ICING TEST

Figure 13 shows in more detail the ducting used on an aircraft intake to achieve the required air flow conditions and permit observation of ice build-up.

PROBES

The probes subdivide into two categories, fixed items and items required to move under operating conditions.

With the former all that is required is to ensure that the correct flow conditions are achieved, check the reading obtained from the probe and record the extent of ice accretion. With the latter it is also necessary to prove that the actuation mechanism still operates under maximum ice conditions.

Figure 14 shows ice accretions on a droplet sizing probe evaluated in the AIT test chamber and Figure 15 shows a flight refuelling probe which was required to extend when "iced-up".

DEVELOPMENT OF HEATED MATS

Another aspect of the work programme has been the development of heated anti-icing mats. In this case it is possible to determine the minimum heat input required for various sections of the heating mat by separately controlling the heat input to sections of the mat. The results of the development programme are then normally confirmed by tests on the production version



FIG 13 INSTALLATION OF AN AIRCRAFT INTAKE

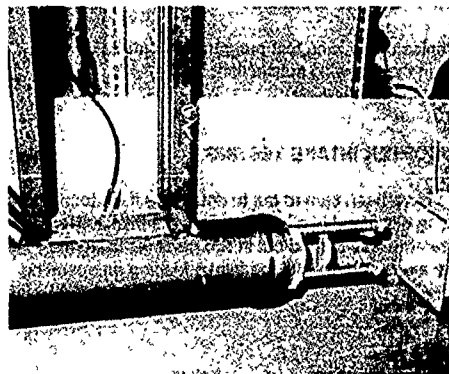


FIG 14 DROPLET SIZING PROBE ICING TEST

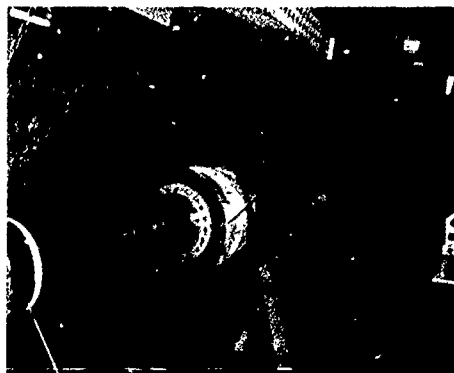


FIG 15 REFUELLING PROBE INSTALLATION

ENGINE INTAKE DUST SEPARATORS

When flown under dusty conditions helicopter engines are fitted with separators at the engine inlet and it is necessary to prove that they do not block with ice. Again the approach adopted is to manufacture ducting to give the required approach conditions, bearing in mind any pitch or yaw requirements, to test as demanded by the JAR etc and measure any change of performance and make a detailed record of the ice formed.

One configuration used for helicopter engine separator assessment is shown in Figure 16 and a photograph of the ice build-up is shown in Figure 17.

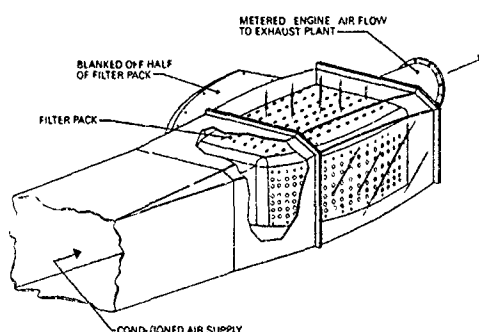


FIG 16 PARTICLE SEPARATOR, TYPICAL CONFIGURATION

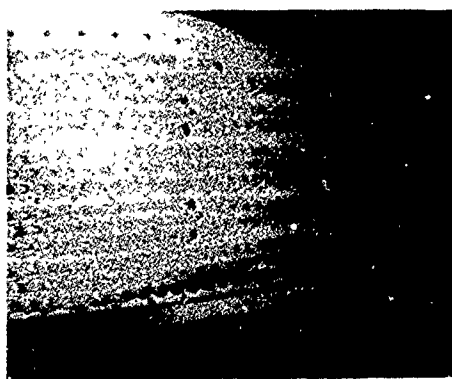


FIG 17 PARTICLE SEPARATOR ICING TEST

SCALE MODELS

As stated earlier one of the main advantages of the facility is its relatively low operating cost. The lower cost results partly from the smaller size and air flows of the facility and of course this can be in some cases a restricting factor.

One way to overcome this problem is to use scale models and this approach has proved very successful in research and development programmes. The use of half linear scale models with appropriate changes to operating conditions where necessary, can reduce the required air mass flow by a factor of four thus bringing many programmes within the scope of the facility.

Figure 18 shows a 50% scale model of an aircraft intake. As the equipment was used for a research/development exercise it was also made with adjustable or replaceable components.

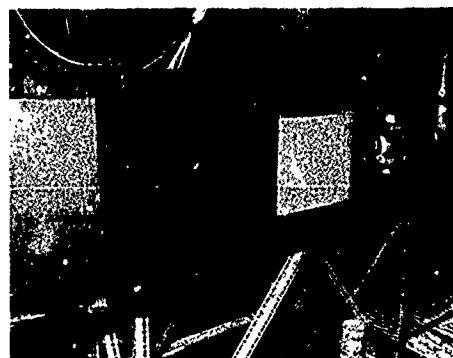


FIG 18 INSTALLATION OF A HALF LINEAR SCALE MODEL INTAKE

CONCLUDING REMARKS

The facility is eminently suitable for either development or certification testing of equipment which requires air flows of 5,7 kg/s or less.

It is possible to simulate accurately the conditions specified in the FAR and JAR and to quickly obtain repeat tests to either evaluate development modifications or check performance repeatability.

Discussion

1. S. Riley, Rolls Royce

The maximum airspeed of your tunnel as a relatively large facility is low. There are many small high speed facilities available. Are there plans to increase its capacity?

Author:

The procedure normally adopted in the AIT altitude test facility is to install air supply ducts sized to give the approach velocity required for the system being evaluated. The main plant limitation is therefore the maximum airflow capability. Whilst there have been several studies into the feasibility of increasing the plant capability, to date they have all being rejected as they would all have negated the main advantage of the present facility, namely, the relatively low operating cost. There is, of course, an ongoing programme for updating the instrumentation and control systems available in the facility.

2. E. Brook, Rolls Royce

You have recently changed from measuring water droplet distributions by oil slides to a laser technique. Have the apparent calibration of your spray nozzle changed? Could you comment on the charge seen, as the certification icing envelopes used by the authorities are based on measurements carried out before modern laser techniques were available?

Author:

We had substantial reservations concerning the change to the laser technique and only decided to recommend the change to customers after a protracted evaluation of the two

systems. Tests carried out by AIT confirm that the laser technique indicates smaller droplet diameters than the oiled slide method. Calibrations in the altitude test facility at Bunsley showed reasonable correlation with the data given by R. G. Keller of the General Electric Company, published in AGARD CP 236, i.e. a spray measured at a volume median diameter of 25 μm by the oil slide technique was shown to have a median diameter of approximately 15 μm by the laser technique.

It follows that larger water droplets are being used than was the case prior to adoption of the laser system for spray characterisation. The accuracy of the oiled slide technique is open to question because of the intrusive nature of the test and the sensitivity of the result to the characteristics of the oil used on the slides. Therefore, since first the laser technique is considered to be more accurate and second the test obtained with the larger droplets would be more rather than less stringent and third as our enquiries showed that the majority of the test facilities in the Western world had already adopted the laser system, it was decided to change to this technique. It is apparent that the test conditions specified by the various authorities for icing certification calibration, should be re-defined using modern laser systems.

3. H. Hoffmann, DLR

Your instrument for the measurement of particle size scattering, is it an own development or the FSSP of PMS?

Author:

No, this is the Malvern equipment. It is commercially available.

A DOCUMENTATION OF VERTICAL AND HORIZONTAL AIRCRAFT SOUNDINGS OF ICING RELEVANT CLOUD PHYSICAL PARAMETERS

by

H.-E. Hoffmann

German Aerospace Research Establishment (DLR)
Institute for Atmospheric Physics
D-8031 Oberpfaffenhofen
Post Wessling/Obb.
Germany

Summary

In a homogeneous st-cloud (in a high pressure area) the total water content TWC is about linearly increasing with increasing distance from the cloud base and obtains its largest value beneath the top (0.39 respectively 0.49 g/m³). The median volume diameter MVD is nearly remaining constant and has predominantly small values (between 15 and 23 µm). The phase of the particles in all st-clouds, evaluated up to now, was fluid. Such a regularity was not found in any of the other types of inhomogeneous clouds of a warm front. Apart from temperature T, which is decreasing nearly linearly in these clouds, too, the course of TWC and MVD is very irregularly. Both the parameters can have several maxima in different distance from the base. The maxima values of TWC can be up to 0.45 g/m³ and those of the MVD up to 460 µm. The phase of the particles could vary between fluid and solid. Not only the vertical structures but also the horizontal structures show great differences of the particle distributions: In the clouds of a high pressure area more than 90% of the particles had diameters between 2 and 32 µm and in the clouds of a warm front more than 49% respectively 99% diameters between 33 and 600 µm.

Notations

D [µm]	Diameter of cloud particles
Fp [km]	Flight path
H [m]	Height above cloud base
MVD [µm]	Median volume diameter of cloud particles
T [°C]	Static air temperature
TWC [g/m ³]	Total water content (water content from fluid and solid particles)

1. Introduction

Since 1983 the "Icing of Aircraft" is investigated in the DLR - Institute for Atmospheric Physics. For this purpose, an aircraft has been equipped as an icing research aircraft (1,2). By the results of icing flights which were conducted with this aircraft, it was tried, before all, to answer the question in which manner the normalized and the aircraft related icing degree is depending on cloudphysical parameters (3,4,5,6). For improving the forecast of icing we tried also during these

icing flights to get informations about the dependence of the icing relevant cloudphysical parameters on cloud parameters. Here, cloud parameters imply the type of clouds and the height above cloud base. We have always got these informations when we could fly through the whole cloud from its top to its base respectively vice versa or when we could fly during one icing flight definite flight pathes in different heights. The data which we have collected during such vertical and horizontal sounding of clouds, together with informations on the meteorological synoptic situation, are serving as input data for a climatology of icing relevant cloud physical parameters producing aircraft related icing degree severe (7,8,9,10,11,12).

After a short description of the measuring procedure in section 2, in section 3 the vertical structure of the cloud physical parameters total water content TWC, temperature T and median volume diameter and in section 4 the horizontal structure of these cloud physical parameters are shown. There is differentiated between Sc, St-clouds in a high pressure area and Sc, As, Ac, Ns-clouds in the range of a warmfront. For each case two example are shown. In section 5, the vertical and the horizontal structures of one of the examples for clouds in a high pressure area and in the range of a warmfront are compared. In the sections 3,4,5, for selected points the particle size distribution is shown, too. The results given in this paper are taken from 10 and 11.

2. Measuring instruments employed and performance of measurements

For the vertical and horizontal structures, the values for the TWC were measured by a Johnson-Williams hot wire instrument, the values for the temperature by a Rosemount platinum-wire instrument, and the values for the MVD by Knollenberg PMS instruments FSSP and OAP. The TWC values used for the particle size distributions are derived from the FSSP and OAP measurements, too.

The measurements were carried out in the course of icing flights which were conducted in a region between the north edge of the Alps and a distance of about 200 km north of it. Each value of the points in the figures is the mean value formed on a flight time of 20 sec. That means a flight distance of about 1.2 km.

3. Results of vertical soundings

3.1 Two examples for Sc, St-clouds in a high pressure area

1. Example

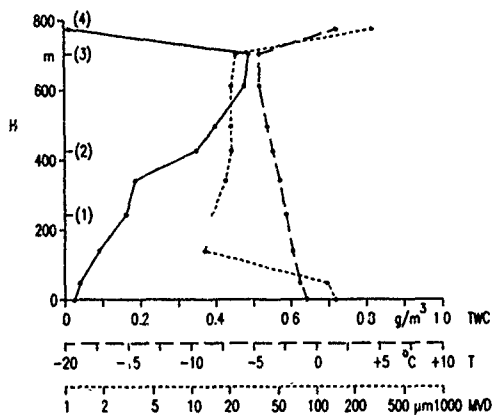


Fig. 1. Total water content TWC, temperature T, and median volume diameter MVD in dependence on height above cloudbase H.

Phase of cloud particles: Fluid

Height of the cloud base: Between 400 and 500 m

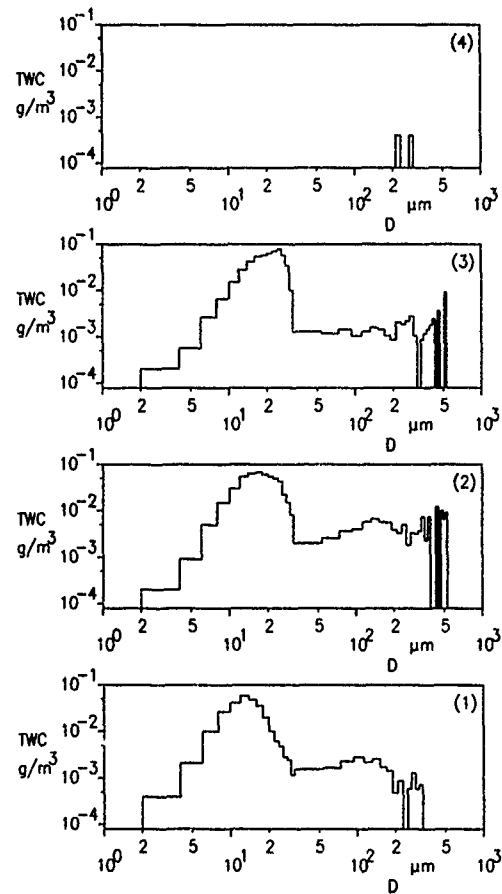


Fig. 2. Total water content TWC in dependence on diameter of particle D for the points (1) to (4) of the vertical structure of fig. 1.

Measuring point No.	Height above cloudbase (m)	TWC (g/m^3)	T ($^{\circ}\text{C}$)	MVD (μm)	\bar{D} (μm)	Number of cloud particles pro cm^3
1	243	0.16	-2.4	15.0	10.3	313.0
2	426	0.35	-3.4	21.0	13.8	266.0
3	704	0.49	-4.5	23.0	14.9	186.0
4	775	0.01	-1.7	280.5	14.1	0.2

Airmass: xPs

Table 1. Some data for the selected measuring points of fig. 1.

2. Example

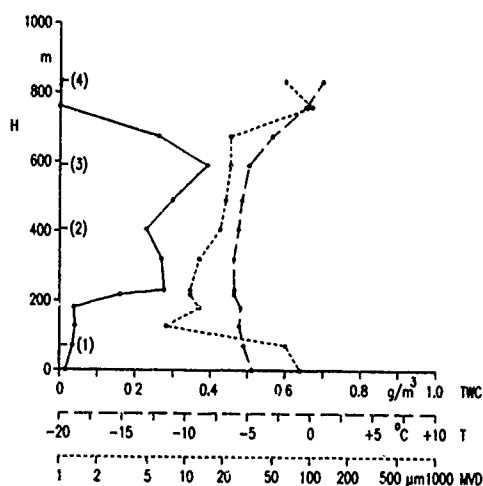


Fig. 3. Total water content TWC, temperature T, and median volume diameter MVD in dependence on height above cloudbase H.

Phase of cloud particles: Fluid
Height of the cloud base: ~400 m

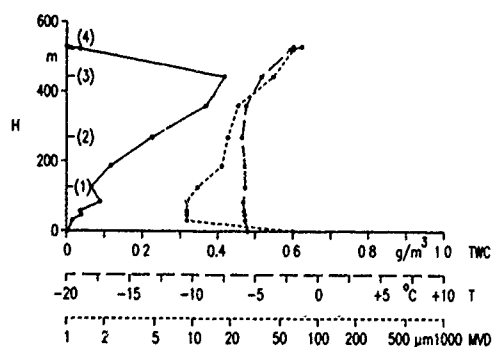


Fig. 4. Total water content TWC, temperature T, and median volume diameter MVD in dependence on height above cloudbase H.

Phase of cloud particles: Fluid
(On the same flight as fig. 3, but about 7 min later and about 5 km alofted)
Height of the cloud base: ~600 m

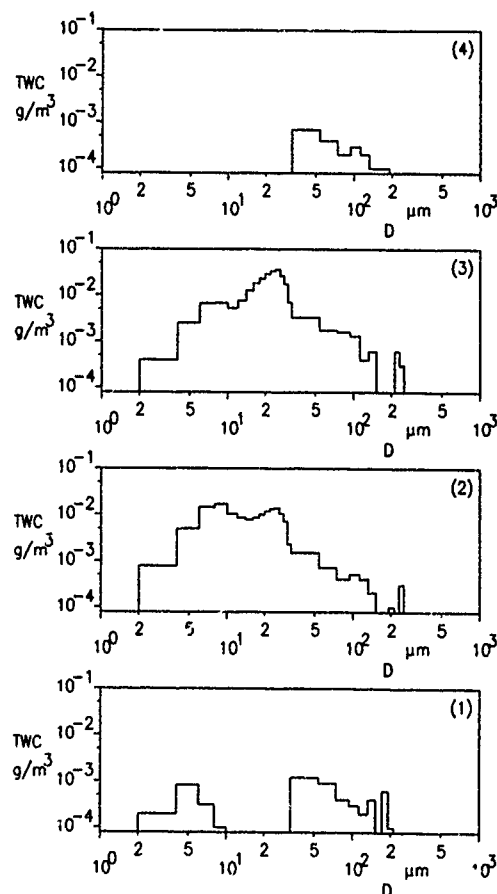


Fig. 5. Total water content TWC in dependence on diameter of particle D for the points (1) to (4) of the vertical structure of fig. 3.

Mea- suring point No.	Height above cloudbase	TWC	T	MVD	\bar{D}	Number of cloud particles
	(m)	(g/m³)	(°C)	(μm)	(μm)	pro cm³
1	71	0.04	-5.3	63.7	4.8	30.0
2	406	0.23	-5.7	19.0	7.2	293.0
3	591	0.39	-4.9	23.0	9.8	173.0
4	833	0.01	+1.0	63.7	67.4	0.03

Airmass. xSp

Table 2. Some data for the selected measuring points of fig. 3.

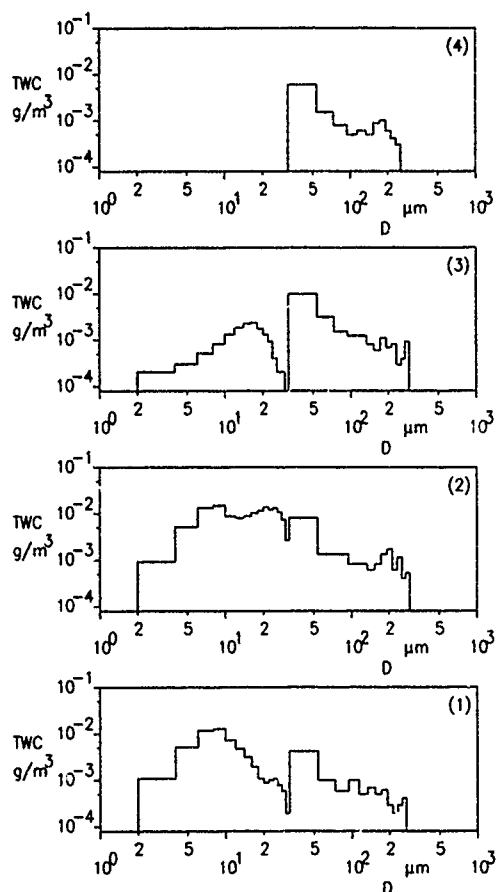


Fig. 6. Total water content TWC in dependence on diameter of particle D for the points (1) to (4) of the vertical structure of fig. 4.

Measuring point No.	Height above cloudbase (m)	TWC (g/m³)	T (°C)	MVD (μm)	\bar{D} (μm)	Number of cloud particles pro cm³
1	126	0.07	-5.8	11.0	6.1	268.0
2	269	0.23	-6.1	19.0	7.3	289.0
3	443	0.42	-4.5	43.9	9.4	34.0
4	522	0.04	-2.2	63.7	57.2	0.2

Airmass: xSp

Table 3. Some data for the selected measuring points of fig. 4.

3.2 Two examples for Sc, Ac, As, Ns-clouds in the range of a warm front

1 Example

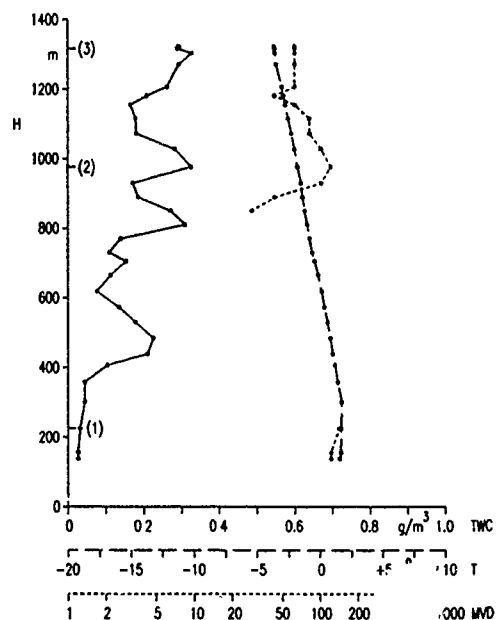


Fig. 7. Total water content TWC, temperature T, and median volume diameter MVD in dependence on height above cloudbase H.

Phase of cloud particles: Fluid

Height of the cloud base: ~1400 m

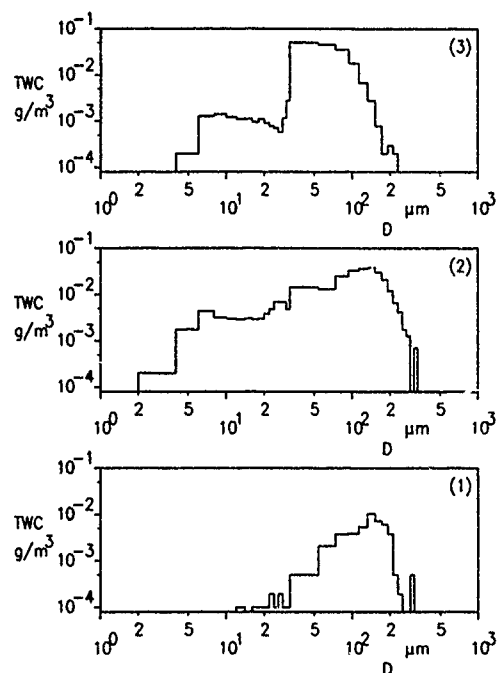


Fig. 8. Total water content TWC in dependence on diameter of particle D for the points (1) to (3) of the vertical structure of fig. 7.

2. Example

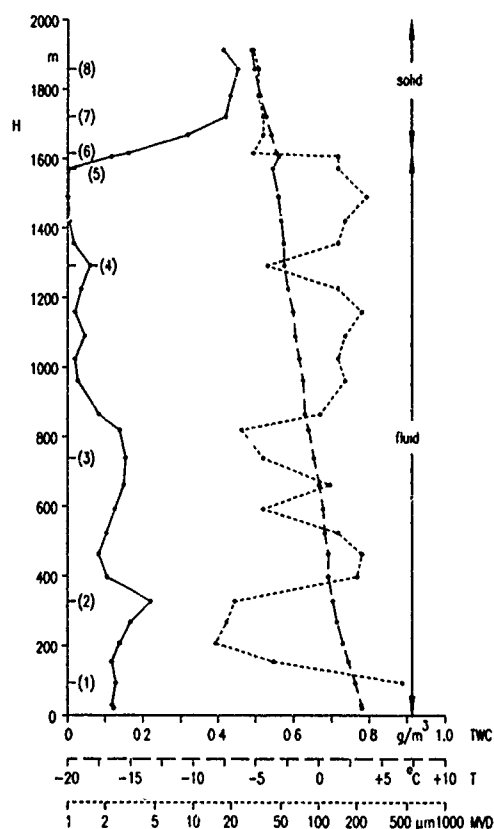


Fig. 9. Total water content TWC, temperature T , and mean volume diameter MVD in dependence on height above cloudbase H .

Phase of cloud particles: Fluid / solid
Height of cloud base: ~1000 m

Measuring point No.	Height above cloudbase (m)	TWC (g/m^3)	T ($^{\circ}\text{C}$)	MVD (μm)	\bar{D} (μm)	Number of cloud particles pro cm^3
1	225	0.03	+1.7	142.6	105.0	0.4
2	976	0.33	-1.7	123.0	19.5	87.0
3	1316	0.29	-3.6	63.7	30.0	21.0

Airmass: mP

Table 4. Some data for the selected measuring points of fig. 7.

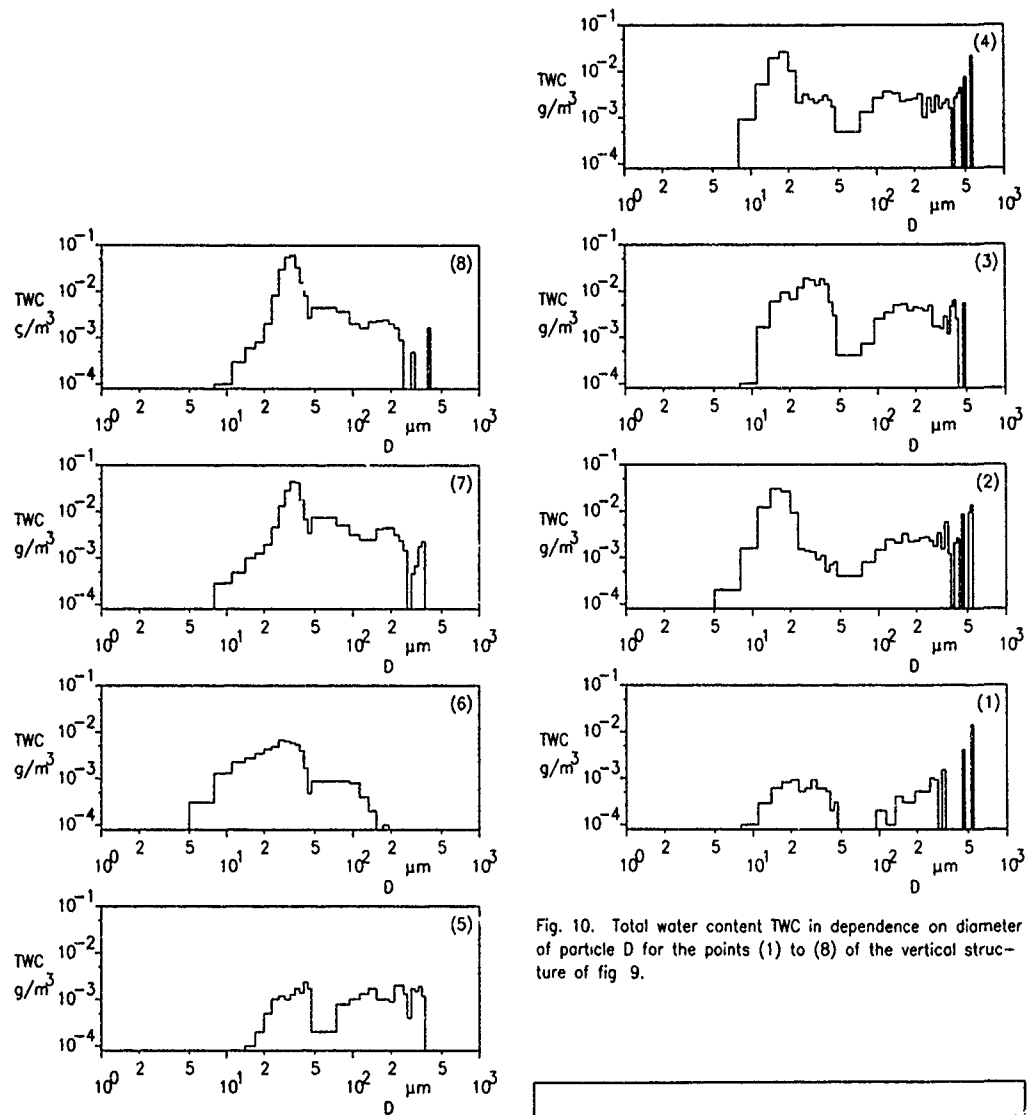


Fig. 10. Total water content TWC in dependence on diameter of particle D for the points (1) to (8) of the vertical structure of fig. 9.

Measuring point No.	Height above cloudbase (m)	TWC (g/m^3)	T ($^{\circ}\text{C}$)	MVD (μm)	\bar{D} (μm)	Number of cloud particles pro cm^3
1	93	0.13	+2.9	46.0	37.4	2.0
2	327	0.22	+1.1	21.5	18.2	44.0
3	738	0.15	-0.3	36.5	34.5	16.0
4	1291	0.06	-2.7	39.5	22.3	30.0
5	1570	0.01	-3.6	142.6	94.9	0.9
6	1615	0.16	-3.3	30.5	17.1	14.0
7	1721	0.42	-4.2	36.5	39.5	12.0
8	1858	0.45	-5.1	33.5	35.5	16.0

Airmass: mS

Table 5. Some data for the selected measuring points of fig. 9.

4. Results of horizontal soundings

4.1 One example for Sc, St-cloud in a high pressure area

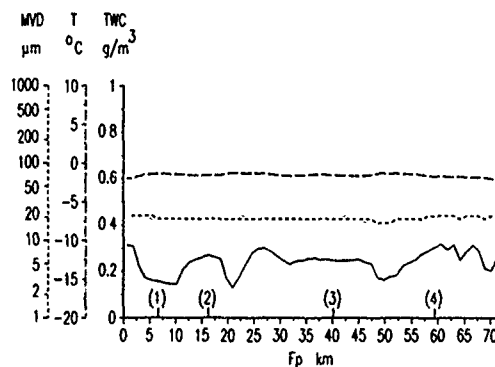


Fig. 11 Total water content TWC, temperature T, and median volume diameter MVD in dependence on flight path Fp in constant flight altitude.
Phase of cloud particles: Fluid
Height above cloudbase: ~450 to 650m
Distance from cloudtop: ~150m
Flight altitude: 1050m

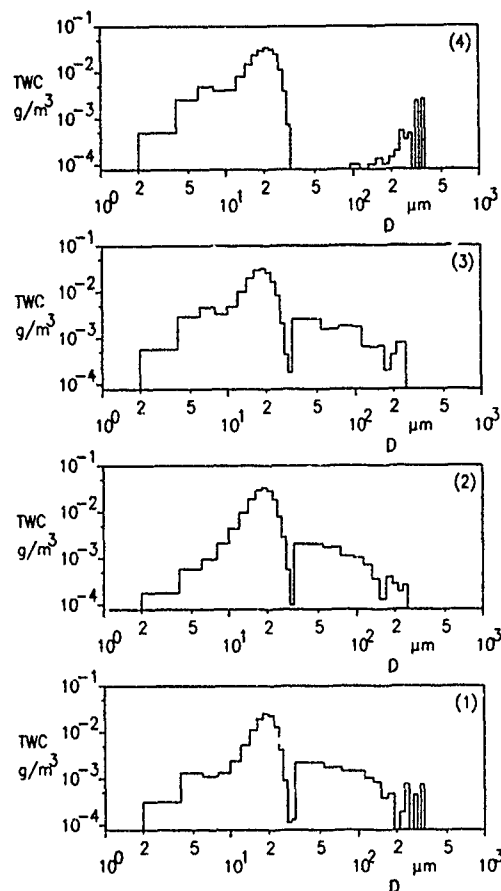


Fig. 12. Total water content TWC in dependence on diameter of particle D for the points (1) to (4) of the horizontal structure of fig. 11.

Measuring point No.	Height above cloudbase (m)	TWC (g/m³)	T (°C)	MVD (μm)	\bar{D} (μm)	Number of cloud particles pro cm³
1	451	0.16	-1.4	19.0	10.3	89.3
2	449	0.27	-1.6	19.0	12.9	86.5
3	449	0.25	-1.5	19.0	9.0	178.3
4	447	0.31	-1.7	21.0	9.4	168.5

Airmass: xSp

Table 6 Some data for the selected measuring points of fig. 11.

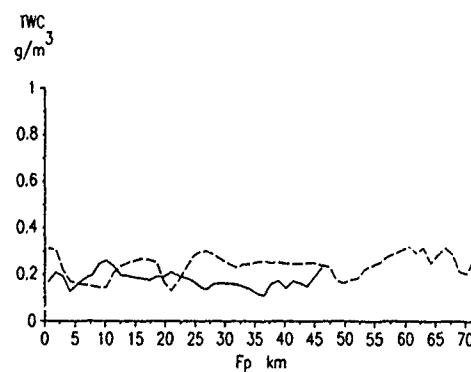


Fig. 13 Total water content TWC in dependence on flight path Fp for two different heights above cloudbase. Phase of cloud particles: Fluid

———— Height above cloudbase: 375 to 575m
----- Height above cloudbase: 450 to 650m

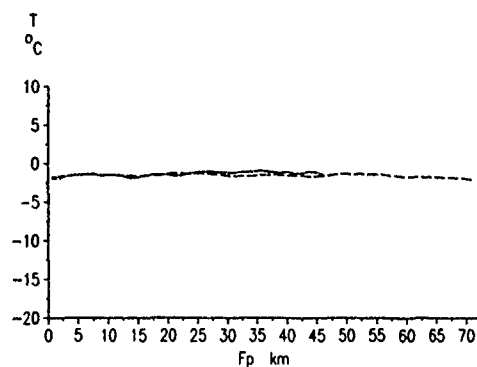


Fig. 14. Temperature T in dependence on flight path F_p for two different heights above cloudbase.
Phase of cloud particles: Fluid

———— Height above cloudbase: 375 to 575m
----- Height above cloudbase: 450 to 650m

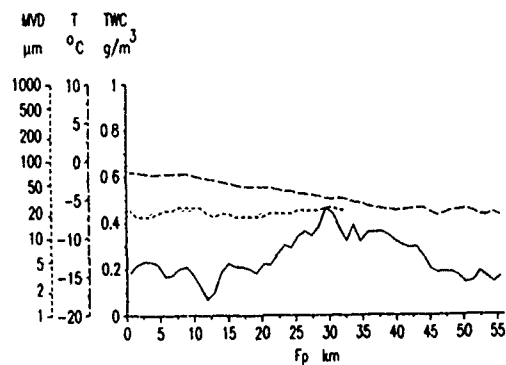


Fig. 16. Total water content TWC, temperature T , and median volume diameter MVD in dependence on flight path F_p in constant flight altitude but deeper penetration into the cloud, caused by continuous ascent of the cloud surface in flight direction
Phase of cloud particles: Fluid
Flight altitude: 1115m
Height above cloudbase: ?
Distance from cloudtop: ?

4.2 One example for Sc, Ac, As, Ns-cloud in the range of a warm front

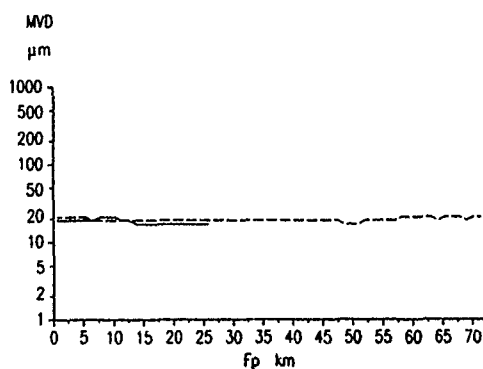


Fig. 15. Median volume diameter MVD in dependence on flight path F_p for two different heights above cloudbase.
Phase of cloud particles: Fluid

———— Height above cloudbase: 375 to 575m
----- Height above cloudbase: 450 to 650m

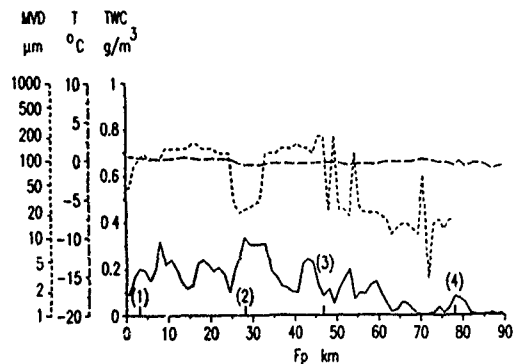


Fig. 17. Total water content TWC, temperature T , and median volume diameter MVD in dependence on flight path F_p .

Phase of cloud particles: Fluid
Height above cloudbase: ~435m
Distance from cloudtop: ?
Flight altitude: 1835m

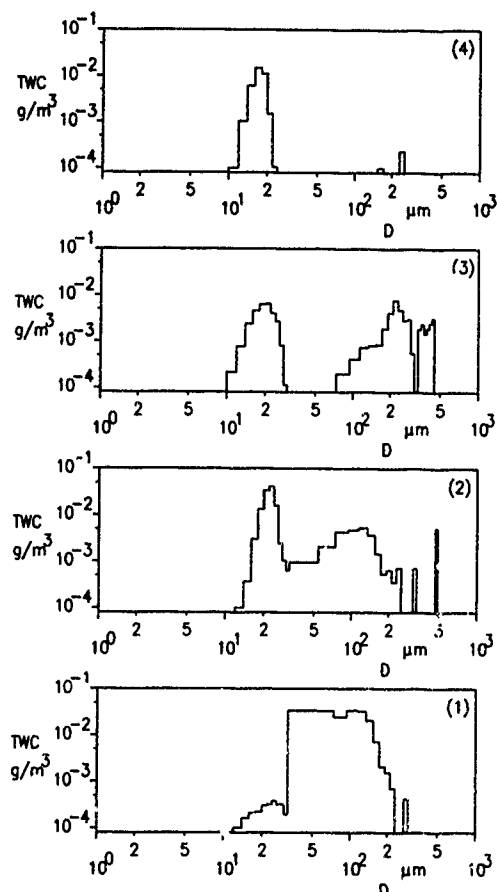


Fig. 18. Total water content TWC in dependence on diameter of particle D for the points (1) to (4) of the horizontal structure of fig. 17.

Measuring point No.	Height above cloudbase (m)	TWC (g/m^3)	T ($^{\circ}\text{C}$)	MVD (μm)	\bar{D} (μm)	Number of cloud particles pro cm^3
1	440	0.20	+0.3	103.3	73.2	1.8
2	438	0.33	-0.6	23.0	26.3	20.9
3	435	0.08	-0.3	202.7	26.9	8.3
4	434	0.08	-0.7	17.0	16.7	14.0

Airmass: mP

Table 7. Some data for the selected measuring points of fig. 17.

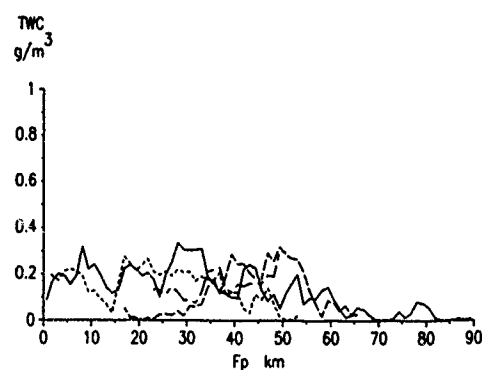


Fig. 19. Total water content TWC in dependence on flight path F_p for four different heights above cloudbase.

Phase of particles: Fluid

— Height above cloudbase: $\sim 435\text{m}$
 - - - Height above cloudbase: $\sim 725\text{m}$
 . . . Height above cloudbase: $\sim 1035\text{m}$
 - . - Height above cloudbase: $\sim 1325\text{m}$

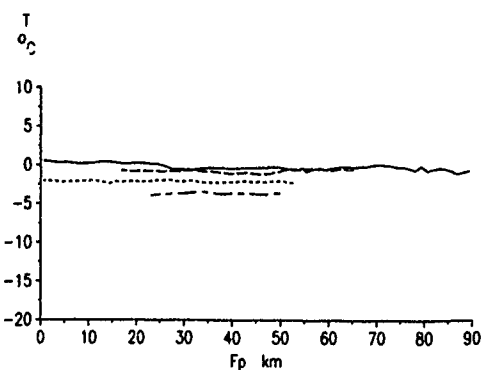


Fig. 20. Temperature T in dependence on flight path F_p for four different heights above cloudbase.

Phase of particles: Fluid

— Height above cloudbase: $\sim 435\text{m}$
 - - - Height above cloudbase: $\sim 725\text{m}$
 . . . Height above cloudbase: $\sim 1035\text{m}$
 - . - Height above cloudbase: $\sim 1325\text{m}$

5. Comparison between representative results of clouds
in a high pressure area and clouds in the range of
a warm front

5.1 Comparison between results of vertical soundings

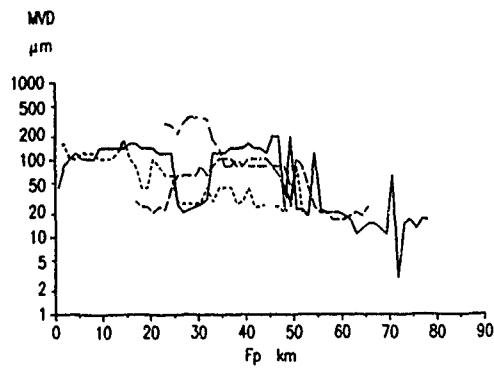


Fig. 21. Median volume diameter MVD in dependence on flight path Fp for four different heights above cloudbase.

Phase of particles: Fluid

- Height above cloudbase: ~435m
- Height above cloudbase: ~725m
- Height above cloudbase: ~1035m
- .-.-.- Height above cloudbase: ~1325m

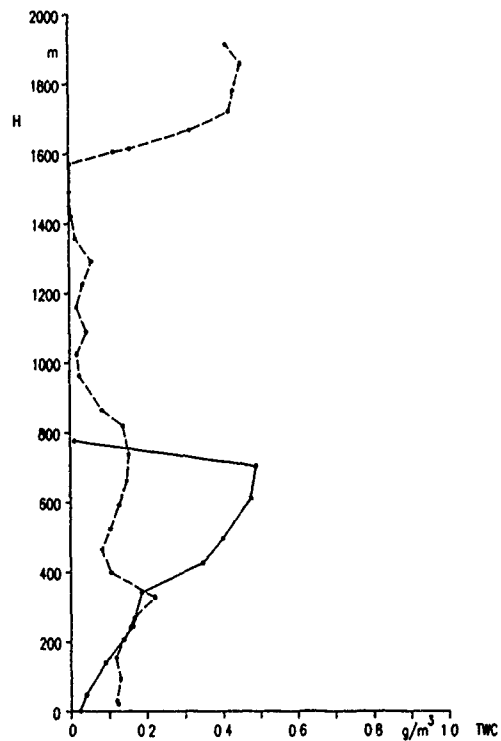


Fig. 22. Total water content TWC in dependence on height above cloudbase H in a high pressure area and in the range of a warmfront.

Phase of cloud particles: Fluid ——— respectively fluid / solid -----
———— In a high pressure area
----- In the range of a warmfront

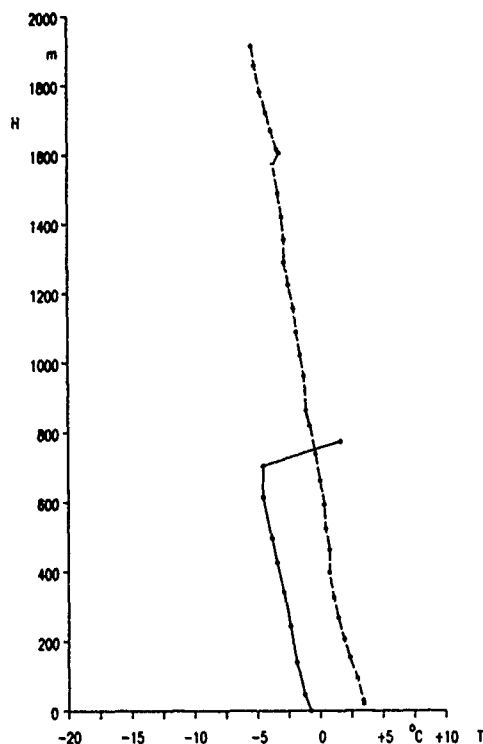
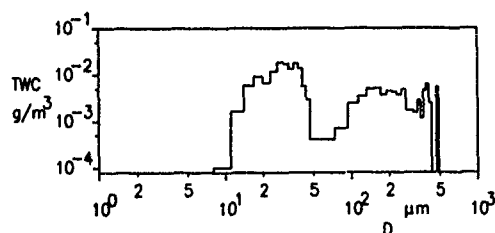
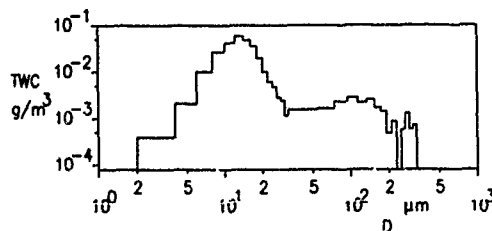


Fig. 23. Temperature T in dependence on height above cloudbase H in a high pressure area and in the range of a warmfront. Phase of cloud particles: Fluid — respectively fluid / solid - - - - .
 — In a high pressure area
 - - - - In the range of a warmfront



In the range of a warmfront



In a high pressure area

Fig. 25. Total water content TWC in dependence on particle diameter D for one point of the vertical structure in a high pressure area and in the range of a warmfront

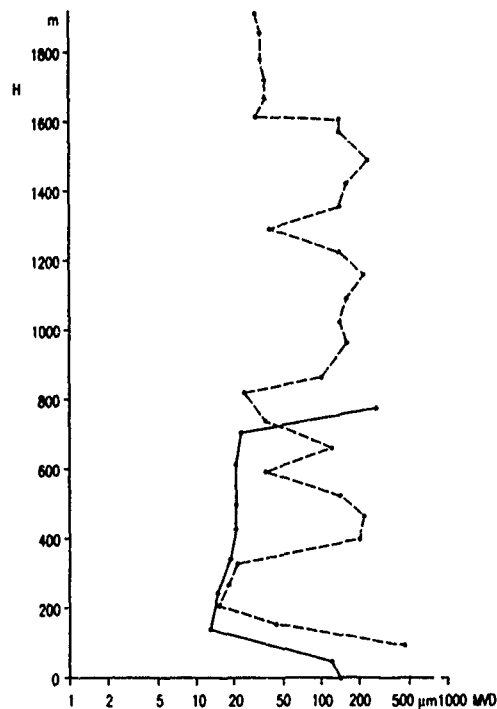
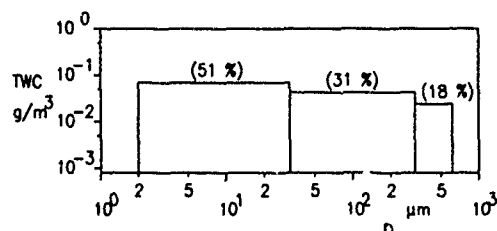
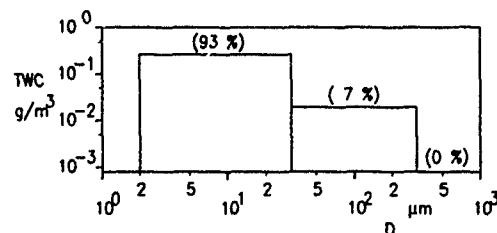


Fig. 24. Median volume diameter MVD in dependence on height above cloudbase H in a high pressure area and in the range of a warmfront. Phase of cloud particles: Fluid — respectively fluid / solid - - - - .
 — In a high pressure area
 - - - - In the range of a warmfront



In the range of a warmfront



In a high pressure area

Fig. 26. Total water content TWC for the particle range 2 to 32 μm , 33 to 310 μm and 311 to 600 μm , and its part on the total water content of all the particles in % for one point of the vertical structure in a high pressure area and in the range of a warmfront.

5.2 Comparison between results of horizontal soundings

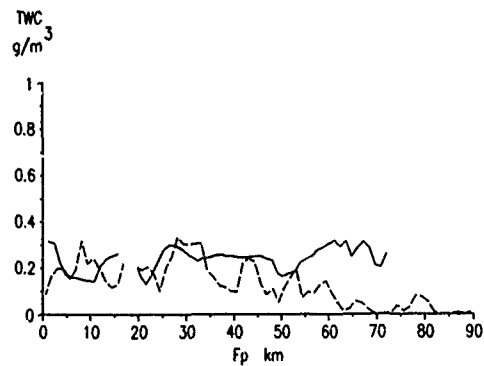


Fig. 27. Total water content TWC in dependence on flight path Fp in constant flight altitude in a high pressure area and in the range of a warmfront. Phase of particles: Fluid

— In a high pressure area
 - - - In the range of a warmfront

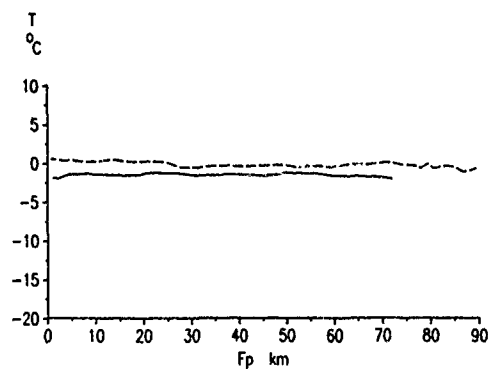


Fig. 28. Temperature T in dependence on flight path Fp in constant flight altitude in a high pressure area and in the range of a warmfront. Phase of particles: Fluid

— In a high pressure area
 - - - In the range of a warmfront

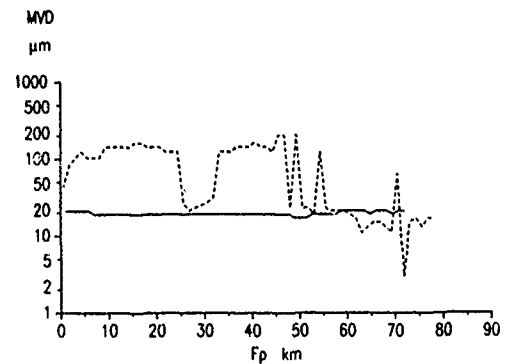


Fig. 29. Median volume diameter MVD in dependence on flight path Fp in constant flight altitude in a high pressure area and in the range of a warmfront. Phase of particles: Fluid

— In a high pressure area
 - - - In the range of a warmfront

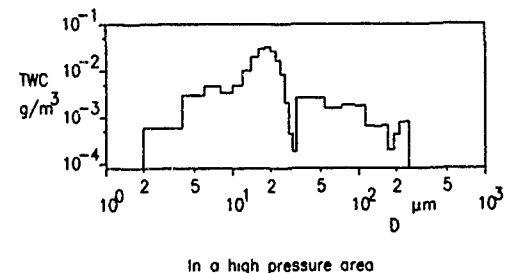
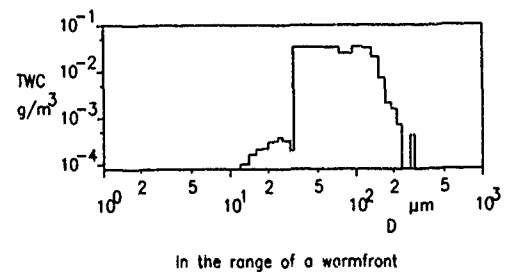


Fig. 30. Total water content TWC in dependence on particle diameter D for one point of the horizontal structure in a high pressure area and in the range of a warmfront.

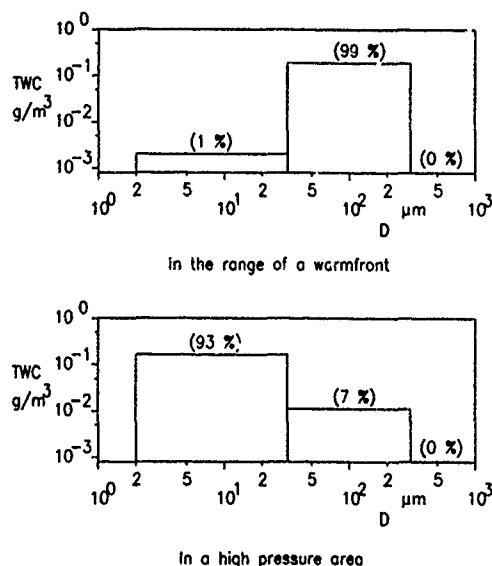


Fig. 31. Total water content TWC for the particle range 2 to 32 μm , 33 to 310 μm and 311 to 600 μm , and its part on the total water content of all the particles in % of one point of the horizontal structure in a high pressure area and in the range of a warmfront.

6. Discussion of the results

The results discussed in this paper were ascertained on icing flights in winter months in altitudes up to $\sim 4000\text{m}$ in a region between the north edge of the Alps and a distance of $\sim 200\text{ km}$ in the north of it.

Results ascertained from the vertical soundings

Total water content TWC of clouds of a high pressure area was about linearly growing with growing distance from cloud base. Its maximum was located directly below the cloud top and attained values between 0.40 and 0.50 g/m^3 (see Fig. 1,3,4,22).

TWC of clouds in the range of a warm front was strongly fluctuating between cloud base and cloud top and had maximum values in different heights. The maximum values were between 0.20 and 0.45 g/m^3 (see Fig. 7,9,22).

Temperature T in clouds of a high pressure area was decreasing linearly with increasing distance from cloud base. Only near the base or near the top, T could increase (see Fig. 1,3,4,23).

T in clouds in the range of a warm front was decreasing with increasing distance from cloud base (see Fig. 7,9,23).

Median volume diameter MVD of clouds of a high pressure area had predominantly small values (between 11 and 23 μm). Only close to cloud base respectively close to cloud top it could get larger values (see Fig. 1,3,4,24).

Up to 90% of the TWC was formed by particles with diameter between 2 and 32 μm (see Fig. 2,5,6,25,26). MVD of clouds in the range of a warm front was strongly fluctuating between small and large values. The maximum values were between 100 and 460 μm (see Fig. 7,9,24). Up to 50% of the TWC was formed by particles with diameter between 33 and 600 μm (see Fig. 8,10,25,26).

The phase of the particles in clouds of a high pressure area was always fluid (see Fig. 1,3,4).

The phase of the particles in clouds in the range of a warm front could vary between fluid and solid (see Fig. 9).

Results ascertained from the horizontal soundings

TWC in the clouds of a high pressure area was varying between values of 0.17 and 0.31 g/m^3 on a flight path of 70km (see Fig. 11,13,27). In the clouds in the range of a warm front the values of TWC were varying between 0 and 0.32 g/m^3 on a flight path of 90 km (see Fig. 17,19,27).

In a special case, when the cloud surface was ascending in flight direction the TWC in the clouds of a high pressure area – when flying in constant altitude – was increasing respectively decreasing in dependence on flight path length (see Fig. 16). Because of ascending surface of cloud – in spite of constant flight altitude – the airplane had flown deeper and deeper into the cloud. Before Fp: 30km the airplane was above the maximum TWC (see Fig. 1), on Fp: 30km the airplane was in the maximum TWC and behind Fp: 30km the airplane was below the maximum TWC.

T in the clouds of a high pressure area and in the range of a warm front was constant in constant heights above cloud base (see Fig. 11,14,20,28). Only in a special case, when the cloud surface was ascending in flight direction T was decreasing when flying in a constant altitude (see Fig. 16).

MVD of the clouds of a high pressure kept constant on small values ($\sim 20\text{ }\mu\text{m}$) (see Fig. 11,29). Up to 93% of the TWC was formed by particles between 2 and 32 μm (see Fig. 30,31).

MVD of the clouds in the range of a warm front was strongly fluctuating between small and large values. The maximum values were between 100 and 200 μm (see Fig. 17,21,29).

Up to 99% of the TWC was formed by particles with diameters between 33 and 310 μm (see Fig. 18,30,31).

The phase of the particles, on the flights discussed here, was always fluid.

References

1. Hoffmann, H.-E.; Demmel, J.: First Stage of Equipping a Type Do 28 as a Research Aircraft for Icing, and First Research Results. ESA-TT-855, 1984.
2. Hoffmann, H.-E.; Demmel, J.: DFVLR's Research Aircraft Do 28, D-IFMP, and its Measuring Equipment. ESA-TT-972, 1986.
3. Forecasters' Guide on Aircraft Icing. Air Weather Service, AWS/TR-80/001, 1980.
4. Hoffmann, H.-E.; Roth, R.; Demmel, J.: Standardized Ice Accretion Thickness as a Function of Cloud Physics Parameters. ESA-TT-1080, 1988.
5. Hoffmann, H.-E.: Icing Degree Moderate to Severe: If and Where in Clouds. ICAS Proceedings, Jerusalem August 28 - September 2, 1988.
6. Hoffmann, H.-E.: The Analysis of Three Icing Flights with Various Ice Accretion Structures when Reaching Icing Degree Severe. ICAS Proceedings, Stockholm September 9-14, 1990.
7. Roach, W.T.; Forrester, D.A.; Crewe, M.E.; Watt, K.F.: An Icing Climatology for Helicopters. Special Investigation Memorandum 12, Meteorological Office, Bracknell, 1984.
8. Hoffmann, H.-E.; Roth, R.: Cloudphysical Parameters in Dependence on Height Above Cloud Base in Different Clouds. Meteorol. Atmos. Phys. 41, 247-254, 1989.
9. Hoffmann, H.-E.: The Horizontal and Vertical Structures of Cloud Physical Parameters. 5th WMO Scientific Conference on Weather Modification and Applied Cloud Physics, Beijing, China, 8-12 May 1989, WMP Report No. 12.
10. Hoffmann, H.-E.; Demmel, J.; Horst, H.; Löbel, H.: A Documentation of Icing-Relevant Cloud Physical Parameters on Vertical Soundings of Stratiform Clouds. DLR - Mitt. 90-07, 1990. (An ESA-Translation in preparation).
11. Hoffmann, H.-E.; Demmel, J.; Horst, H.; Stingl, J.: A Documentation of Icing-Relevant Cloud Physical Parameters on Horizontal Soundings of Stratiform Clouds. (DLR - Report in preparation)

rameters on Horizontal Soundings of Stratiform Clouds. (DLR - Report in preparation)

12. Hoffmann, H.-E.: A Climatology for Cloud Physical Parameters Causing Aircraft Related Icing Degree Severe. (DLR - Report in preparation)

Discussion

1. M. Holmes, RAE

As a result of your investigations, do you believe that the FAA standard clouds are still representative of what occurs in the real environment?

Author:

The FAA standards for icing clouds are not representative for the real atmosphere.

2. R. Toogood, Pratt and Whitney Canada

You mentioned that your measurements indicate variance with the FAA 25, App C atmospheric conditions. Would you agree then that your measurements are also at variance with the JAR atmospheric definitions?

Are the results of your research being coordinated with the new effort in the United States to re-examine the definition of the icing atmosphere?

Author:

Our measurements are at variance with the FAA and also with the JAR atmospheric icing conditions.

After each yearly DLR Icing Flight Season we are sending special lists with our icing results to the University of Dayton respectively to the Naval Research Lab. in Washington. They are collecting new icing data in a contract from FAA to re-examine the definitions of the icing atmosphere.

3. V. Garratt, RAE

I am not sure how you differentiate between solid and liquid particles.

Author:

This is our most important problem. We apply two solutions: At first observations by the pilots or flight engineers, secondly with a back scatter device to determine the normalized visibility. The results of both are only qualitative. The percentage between solid and liquid particles cannot be determined.

DEVELOPMENTS IN ICING TEST TECHNIQUES FOR AEROSPACE APPLICATIONS IN THE RAE PYESTOCK ALTITUDE TEST FACILITY

M Holmes, V E W Garratt, R G T Drage
Propulsion Department, Royal Aerospace Establishment
Pyestock, Hants. GU14 OLS, England

ABSTRACT

The altitude test facilities at RAE Pyestock are used in support of clearance of aero-engines, intakes and helicopter rotors to operate under severe icing conditions. An important aspect of the work is the simulation of the wet icing cloud in terms of water concentration, mean droplet size and spectrum. Water spray rakes or booms have been developed for this activity and individual nozzles calibrated in a purpose built wind tunnel. A laser particle sizer has been used to calibrate typical spray nozzles and attempts made to establish a traceable standard. Although this paper mainly deals with the development of cloud simulation, it also includes a short description of the facilities and the capability for monitoring ice formation and shedding.

1 INTRODUCTION

Safe operation of civil and military aircraft and helicopters in weather conditions which can cause ice build-up on engine intakes, engine fan, compressor and helicopter rotor blades is a prime concern of the air worthiness authorities. Regulations have therefore been produced in Europe and the USA which identify the test conditions with which aerospace vehicles in ground-based facilities must comply before clearance to fly in icing conditions is given. The advantages of gaining test evidence on ground-based facilities prior to flight testing is that they can provide specified, consistent and repeatable test conditions irrespective of the prevailing weather. They also permit the use of non-flightworthy test vehicles, all of which contribute towards a considerable reduction in time and cost to obtain clearance for flight in ice-forming conditions.

Such test facilities exist at the Royal Aerospace Establishment, England, in the form of two of the altitude test cells at Pyestock. These were primarily intended for steady-state and transient performance evaluation of air breathing missile and aero engines, but a capability for icing tests was recognised and incorporated at the design stage. Although there has been long experience of icing tests extending over twenty years, development of techniques, instrumentation and monitoring

equipment is a continuing process and significant improvements have recently been introduced. These are centred on one of the most important elements of the whole process, the simulation of the defined cloud.

Some icing clouds consist of a mixture of supercooled water droplets and particles of dry ice and completely different techniques are used for producing these two components of the cloud. Ice particles are produced by milling chips off prepared ice blocks and introducing them into the main air flow upstream of the liquid water injection point. However, customers seldom specify a requirement for dry ice and the subject has therefore not attracted quite the same development effort as the production of water droplets. It is thus not given much prominence in this paper. Water droplets are produced using an array of spray nozzles placed in the cold inlet air stream. The droplets rapidly lose heat to their cold surroundings to become supercooled, as in the natural cloud, retaining their liquid state until impact with an object triggers solidification.

Apart from the difficulty of producing a consistent uniformly distributed spray pattern across the duct, which may be up to 2.6m in diameter, there is the problem of measuring the droplet size distribution itself. Although this should ideally be done whilst the test is in progress, the practice at RAE has been to calibrate individual nozzles in a controlled environment in a low speed wind tunnel especially adapted for this purpose. A laser particle sizer has been used to good effect in this work.

This paper begins by reviewing the icing certification regulations, noting any differences between the various regulatory authorities and the effect this can have on setting up test conditions. The test facilities at Pyestock are then described together with a brief description of the capability for monitoring ice formation and shedding. Finally, the development of water spray rakes is discussed, with particular attention paid to the calibration of spray nozzles and the development of special equipment for that purpose.

2 REVIEW OF ICING REGULATIONS

Icing tests at Pyestock form part of an overall icing certification programme agreed between the manufacturer and one or more of the three regulatory authorities empowered to grant the relevant operational clearance for aerospace vehicles manufactured and/or tested in the United Kingdom (UK). These authorities are:-

(a) The UK Ministry of Defence Procurement Executive (MOD(PE)) which deals with military equipment covered by the appropriate Defence Standard (Ref 1).

(b) The British Civil Aviation Authority (CAA) which administers the Joint (European) Aircraft Requirements (JAR) applicable to modern transport aircraft and propulsion systems (Ref 2 and 3) and also the old British Civil Aircraft Requirements which still apply to types originally certified to these regulations.

(c) The Department of Transportation of the United States of America (USA) Federal Aviation Administration which issues Federal Aviation Regulations (FAR) (Ref 4) and associated Advisory Circulars which are applicable to UK manufactured aerospace equipment which is required to operate in America.

The nature of the regulations, which applies to all authorities, demands that clearance to operate in icing conditions is dependant on a three-part assessment. The first requirement is for an in-depth theoretical analysis of the susceptible icing areas on the flight vehicle at the most severe atmospheric conditions which may produce ice accretion and their affect on the vehicle as a whole. This is followed, wherever possible, by full-scale rig tests at these critical conditions and, finally, flight tests are performed in real icing environments. The total programme should be agreed between the aerospace manufacturer and the airworthiness authorities, but the demonstration of satisfactory operation under simulated conditions is the sole responsibility of the manufacturer under the scrutiny of the appropriate authority's officials or their delegates.

All three regulatory authorities refer to the same two standard wet icing atmospheres detailed in Refs 5 to 8. These are the Maximum Continuous icing conditions relating to long tracts of stratiform cloud and the Maximum Intermittent icing typical of short span cumuliiform cloud, illustrated in Fig 1. Both are based on a statistical treatment

of actual meteorological data by the National Advisory Committee in Aeronautics (NACA) contained in Refs, 6, 7 and 8. Ref 6 gives two sets of curves depicting cloud liquid water content (LWC) versus mean effective droplet diameter or volume median diameter, (VMD), over an ambient temperature range of 0°C to -30°C for continuous maximum icing and 0°C to -40°C for intermittent maximum icing. Ref 7 gives two curves of LWC factor versus cloud horizontal extent to allow for duration of flight in icing conditions and Ref 8 is the source for plots of ambient temperature versus pressure altitude.

The spectrum of droplet sizes to be employed for demonstrating compliance with icing regulations is not strictly defined. Probably because it would be very difficult, if not impossible, to simulate the range of sizes which occur in real clouds. The droplet spectra tabled in Def Stan 00-970 and AC 20-73 all plot as normal distributions and are aimed at the theoretical assessment of the icing hazard in terms of water catch rate (20 micron droplets) and water impingement limits (50 micron droplets).

At Pyestock, the practical operating conditions recommended for the air blast spray nozzles are those which produce a near normal size/volume distribution; that is, as far as possible, bimodal distributions are avoided as giving unrepresentative icing conditions.

In general, the icing test requirements for the civil aircraft authorities quoted show very close agreement and it would appear that there is a gradual convergence towards a common policy covering all aspects of clearance to operate in natural icing conditions.

The main differences at the moment lie in the requirements for the simulated conditions for testing rotorcraft and those for testing turbine engines. In the former, the CAA has reduced the severity of the icing atmosphere below 3000 m from that quoted in Refs 3 to 6. In the latter, whereas the CAA/JAR requires simulated altitudes, forward speeds and engine powers for the flight regime under scrutiny, the FAA states that compliance with regulations can be adequately demonstrated over a range of engine powers at ground level static conditions but with considerably increased liquid water concentrations.

3 DESCRIPTION OF ICING FACILITIES

The altitude test facilities at Pyestock, pictured from overhead in Fig 2, consist

of five test cells which are provided with air from a central compressor house at the pressure and temperature corresponding to the required altitude and Mach Number conditions. Exhauster-compressors in the same building extract the exhaust gases and depress the pressure in the test chamber to the required altitude. The test vehicle, be it aero engine or test rig, is mounted in the test cell and measurements of pressures, temperatures, fuel flow, thrust, etc are taken by a computer-controlled data-gathering and analysis system.

Of the four test cells currently in commission, two have the capability of conditioning their inlet air to the sub zero temperatures required for simulating icing conditions. These are Cells 3 and 3 West, the former being used primarily for testing military engines and the latter for testing large civil fan engines. For wet icing tests a water spray rake is mounted in the cell air inlet duct which is used to inject a cloud of water droplets into the airstream ahead of the test vehicle. An installation diagram of such an arrangement is shown in Fig 3. Both facilities have large test chambers; Cell 3 is 6m diameter and Cell 3 West, which has a diameter of 7.6m, is big enough to accommodate a helicopter fuselage (less rotors) as well as the latest civil fan engines. A majority of the aero engine testing is done in the connected mode, in which all of the inlet air flows through a duct into the front of the engine. Whenever plant capacity allows, however, it is preferred to test engines in conjunction with their intakes in the free jet mode, a method which is always applied to helicopter rigs. For this technique, air is discharged from a subsonic nozzle to envelope the test vehicle thus giving a better representation of the free-stream flow field presented to it.

There are significant differences between the two cells in the way the inlet air is conditioned, which affects the test envelopes that can be covered and the relationship between the simulated and natural icing conditions. In Cell 3, air is drawn from atmosphere and dried by passing through silica gel beds into the facility compressors, which then feed a proportion of the high pressure air after a further drying process into a cold air turbine (CAT) thereby reducing its temperature to a minimum value of -70°C . This is then mixed with warm air in a chamber adjacent to the test cell to produce the required inlet air temperature. In Cell 3 West, air is induced from atmosphere into a 3-stage

cross-flow heat exchanger containing pipes through which an aqueous ammonia solution at temperatures down to -52°C is circulated. The ammonia is stored in two 500 tonne capacity insulated tanks which provide a reservoir to maintain cold conditions for the duration of a test. The tanks are recharged by a refrigeration plant over a 24-hour period. Thus, whereas Cell 3 can be provided with cold air for periods of 3 to 4 hours, limited only by air drying capacity, the duration of tests in Cell 3 West is limited by the rate of circulation of the stored coolant to between half an hour and three hours. The actual time 'on condition' is determined by the required air mass flow, its temperature and the quantity of water in the ambient atmosphere.

In Cell 3 West, the consequence of not drying the inlet air prior to entering the cooler is that some of the entrained water vapour is deposited on the cooler tubes in the form of frost which progressively builds up until its effect on the natural frequency of the tubes is to cause them to resonate in the air stream leading to curtailment of the test. This phenomenon is a function of the atmospheric water vapour content, air flow, air inlet temperature and duration but is restrictive in practice only on the largest civil fan engines at lower altitudes, ie where air flow demand is greatest. The frost particles also have a tendency to shed suddenly when the air flow is increased, such as during a slam acceleration of the engine under test, unintentionally producing a dense cloud of ice particles which is unrepresentative for the scheduled wet icing test.

A further difference between these two inlet conditioning systems is the effect on humidity. Ideally, the relative humidity of the air should be between 85 to 95% at the point where the droplets are injected so as to minimise the evaporation of droplets. Cell 3 has an advantage in this respect as the air is initially dried and brought up to the desired humidity using a steam injection system. Cell 3 West, on the other hand, has to accept whatever humidity levels occur following partial freeze-drying of ambient air during its passage through the cooler. Experience shows, however, that by avoiding icing tests on particularly humid or very dry days, and even choosing most favourable times of the day, that this is not a too serious drawback. Humidity is monitored using a Michell cooled mirror dew point probe placed in the low velocity air upstream of the spray rake which provides dew point temperatures from which

the relative humidity at the water spray rake is then automatically calculated.

The icing cloud is produced by a number of air blast water spray nozzles placed in horizontal rows about 127 mm apart on an array of arms forming a sturdy structure, which contain the water feed and air supply to individual nozzles. Fig 4 shows a typical installation of a spray rake. Three rake assemblies are available ranging from one with 37 nozzles for a 0.9 m dia duct to one with 242 nozzles for a 2.4 m dia duct. A new rake for the future family of large civil engine will require 310 nozzles for a 2.64 m dia duct. The water supply is demineralised and held in a tank at about 20°C pressurised to 690 kPa (100 lb.in² abs), flow being controlled by remotely-operated valves. The water injection system is deceptively complicated and has been the subject of extensive development at Pyestock over many years, justifying a separate description of it and its calibration in the following sections.

The overall spray pattern of the various water injection rakes is checked in the test chamber. This is achieved by mounting a target grid of rods downstream of the spray rake and blowing air at a temperature no higher than -15°C with both high and low water flow rates. The low temperature ensures that all droplets impacting on the grid will freeze and the resulting ice accretion pattern when examined after 3 to 5 minutes of water injection gives an excellent indication of the uniformity of the spray.

Dry ice particles are introduced into the test cell in a totally different way, upstream of the water spray rake. They are produced by milling ice blocks which have been moulded and then cured for several days at -20°C. The required number of cured blocks are loaded onto a variable speed conveyor inside a pre-cooled chamber and are moved into contact with a variable speed multi-blade cutter. The resulting ice particles, which are approximately 1 mm in size, are collected and fed into the main airstream through 26 distribution tubes of varying lengths.

Before dealing with the subject of producing and measuring water droplets, mention must first be made of the extensive facilities for viewing ice accretion and its subsequent shedding from the test vehicle. Five channels of closed circuit TV are available for remote viewing and recording on tape. One of these channels can provide a strobed view of rotating parts, such as the fan blades

or entry spinner of an engine. Remotely operated high definition still camera shots are also taken for record purposes, typical of which is Fig 5, whilst high-speed cine up to 1200 frames per sec is available for recording the ice shedding and resulting particle trajectories associated with the post-icing engine accelerations. For connected tests, camera viewing windows are mounted in the inlet duct. These are kept frost and mist free by electro-thermal heating.

4 PRODUCTION AND MEASUREMENT OF WATER DROPLETS

4.1 Spray nozzle

Airblast atomising nozzles are used to produce a cloud of water droplets, a typical nozzle being shown in Fig 6 comprising a central water nozzle surrounded by an annular air passage. Three different sizes of water nozzles are currently available depending on the LWC range required. The water jet emerges at a low velocity compared with its enveloping air jet, this high relative velocity promoting the break-up of the water into fine droplets. A noteworthy feature of this nozzle is the protrusion of the water nozzle from the air cap face, which allows the water flow to be set largely independently of the airflow although there is some increase in water flow with atomising air pressure due to the 'ejector' effect. If, as in some nozzle designs the water nozzle is withdrawn into the air cap, then the water flow can be strongly influenced by the atomising air pressure.

The other main parameter in producing the required droplet VMD is the atomising air pressure. This is measured by means of hypodermic tubes inserted into two of the control spray arms connected to separate pressure transducers, ensuring that the pressure is measured as near as possible to the actual nozzles. Because of the low airflow rates, the arms act as plenum chambers. The mean of these measurements is taken as representative of the whole rake and the atomising air pressure is set using the difference between this and the rake duct static pressure.

4.2 Water flow control

The control and accurate measurement of the water flow through the spray rake is important both for the realisation of the specified LWC and the production of correct droplet VMD. The water flowmeters used for this purpose are either of the Pelton wheel or turbine type and are calibrated before each icing installation

using a dedicated traceable gravimetric calibration system. On the large rake there is a fundamental problem in that a head difference of up to 2.4 m between the top and bottom arms causes unequal water flows if not corrected. The current method of solution uses constant level weir chambers on each arm in which the water levels are maintained by optical sensors controlling valves in the water feed line, shown in Fig 7. The water is displaced from the chambers by pressurising them with nitrogen gas. Whilst very successful in producing equal flows to the spray nozzles, this system is subject to pulsations in the water supply to the weir chambers caused by the continual opening and closing of the valves in the feed lines. This has made the on-line measurement of total water flow difficult. New improved methods of flow control are currently under development.

4.3 Spray calibration facility

The water droplets should preferably be measured in the test cell close to the test vehicle, but in practice this has not been found to be feasible in a large-scale engineering environment not conducive to the use of delicate instruments. The alternative solution is to calibrate individual spray nozzles in a separate facility. At Pyestock, this comprises an open circuit wind tunnel having a 0.37 m² working section connected to exhausters compressors with capacity to generate up to 80 m/s air velocity over a twin nozzle spray mast, as shown in Fig 8. A laser particle-sizer produced by Malvern Instruments is mounted at the side of the working section with its beam directed through the droplet cloud shown in Fig 9. This instrument's principle of operation is the measurement of the diffracted laser light pattern generated by the droplet cloud intercepting the laser beam, Ref 9. The pattern is then converted into a droplet volume spectrum by Malvern Instruments proprietary software using an Olivetti computer. A typical computer output showing the spray analysis is shown in Fig 10. As can be appreciated, this widely accepted instrument, Refs 10 and 11, is a major advance on earlier techniques based on the use of oiled or coated glass slides on which droplets were captured and photographed for later analysis. The laborious task of sizing a few hundred droplets under a microscope against a standard graticule did not lend itself to accurate and repeatable measurements of a large number of samples. The laser instrument, on the other hand, is non-intrusive, on-line, counts many

thousands of droplets in a few seconds and can be operated remotely.

Various lenses can be used with the instrument covering different particle size ranges and working distances. The latter is defined as that distance from the lens which must contain all the spray. Experience has shown that the best working arrangement is with a 300mm lens giving a working distance of 400mm and a particle (droplet) size range of 5.8 to 564 microns. This working distance accords well with the 610mm tunnel width. The lower droplet size limit of 5.8 microns is not a disadvantage in practice as any volume of liquid contained below this size would generally be a very small proportion of the total in the distributions typically used for icing cloud simulations. Additionally, the Malvern software takes some account of the undersize droplets.

The Malvern particle sizer has become a widely accepted method of particulate measurement and is generally self checking in that mis-alignment or dirty lenses are immediately obvious. However, a Verification Reticule is also used as an additional functional check. This consists of an optical glass flat which can be attached to the receiving lens of the particle sizer on which about 10000 chrome dots of known sizes are deposited randomly within an 8mm diameter circular area. The VMD of this array is initially determined by the manufacturers within a specified tolerance of ± 2 microns. If the particle sizer repeats this measurement within the above tolerance then it can be concluded that the system is functioning correctly. With such a complex opto-electronic system this alone is of great worth. However, initially it was thought that the reticule might also serve as a much needed transfer standard for forward diffraction particle sizers. Unfortunately, a thorough investigation by the National Physical Laboratory (UK) showed that this was not feasible for various reasons, eg the random overlapping of the dots make the accurate independent calculation of the VMD impossible.

5 TYPICAL SPRAY NOZZLE CALIBRATIONS

5.1 Nozzle characteristic curves

The presentation of spray calibration facility results in the form of nozzle characteristics (Fig 11) at constant water flow rates has marked advantages. The data gathering is expedited by only needing to change the air pressure significantly at each test point. Generally, the whole curve can be covered

in about thirty minutes of testing with about fifteen test points. The form of the line is well defined with little scatter making for excellent overall accuracy. The asymptotic curves clearly show the operational limits of the nozzles. For instance, a required VMD becomes impossible to achieve above a certain water flow for a given size nozzle irrespective of atomising air pressure. If the LWC is too high, a larger (water) nozzle becomes necessary to produce a 20 micron VMD, say.

This is further illustrated by the 20 micron working curves shown in Fig 12 comparing four different size nozzles. These show that the limit of water flow which can produce a 20 micron VMD varies from 10.4 litre/h for a 0.41 mm dia nozzle to 16.3 litre/h for a 0.91 mm dia nozzle.

5.2 Effect of main stream air velocity

As well as the main parameters of water flow rate and atomising air pressure, it has been observed that the main air stream velocity over the spray rake also influences droplet size, which reduces as air velocity increases. The reason for this is not fully understood, but may be due to the increased turbulence causing secondary atomisation. An investigation of this effect was thus undertaken and the results of VMD vs tunnel air speed over a range of nozzle water flows are shown in Fig 13. It can be seen that this effect is quite appreciable which justifies the use of a tunnel for such work rather than operating in still air. One interesting feature of these results is that the higher the water flow the earlier, in terms of air speed, does the effect commence. A factor in this may be the increasing momentum of the water jet allowing it to persist, so giving the secondary turbulence longer in which to have an effect.

5.3 Effect of main stream air temperature

As the demineralised water supply fed to the spray rake is maintained at 20°C to prevent it freezing before or on reaching the nozzle, it may be questioned if the droplets have become supercooled and/or reached air stream temperature by the time they arrive at the target, as they would in a natural cloud. This is important because Ref 12, for instance, shows that ice accretion takes different forms depending on the state of the droplets at impact. Theoretical studies at Pyestock, some results from which are given in Fig 14, suggest that while a 10 micron droplet comes to thermal equilibrium in a

-5°C air stream in under a metre or so, a 30 micron droplet with 27 times more mass, might require 5 metres, although it would still be supercooled within about a metre.

From this point of view, the separation between the spray rake and the target needs to be greater than 5 m to ensure representative ice accretion, especially with a broad droplet spectrum or a VMD greater than 20 micron.

An intrinsic problem with this theoretical analysis is that the initial heat transfer is strongly dependant on the droplet to air stream relative horizontal velocity. As the emergent water jet, before break-up, is surrounded by the (warm) atomising air it cannot be known precisely at what velocity the drop is actually formed and exposed to the cold air stream. The way round this has been to consider the two possible extremes of initial droplet velocity, ie zero and main air stream velocity, and produce two cooling curves where the true state of affairs lies somewhere in-between. For the purposes of this paper and to illustrate simply the comparative thermal history of three different drop sizes, only the zero velocity case has been presented.

6 CONCLUDING REMARKS

Although a solid data base on the Pyestock spray nozzles has been achieved there is considerable scope for further work mainly through extending the capability of the spray calibration facility.

The present air velocity limit of 76 m/s is not fully representative of the velocities used in the actual icing tests, and as previously mentioned, this parameter can affect the droplet VMD. It is intended to increase this velocity by reducing the tunnel area by means of an insert. This will consist of a tube of 0.4 m dia supported and sealed centrally in the existing tunnel. Provision will be made for the Malvern transmitting and receiving lenses to be sealed into this tube. In this way the tunnel air velocity can be increased to 150 m/s.

All the measurements reported on here have been made with the spray bar 0.7 m from the laser beam. This distance is often exceeded in icing tests and the effect of this is not known and needs to be investigated. Increased evaporation or coalescence may occur, changing the VMD. The present tunnel arrangement only allows fairly small changes in this sampling distance and therefore a scheme has been suggested whereby a group of nozzles is

supported on a 'sting'. This sting is then introduced at the mouth of the tunnel and can be inserted varying distances downstream into the working section of the tunnel, giving a maximum separation of 4.8 m.

As the tunnel air velocity and the nozzle to laser beam distance increases so does the spray become more diffuse. On the standard Malvern instrument it is necessary for the spray to obscure 10 to 30% of the laser beam to give sufficient scattering signal. Because of the very low water flows sometimes specified in the icing tests, even the use of two spray nozzles has not always allowed this criterion to be strictly satisfied. For this reason the Pyestock particle sizer has had an extra amplification stage fitted allowing the obscuration to go as low as 2%.

However, it is envisaged that with the increased tunnel speed and separation even this may not be sufficient. Therefore the enhancement scheme will provide two representative groups of five and seven nozzles. These will be sting mounted complete with their air and individual water supplies, and will afford the option of choosing any number of active nozzles within each group thereby permitting the obscuration to be adjusted depending on water flow rate, target distance and tunnel air velocity.

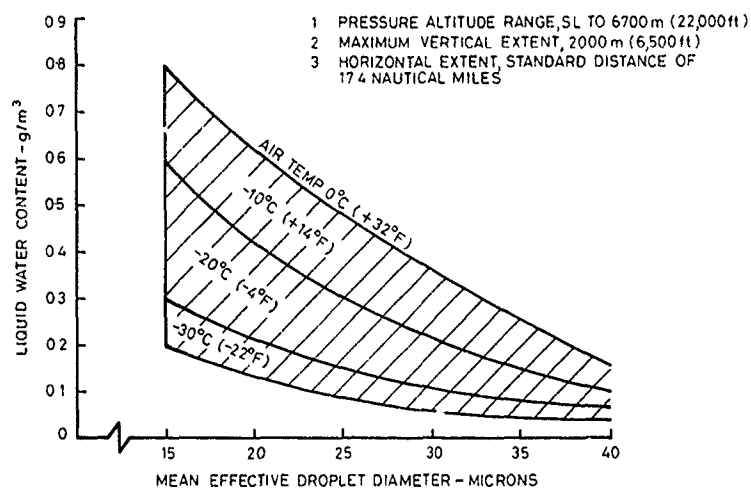
Future work at RAE will thus continue to be aimed at meeting customer requirements and satisfying the evolving demands of the international regulatory authorities. In this respect, a document about to be published by the FAA entitled "The Aircraft Icing Technology Handbook" should stimulate international efforts towards producing a single comprehensive set of icing requirements aimed at worldwide application. International effort might also be appropriate to update the existing icing cloud characteristics bearing in mind that these are based on data gathered nearly forty years ago using flight instrumentation far less precise than modern equipment. Perhaps this should be extended to other parts of the globe not previously surveyed. The test facilities at Pyestock could play a role in this work by evaluating the latest flight-standard instruments.

REFERENCES

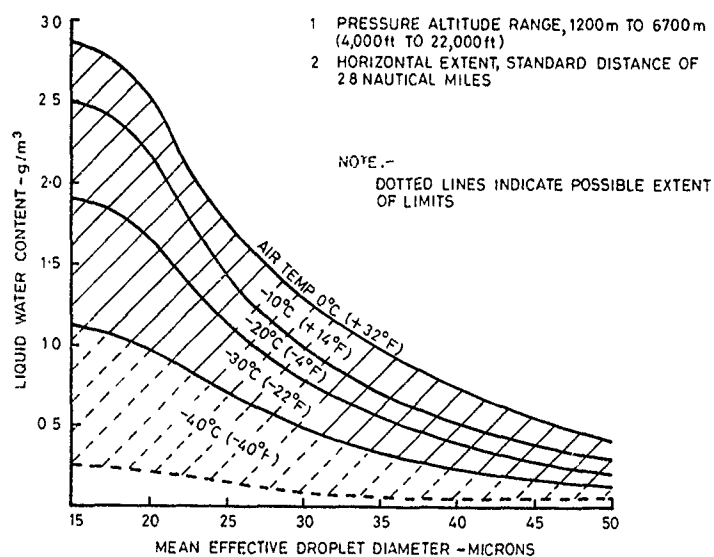
- 1 Defence Standards: 00-970 Vol 1 Aircraft, Vol 2 Rotorcraft and 00-971 Engines, 1983

- 2 Joint Airworthiness Requirements: JAR-2S large aircraft and JAR-E engines, 1986.
- 3 British Civil Airworthiness Requirements: BCAR 29 rotorcraft (post 17.12.86), BCAR-G rotorcraft (pre 17.12.86) and Paper G610 Issue 2 18.9.81 rotorcraft.
- 4 Federal Aviation Regulations: Airworthiness Standards Part 25 transport category airplanes, Part 27 normal category rotorcraft, Part 29 transport category rotorcraft and Part 33 aircraft engines.
- 5 Aircraft ice protection. FAA advisory circular AC 20.73 1971.
- 6 Continuous maximum and intermittent maximum atmosphere icing conditions: liquid water content versus mean effective drop diameter. NACA TN 1855, 1949.
- 7 Continuous maximum and intermittent maximum atmospheric icing conditions: liquid water content versus cloud horizontal distance. NACA TN 2738, 1952.
- 8 Continuous maximum and intermittent maximum atmospheric icing conditions: ambient temperature versus pressure altitude. NACA TN 2569, 1951.
- 9 Swithenbank, et al, "A laser diagnostic technique for the measurement of droplet and particle size distribution". Progress in Astronautics and Aeronautics 53 (1977) 421.
- 10 Dodge, L.G. and Cerwin, W.A., "Liquid particle size measurement techniques". ASTM STP 848 edited by Tishkoff, Ingebo and Kennedy, 1984.
- 11 Ugur Tuzun, Farhad A Farhadpour, "Comparison of Light Scattering with other Techniques for Particle Size Measurement". Particle Characterization 2 (1985) p104-112.
- 12 Marck, C J and Bartlett, C S., "Stability relationship for waterdroplet crystallization within NASA Lewis icing spray nozzle". AIAA-88-0289 26th Aerospace Sciences Meeting, Nevada, 1988.

Copyright ©, Controller HMSO London (1990)



STRATIFORM CLOUDS



CUMULIFORM CLOUDS

FIG 1 CLOUD CHARACTERISTICS



FIG 2 AERIAL VIEW OF TEST FACILITY

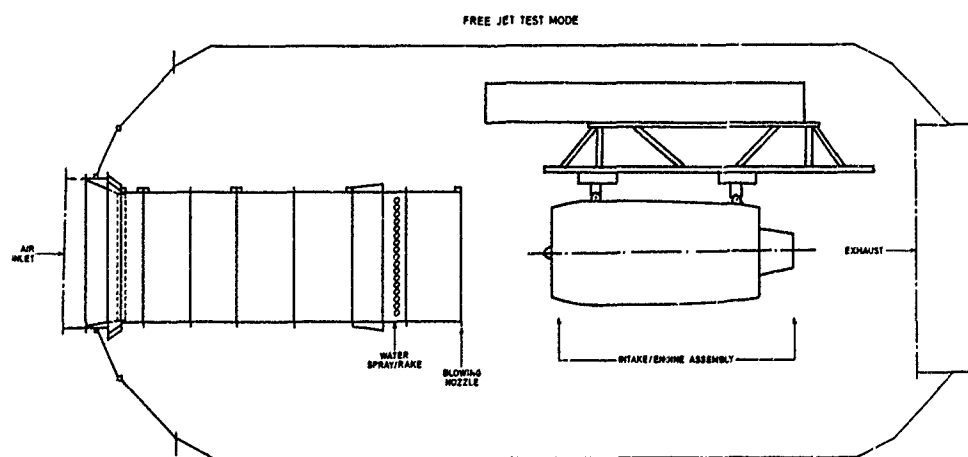


FIG 3 TYPICAL ENGINE INSTALLATION

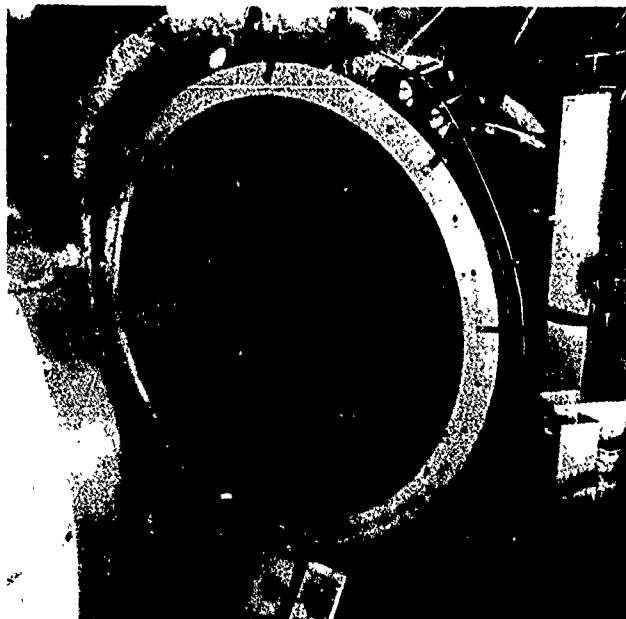


FIG 4 SPRAY RAKE INSTALLATION



FIG 5 ICE BUILD-UP ON ENGINE INLET

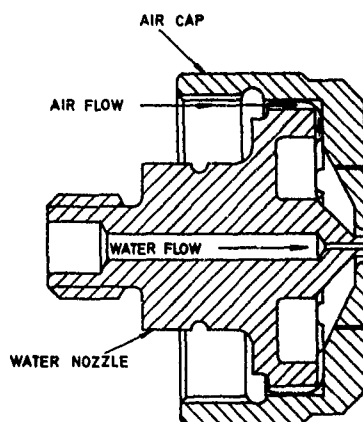


FIG 6 TYPICAL SPRAY NOZZLE

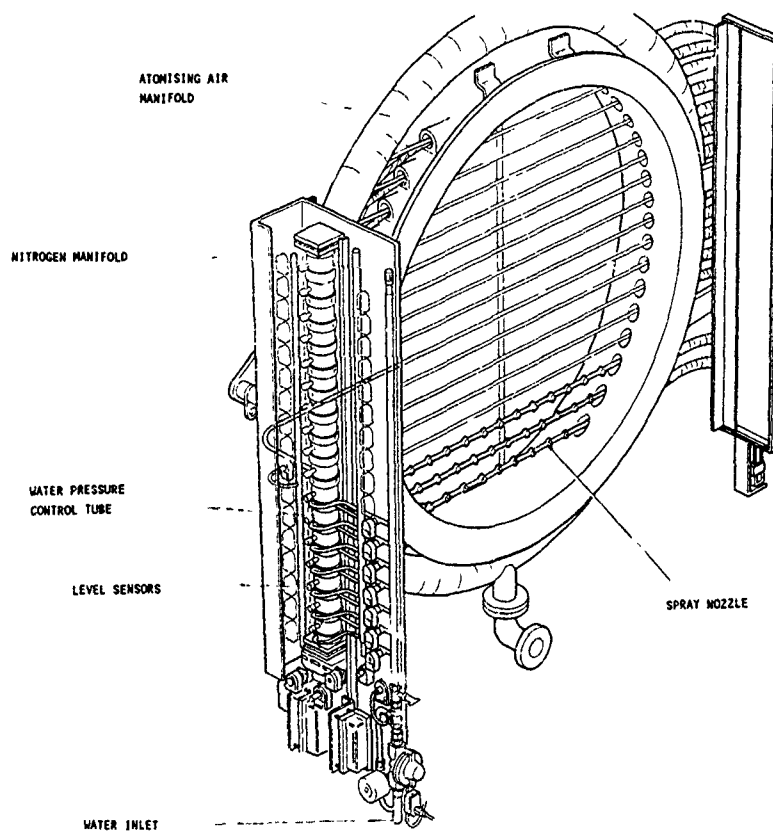


FIG 7 SPRAY RAKE AND CONTROL SYSTEM

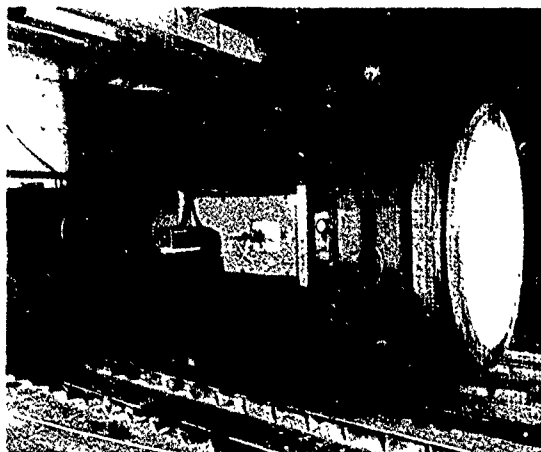
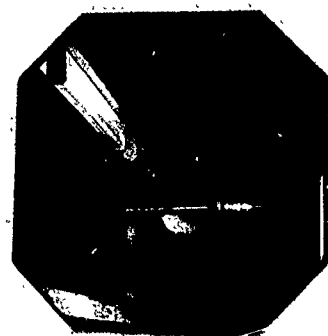
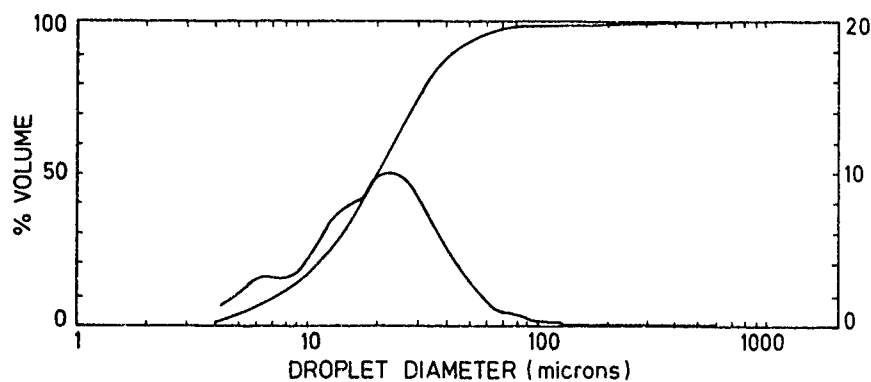


FIG 8 SPRAY CALIBRATION TUNNEL

FIG 9 TUNNEL
WORKING SECTION

Malvern Instruments MASTER Particle Sizer M6 10

Size microns	% under	Size band microns	%	Result source	
564.0	100.0			Record No.	= int0604
261.6	100.0	564.0	261.6	Focal length	= 20
160.4	99.9	261.6	160.4	Experiment type	= 300 mm
112.8	99.8	160.4	112.8	Volume distribution	
84.3	99.5	112.8	84.3	Beam length	= 14.3 mm
64.6	98.2	84.3	64.6	Obscuration	= 0.0338
50.2	94.9	64.6	50.2	Volume Conc.	= 0.0012%
39.0	88.2	50.2	39.0	Log Diff.	= 2.74
30.3	76.8	39.0	30.3	Model Indp	
23.6	61.1	30.3	23.6	D(v,0.5)	= 20.0 um
18.5	45.0	23.6	18.5	D(v,0.9)	= 41.2 um
14.5	31.8	18.5	14.5	D(v,0.1)	= 7.3 um
11.4	21.1	14.5	11.4	D(4,3)	= 22.1 um
9.1	14.4	11.4	9.1	D(3,2)	= 14.7 um
7.2	9.8	9.1	7.2	Span	= 1.7
5.8	5.3	7.2	5.8	Spec. surf. area	
				0.4361 sq. m./cc.	

System number 1973 Diode jp035A

FIG 10 SPRAY DROPLET SIZE DISTRIBUTION

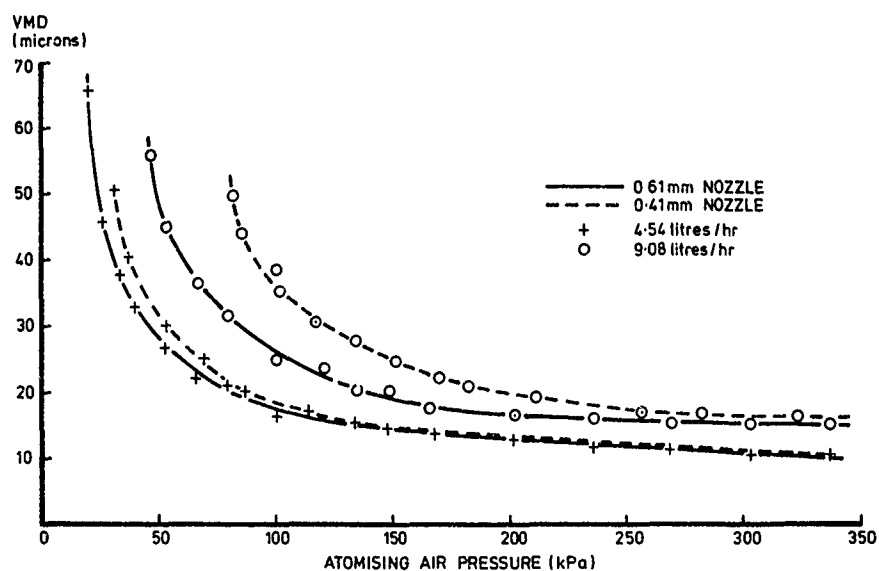


FIG 11 SPRAY NOZZLE CHARACTERISTICS

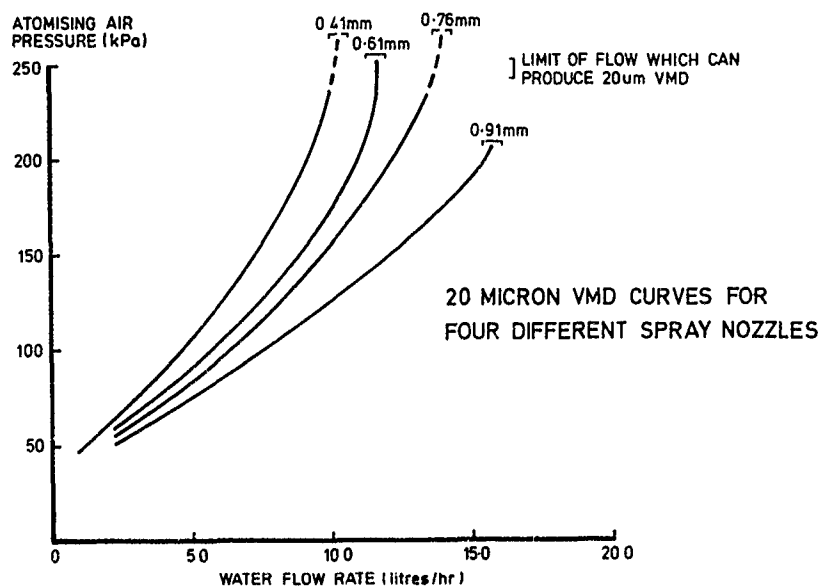


FIG 12 EFFECT OF SPRAY NOZZLE SIZE

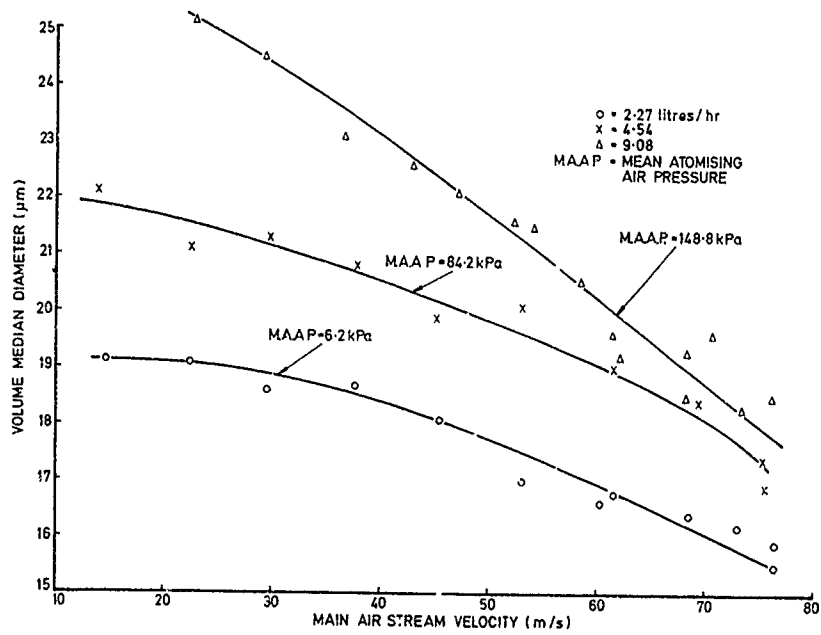


FIG 13 EFFECT OF TUNNEL VELOCITY

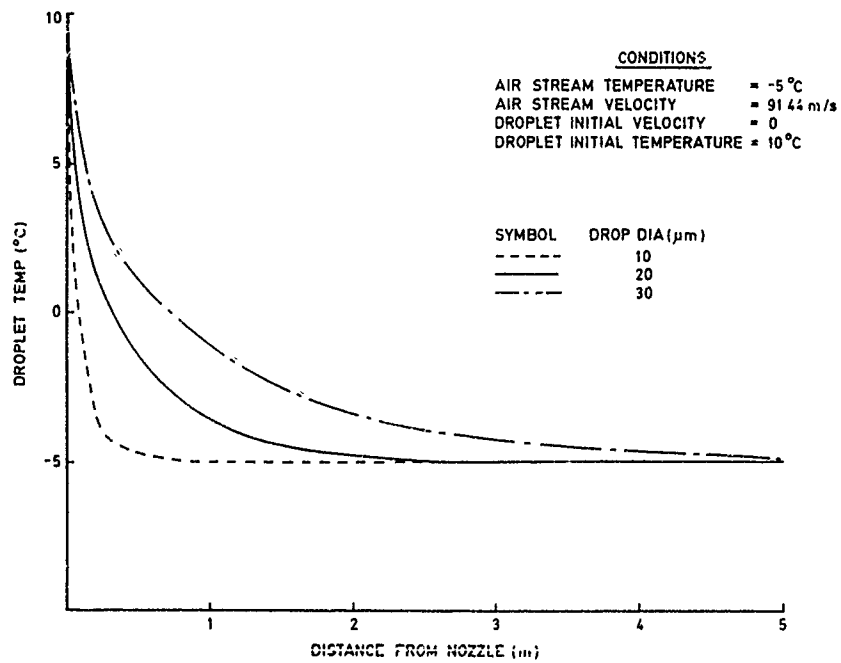


FIG 14 DROPLET TEMPERATURE REDUCTION

Discussion

1. W. Grabe, NRC Ottawa

Are the nozzles on a horizontal bar individually controllable and have you found flow graduations from the inlet to the outlet side?

After calibration of a nozzle in a calibration tunnel, do you check it in a test situation and do you then adjust for differences?

Author:

The water flow to individual nozzles is not controlled during a test, but the nozzles could be blanked off prior to a test if some bias to the cloud pattern is required. A metal grid is used to collect ice downstream of the spray nozzles to check whether the distribution meets the requirements.

We do not check the calibration done in the wind tunnel against measurements taken in the test chamber, as the latter presents a harsh environment for precision measuring equipment. The most influential parameters (air velocity, atomizing air pressure) are controlled in the calibration tunnel, and we have no evidence that additional droplet size measurements in the test chamber are justified.

2. E. Brook, Rolls Royce

You have looked at the variation of droplet size with air velocity in your calibration tunnel, but your calibration is carried out at sea level. Have you looked at the variation of

droplet size during the tests at high altitude?

As you have not, are you satisfied that the parameters you use for setting up the droplet size give correct droplet sizes during the tests at high altitudes?

Author:

It is the practice at RAE to allow for the effect of low pressure at altitude on atomization performance by testing nozzles in a low pressure chamber. However, by setting air pressure by the pressure difference between ambient and nozzle air supply we are confident that calibration in the wind tunnel is applicable to altitude.

3. C. Scott Bartlett, Sverdrup Technology

In reference to your data showing a strong influence of droplet injection station air velocity on test section droplet size, could you comment if this result could be attributed to instrument error and, if not, can you offer an idea of what process might cause the effect?

Author:

RAE are confident that instrument error is not responsible for the influence of air velocity on mean droplet size when using the Malvern instrument, although some other instruments are known to be sensitive to droplet velocity. This is a result of the basic principle of operation of the Malvern instrument that produces a stationary diffraction image of a moving droplet. The effect could result from the reasons mentioned in paragraph 5.2 of the paper.

ENTREE D'AIR D'HELICOPTERES PROTECTION POUR LE VOL EN CONDITIONS NEIGEUSES OU GIVRANTES

par
Xavier de la SERVETTE
et
Philippe CABRIT

AEROSPATIALE
Division Hélicoptères
13725 Marignane Cedex
France

ABSTRACT

La fonction principale d'une entrée d'air est d'assurer l'alimentation correcte du moteur ; de plus, celle-ci doit assurer la protection du moteur contre les effets de l'humidité atmosphérique et des objets extérieurs, afin de garantir la sécurité du vol quelles que soient les conditions extérieures. Le comportement des différents types d'entrée d'air utilisés sur hélicoptère en conditions de neige et de givre est présenté, en insistant sur les conditions critiques liées à chacune des solutions. L'expérimentation étant indispensable pour l'étude de ce type de phénomène, des moyens d'essais spécifiques ont été développés ; ils permettent maintenant de simuler toutes les conditions critiques de neige ou de givre identifiées ; la qualité de simulation a été prouvée par des essais de recoupement en conditions naturelles.

1) INTRODUCTION

Le vol tout temps sans restriction opérationnelle est un objectif inéluctable pour tout véhicule aéronautique. Les hélicoptères n'échappent pas à cette règle, et les constructeurs ont certifié des appareils en condition de vol I.F.R., et, plus récemment, sans restriction en conditions givrantes.

Aujourd'hui, l'utilisation opérationnelle d'hélicoptères avec des conditions météorologiques adverses devient de plus en plus courante au fur et à mesure que les opérateurs prennent confiance dans les qualités de leur matériel.

L'ensemble des travaux effectués pour assurer la certification des appareils en vol tout temps (plusieurs années dans le cas du Puma et du Super Puma), associé à l'expérience acquise en service a permis d'améliorer de manière très significative la connaissance du comportement des entrées d'air en conditions de neige et de givrage et des risques associés à ces conditions. Un bon exemple de cette tendance est donné par l'évolution du règlement F.A.R. en ce qui concerne la protection des entrées d'air en vol sous la neige : initialement, aucune mention de cette condition n'était faite dans le règlement, et des appareils tels que le Super Frelon ont été certifiés, sans aucun essai à la neige. Puis, la notion de neige a été introduite dans les paragraphes de la FAR 27-1093 et 29-1093, et enfin, l'AC 29-2 change 2 propose des essais de démonstration particulièrement difficiles à réaliser (1 h 30 d'essai sous la neige tombante avec une visibilité inférieure à 1/4 mile...).

Le but de ce document est de synthétiser l'expérience acquise par Aérospatiale en ce qui concerne la protection des entrées d'air, en conditions de neige et de givre. En particulier, les conditions critiques de neige et de givre déterminées sur les différentes entrées d'air récemment développées par Aérospatiale seront citées. De plus, les moyens spécifiques d'essais développés récemment pour étudier et justifier les entrées d'air seront décrits.

2) CONCEPTION D'UNE ENTREE D'AIR

2.1 Fonctions d'une entrée d'air

La fonction principale d'une entrée d'air est d'assurer l'alimentation correcte du moteur en air dans tout le domaine et les attitudes de vol revendiqués pour l'hélicoptère. Un certain nombre de critères doit être respecté afin de garantir le bon fonctionnement du moteur (indices de distorsion en pression et en température en particulier) et d'autres doivent être optimisés pour améliorer les performances de l'appareil (perte de charge entrée d'air, traînée y compris traînée y compris traînée de captation etc...).

Par ailleurs, l'entrée d'air hélicoptère doit assurer la protection du moteur contre les corps étrangers (contre le sable (dans certains cas d'utilisation spécifiques où les dégradations des moteurs sont très rapides), et contre les effets de l'humidité atmosphérique).

Il convient aussi de prendre en compte l'aspect bruit externe dans la définition de l'entrée d'air.

Enfin, comme pour tous les éléments de l'hélicoptère, l'ensemble d'entrée d'air doit être réalisable en production : à un coût et une masse maximum, présenter une bonne fiabilité, et ne pas pénaliser les opérations de maintenance.

Il apparaît donc que la fonction protection contre la neige et le givre de l'entrée d'air est certes une fonction prépondérante pour la sécurité de l'appareil et indispensable à ce titre, mais qu'elle ne peut en aucun cas être le seul critère de dimensionnement ; on obtiendrait alors une "mauvaise" entrée d'air peu performante, et pouvant peut-être mettre en cause la sécurité du vol au travers d'autres critères, tels que des instabilités de fonctionnement moteur, par exemple.

2.2 Principaux types d'entrée d'air

Les différentes fonctions d'une entrée d'air étant très variées, et sa forme très fortement dépendante de l'architecture générale de l'hélicoptère (position et nombre des moteurs, forme fuselage et capotages, recirculation gaz d'échappement dans le flux rotor, etc...), et du moteur, il n'est pas possible d'envisager une forme universelle d'entrée d'air. On peut cependant dégager 2 familles :

1) Entrées d'air statique

Leur plan d'entrée est grossièrement parallèle à l'écoulement d'air en vol d'avancement (Cf Fig 1).

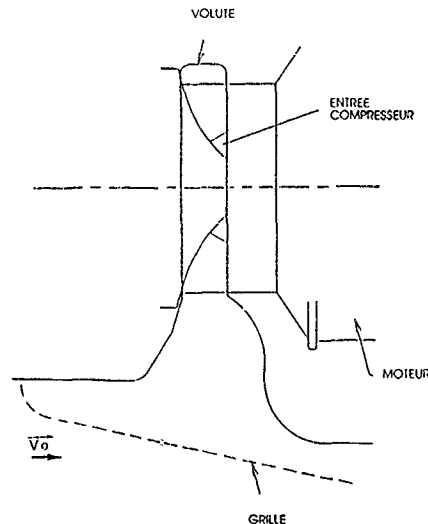


Figure 1. ENTREE D'AIR STATIQUE

Les entrées d'air statique présentent des avantages qui sont :

- simplicité
- faible masse
- moins de risques d'ingestion de corps étrangers
- traînée de l'appareil réduite par une meilleure intégration au profil du fuselage.

Bien conçue, et après optimisation, une telle entrée d'air est capable de récupérer une partie (jusqu'à 50 %) de la pression dynamique du vol d'avancement. Par contre, l'indice de distorsion des pressions dans le plan du compresseur et le risque d'absorption d'air chaud restent en général plus importants que dans le cas d'une entrée d'air dynamique.

La configuration optimale est alors définie par :

- un rayon de courbure de la lèvre amont de l'entrée d'air très important afin d'éviter le décollement des filets d'air et de récupérer une partie de la pression dynamique à grande vitesse.

Cette configuration, dans la mesure où la conception générale de l'appareil permet d'éviter la réingestion d'air chaud, constitue un excellent compromis du point de vue performances de l'appareil.

2) Entrées d'air dynamique

Leur plan d'entrée fait face à l'écoulement d'air en vol d'avancement (Cf Fig 2).

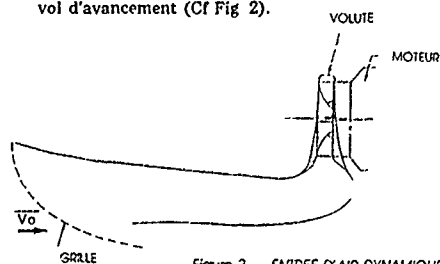


Figure 2. ENTREE D'AIR DYNAMIQUE

Les entrées d'air dynamique permettent de récupérer la pression dynamique en vol d'avancement et d'obtenir une très faible distorsion de pression dans le plan d'entrée du compresseur.

Le dimensionnement optimal est déterminé par :

- la position frontale des entrées d'air par rapport aux capots, ce qui implique parfois l'installation de longs conduits (plus difficiles à installer et plus lourds). La perte de charge propre aux conduits est alors compensée en vol stationnaire par l'absence de recyclage de gaz chauds, en vol d'avancement par la récupération de pression dynamique et la non-absorption de la couche limite,
- le profil des lèvres d'entrée d'air doit être suffisamment épais et d'une forme qui évite tout décollement des filets d'air que ce soit en vol stationnaire ou en vol d'avancement.

Les entrées d'air dynamique sont bien adaptées à des moteurs à entrée d'air axiale, et à des hélicoptères dont la vitesse de croisière est élevée.

2.3 Protection de l'entrée d'air

La fonction "protection du moteur par l'entrée est souvent globale, et il est difficile de séparer la protection contre l'humidité atmosphérique des autres cas (corps étrangers en particulier). Pour cette raison, les diverses protections sont mentionnées, mais seules celles concernant l'humidité atmosphérique sont détaillées.

Le chapitre 3 décrira les conditions précises de neige et de givre qui doivent être démontrées, mais il convient dès maintenant de rappeler les différentes formes d'humidité atmosphérique qu'un hélicoptère peut rencontrer :

- 1) La pluie, qui est de l'eau sous forme liquide, présente dans l'atmosphère en gouttes de gros diamètre, et avec une température ambiante positive. La réalisation de l'entrée d'air d'un hélicoptère doit être telle qu'il n'y ait pas de risque de drainage vers le moteur d'eau collectée sur le fuselage. Dans ce cas les démonstrations effectuées par les motoristes pour la certification moteur permettent de démontrer le bon fonctionnement.
- 2) La pluie verglaçante, qui est de la pluie survenant par une température extérieure négative. Cette configuration entraîne des captations très rapides sur l'ensemble de la structure de l'hélicoptère, et aujourd'hui, aucun hélicoptère ne peut être justifié dans ces conditions. Ce cas est donc cité pour mémoire et il ne sera pas pris en compte dans la suite de cet exposé.
- 3) Le givrage, qui est la présence d'eau liquide dans l'atmosphère à une température inférieure à 0°C, sous la forme de gouttelettes de petit diamètre (de 10 à 40 microns). L'état "eau liquide" avec une température extérieure négative étant instable, les gouttelettes se transforment en glace dès qu'elles entrent en contact avec un objet quelconque. Ce phénomène peut entraîner des captations très importantes sur la structure hélicoptère et dans les entrées d'air moteur, susceptibles d'induire des endommagements ou des arrêts moteur.

4) La neige, qui est la présence d'eau solide (glace) dans l'air à température inférieure à 0°C, sous la forme de cristaux. La forme des cristaux peut varier de manière très importante en fonction de la température extérieure et de la transformation de la neige (cas de neige soulevée par le rotor). On peut grossièrement dire que lorsque la température est basse, les cristaux sont petits et peu collants, et que lorsqu'elle est proche de 0°C, la tendance inverse peut être observée, pouvant entraîner des accumulations importantes sur la structure ou les entrées d'air.

Différents systèmes sont couramment utilisés pour assurer la protection globale des entrées d'air :

1) Système de chauffage

Le principe est simple et permet de s'affranchir des problèmes liés à l'humidité atmosphérique pour des températures inférieures à 0°C en évitant la formation de captation de glace. Il présente l'inconvénient de nécessiter des apports d'énergie importants, qui peuvent être réduits s'il est possible de seulement dégivrer périodiquement l'entrée d'air (dégivrage au lieu d'antigivrage). Il faut alors que le moteur présente une capacité d'ingestion de morceaux de glace suffisante sans dégradation du moteur et sans perte de puissance. Un moyen complémentaire de protection contre l'ingestion de corps étrangers doit être associé au simple chauffage.

2) Système à impulsion

C'est un système de dégivrage qui, au lieu de décoller les captations par chauffage, assure cette fonction par choc. Ce système n'est vraiment efficace que lorsque l'épaisseur de captation atteint plusieurs millimètres, et la majorité des petits turbomoteurs d'hélicoptère n'ont pas de capacité d'ingestion suffisante.

3) Système à inertie

Le principe consiste à donner à l'air une composante de rotation, afin de centrifuger les particules (eau, sable, corps étrangers, glace) contenues dans celui-ci. Cette mise en rotation peut être obtenue à partir d'une série de vortex montés sur un panneau (Cf Fig. 3) (très bonne efficacité au sable, mais perte de charge importante), ou bien dans l'entrée d'air moteur (I.P.S.) (Cf Fig 4) (efficacité de séparation moins bonne, mais perte de charge moins importante). Dans certains cas, des déflecteurs sont placés dans l'entrée d'air hélicoptère pour assurer cette fonction. Dans tous les cas, il est nécessaire d'y associer un ensemble d'extraction des particules centrifugées soit par ventilateur, soit par effet de trompe. Ces systèmes sont efficaces en ce qui concerne la protection contre les objets étrangers (y compris les morceaux de glace), mais il est souvent nécessaire d'y associer un antigivrage de certaines parties pour assurer une protection complète.

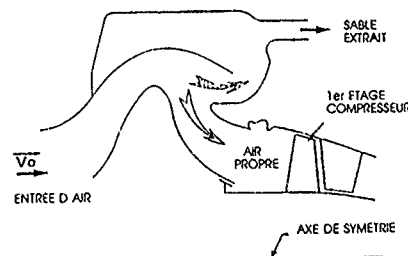
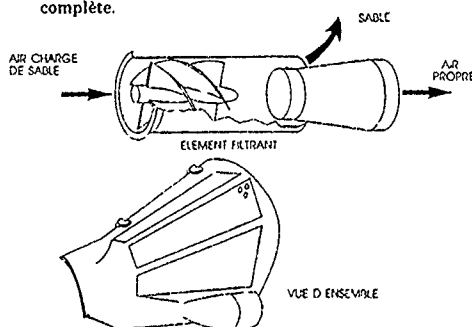


Figure 4 SEPARATEUR DE PARTICULES INTEGRE

4) Système à grille

Une grille placée sur l'entrée d'air permet de protéger efficacement le moteur contre les éléments étrangers, sauf lorsque les conditions extérieures imposent l'utilisation d'un filtre anti-sable spécifique (cas relativement limités). De plus, cette grille assure une protection efficace en condition de givrage puisqu'elle capte les gouttelettes d'eau surfondues présentes dans l'air. Pour assurer l'alimentation du moteur en cas de colmatage de la grille, il est nécessaire dans certains cas de prévoir un by-pass en arrière de la grille.

Pour le vol sous la neige, la grille protège le moteur contre l'ingestion de captations accumulées sur un point de la cellule et pouvant se détacher, par contre, elle n'assure aucune protection intrinsèque dans cette condition car la neige n'accroche pas sur la grille ; le bon fonctionnement dépend alors de la forme du conduit d'entrée d'air.

Il apparaît donc qu'une grille externe, placée sur l'entrée d'air, permet de protéger efficacement le moteur dans la majorité des cas, il existe cependant des conditions pour lesquelles cette protection peut être incomplète (neige par exemple), et des captations peuvent se produire dans l'entrée d'air. Il est alors possible de placer une seconde grille à proximité du moteur, qui évitera l'ingestion par celui-ci de captations formées dans les conduits d'entrée d'air ; différents essais ont démontré que la protection apportée par la grille externe était suffisante pour éviter tout colmatage dans l'entrée d'air ou sur la grille interne. Un exemple de protection d'entrée d'air à l'aide de 2 grilles est présenté sur la figure 5

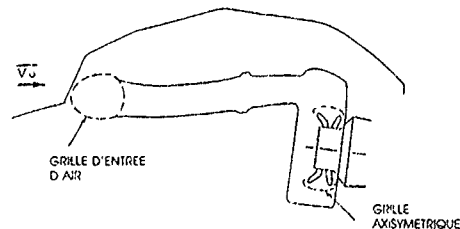


Figure 5 EXEMPLE DE SYSTEME DE PROTECTION A DOUBLE GRILLE

L'avantage principal des protections à base de grille est que la perte de charge apportée par ces dernières est relativement faible (elles ont de plus tendance à améliorer les indices de distorsion), et que c'est un système passif ne nécessitant aucun apport d'énergie et d'une fiabilité quasi infinie. De plus, la pénalité en masse est négligeable comparée aux autres solutions. Ces différents éléments ont conduit Aérospatiale à retenir ce principe de protection sur tous les hélicoptères récemment conçus, bien que leur mise au point soit plus délicate que les autres systèmes et qu'un certain nombre de conditions critiques doit être démontré.

3) CONDITIONS DE NEIGE ET DE GIVRE A JUSTIFIER - POINTS CRITIQUES

3.1 Conditions givrantes

L'atmosphère givrante est définie traditionnellement par la FAR 25 annexe C ou la FAR 29 annexe C auxquelles s'ajoutent des exigences de fonctionnement au sol en brouillard givrant (FAR 29-1093 b2).

La FAR définit les combinaisons de température extérieure, concentration d'eau, diamètre de gouttelettes, et taille de nuage qui doivent être démontrées.

D'une manière générale on peut dire que les captations sont d'autant plus importantes que la concentration est élevée, la température faible, et le temps d'exposition au nuage givrant important. Il convient cependant de rappeler que la concentration maxi diminue avec la température.

Les points critiques à couvrir, plus particulièrement au cours de la justification de l'entrée d'air dépendent largement du type de protection retenu :

- 1) Si la protection est un anti-givrage par chauffage, il est nécessaire de démontrer son bon fonctionnement dans les conditions de température minimale revendiquées, avec la concentration d'eau maximale ; de plus, la source d'énergie de chauffage doit être ajustée au niveau minimum que l'on peut rencontrer en vol (régime moteur minimum pour chauffage à P2, tension minimum pour chauffage électrique). Il peut être nécessaire, dans certains cas, de couvrir certains défauts de fonctionnement du système de chauffage si une fiabilité suffisante ne peut pas être démontrée.

On mentionnera enfin la vérification du non-endommagement de l'ensemble entrée d'air en fonctionnement à la température maximale d'utilisation du dégivrage, et avec une alimentation en énergie maximale.

Un des points devant être vérifié pendant les essais est l'absence de point froid en aval d'une zone chauffée, car la probabilité de recongélation est élevée.

- 2) Dans le cas de dégivrage par chauffage, les points exposés ci-dessus sont applicables, mais il faut y associer la recherche des conditions où le taux de captation est le plus important.
- 3) Pour un dégivrage par impulsion, deux conditions peuvent être critiques : celle correspondant au taux de captation maximum, et le cas de température proche de 0°C, avec lesquelles les captations sont relativement molles et moins sensibles aux accélérations générées par les impulsions.
- 4) Contrairement au cas des protections par chauffage, les grilles ne présentent pas de problèmes d'une manière générale à faible température : les captations sur les fils de la grille sont dures et se détachent lorsqu'elles atteignent une certaine épaisseur, ce qui permet de démontrer une durée de fonctionnement sans limitation. On doit cependant vérifier dans ces conditions qu'il n'y a pas de risque de colmatage de l'ensemble de l'entrée d'air par les captations se produisant sur la grille.

Deux cas sont à considérer :

Vol à grande vitesse ($V > 70$ kts)

Le tube de courant alimentant l'entrée d'air est concentré ce qui entraîne le passage d'une grande quantité d'air donc d'eau à travers une surface de grille faible. La zone intéressée se colmate alors rapidement et l'alimentation du moteur s'effectue alors par la zone restée propre.

Pour traverser cette zone les filets d'air sont défléchis et cela entraîne une séparation des gouttelettes avant le passage au travers de la grille, celle-ci reste claire de captation dans certaines zones (Cf Fig. 6). La formation de ce bouclier est rapide, donc peu de gouttes surfondues pénètrent à l'intérieur du conduit d'entrée d'air.

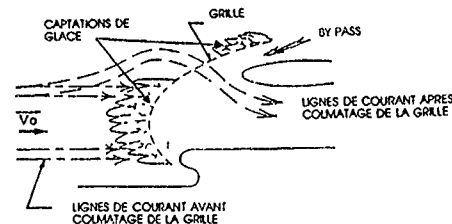


Figure 6. PROTECTION ANTIGIVRE PAR GRILLE
EN VOL D'AVANCEMENT

Vol à faible vitesse ($V < 30$ kts)

Les lignes de courant sont beaucoup plus espacées et on observe un colmatage beaucoup plus lent de la grille mais plus uniforme (Fig. 7). Si le débit d'air par unité de surface n'est pas trop élevé, la grille peut rester poreuse, les captations sur les fils du grillage assurant une déflexion suffisante pour éviter le colmatage du passage entre les dépôts de glace. Un dimensionnement adéquat de la grille ou l'installation d'un by-pass permet d'assurer l'alimentation correcte du moteur.

La formation de la protection naturelle par les captations de glace est plus lente que dans le cas de la grande vitesse ce qui entraîne la pénétration dans le conduit d'entrée d'air d'une plus grande quantité de givre. Les accumulations éventuelles doivent pouvoir être intégrées par le moteur sans trouble de fonctionnement.

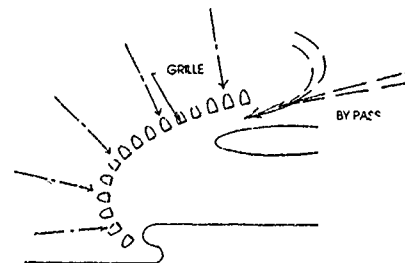
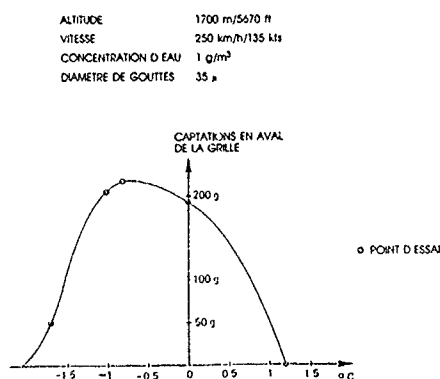


Figure 7. PROTECTION ANTIGIVRE PAR GRILLE
A BASSE VITESSE

Lorsque la température est supérieure à -5°C , la forme des captations sur la grille évolue : celles-ci deviennent beaucoup plus larges et accrochées autour des fils de grille, alors qu'à faible température, la captation se forme à partir du point d'arrêt et en amont de celui-ci ; le colmatage de la grille est souvent rapide car les vides de maille sont remplis par la glace. Ce phénomène s'explique par un retard à la congélation dû à un trop faible écart de température entre l'ambiante et 0°C pour obtenir une congélation instantanée (voir travaux de simulation de ce point dans le paragraphe 5). Pour des températures très proches de 0°C , le retard peut être suffisamment important pour que la grille capte partiellement les gouttelettes d'eau surfondue et que par contre des captations se produisent dans le conduit d'entrée d'air et puissent induire des instabilités de fonctionnement du moteur. Ce phénomène ne se produit que dans un domaine de température très étroit (de l'ordre de $1,5^{\circ}\text{C}$), et il est largement dépendant de la forme de la grille et de sa position relativement à l'entrée d'air. La figure 8 présente une courbe expérimentale donnant des captations relevées en aval de la grille en fonction de la température.

EFFET DE LA TEMPERATURE



Une attention particulière doit donc être apportée à la vérification du bon fonctionnement de l'entrée d'air à température très proche de 0°C .

3.2 Neige

Les conditions d'homologation des hélicoptères en vol sous la neige ont été précisées par l'indice 2 de l'Advisory Circular 29.2.

Outre la vérification du bon fonctionnement de l'entrée d'air pour différents types de neige et de température, il est nécessaire de faire un vol d'une heure et demie dans des conditions de précipitation extrêmes (visibilité inférieure à 400m sans brouillard représentant environ 1 g/m³), et comportant 5 mm de stationnaire en neige recirculante, ainsi qu'un 1 heure de vol de croisière, le reste du temps étant des opérations de roulage ou d'attente au sol.

Il est très difficile de trouver dans la nature des conditions de concentration requises par ce texte ; de plus, la condition de vol en stationnaire neige recirculante ne correspond pas à un cas de vol opérationnel car la visibilité dans ces conditions nulle et aucun pilote ne restera dans de telles conditions. Ceci montre donc la sévérité de exigences vis à vis des conditions réelles d'utilisation.

Les problèmes de fonctionnement en vol sous la neige d'entrée d'air d'hélicoptère peuvent être de 2 types :

1) absorption par l'entrée d'air moteur de "paquets" de neige qui se détachent de la cellule, entraînant une instabilité moteur. Tous les principes de protection d'entrée d'air efficaces contre l'ingestion de corps étrangers protègent correctement l'entrée d'air ; il peut être nécessaire de doubler les grilles dans certaines zones pour garantir un bon fractionnement des accumulations de neige. Les risques les plus importants de captation sur la structure en vol sous la neige sont présents lorsque la température extérieure est proche de 0°C (gros flocons collants) et lorsque la concentration est élevée.

Dans certains cas, un antigivrage très efficace du pare-brise peut entraîner le dégel de la neige, puis son regel sur la structure, avec formation de captations importantes.

2) accrochage de neige en un point du conduit d'entrée d'air, et développement d'une captation susceptible d'être ingérée par le moteur.

Ce phénomène n'apparaît pas systématiquement et est lié à la forme des conduits et à la température de la neige. D'une manière générale, aucun problème de développement de captation n'est rencontré lorsque le conduit ne présente pas de point d'arrêt (coude ou accident de surface) ; dans ce cas, aucune protection spécifique n'est requise. Par contre, si le profil d'entrée d'air est accidenté, il y a formation de captation liée au transfert thermique neige/paroie d'entrée d'air. Nous avons pu mettre en évidence cette relation au cours d'essais où l'on reproduisait ou non l'ambiance thermique autour de l'entrée d'air. Dans un cas, des captations très importantes étaient relevées, et dans l'autre, aucune, pour les mêmes conditions d'essai. Nous analysons ce phénomène de captation comme dû à un dégel de la neige au niveau du point d'arrêt (au contact du conduit), suivi d'un regel en aval sur un point "froid" où l'accumulation se produit.

Les conditions les plus critiques pour ce cas de figure sont lorsque la température extérieure est très proche de 0°C , et qu'il neige, ou lorsque l'hélicoptère fait un stationnaire en neige recirculante, avec une température extérieure légèrement positive ; ce dernier cas est de loin le plus difficile, car on associe la concentration de neige élevée due à la recirculation du rotor avec les conditions de température critiques.

Les protections à base de chauffage sont moins sensibles à ce problème pour des températures proches de 0°C , mais des phénomènes de dégel - regel peuvent se rencontrer à plus faible température, avec le chauffage minimum. Dans la majorité des cas, c'est ce point qui dimensionne la puissance de chauffage (il faut plus d'énergie pour faire fondre la neige que pour se protéger du givrage à isotherme extérieure). Un point favorable est toutefois à mentionner, car à faible température, les flocons sont moins denses, et impactent donc moins sur les accidents du conduit d'entrée d'air ; cet avantage n'existe qu'en neige tombante, et non pas de la neige recirculante.

Le point de neige à température proche de 0°C est aussi le point critique des systèmes de dégivrage par impulsion, car les captations sont très molles et peu sensibles au choc.

Les systèmes à inertie, de par leur forme, nécessitent une protection contre la neige (chauffage pour I.P.S.). Il est possible de s'en affranchir dans le cas des filtres type vortex en montant ces derniers parallèlement à l'écoulement d'air. Il y a alors effet de séparation de la neige en vol d'avancement.

Comme ceci a déjà été mentionné ci-dessus, les grilles sont totalement transparentes aux flocons de neige ; elles n'assurent une protection qu'en arrêtant les captations qui peuvent se former en amont de la grille.

C'est une des raisons pour lesquelles une seconde grille est montée dans certains cas au plus près de l'entrée d'air moteur ; elle évite l'ingestion par celui-ci de captations qui peuvent se former dans les conduits d'entrée d'air (voir paragraphe 2.3 et figure 5).

4) MOYENS D'ESSAIS UTILISES POUR ETUDIER LA PROTECTION DES ENTREES D'AIR

4.1. Moyens d'essais au givre :

Les essais de mise au point et de certification en givrage des entrées d'air d'hélicoptère s'effectuent depuis de nombreuses années dans des souffleries permettant de reproduire les conditions givrantes naturelles par pulvérisation d'eau dans un courant d'air froid.

En France, les essais sont effectués par le CEP_R de Saclay dans des installations (Cf Fig. 9) permettant de reproduire la vitesse de vol, la température, l'altitude, l'hygrométrie, le diamètre des gouttelettes et la concentration d'eau.

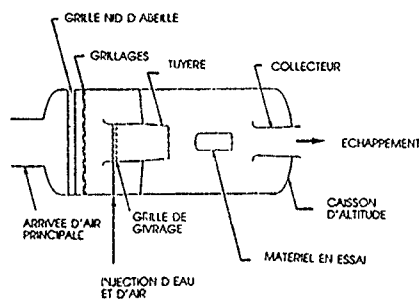


Figure 9 BANC DE GIVRAGE DU CEP_R DE SACLAY

L'essai est effectué à l'aide d'un bâti d'essai reproduisant l'installation motrice (moteur, capotages, entrée d'air et système de protection). Les conditions qui étaient utilisées jusqu'il y a quelques années pour couvrir les exigences de certification d'hélicoptère ne volant pas en conditions givrantes prévues, étaient :

Vitesse 50 à 130 kts
température -5 à -30°C

Avec l'évolution des conditions d'utilisation des hélicoptères, le CEP_R a fait évoluer les plages d'essais possibles pour entrées d'air hélicoptère.

Tout d'abord le domaine de vitesse a été abaissé à 10 kts ce qui permet une simulation satisfaisante du stationnaire. Ceci nécessite, outre l'établissement d'un écoulement stable dans la soufflerie givrante, de réaliser un nuage givrant homogène avec des quantités d'eau injectées faibles (utilisation d'un petit nombre d'injecteurs adaptés à ces conditions particulières). Afin de garantir une bonne simulation, il est apparu nécessaire de vérifier l'écoulement d'air autour de la maquette et de le comparer à celui relevé en stationnaire sur hélicoptère (visualisation par fils de laine). D'autre part les bancs d'essais ont été instrumentés et calibrés pour effectuer des essais pour une température proche de 0°C.

Dans les deux cas, il a été mis en évidence la nécessité de disposer d'un modèle théorique permettant d'évaluer l'influence des paramètres d'essai sur la qualité de la simulation au niveau de la maquette en essai.

En effet le nuage givrant est réalisé par la pulvérisation de l'eau nécessaire à température positive dans un courant d'air dont la saturation en eau peut ne pas être totale.

Pour aboutir à une simulation satisfaisante d'un nuage givrant il est nécessaire que les gouttelettes arrivent dans la section d'essai en état de surfusion (température inférieure à 0°C) à une vitesse voisine de celle de l'écoulement et que l'évaporation dans l'écoulement non saturé ne remette pas en cause la concentration d'essai. Le modèle mis au point par le CEP_R montre :

- L'importance du temps de transit entre grille et maquette pour les essais proches de 0°C, en effet une distance grille/maquette trop faible conduit à grande vitesse à un nuage ne contenant qu'une partie des gouttelettes en surfusion
- L'effet de l'hygrométrie sur la concentration pour les essais à basse vitesse et à température proche de 0°C, la concentration peut être réduite par des facteurs de l'ordre de 50 % par l'évaporation des gouttelettes entre grille et maquette. Dans ce cas la température des gouttelettes est inférieure à celle de l'écoulement.
- L'hygrométrie insuffisante, donc l'évaporation, n'a pas un effet déterminant sur les diamètres de gouttes.

Les résultats obtenus permettent de mettre en évidence les paramètres de réglage importants pour chaque type d'essai et d'apporter pour chaque point d'essai effectué les facteurs correctifs correspondant aux conditions d'essai réellement rencontrées.

Ces travaux effectués par le CEP_R à la fois sur le domaine d'utilisation des bancs d'essais et l'analyse des conditions d'essai permettent de disposer d'un moyen d'essai en givrage artificiel bien adapté aux conditions particulières des entrées d'air d'hélicoptère.

Des recoupements effectués sur différentes entrées d'air entre le comportement observé en simulation au banc et en conditions naturelles ou sur d'autres moyens d'essai, démontrent une bonne représentativité du banc CEP_R, y compris à basse vitesse à une température proche de 0°C. Ce moyen d'essai peut être exclusivement utilisé en certification.

4.2 Moyens d'essai à la neige

4.2.1 Essai en conditions naturelles :

Le seul moyen d'essai actuellement reconnu pour la certification des hélicoptères à la neige est l'essai en condition de neige naturelle. Les exigences de certification nécessitent d'obtenir les conditions suivantes :

- averse de neige importante (visibilité réduite à 400 m sans brouillard)
- durée de ces conditions : 1 h à 1 h 30
- conditions critiques de température (en général autour de 0°C).

Afin d'effectuer ces essais avec un niveau de sécurité satisfaisant, ces conditions météorologiques doivent être rencontrées dans des zones où il est possible de voler à grande vitesse avec une visibilité réduite (ce qui exclut pratiquement les zones de haute montagne).

La recherche de ces conditions obligatoirement en période hivernale peut nécessiter plusieurs semaines avec des déplacements sur de grandes distances afin de s'adapter aux évolutions de la météorologie. Pour cela, ce type d'essai ne peut être réservé qu'au parcours final de certification et il est donc nécessaire pour les constructeurs de disposer de moyens de développement permettant de s'assurer de la validité des protections choisies.

La condition de neige naturelle qui peut être trouvée le plus aisément est le vol stationnaire dans le nuage de neige soufflée par le rotor de l'hélicoptère (neige recirculante). En effet il suffit de trouver une zone recouverte de neige fraîche et un essai est possible avec une épaisseur très faible au-dessus de laquelle l'hélicoptère peut se déplacer afin d'être toujours au-dessus de la couche de neige fraîche (le souffle du rotor ayant pour effet de "balayer" la neige autour de l'appareil).

Des conditions favorables pour effectuer des essais en neige recirculante peuvent être trouvées aisément pendant la saison hivernale même après une averse de neige de faible importance. Toutefois l'obtention des conditions les plus critiques pour ce type d'essai correspond en général à une température de l'air légèrement positive, la neige ne peut alors être soulevée par le rotor que si celle-ci est restée en surface suffisamment froide pour éviter l'agglomération des flocons. Dans ce cas il est nécessaire que la chute de neige ait lieu à température négative et soit suivie d'une légère élévation de température de l'air ambiant : cette condition n'est rencontrée que rarement au cours d'un hiver, même dans une zone où les chutes de neige sont fréquentes.

Les points d'essai en neige recirculante, bien que ne permettant pas la démonstration complète nécessaire à la certification d'une nouvelle entrée d'air, peuvent être intégrés dans le programme de certification de l'hélicoptère. Il convient toutefois de faire les remarques suivantes sur ce type d'essai :

- La concentration de neige pendant un essai en neige recirculante est très élevée (de l'ordre de 3 à 4 fois celle des averses de neige les plus sévères)

- Le fonctionnement prolongé dans ces conditions (au-delà de 10 secondes) ne constitue pas une condition d'utilisation normale de l'hélicoptère. En effet il s'agit d'évoluer très près du sol en l'absence totale de visibilité, ce qui n'est possible que sur un terrain bien dégagé avec des repères au sol qui ne sont pas cachés par la neige. La phase de 5 minutes prévue dans l'essai type recommandé par la FAA permet de couvrir avec des marges très importantes les conditions normales d'utilisation dans ces conditions correspondant à l'atterrissage et au décollage sur un terrain enneigé ;

- Les conditions de vol à faible vitesse ne sont pas nécessairement, malgré la concentration plus élevée, parmi les plus sévères pour le fonctionnement de l'entrée d'air. En effet le champ aérodynamique différent, pour certains types d'entrée d'air, de celui existant en vol de croisière n'entraîne pas une concentration de neige dans les mêmes zones des conduits. D'autre part la faible vitesse d'avancement ne favorise pas l'accumulation de neige sur les mêmes zones de la structure qu'en vol rapide et ne favorise pas le détachement de ces éventuelles accumulations qui pourraient être ingérées par les moteurs.

A ce jour, les essais de certification en vol sous la neige doivent être effectués sur un hélicoptère en vol en conditions naturelles. L'expérience montre que le spectre recommandé par la FAA est un objectif très difficile à réaliser. Il est donc nécessaire de développer des moyens complémentaires de démonstration : ceux-ci peuvent comprendre des essais au banc (voir paragraphe suivant) et des essais spécifiques aux appareils. Le vol prolongé en stationnaire neige recirculante est un moyen complémentaire très efficace car il permet relativement facilement de mettre en évidence les points "sensibles" d'une entrée d'air ; des visualisations par endoscope sont une aide appréciable pour ce type d'essai. La justification d'un temps prolongé (supérieur à 10 minutes) en vol en neige recirculante apporte une grande confiance sur la qualité de la protection, mais celle-ci doit être confirmée en vol d'avancement. Par contre, la non justification d'un temps prolongé ne signifie pas nécessairement que la protection de l'entrée d'air n'est pas certifiable : il peut en effet exister dans certains cas des effets de seuil avec des concentrations élevées, au-delà desquels des captations peuvent se développer dans l'entrée d'air.

Nous considérons qu'un autre moyen complémentaire de démonstration est le vol en conditions réelles de neige, telles qu'elles peuvent être rencontrées lorsque l'équipage recherche les "conditions FAA". Il y a alors accumulation d'expérience en vol sous la neige dans des conditions de neige très diverses, avec des durées d'exposition variables, suivies ou non de réchauffage, des vitesses de vol adaptées à la visibilité, etc... Le bon fonctionnement de l'installation motrice pendant ces vols est un élément important à prendre en compte pour la justification de l'entrée d'air.

4.2.2 Essais artificiels

Il est très vite apparu indispensable de disposer de moyens d'essai artificiels pour étudier le comportement à la neige des entrées d'air, afin de réduire les coûts de développement, mais aussi pour permettre de faire des essais comparables entre eux (température ambiante, concentration, qualité de neige) et donc de juger de l'influence de différents paramètres.

Les essais peuvent être effectués sur un hélicoptère complet ou sur un bâti d'essai, comprenant l'entrée d'air et son environnement (y compris environnement thermique (Cf Fig. 10), avec un ventilateur assurant le débit d'air moteur. Cette dernière solution est de loin la plus souple, et, avec quelques précautions, permet de garantir une bonne simulation. Les essais au banc permettent de faire un grand nombre d'observations (forme et position des captations éventuelles), et de mesures (température de paroi en particulier).

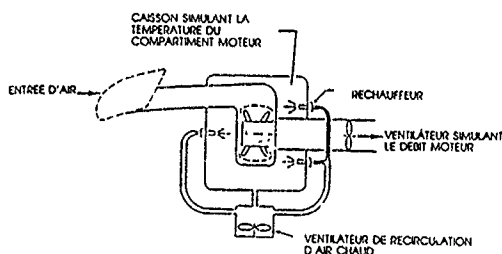


Figure 10. ESSAI MOTEUR AU BANC

La méthodologie d'essai suivante a été mise au point:

1) Méthode d'ingestion

Il s'agit de pulvériser dans l'air aspiré par le moteur de la neige à la concentration voulue. La neige est pulvérisée par brossage devant l'entrée du moteur à l'entrée du ventilateur projetant la neige dans la zone de l'entrée d'air (Cf Fig. 11). La pulvérisation de neige s'effectue par brossage manuel, cette solution qui peut paraître très artisanale permet le maximum de régularité et s'adapte aisément à tous les types de neige. Elle a donc été retenue pour tous les essais à basse vitesse. Dans le cas où l'on veut intégrer l'effet de la vitesse de l'appareil, il est nécessaire de souffler de la neige à l'amont des capotages avec un ventilateur, mais il est quasiment impossible de garantir une concentration précise au droit de l'entrée d'air.

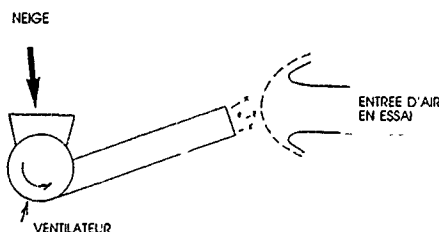


Figure 11 : INGESTION ARTIFICIELLE DE NEIGE DANS UNE ENTRÉE D'AIR

2) Neige utilisée

La neige utilisée qui est collectée avant l'essai peut être de la neige naturelle fraîche ou de la neige artificielle. Cette dernière solution permet d'effectuer les essais en chambre climatique et donne ainsi le maximum de souplesse dans le choix des conditions d'essai.

La neige artificielle est réalisée à l'aide de canons de neige utilisés dans les stations de ski (canon à eau pulvérisée et air comprimé, canon à eau pulvérisée sur un ventilateur). La meilleure qualité de neige est obtenue pour les températures d'air inférieures à -10°C . La neige fabriquée est stockée dans la chambre climatique pour être utilisée dans les heures qui suivent lorsque la température de l'essai est obtenue (en général les conditions critiques sont situées près de 0°C). Cette méthode est préférable à l'utilisation directe du canon à neige sur le matériel en essai ; en effet :

- 1) L'essai est effectué à la température désignée (y compris au voisinage de 0° et même à température légèrement positive par réchauffage de la chambre climatique juste avant l'essai)
- 2) La concentration de neige est bien maîtrisée.
- 3) Il n'y a pas de superposition de phénomènes parasites comme le givrage des grilles d'entrée d'air par l'eau surfondue contenue dans le nuage produit par le canon à neige.

Il est à noter que la neige artificielle ne forme pas de flocons et présente donc des différences par rapport à la neige naturelle tombante. Par exemple la relation traînée/masse des particules est différente (vitesse de chute dans l'air 2 à 3 fois plus importante), cet élément est donc à prendre en compte dans des dispositifs séparateurs à inertie.

Des essais de comparaison ont été effectués à iso-conditions d'essai avec de la neige artificielle et de la neige naturelle. Ces essais ont montré un comportement qualitatif identique (captations aux mêmes endroits) mais quantitativement légèrement différent (captations plus sévères avec de la neige artificielle). Ceci peut s'expliquer par :

- 1) Des impacts plus nombreux sur les parois des conduits coudés (déflexions moins importantes des particules).
- 2) Un accrochage plus facile des particules sur les aspérités des parois
- 3) Echange thermique plus facile entre cristaux et parois favorisant la fusion partielle de l'eau et donc l'adhésion de la particule.

D'autres essais ont été effectués afin de comparer les résultats obtenus au banc avec ceux de vol. On retrouve globalement le même écart qu'entre essai en neige naturelle et en neige artificielle.

L'expérience accumulée au cours des années récentes nous amène dorénavant à mettre au point la protection à la neige de l'entrée d'air au banc, puis de vérifier en vol le bon fonctionnement de la protection. Cette démarche a été suivie sur 3 installations motrices différentes et aucun comportement particulier non décelé au banc n'a été noté au cours des essais en vol.

5) CONCLUSION

La part des travaux de développement d'une entrée d'air liée à la protection contre la neige et le givre a très nettement augmenté au cours des dernières années. Initialement, les études ont été menées de manière très empirique, à partir d'essais effectués directement sur hélicoptère. Ce moyen d'investigation étant très limité, des bancs d'essai spécifiques ont été développés afin de simuler toutes les conditions critiques connues. Ces bancs apportent des résultats suffisamment fiables pour permettre à eux seuls d'effectuer toute la certification en conditions givrantes de l'entrée d'air, et limiter les essais en neige naturelle aux simples essais de certification (vérification des résultats obtenus au banc).

Les différents essais effectués sur plusieurs définitions d'entrée d'air ont permis de constituer une banque de résultats qui servent de base à l'établissement de moyens de calcul prévisionnel.

L'amélioration de nos connaissances du fonctionnement de la protection des entrées d'air contre la neige et le givre a modifié le processus classique de définition d'une entrée d'air qui était essentiellement centré sur l'optimisation aérodynamique. Aujourd'hui, nous intégrons dès le début du développement des travaux et essais concernant la protection et donc de définir une entrée d'air globalement plus performante.

Les travaux effectués par Aérospatiale dans les 4 dernières années sur la protection des entrées d'air ont été menés sur 4 installations motrice différentes et représentent environ 60 heures d'essai en soufflerie givrante, 40 heures en chambre climatique neige, et 4 campagnes d'essais en vol à la neige. Ils ont permis d'optimiser le concept de protection par grille qui est à notre sens le plus performant, tant au niveau masse, perte de puissance associée, que pour la fiabilité de la protection.

Discussion

1. A. Spirk, MTU

Have you — in the case of partial accretion of ice on the inlet screen — observed pressure distortion at the position of the engine inlet?

Can you indicate the additional pressure loss caused by a blocked inlet screen, for high engine power level, i.e. high inlet air flow?

Author:

The effect of an eventual pressure inlet distortion due to the ice accretion on the screen is checked in two ways. At the end of the icing test point it is checked that the engine is able to accelerate satisfactorily surge free with the accretion on the screen. Secondly during the air inlet pressure distortion tests, a test point is conducted with the simulation of the screen clogging.

Generally the pressure loss through the iced screen does not exceed 5% of the atmospheric pressure. But in most of the test points, the loss remained below this value.

2. ??

Can you give me an indication about the pressure loss that occurs at fully iced inlets at high mass flows?

Author:

It should not be more than 5% of the atmospheric pressure. But in most of the test points the loss remains below this value.

35-10

REPORT DOCUMENTATION PAGE			
1. Recipient's Reference	2. Originator's Reference	3. Further Reference	4. Security Classification of Document
	AGARD-CP-48Q	ISBN 92-835-0618-9	UNCLASSIFIED
5. Originator	Advisory Group for Aerospace Research and Development North Atlantic Treaty Organization 7 rue Ancelle, 92200 Neuilly sur Seine, France		
6. Title	LOW TEMPERATURE ENVIRONMENT OPERATIONS OF TURBOENGINES (DESIGN AND USER'S PROBLEMS)		
7. Presented at	the Propulsion and Energetics Panel 76th Symposium held in Brussels, Belgium, 8th—12th October 1990.		
8. Author(s)/Editor(s)	Various		9. Date May 1991
10. Author's/Editor's Address	Various		11. Pages 386
12. Distribution Statement	This document is distributed in accordance with AGARD policies and regulations, which are outlined on the back covers of all AGARD publications.		
13. Keywords/Descriptors			
Turboengine design Turboengine operations Icing Cold weather starting Anti-icing systems		Low temperature operations Icing tests Ice tolerant design Ice protection Low temperature ignition	
14. Abstract			
<p>The Conference Proceedings contain the 33 papers presented at the Propulsion and Energetics Panel 76th Symposium on "Low Temperature Environment Operations of Turboengines (Design and User's Problems)", which was held 8th—12th October 1990 in Brussels, Belgium.</p> <p>The Symposium was composed of the following sessions: Cold Weather Operational Experience and Requirements (6); System Design Considerations (14); Fuel Effects and Lubricants Behaviour (5); Icing Conditions and Testing (8). Questions and answers of the discussions follow each paper in the Proceedings.</p> <p>Both the engine designers and the users made ample use of this Symposium to exchange their views of the state of their art and their experience within and between their respective communities. The papers presented and the discussions represent a significant contribution to improved cold weather tolerant and anti-icing design and to safer aircraft operation in a low temperature environment. A case was also made for advanced and larger dedicated testing facilities, and some specialized software developments were indicated.</p>			

<p>AGARD Conference Proceedings 480 Advisory Group for Aerospace Research and Development, NATO LOW TEMPERATURE ENVIRONMENT OPERATIONS OF TURBOENGINES (DESIGN AND USER'S PROBLEMS) Published May 1991 386 pages</p> <p>The Conference Proceedings contain the 33 papers presented at the Propulsion and Energetics Panel 76th Symposium on "Low Temperature Environment Operations of Turboengines (Design and User's Problems)", which was held 8th-12th October 1990 in Brussels, Belgium.</p> <p>P.T.O.</p>	<p>AGARD-CP-480</p> <p>Turboengine design Turboengine operations Icing Cold weather starting Anti-icing systems Low temperature operations Icing tests Ice tolerant design Ice protection Low temperature ignition</p>	<p>AGARD Conference Proceedings 480 Advisory Group for Aerospace Research and Development, NATO LOW TEMPERATURE ENVIRONMENT OPERATIONS OF TURBOENGINES (DESIGN AND USER'S PROBLEMS) Published May 1991 386 pages</p> <p>The Conference Proceedings contain the 33 papers presented at the Propulsion and Energetics Panel 76th Symposium on "Low Temperature Environment Operations of Turboengines (Design and User's Problems)", which was held 8th-12th October 1990 in Brussels, Belgium.</p> <p>P.T.O.</p>	<p>AGARD-CP-480</p> <p>Turboengine design Turboengine operations Icing Cold weather starting Anti-icing systems Low temperature operations Icing tests Ice tolerant design Ice protection Low temperature ignition</p>
<p>AGARD Conference Proceedings 480 Advisory Group for Aerospace Research and Development, NATO LOW TEMPERATURE ENVIRONMENT OPERATIONS OF TURBOENGINES (DESIGN AND USER'S PROBLEMS) Published May 1991 386 pages</p> <p>The Conference Proceedings contain the 33 papers presented at the Propulsion and Energetics Panel 76th Symposium on "Low Temperature Environment Operations of Turboengines (Design and User's Problems)", which was held 8th-12th October 1990 in Brussels, Belgium</p> <p>P.T.O.</p>	<p>AGARD-CP-480</p> <p>Turboengine design Turboengine operations Icing Cold weather starting Anti-icing systems Low temperature operations Icing tests Ice tolerant design Ice protection Low temperature ignition</p>	<p>AGARD Conference Proceedings 480 Advisory Group for Aerospace Research and Development, NATO LOW TEMPERATURE ENVIRONMENT OPERATIONS OF TURBOENGINES (DESIGN AND USER'S PROBLEMS) Published May 1991 386 pages</p> <p>The Conference Proceedings contain the 33 papers presented at the Propulsion and Energetics Panel 76th Symposium on "Low Temperature Environment Operations of Turboengines (Design and User's Problems)", which was held 8th-12th October 1990 in Brussels, Belgium.</p> <p>P.T.O.</p>	<p>AGARD-CP-480</p> <p>Turboengine design Turboengine operations Icing Cold weather starting Anti-icing systems Low temperature operations Icing tests Ice tolerant design Ice protection Low temperature ignition</p>

<p>The Symposium was composed of the following sessions: Cold Weather Operational Experience and Requirements (6); System Design Considerations (14); Fuel Effects and Lubricants Behaviour (5); Icing Conditions and Testing (8). Questions and answers of the discussions follow each paper in the Proceedings.</p> <p>Both the engine designers and the users made ample use of this Symposium to exchange their views of the state of their art and their experience within and between their respective communities. The papers presented and the discussions represent a significant contribution to improved cold weather tolerant and anti-icing design and to safer aircraft operation in a low temperature environment. A case was also made for advanced and larger dedicated testing facilities, and some specialized software developments were indicated.</p> <p>ISBN 92-835-0618-9</p>	<p>The Symposium was composed of the following sessions: Cold Weather Operational Experience and Requirements (6); System Design Considerations (14); Fuel Effects and Lubricants Behaviour (5); Icing Conditions and Testing (8). Questions and answers of the discussions follow each paper in the Proceedings.</p> <p>Both the engine designers and the users made ample use of this Symposium to exchange their views of the state of their art and their experience within and between their respective communities. The papers presented and the discussions represent a significant contribution to improved cold weather tolerant and anti-icing design and to safer aircraft operation in a low temperature environment. A case was also made for advanced and larger dedicated testing facilities, and some specialized software developments were indicated.</p> <p>ISBN 92-835-0618-9</p>
<p>The Symposium was composed of the following sessions: Cold Weather Operational Experience and Requirements (6); System Design Considerations (14); Fuel Effects and Lubricants Behaviour (5); Icing Conditions and Testing (8). Questions and answers of the discussions follow each paper in the Proceedings.</p> <p>Both the engine designers and the users made ample use of this Symposium to exchange their views of the state of their art and their experience within and between their respective communities. The papers presented and the discussions represent a significant contribution to improved cold weather tolerant and anti-icing design and to safer aircraft operation in a low temperature environment. A case was also made for advanced and larger dedicated testing facilities, and some specialized software developments were indicated.</p> <p>ISBN 92-835-0618-9</p>	<p>The Symposium was composed of the following sessions: Cold Weather Operational Experience and Requirements (6); System Design Considerations (14); Fuel Effects and Lubricants Behaviour (5); Icing Conditions and Testing (8). Questions and answers of the discussions follow each paper in the Proceedings.</p> <p>Both the engine designers and the users made ample use of this Symposium to exchange their views of the state of their art and their experience within and between their respective communities. The papers presented and the discussions represent a significant contribution to improved cold weather tolerant and anti-icing design and to safer aircraft operation in a low temperature environment. A case was also made for advanced and larger dedicated testing facilities, and some specialized software developments were indicated.</p> <p>ISBN 92-835-0618-9</p>

AGARD

NATO - OTAN

7 RUE ANCELLE • 92200 NEUILLY-SUR-SEINE

FRANCE

Téléphone (1)47.38.57.00 • Télex 610 176

Télécopie (1)47.38.57.99

DIFFUSION DES PUBLICATIONS

AGARD NON CLASSIFIEES

L'AGARD ne détient pas de stocks de ses publications, dans un but de distribution générale à l'adresse ci-dessus. La diffusion initiale des publications de l'AGARD est effectuée auprès des pays membres de cette organisation par l'intermédiaire des Centres Nationaux de Distribution suivants. A l'exception des Etats-Unis, ces centres disposent parfois d'exemplaires additionnels; dans les cas contraire, on peut se procurer ces exemplaires sous forme de microfiches ou de microcopies auprès des Agences de Vente dont la liste suit

CENTRES DE DIFFUSION NATIONAUX

ALLEMAGNE

Fachinformatikszentrum,
Karlsruhe
D-7514 Eggenstein-Leopoldshafen 2

BELGIQUE

Coordonnateur AGARD-VSL
Etat-Major de la Force Aérienne
Quartier Reine Elisabeth
Rue d'Evere, 1140 Bruxelles

CANADA

Directeur du Service des Renseignements Scientifiques
Ministère de la Défense Nationale
Ottawa, Ontario K1A 0K2

DANEMARK

Danish Defence Research Board
Ved Idraetsparken 4
2100 Copenhagen Ø

ESPAGNE

INTA (AGARD Publications)
Pintor Rosales 34
28008 Madrid

ETATS-UNIS

National Aeronautics and Space Administration
Langley Research Center
M/S 180
Hampton, Virginia 23665

FRANCE

O.N.E.R.A. (Direction)
29, Avenue de la Division Leclerc
92320, Châtillon sous Bagneux

GRECE

Hellenic Air Force
Air War College
Scientific and Technical Library
Dekelia Air Force Base
Dekelia, Athens TGA 1010

ISLANDE

Director of Aviation
c/o Flugrad
Reykjavik

ITALIE

Aeronautica Militare
Ufficio del Delegato Nazionale all'AGARD
3 Piazzale Adenauer
00144 Roma EUR

LUXEMBOURG

Voir Belgique

NORVEGE

Norwegian Defence Research Establishment
Attn: Biblioteket
P.O. Box 25
N-2007 Kjeller

PAYS-BAS

Netherlands Delegation to AGARD
National Aerospace Laboratory NLR
Kluuyverweg 1
2629 HS Delft

PORTUGAL

Portuguese National Coordinator to AGARD
Gabinete de Estudos e Programas
CLAFIA
Base de Alfragide
Alfragide
2700 Amadora

ROYAUME UNI

Defence Research Information Centre
Kentigern House
65 Brown Street
Glasgow G2 8EX

TURQUIE

Millî Savunma Başkanlığı (MSB)
ARGE Daire Başkanlığı (ARGE)
Ankara

LE CENTRE NATIONAL DE DISTRIBUTION DES ETATS-UNIS (NASA) NE DETIENT PAS DE STOCKS DES PUBLICATIONS AGARD ET LES DEMANDES D'EXEMPLAIRES DOIVENT ETRE ADRESSEES DIRECTEMENT AU SERVICE NATIONAL TECHNIQUE DE L'INFORMATION (NTIS) DONT L'ADRESSE SUIT.

AGENCES DE VENTE

National Technical Information Service
(NTIS)
5285 Port Royal Road
Springfield, Virginia 22161
Etats-Unis

ESA/Information Retrieval Service
European Space Agency
10, rue Mario Nikis
75015 Paris
France

The British Library
Document Supply Division
Boston Spa, Wetherby
West Yorkshire LS23 7BQ
Royaume Uni

Les demandes de microfiches ou de photocopies de documents AGARD (y compris les demandes faites auprès du NTIS) doivent comporter la dénomination AGARD, ainsi que le numéro de série de l'AGARD (par exemple AGARD-AG-315). Des informations analogues, telles que le titre et la date de publication sont souhaitables. Veuillez noter qu'il y a lieu de spécifier AGARD-R-n-n et AGARD-AR-n-n lors de la commande de rapports AGARD et des rapports consultatifs AGARD respectivement. Des références bibliographiques complètes ainsi que des résumés des publications AGARD figurent dans les journaux suivants:

Scientific and Technical Aerospace Reports (STAR)
publié par la NASA Scientific and Technical
Information Division
NASA Headquarters (NTI)
Washington D.C. 20546
Etats-Unis

Government Reports Announcements and Index (GRA&I)
publié par le National Technical Information Service
Springfield
Virginia 22161
Etats-Unis
(accessible également en mode interactif dans la base de
données bibliographiques en ligne du NTIS, et sur CD-ROM)



Imprimé par Specialised Printing Services Limited
40 Chigwell Lane, Loughton, Essex IG10 3TZ

AGARD

NATO OTAN

7 RUE ANCELLE - 92200 NEUILLY-SUR-SEINE

FRANCE

Telephone (1)47.38.57.00 • Telex 610 176

Telefax (1)47.38.57.99

DISTRIBUTION OF UNCLASSIFIED

AGARD PUBLICATIONS

AGARD does NOT hold stocks of AGARD publications at the above address for general distribution. Initial distribution of AGARD publications is made to AGARD Member Nations through the following National Distribution Centres. Further copies are sometimes available from these Centres (except in the United States), but if not may be purchased in Microfiche or Photocopy form from the Sales Agencies listed below.

NATIONAL DISTRIBUTION CENTRES

BELGIUM

Coordonnateur AGARD — VSL
Etat-Major de la Force Aérienne
Quartier Reine Elisabeth
Rue d'Evere, 1140 Bruxelles

LUXEMBOURG

See Belgium

NETHERLANDS

Netherlands Delegation to AGARD
National Aerospace Laboratory, NLR
Kluwerweg 1

CANADA

Director Scientific In-
Dept of National De-
Ottawa, Ontario K1L

NASA

National Aeronautics and
Space Administration

Washington, D.C.
20546

Postage and Fees Paid
National Aeronautics and
Space Administration
NASA-451

Official Business
Penalty for Private Use \$300



DENMARK

Danish Defence Res-
Ved Idraetsparken 4
2103 Copenhagen C

**SPECIAL FOURTH CLASS MAIL
BOOK**

FRANCE

O.N.E.R.A. (Directi-
29 Avenue de la Di-
92320 Châtillon

L1 001 AGARDCP480910819S002672D

DEPT OF DEFENSE

DEFENSE TECHNICAL INFORMATION CENTER

ATTN: DTIC-FDAB/JOYCE CHIRAS

CAMERON STATION BLDG 5

ALEXANDRIA VA 223046145

GERMANY

Fachinformationsz-
Karlsruhe
D-7514 Eggenstein

GREECE

Hellenic Air Force
Air War College
Scientific and Tech
Dekelia Air Force L
Dekelia, Athens TGA 1010

ICELAND

Director of Aviation
c/o Flugrad
Reykjavik

UNITED KINGDOM

Defence Research Inf. mation Centre
Kentigern House
65 Brown Street
Glasgow G2 8EX

ITALY

Aeronautica Militare
Ufficio del Delegato Nazionale all'AGARD
3 Piazza Adenauer
00144 Roma/EUR

UNITED STATES

National Aeronautics and Space Administration (NASA)
Langley Research Center
M/S 180
Hampton, Virginia 23665

THE UNITED STATES NATIONAL DISTRIBUTION CENTRE (NASA) DOES NOT HOLD
STOCKS OF AGARD PUBLICATIONS, AND APPLICATIONS FOR COPIES SHOULD BE MADE
DIRECT TO THE NATIONAL TECHNICAL INFORMATION SERVICE (NTIS) AT THE ADDRESS BELOW.

SALES AGENCIES

National Technical
Information Service (NTIS)
5285 Port Royal Road
Springfield, Virginia 22161
United States

ESA/Information Retrieval Service
European Space Agency
10, rue Mario Nikis
75015 Paris
France

The British Library
Document Supply Centre
Boston Spa, Wetherby
West Yorkshire LS23 7BQ
United Kingdom

Requests for microfiches or photocopies of AGARD documents (including requests to NTIS) should include the word 'AGARD' and the AGARD serial number (for example AGARD-AG-315). Collateral information such as title and publication date is desirable. Note that AGARD Reports and Advisory Reports should be specified as AGARD-R-nnn and AGARD-AR-nnn, respectively. Full bibliographical references and abstracts of AGARD publications are given in the following journals:

Scientific and Technical Aerospace Reports (STAR)
published by NASA Scientific and Technical
Information Division
NASA Headquarters (NTT)
Washington D.C. 20546
United States

Government Reports Announcements and Index (GRA&I)
published by the National Technical Information Service
Springfield
Virginia 22161
United States
(also available online in the NTIS Bibliographic
Database or on CD-ROM)



Printed by Specialised Printing Services Limited
40 Chigwell Lane, Loughton, Essex IG11 7TZ

ISBN 92-835-0618-9